

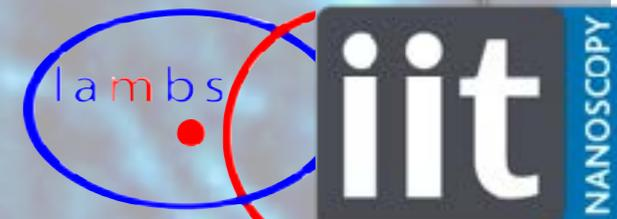
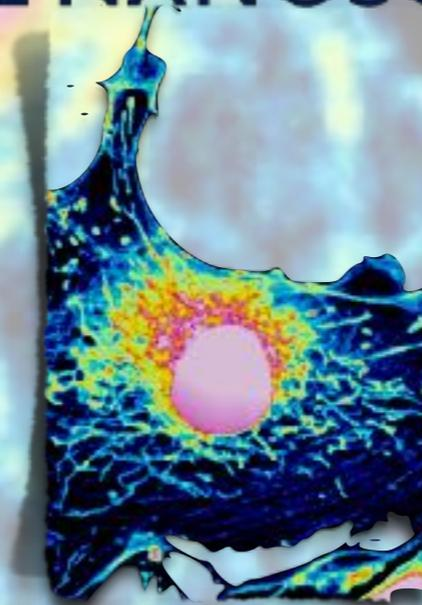


The Abdus Salam
International Centre
for Theoretical Physics

The Extra Microscope

Alberto Diaspro

ISTITUTO ITALIANO DI TECNOLOGIA
OPTICAL NANOSCOPY

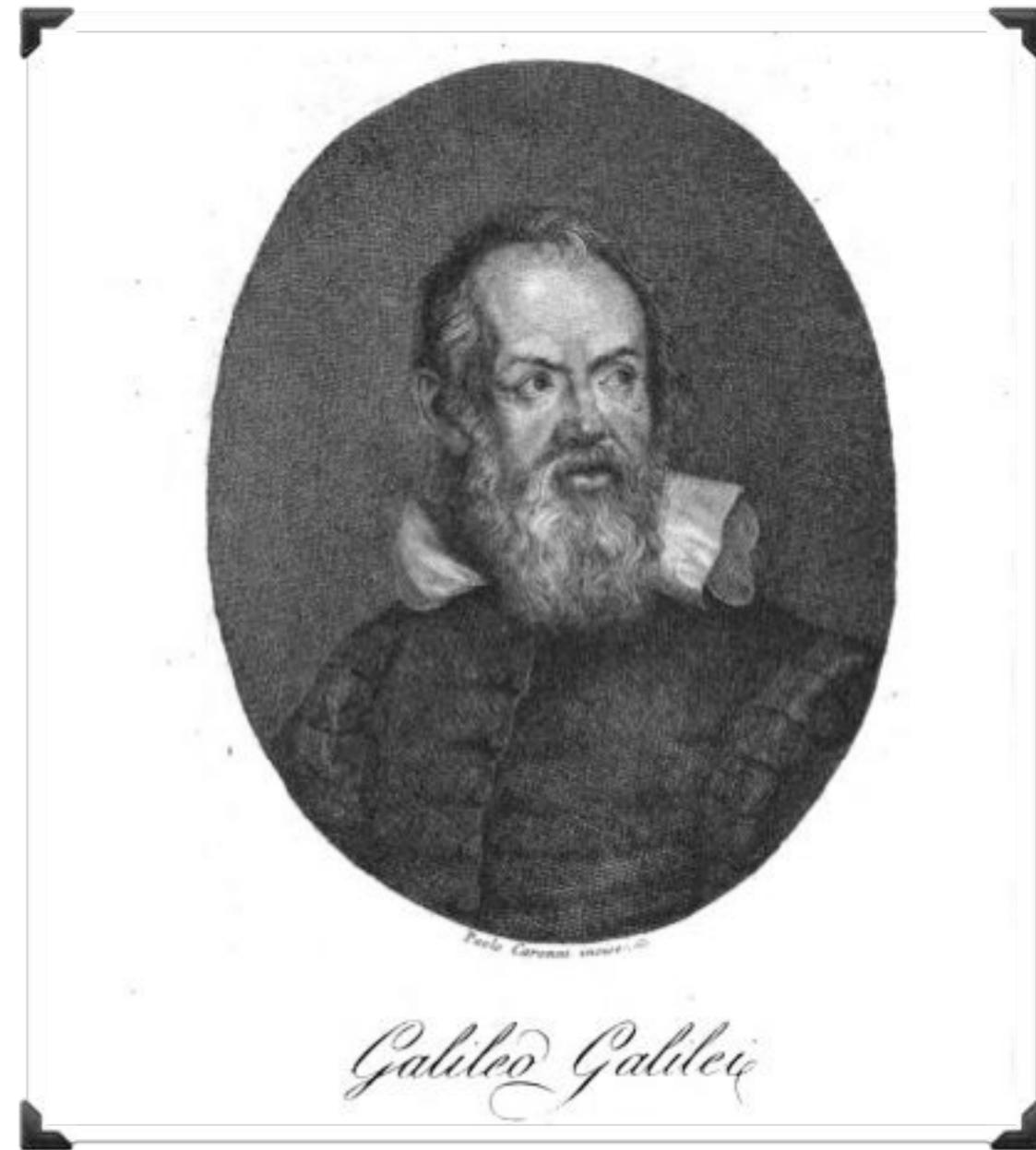


MICROSCOPIUM EXTRAORDINARIUM NOMINARE LIBUIT...

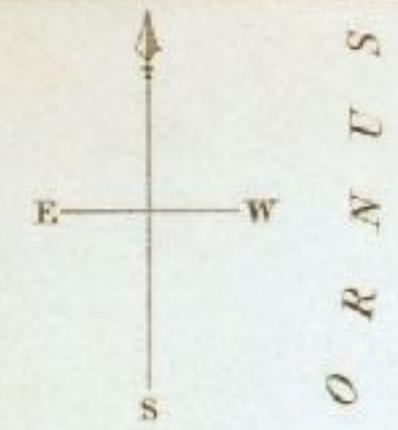
...microscopium nominare libuit...Faber, Lincei, 1625



Since the early years of the Galileo Galilei's "Occhialino" - "*un occhialino per veder da vicino le cose minime*" - brilliantly renamed, on April 13th 1625 in a letter written to Federico Cesi, as "Microscopium" by Johannes Faber (1574-1629), it was evident the potential of such an optical tool.



Ottavio Leoni, portrait of Galileo Galilei, 1624



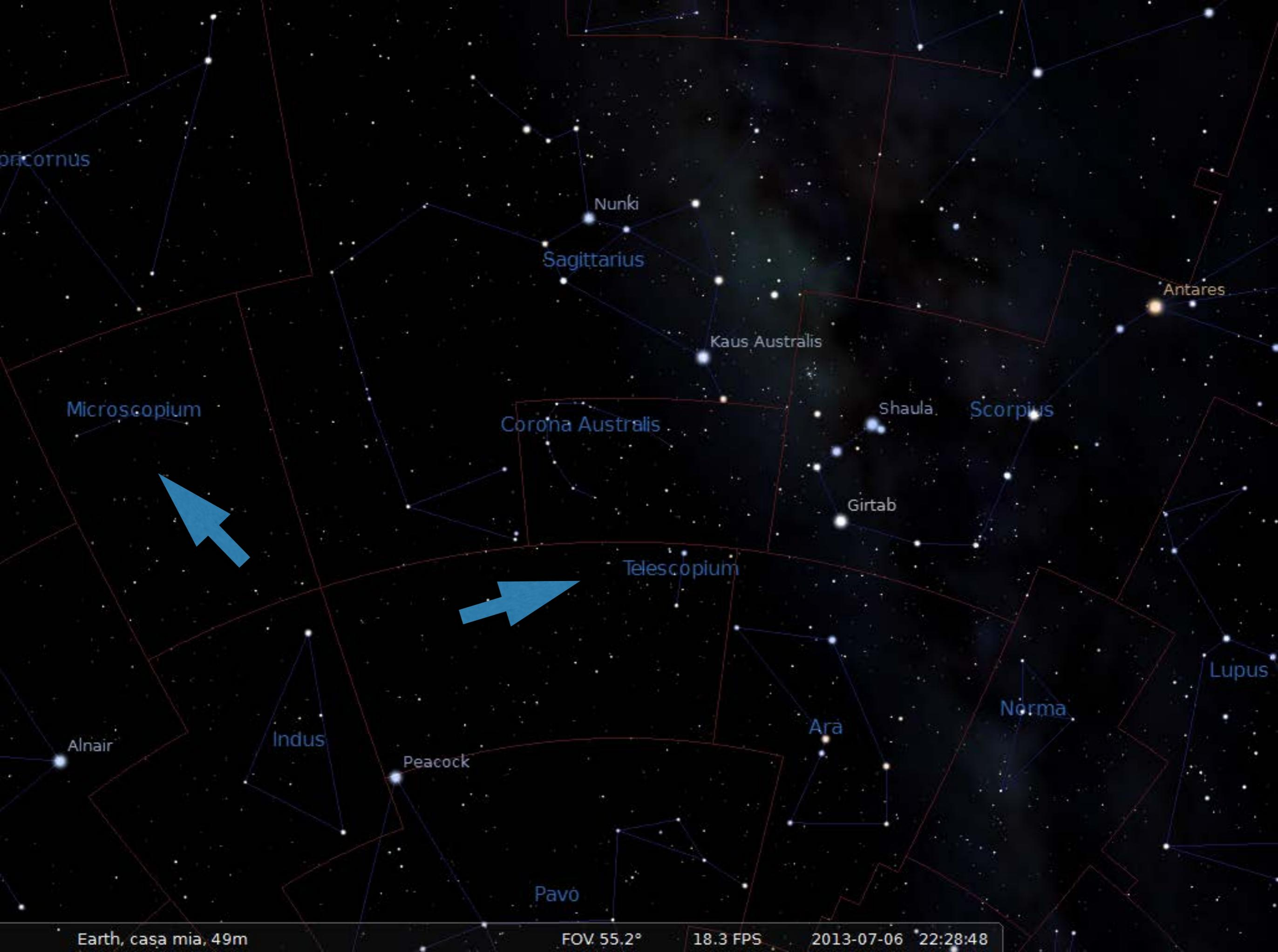
APRIL CORNUS
BALLON AEROSTAT.



ANTINOUS
SCUTUM
SOBIESKI
CORPUS
SAGITTARIUS
PAVO
ARA

MICROSCOPIUM. AND TELESCOPIUM.

Sculp. Hall, sculp.



Orion

Nunki

Sagittarius

Antares

Kaus Australis

Microscopium

Corona Australis

Shaula

Scorpius

Girtab

Telescopium

Lupus

Alnair

Indus

Peacock

Ara

Norma

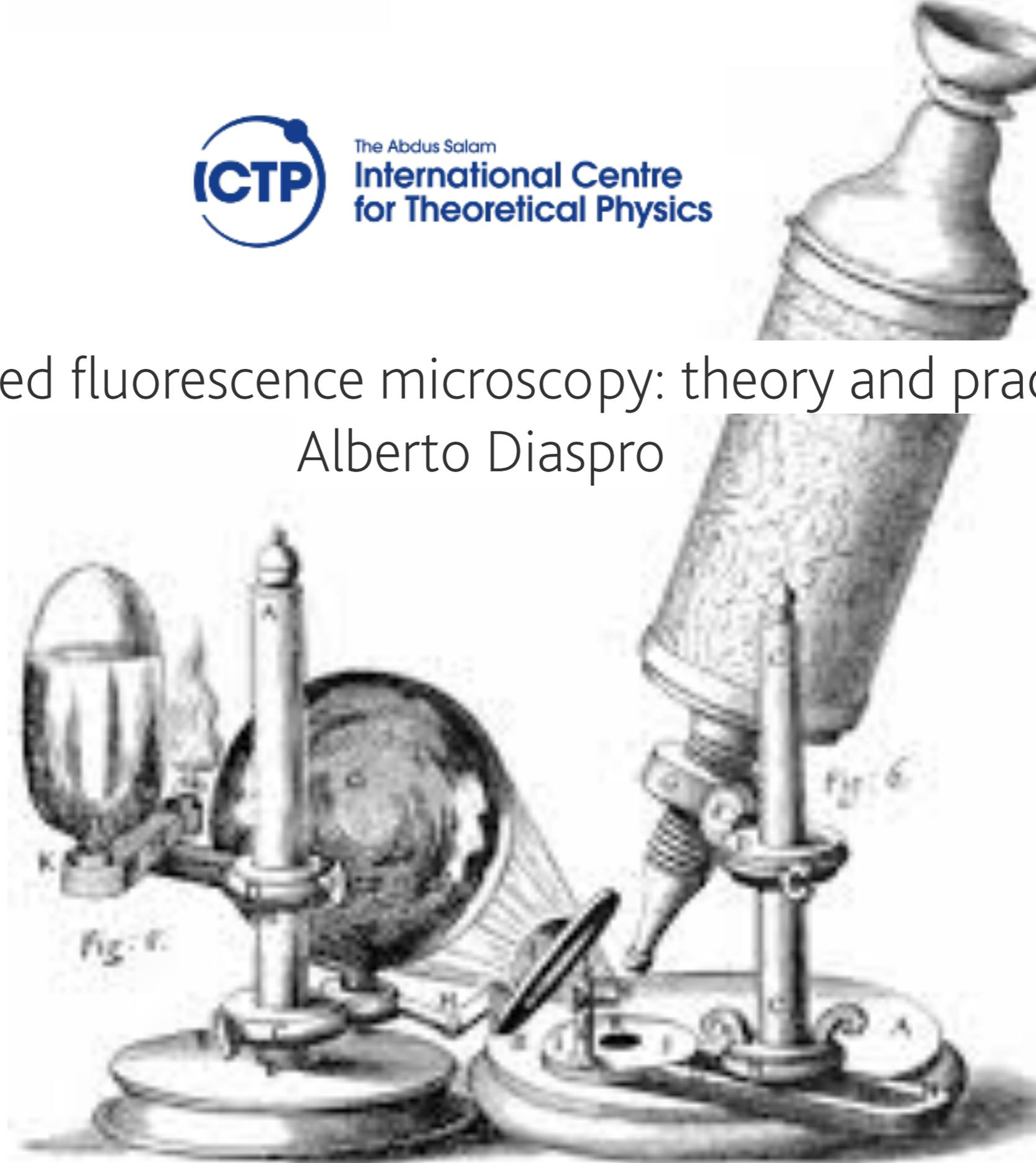
Pavo

"Sometimes you can observe
a lot by watching."
— Yogi Berra, catcher



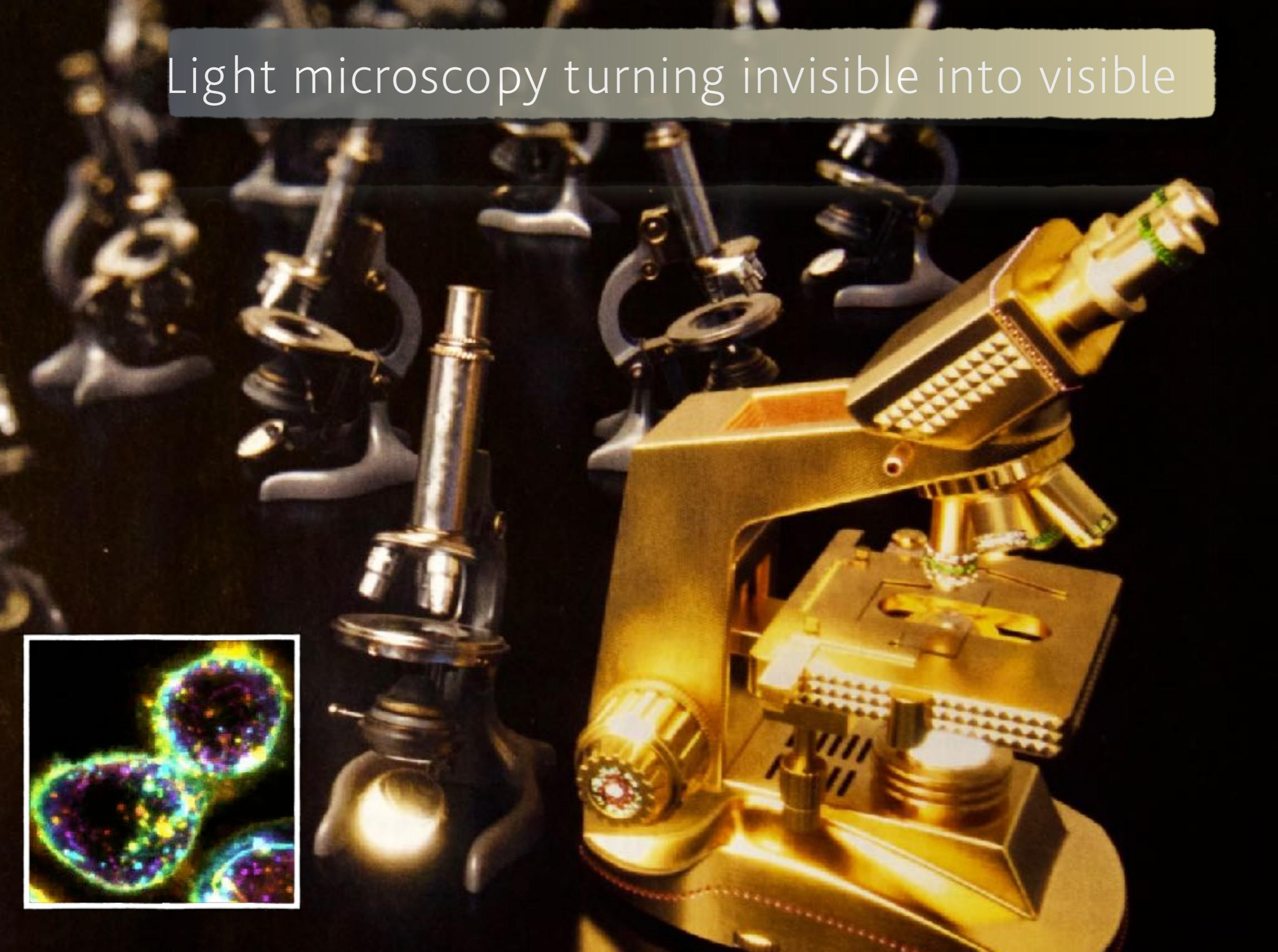
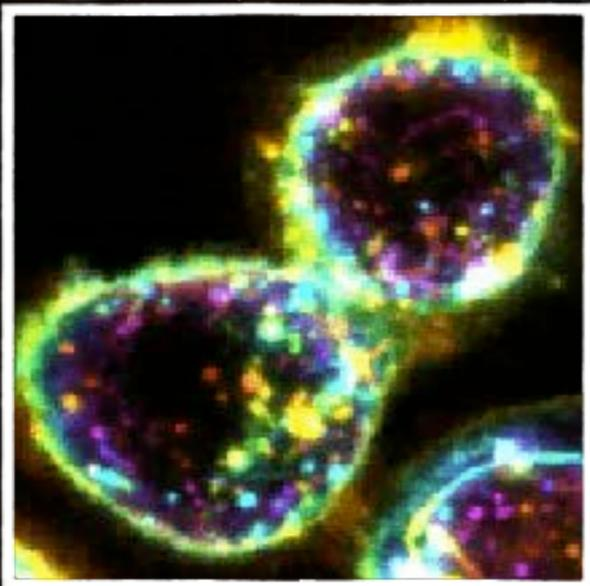
Advanced fluorescence microscopy: theory and practice

Alberto Diaspro

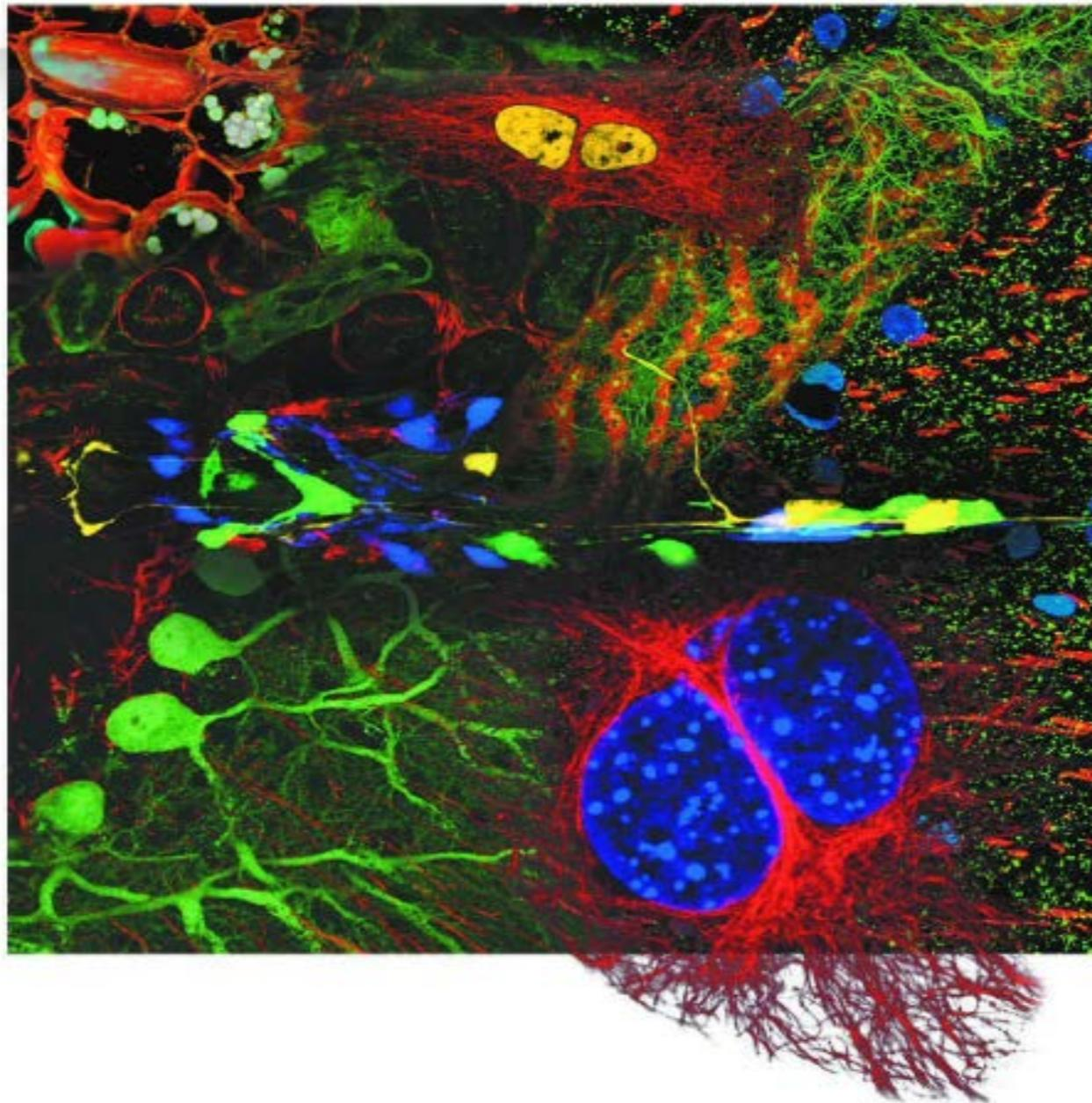


https://www.youtube.com/watch?v=h0jFSHz_5Rc

Light microscopy turning invisible into visible



Light microscopy turning invisible into visible

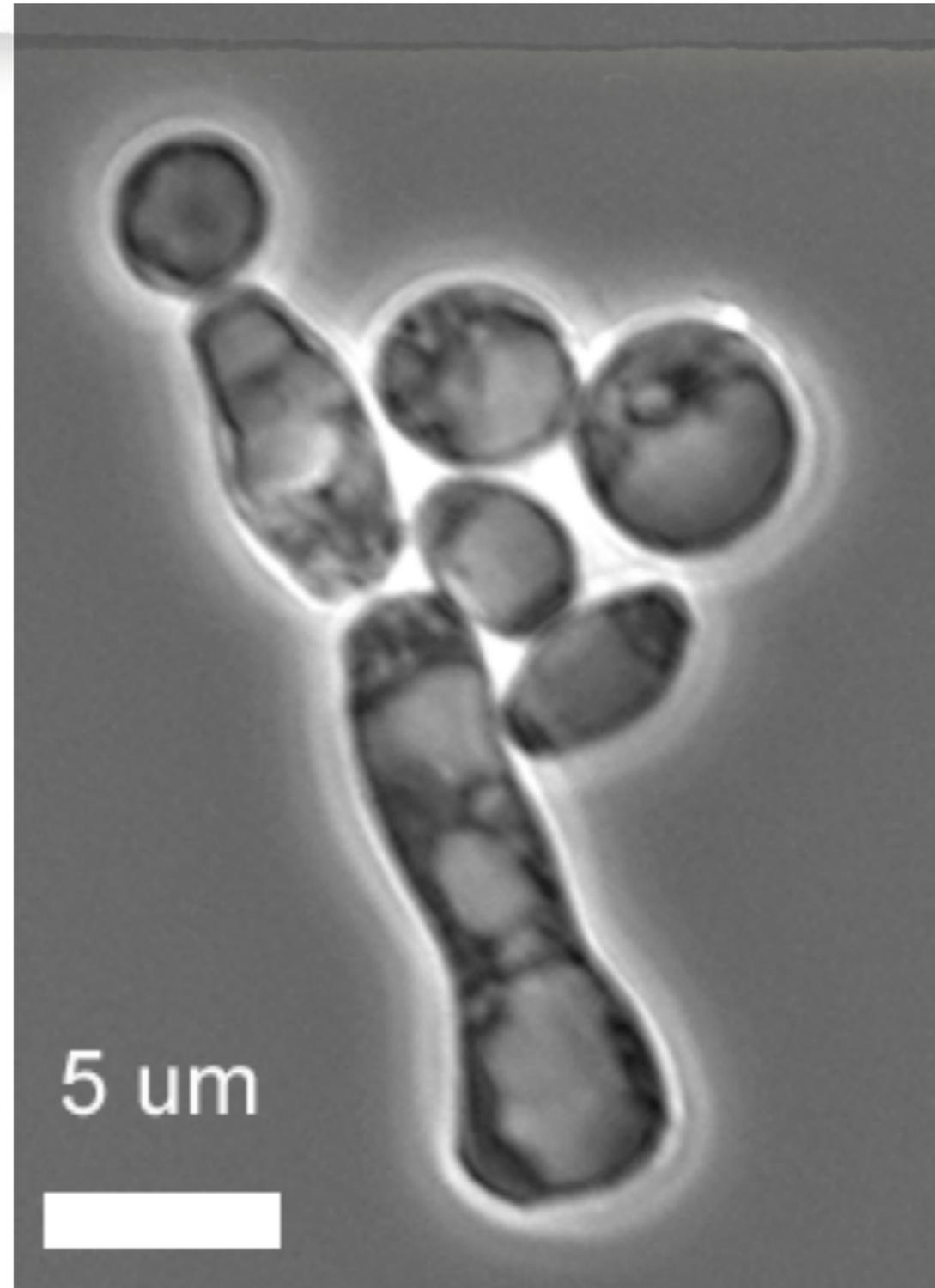


A microscope is an instrument magnifying objects by means of a specific interaction – more commonly by means of lenses – so as to capture details invisible to the naked eye.

(Oxford dictionary, after Colin Sheppard)

SLIDE CREDIT: leica microsystems

Light microscopy turning invisible into visible

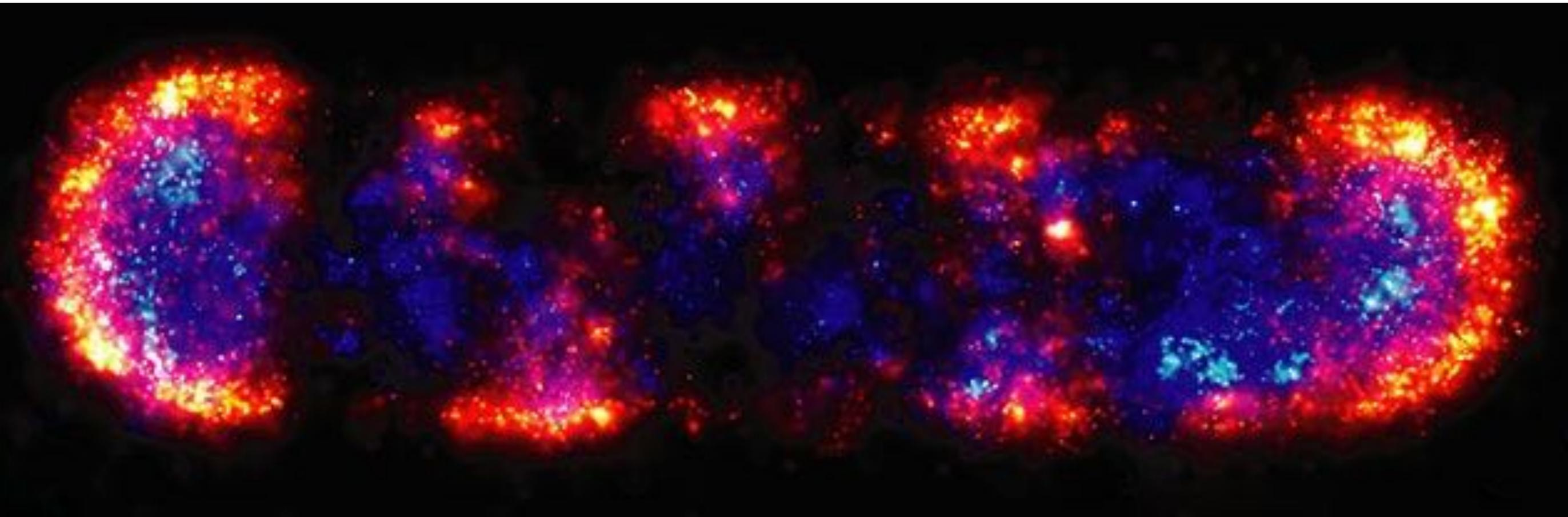


Light microscopy turning invisible into visible

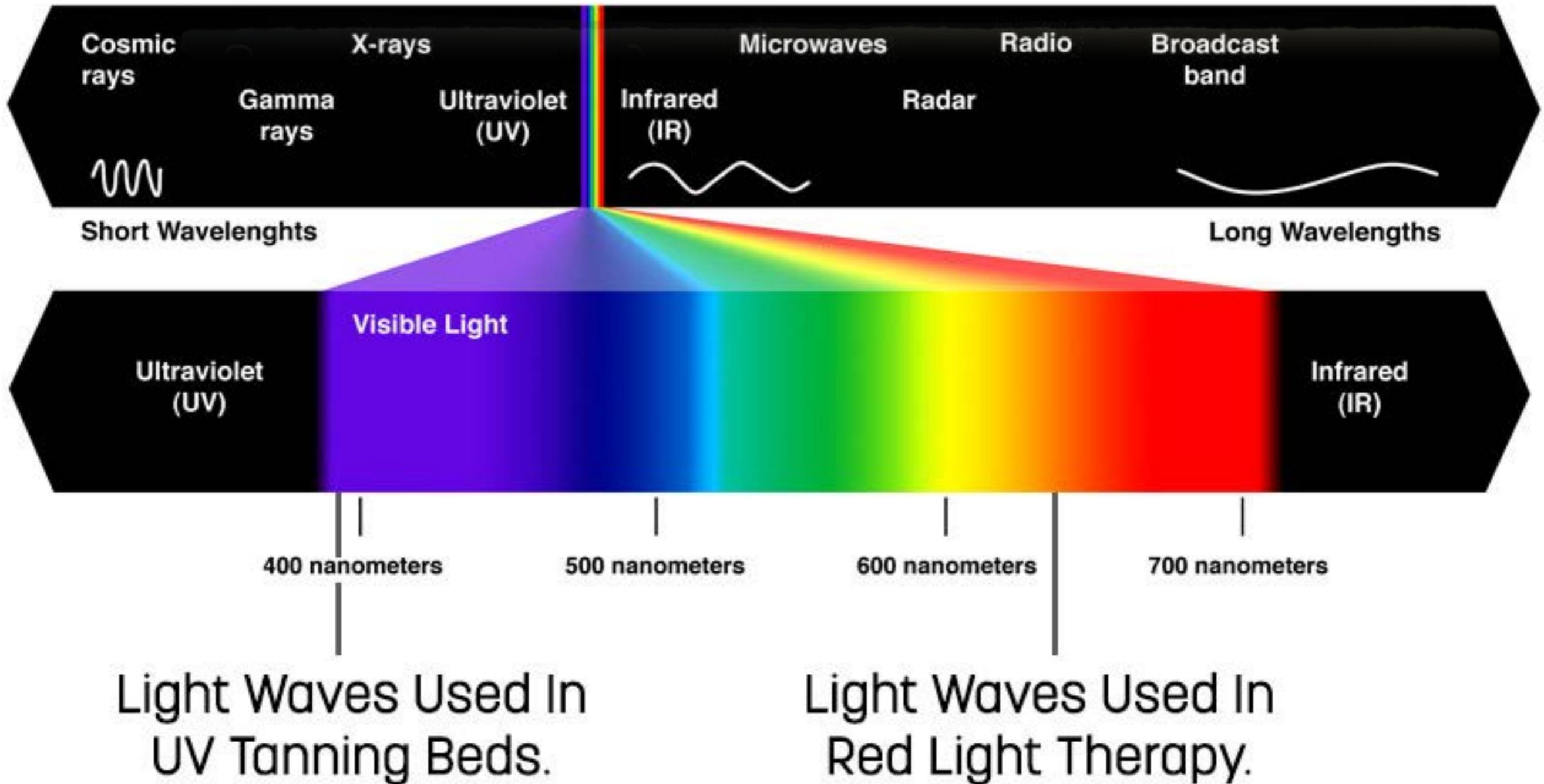


Light microscopy turning invisible into colors

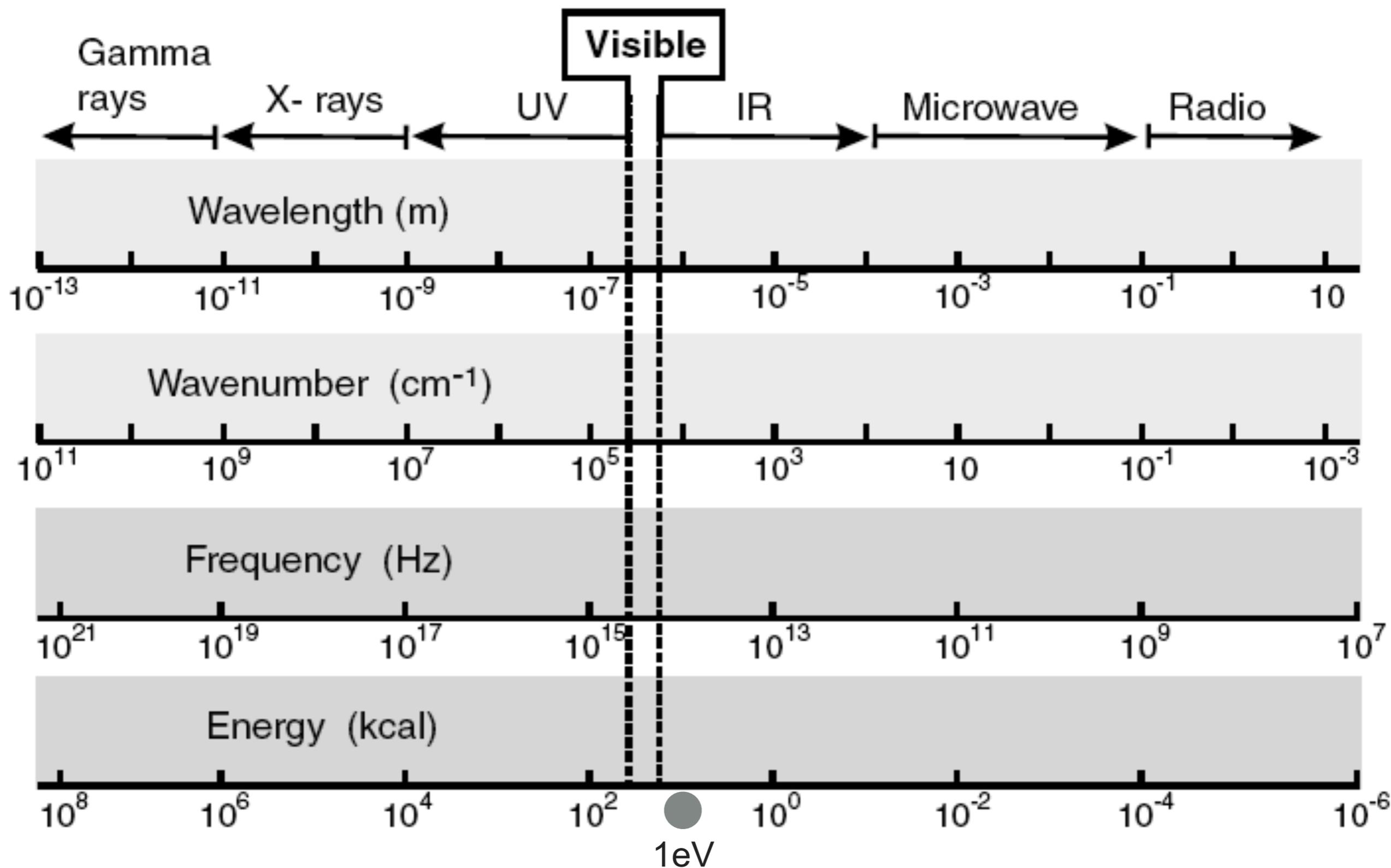
0 1 2 3



Light microscopy turning invisible into visible

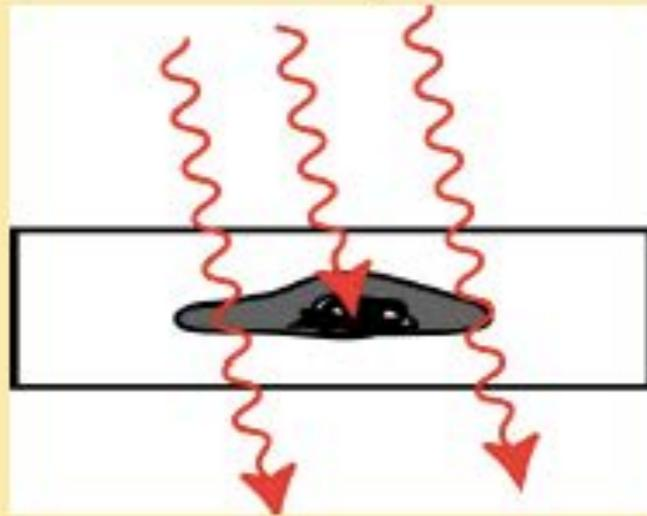


<http://www.tanunique.net/tropical-topics/230-what-is-red-light-therapy.html>

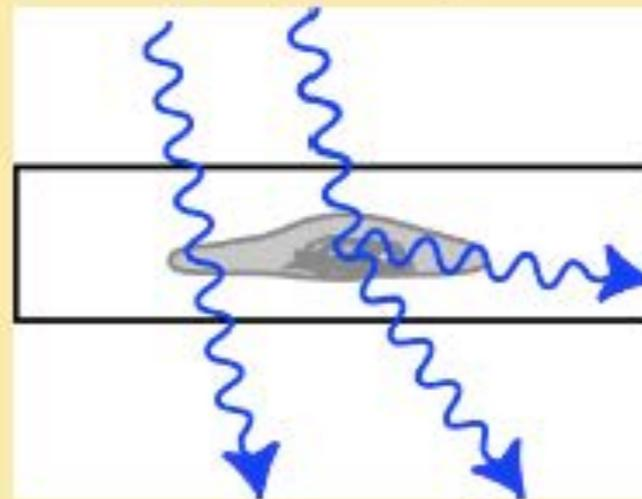


Possible Interactions with Light

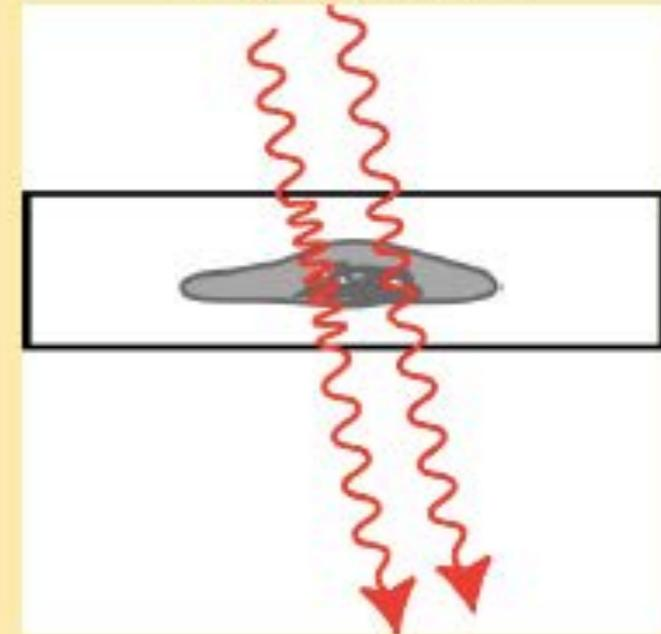
A. Absorption



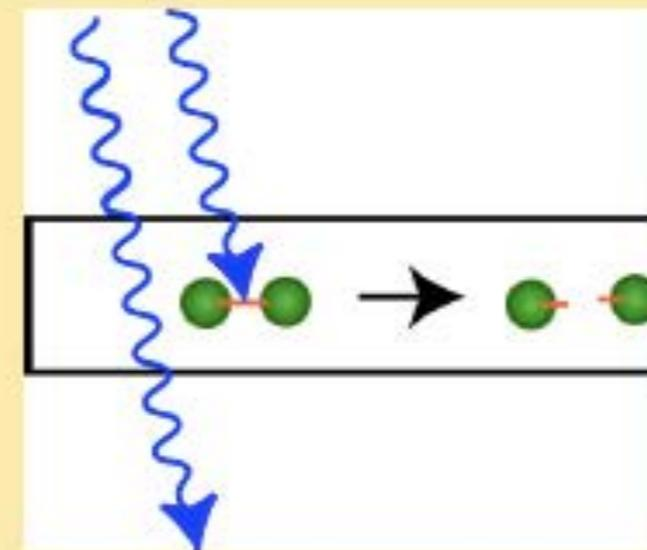
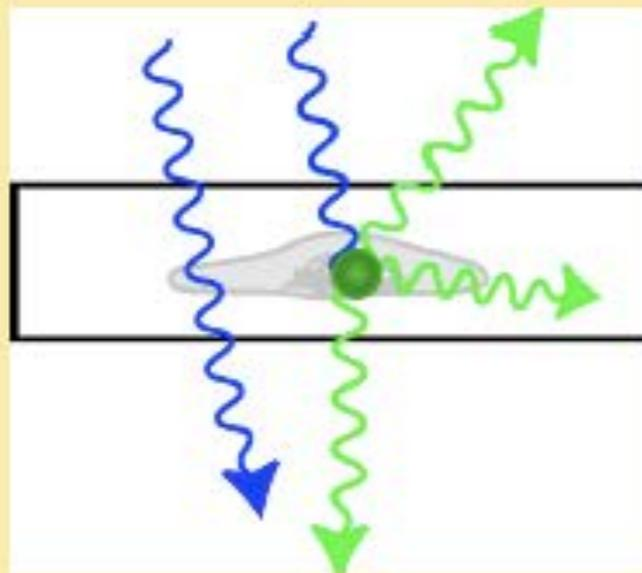
B. Scattering



C. Interference

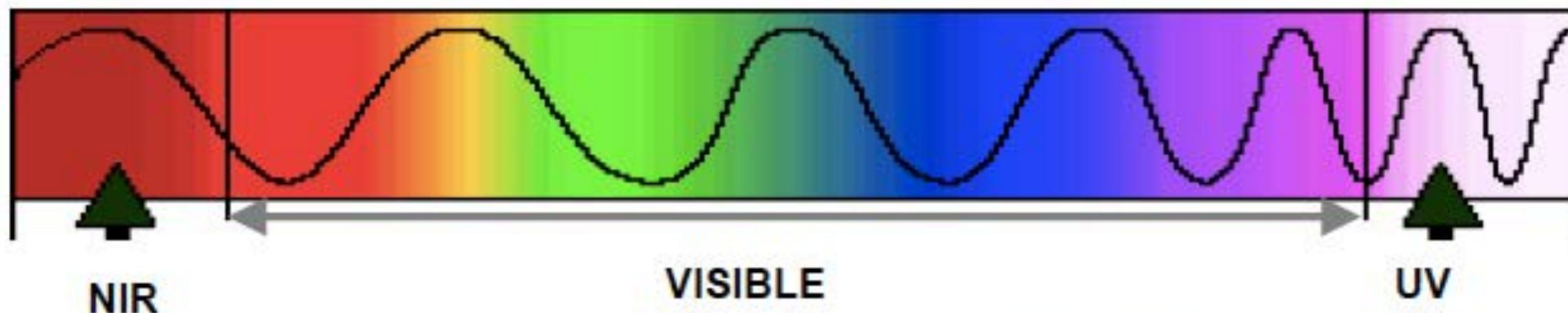


D. Fluorescence



E. Light-Induced Processes

Absorbers in Tissue



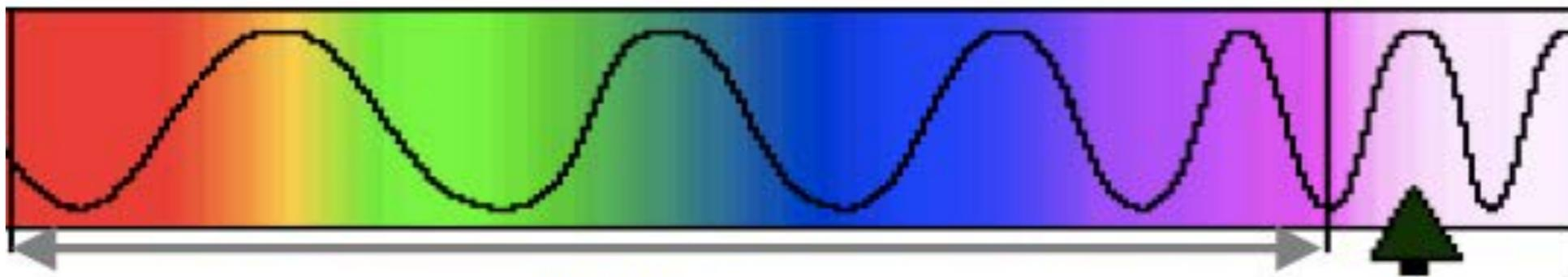
• NIR

- Hemoglobin
- Lipids
- Water

• UV-VIS

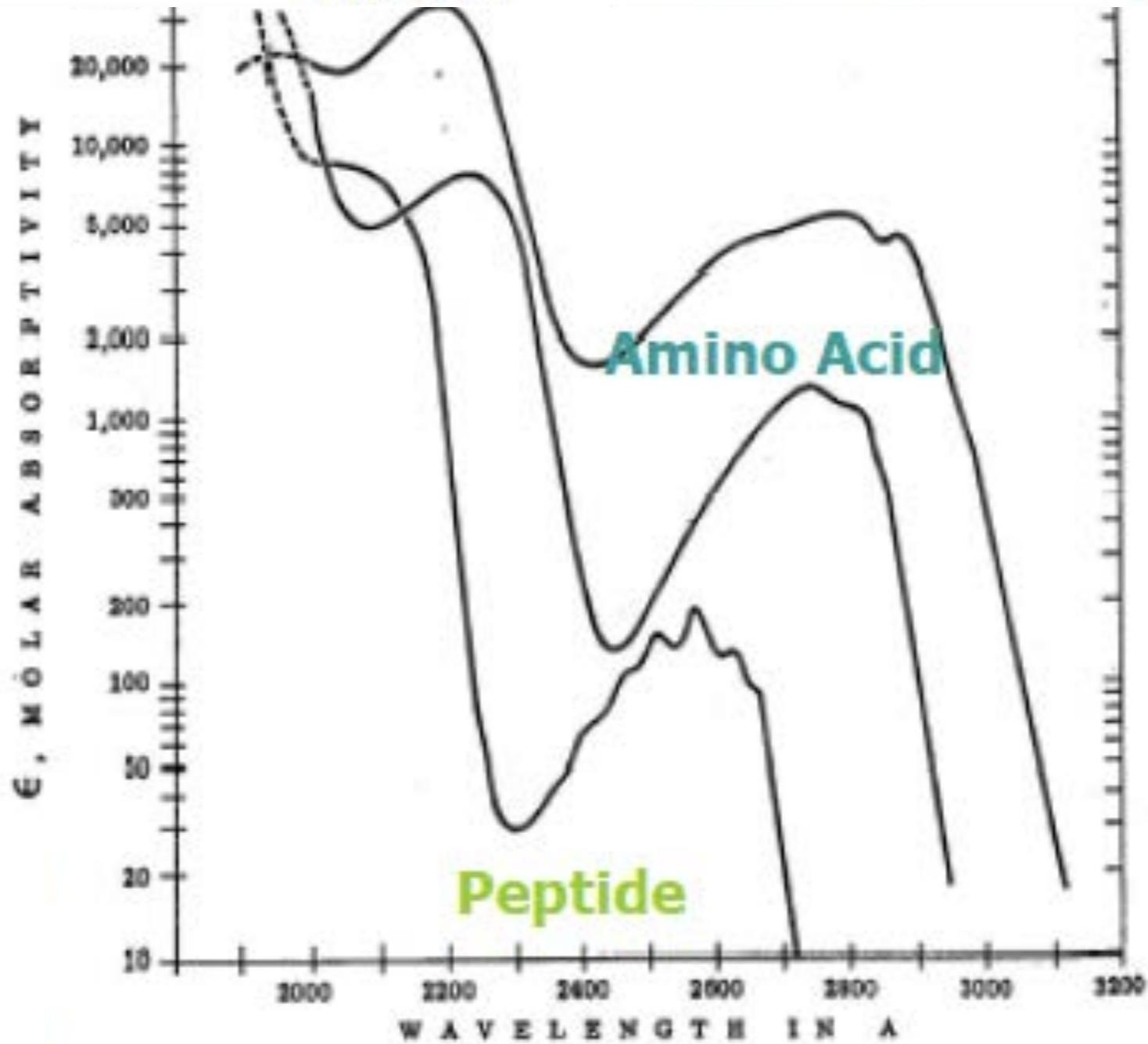
- DNA
- Hemoglobin
- Lipids
- Structural protein*
- Electron carriers*
- Amino acids*

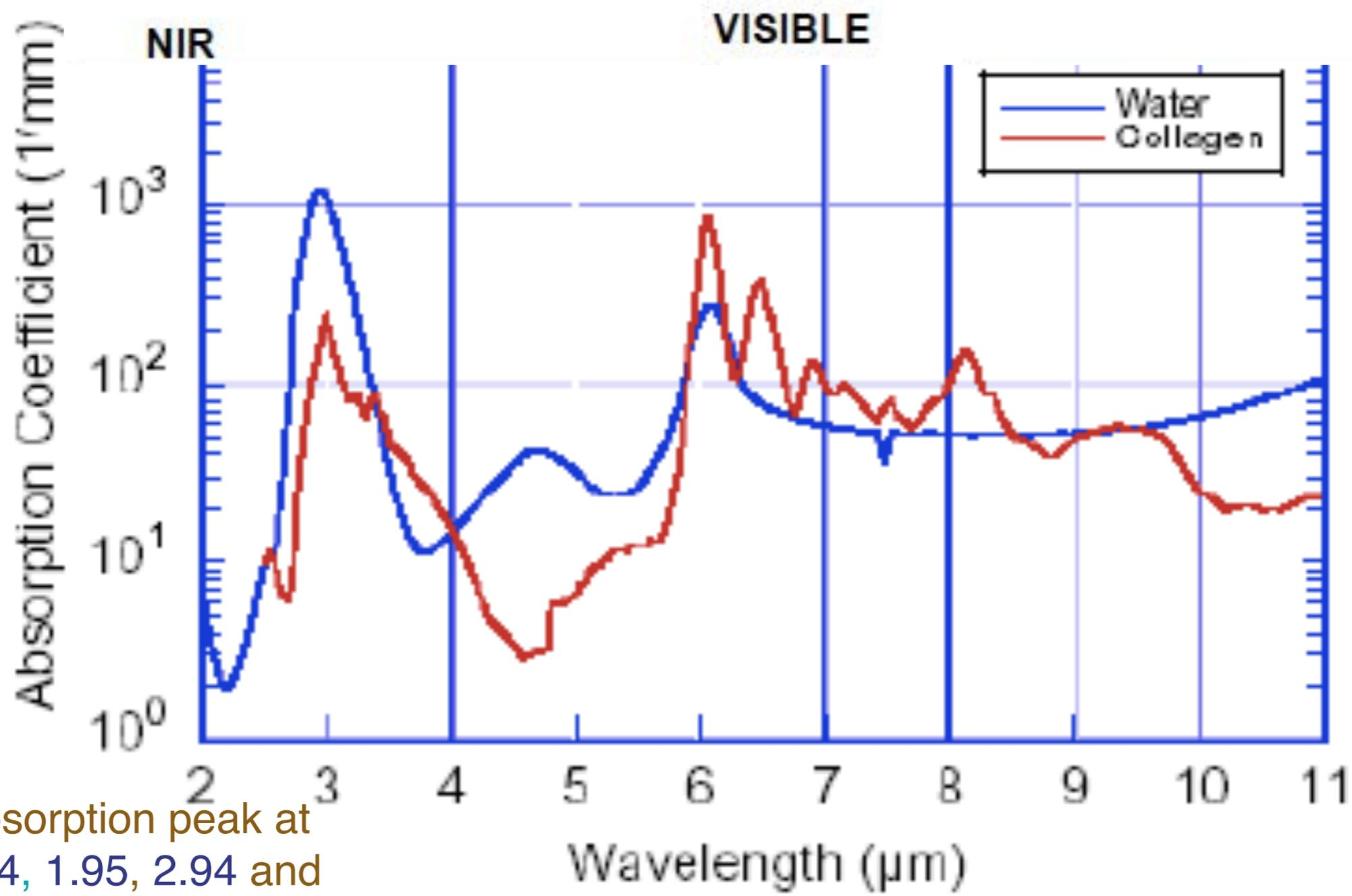
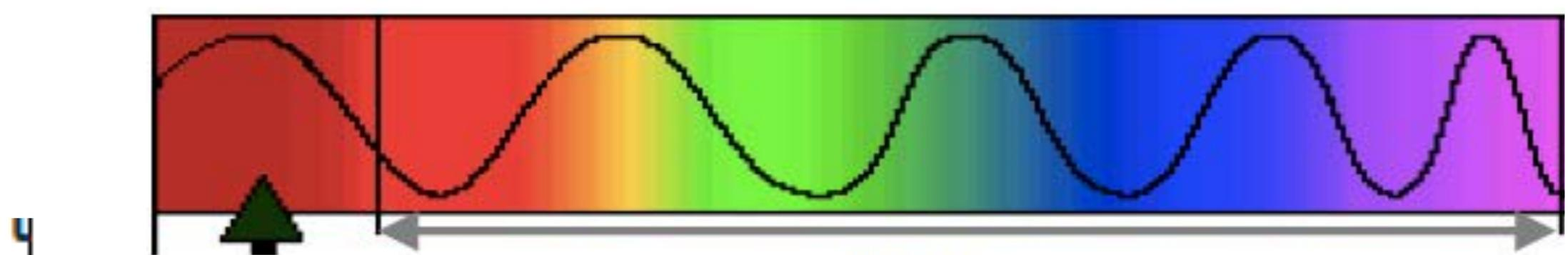
* Absorbers that fluoresce when excited in the UV-VIS



VISIBLE

UV

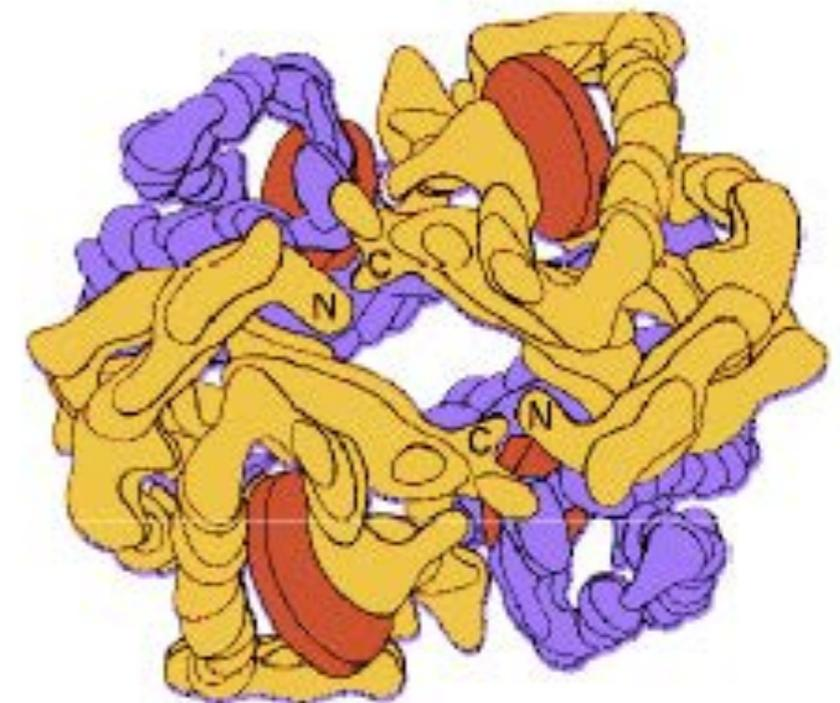
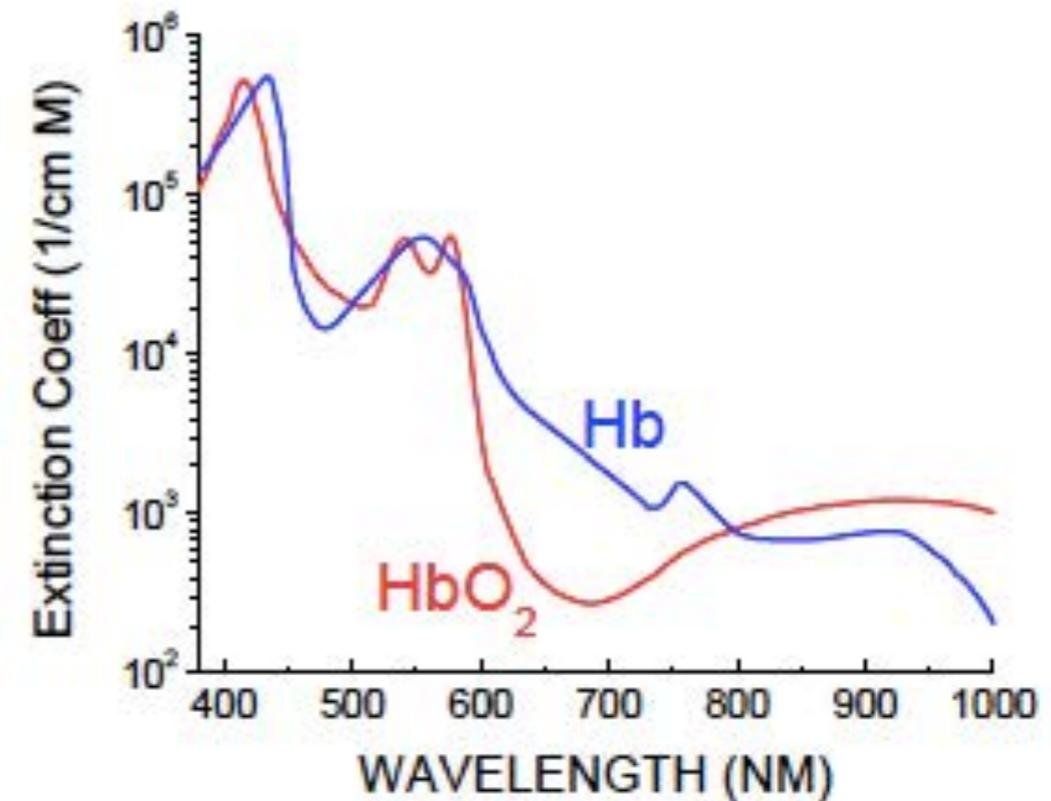


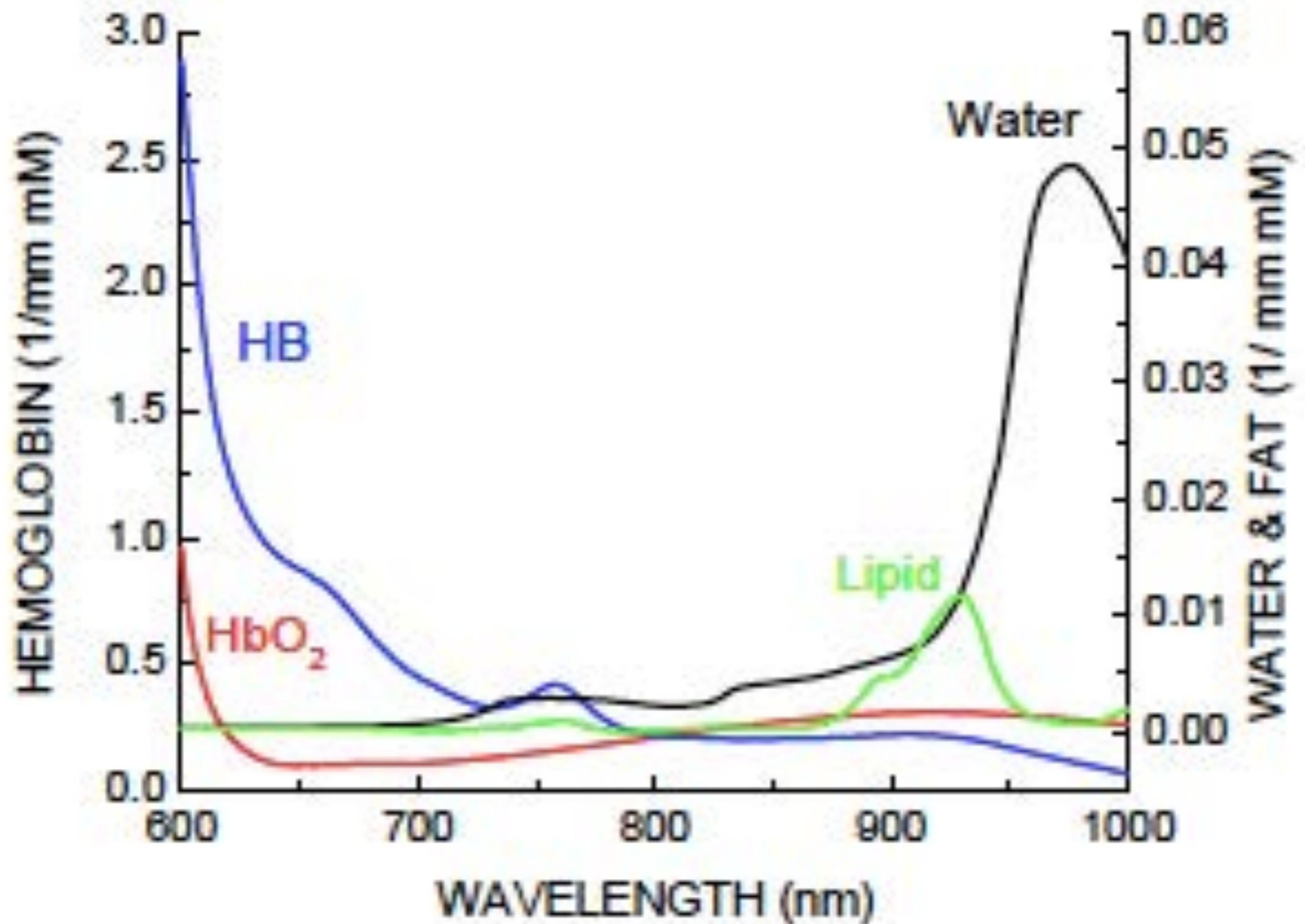


Water absorption peak at 0.96, 1.44, 1.95, 2.94 and 6.1 μm

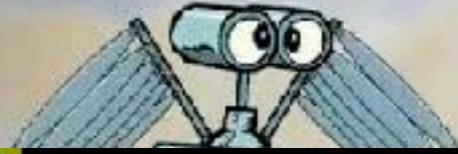
Hemoglobin

- **Responsible for oxygen transport**
 - HbO₂ and Hb
 - oxygen saturation is an indicator of oxygen delivery and utilization as well as metabolic activity
- **Deoxyhemoglobin has lower absorption than oxyhemoglobin in the blue and green**
 - Bright red arterial blood
 - Bluish venous blood
- **Absorption peaks for HbO₂**
 - 418, 542, 577, and 925 nm
- **Absorption peaks for Hb**
 - 550, 758, 910 nm





Alberto Diaspro, Nanoscopy, Istituto Italiano di Tecnologia



Bernd Rieger & Sjoerd Stallinga
Department of Imaging Physics
TU Delft

animation by Mooves

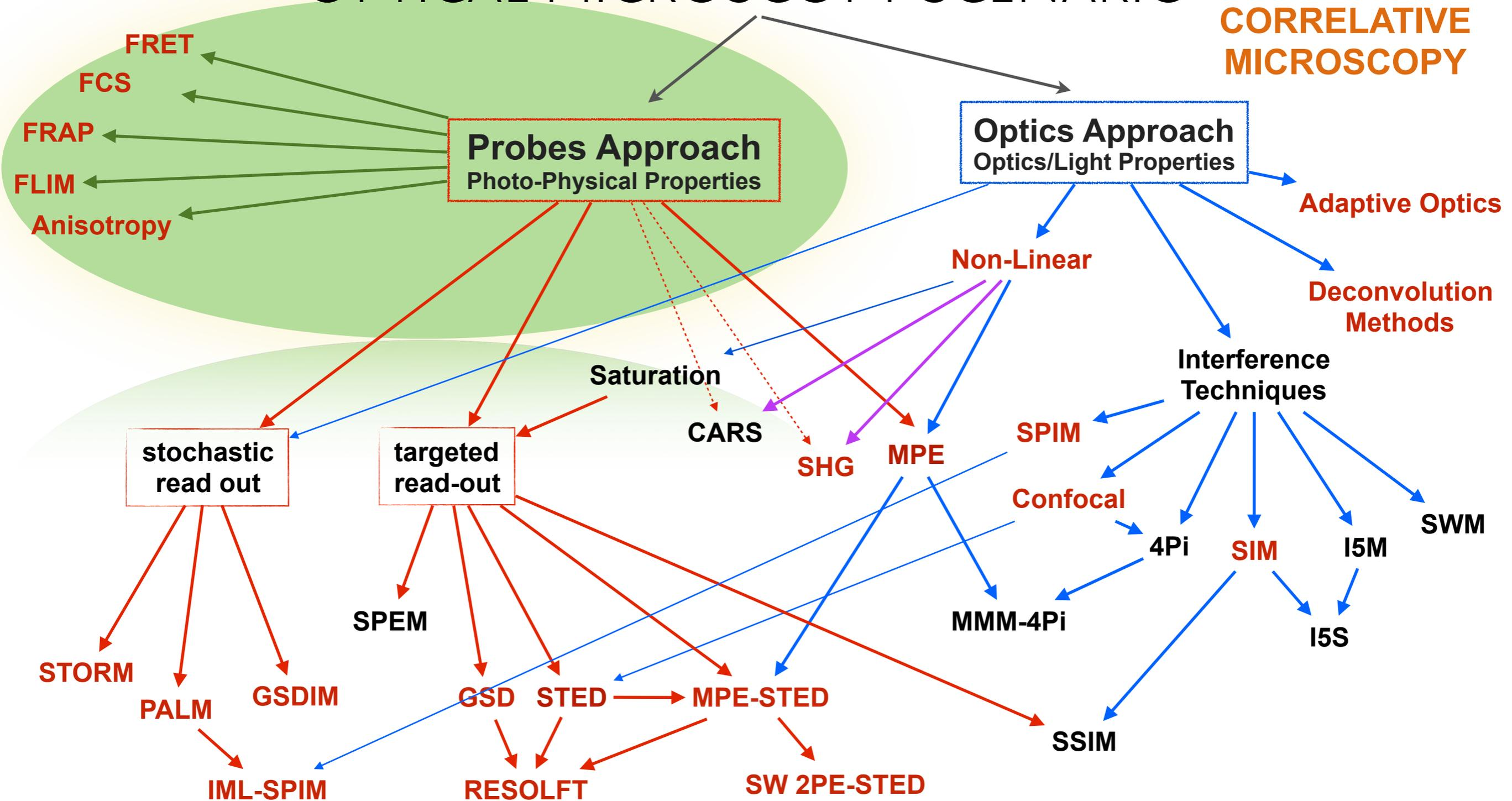


Optical microscope

- Objective lens
 - Numerical aperture ($n \sin \alpha$)
 - Air / oil immersion / water immersion
 - Corrected for cover slip (No. 1 $\frac{1}{2}$ = 0.17mm) or not
 - Corrected for infinity or not
 - e.g 100X 1.4NA Oil 0.17/ ∞
- Eyepiece
- Illumination system
 - Condenser
 - Aperture stop (diaphragm)
 - Field stop

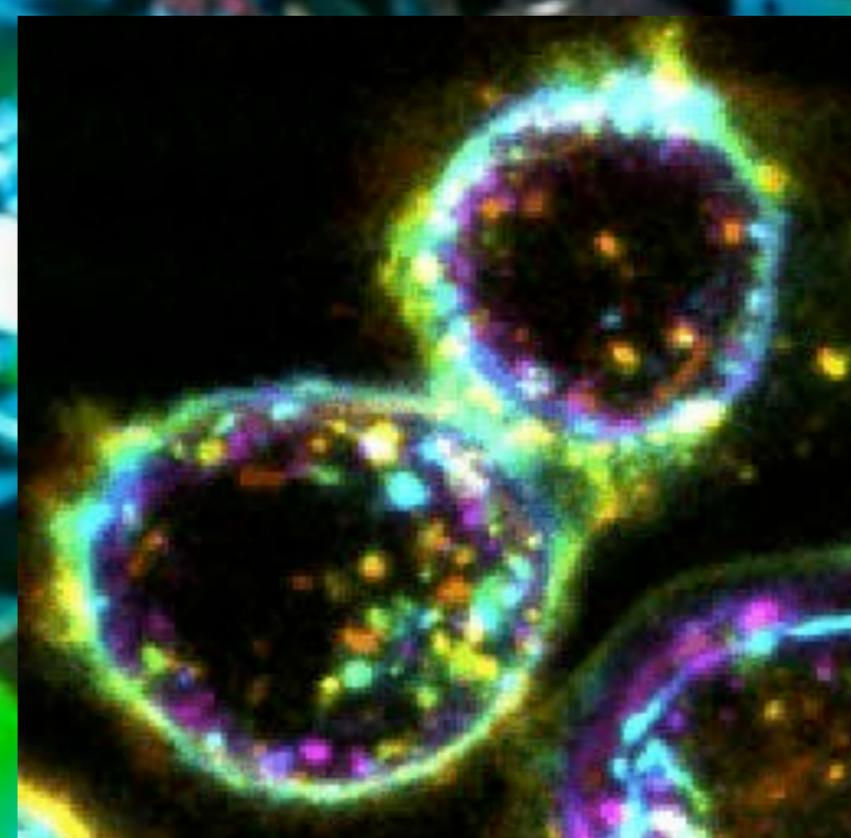
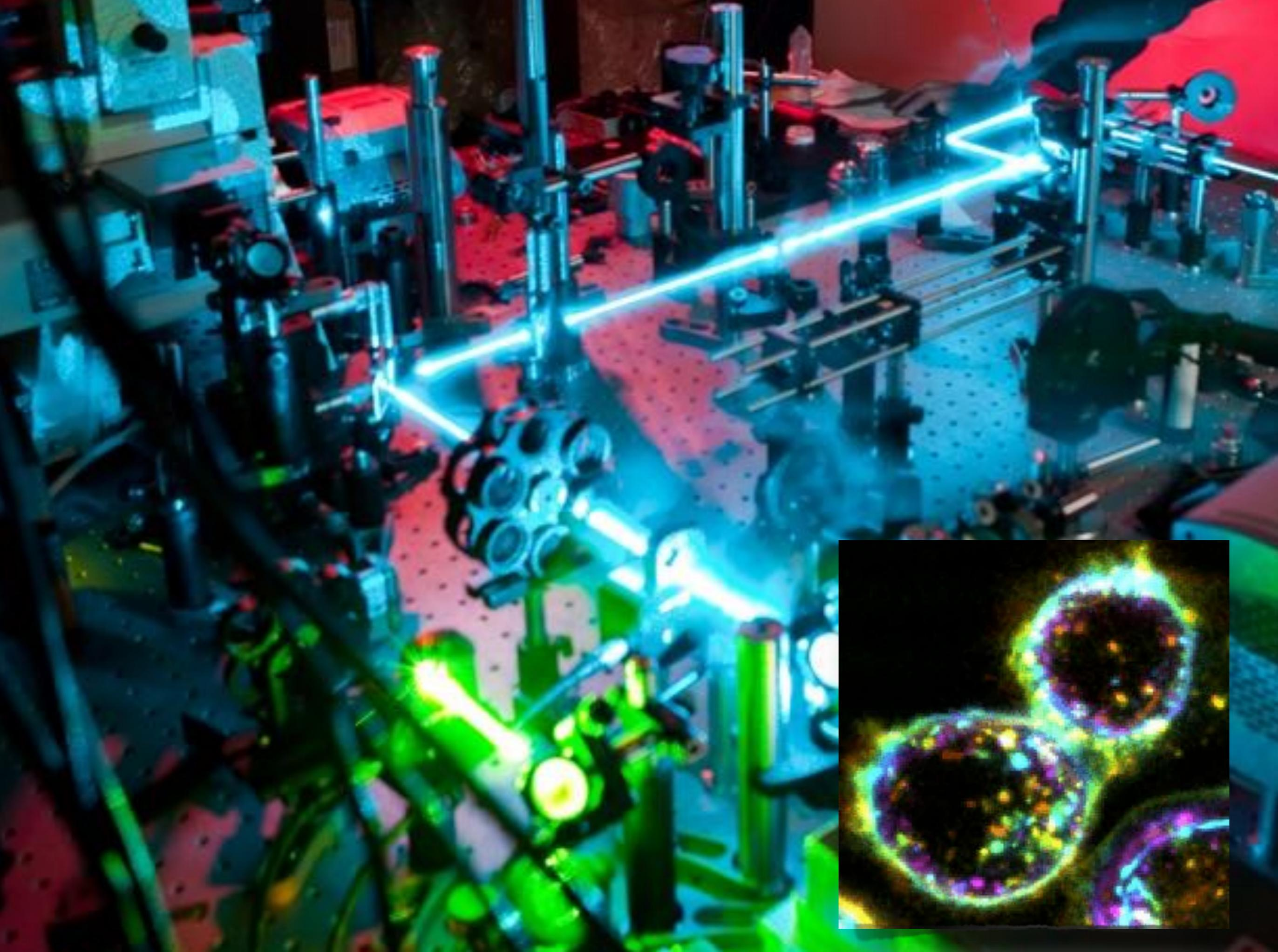


OPTICAL MICROSCOPY SCENARIO



***MUELLER matrix microscopy**

Y. Garini, B. J. Vermolen, I.T. Young, From micro to nano: recent advances in high-res microscopy, Curr.Op. iBiotech. 16, 3 (2005)
 A. Diaspro, Circumventing the diffraction limit. Il Nuovo Saggiatore, 30(5) 45 (2014).





Michelangelo Buonarroti, Giudizio Universale(1536-1541) Cappella Sistina, Vaticano

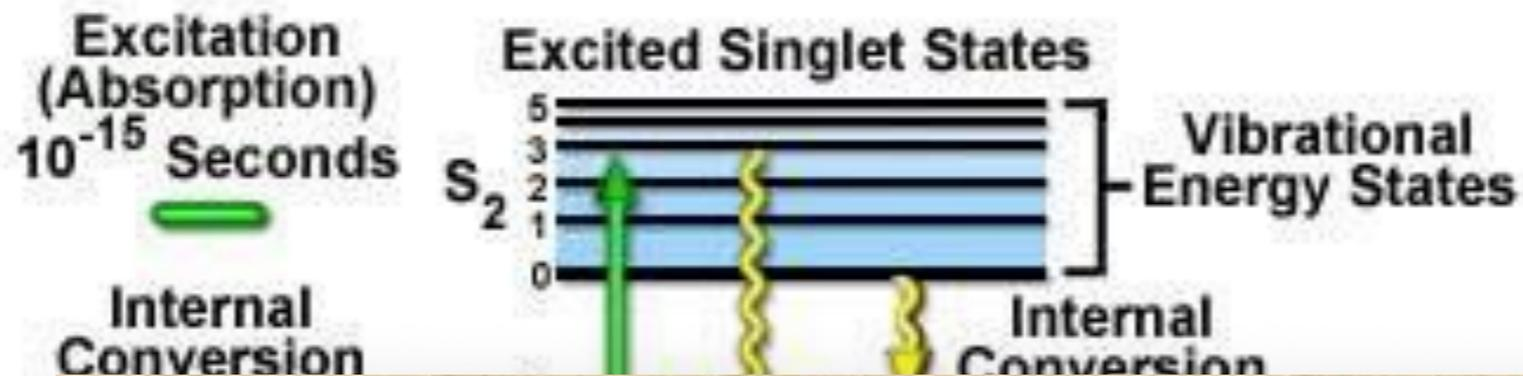
Fluorescence microscopy has become an indispensable tool in cell biology because of its unique advantages: it is a largely non-invasive technique, it can probe the deeper layers of a specimen at ambient conditions and enables spectroscopic diagnosis with chemical sensitivity

5 μm

fluorescence

Slide credit for Fluorescence slides(adapted): David Jameson

Jablonski Energy Diagram



What is fluorescence?

FLUORESCENCE is the light emitted by an atom or molecule after a finite duration subsequent to the absorption of electromagnetic energy.

Specifically, the emitted light arises from the transition of the excited species from its first excited electronic singlet level to its ground electronic level. (usually)

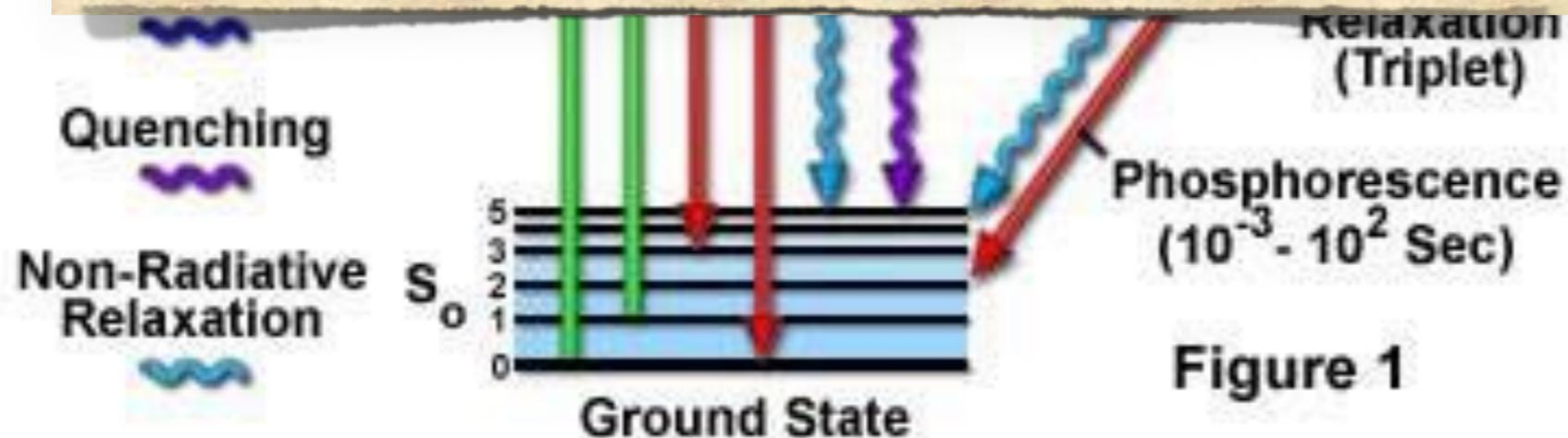
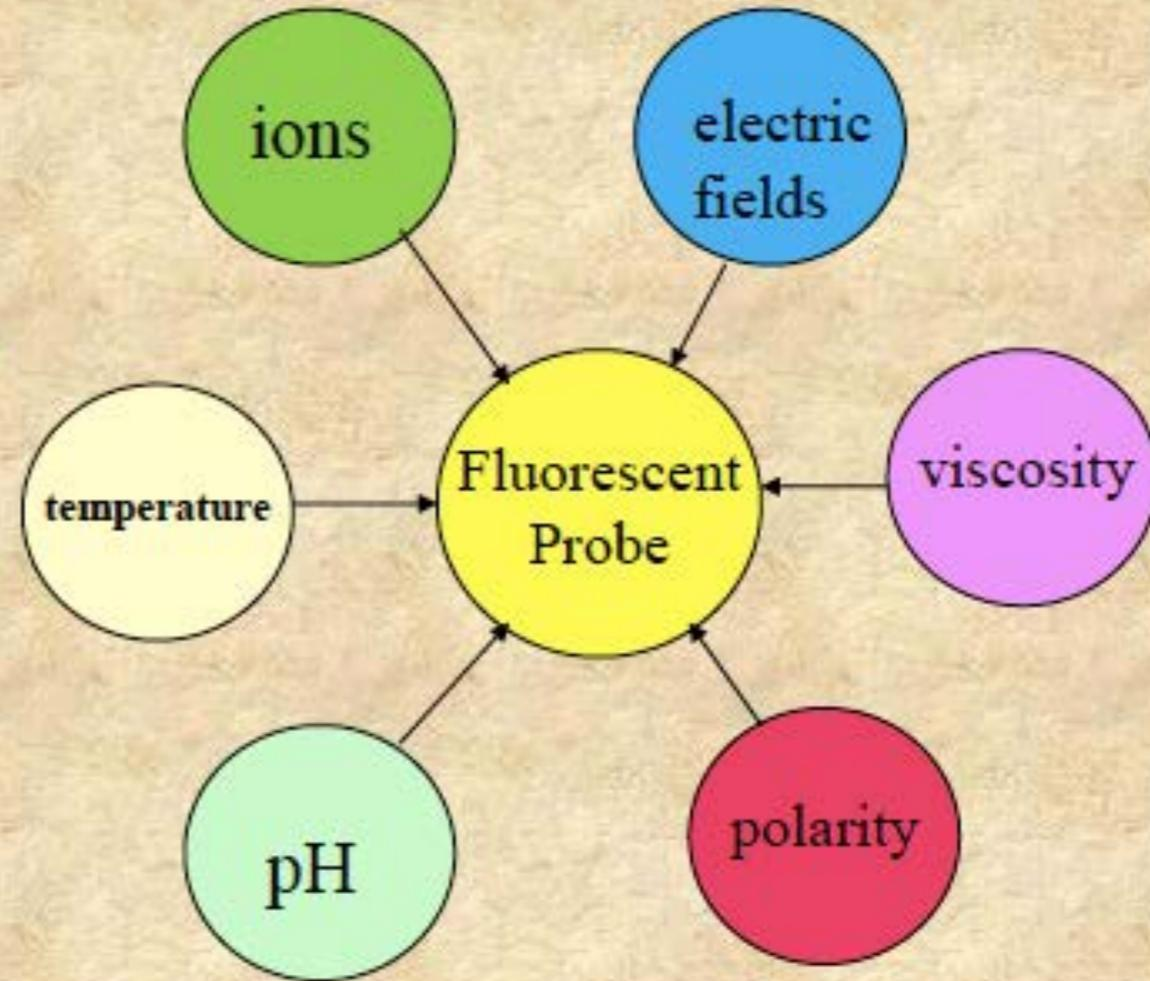


Figure 1

fluorescence

Why fluorescence?

- its pretty!
- it provides information on the molecular environment
- it provides information on dynamic processes on the nanosecond timescale

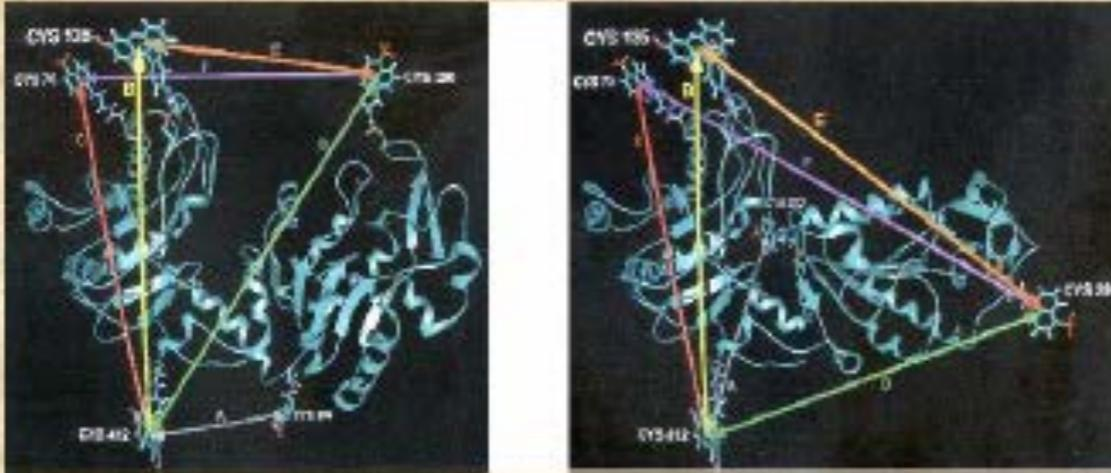


Fluorescence Probes are essentially molecular stopwatches which monitor *dynamic* events which occur during the excited state lifetime – such as movements of proteins or protein domains

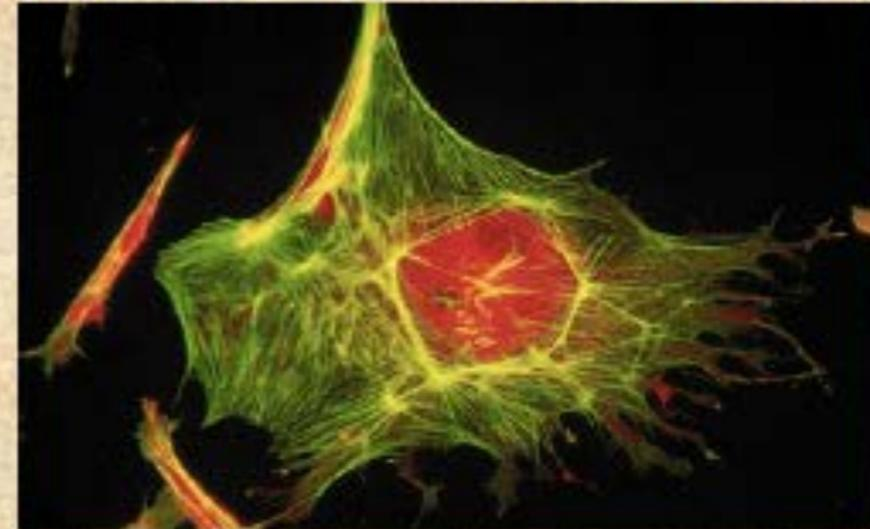
fluorescence

Experimental Systems Accessible to Fluorescence

Molecular structure and dynamics



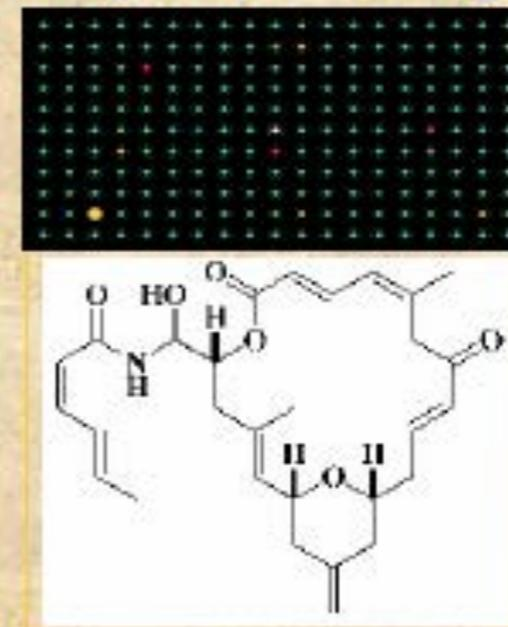
Cell organization and function



Live Animals



Engineered surfaces

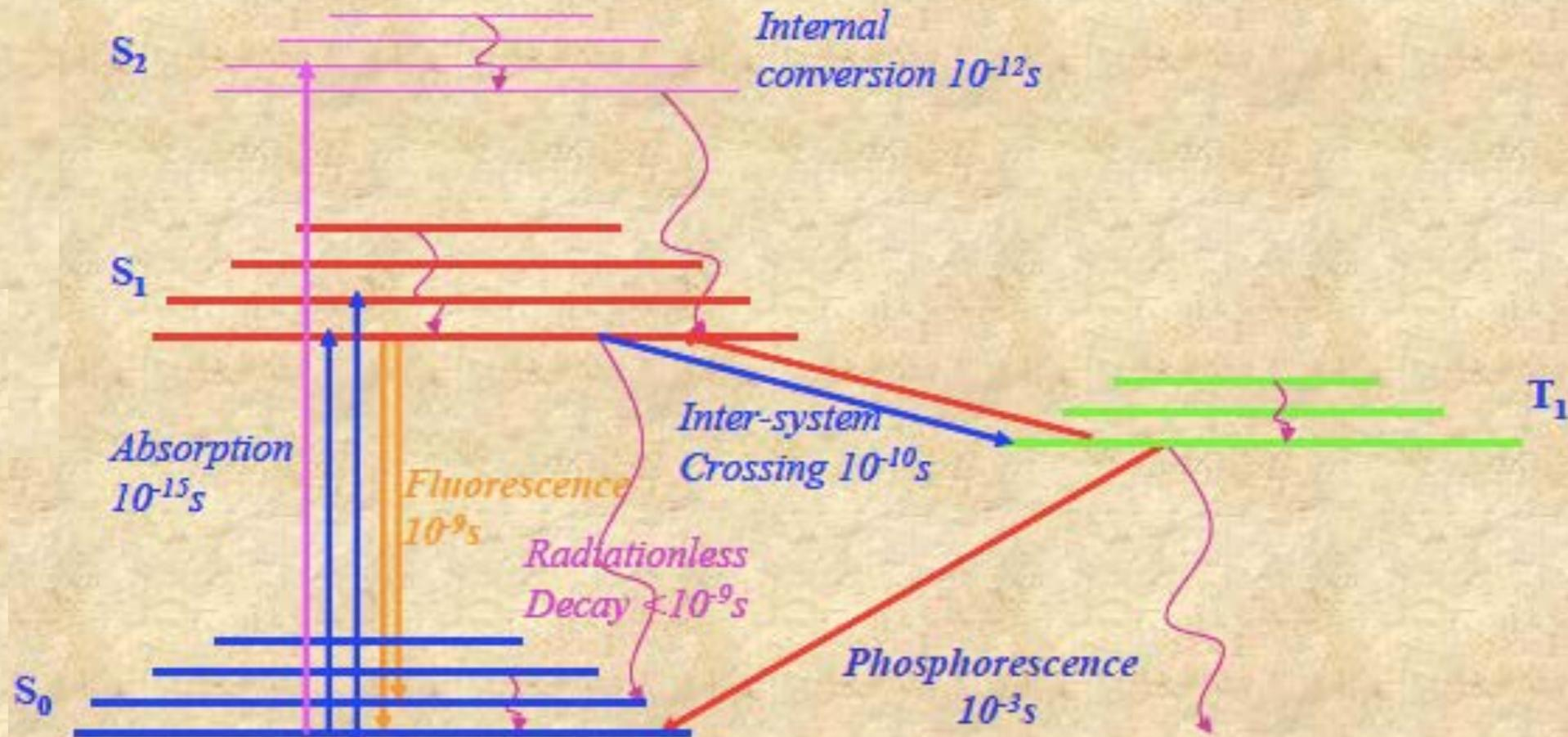


*High throughput
Drug discovery*

fluorescence

The Perrin-Jablonski Diagram

The life history of an excited state electron in a luminescent probe



Key points:

- ✓ Excitation spectra are mirror images of the emission spectra
- ✓ Emission has lower energy compared to absorption
- ✓ Triplet emission is lower in energy compared to singlet emission
- ✓ Most emission/quenching/FRET/chemical reactions occur from the lowest vibrational level of $[S]_1$

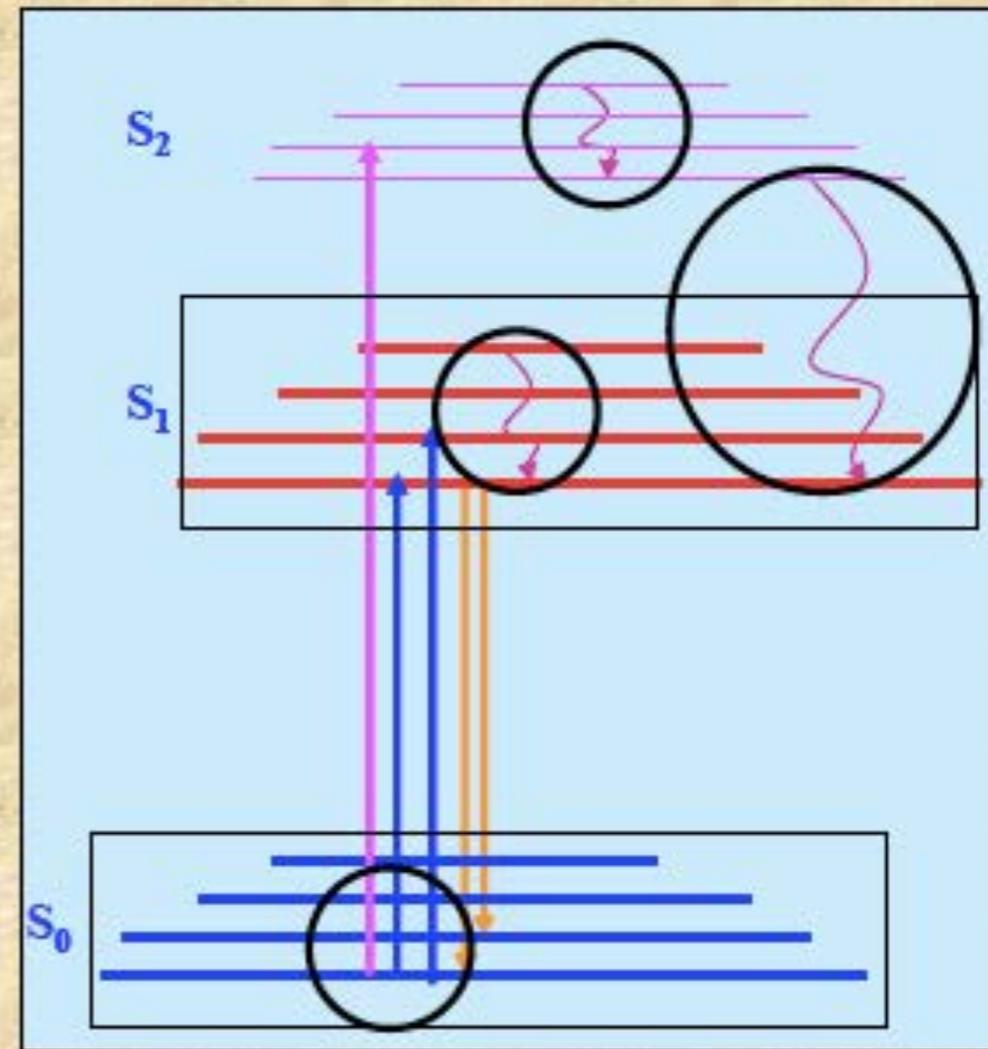
GM

fluorescence

Specifically, although the fluorophore may be excited into different singlet state energy levels (e.g., S_1 , S_2 , etc) rapid thermalization invariably occurs and emission takes place from the lowest vibrational level of the first excited electronic state (S_1). This fact accounts for the independence of the emission spectrum from the excitation wavelength.

The fact that ground state fluorophores, at room temperature, are predominantly in the lowest vibrational level of the ground electronic state (as required from Boltzmann's distribution law) accounts for the Stokes shift.

Finally, the fact that the spacings of the energy levels in the vibrational manifolds of the ground state and first excited electronic states are usually similar accounts for the fact that the emission and absorption spectra (plotted in energy units such as reciprocal wavenumbers) are approximately mirror images

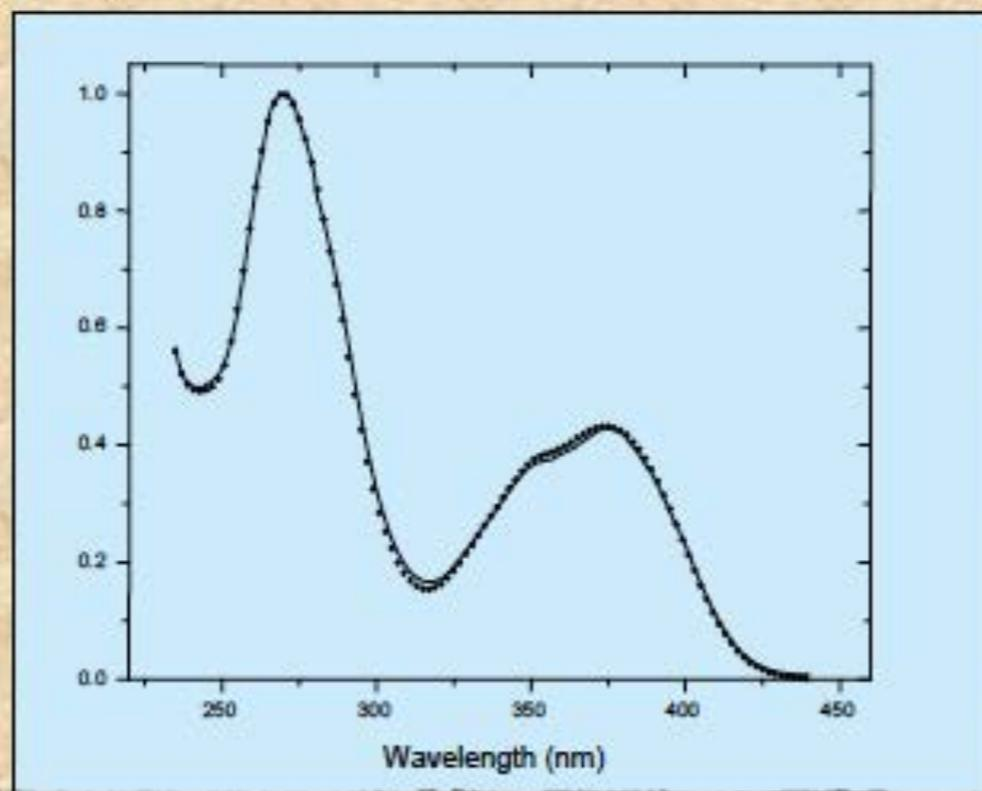


fluorescence

The fluorescence excitation spectrum

The relative efficiencies of different wavelengths of incident light to excite fluorophores is determined as the excitation spectrum. In this case, the excitation monochromator is varied while the emission wavelength is kept constant if a monochromator is utilized - or the emitted light can be observed through a filter.

If the system is "well-behaved", i.e., if the three general rules outlined above hold, one would expect that the excitation spectrum will match the absorption spectrum. In this case, however, as in the case of the emission spectrum, corrections for instrumentation factors are required.



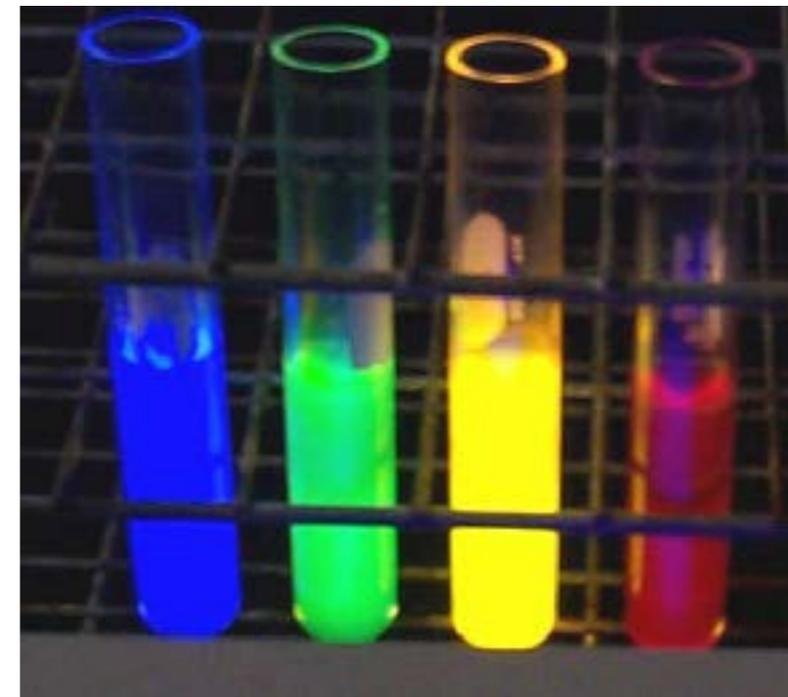
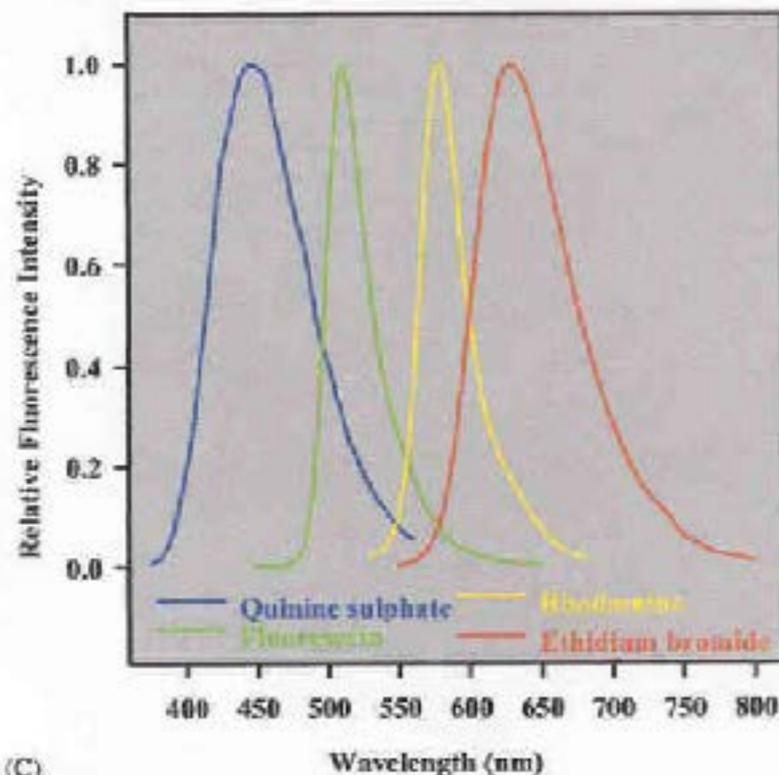
Overlay of Absorption Spectrum and Corrected Excitation Spectrum for ANS in ethanol

fluorescence

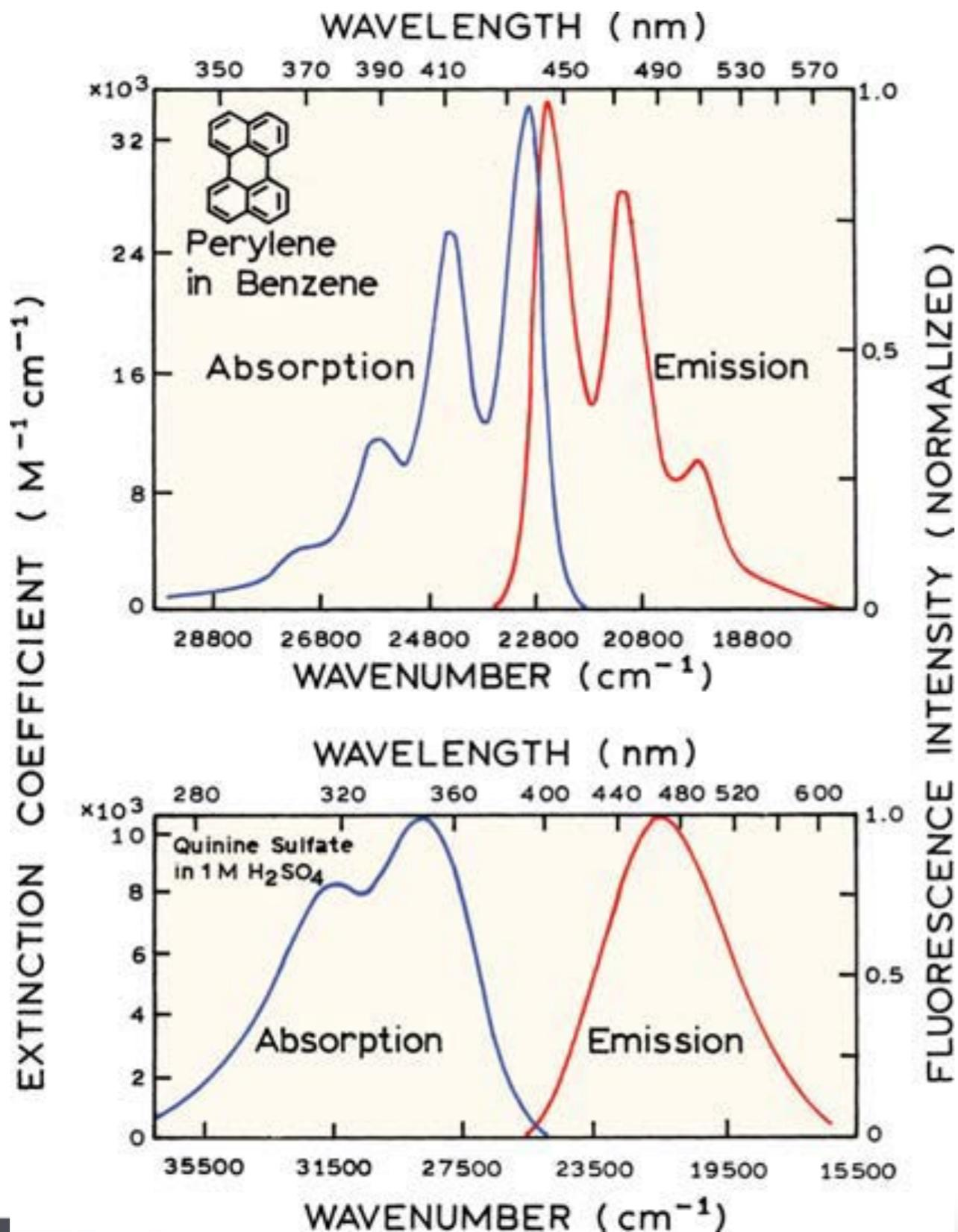
1) *In a pure substance existing in solution in a unique form, the fluorescence spectrum is invariant, remaining the same independent of the excitation wavelength*

2) *The fluorescence spectrum lies at longer wavelengths than the absorption*

3) *The fluorescence spectrum is, to a good approximation, a mirror image of the absorption band of least frequency*

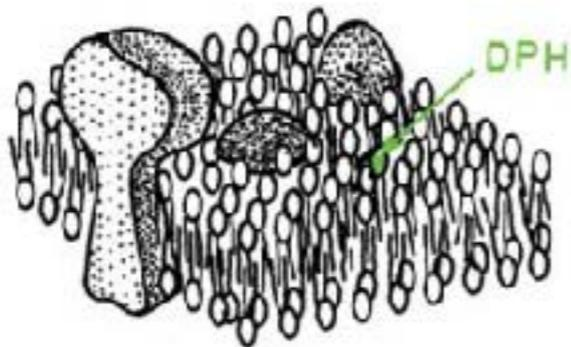
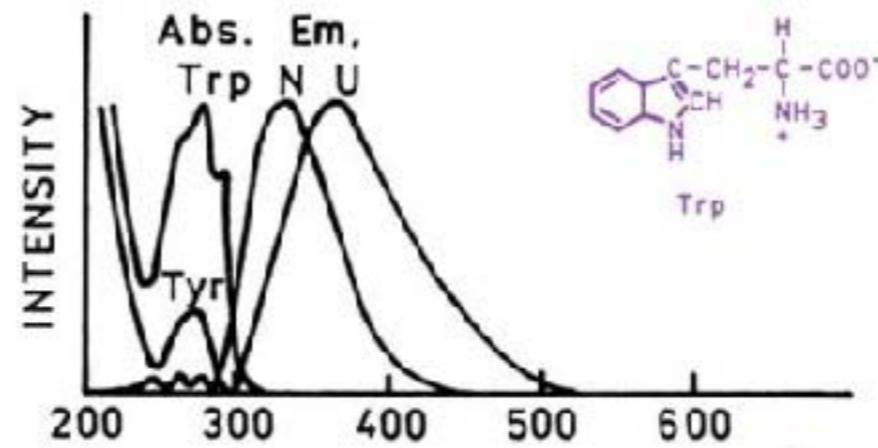
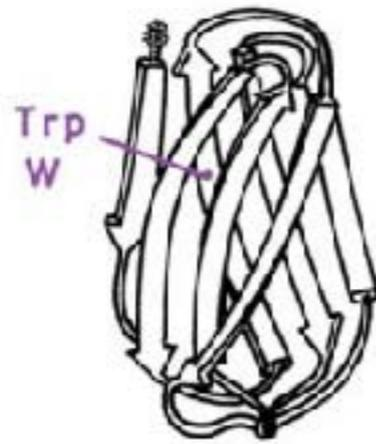


fluorescence

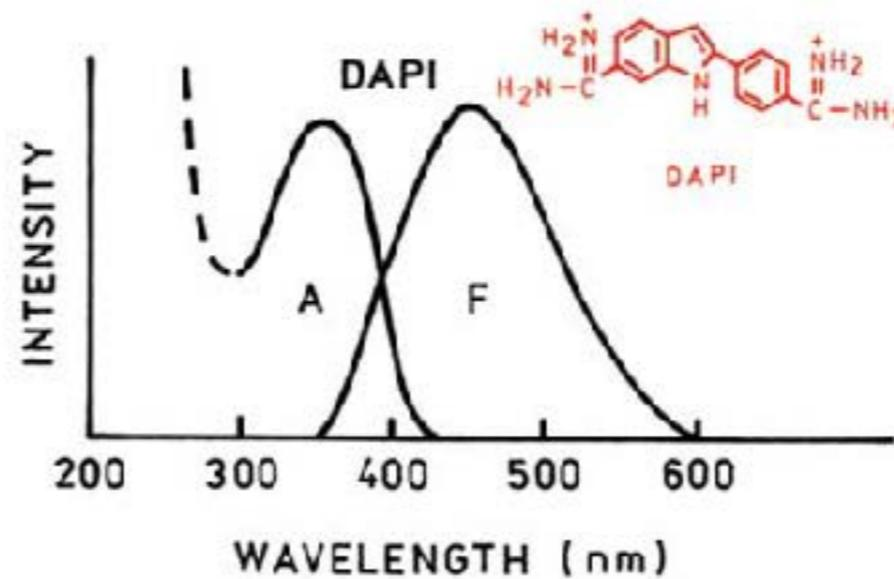
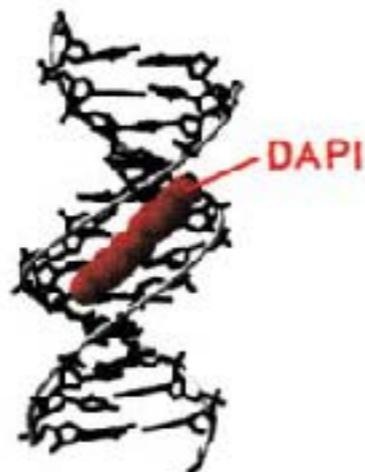
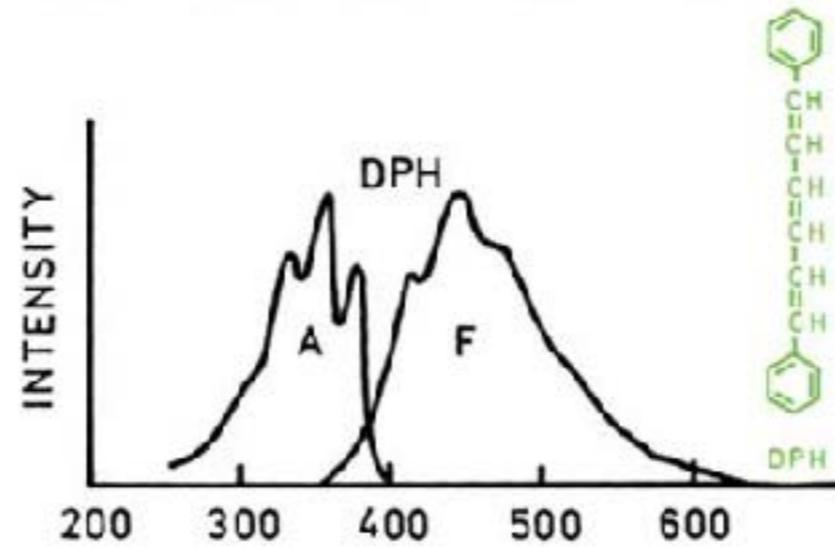


Professor Alexander Jablonski (1898–1980), circa 1935. Courtesy of his daughter, Professor Danuta Frackowiak.

fluorescence



diphenylhexatriene (DPH)



fluorescence

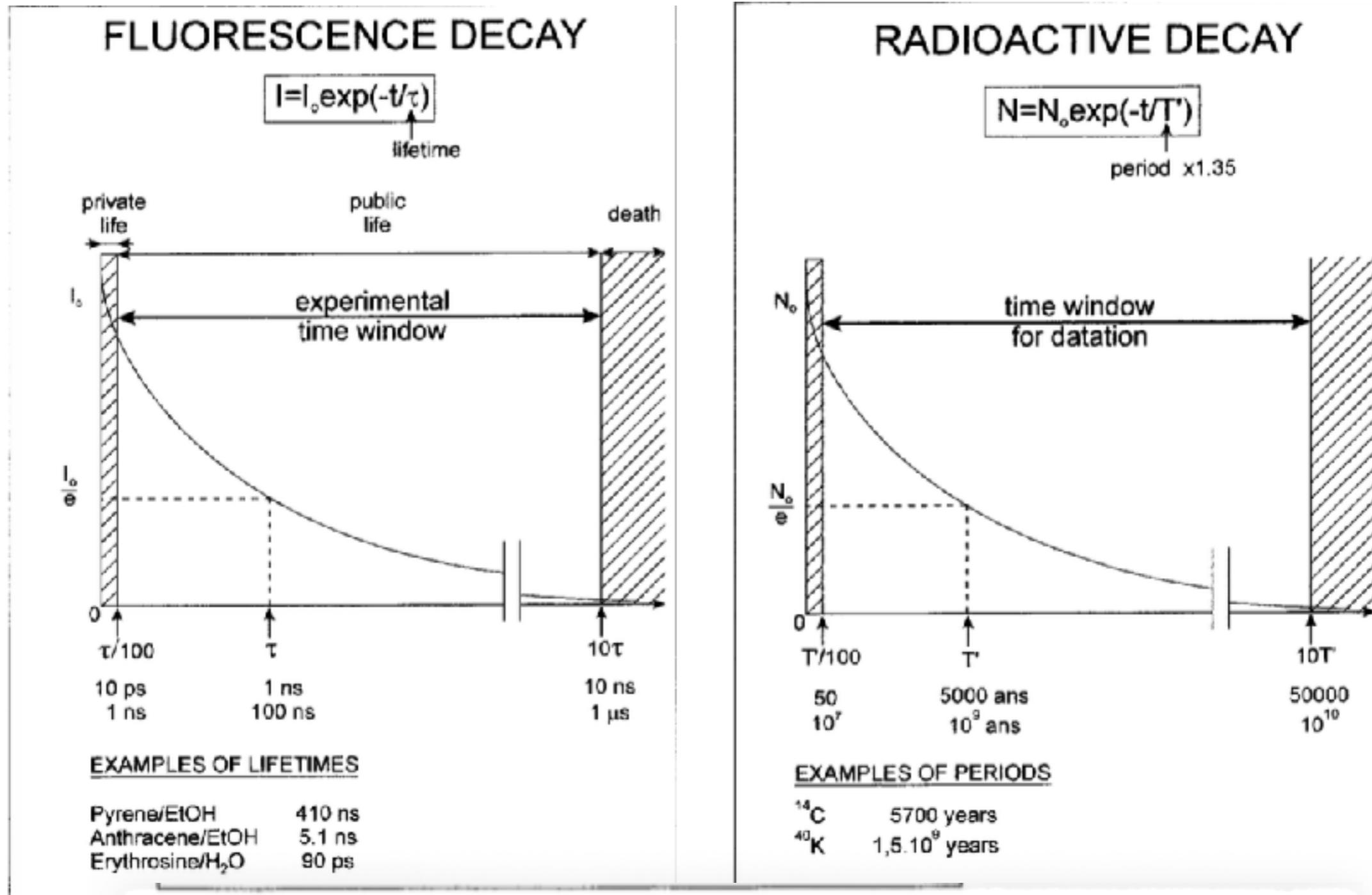


Fig. 3.2. Decay of fluorescence intensity and analogy with radioactive decay. Note that the lifetime τ is the time needed for the concentration of molecular entities to decrease to 1/e of its original value, whereas the radioactive

period T is the time needed for the number of radioactive entities to decrease to $\frac{1}{2}$ of its original value. Therefore, T' (the decay time constant equivalent to the lifetime) is equal to $1.35T$.

fluorescence

Quantum Yield

The quantum yield of fluorescence (QY) is dependent on the **rate of the emission process** divided by the sum of the **rates of all other deactivation processes**

$$QY = k_f / k_f + k_i + k_x$$

k_f is the rate of fluorescence, k_i is the rate of radiationless decay and k_x is the rate of intersystem crossing.

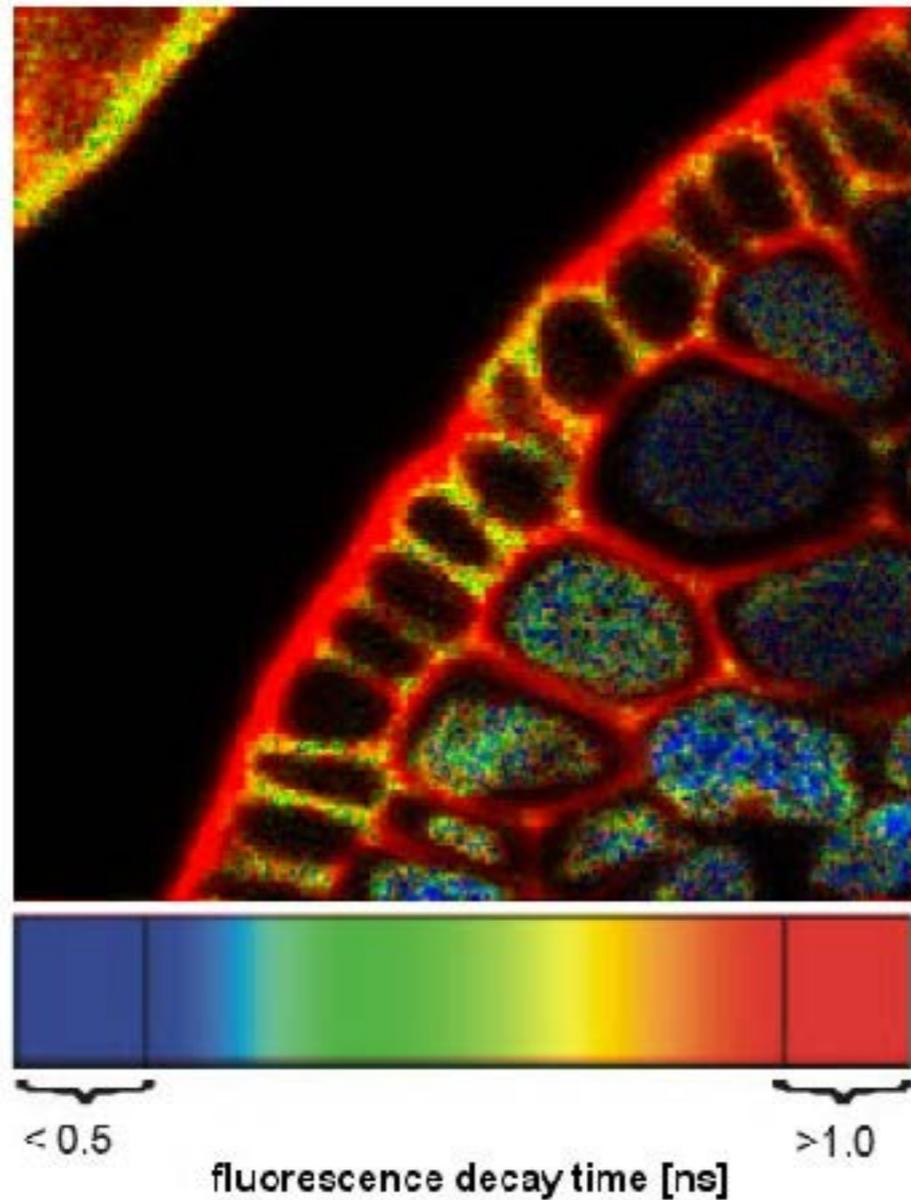
Another way to think about QY is:

$QY = \text{Number of emitted photons} / \text{Number of absorbed photons}$

If the rates of the deactivation processes are slow compared to k_f then the **QY is high**

However, if the rates of these other processes are fast compared to k_f then **QY is low**

fluorescence



$$Q = \frac{k_f}{k_f + k_i}$$

$$\tau = \frac{1}{k_f + k_i}$$

➤ Lifetime

The average time spent in the excited state before returning to the ground state

fluorescence

Absorption and emission processes are almost always studied on *populations* of molecules and the properties of the supposed typical members of the population are deduced from the macroscopic properties of the process.

In general, the behavior of an excited population of fluorophores is described by a familiar rate equation:

$$\frac{dn^*}{dt} = -n^* \Gamma + f(t)$$

where n^* is the number of excited elements at time t , Γ is the rate constant of emission and $f(t)$ is an arbitrary function of the time, describing the time course of the excitation. The dimensions of Γ are sec^{-1} (transitions per molecule per unit time).

fluorescence

If excitation occurs at $t = 0$, the last equation, takes the form:

$$\frac{dn^*}{dt} = -n^* \Gamma$$

and describes the decrease in excited molecules at all further times. Integration gives:

$$n^*(t) = n^*(0) \exp(-\Gamma t)$$

The lifetime, τ , is equal to Γ^{-1}

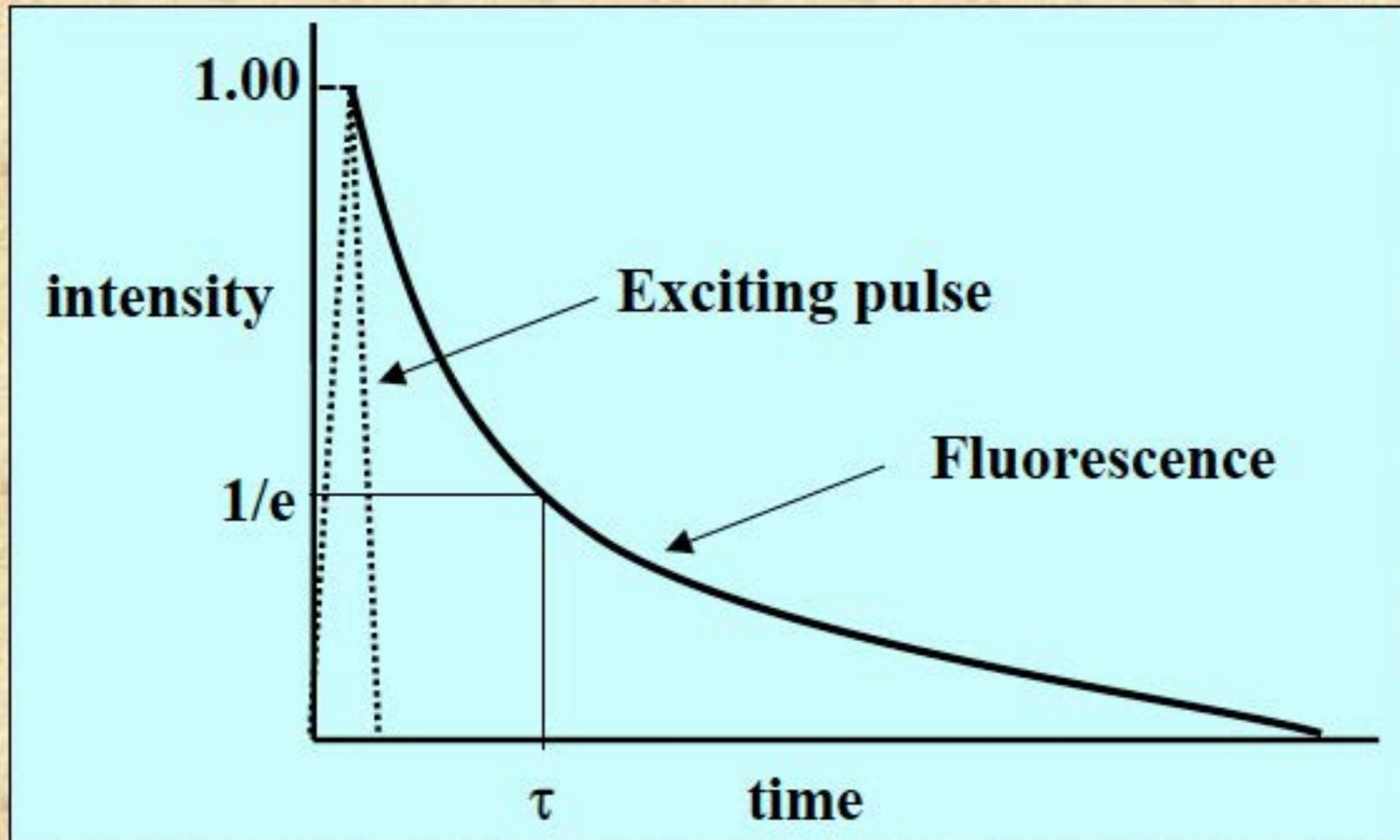
If a population of fluorophores are excited, the lifetime is the time it takes for the number of excited molecules to decay to $1/e$ or 36.8% of the original population according to:

$$\frac{n^*(t)}{n^*(0)} = e^{-t/\tau}$$

fluorescence

In pictorial form:

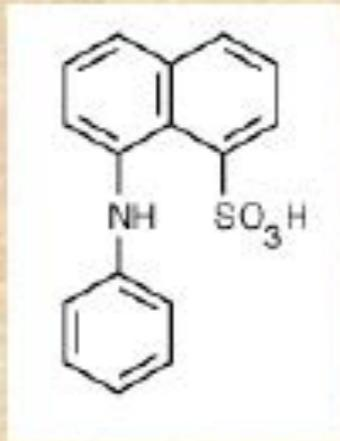
$$\frac{n^*(t)}{n^*(0)} = e^{-t/\tau}$$



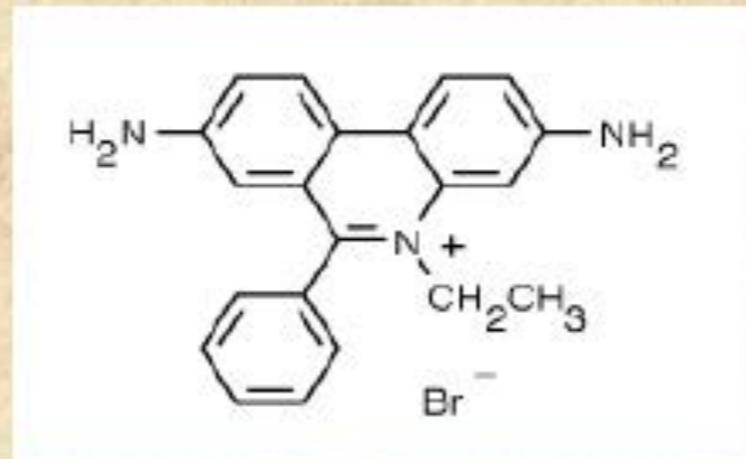
fluorescence

The lifetime and quantum yield for a given fluorophore is often dramatically affected by its environment.

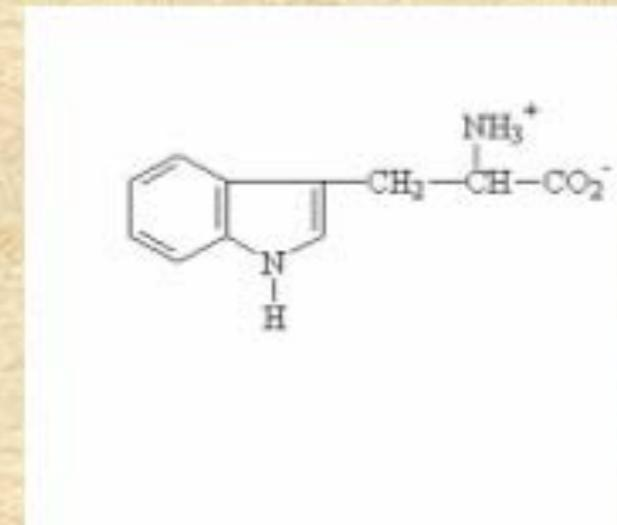
Examples of this fact would be NADH, which in water has a lifetime of ~ 0.4 ns but bound to dehydrogenases can be as long as 9 ns.



ANS in water is ~ 100 picoseconds but can be 8 – 10 ns bound to proteins



Ethidium bromide is 1.8 ns in water, 22 ns bound to DNA and 27 ns bound to tRNA



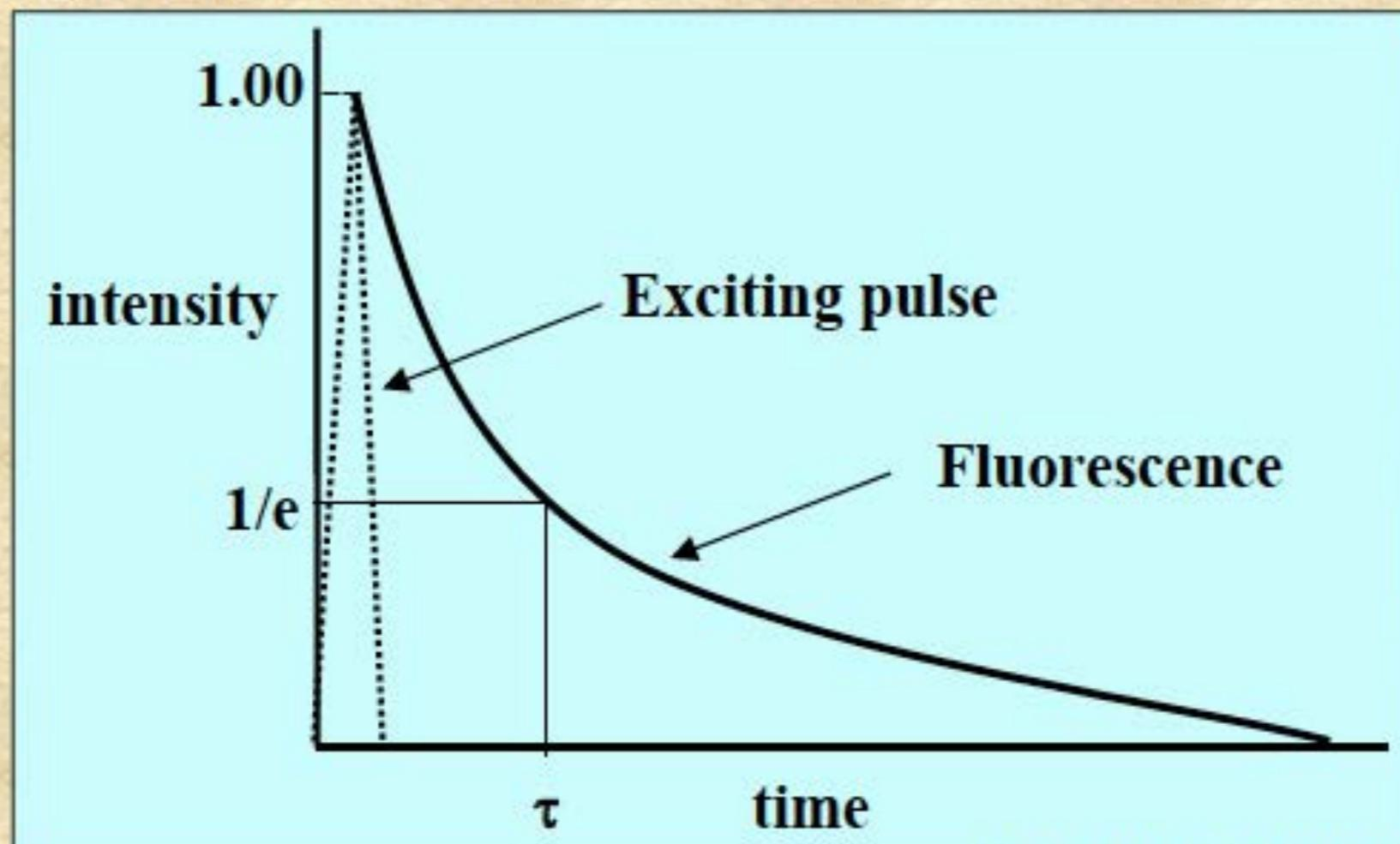
The lifetime of tryptophan in proteins ranges from ~ 0.1 ns up to ~ 8 ns

fluorescence

David Jameson

Excited state lifetimes have traditionally been measured using either the *impulse* response or the *harmonic* response method. In principle both methods have the same information content. These methods are also referred to as either the “time domain” method or the “frequency domain” method.

In the *impulse* (or pulse) method, the sample is illuminated with a short pulse of light and the intensity of the emission versus time is recorded. Originally these short light pulses were generated using *flashlamps* which had widths on the order of several nanoseconds. Modern laser sources can now routinely generate pulses with widths on the order of picoseconds or shorter.



Principles of Fluorescence Techniques 2011

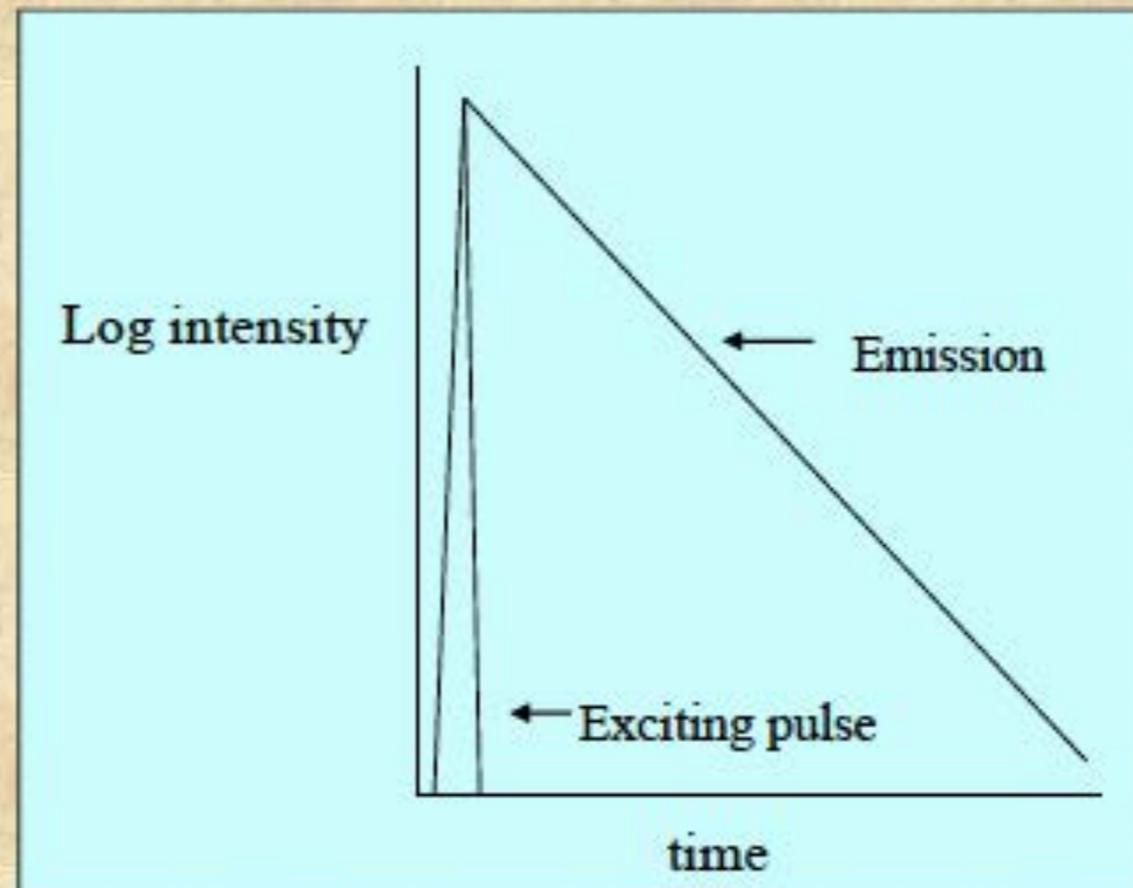
fluorescence

As shown in the intensity decay figure, the *fluorescence* lifetime, t , is the time at which the intensity has decayed to $1/e$ of the original value. The decay of the intensity with time is given by the relation:

$$I_t = \alpha e^{-t/\tau}$$

Where I_t is the intensity at time t , α is a normalization term (the pre-exponential factor) and τ is the lifetime.

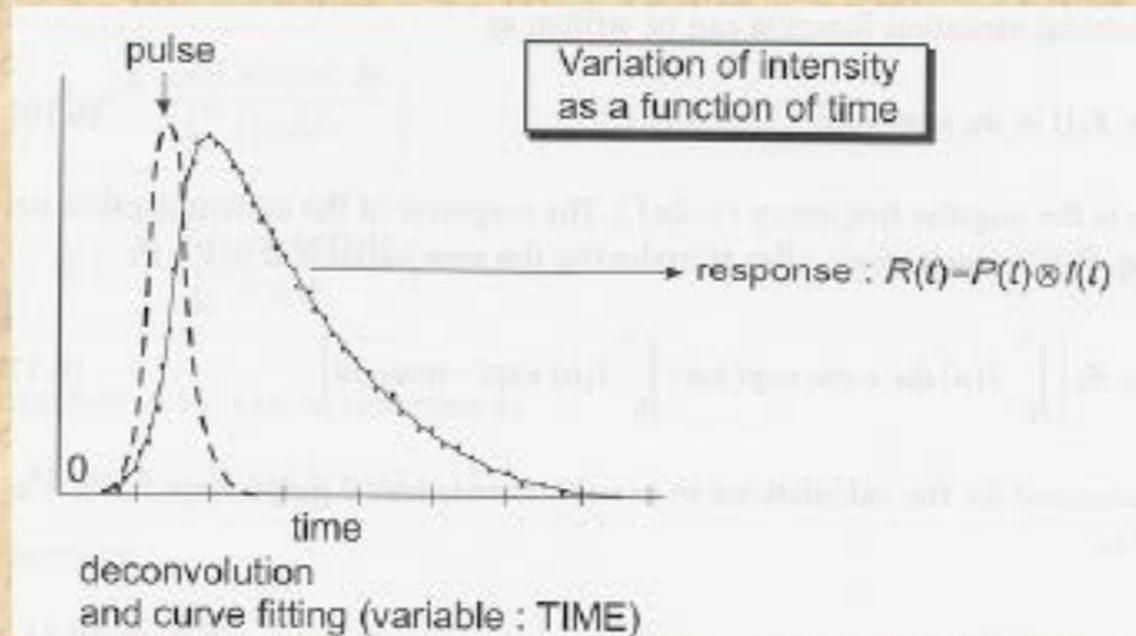
It is more common to plot the fluorescence decay data using a logarithmic scale as shown here.



fluorescence

If the decay is a single exponential and if the lifetime is long compared to the exciting light then the lifetime can be determined directly from the slope of the curve.

If the lifetime and the excitation pulse width are comparable some type of *deconvolution* method must be used to extract the lifetime.



Great effort has been expended on developing mathematical methods to “deconvolve” the effect of the exciting pulse shape on the observed fluorescence decay.

With the advent of very fast laser pulses these deconvolution procedures became less important for most lifetime determinations, although they are still required whenever the lifetime is of comparable duration to the light pulse.

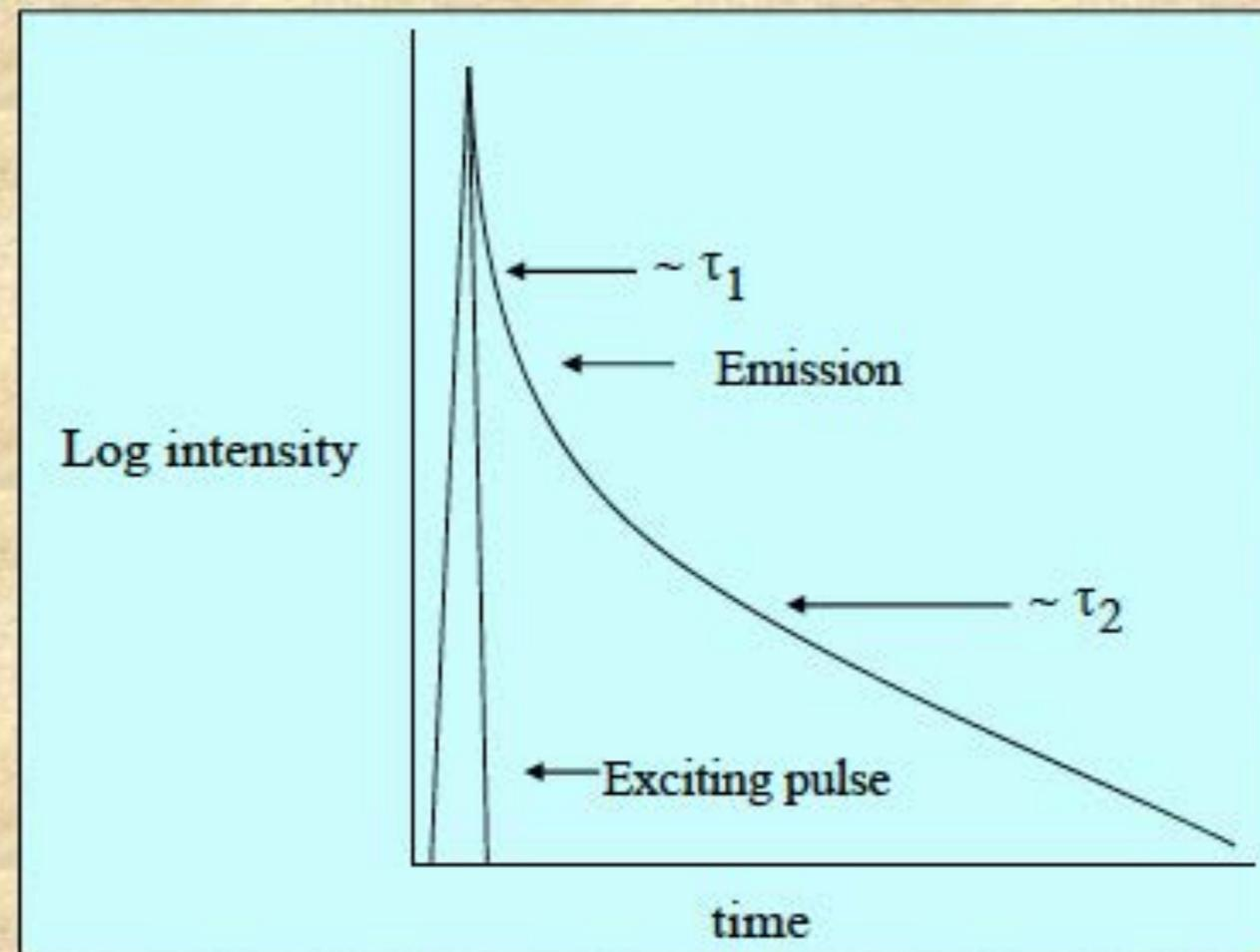
fluorescence

If the decay is multiexponential, the relation between the intensity and time after excitation is given by:

$$I(t) = \sum_i \alpha_i e^{-t/\tau_i}$$

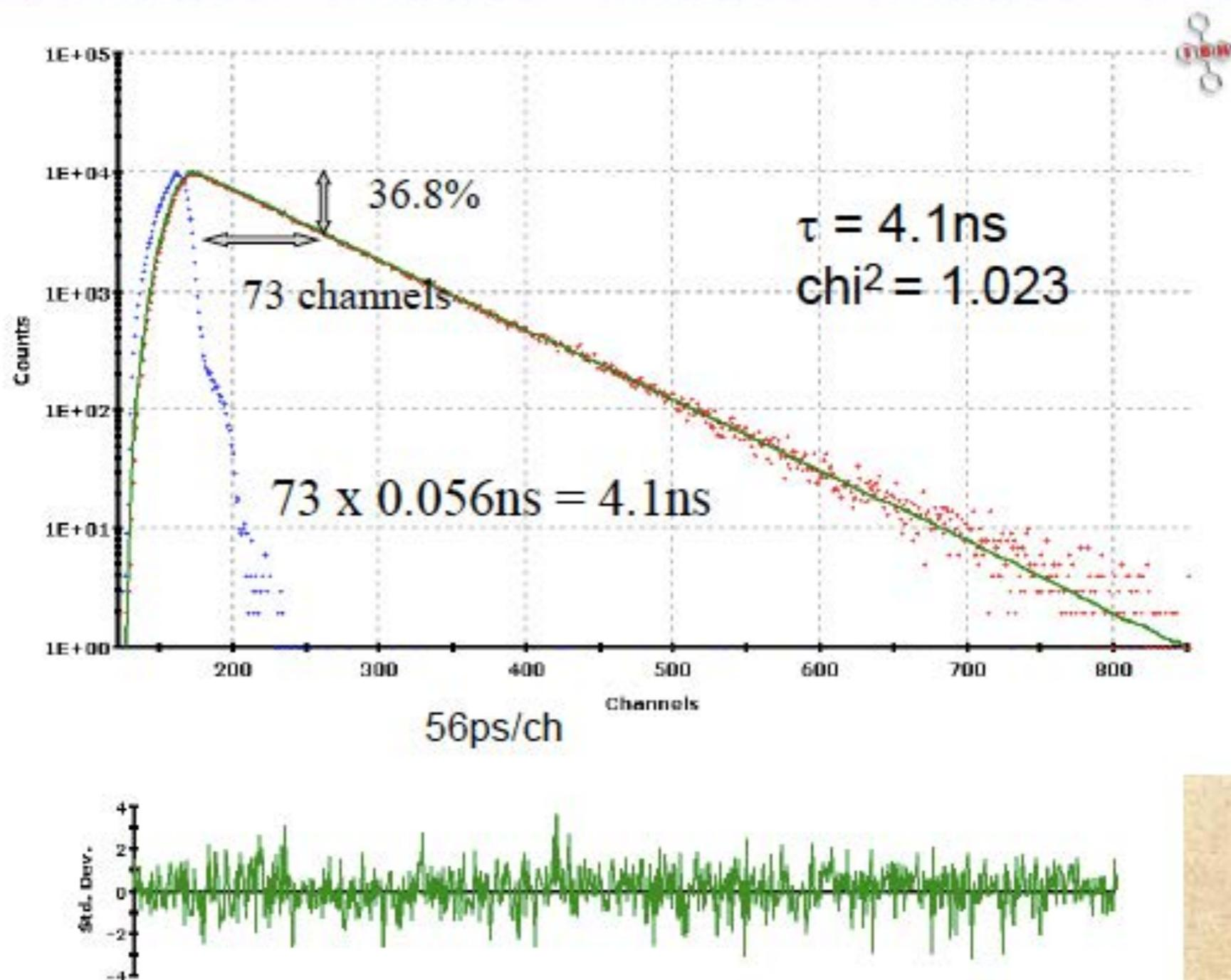
One may then observe data such as those sketched below:

Here we can discern at least two lifetime components indicated as τ_1 and τ_2 . This presentation is oversimplified but illustrates the point.



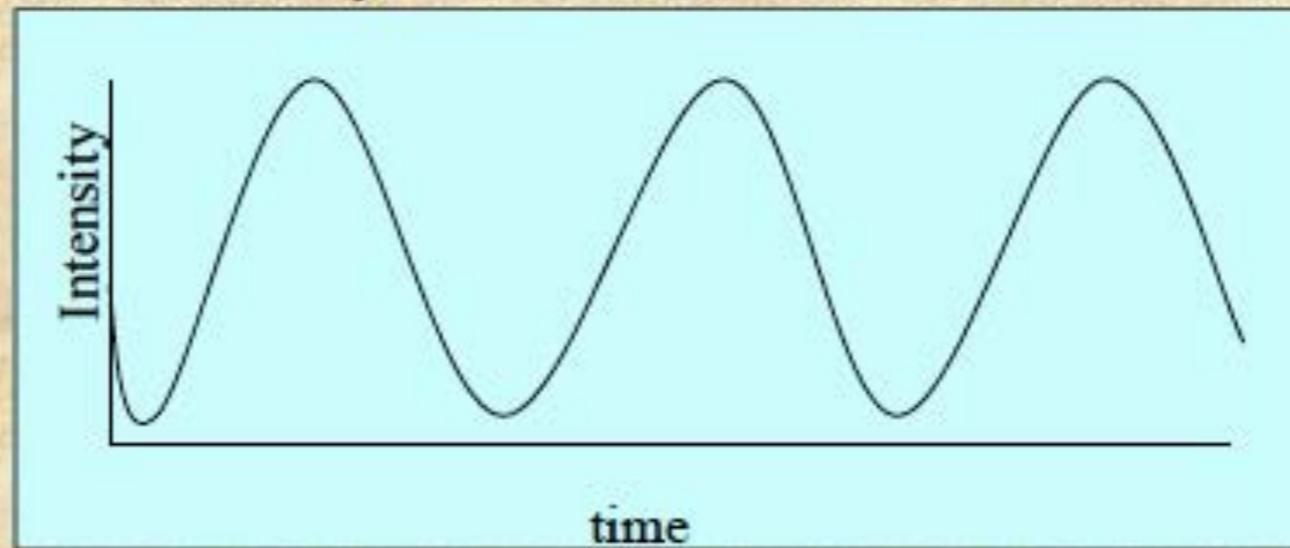
fluorescence

Here are pulse decay data on anthracene in cyclohexane taken on an IBH 5000U Time-correlated single photon counting instrument equipped with an LED short pulse diode excitation source.



fluorescence

In the harmonic method (also known as the phase and modulation or frequency domain method) a continuous light source is utilized, such as a laser or xenon arc, and the intensity of this light source is modulated sinusoidally at high frequency as depicted below. Typically, an *electro-optic* device, such as a *Pockels cell* is used to modulate a continuous light source, such as a CW laser or a xenon arc lamp. Alternatively, LEDs or laser diodes can be directly modulated.



In such a case, the excitation frequency is described by:

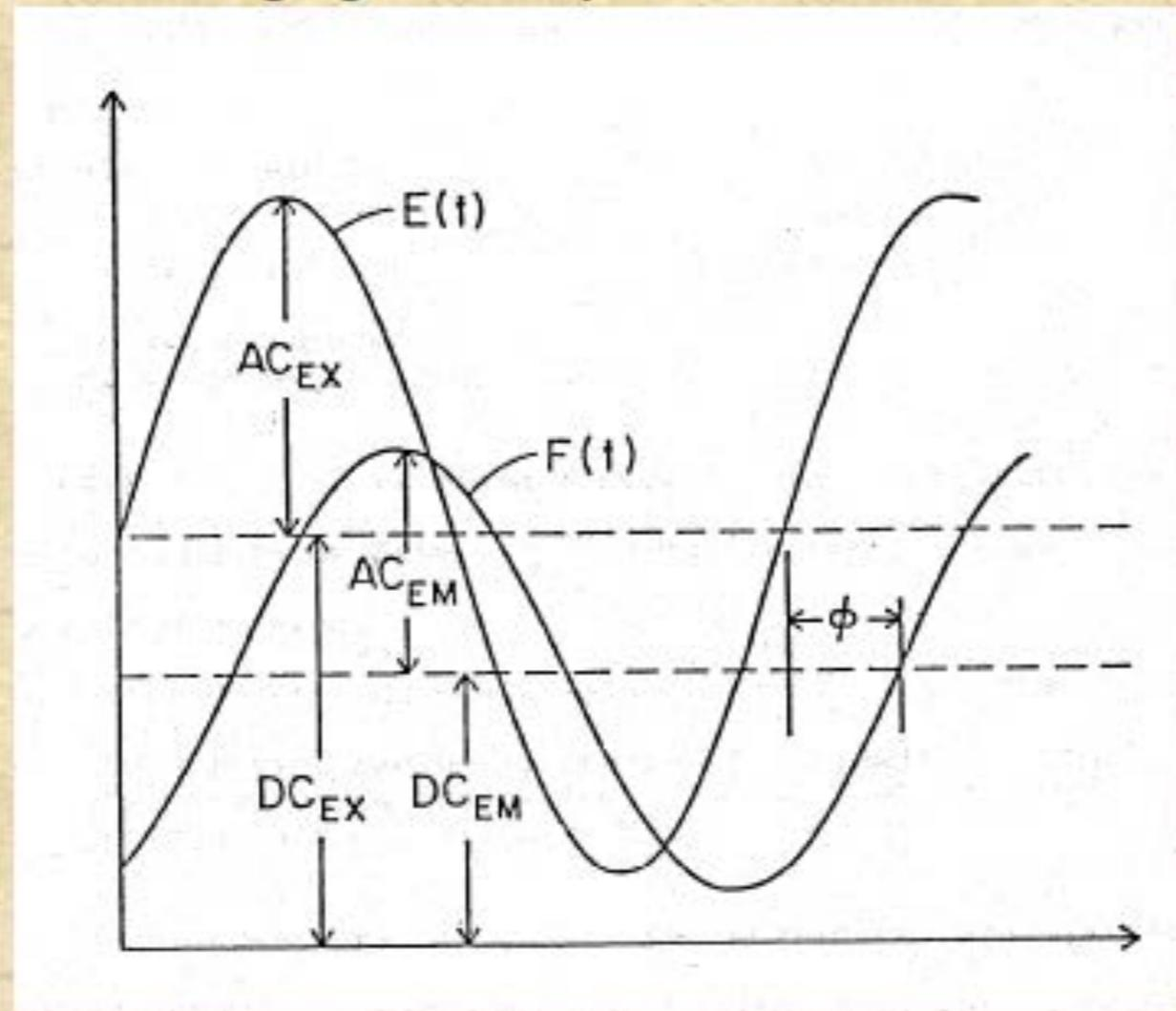
$$E(t) = E_0 [1 + M_E \sin \omega t]$$

$E(t)$ and E_0 are the intensities at time t and 0 , M_E is the modulation factor which is related to the ratio of the AC and DC parts of the signal and ω is the angular modulation frequency.

$\omega = 2\pi f$ where f is the linear modulation frequency

fluorescence

Due to the persistence of the excited state, fluorophores subjected to such an excitation will give rise to a modulated emission which is shifted in phase relative to the exciting light as depicted below.



This sketch illustrates the phase delay (ϕ) between the excitation, $E(t)$, and the emission, $F(t)$. Also shown are the AC and DC levels associated with the excitation and emission waveforms.

fluorescence

One can demonstrate that:

$$F(t) = F_0 [1 + M_F \sin(\omega t + \phi)]$$

This relationship signifies that measurement of the phase delay, ϕ , forms the basis of one measurement of the lifetime, τ . In particular one can demonstrate that:

$$\tan \phi = \omega \tau$$

The *modulations* of the excitation (M_E) and the emission (M_F) are given by:

$$M_E = \left(\frac{AC}{DC} \right)_E \quad \text{and} \quad M_F = \left(\frac{AC}{DC} \right)_F$$

The *relative modulation*, M , of the emission is then:

$$M = \frac{(AC/DC)_F}{(AC/DC)_E}$$

τ can also be determined from M according to the relation: $M = \frac{1}{\sqrt{1 + (\omega \tau)^2}}$

fluorescence

Using the *phase shift* and *relative modulation* one can thus determine a *phase lifetime* (τ_p) and a *modulation lifetime* (τ_M).

If the fluorescence decay is a single exponential, then τ_p and τ_M will be equal at all modulation frequencies.

If, however, the fluorescence decay is multiexponential then $\tau_p < \tau_M$ and, moreover, the values of both τ_p and τ_M will depend upon the modulation frequency, i.e.,

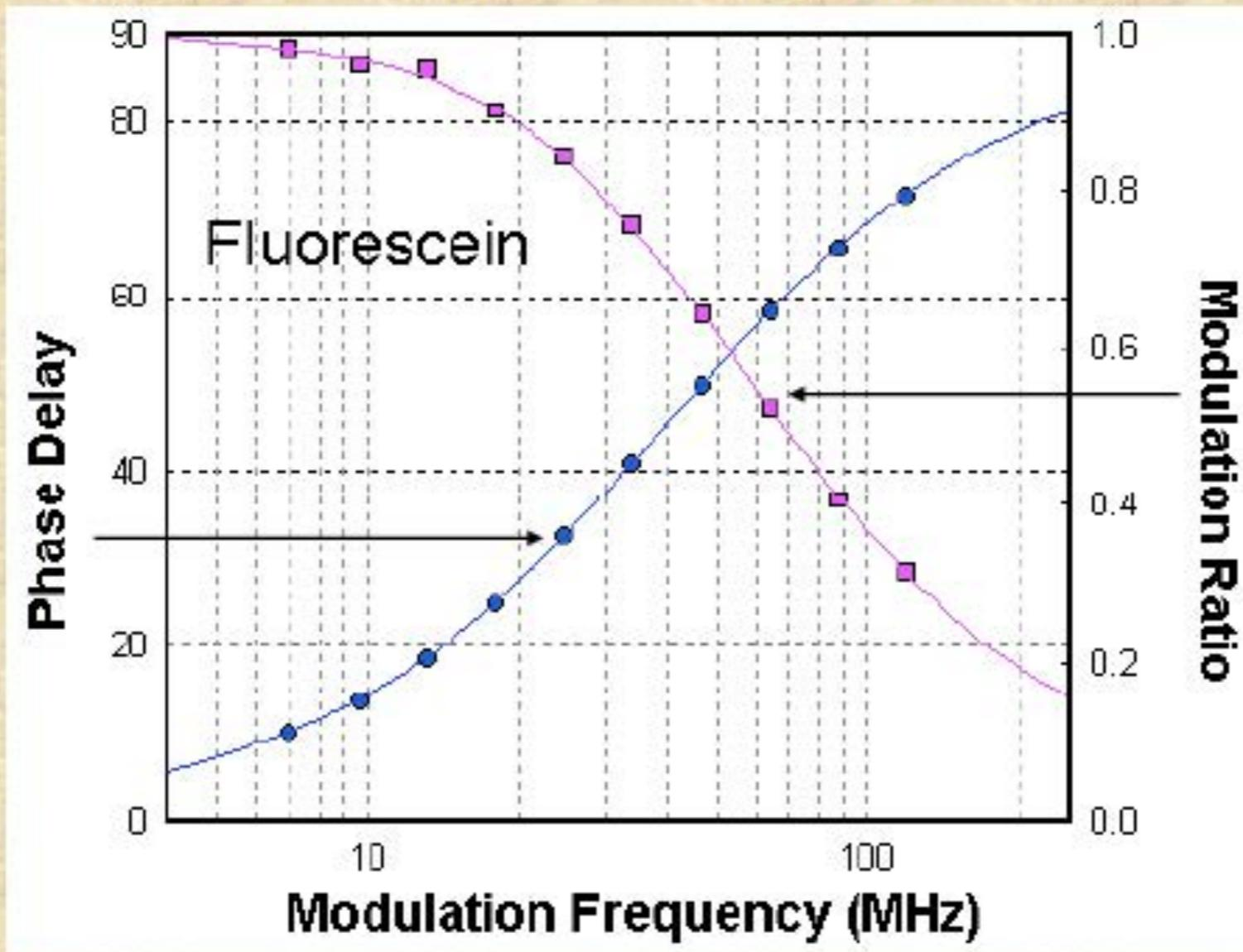
$$\tau_p(\omega_1) < \tau_p(\omega_2) \quad \text{if } \omega_1 > \omega_2$$

To get a feeling for typical phase and modulation data, consider the following data set.

Frequency (MHz)	τ_p (ns)	τ_M (ns)
5	6.76	10.24
10	6.02	9.70
30	3.17	6.87
70	1.93	4.27

fluorescence

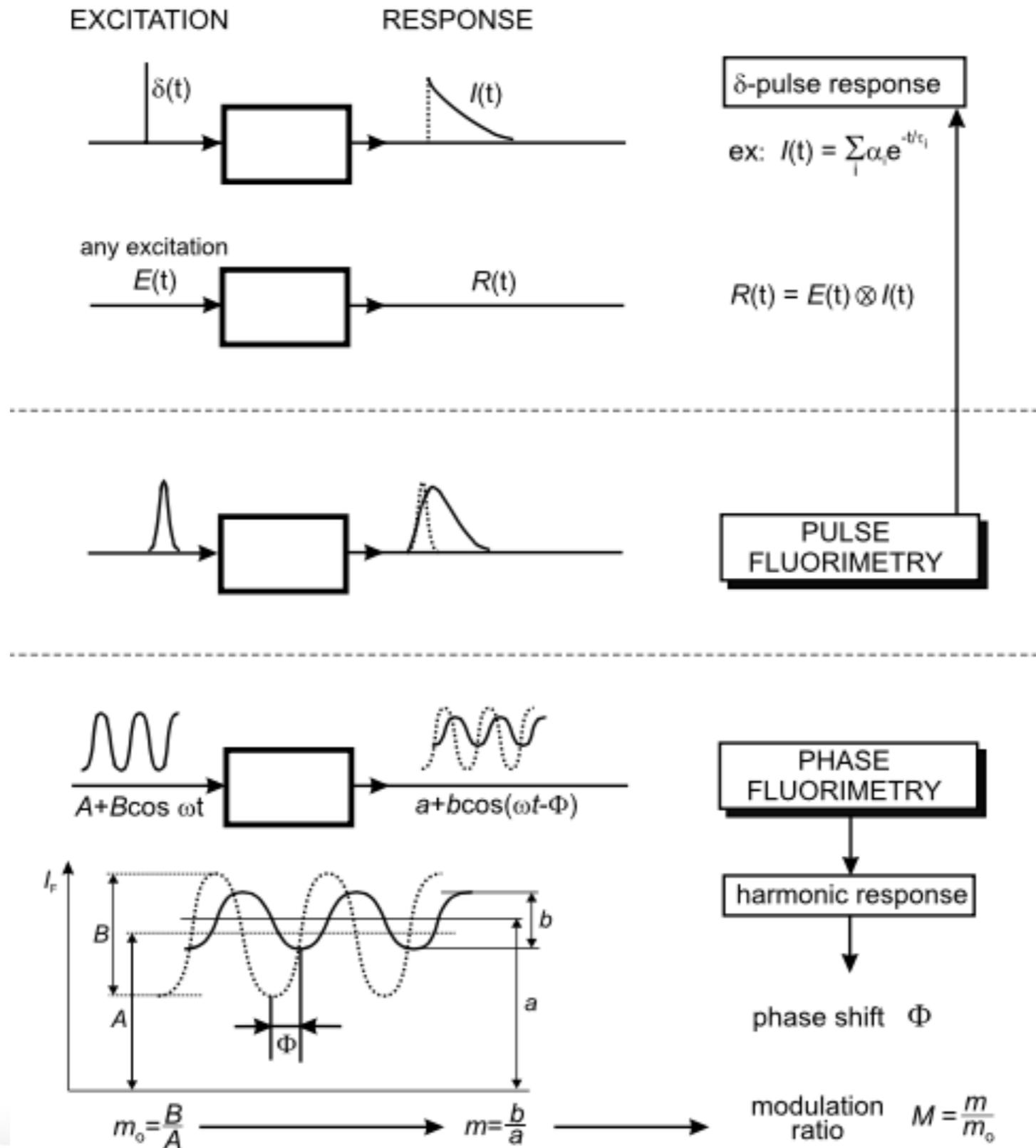
Multifrequency phase and modulation data are usually presented as shown below:



The plot shows the frequency response curve (phase and modulation) of Fluorescein in phosphate buffer pH 7.4 acquired on an ISS Chronos using a 470 nm LED. The emission was collected through a 530 high pass filter. The data is best fitted by a single exponential decay time of 4 ns.

fluorescence

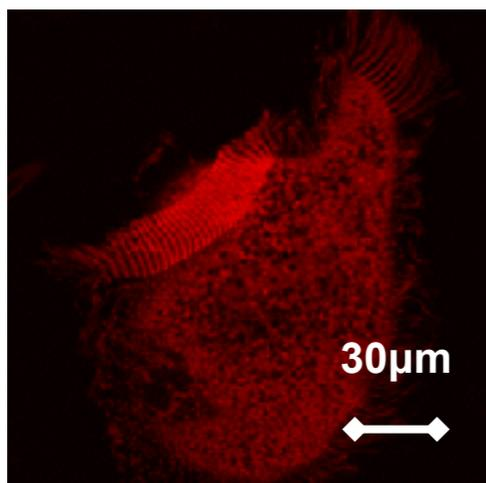
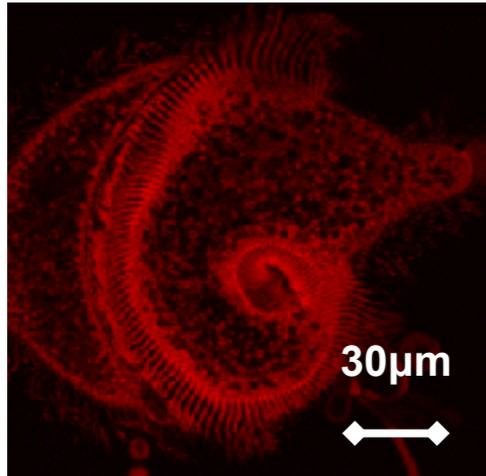
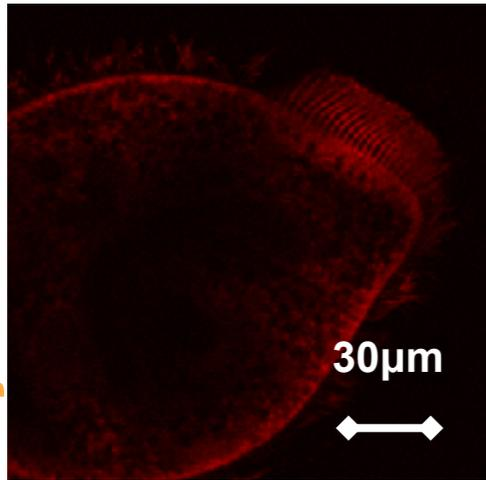
Slide credit for Fluorescence slides(adapted): David Jameson



FLIM on Biological system

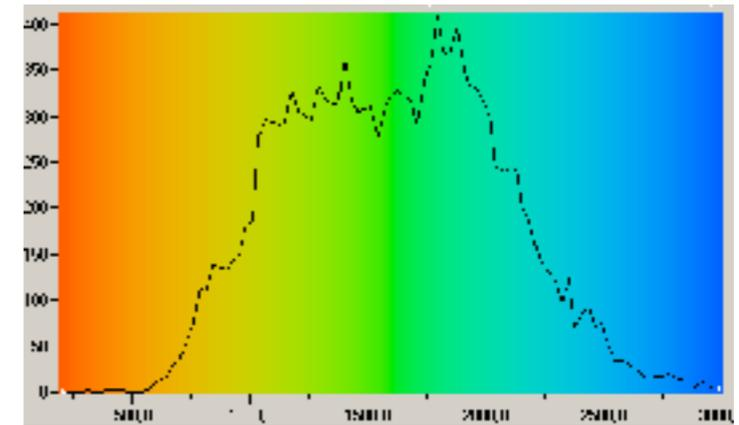
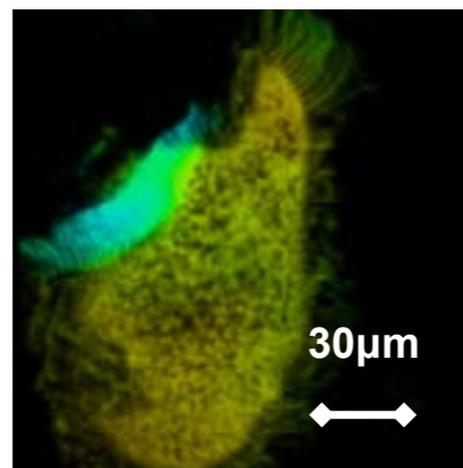
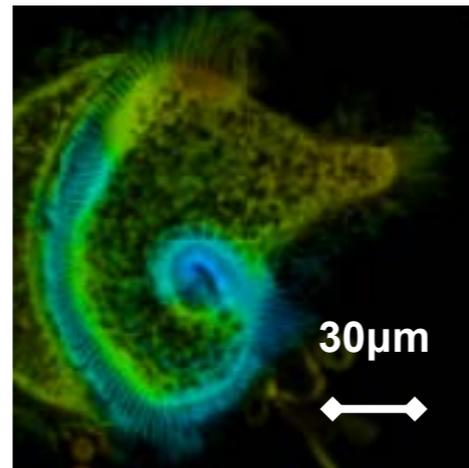
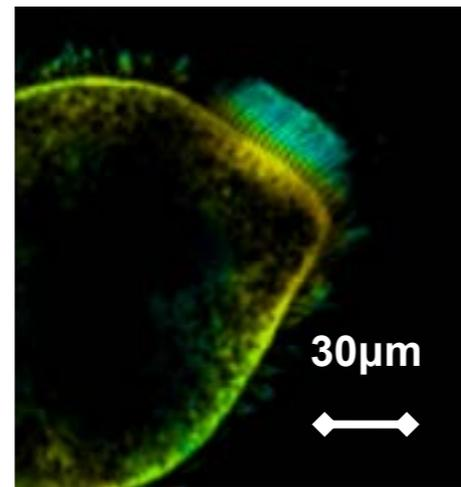
Giuliano Colombetti, IBF CNR, Pisa

Fluorescence intensity



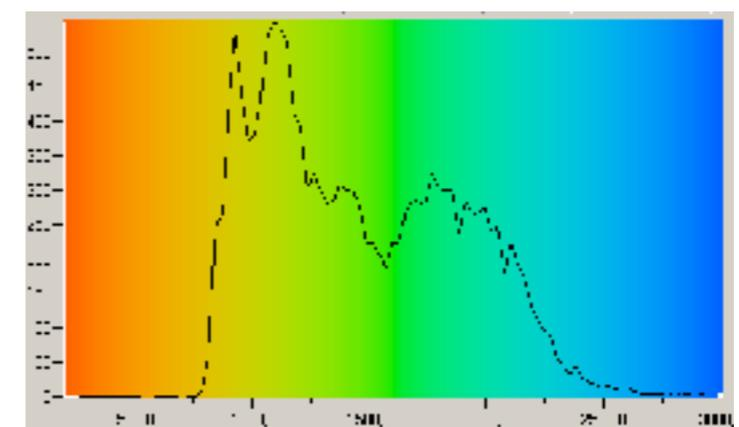
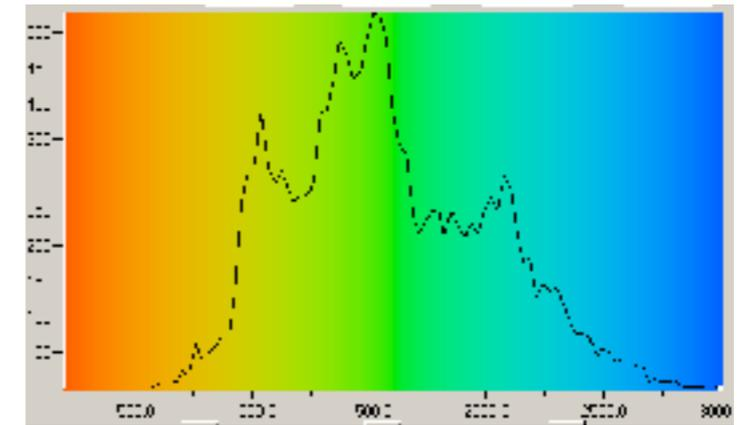
Credits: Mattia Pesce

Fluorescence Life time imaging



200ps

3000ps

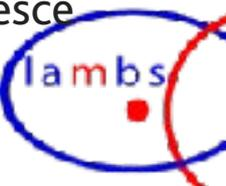


Credits: Mattia Pesce

Ciliated Protozoa (Fabrea Salina)

Colombetti G., Checcucci G., Lucia S., Usai C., Ramoino P., Bianchini P., Pesce M., Vicidomini G., Diaspro A. (2007). *Microsc Res Tech.* 70(12), 1028–33

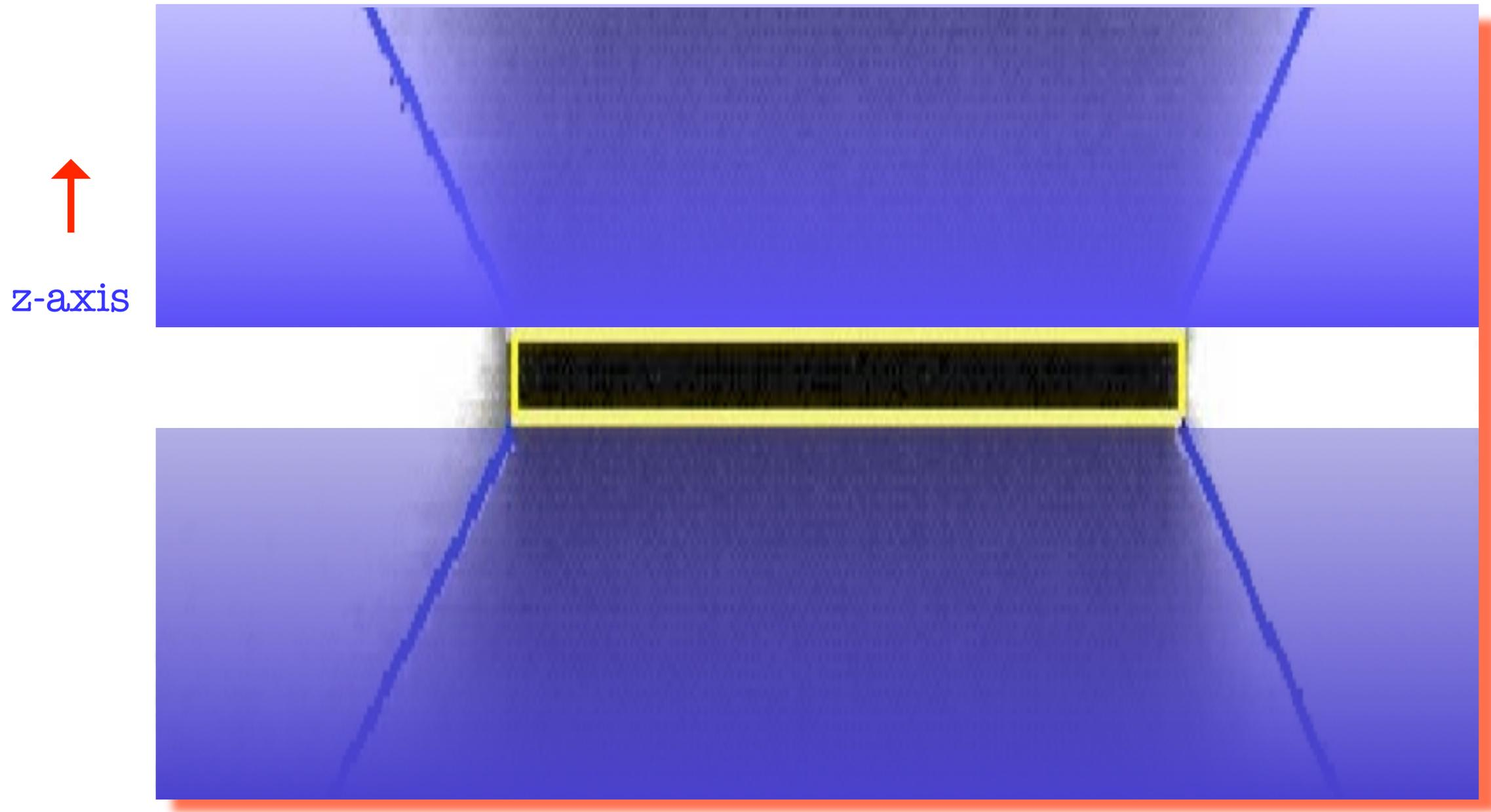
Alberto Diaspro, Nanoscopy, Istituto Italiano di Tecnologia



copyright Darwin/Eligio Paoni

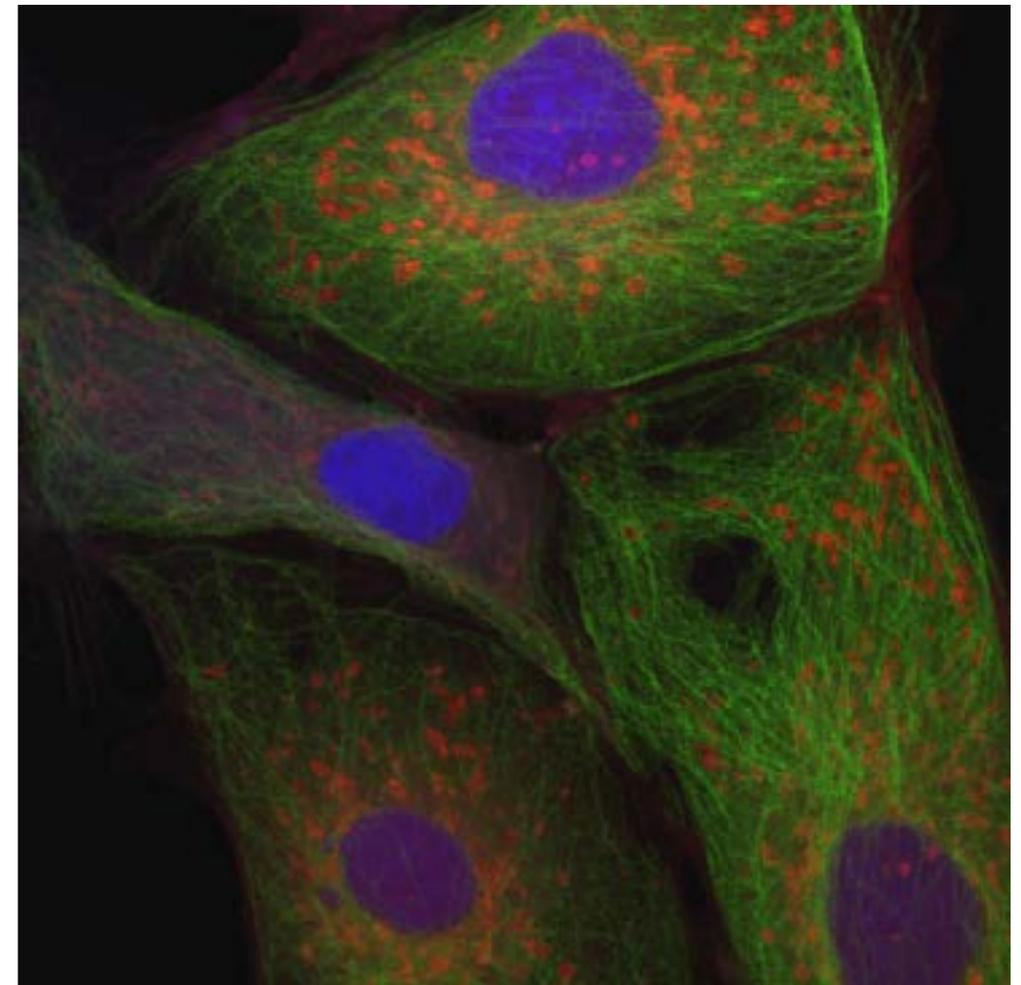
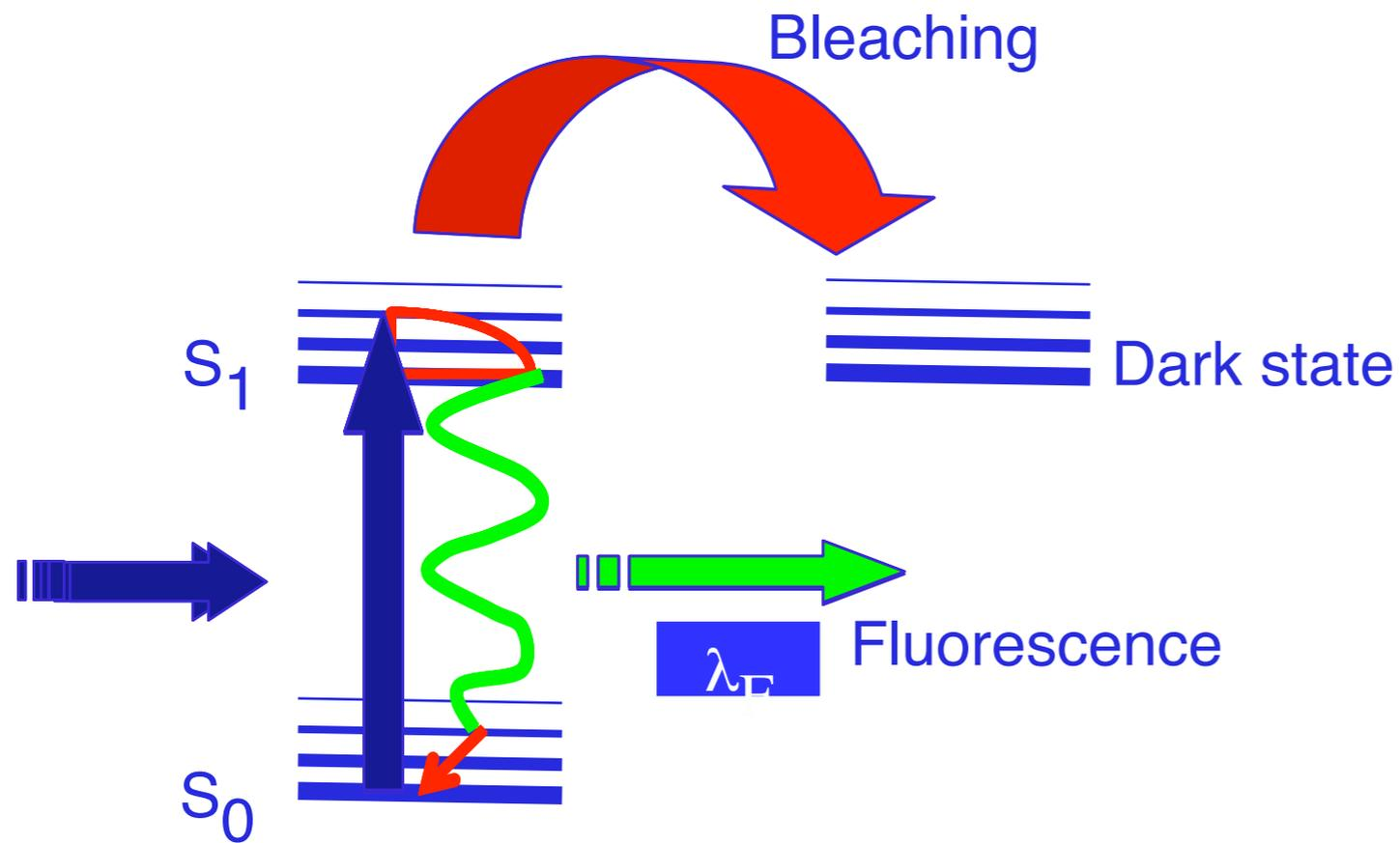


photobleaching



Diaspro A. et al., Photobleaching, in Handbook of Confocal Microscopy (J.Pawley ed.), Plenum, NEW edition, 2006

photobleaching



Diaspro A. et al., Photobleaching, in Handbook of Confocal Microscopy (J.Pawley ed.), Plenum, NEW edition, 2006

Image Credit: Giovanni Giozzet Olympus

photobleaching

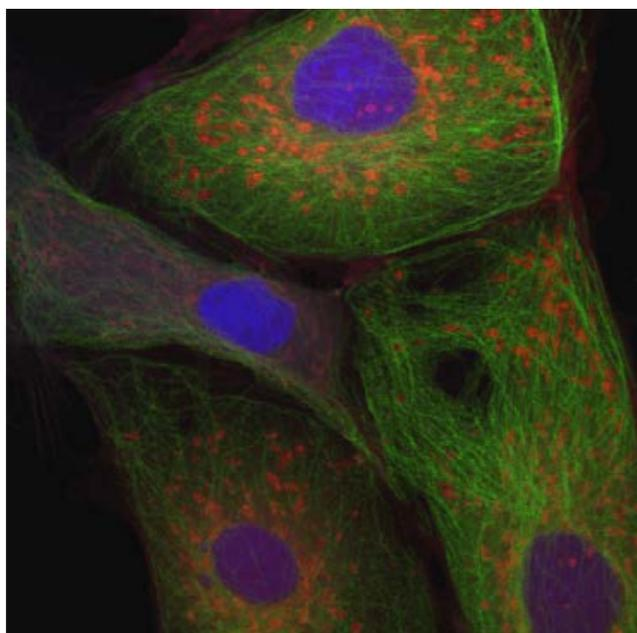
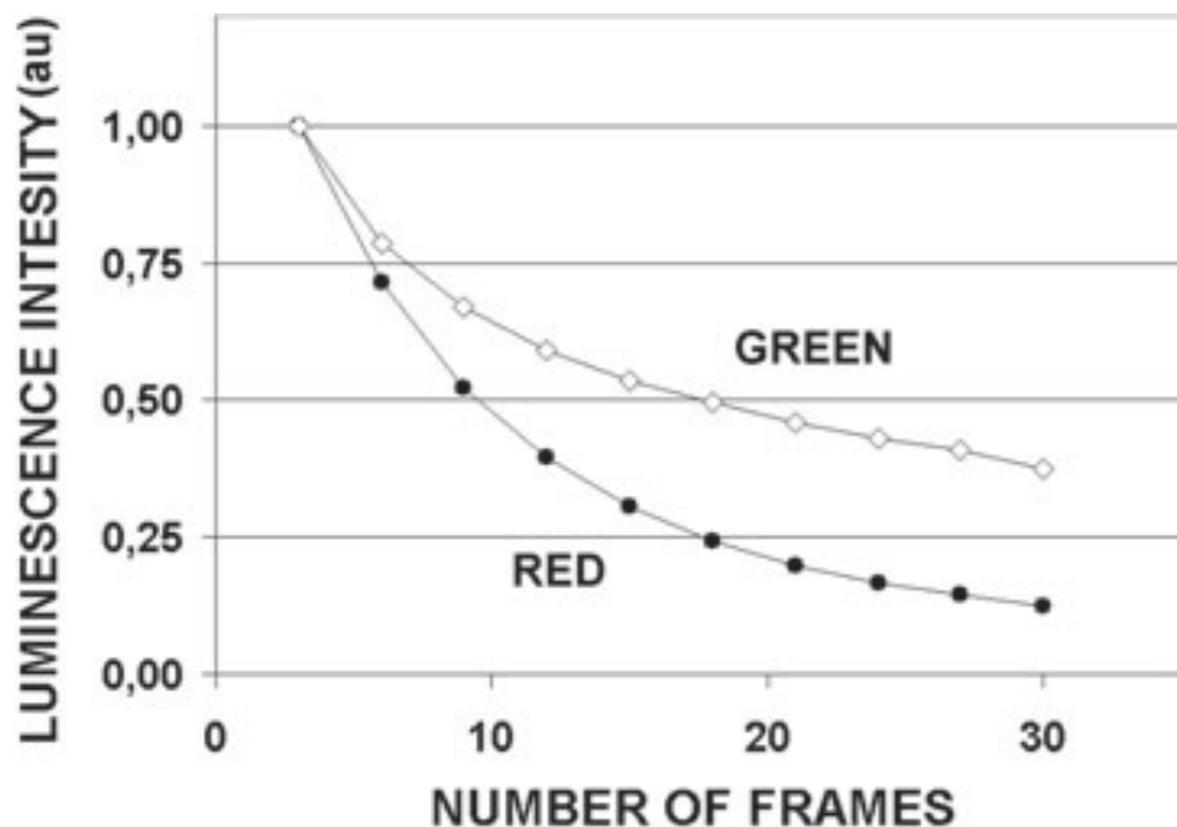
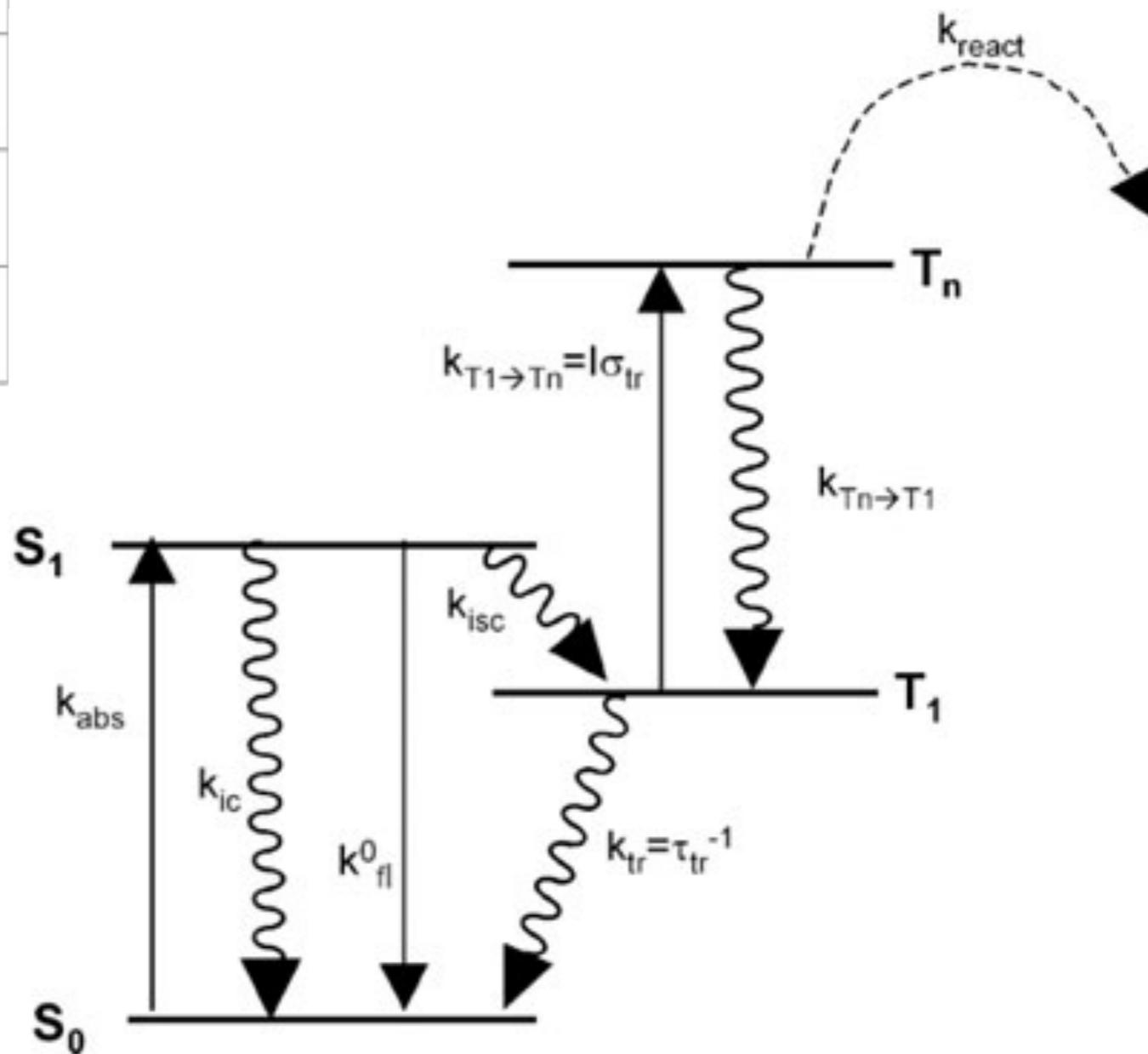
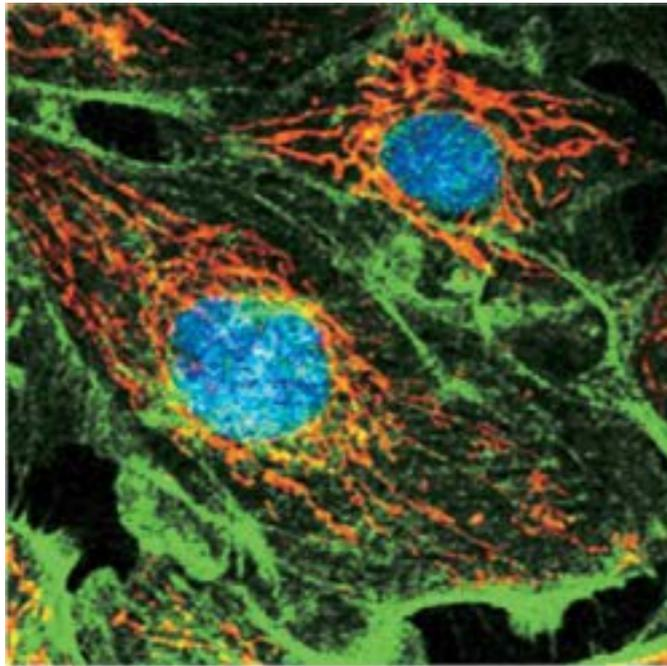


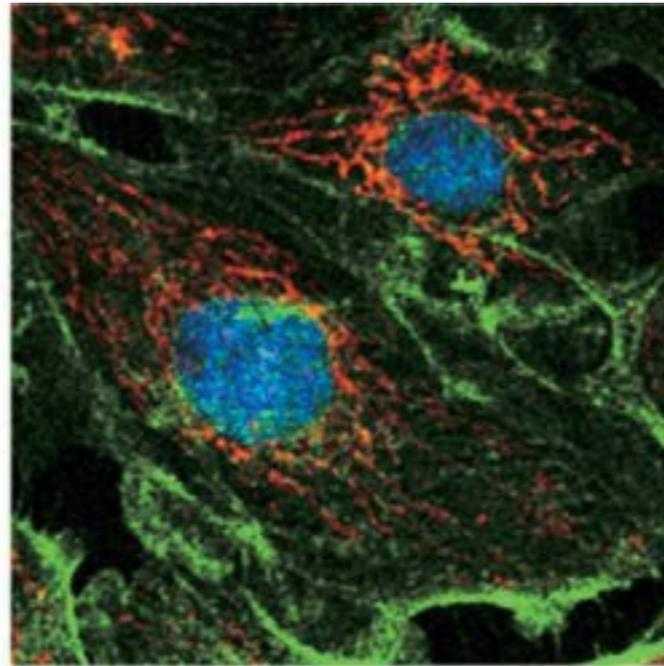
Image Credit: Giovanni Giozzet Olympus



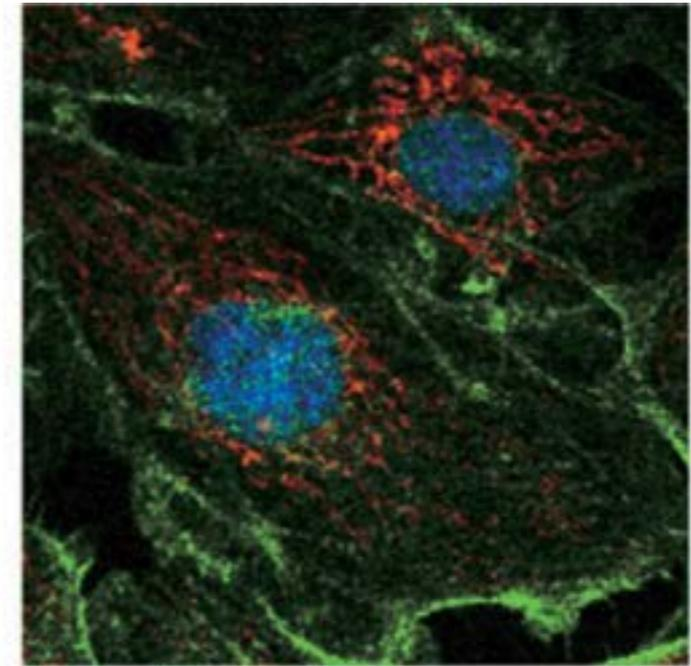
photobleaching



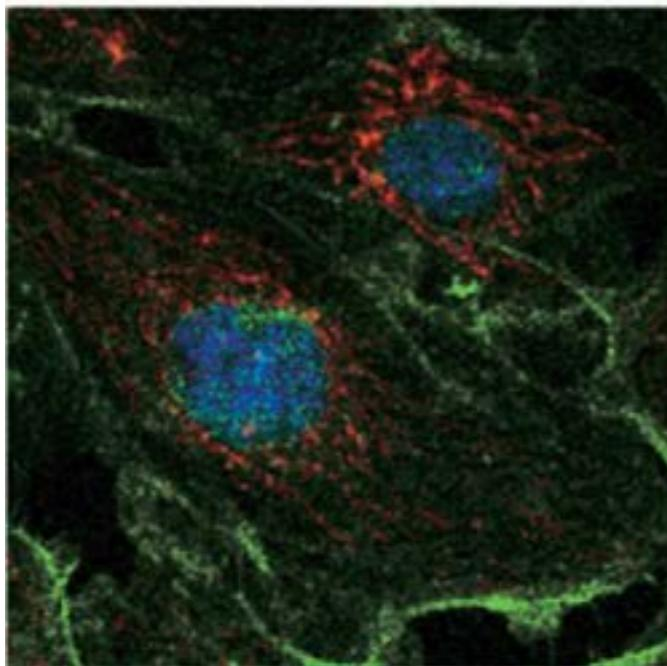
t=0 min



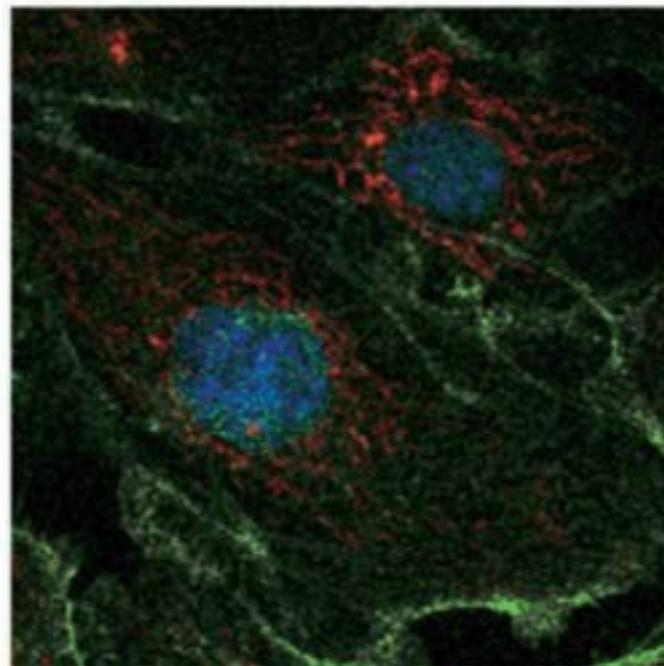
t=4 min



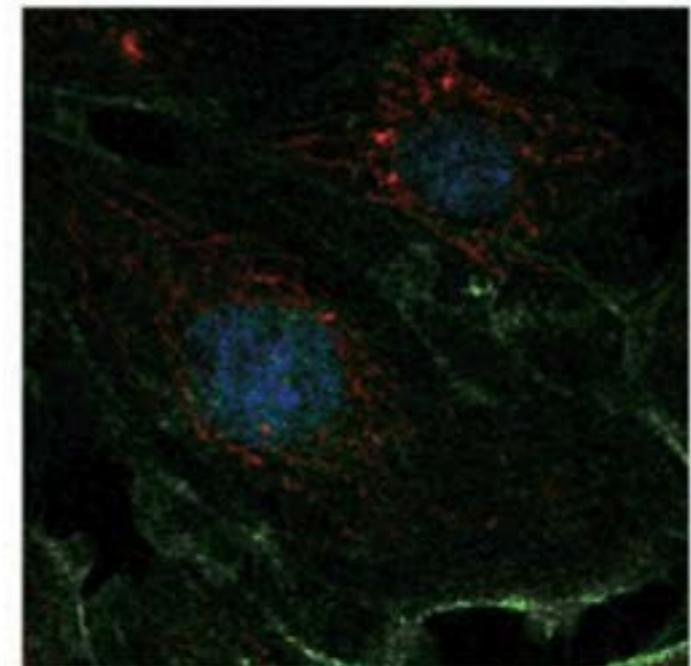
t=8 min



t=12 min



t=16 min

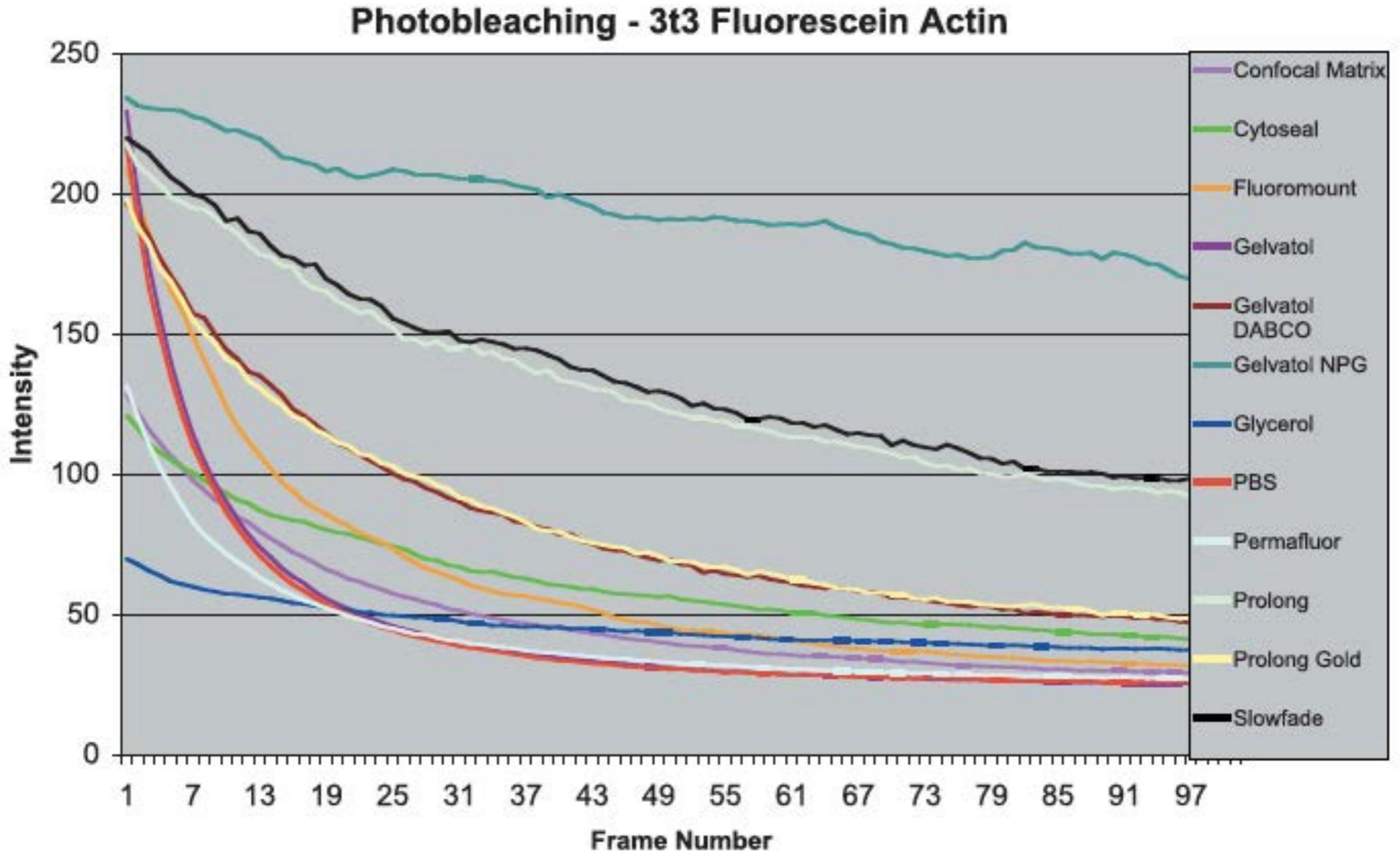


t=20 min

Diaspro A. et al., Photobleaching, in Handbook of Confocal Microscopy (J.Pawley ed.), Plenum, NEW edition, 2006

Alberto Diaspro, Nanoscopy, Istituto Italiano di Tecnologia

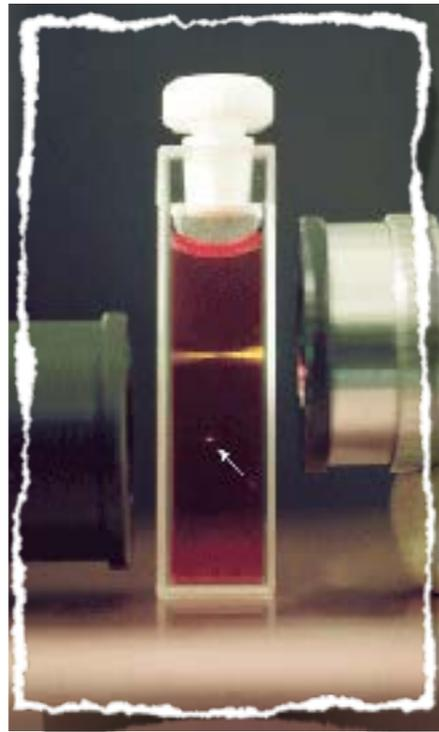
photobleaching



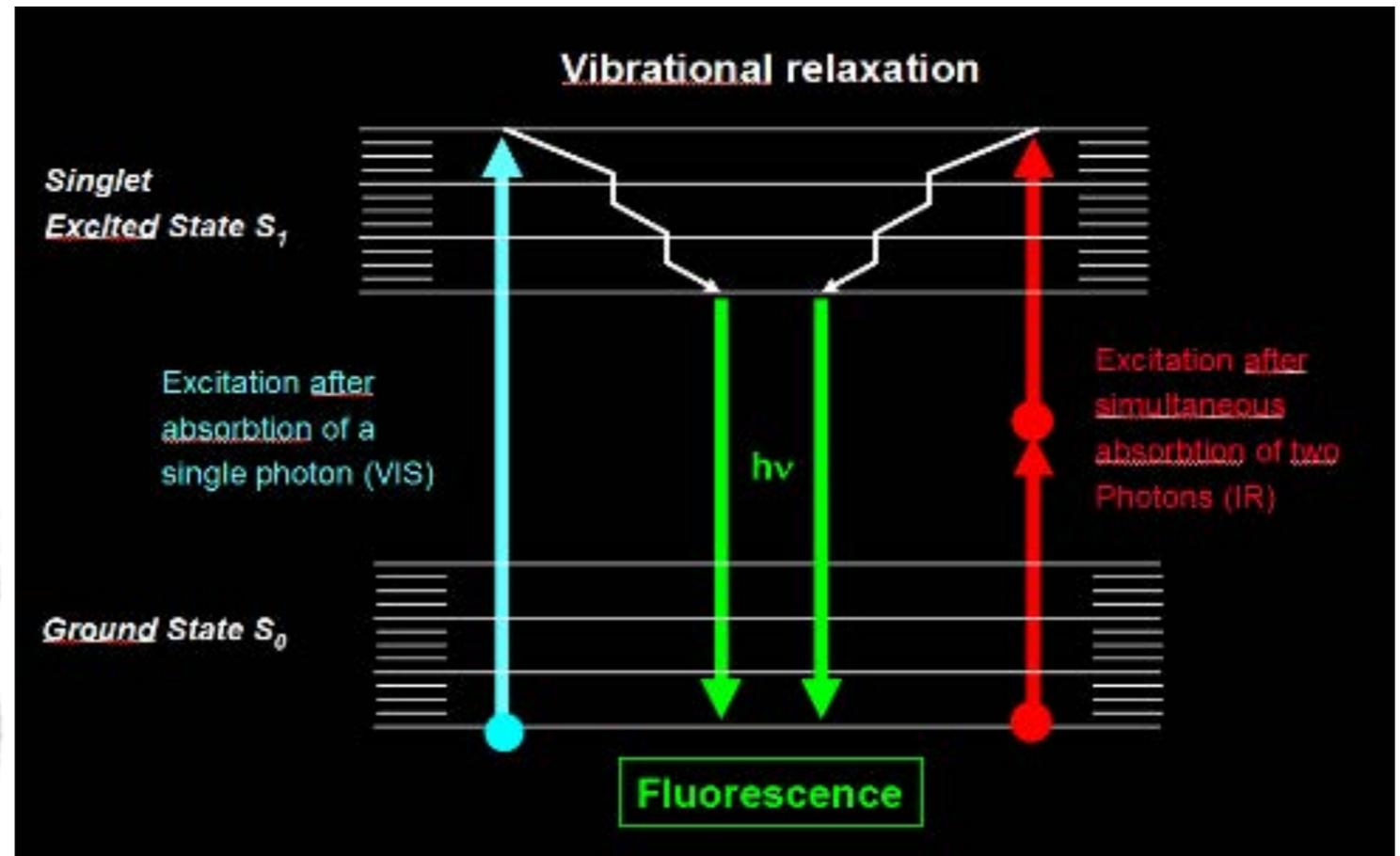


fluorescence

non linear excitation



Credit:BRAD AMOS
MRC UK



Sheppard CJR and Kompfner R. *Applied Optics* .17: 2879–2882 (1978)
Denk, W., Strickler, J.H. & Webb, W.W. *Science* 248, 73–76 (1990).

Maria Göppert-Mayer predicted that an atom or a molecule could interact with two photon(s) simultaneously by absorbing them in the very same quantum event (1929).

Diaspro et al., *Quart. Rev. .Biophys.* (2005) 38 (2): 1-72 .

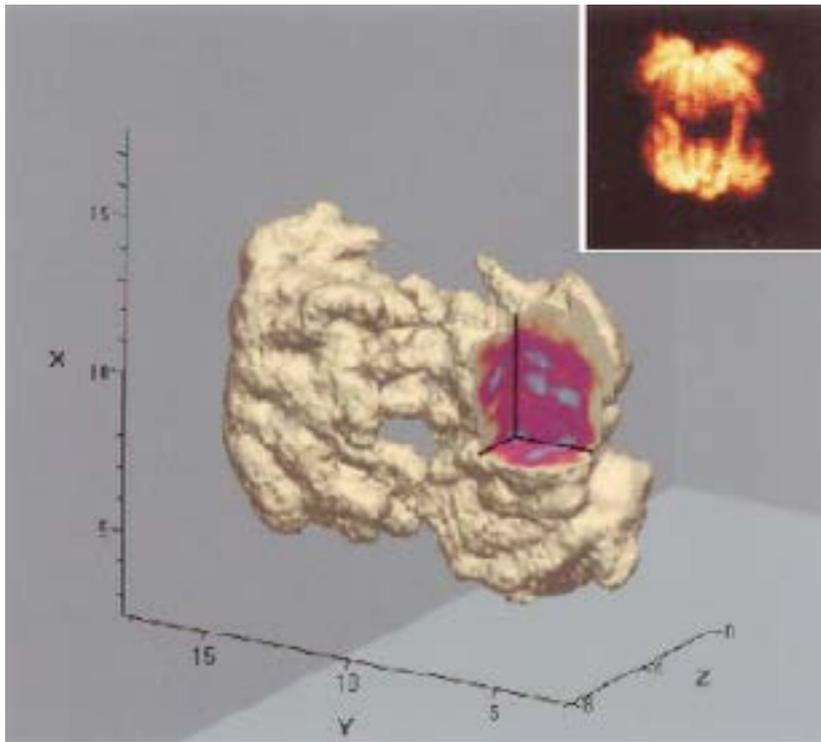
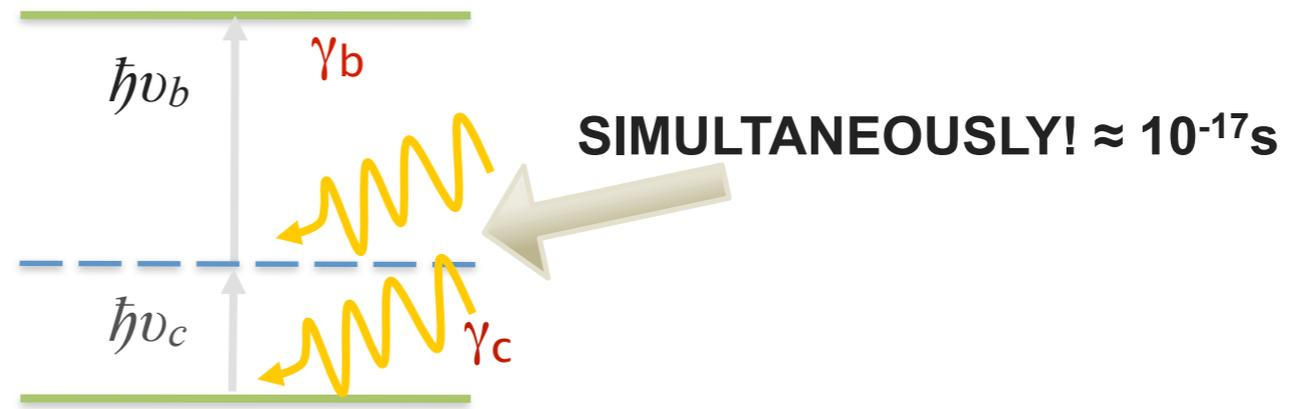
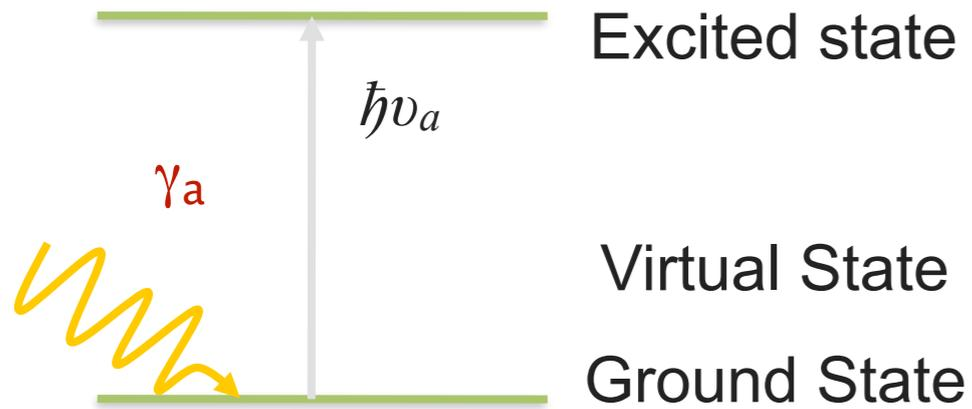


Movie credit: P.Sapuppo, E.Cocchia Leica Microsystems

non linear excitation

Denk, W., Strickler, J. H., & Webb, W. W. (1990). Science, 248(4951), 73-76

Sheppard CJR, Kompfner R (1978). Appl. Opt. 17, 2879-2882



CW-two-photon excited 3D-data stack after volume rendering taken of DAPI-stained mouse fibroblast DNA undergoing mitosis taken with 210mw.

$$I_f \propto n_a \propto \langle P \rangle^2$$

$$n_a \approx \frac{\sigma \langle P \rangle^2}{\tau_p f_p} \left(\frac{N.A.^2}{2 \hbar c \lambda} \right)^2$$

n_a = number of absorbed photons per molecule

σ = two Photon cross section $10^{-48} - 10^{-50} \text{ cm}^4 \text{ photon}^{-1} \text{ molec}^{-1}$

τ_p = pulse width 100 fs

f_p = pulse repetition rate ~80 Mhz

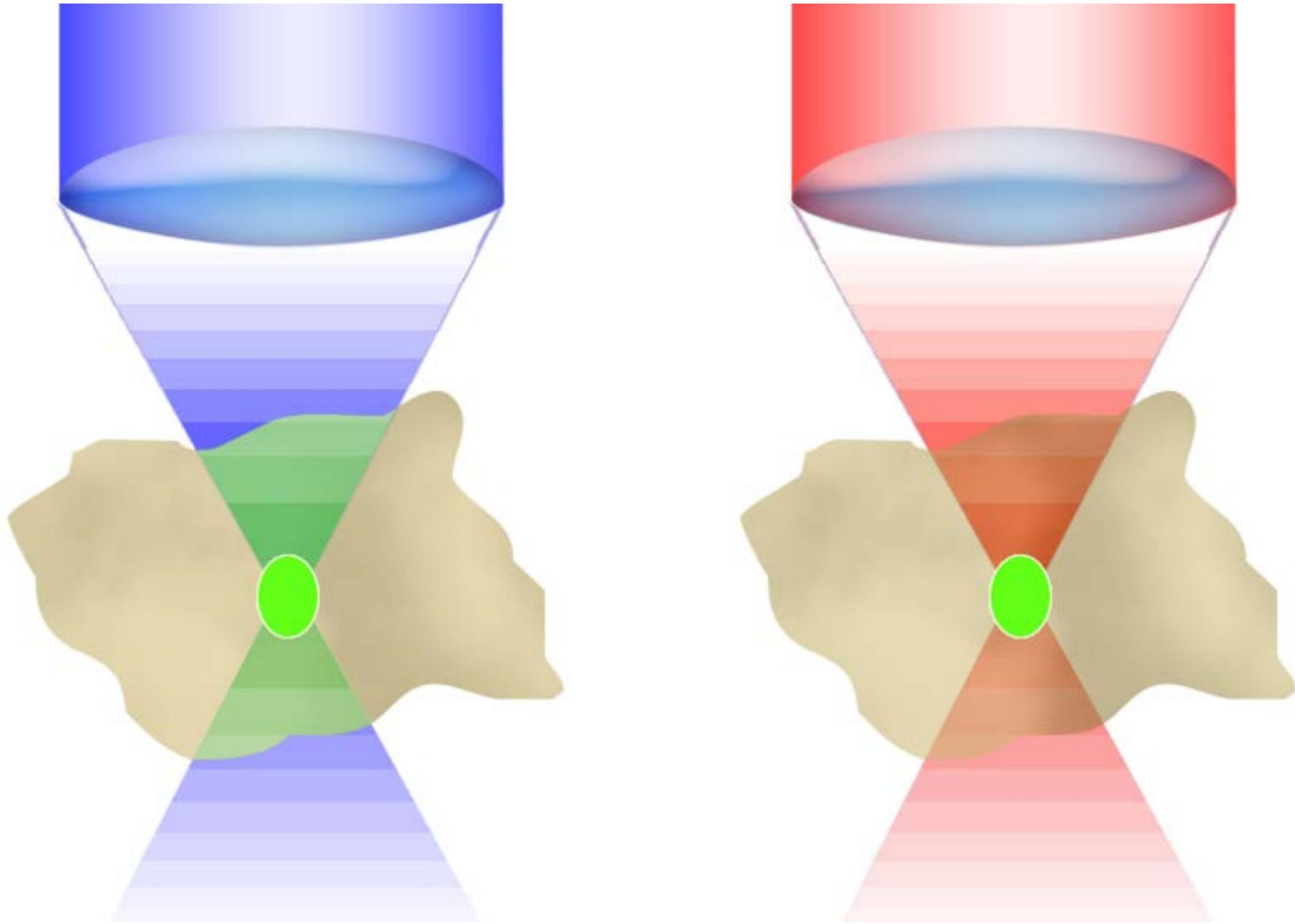
N.A. = lens numerical aperture ~1.2/1.4

$\langle P \rangle$ = average incident power ~20mW

Booth, M. J., & Hell, S. W. (1998) "Continuous wave excitation two-photon fluorescence microscopy exemplified with the 647-nm ArKr laser line", Journal of Microscopy 190(Pt 3), 298-304.

P. Bianchini and A. Diaspro, (2012) "Fast scanning STED and two-photon fluorescence excitation microscopy with continuous wave beam," Journal of Microscopy 245(3), 225-228

non linear microscopy



Diaspro et al., Quart. Rev. .Biophys. (2005) 38 (2): 1-72 .

Alberto Diaspro, Nanoscopy, Istituto Italiano di Tecnologia

two-photon excitation (2pe) microscopy

Simply Winnie Pooh Philosophy: Two are better than one!



A. Diaspro (ed.), (2001) "Confocal and Two-photon Microscopy. Wiley, NY, 1-567.

two-photon excitation (2pe) microscopy



A. Diaspro (ed.), (2001) "Confocal and Two-photon Microscopy. Wiley, NY, 1-567.

Diaspro A: Two-photon fluorescence excitation. A new potential perspective in flow cytometry. *Minerva Biotechnologica* 1998, **11**: 87-92.

two-photon excitation (2pe) microscopy



Giuseppe Pellizza da Volpedo (1868–1907)

Il quarto stato (1901), olio su tela, 293x545 cm, Milano, Civica Galleria d'Arte Moderna

two-photon excitation (2pe) microscopy



(Credit: CLAUDIA DIASPRO from JOVANOTTI'S POP CONCERT)

A.Diaspro et al., (2006) Biomedical Engineering On Line (BMEOL), 5(1):36..

This article can be downloaded for free from: <http://www.biomedical-engineering-online.com/content/5/1/36>

Resonant scanning optical microscope

15 September 1978 / Vol. 17, No. 18 / APPLIED OPTICS 2879

C. J. R. Sheppard and R. Kompfner



SCANNING OPTICAL MICROSCOPE

1931

1977

1990

Two-Photon Laser Scanning Fluorescence Microscopy

WINFRIED DENK,* JAMES H. STRICKLER, WATT W. WEBB

Molecular excitation by the simultaneous absorption of two photons provides intrinsic three-dimensional resolution in laser scanning fluorescence microscopy. The excitation of fluorophores having single-photon absorption in the ultraviolet with a stream of strongly focused subpicosecond pulses of red laser light has made possible fluorescence images of living cells and other microscopic objects. The fluorescence emission intensity varies quadratically with the excitation intensity so that fluorescence and photobleaching were confined to the vicinity of the focal plane as expected for cooperative two-photon excitation. This technique also provides unprecedented capabilities for three-dimensional, spatially resolved photochemistry, particularly photolytic release of caged effecter molecules.

WE REPORT THE APPLICATION OF two-photon excitation of fluorophores (1) to laser scanning microscopy (LSM) (2). In LSM, the laser is focused to a diffraction-limited beam waist (<1 μm in diameter and is raster-scanned across a specimen. Confocal LSM provides depth discrimination and improves spatial resolution within the plane of focus by focusing the image through the same system. The two-photon excitation of fluorophores (3) and the use of femtosecond laser pulses (4) to excite a small area of the specimen (5) have made it possible to perform good laser scanning microscopy (6) with ultraviolet (UV) excitation. Fluorophores that absorb and emit in the visible (7). Confocal scanning images with fluorophores and fluorescent chemical indicators that are excited by the ultraviolet (UV) part of the spectrum have not appeared, however, largely because of the lack of suitable microscope lenses, which must be chromatically corrected and transparent for both

absorption and emission wave lengths (4, 5). Anticipated photodamage to living cells and the limitations of UV lasers have also inhibited this approach. Two-photon molecular excitation (7, 8) is made possible by the very high local instantaneous intensity provided by the tight focusing in an LSM combined with the temporal concentration of a femtosecond pulsed laser (9) (CPM) producing a stream of pulses with a pulse duration (τ_p) of about 100 fs at a repetition rate (f_r) of about 80 MHz; the probability becomes appreciable for a dye molecule to absorb two long-wavelength (λ_{exc}) photons simultaneously, thus combining their energy in order to reach its excited state. Assuming a typical two-photon cross section (σ₂) of σ₂ = 10⁻⁵⁰ m²/s per photon with the above pulse parameters and the beam focused by a lens of numerical aperture A = 1.4, we calculated that an average incident laser power (P₀) of ~50 mW would saturate the fluorescence output at the rate of one absorbed photon

Two-photon excitation STED microscopy

Gael Moneron and Stefan W. Hell*

Department of Neurosciences, Max-Planck Institute for Biophysical Chemistry, Am Fassberg 11, 37077 Göttingen, Germany

Abstract: We report sub-diffraction resolution in two-photon excitation (2PE) fluorescence microscopy achieved by merging this technique with stimulated-emission depletion (STED). We demonstrate an easy-to-implement and promising laser combination based on a short-pulse laser source for two-photon excitation and a continuous-wave (CW) laser source for resolution enhancement. Images of fluorescent nanoparticles and the immunostained transcription regulator NFκB in mammalian cells exhibit resolutions of 50 nm and ~70 nm in the focal plane, corresponding to a 4–5.4-fold improvement over the diffraction limit.

©2009 Optical Society of America
OCIS codes (180.1750) Confocal microscopy; (180.2520) Fluorescence microscopy; (180.4150) Nanoscale microscopy; (180.8100) Scanning microscopy; (180.9200) Three-dimensional microscopy; (110.2130) Microscopy.

References and links

1. W. Denk, J. H. Strickler, and W. W. Webb, "Two-photon laser scanning fluorescence microscopy," *Science* **248**(4971), 73–75 (1990).
2. S. W. Hell and J. Wichmann, "Breaking the diffraction resolution barrier by stimulated emission depletion microscopy," *Optics Letters* **19**(13), 755–757 (1994).

Neurotechnique

Superesolution Imaging in Biological Systems Using Stimulated-Emission Depletion Two-Photon Laser Scanning Microscopy

Jun-Bil Dimp,† Kevin T. Takasaki,† and Leonardo L. Sabatini*
†Department of Neurobiology, Harvard Medical School, Cambridge, MA 02138, USA
*Program in Neurobiology, Harvard University, Cambridge, MA 02138, USA
Correspondence: sabatini@fas.harvard.edu
DOI: 10.1093/neuro/nfn017

Stimulated-emission depletion (STED) microscopy is a superresolution technique that allows imaging beyond the diffraction limit by using near-infrared (NIR) lasers for both pulsed two-photon excitation and continuous-wave stimulated emission depletion (STED). Furthermore, we demonstrate that

Single-wavelength two-photon excitation-stimulated emission depletion (SW2PE-STED) superresolution imaging

Paolo Bianchini*, Benjamin Harke*, Silvia Galiani†, Giuseppe Micidomini† and Alberto Diaspro*^{1,2}

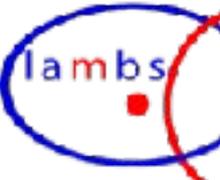
*Department of Nanophysics, Istituto Italiano di Tecnologia, 16100 Genoa, Italy; †Department of Physics, University of Genoa, 16100 Genoa, Italy

Edited by David A. Weitz, Harvard University, Cambridge, MA, USA; Received 15 May 2011; accepted 15 November 2011

We developed a new class of two-photon excitation-stimulated emission depletion (2PE-STED) optical microscope. In this work, we show the opportunity to perform superresolved fluorescence imaging, exciting and stimulating the emission of a fluorophore with a single-wavelength laser. The key point of the microscope lies on finding a wave with a nonzero cross-section for 2PE and STED processes. In this paper, we describe the principle of the microscope and the experimental setup. The key point of the microscope lies on finding a wave with a nonzero cross-section for 2PE and STED processes. In this paper, we describe the principle of the microscope and the experimental setup.

2009

2012

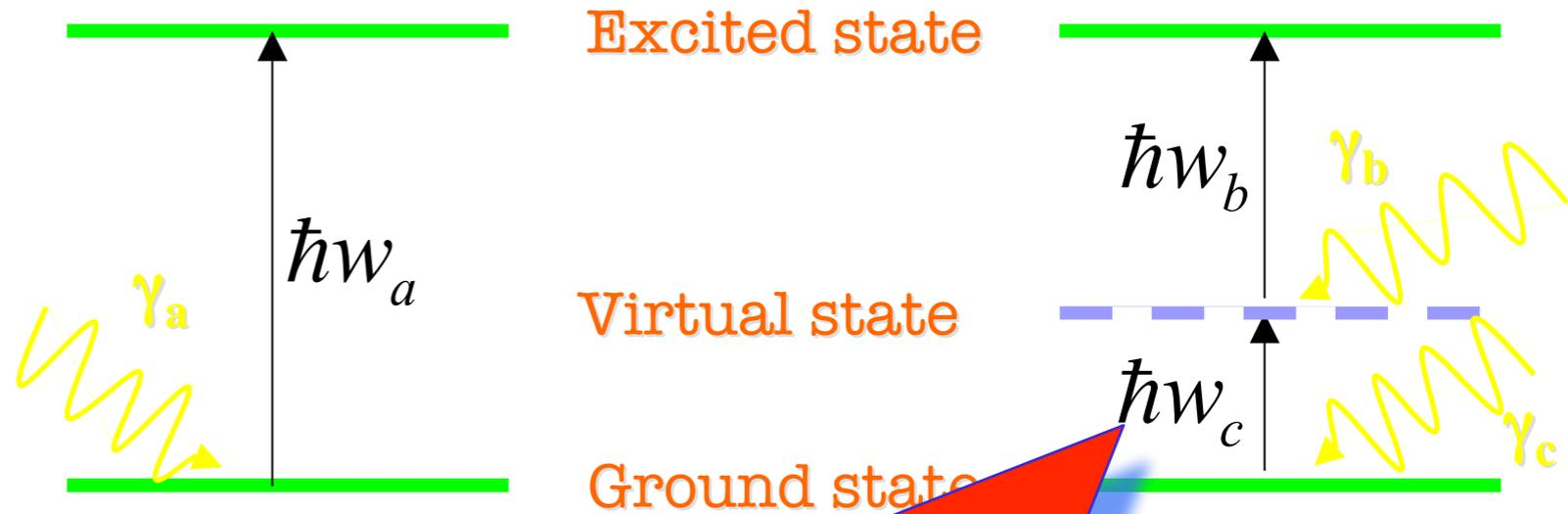


two-photon excitation (2pe) microscopy

MARIA GOEPPERT MAYER

The shell model

Nobel Lecture, December 12, 1963



SIMULTANEOUSLY!

10^{-17} s

Maria Göppert-Mayer predicted that an atom or a molecule could interact with two photons simultaneously by absorbing them in the very same quantum event.

two-photon excitation (2pe) microscopy

History

- 1931: Prediction of two-photon absorption by Maria Göppert-Mayer
- 1961: Experimental observation of two-photon excitation in $\text{CaF}_2:\text{Eu}^{2+}$
- **1978: Proposal of application of TPE and other NLE to scanning microscopy**
(Colin Sheppard, Oxford)
- 1990: First successful realization of two-photon laser scanning fluorescence microscopy
(Winfried Denk at W.Webb Lab, Cornell University)

Physics background

- Description by means of perturbation theory:

$$\text{e.g. } H' = e \mathbf{r} \cdot \mathbf{E} \text{ (spatially odd function)}$$

A.Diaspro (ed.), (2001) "Confocal and Two-photon Microscopy. Wiley, NY, 1-567.

two-photon excitation (2pe) microscopy



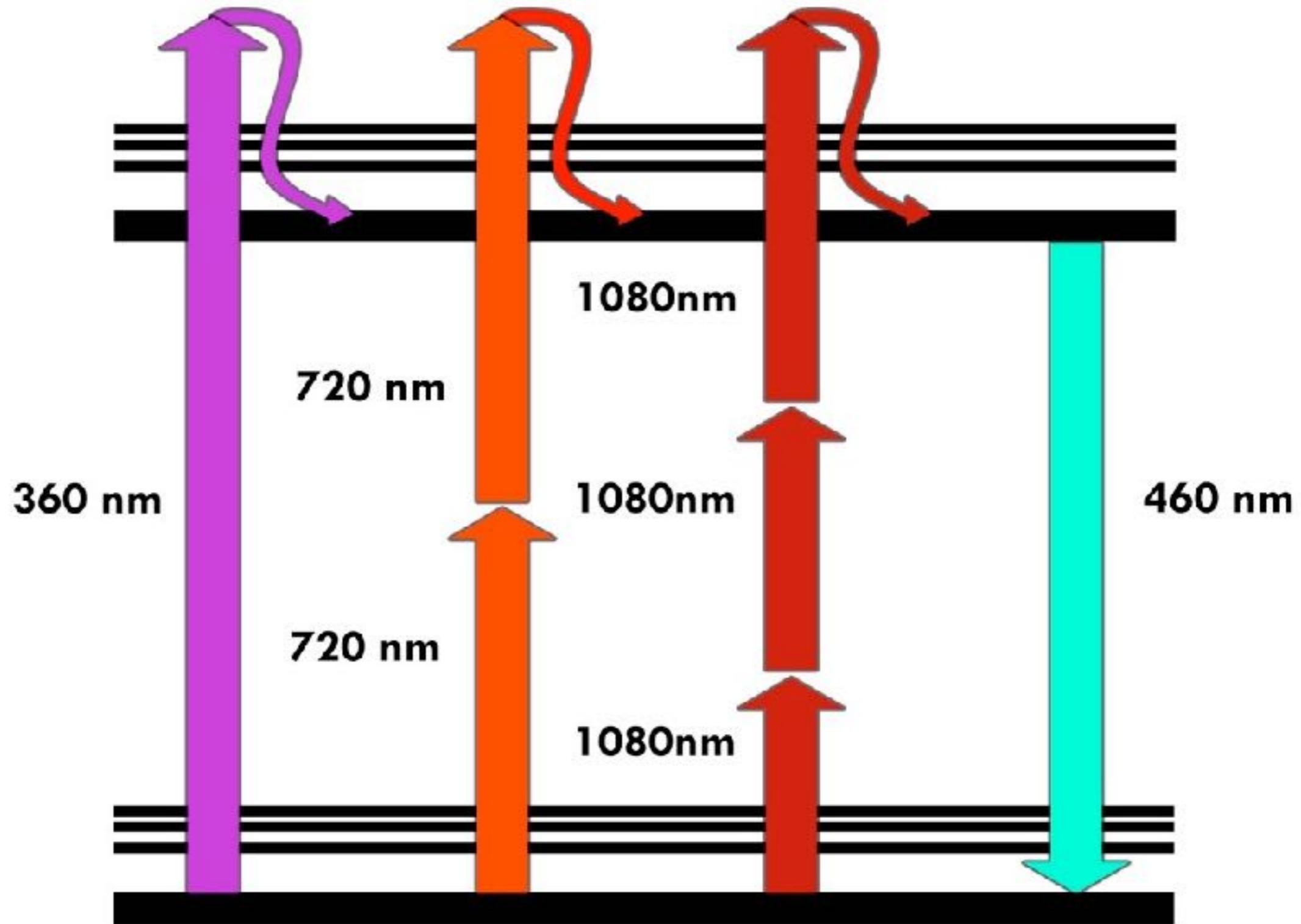
$$E_a = E_b + E_c$$

$$\lambda_a = \left(\frac{1}{\lambda_b} + \frac{1}{\lambda_c} \right)^{-1}$$



Movie Credit: Elio Cocchia Fabrizio Papalia, Paolo Sapuppo - LEICA Microsystems

two-photon excitation (2pe) microscopy



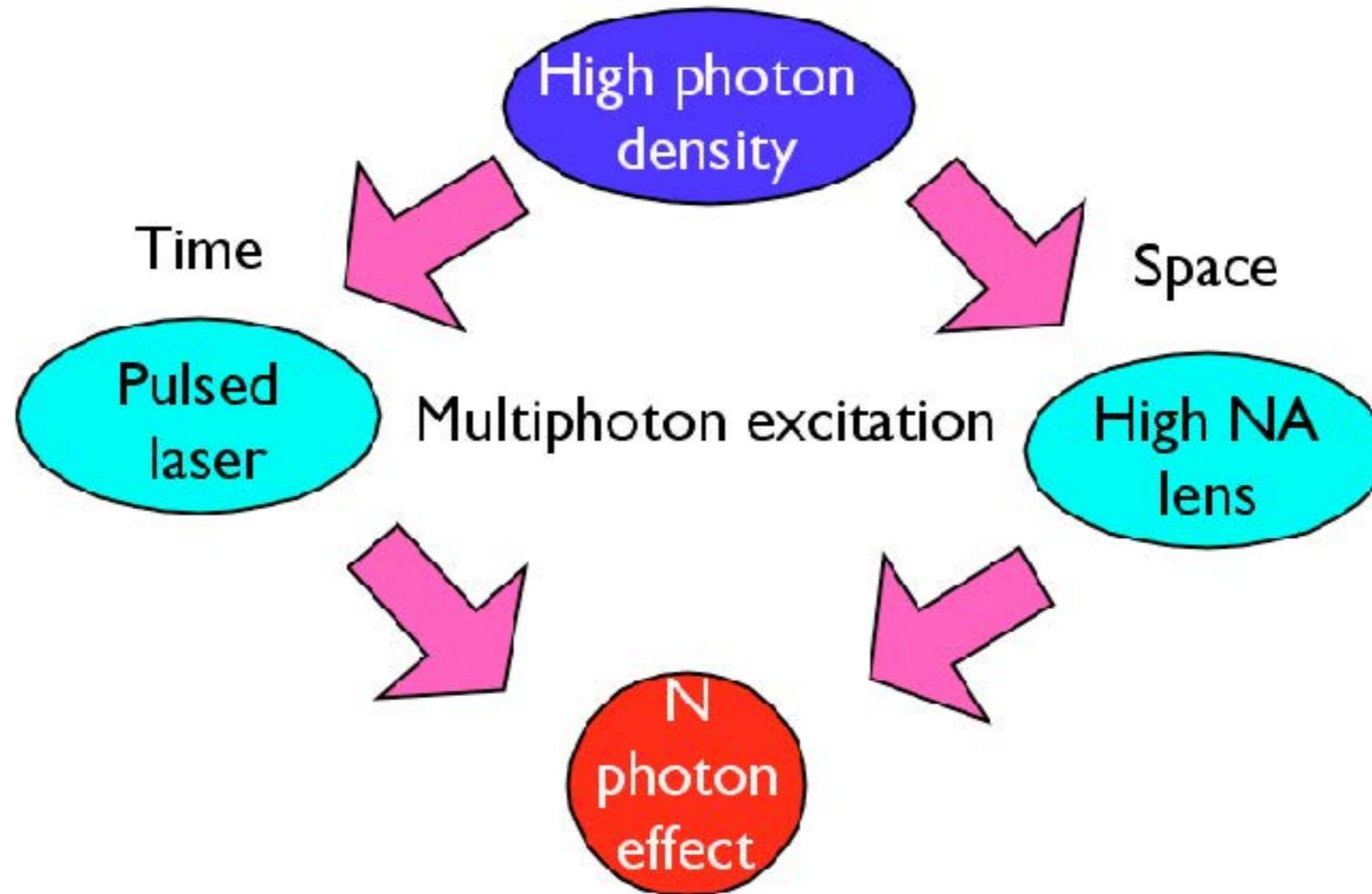
two-photon excitation (2pe) microscopy



IN BRIGHT SUNLIGHT, A MOLECULE OF RHODAMINE B, AN EXCELLENT 1-OR 2-PHOTON ABSORBER, ABSORBS A PHOTON THROUGH A 1-PHOTON PROCESS ABOUT ONCE A SECOND, A PHOTON PAIR BY 2-PHOTON ABSORPTION EVERY 10 MILLION YEARS...

Denk and Svoboda (1997) Neuron, 18:351

two-photon excitation (2pe) microscopy

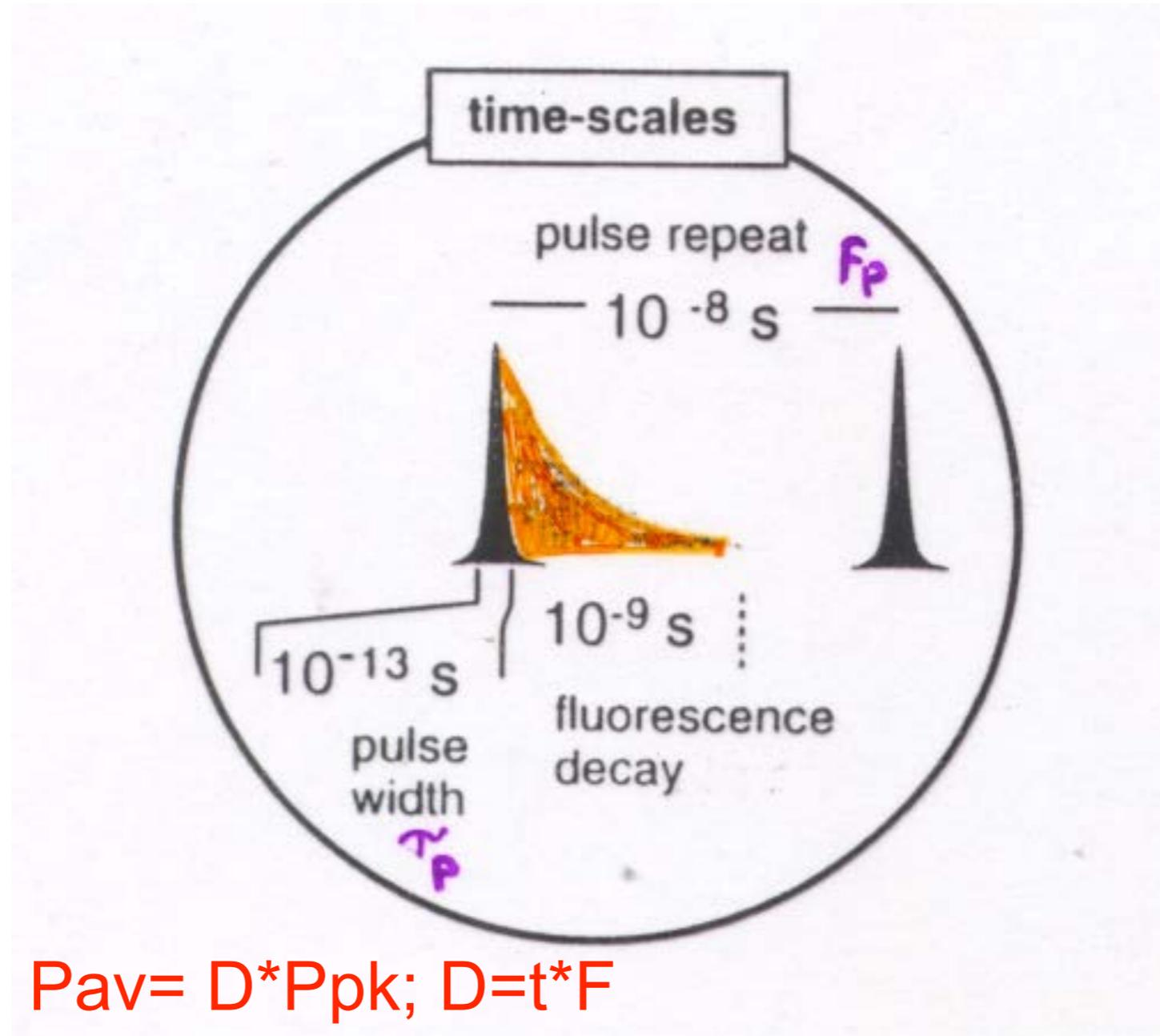


A.DIASPRO, ET AL. (2005) QUART. REV. .BIOPHYS.,VOL.38, NR.2, PP.1-72.

Diaspro A: Two-photon fluorescence excitation. A new potential perspective in flow cytometry. *Minerva Biotecnologica* 1998, 11: 87-92.

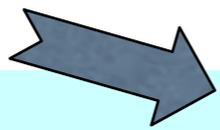
two-photon excitation (2pe) microscopy

CORE ELEMENTS ARE LASER SOURCES



$$P_{av} = D * P_{pk}; D = t * F$$

two-photon excitation (2pe) microscopy


$$n_a = \frac{\sigma \langle P \rangle^2}{\tau_p f_p^2} \left(\frac{N.A.^2}{2\hbar c \lambda} \right)^2$$

$$I_f \propto n_a \propto \langle P \rangle^2$$

n_a = no. of absorbed photons per molecule

σ = two-photon cross-section 10^{-48} - 10^{-50}
 $\text{cm}^4 \text{s photon}^{-1} \text{molec}^{-1}$

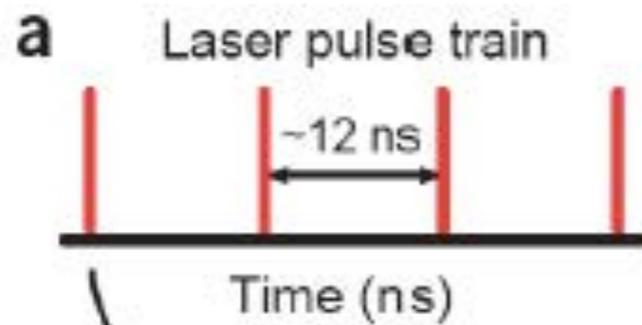
τ_p = pulse width ~ 100 fs

f_p = pulse repetition rate ~ 80 MHz

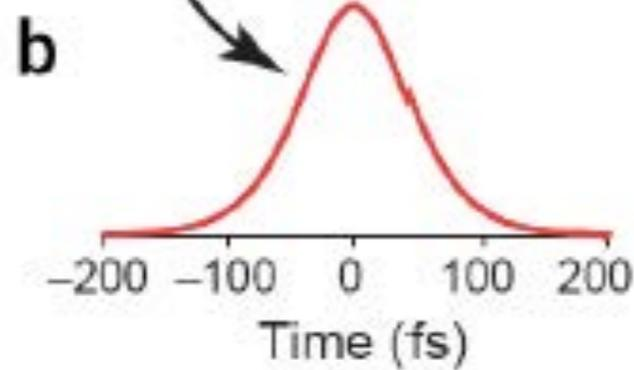
NA = lens numerical aperture $\sim 1.2 - 1.4$

$\langle P \rangle$ = average incident power ~ 20 mW

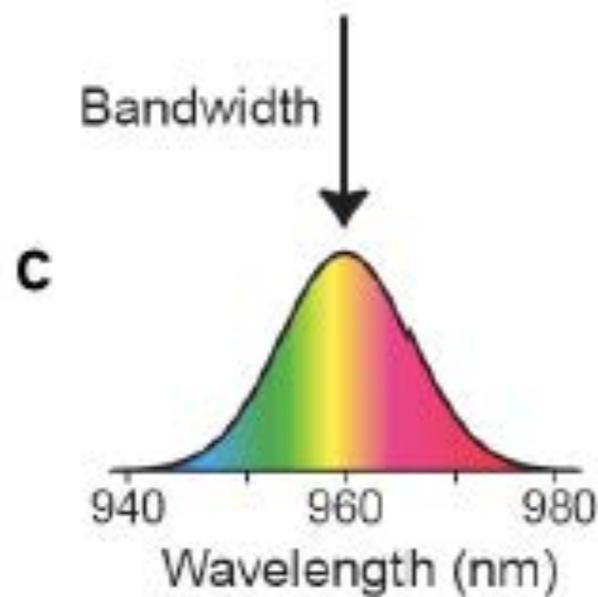
Denk, W., Strickler, J.H. & Webb, W.W. *Science* **248**, 73-76 (1990).



80 MHz repetition rate



FWHM 100 fs – time

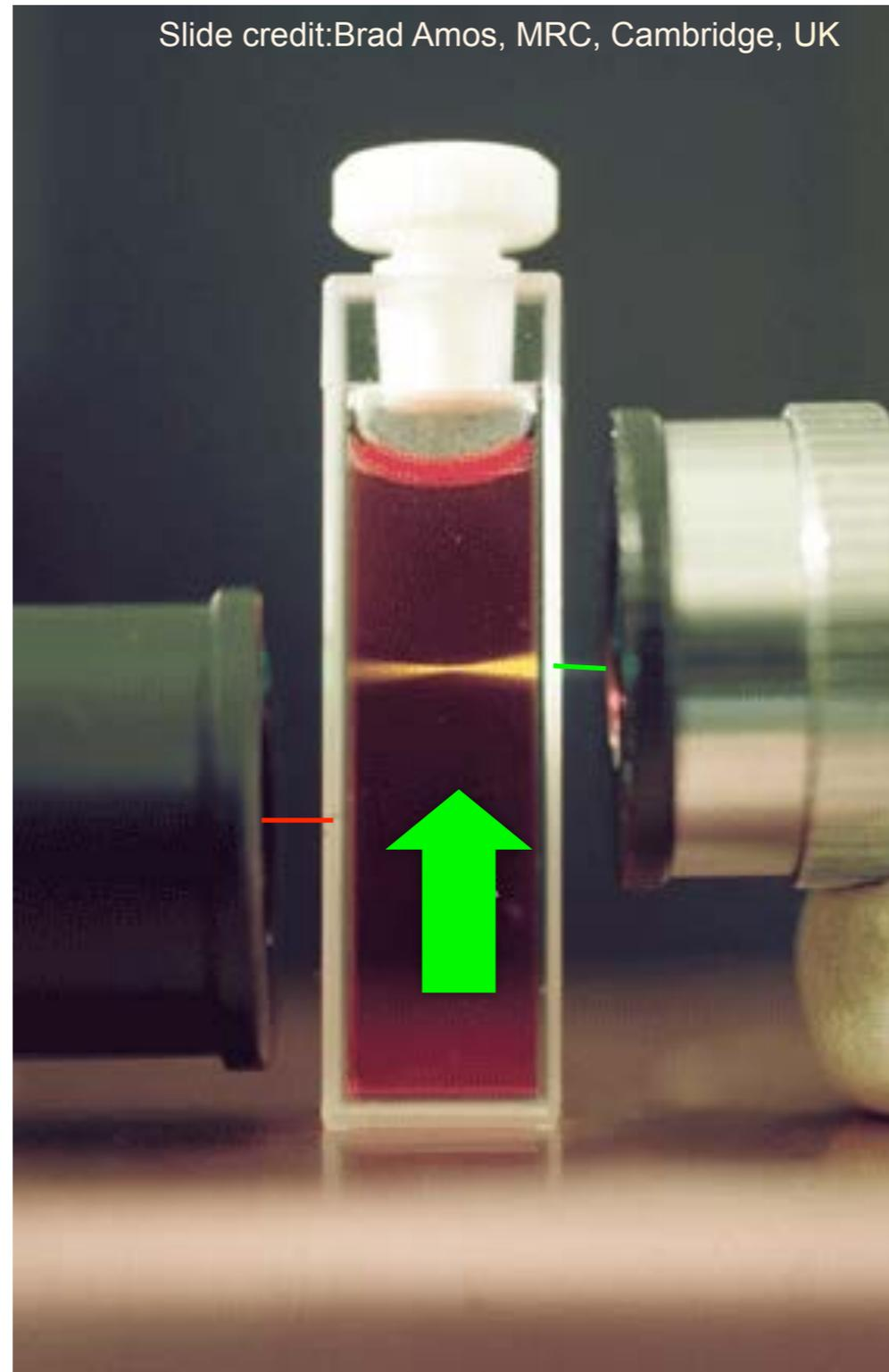


FWHM 10 – 15 nm

Short pulses of monochromatic light have colors! - Spectral components

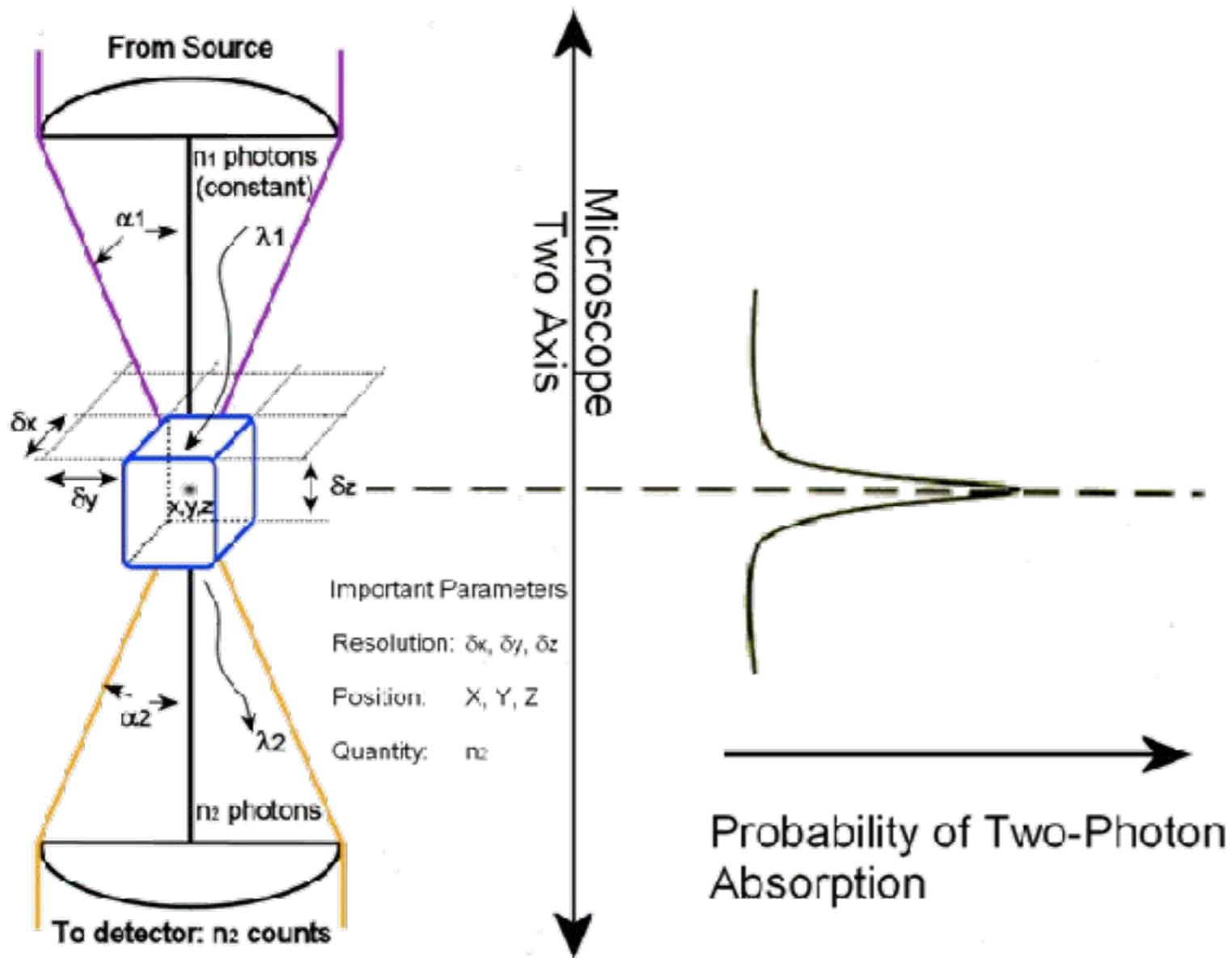
Nat. Biotech. Vol 21 No 11, 2003, Zipfel et al. Nonlinear magic: multiphoton microscopy in the biosciences

two-photon excitation (2pe) microscopy

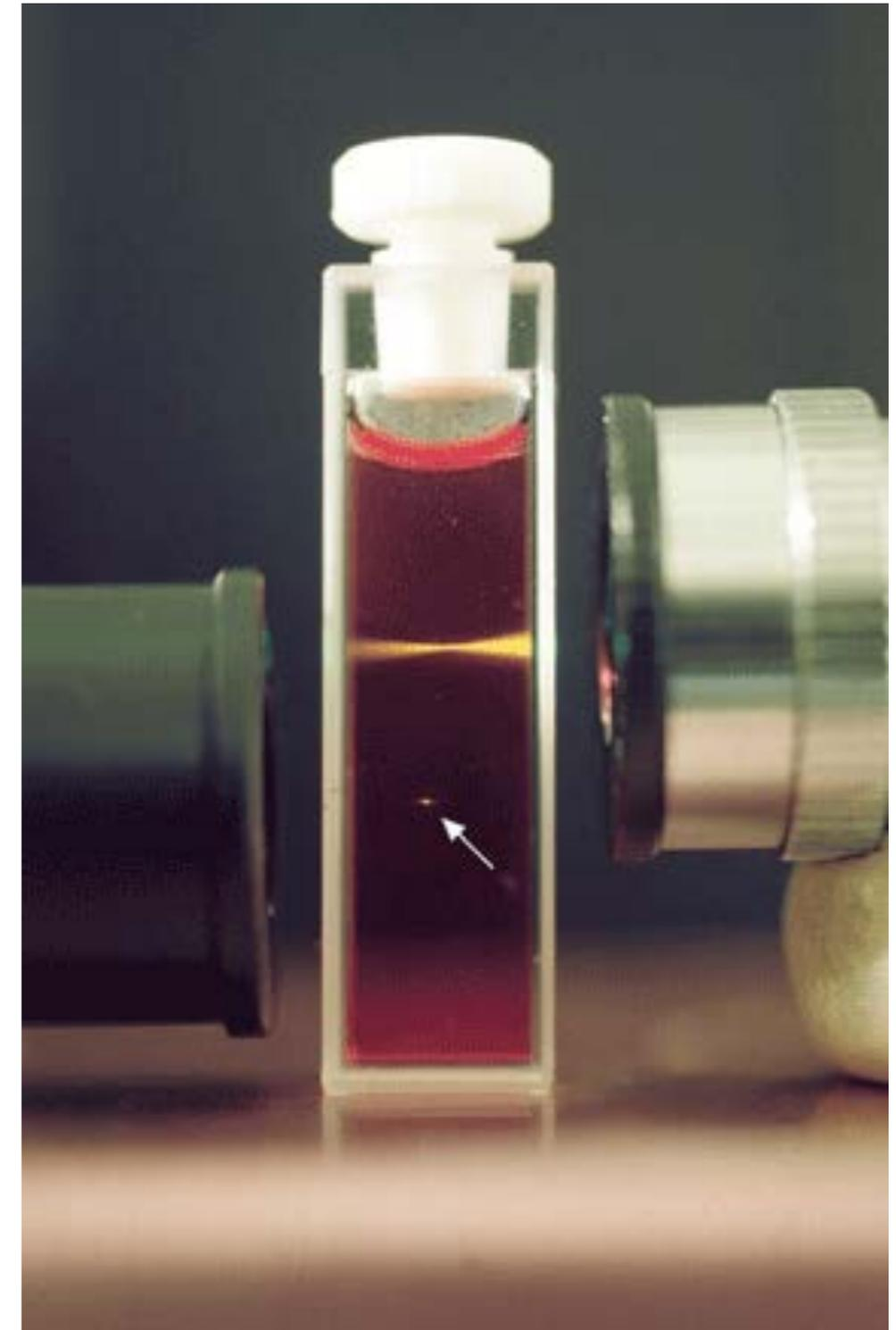


A. DIASPRO, ET AL. (2005) QUART. REV. .BIOPHYS., VOL.38, NR.2, PP.1-72.

two-photon excitation (2pe) microscopy

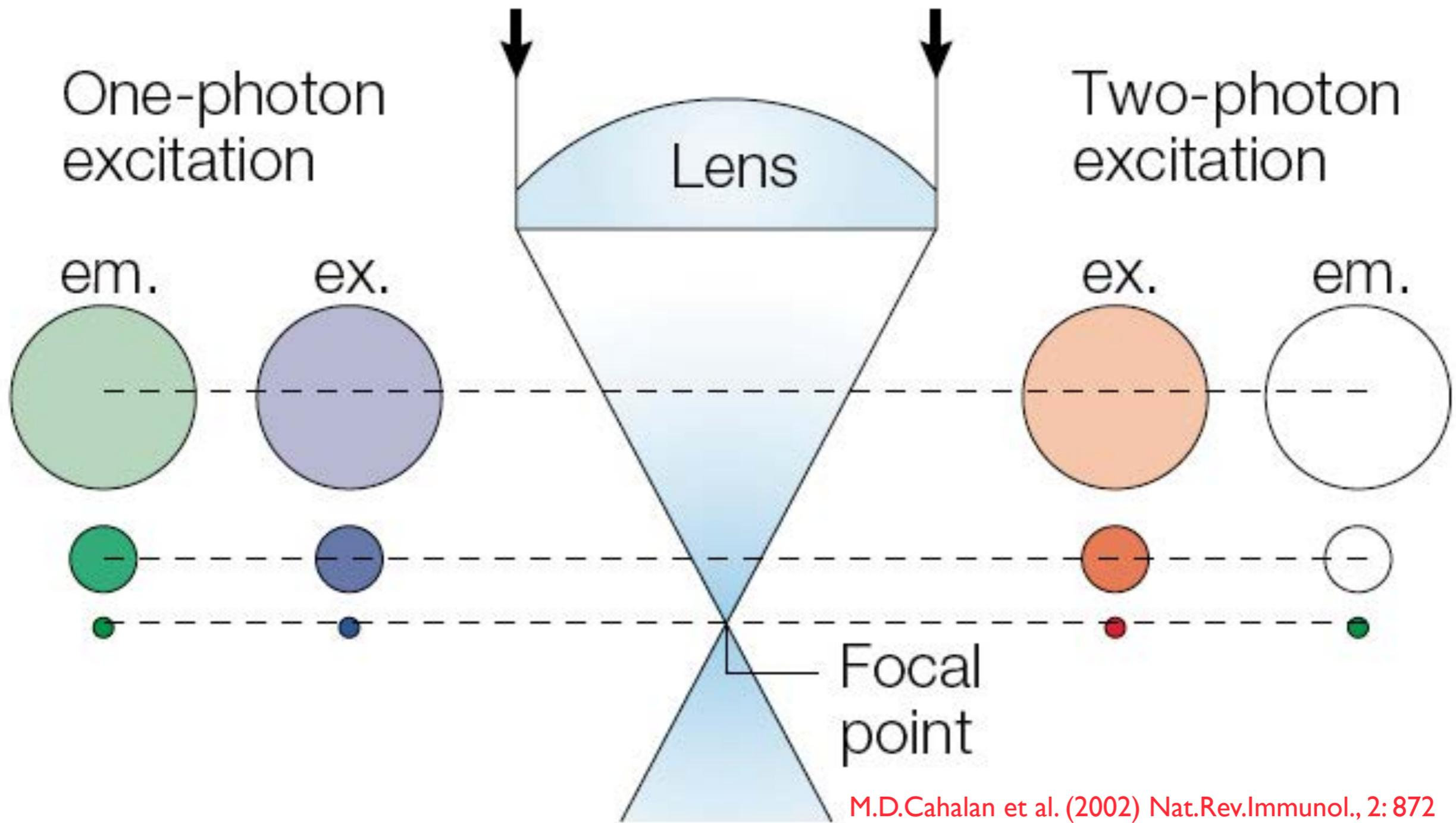


Slide credit: Jim Pawley's Handbook

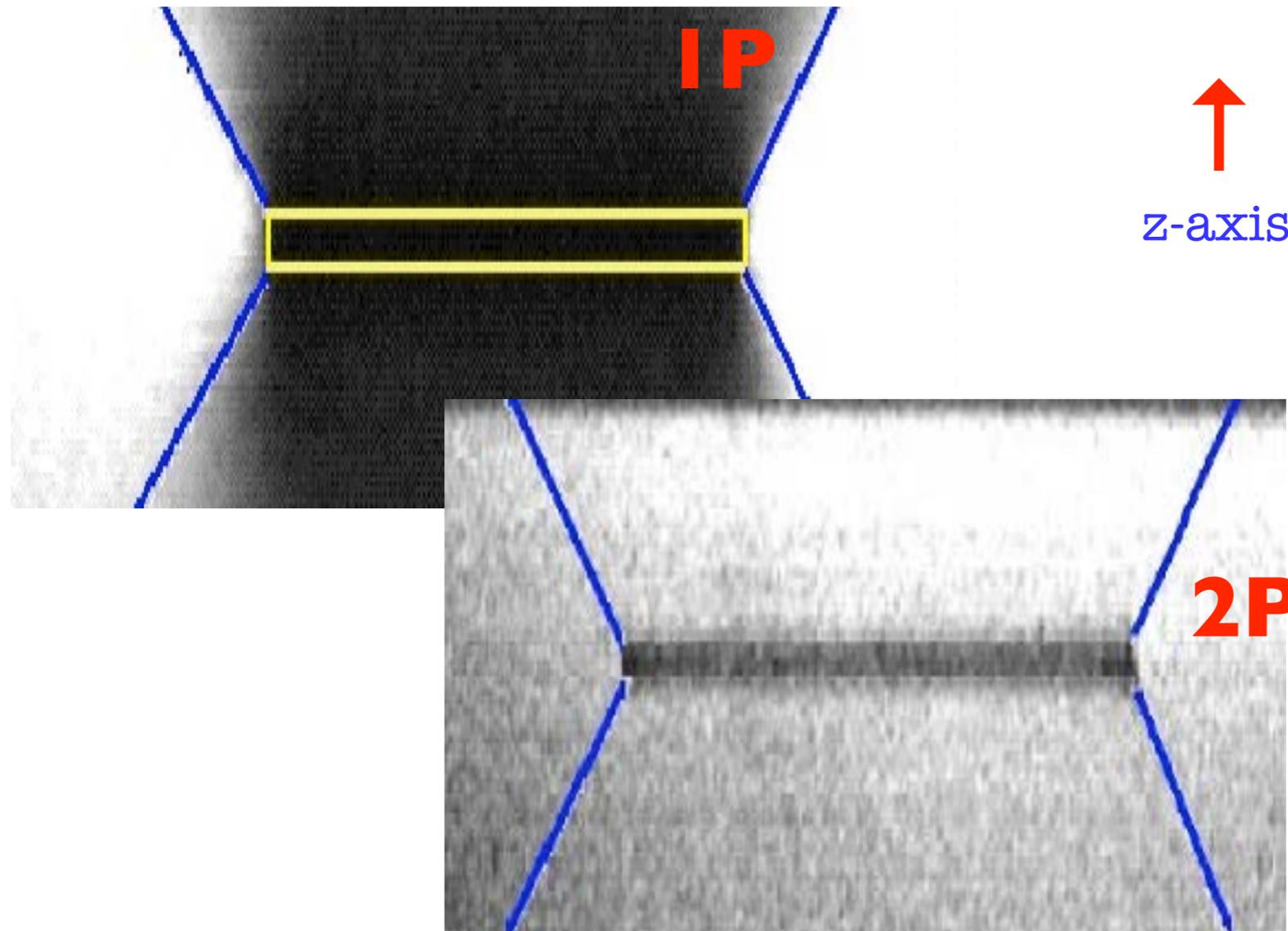


Slide credit: Brad Amos, MRC, Cambridge, UK

two-photon excitation (2pe) microscopy



two-photon excitation (2pe) microscopy



Slide credit: David Piston, Vanderbilt University

two-photon excitation (2pe) microscopy

$$n_a = \frac{\sigma \langle P \rangle^2}{\tau_p f_p^2} \left(\frac{N.A.^2}{2\hbar c \lambda} \right)^2$$

$$I_f \propto n_a \propto \langle P \rangle^2$$

n_a = no. of absorbed photons per molecule

σ = two-photon cross-section 10^{-48} - 10^{-50}
 $\text{cm}^4 \text{s photon}^{-1} \text{molec}^{-1}$

τ_p = pulse width ~ 100 fs

f_p = pulse repetition rate ~ 80 MHz

NA = lens numerical aperture $\sim 1.2 - 1.4$

$\langle P \rangle$ = average incident power ~ 20 mW

Denk, W., Strickler, J.H. & Webb, W.W. *Science* **248**, 73-76 (1990).

two-photon excitation (2pe) microscopy

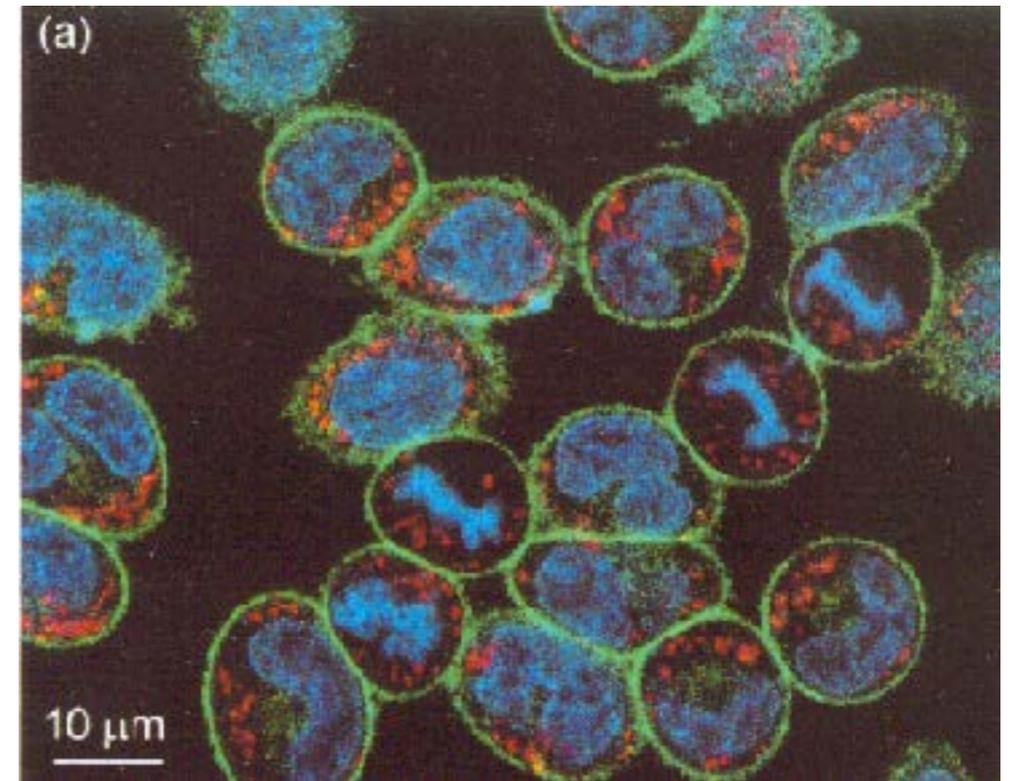
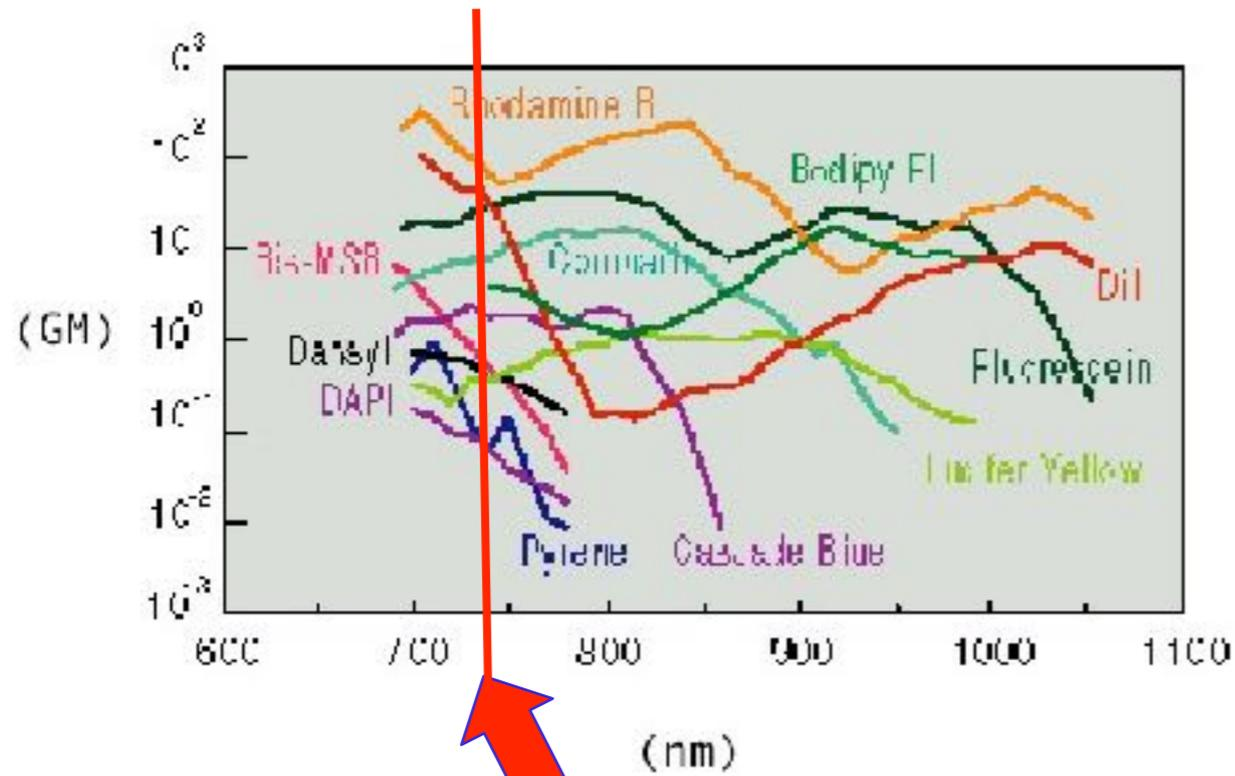
Order of magnitude estimation of MPE cross sections. j, k, l are the intermediate states. τ_j , τ_k , and τ_l represent the corresponding lifetimes of the intermediate states. ¶

$$\delta_{lp} = 10^{-16} \text{ cm}^2$$

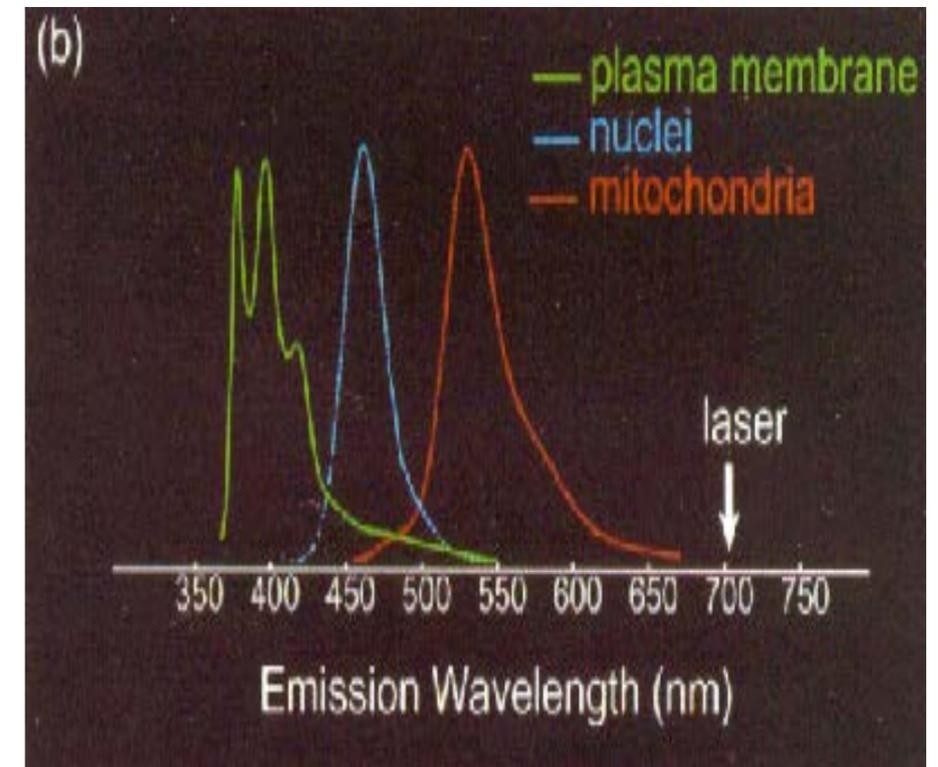
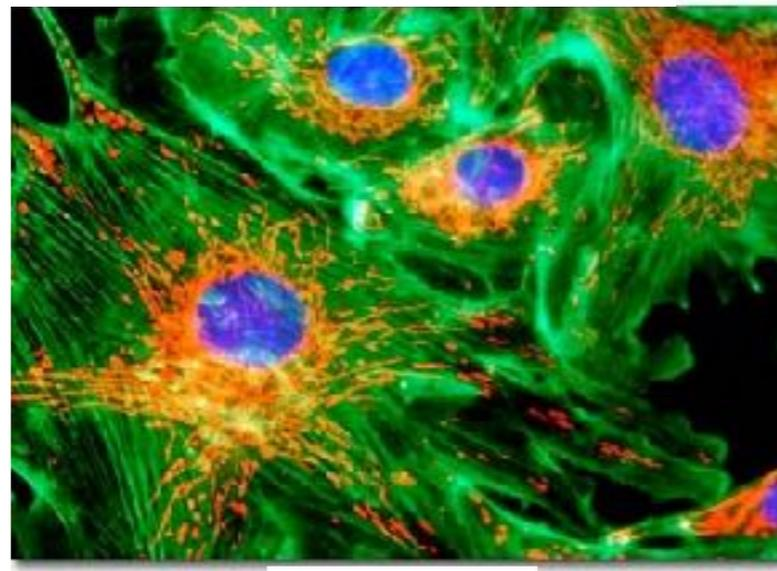
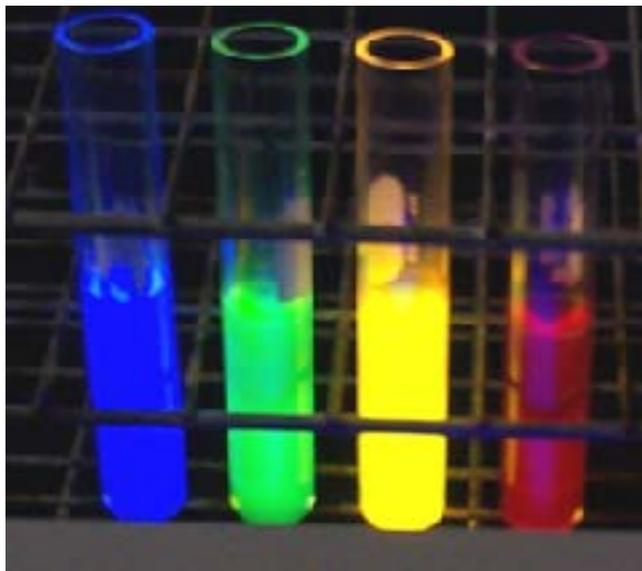
$n\text{PE}$	approximate expression	estimated cross-section ¶
2PE	$\sigma_2 = \sigma_{ij} \sigma_{jf} \tau_j$	$10^{-49} \text{ cm}^2 (\text{photons} / \text{cm}^2 \text{ s})^{-1}$
3PE	$\sigma_3 = \sigma_{ij} \sigma_{jk} \sigma_{kf} \tau_j \tau_k$	$10^{-82} \text{ cm}^2 (\text{photons} / \text{cm}^2 \text{ s})^{-2}$
4PE	$\sigma_3 = \sigma_{ij} \sigma_{jk} \sigma_{kl} \sigma_{if} \tau_j \tau_k \tau_l$	$10^{-115} \text{ cm}^2 (\text{photons} / \text{cm}^2 \text{ s})^{-3}$

Table credit: Chris Xu

two-photon excitation (2pe) microscopy



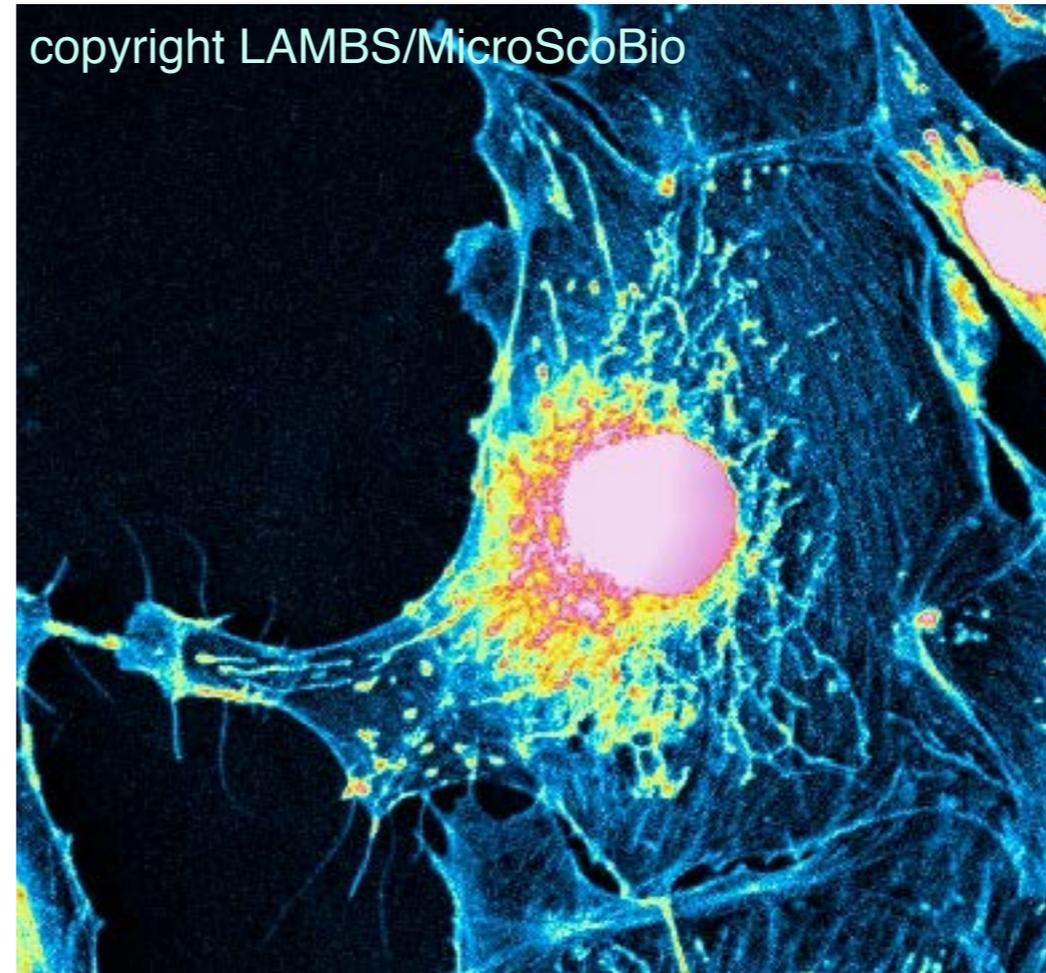
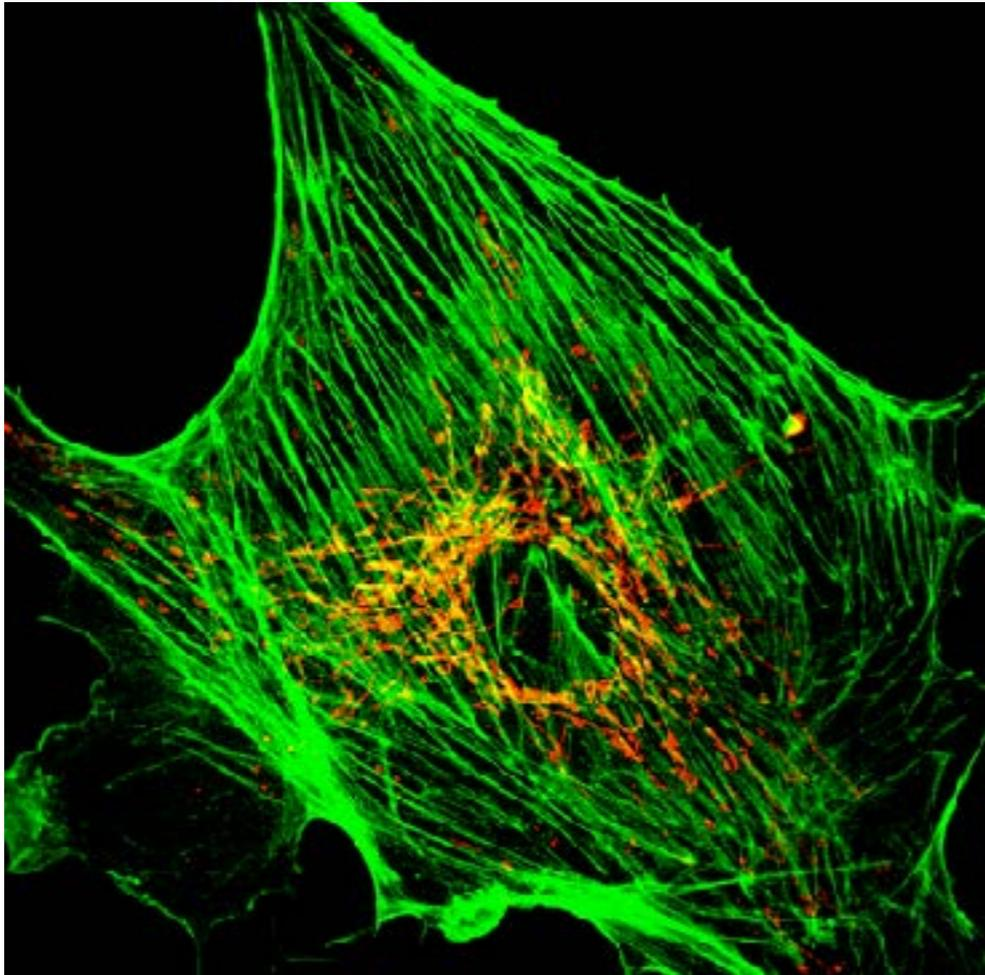
MULTIPLE FLUORESCENCE BY ONE WAVELENGTH EXCITATION



Xu C. et al., Bioimaging, 4, 198-207, 1996

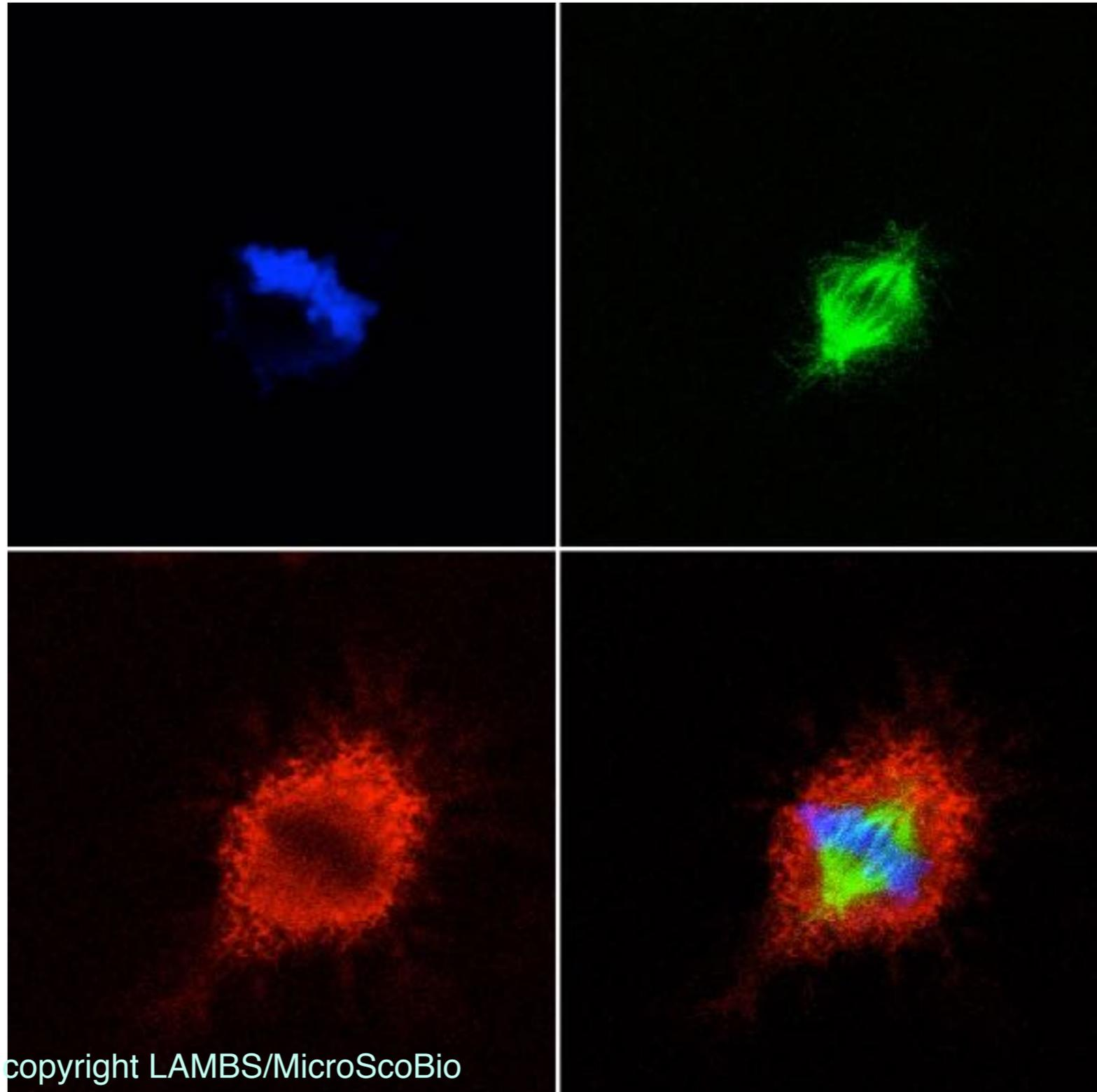
two-photon excitation (2pe) microscopy

Confocal (left) and TPE (right) multiple fluorescence.



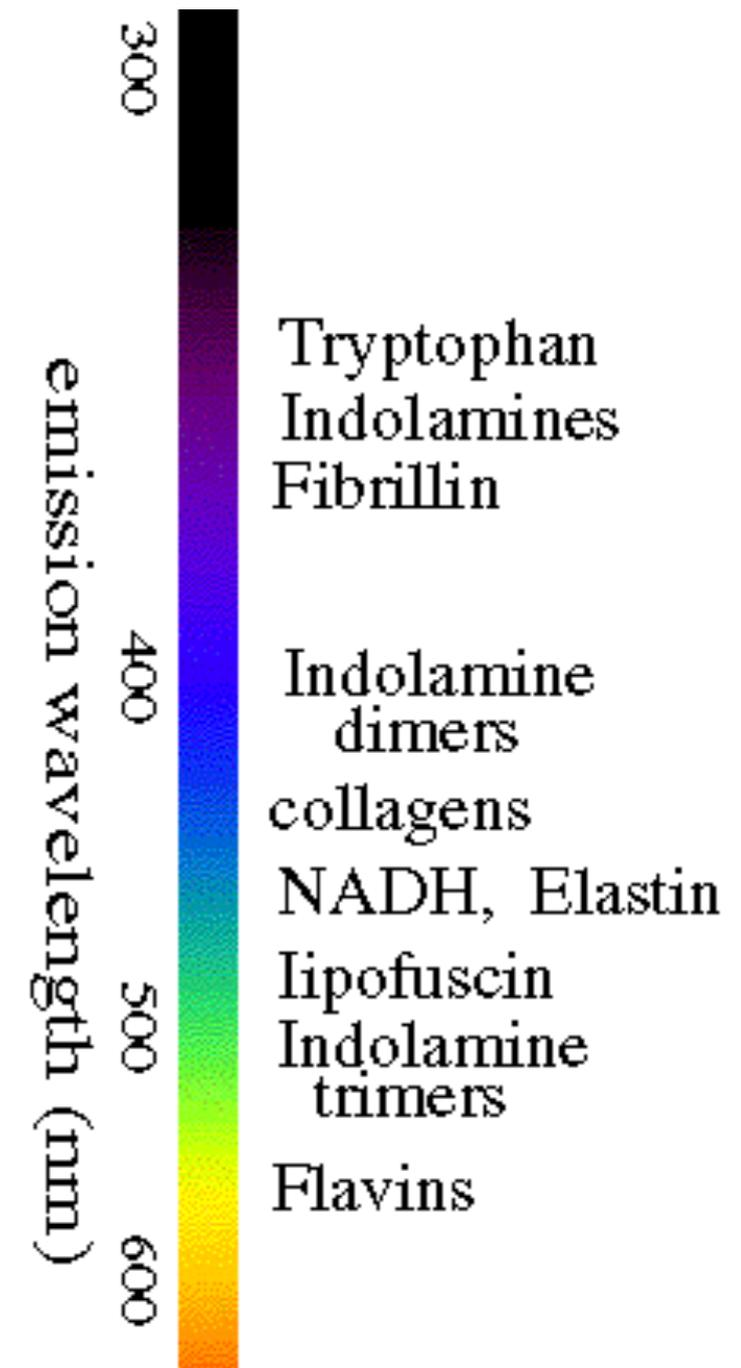
Cells are labelled with DAPI (DNA), mitotracker red (mitochondria) and bodipy (actin); F-14780 Molecular Probes slide.

two-photon excitation (2pe) microscopy



two-photon excitation (2pe) microscopy

INTRINSIC EMITTERS	λ (nm)	δ_2
GFP wt	800-850	~ 6
GFP S65T	~ 960	~ 7
BFP	780/820	-
CFP	780/840	-
YFP	860/900	-
EGFP	940-1000	~ 250
<u>DsRed-Coral Red</u>	960-990	~ 20-110
<u>Citrine-Coral yellow</u>	950	~ 70
<u>Phycoerythrin</u>	1064	~ 300
<u>Flavins</u>	~ 700-730	~ 0.1-0.8
NADH	~ 690-730	~ 0.02-0.09
Retinol	700-830	~0.07
Pyridoxine	690-710	~0.008
Folic acid	700-770	~0.007
<u>Lipofuscin</u>	700-850	-
<u>Collagen, Elastin</u>	700-740	-
<u>Qdots</u>	700-1000	~ 2000-47000

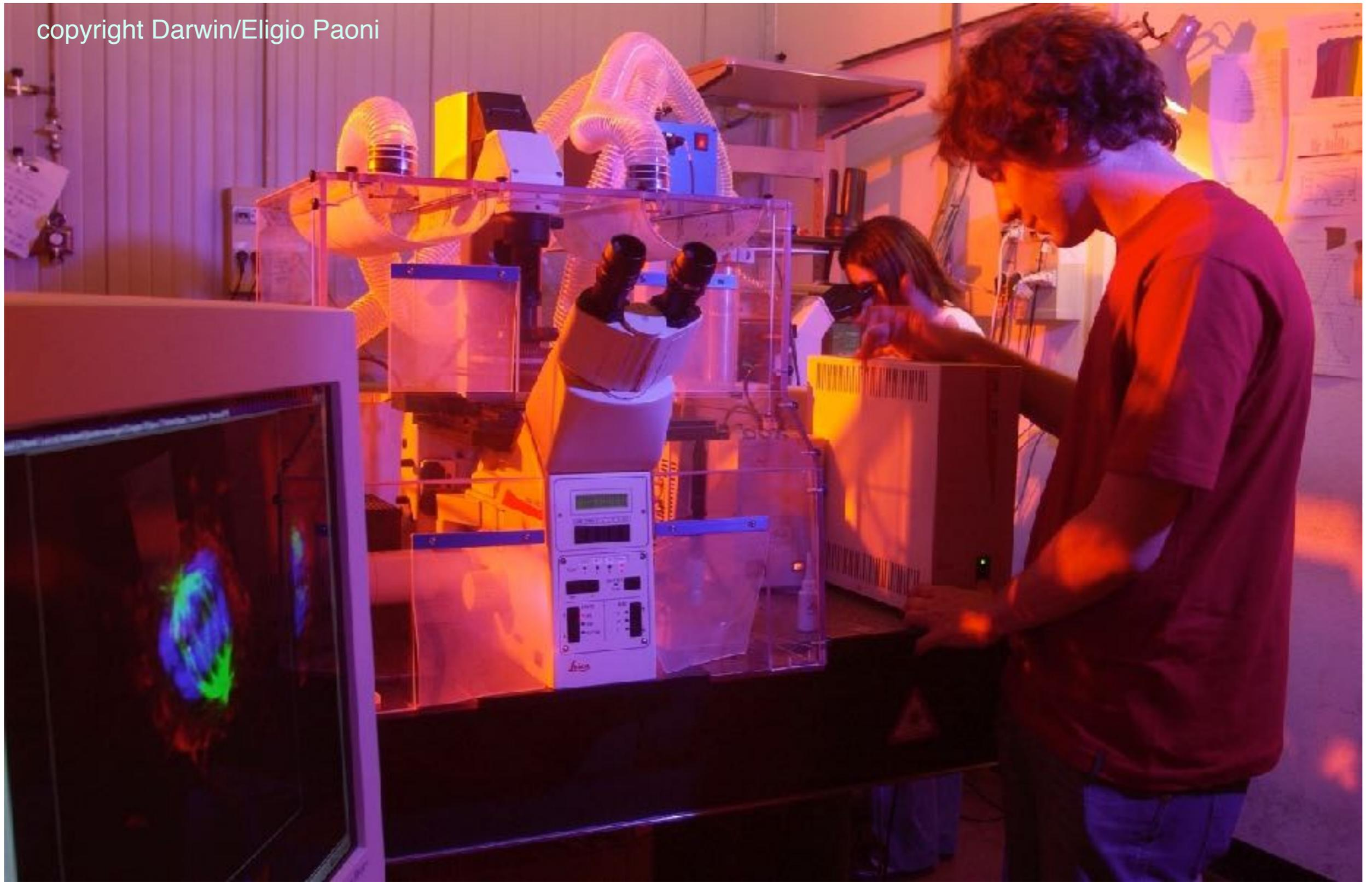


<http://www.biomedical-engineering-online.com/home/>

A. Diaspro et al. , Multi-photon excitation microscopy. BioMedical Engineering OnLine 2006, 5:36 (6Jun2006)

3D sequence collected at LAMBS, sample
courtesy of Paola Ramoino, DIPTERIS

copyright Darwin/Eligio Paoni



spectral separation

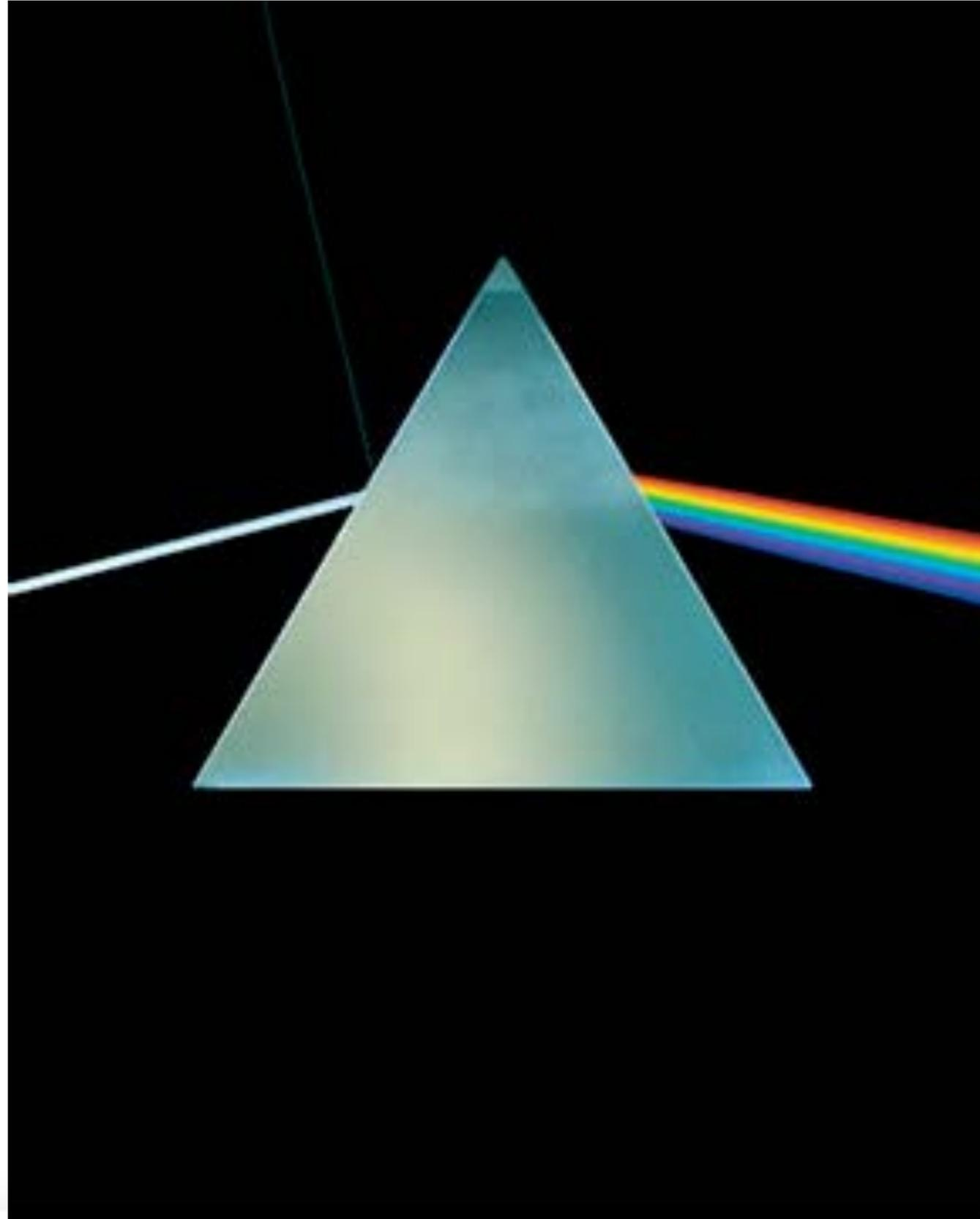
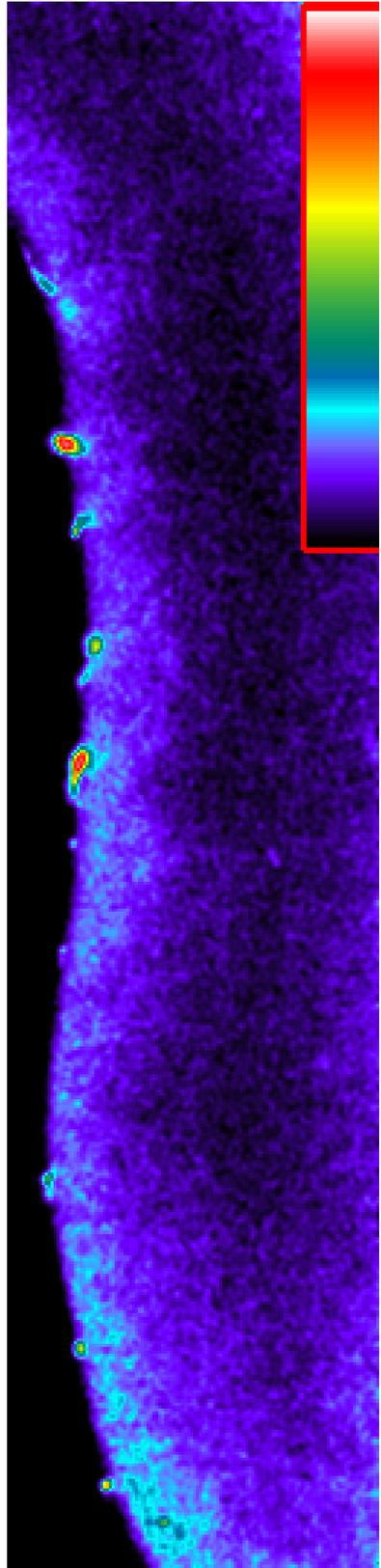
“There were 5 characters...6 considering ...ice” (D.Pennac, La Fata Carabina)



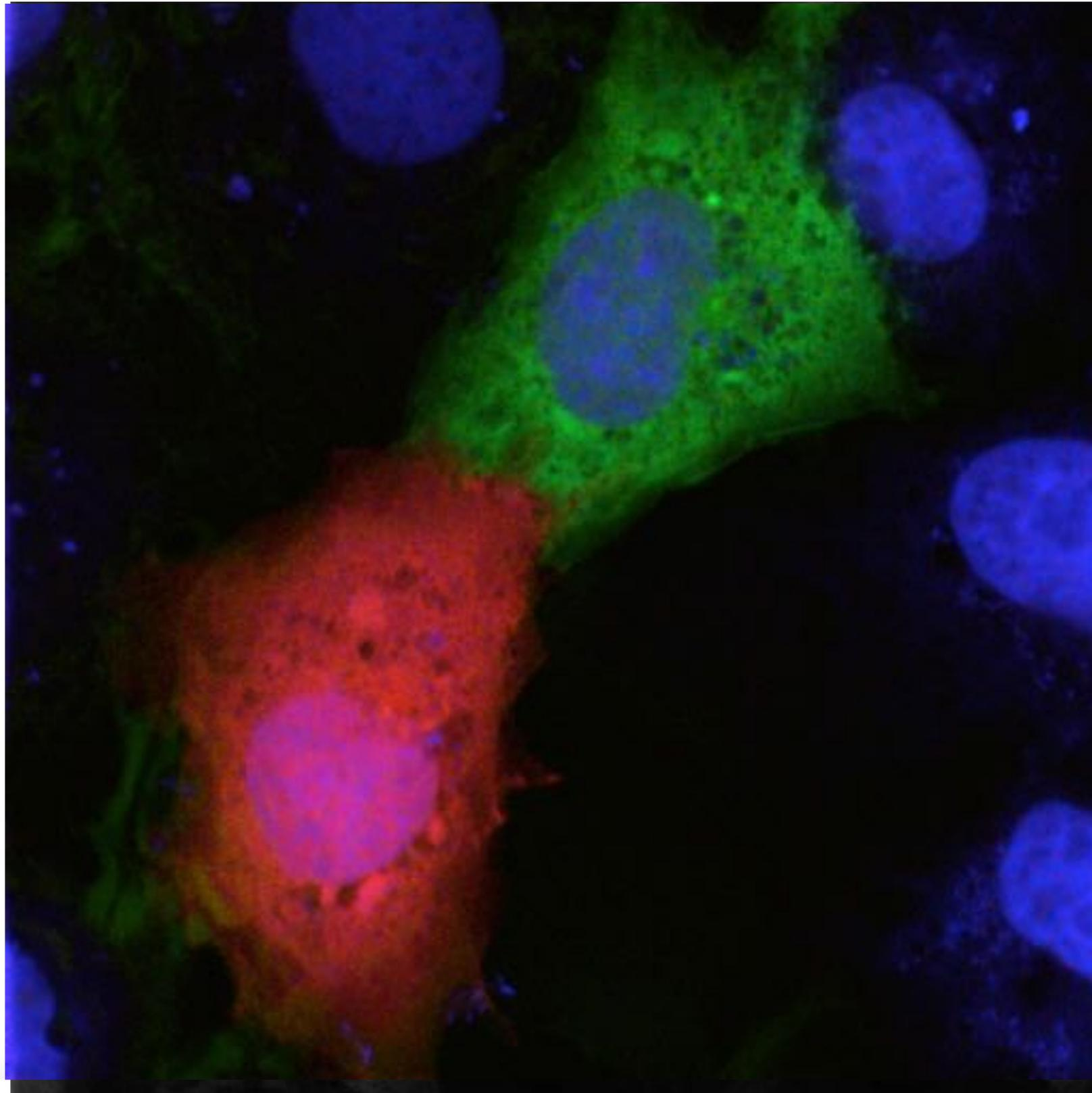
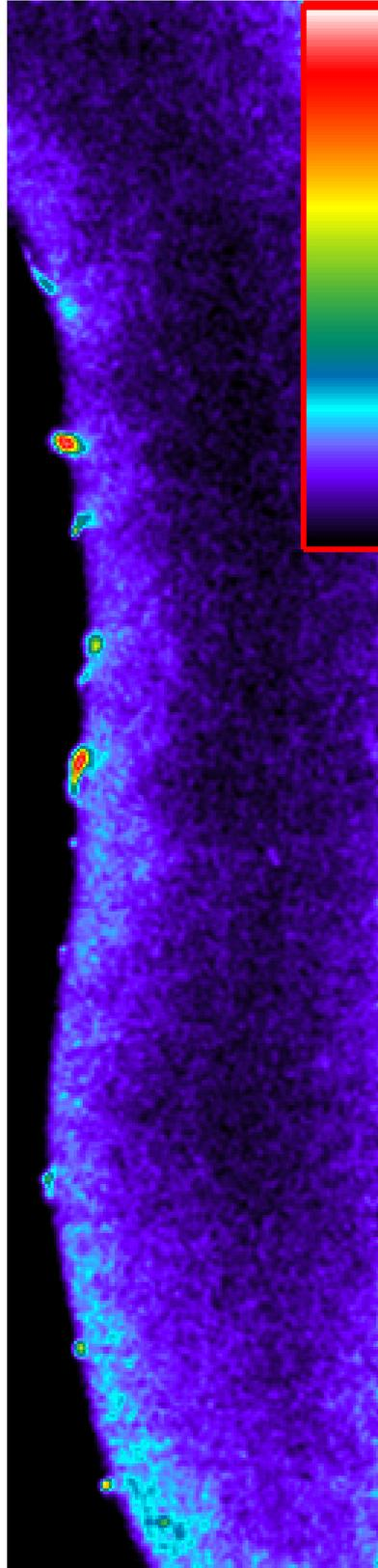
Burano, da [“laRepubblica.it”](http://laRepubblica.it)

Alberto Diaspro, Nanoscopy, Istituto Italiano di Tecnologia

spectral separation

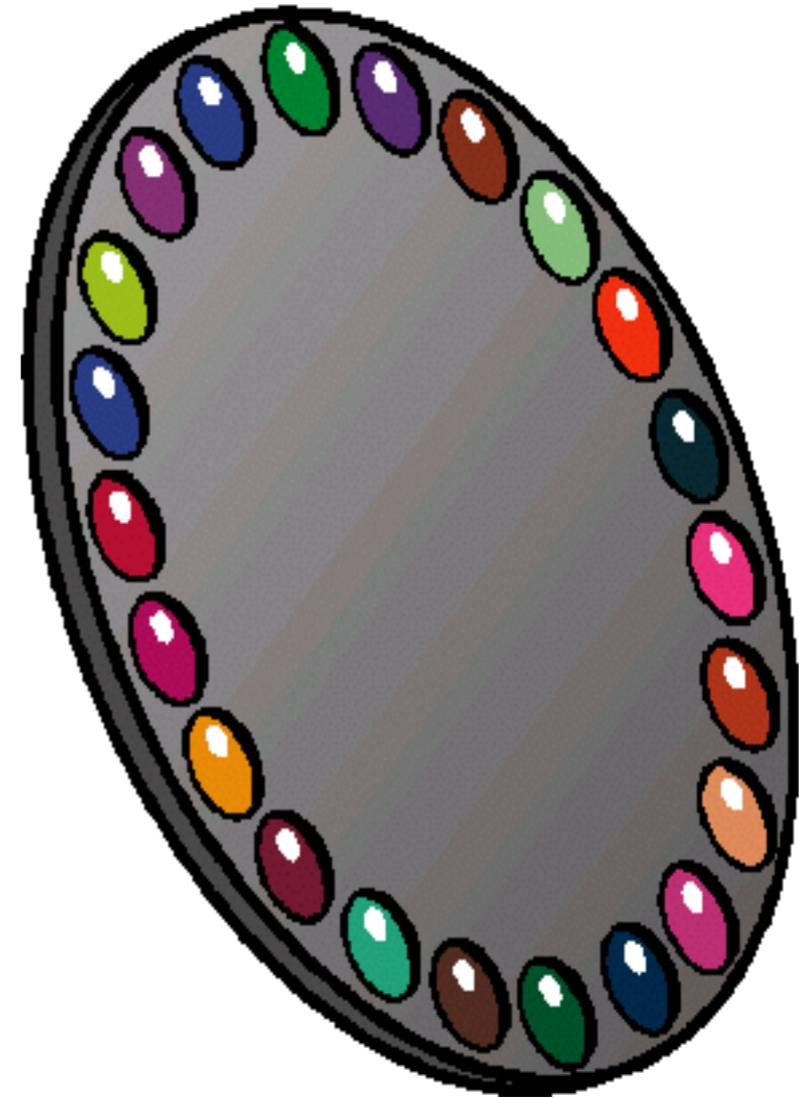
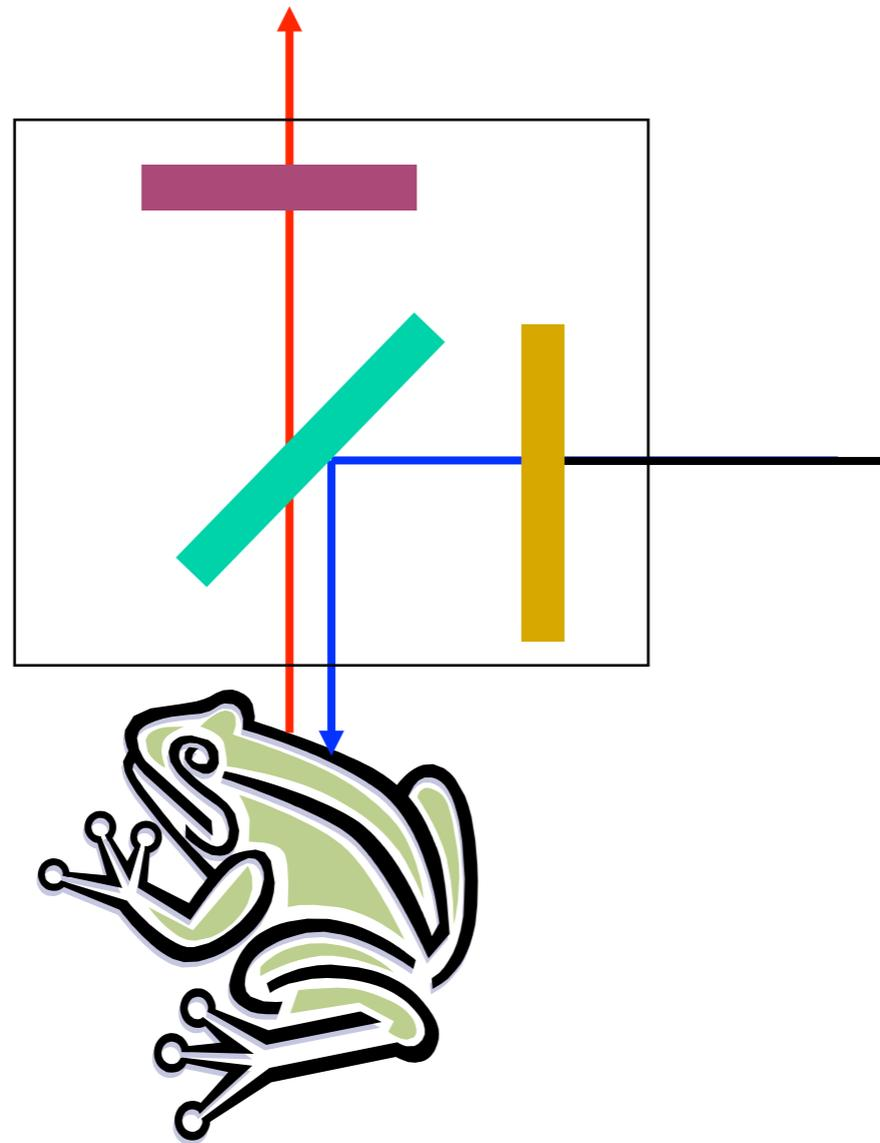
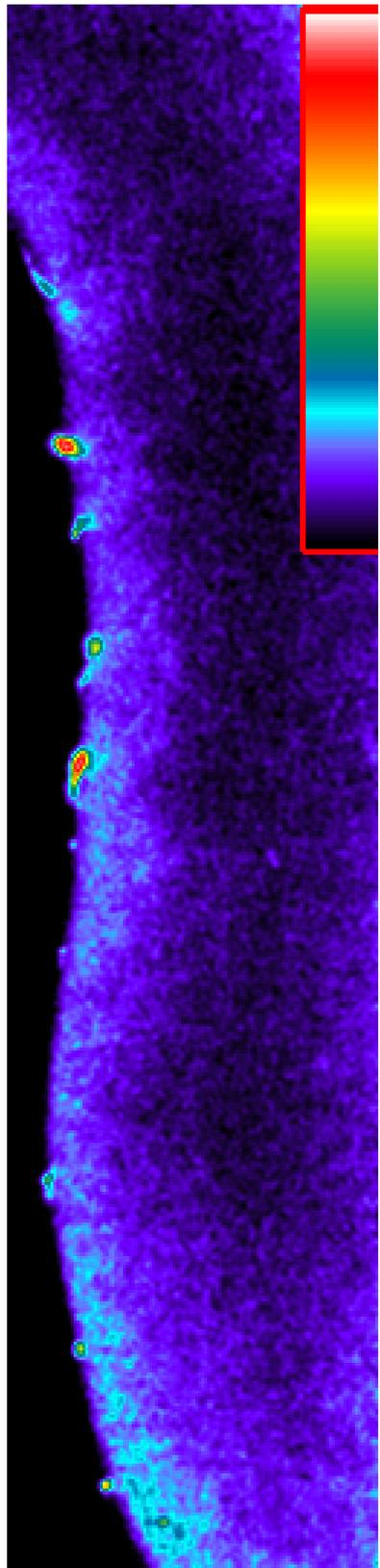


spectral separation



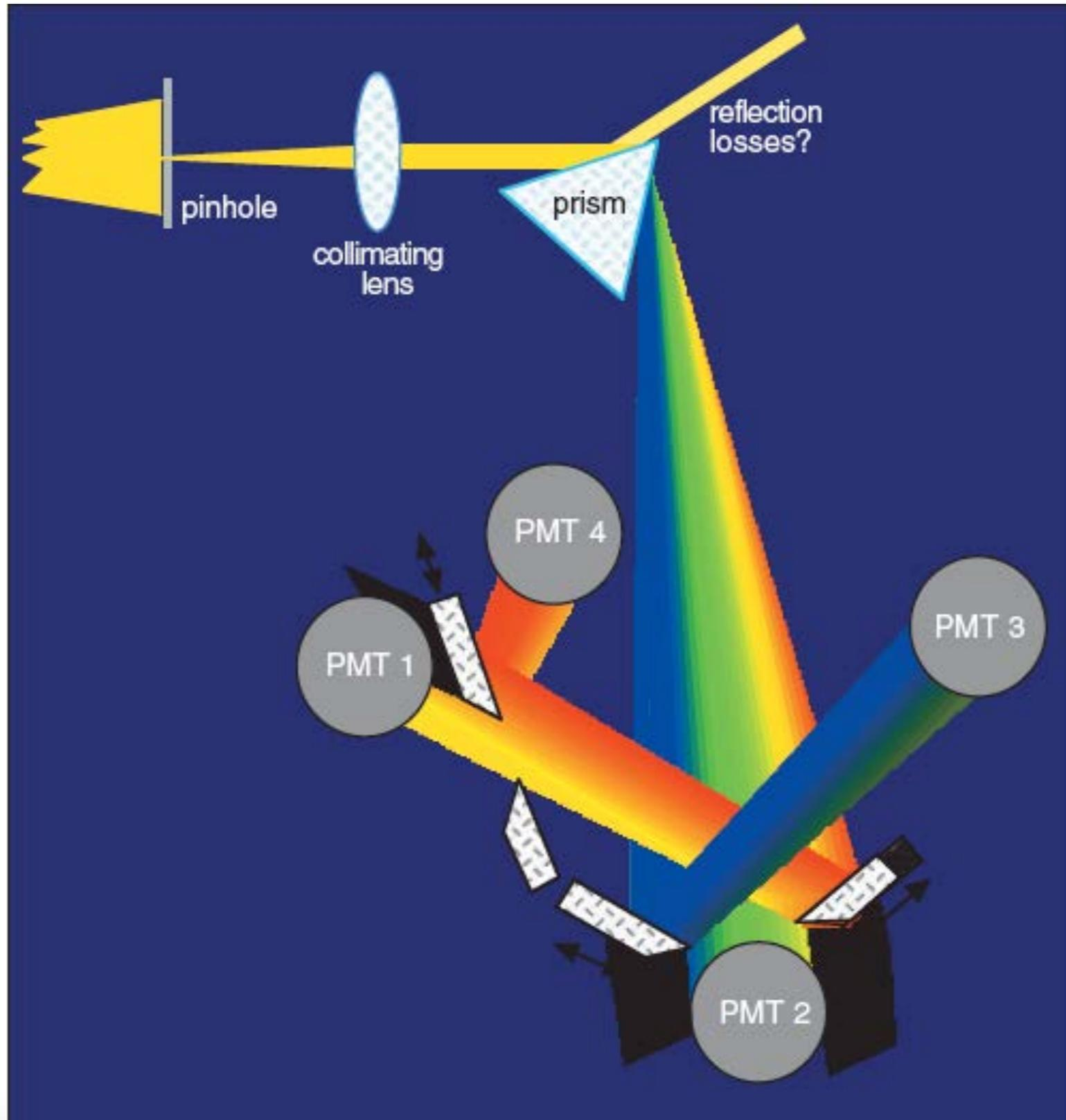
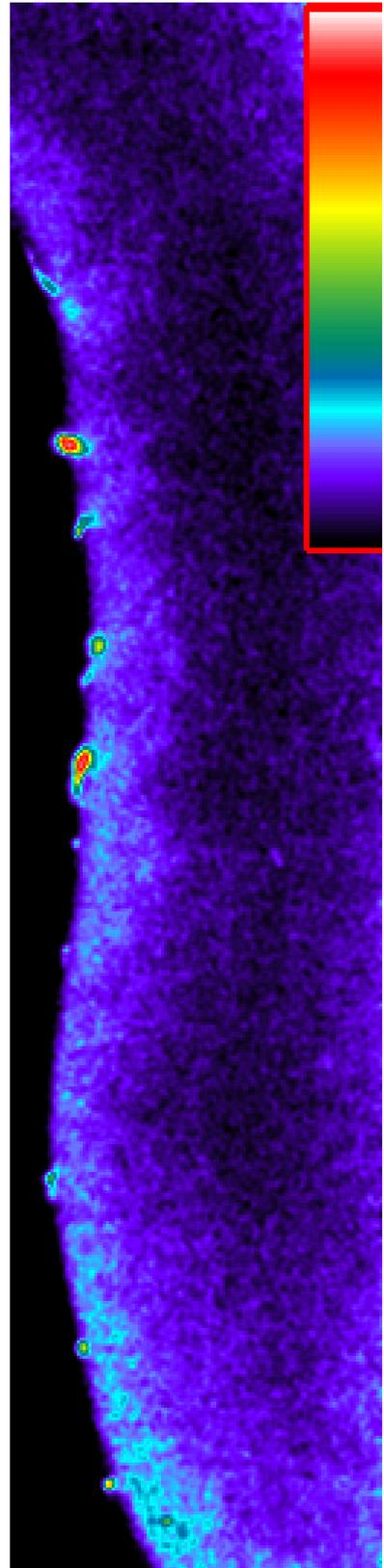
Alberto Diaspro, Nanoscopy, Istituto Italiano di Tecnologia

spectral separation



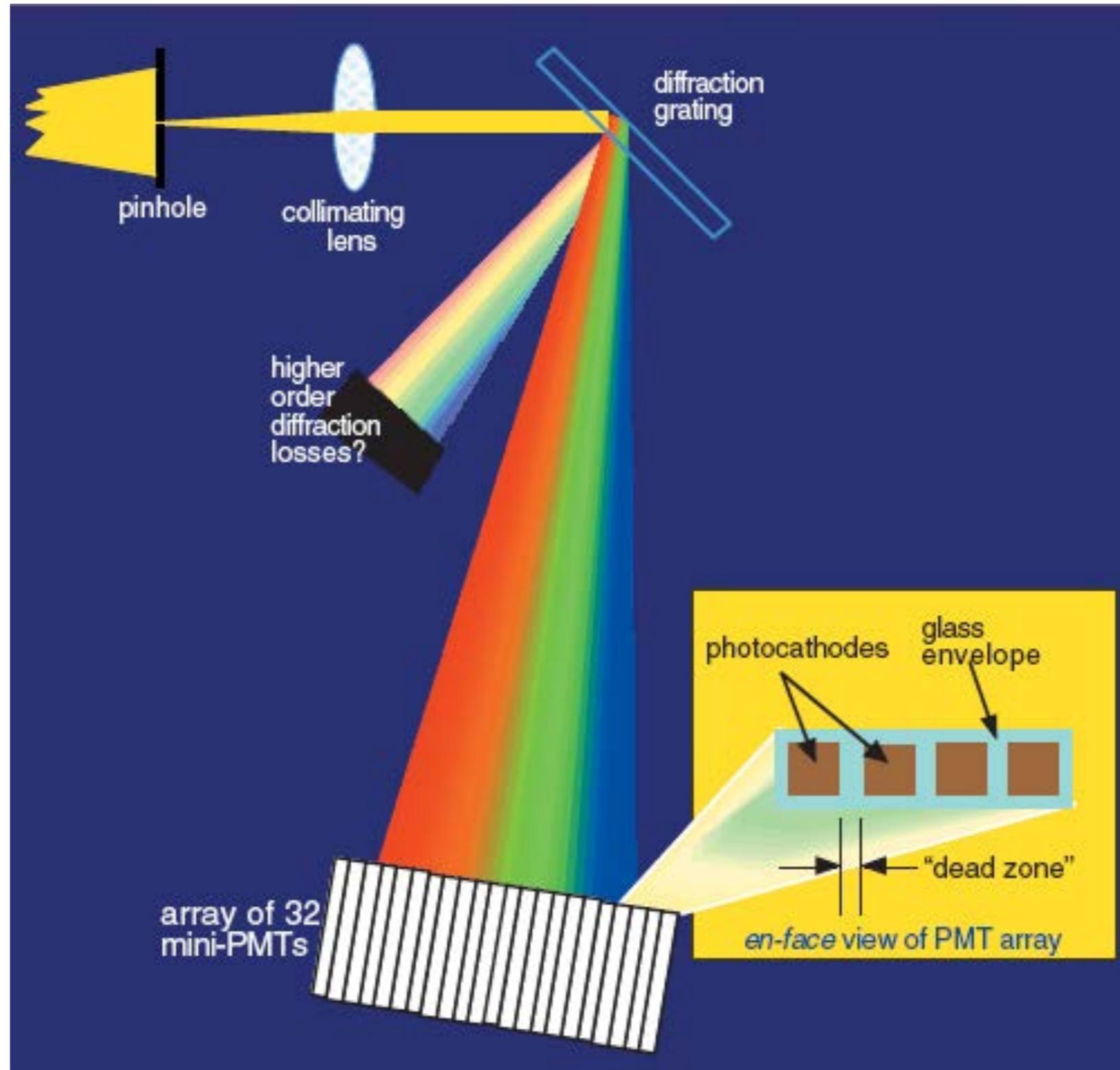
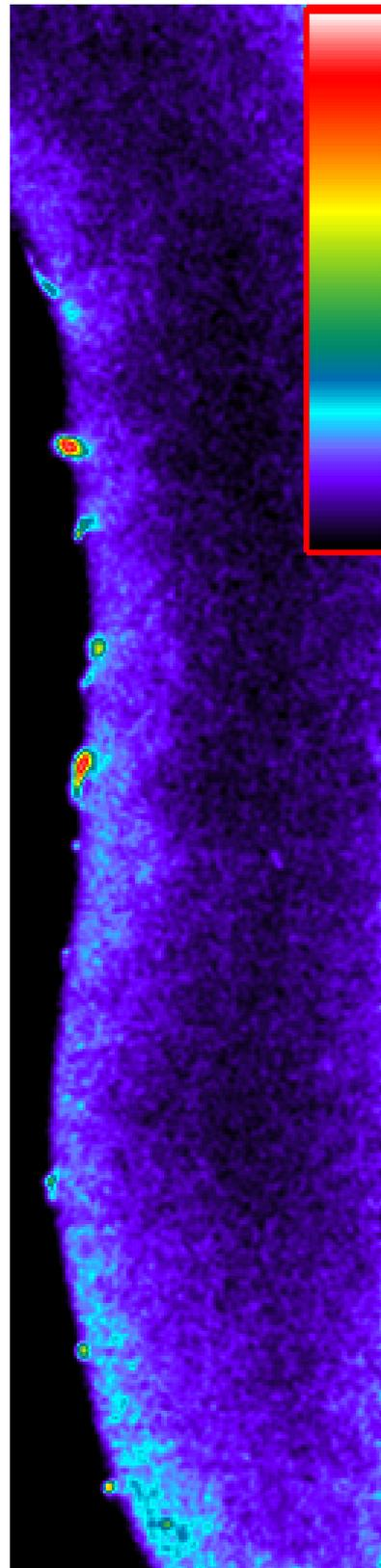
Slide credit: Rolf Borlinghaus, Leica Microsystems

spectral separation



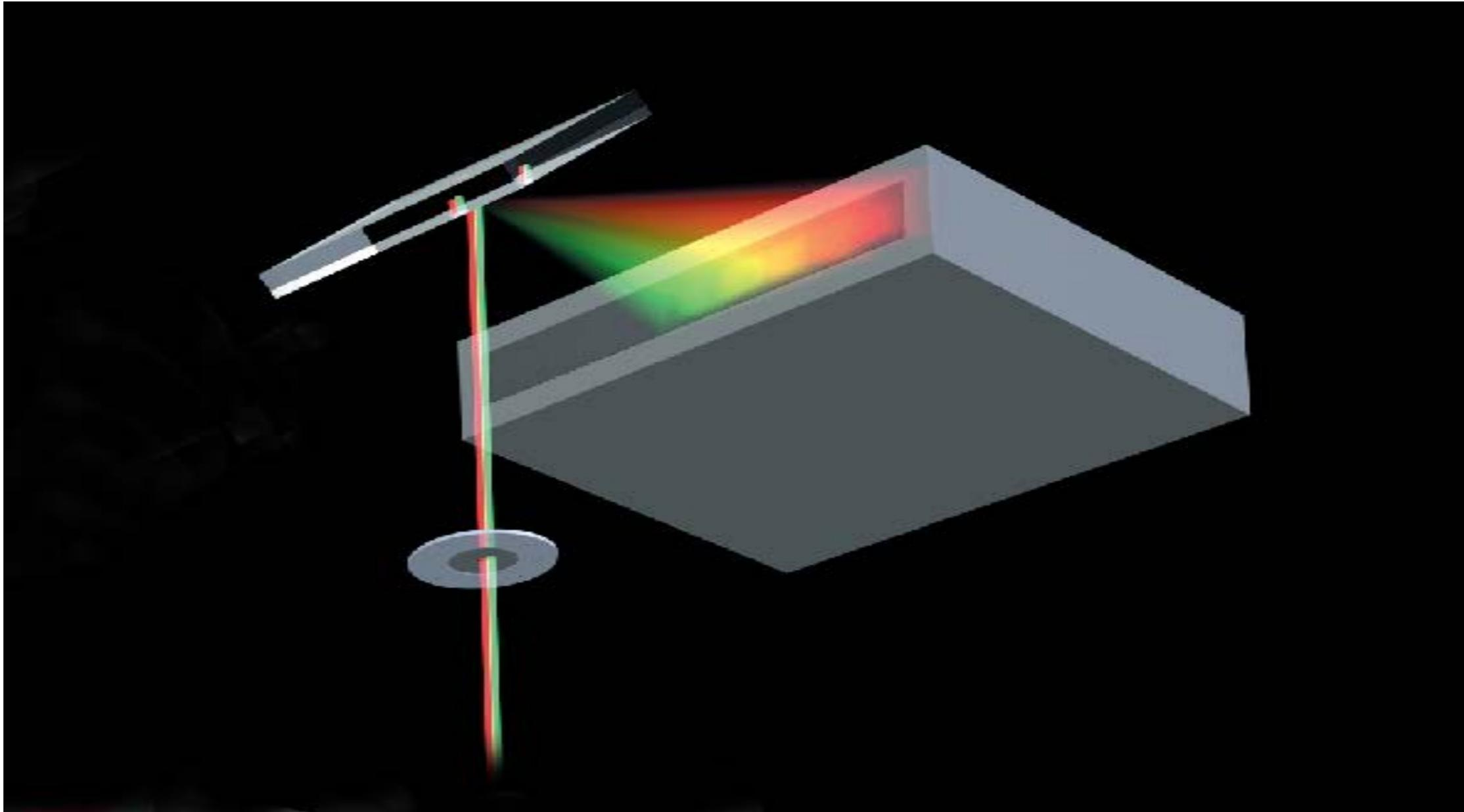
Alberto Diaspro, Nanoscopy, Istituto Italiano di Tecnologia

spectral separation



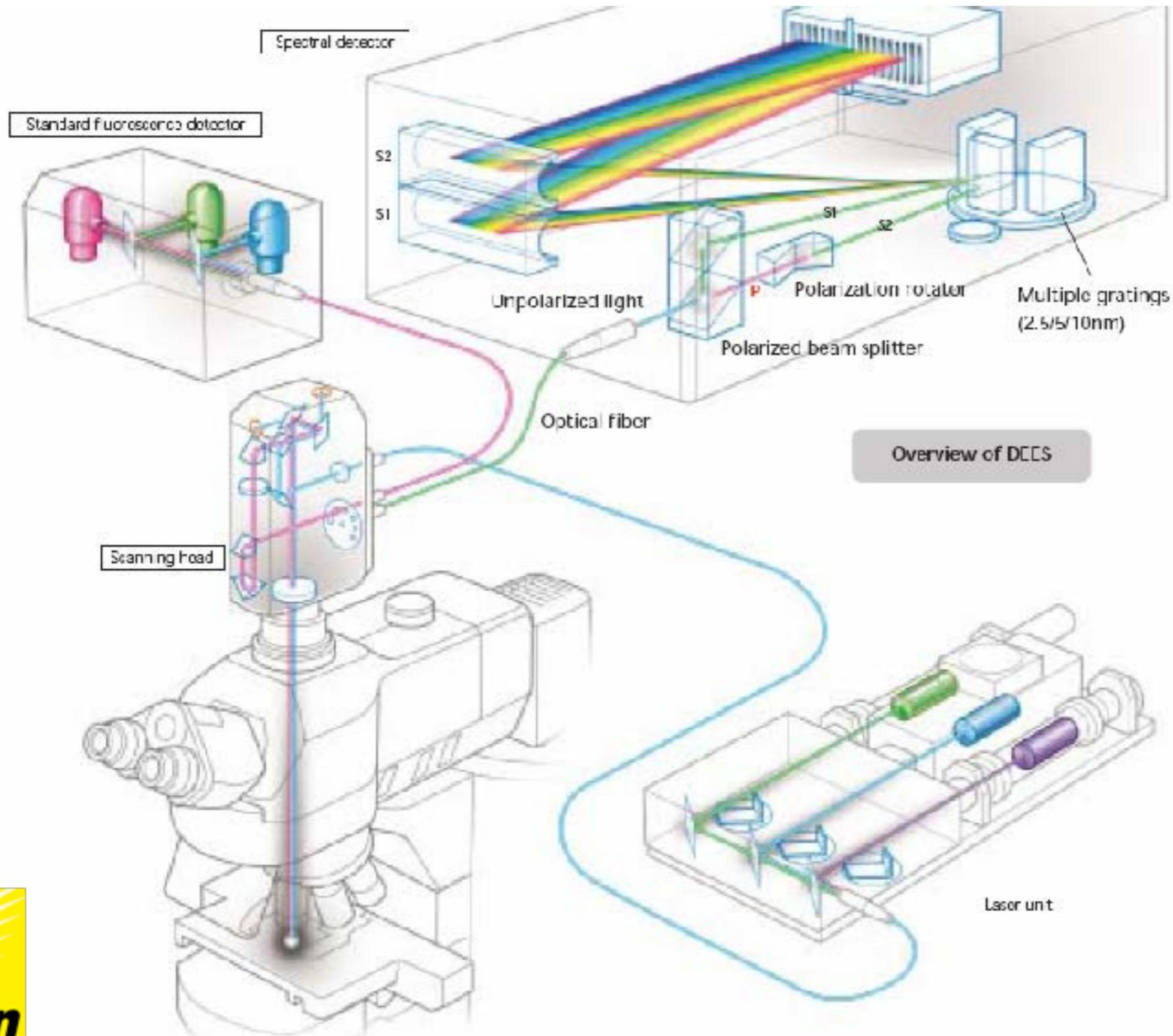
spectral separation

LSM 510 META



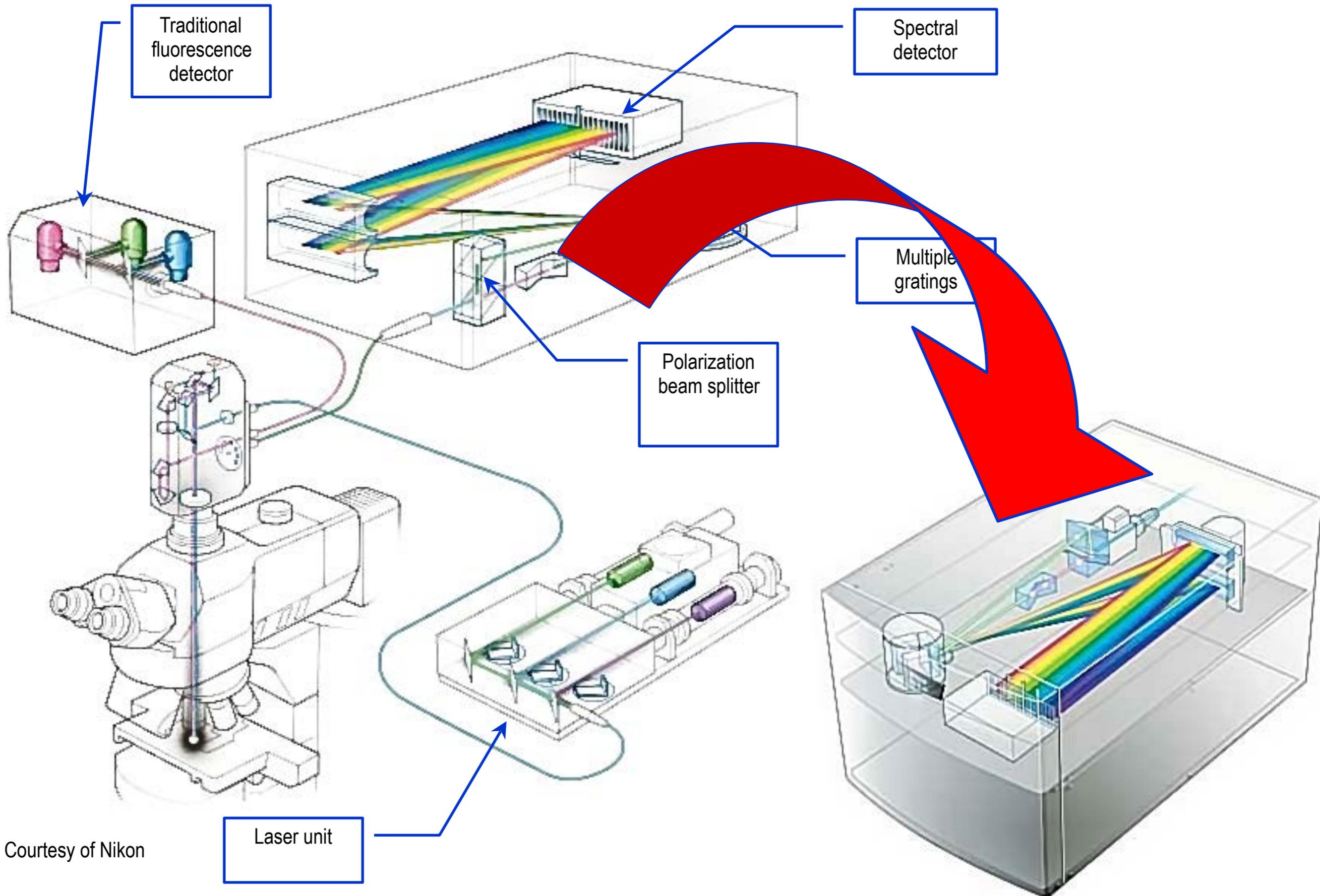
Alberto Diaspro, Nanoscopy, Istituto Italiano di Tecnologia

spectral separation

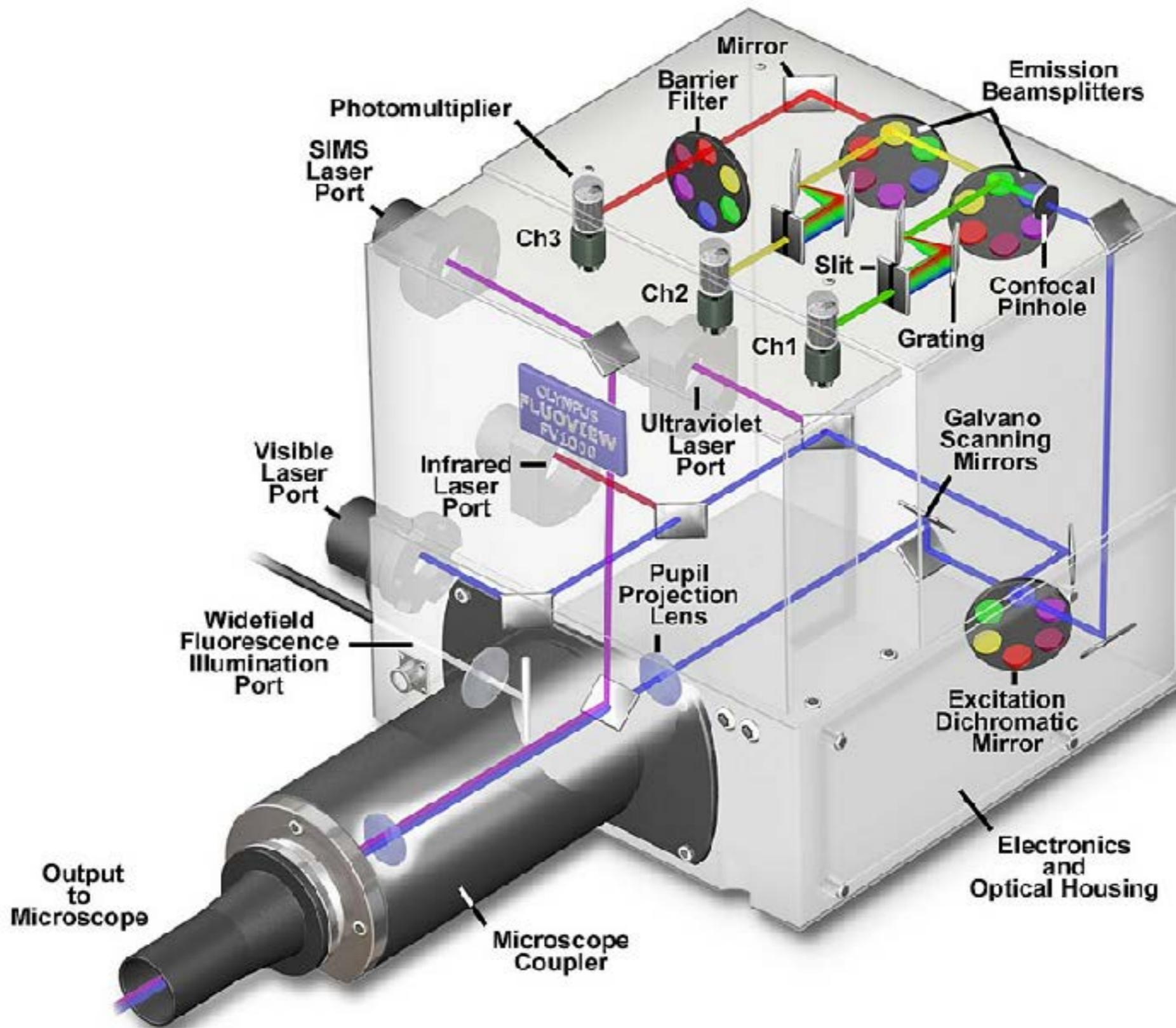


(credit:Nikon)

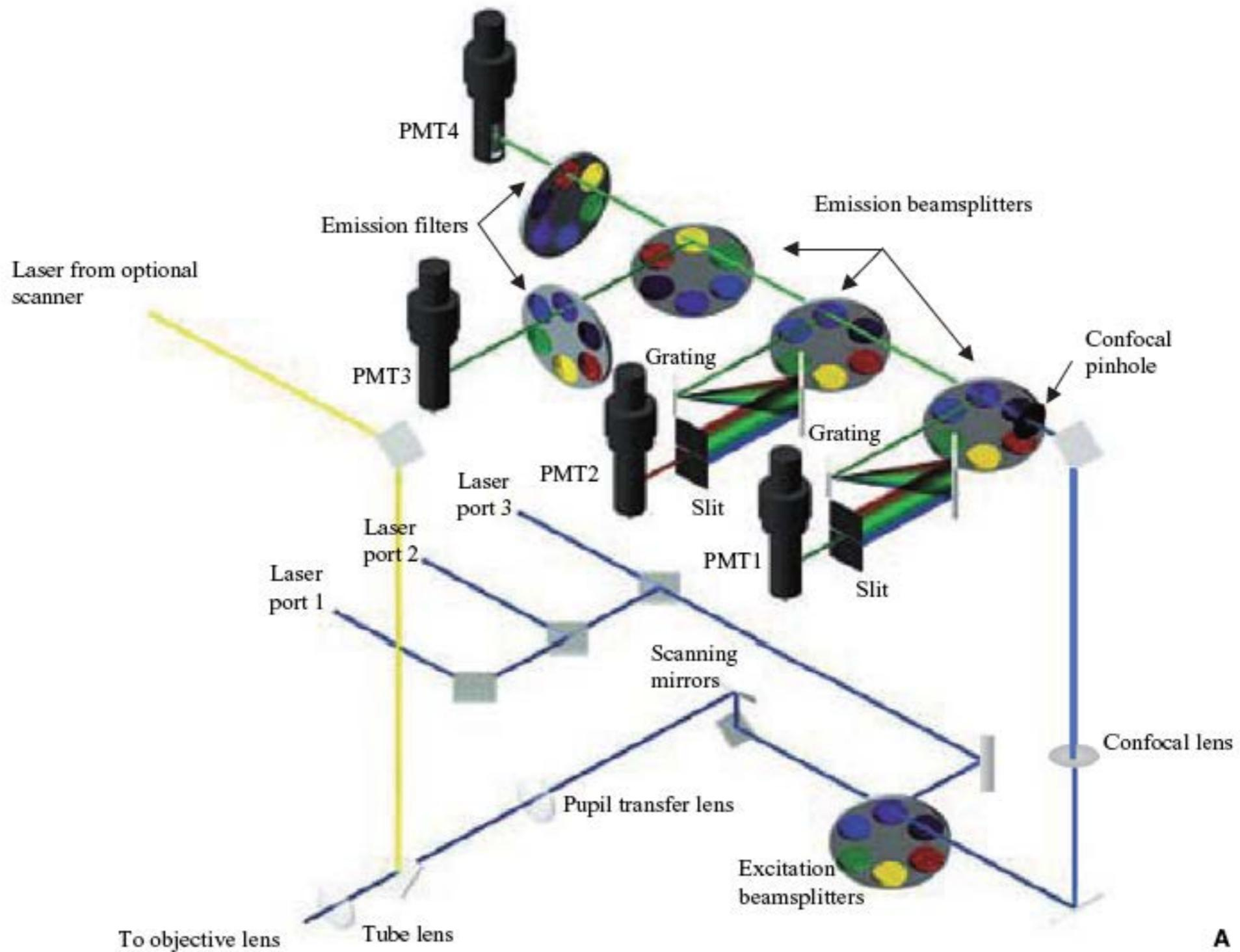
Spectral confocal systems



Olympus spectral confocal system



spectral separation



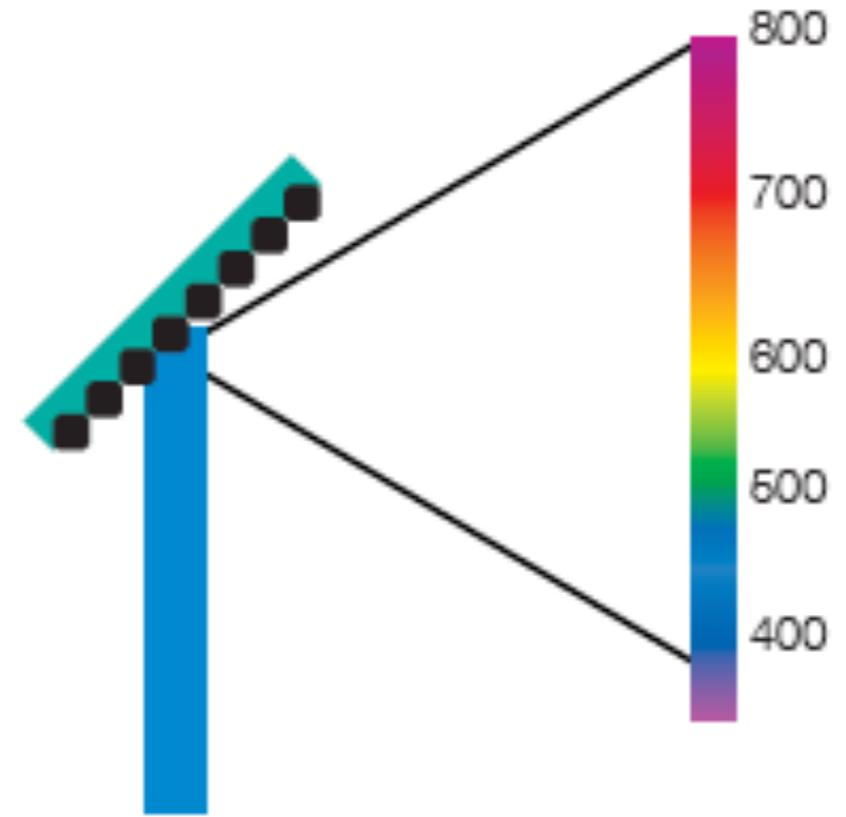
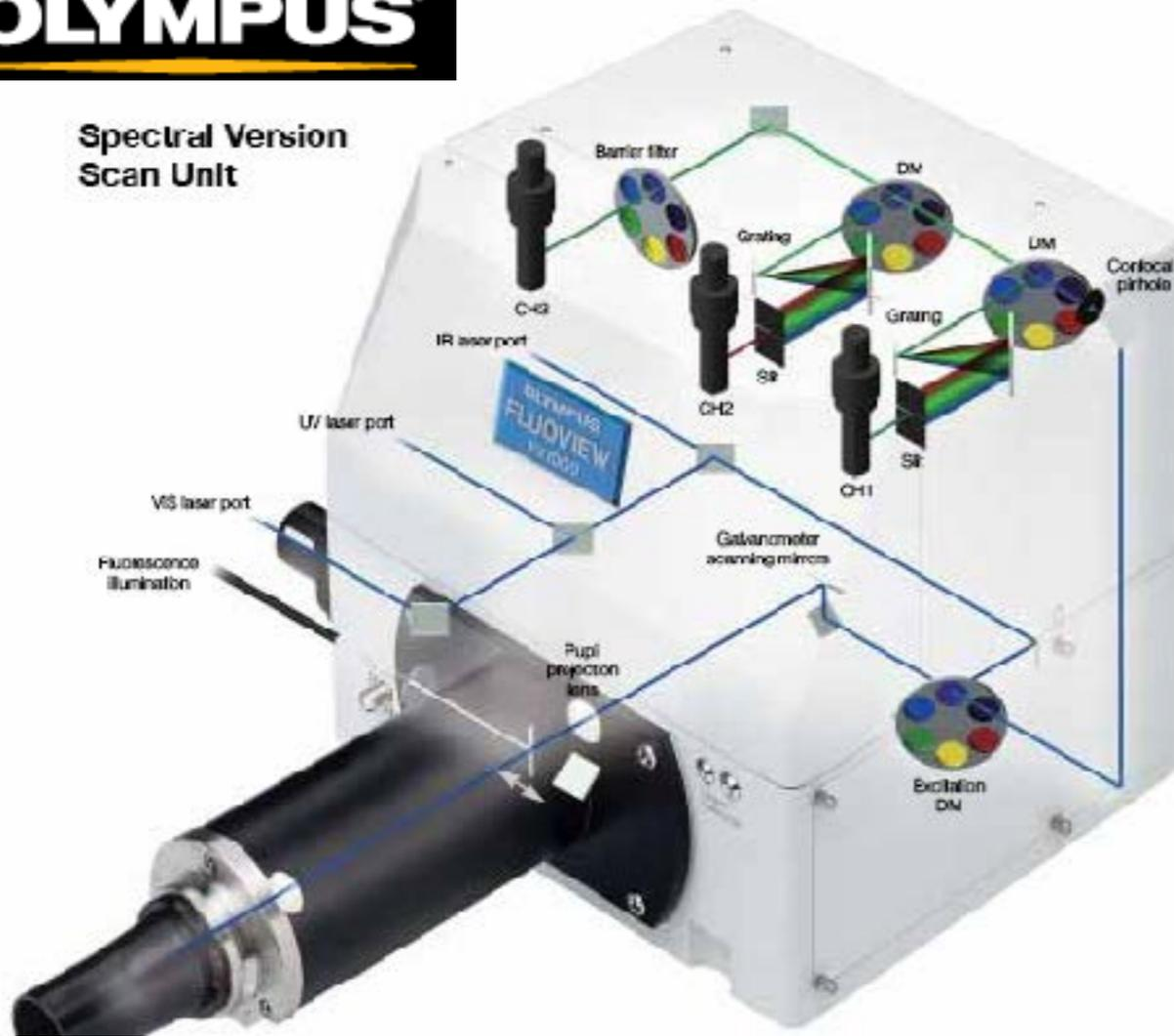
Slide credit: Handbook of Confocal Microscopy (J.Pawley ed.), Plenum, NEW edition, 2006

Alberto Diaspro, Nanoscopy, Istituto Italiano di Tecnologia

spectral separation

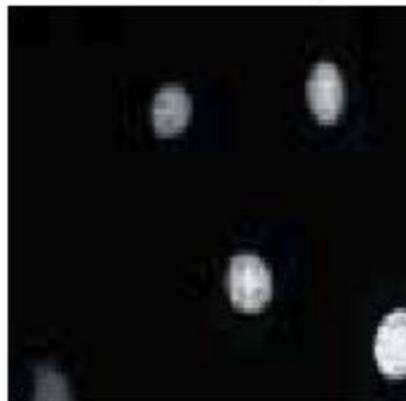


Spectral Version Scan Unit



Grating

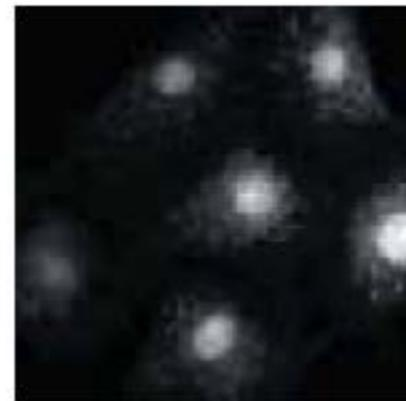
XYλ series, wavelength range 495-695nm



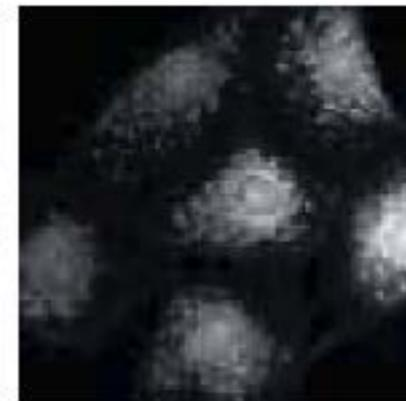
495nm - 515nm



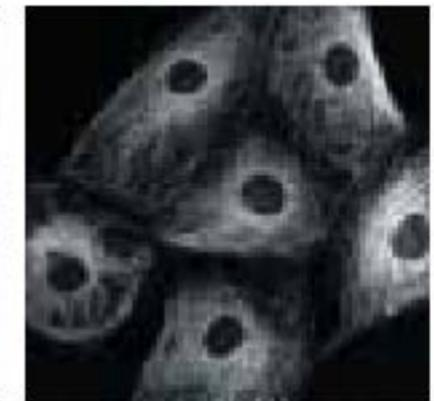
505nm - 525nm



535nm - 555nm

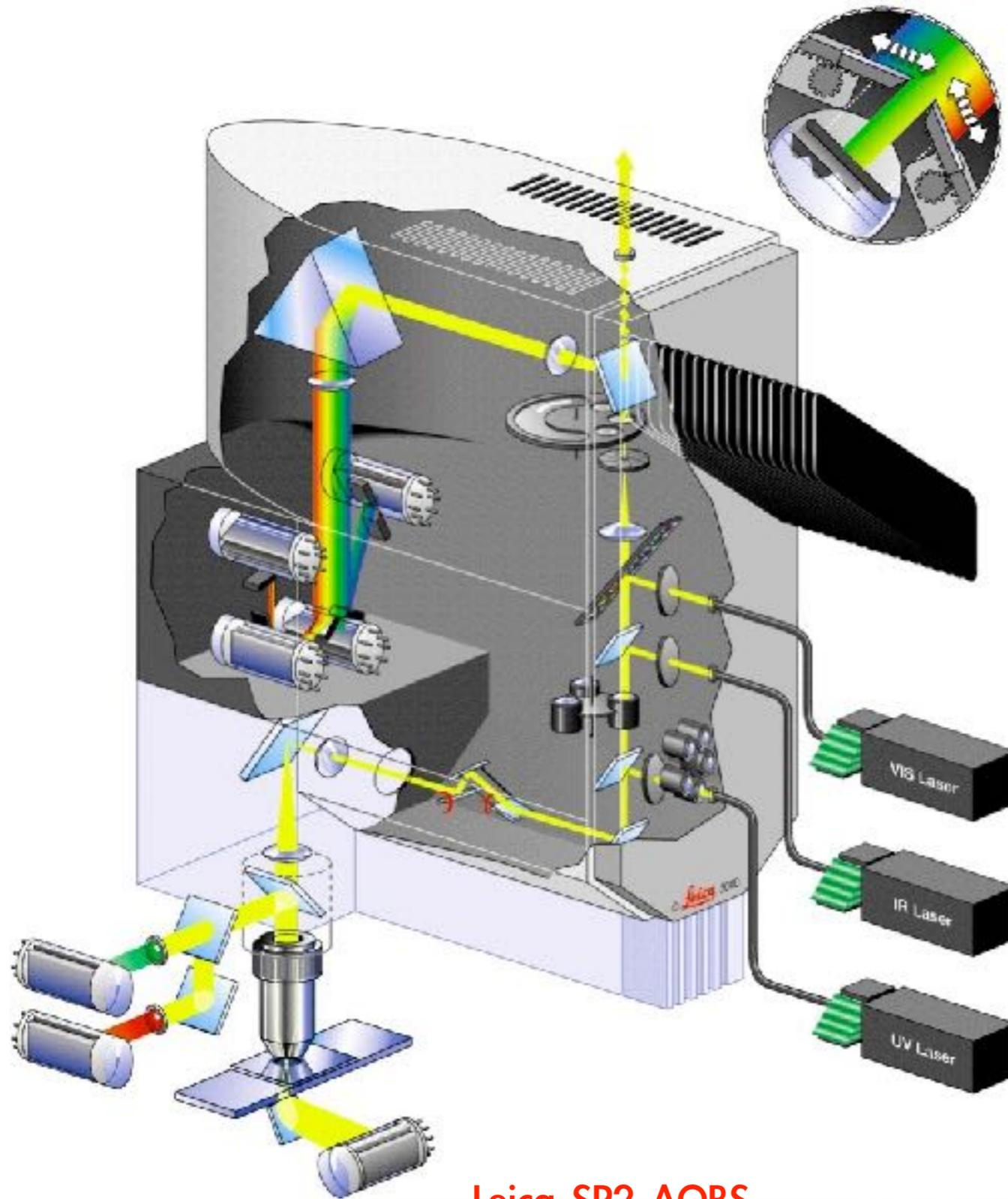


565nm - 585nm

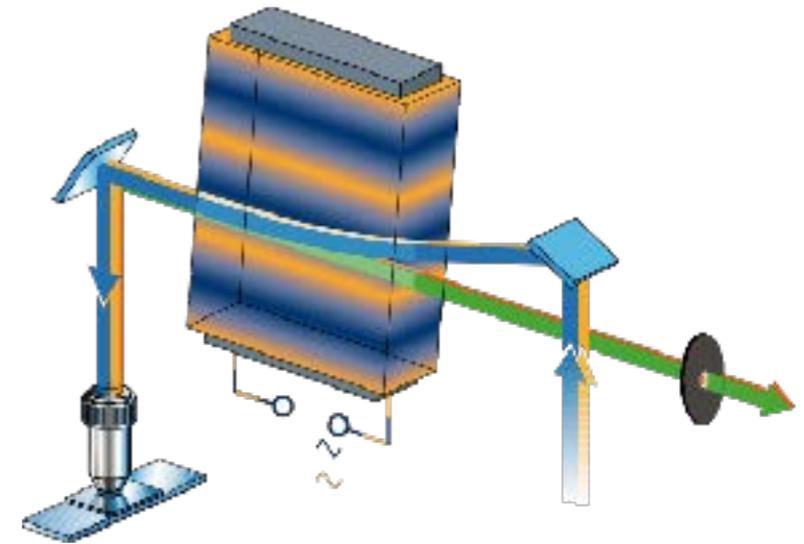


595nm - 615nm

spectral separation

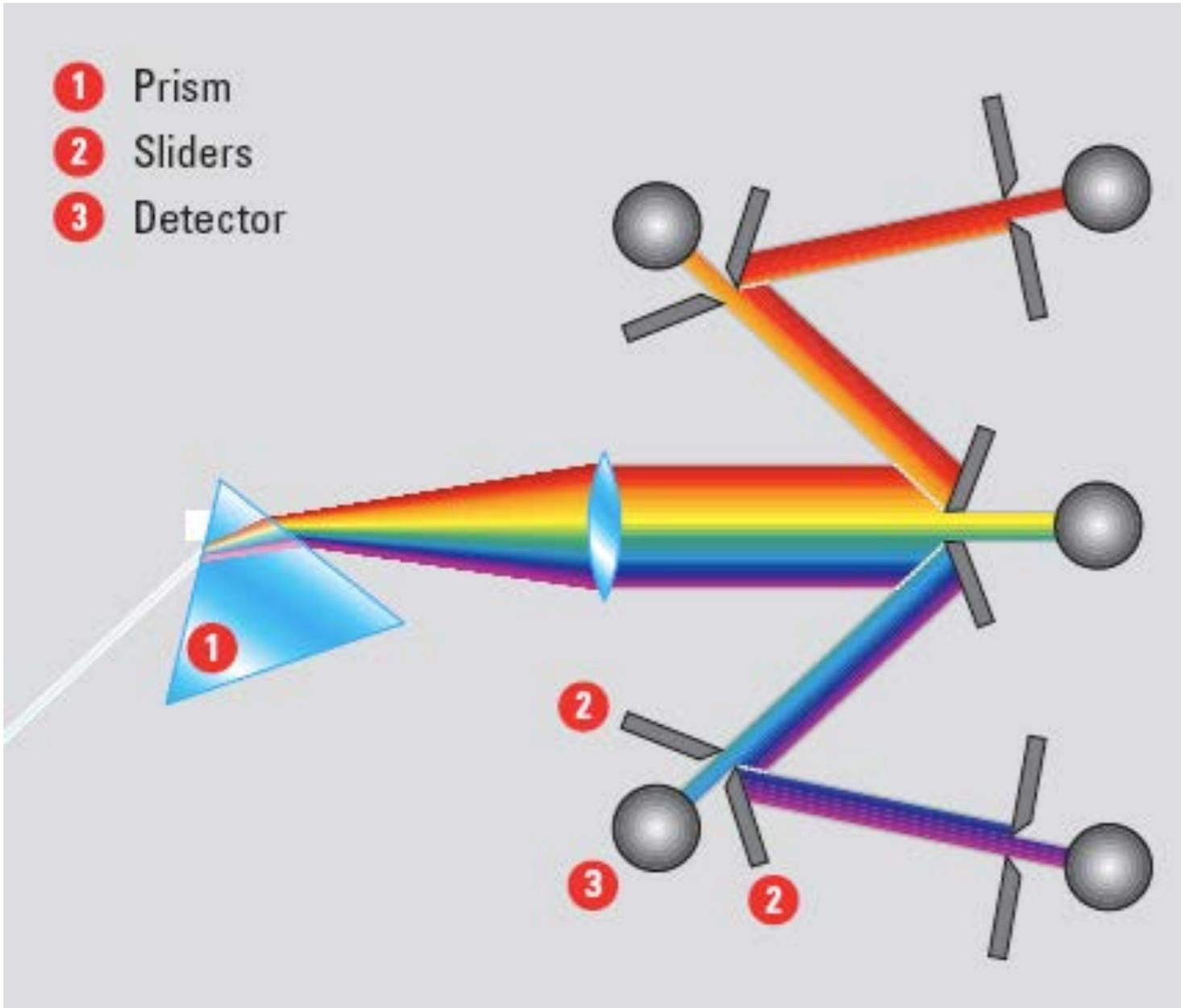


Leica SP2 AOBS



(credit: Leica microsystems)

spectral separation



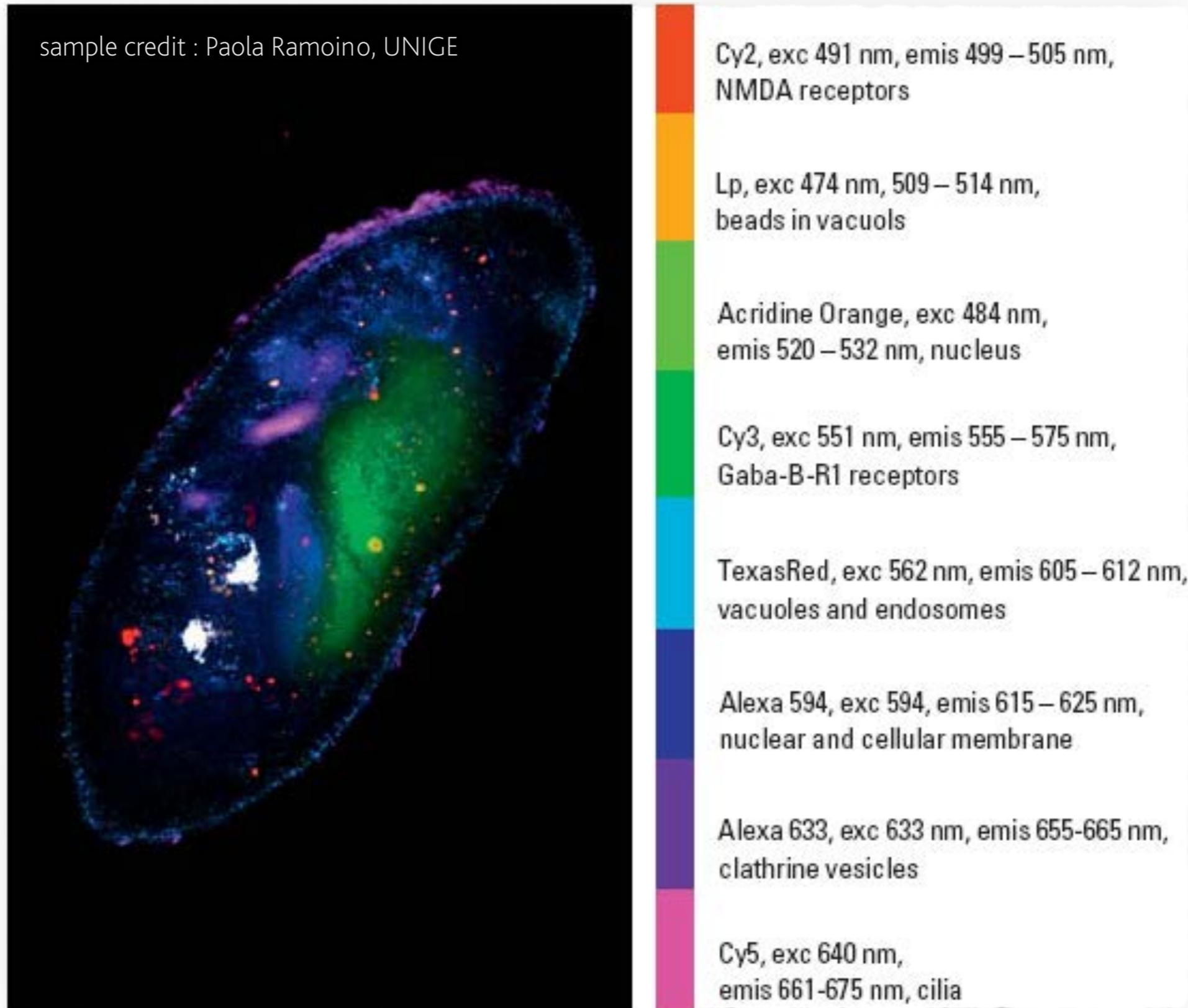
Larval state of the marine polychaete *Platynereis*

TCS SP5 resonant scanner 71 Hz framerate.
Beating cilia in reflected light and DiI-Fluorescence together with transmitted light.

Courtesy of Kristin Tessmar und Detlev Arendt
European Molecular Biology Laboratory (EMBL)
Heidelberg, Germany

Leica
MICROSYSTEMS

spectral separation



fluorescence

FL will provide information related to environmental and boundary conditions.

FRET measurements can be used to monitor protein binding or structural changes.

FRAP measurements can be used to monitor macromolecule diffusion at high spatial localization.

FCS at different time scale provides information on flickering of fluorescent molecules (1-100 micros), diffusion (100 micros-1 ms), and photobleaching (> 1 ms).

FCS allows direct comparison with in vivo condition at single molecule level.

SMD allows single molecule studies.

SHG allows structural studies and does not require any staining.

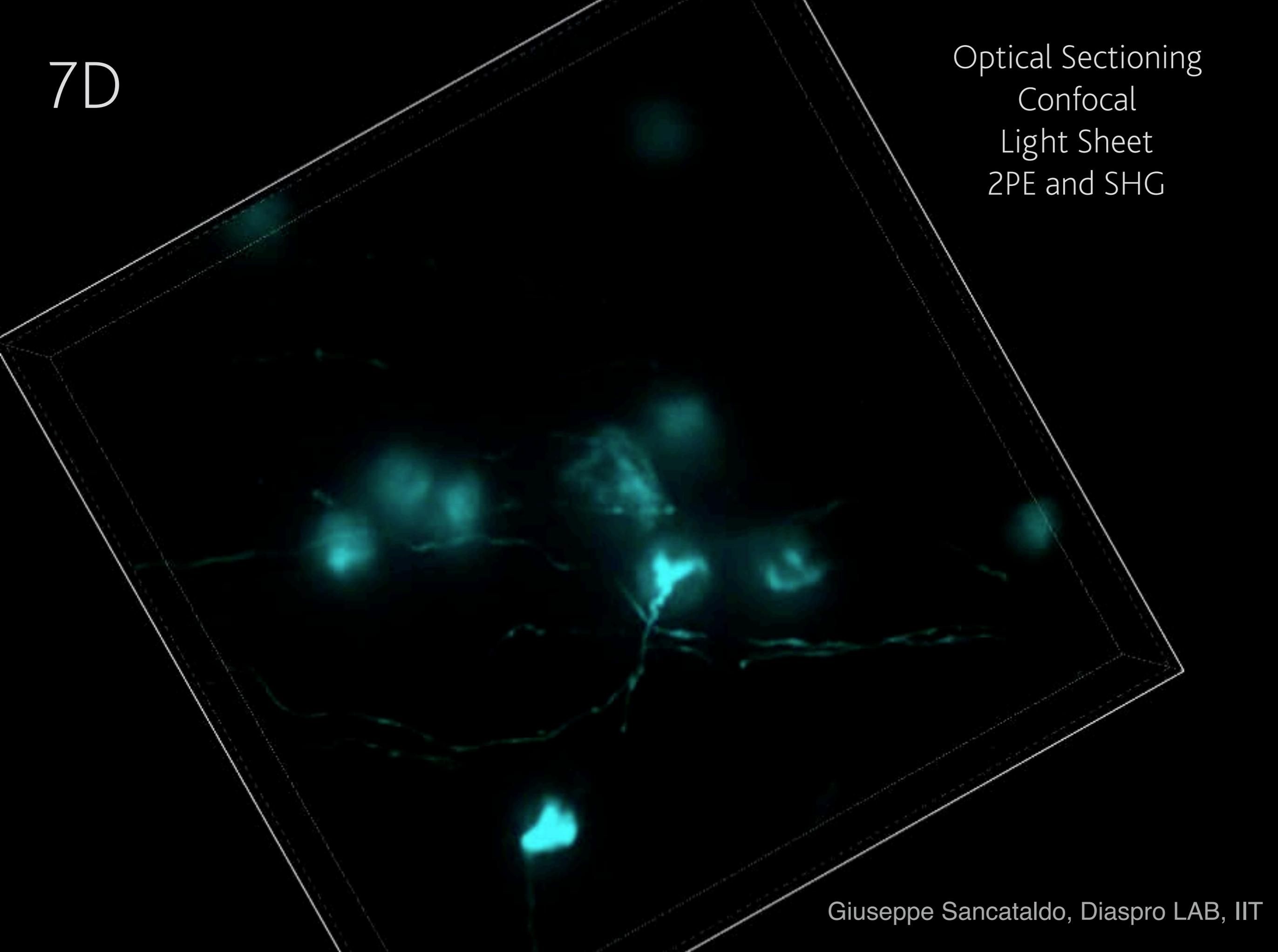
“C'erano 5 personaggi...6 contando la lastra di ghiaccio” (D.Pennac, La Fata Carabina)



7D (x-y-z-t-lambda-tau-chi)

7D

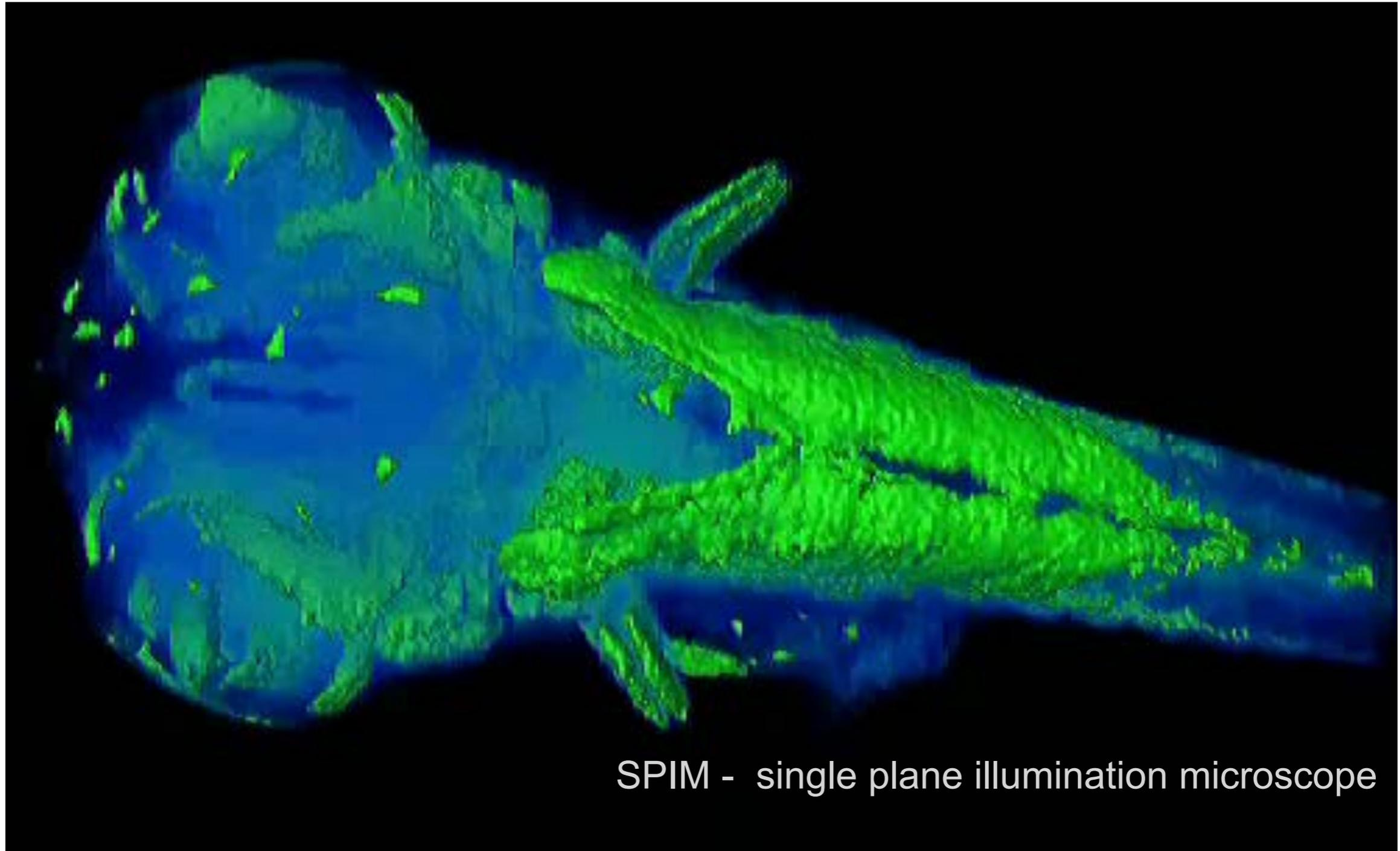
Optical Sectioning
Confocal
Light Sheet
2PE and SHG



7D

3D

3D rendered movie of the Medaka embryo.



SPIM - single plane illumination microscope

J. Huiskens, J. Swoger, F. Del Bene, J. Wittbrodt and [E.H.K. Stelzer](#), Science 305, 1007 -1009 (2004)

Alberto Diaspro, Nanoscopy, Istituto Italiano di Tecnologia

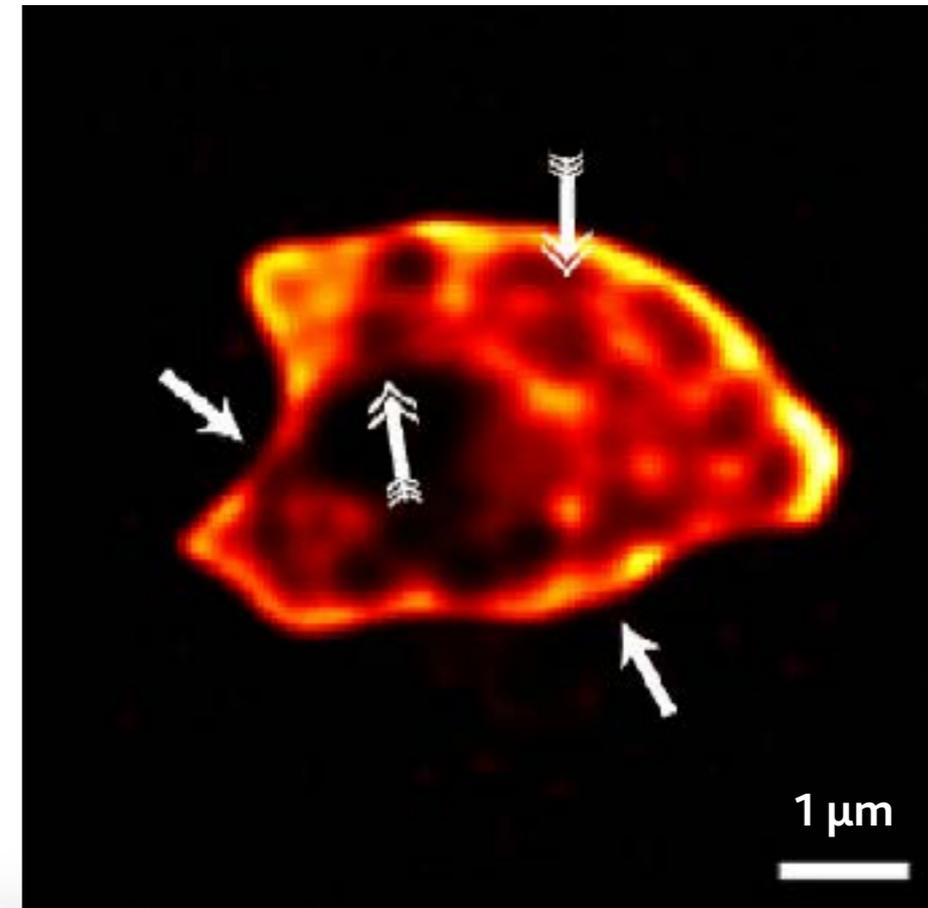
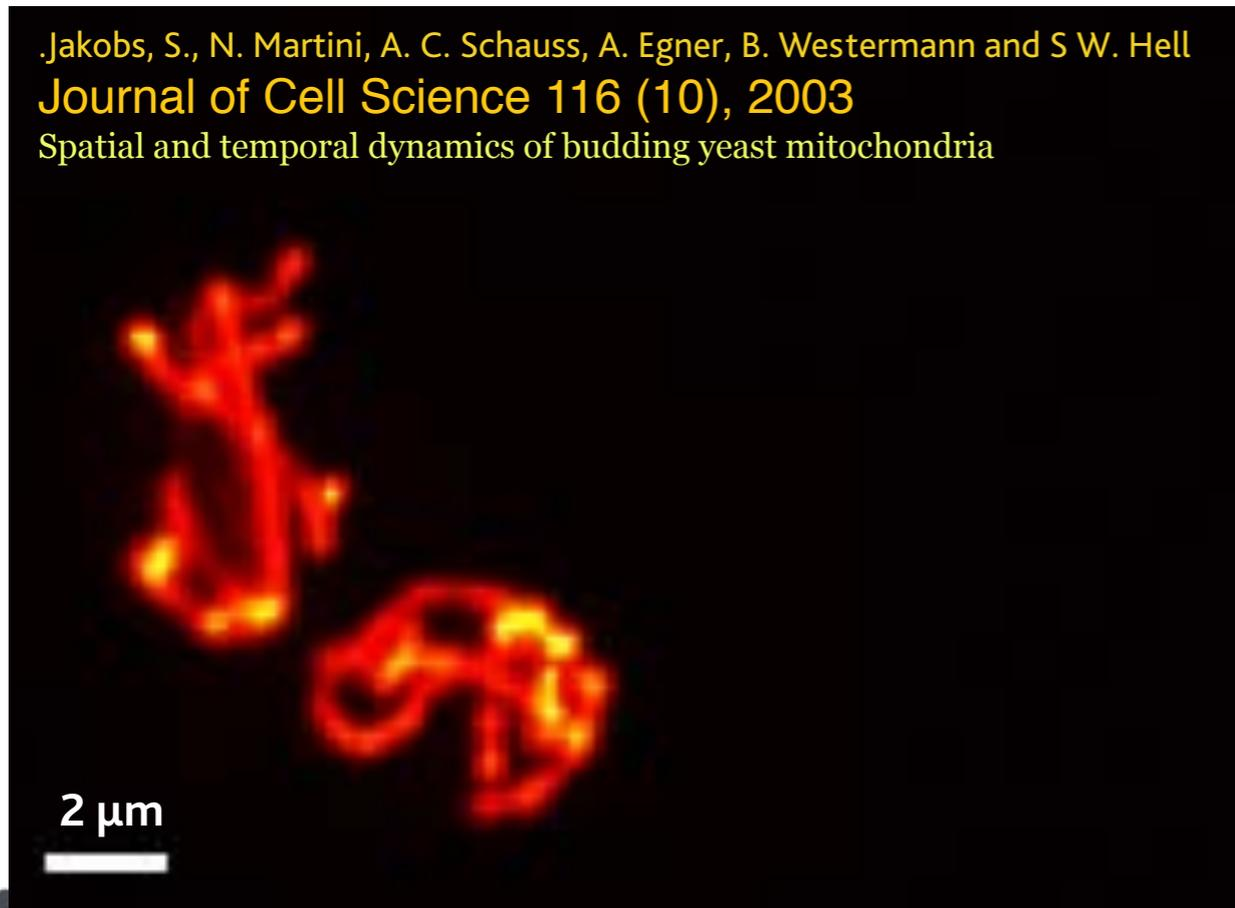
7D

4D



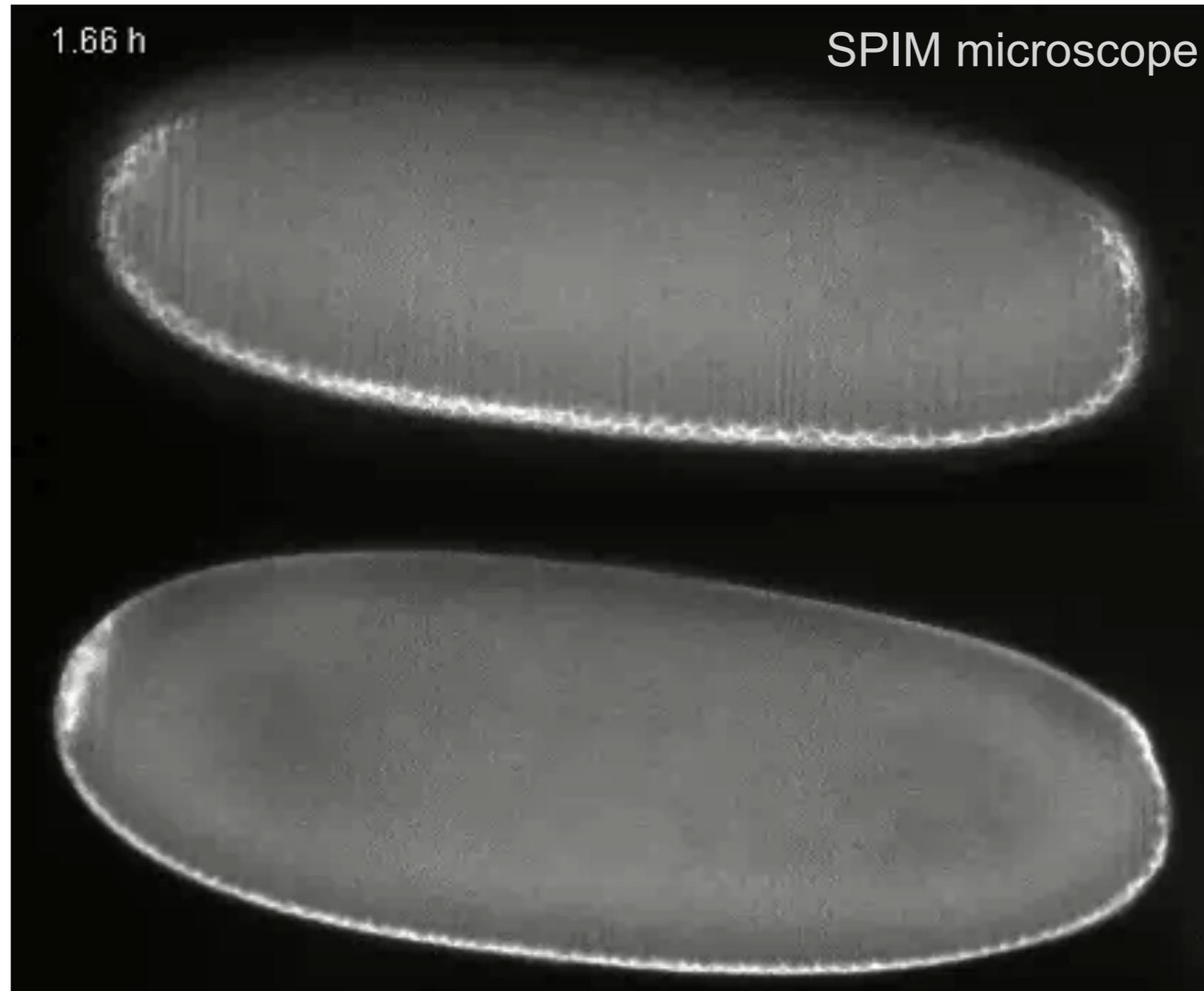
Stefan Hell's lab - <http://www.nanoscopy.de/>

Jakobs, S., N. Martini, A. C. Schauss, A. Egner, B. Westermann and S W. Hell
Journal of Cell Science 116 (10), 2003
Spatial and temporal dynamics of budding yeast mitochondria



7D

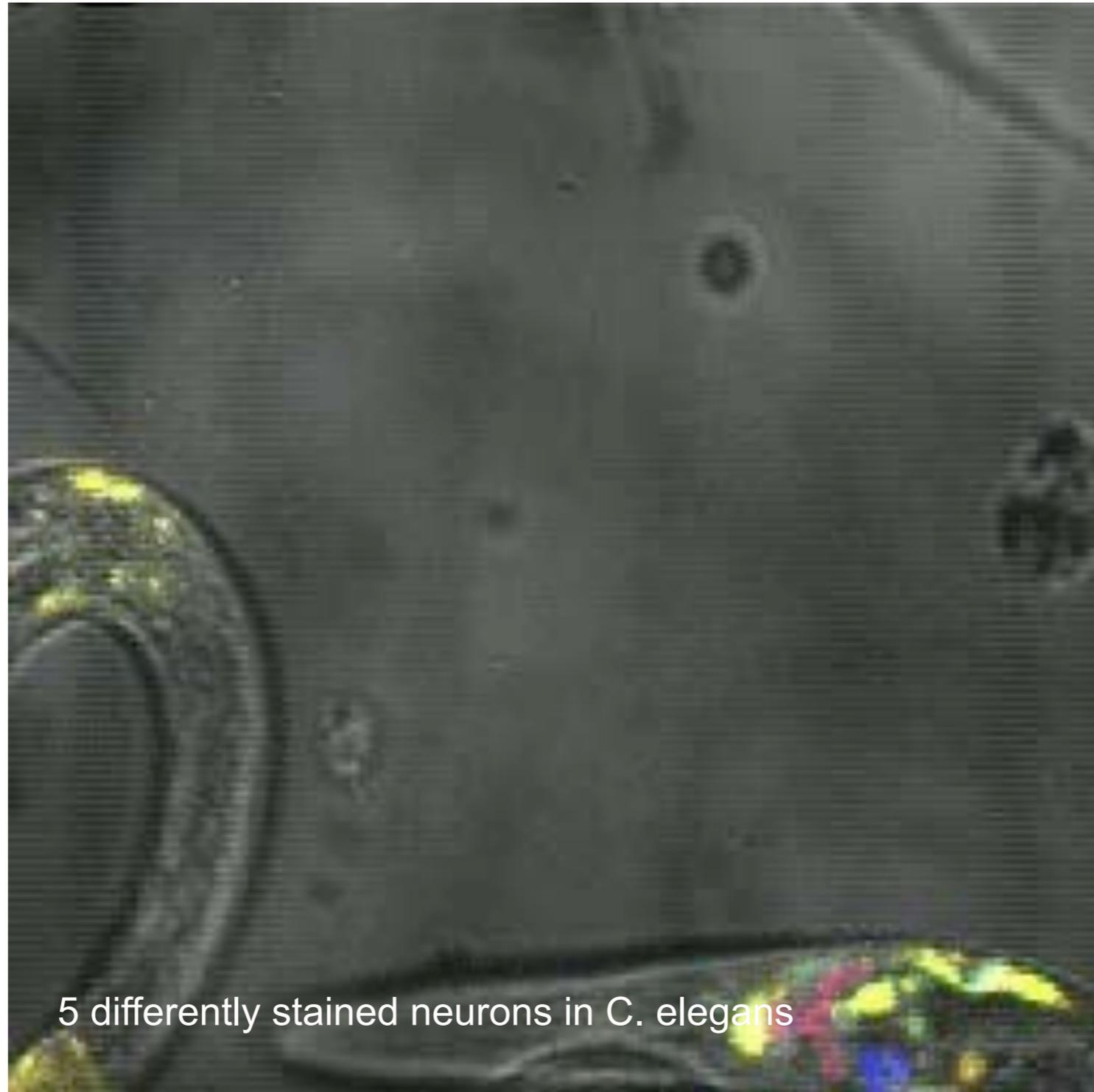
4D Time-lapse imaging of *Drosophila melanogaster* embryogenesis



J. Huisken, J. Swoger, F. Del Bene, J. Wittbrodt and E.H.K. Stelzer, Science 305, 1007 -1009 (2004)

7D

5D



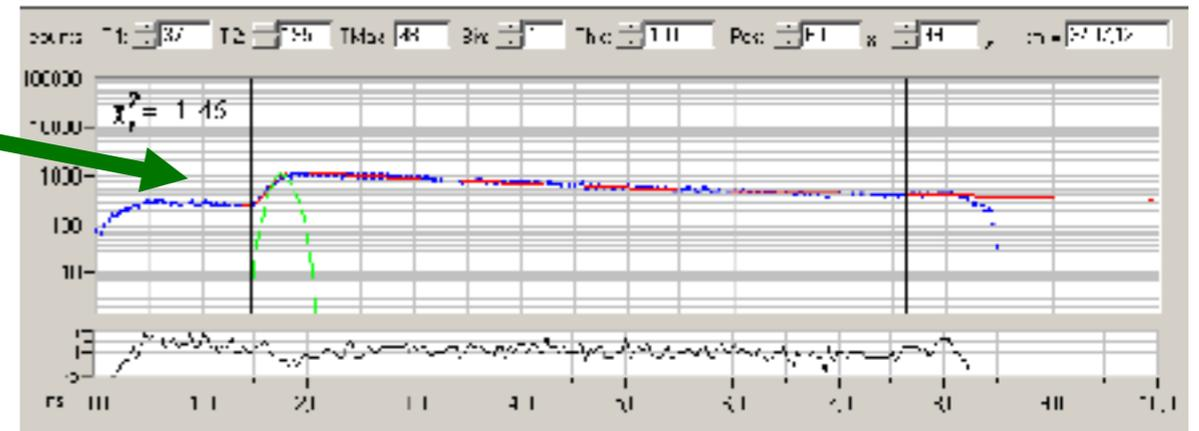
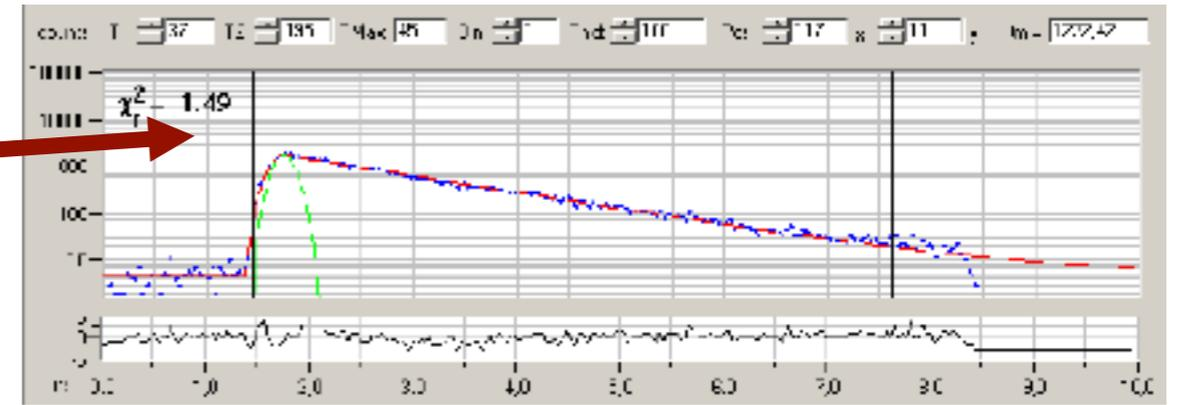
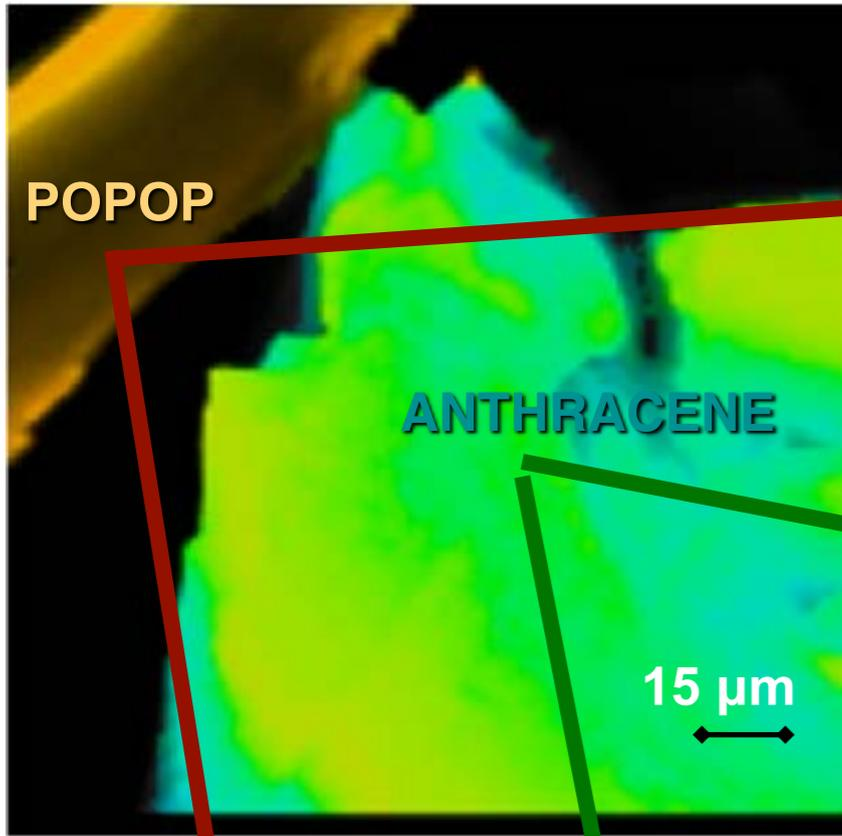
5 differently stained neurons in C. elegans

TCS SP5 resonant scanner 50 Hz framerate. Simultaneous record of CFP, GFP, YFP, DsRed, DiD and transmitted light.

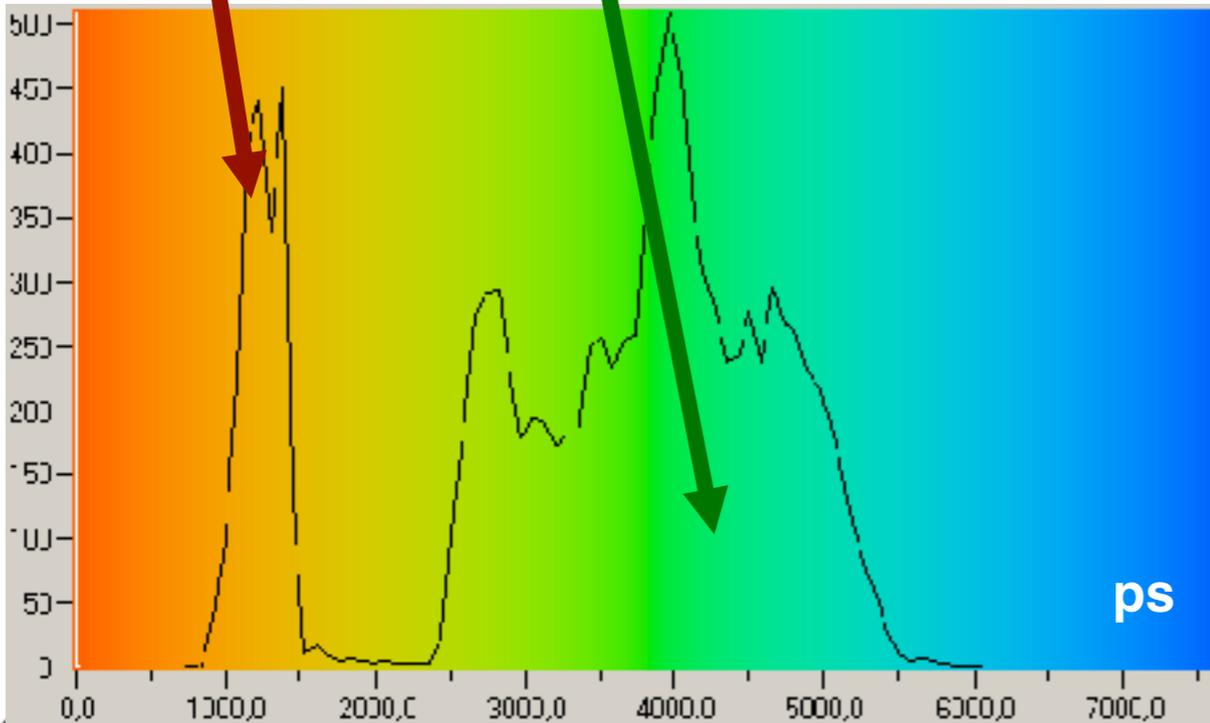
Credits: LEICA microsystems and Dr. Harald Hutter, Max Planck Institute (MPI) for Medical Research, Heidelberg, Germany
Alberto Diaspro, Nanoscopy, Istituto Italiano di Tecnologia



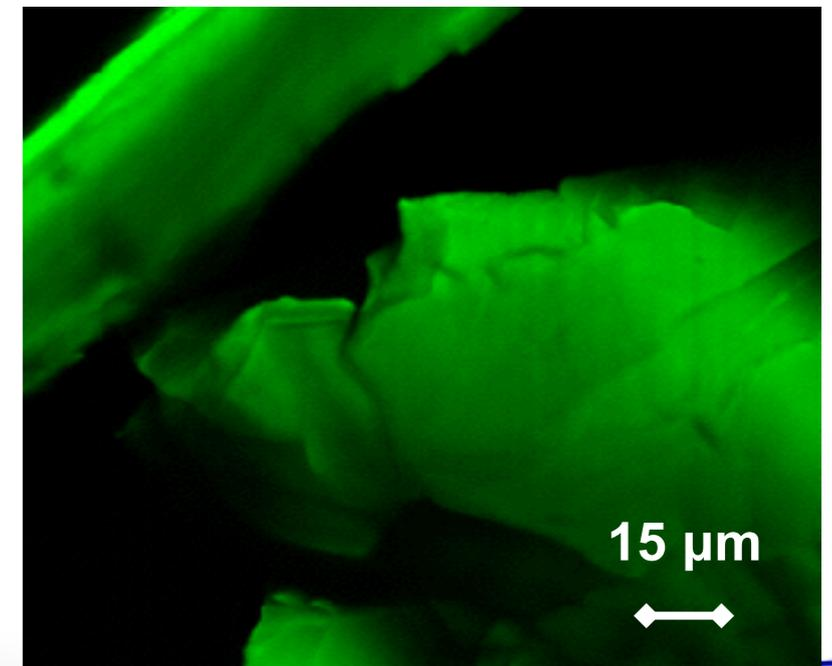
7D



copyright LAMBS MicroScoBio

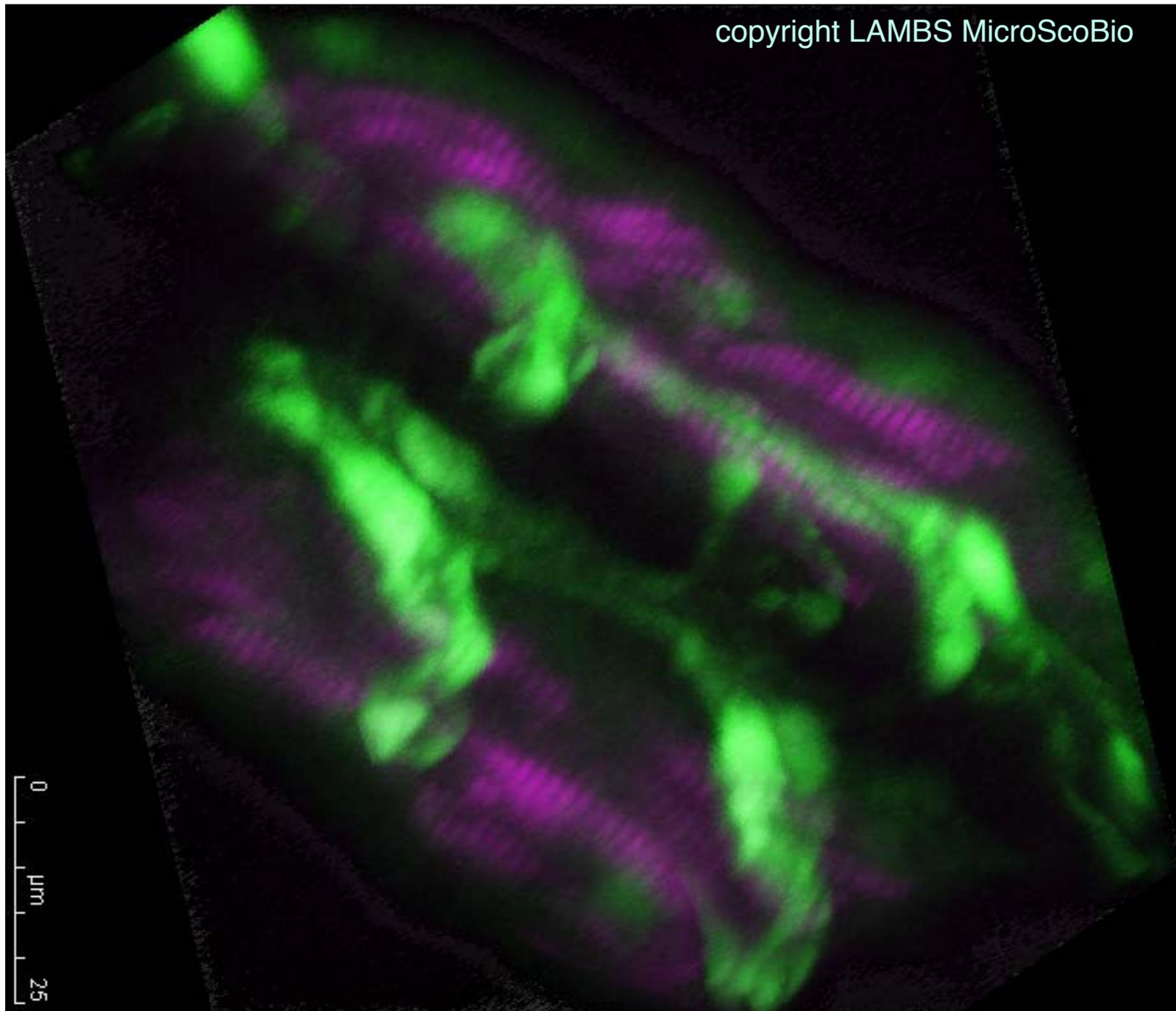


6D

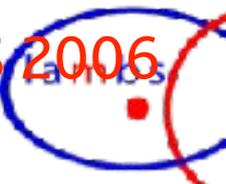


7D

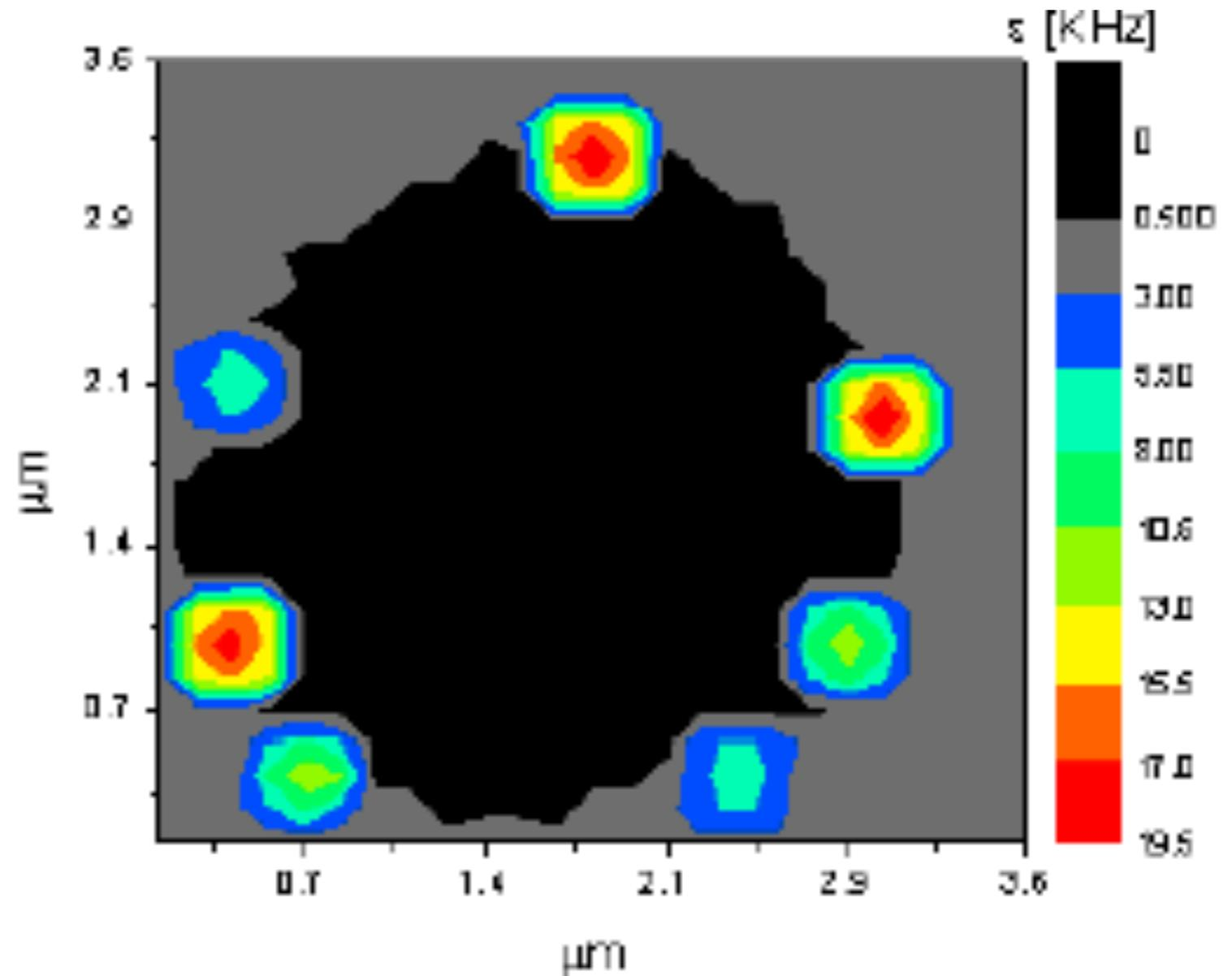
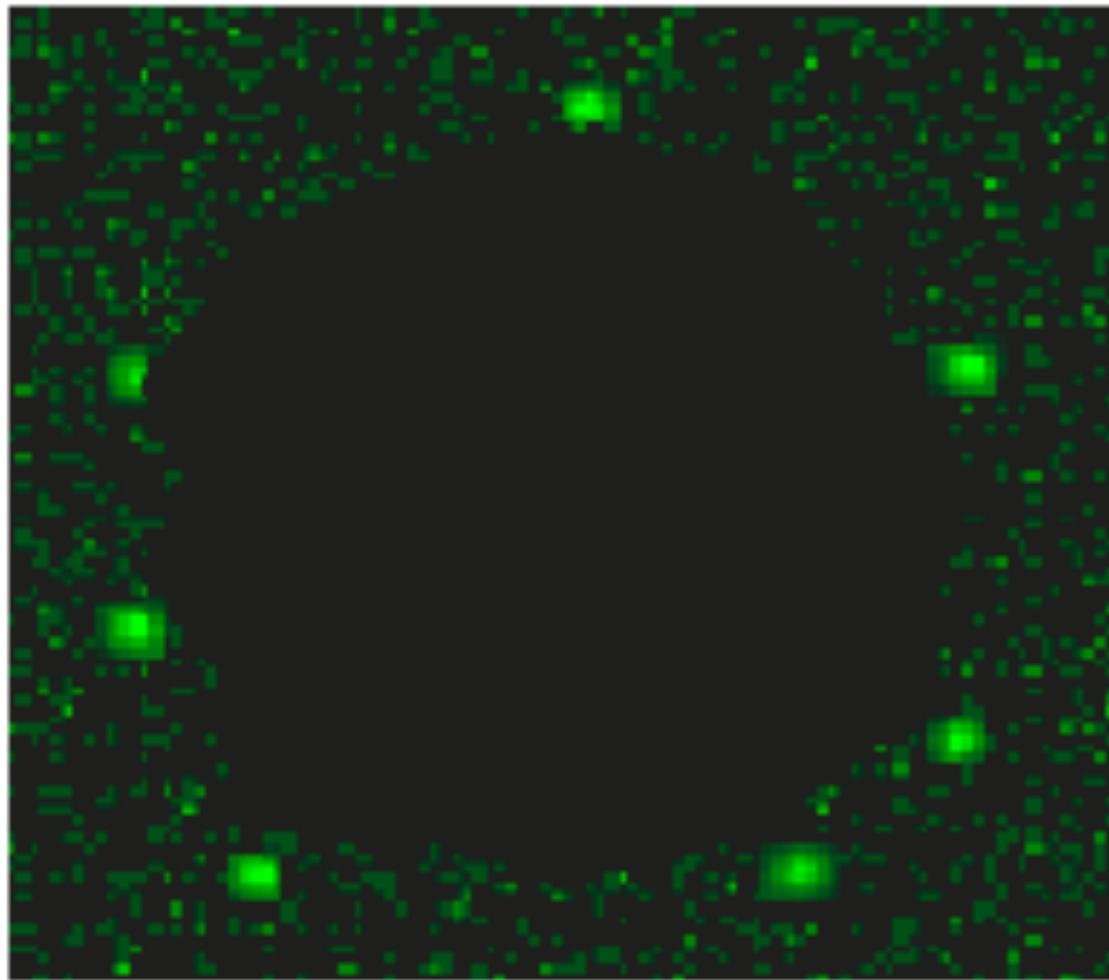
7D



SHG from muscle fibers from the Zebrafish tail and EGFP fluorescence - Paolo Bianchini, LAMBS 2006
Alberto Diaspro, Nanoscopy, Istituto Italiano di Tecnologia



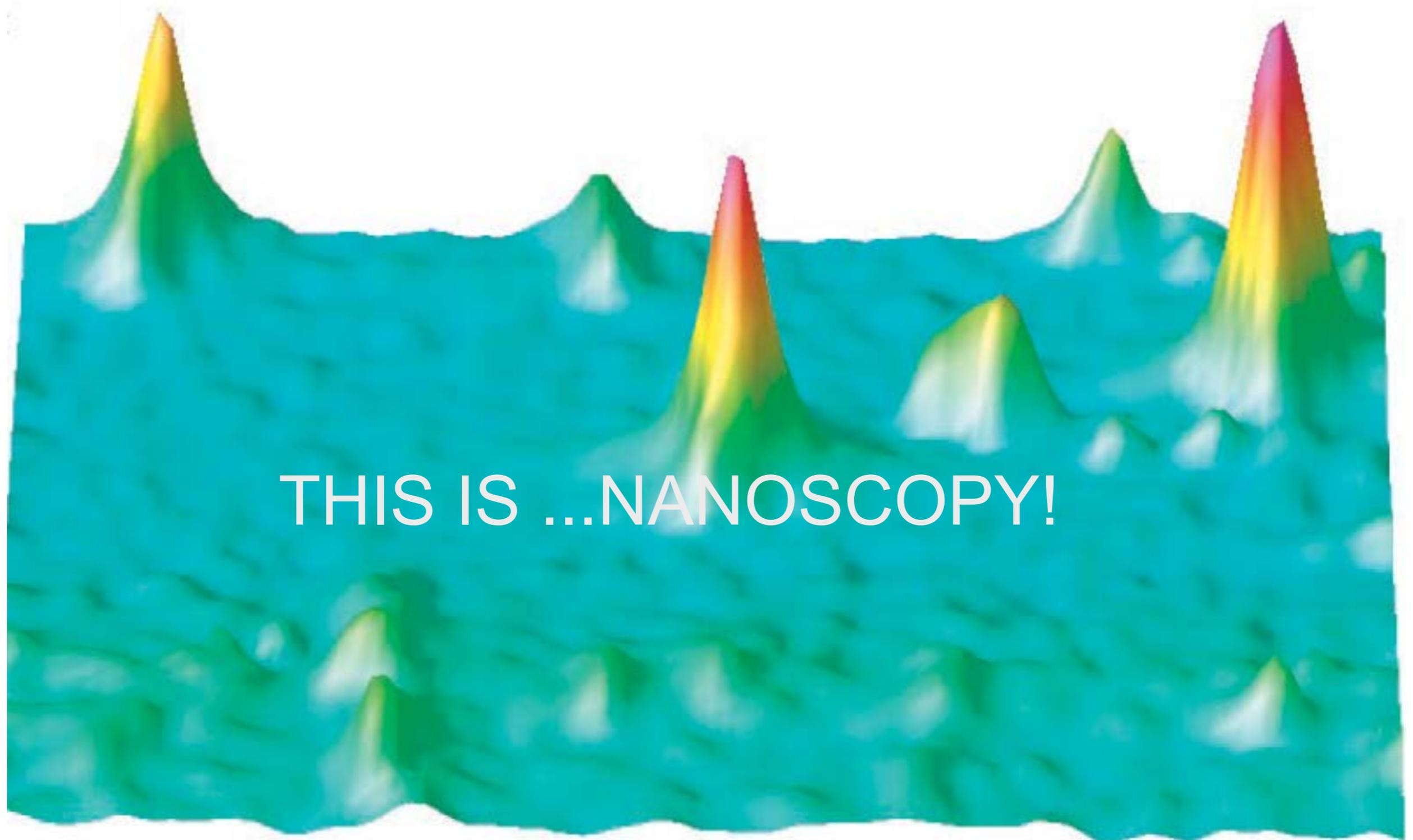
7D and more



Single GFPmut2 molecules fluorescence (bright green) and brightness after incorporation in a poly-electrolyte matrix built on amorphous calcium carbonate (dark sphere). The field of view is $3.6 \times 3.6 \mu\text{m}$.

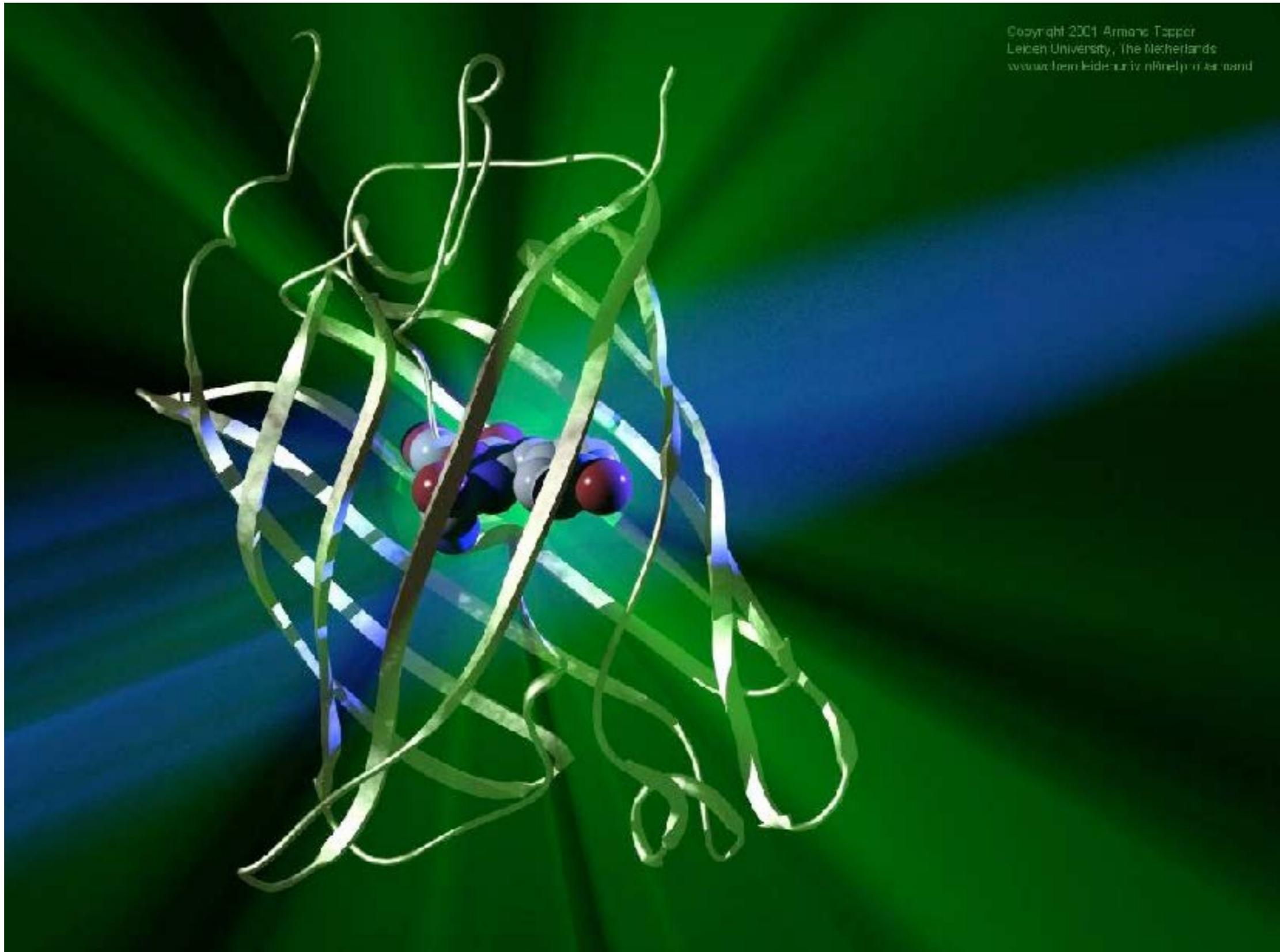
Diaspro A., et al. (2006) Optics Express, Vol. 14(21).

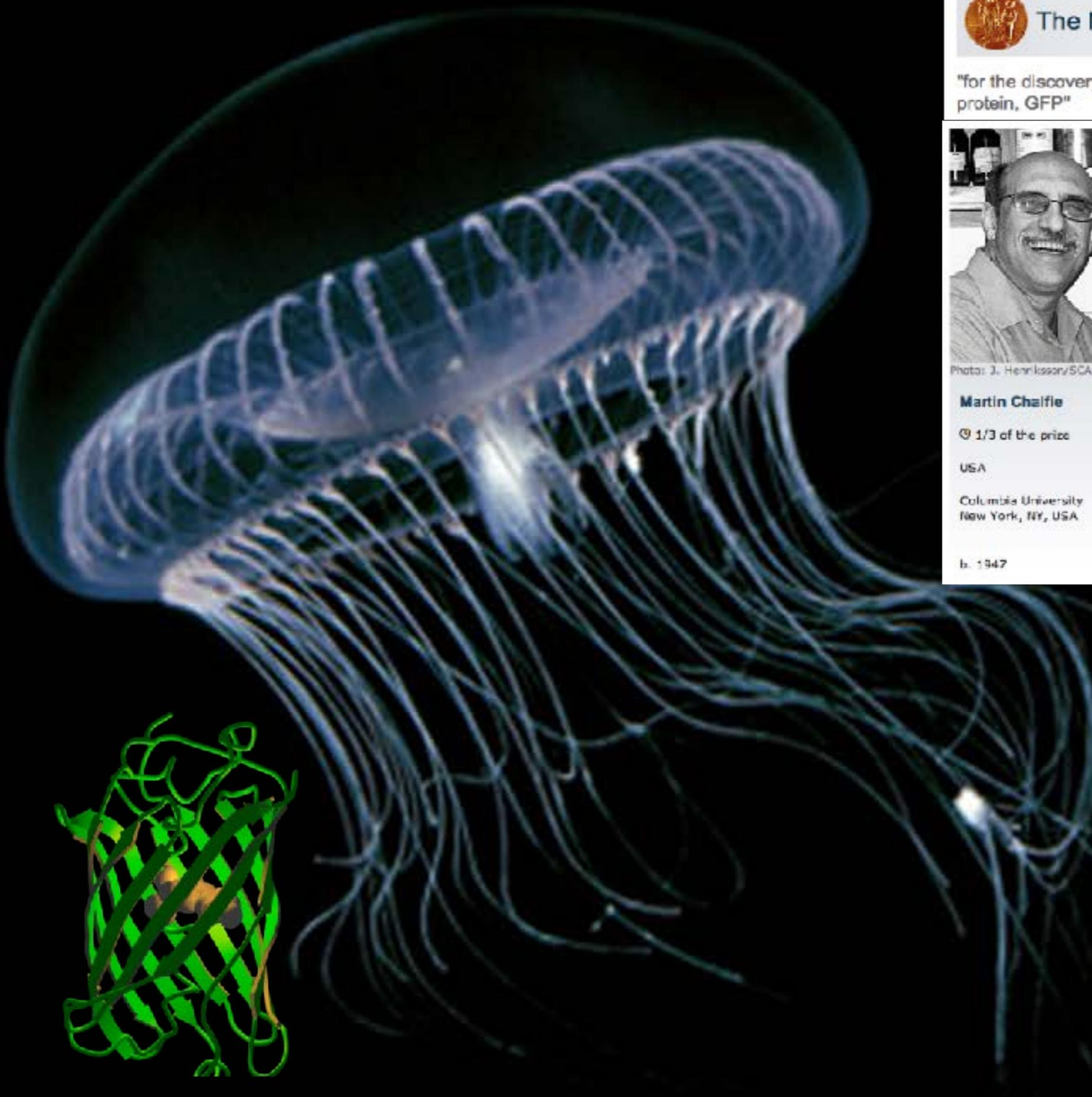
7D and more



Hybrid space-frequency image of single molecules of pentacene. Moerner WE, Orrit M. (1999) Science 283(5408):1670-6

GREEN FLUORESCENT PROTEIN





The Nobel Prize in Chemistry 2008

"for the discovery and development of the green fluorescent protein, GFP"



Photo: J. Henriksdottir/SCANPIX

Martin Chalfie

1/3 of the prize

USA

Columbia University
New York, NY, USA

b. 1947



Photo: UCSD

Roger Y. Tsien

1/3 of the prize

USA

University of California
San Diego, CA, USA

b. 1952



Photo: J. Henriksdottir/SCANPIX

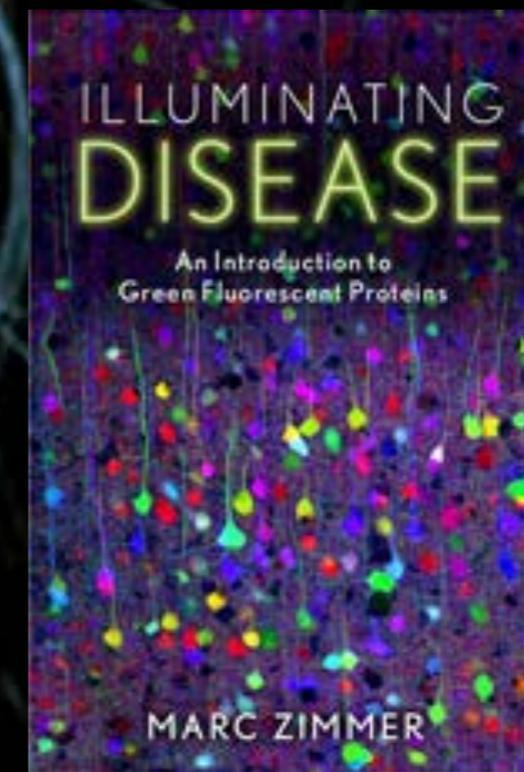
Osamu Shimomura

1/3 of the prize

USA

Marine Biological
Laboratory (MBL)
Woods Hole, MA, USA

b. 1928

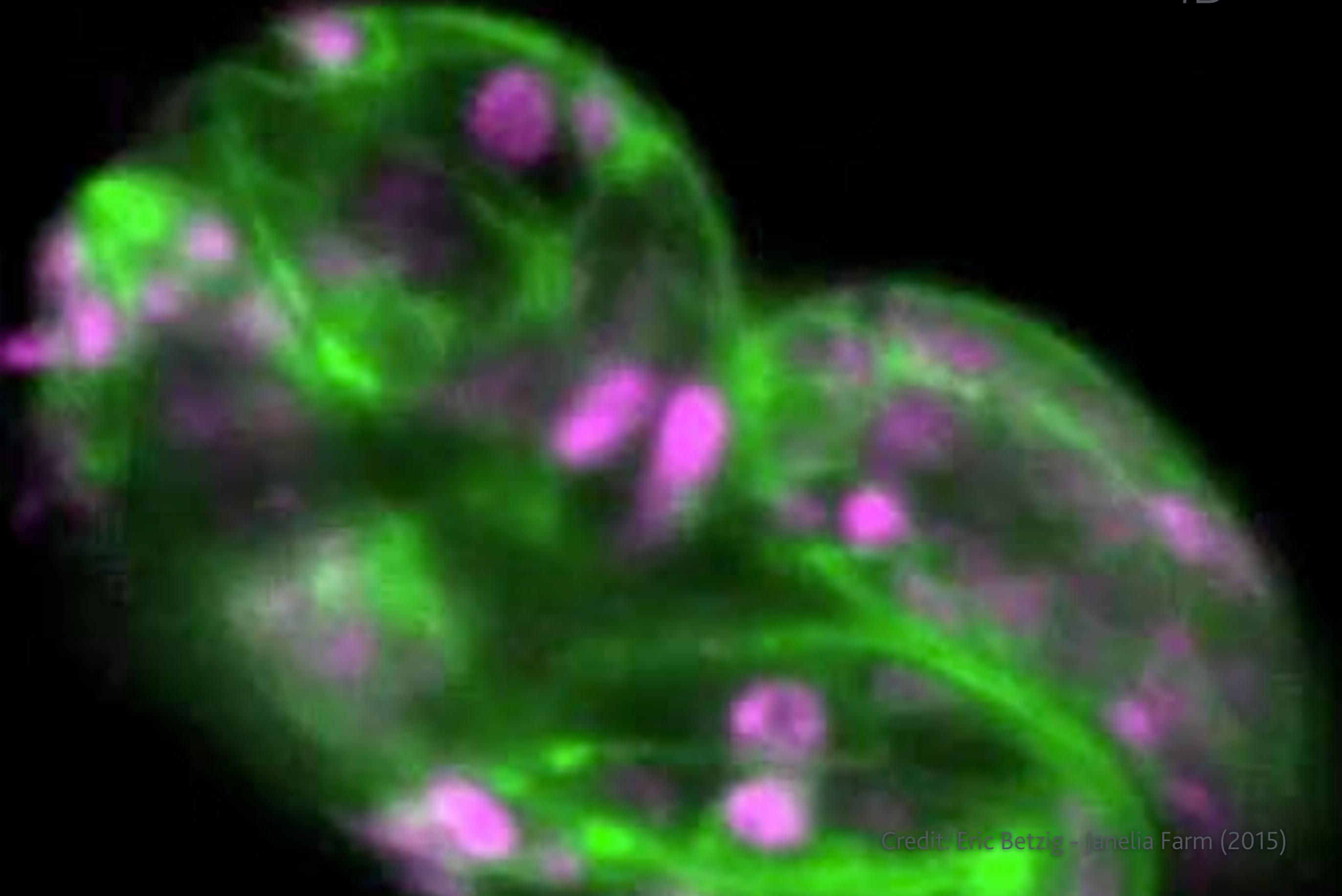


Credit: M Chalfie - Nobel Laureate 2008



C. Elegans PH-GFP H2B-mCherry

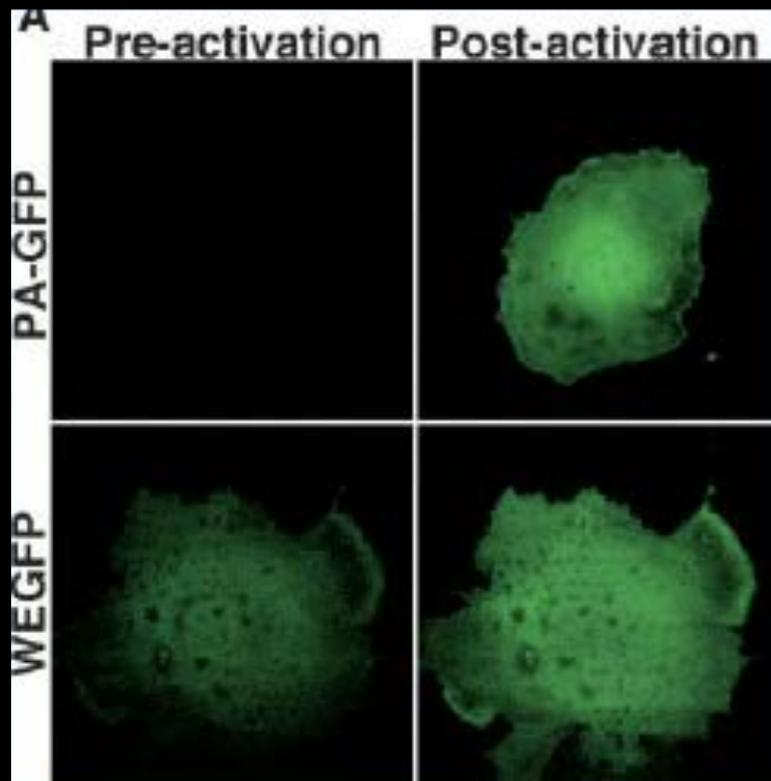
4D



Credit: Eric Betzig - Janelia Farm (2015)

Directed Mutagenesis of Photoactivated Fluorescent Proteins (PA-FPs)

increased on/off contrast of PA-GFP



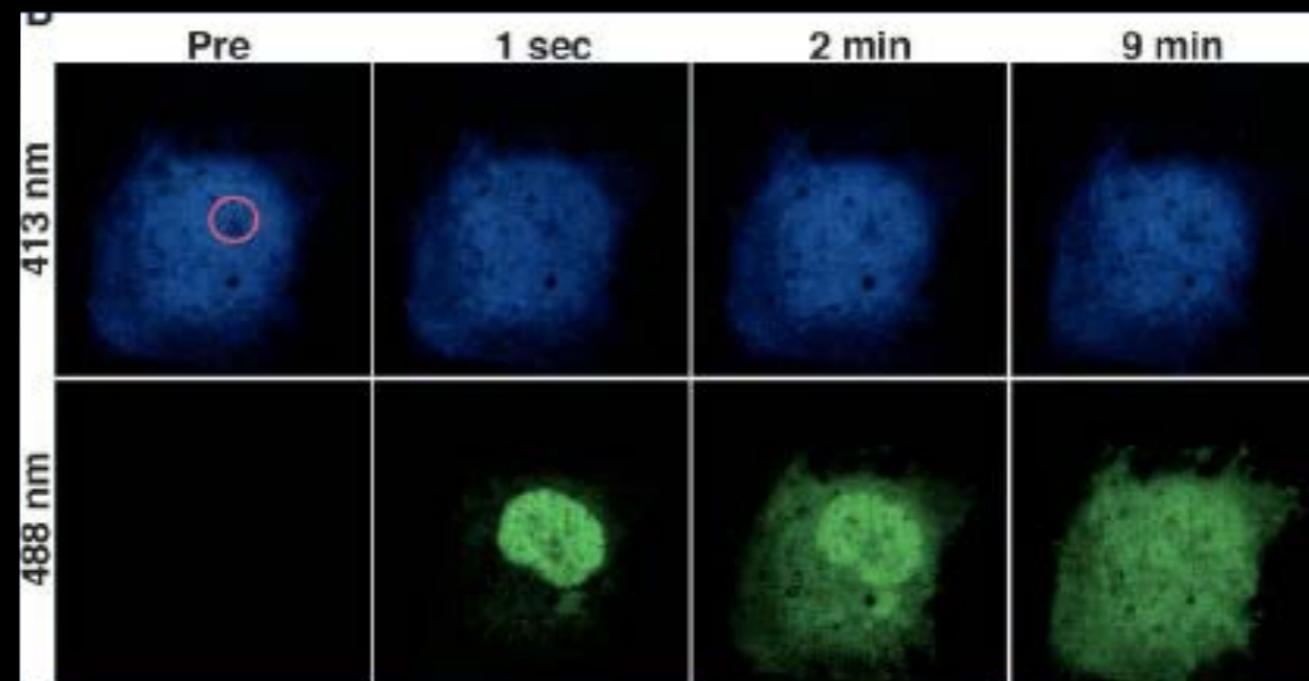
Jennifer
Lippincott-
Schwartz



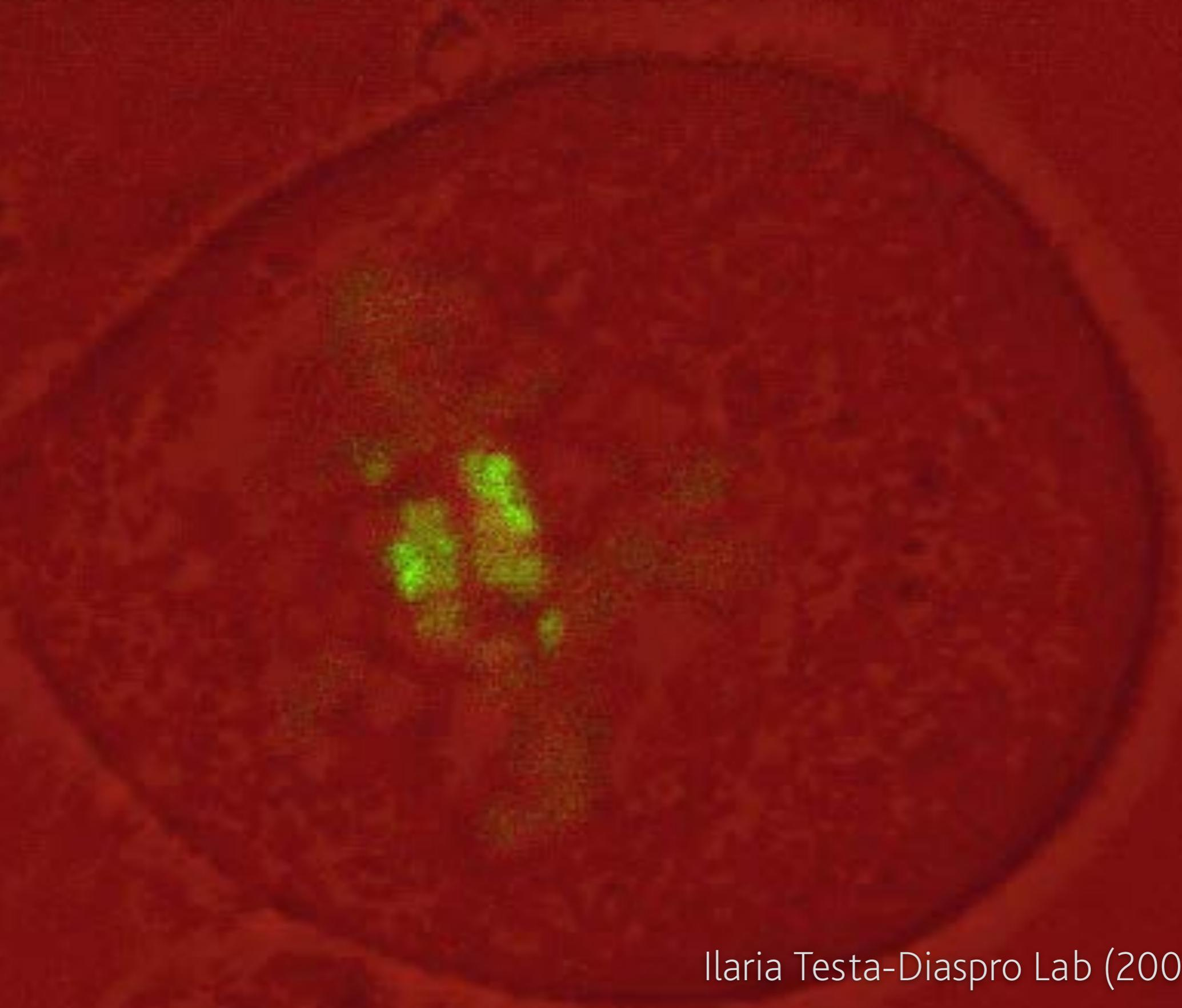
George
Patterson



pulse chase: nuclear vs cytosolic diffusion



G.H. Patterson, J. Lippincott-Schwartz, *Science* **297**, 1873 (2002)



Single molecule

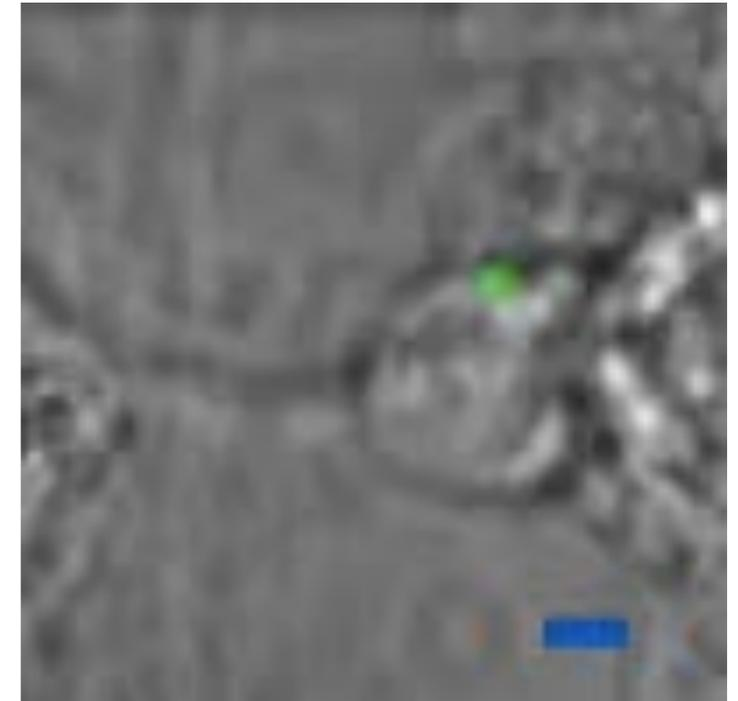
Localization precision
depends
on the number of photons
 N detected
over background

$$\sigma \sim 1/\sqrt{N}$$

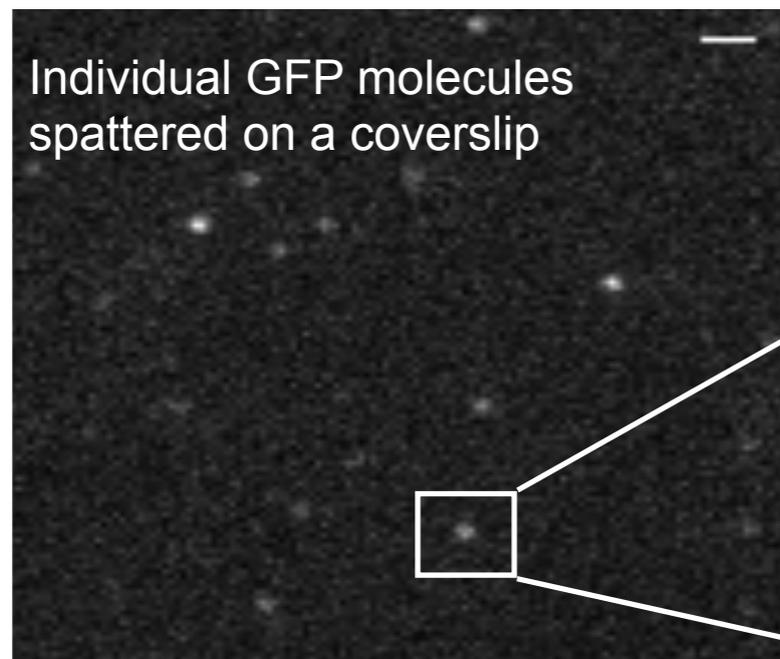
How does a single molecule look like

How do we recognize a single molecule?

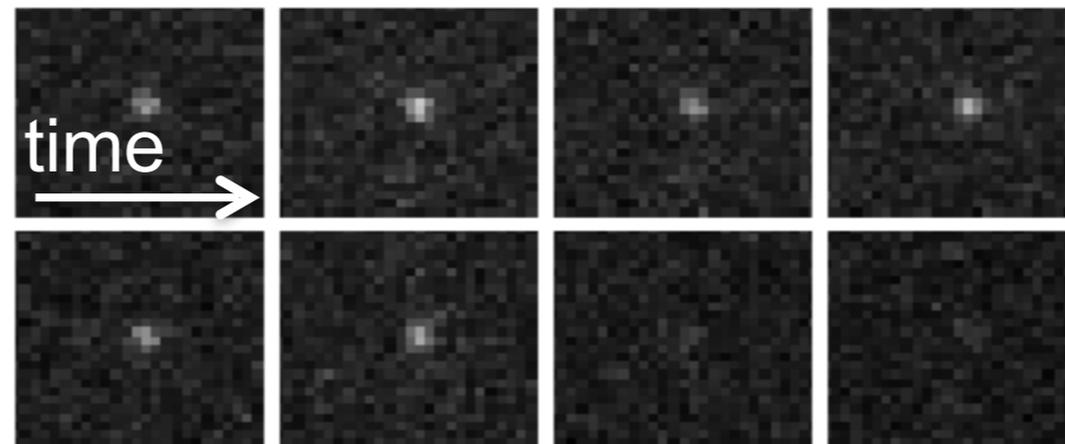
Single molecules disappear after emitting N photons.



Diffusion of GABA receptor in living neuron



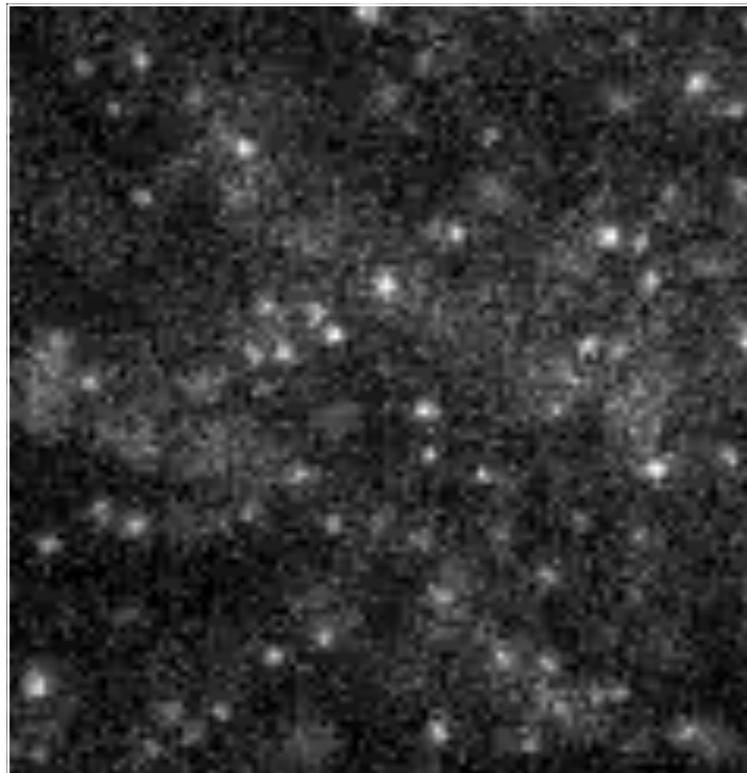
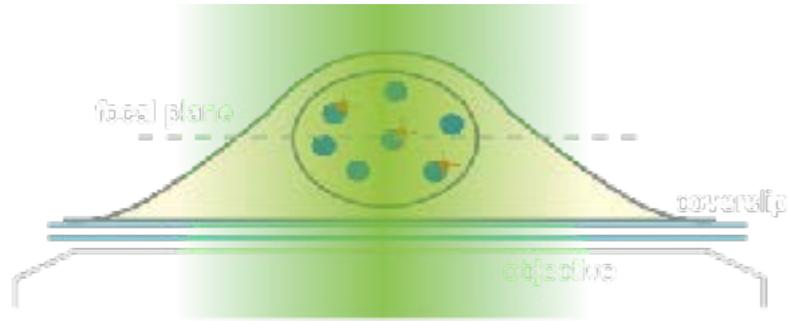
Individual GFP molecules spattered on a coverslip



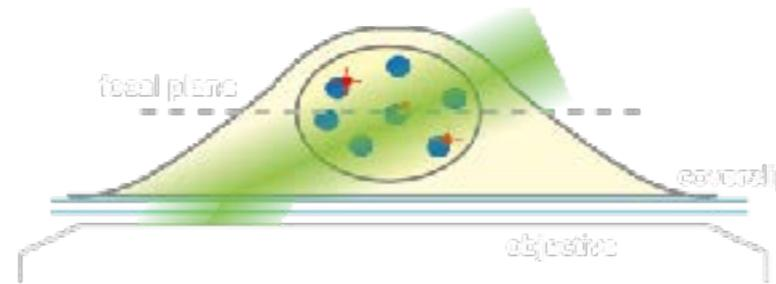
Single molecule

slide credit: Davide Mazza

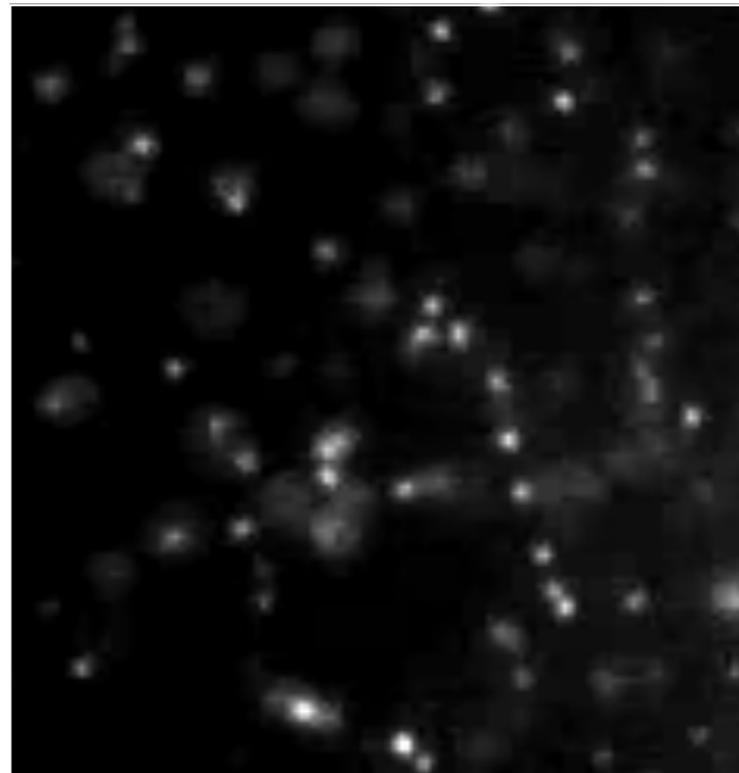
WIDEFIELD ILLUMINATION



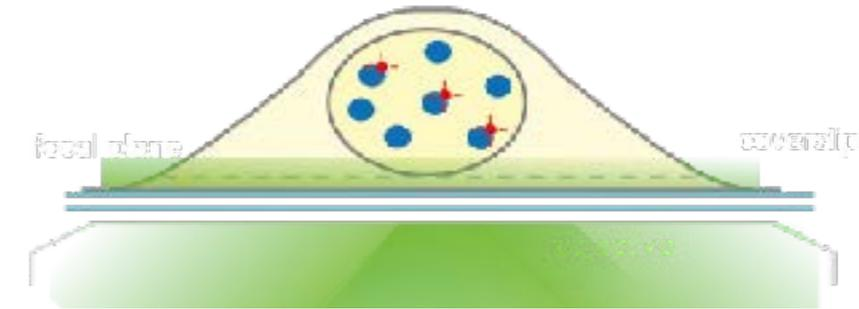
INCLINED (HILO) ILLUMINATION



Tokunaga et al., Nat. Methods 2007

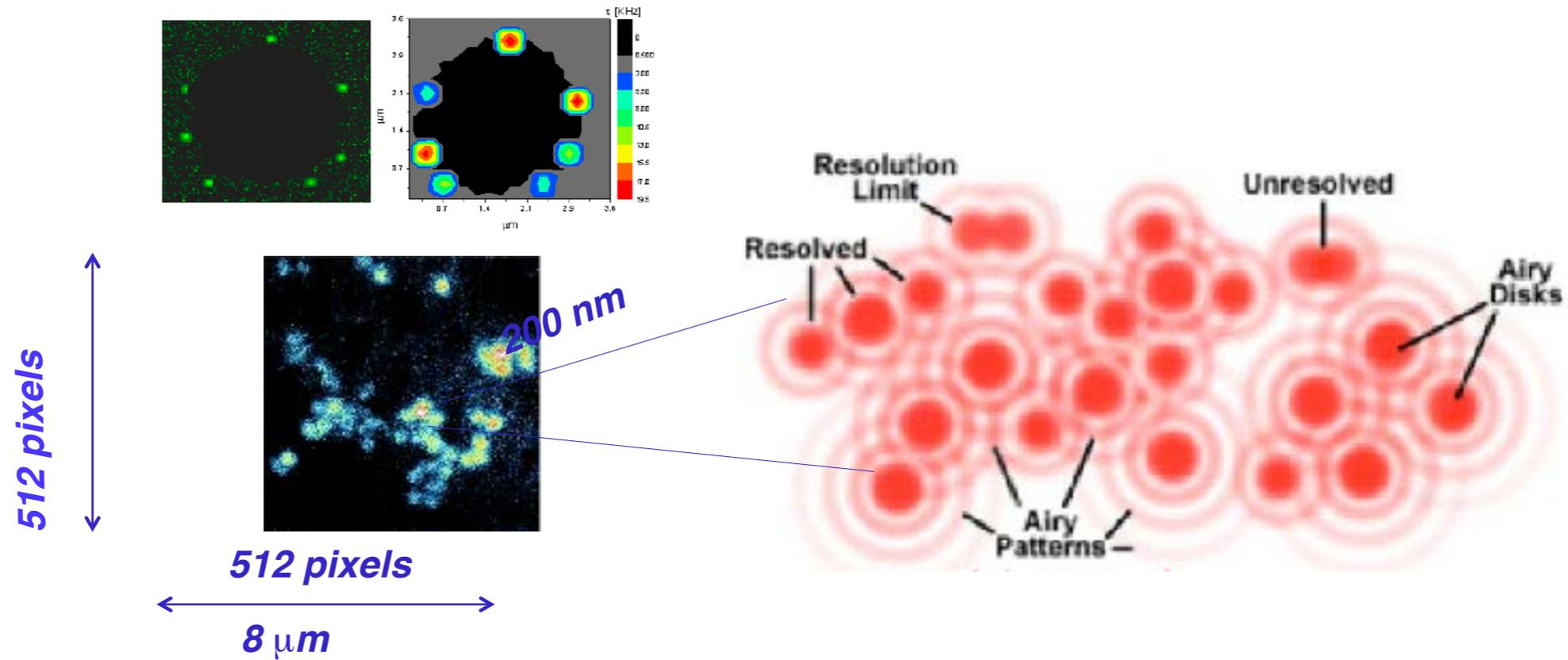


TIRF ILLUMINATION



Images of 100nm fluorescent beads in aqueous solution - Frame rate 100fps

Single molecule structure is still not resolved

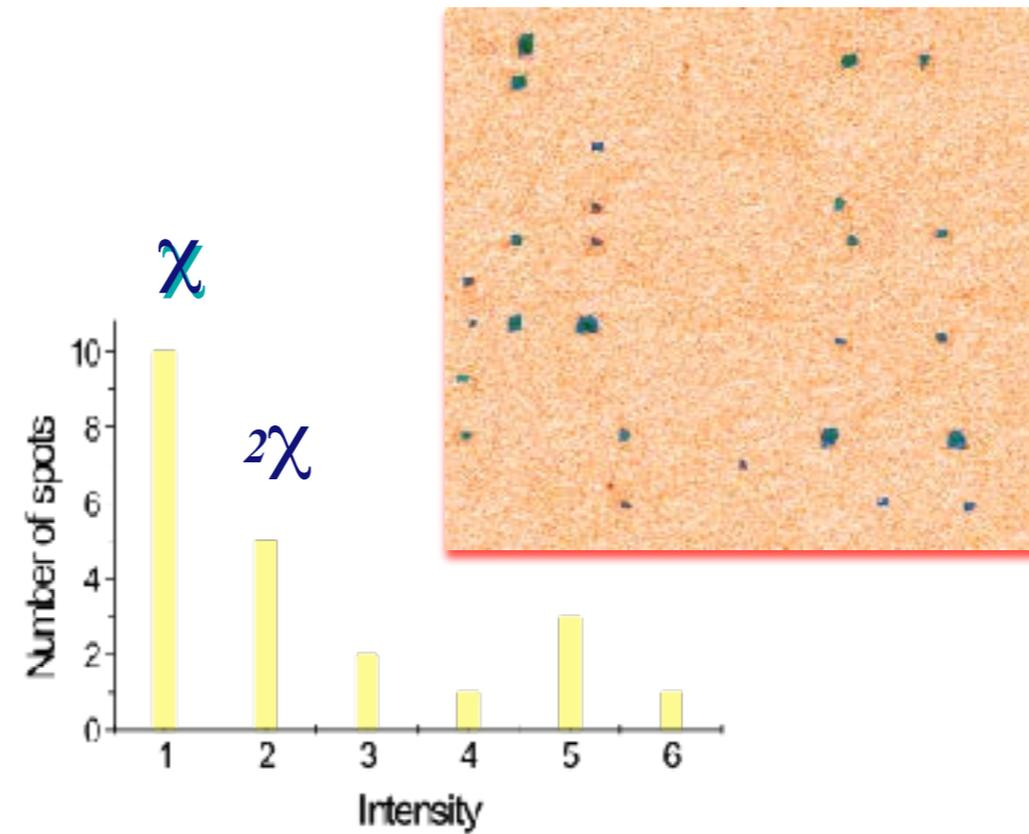
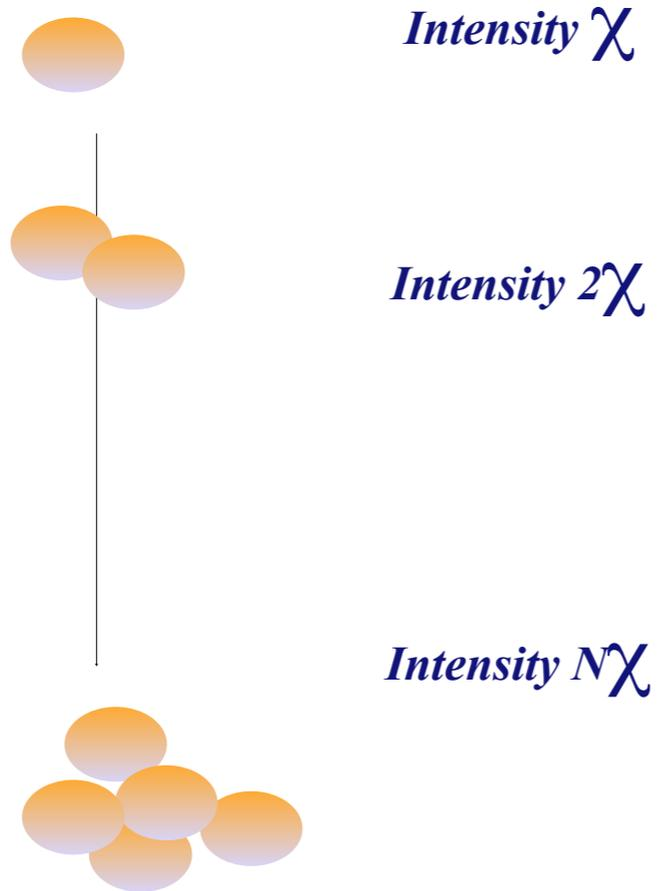


Micr. Res. Tech. (2002) 55:359-4

Diaspro Lab -LAMBS - Dept. Physics

Micr. Res. Tech., 55:359-364 (2002)
Biophysical J., 84 (2003).
J.Phys.D,36 (2003).

Single Molecule Imaging

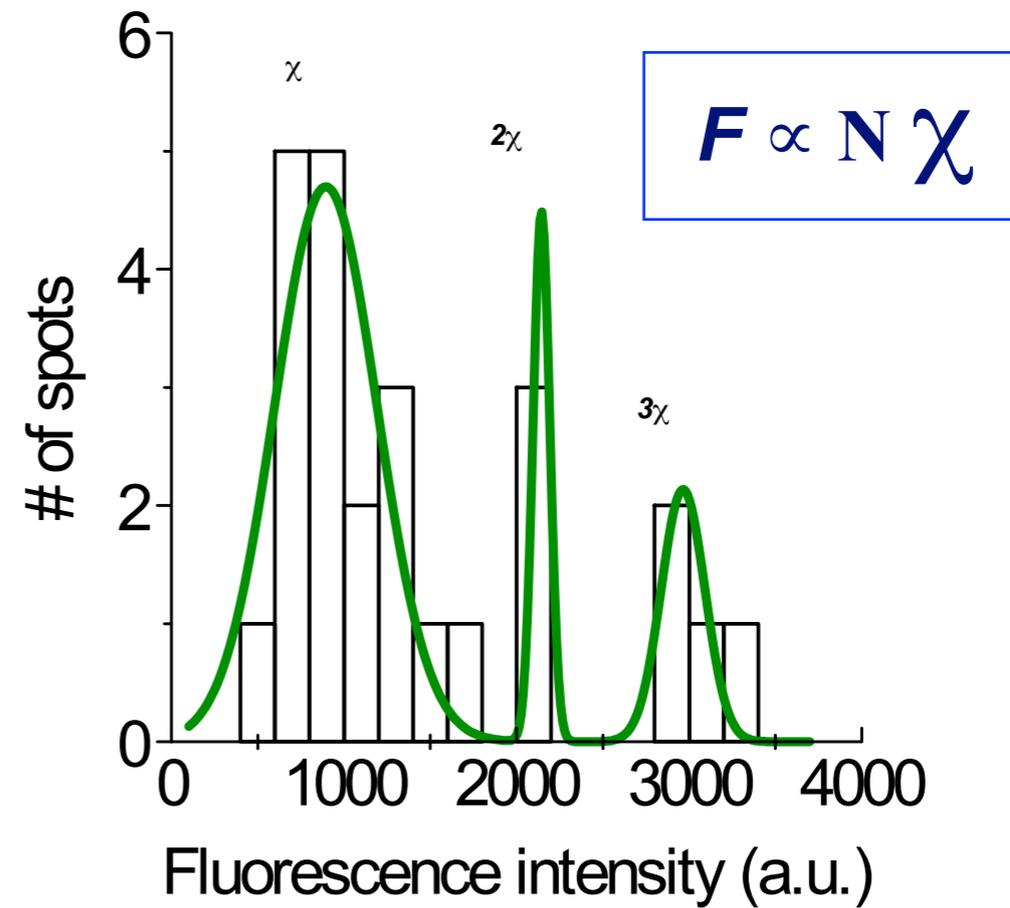
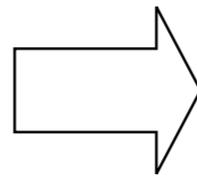
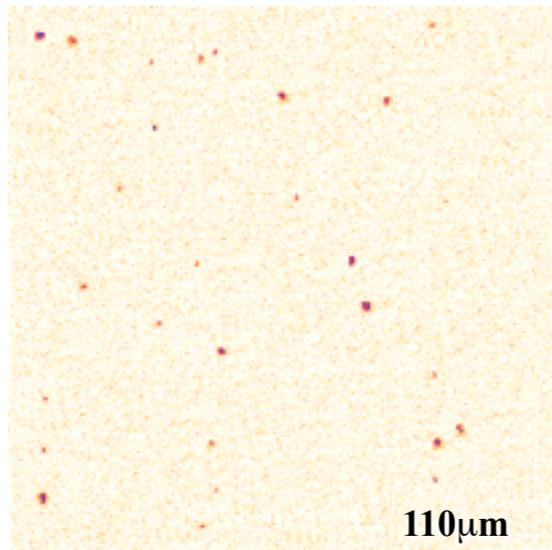


N = number of molecules

Micr. Res. Tech. (2002) 55:359-4

Single Molecule Imaging

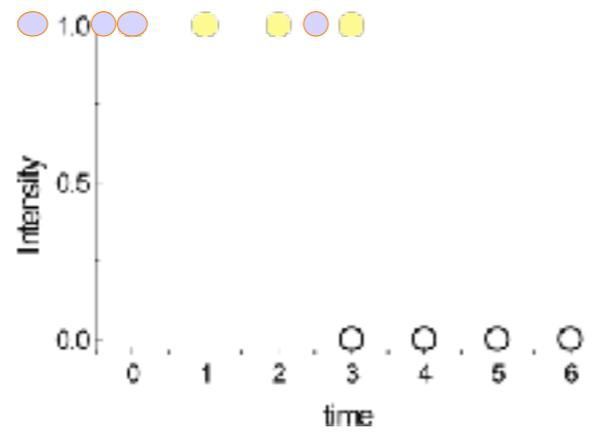
Fluorescein $c=1\mu\text{M}$ @ 8mW



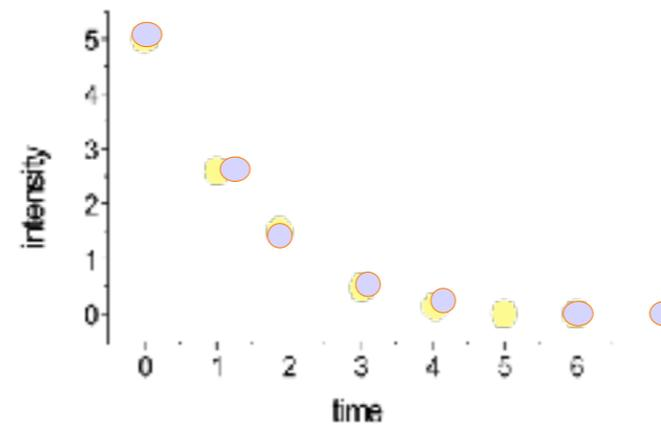
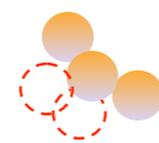
Micr. Res. Tech. (2002) 55:359-4

Single Molecule Imaging

Single Molecule



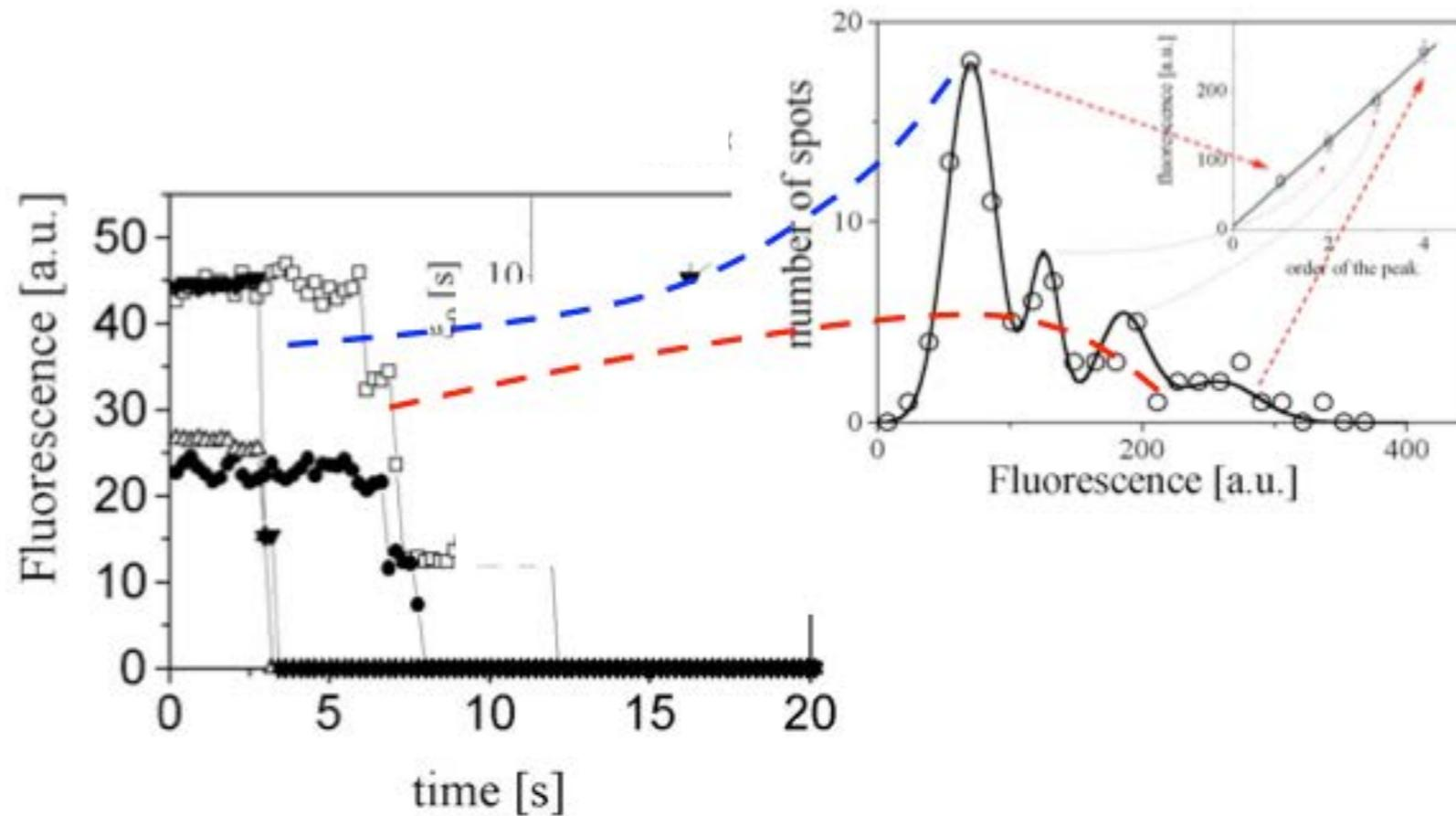
Aggregates



Micr. Res. Tech. (2002) 55:359-4

Single Molecule Imaging

Single Molecule Photobleaching of Sparse Aggregates



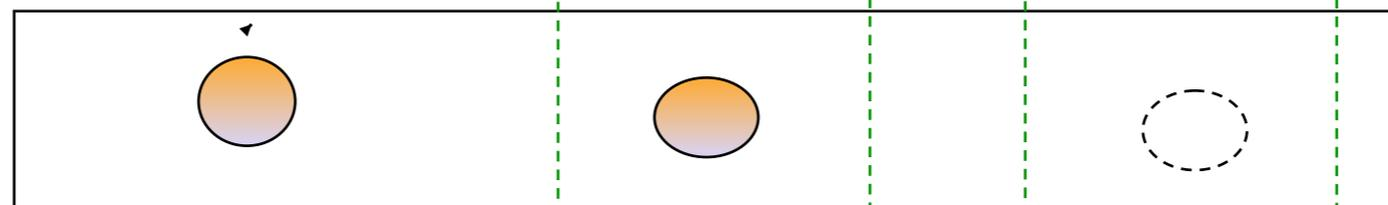
Biophys J. 2003 Jan;84(1):588-98

Single Molecule Imaging

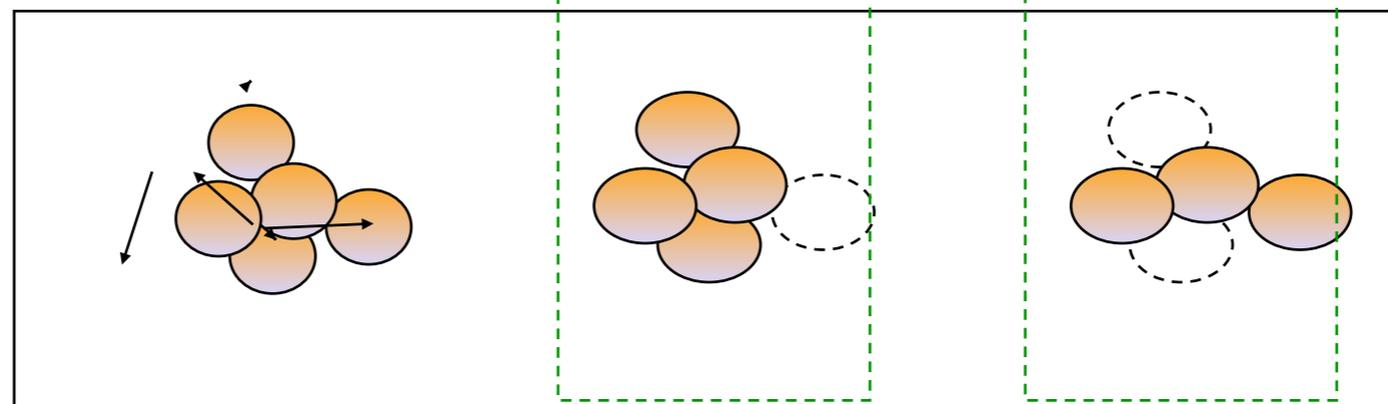
Fluorescence Polarization

Emission Polarization

Single Molecule



Aggregates



J Biomed Opt. (2003) 8(3):391-5

2PE and GFP

Multi-photon switching dynamics of single green fluorescent proteins

G. Chirico,¹ F. Cannone,¹ A. Diaspro,² S. Bologna,³ V. Pellegrini,⁴ R. Nifosì,⁴ and F. Beltram⁴

¹*INFM and Department of Physics, University of Milano Bicocca, Piazza della scienza 3, 20126 Milano, Italy*

²*INFM and Department of Physics, University of Genoa, Via Dodecaneso 33, 16146 Genova, Italy*

³*Department of Biochemistry and Molecular Biology, University of Parma, 43100 Parma, Italy*

⁴*NEST-INFM and Scuola Normale Superiore, Piazza dei Cavalieri 7, I-56126 Pisa (Italy)*

(Dated: February 19, 2004)

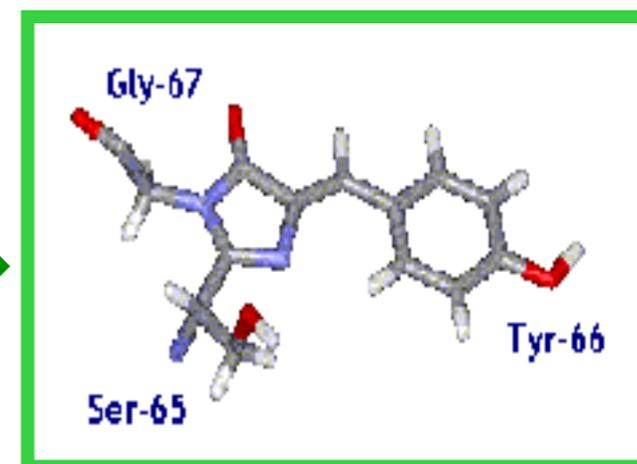
Multi-photon driven photo-switching between dark and bright (fluorescent) states of a green fluorescent protein (GFP) mutant is demonstrated. A single-molecule investigation shows the existence of two distinct bright states that display sharp two-photon cross-section bands peaked at 780nm and at 870nm. Fluorescence of these two species can be independently switched on and off. These results highlight a new photoconversion pathway for photochromic GFPs and can have significant applications in multi-photon confocal microscopy and in optical data-storage architectures.

CHIRICO G., CANNONE F., DIASPRO A., BOLOGNA S., PELLEGRINI V., NIFOS R., BELTRAM F. (2004). PHYSICAL REVIEW E, STATISTICAL, NONLINEAR, AND SOFT MATTER PHYSICS. vol. 70, pp. 03-0901

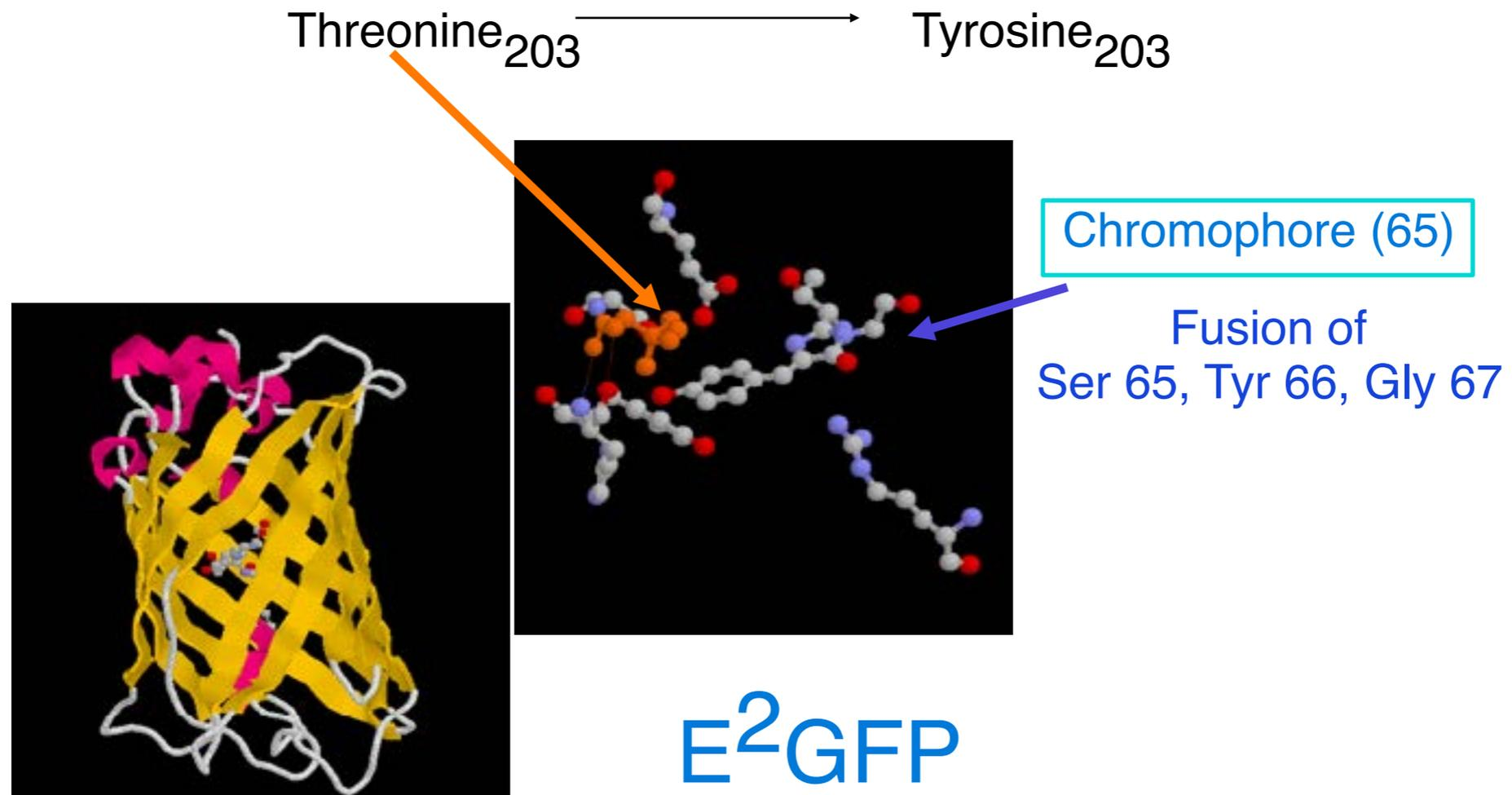
CHIRICO G., DIASPRO A., CANNONE F., COLLINI M., BOLOGNA S., PELLEGRINI V., BELTRAM F. (2005). Selective fluorescence recovery after bleaching of single E2GFP proteins induced by two-photons excitation. CHEMPHYSICHEM. vol. 6, pp. 328-335



238 AA
11 β -barrel ; 4 α -helices
Gly-67, Tyr-66, Ser-65



2PE and GFP



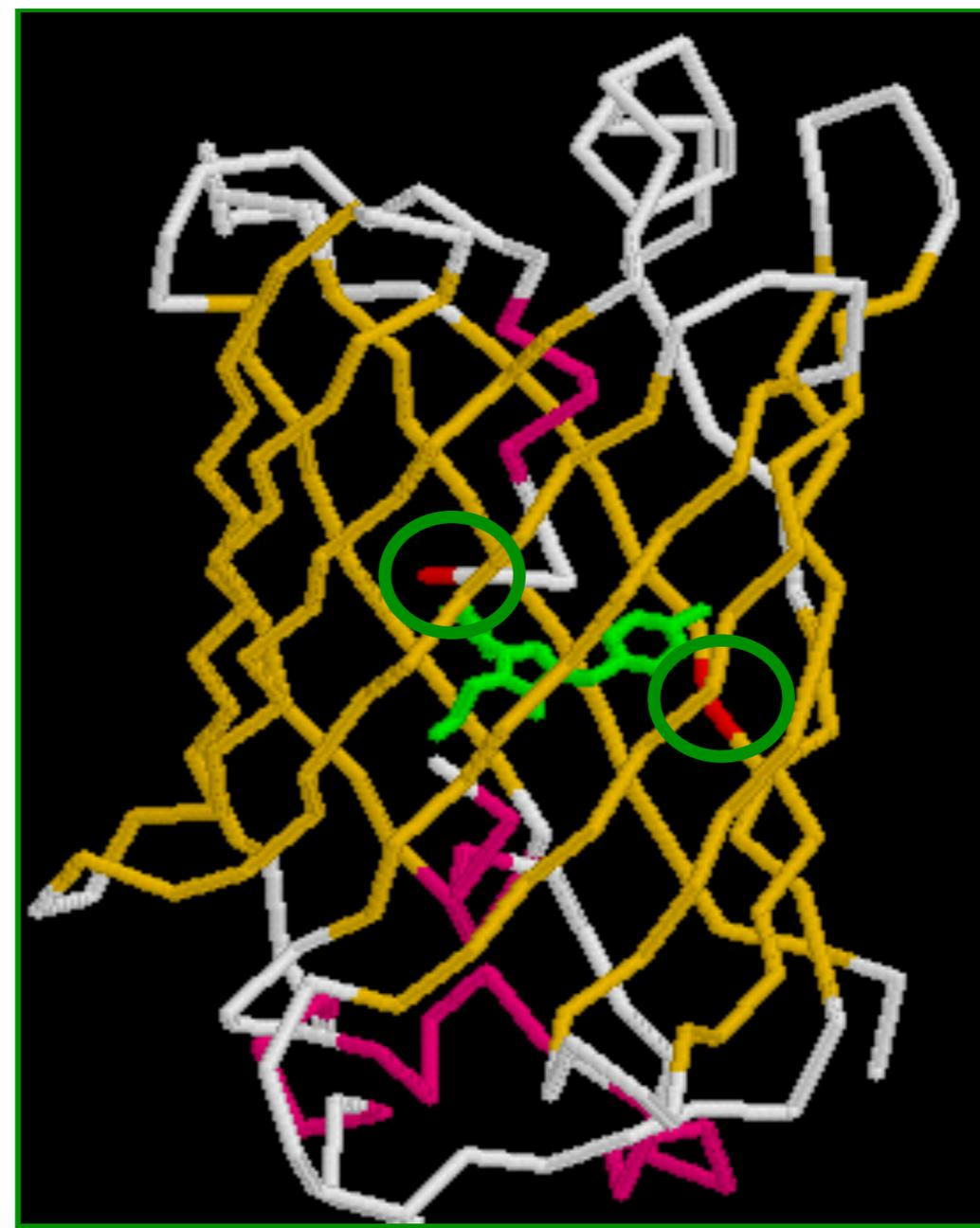
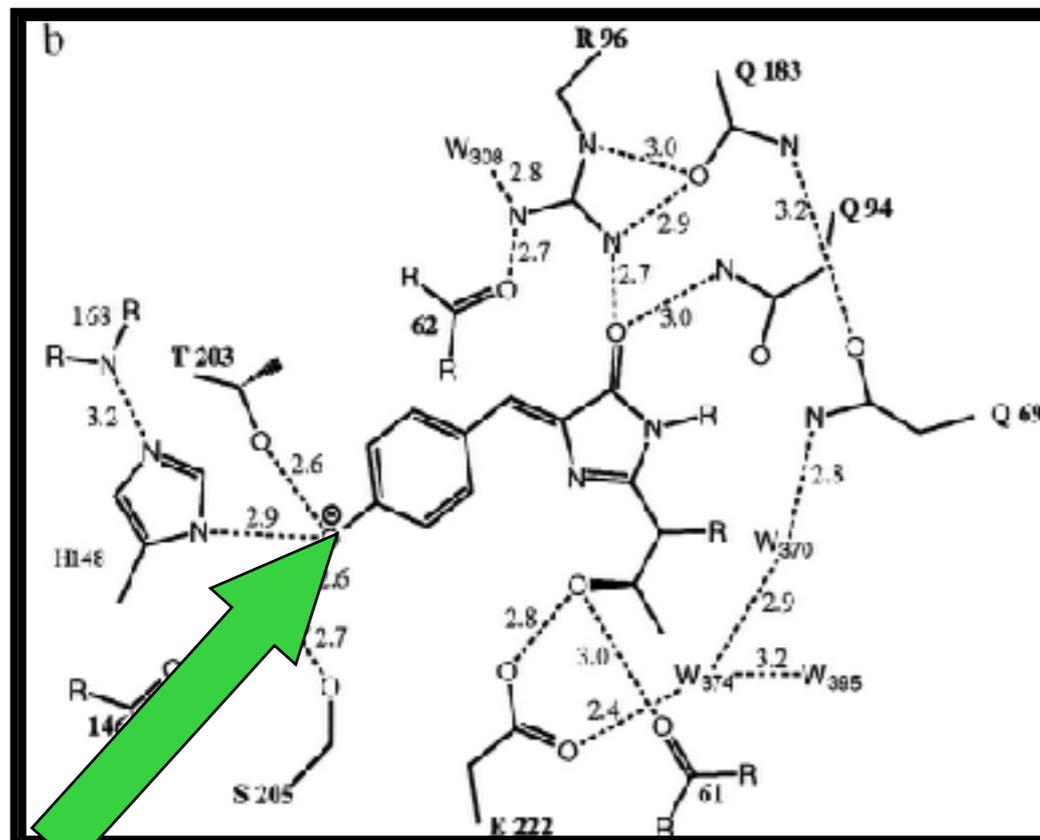
Cinelli RA, Ferrari A, Pellegrini V, Tyagi M, Giacca M, Beltram F., Photochem Photobiol. 2000 Jun;71(6):771-6.

2PE and GFP

Switchable - GFP

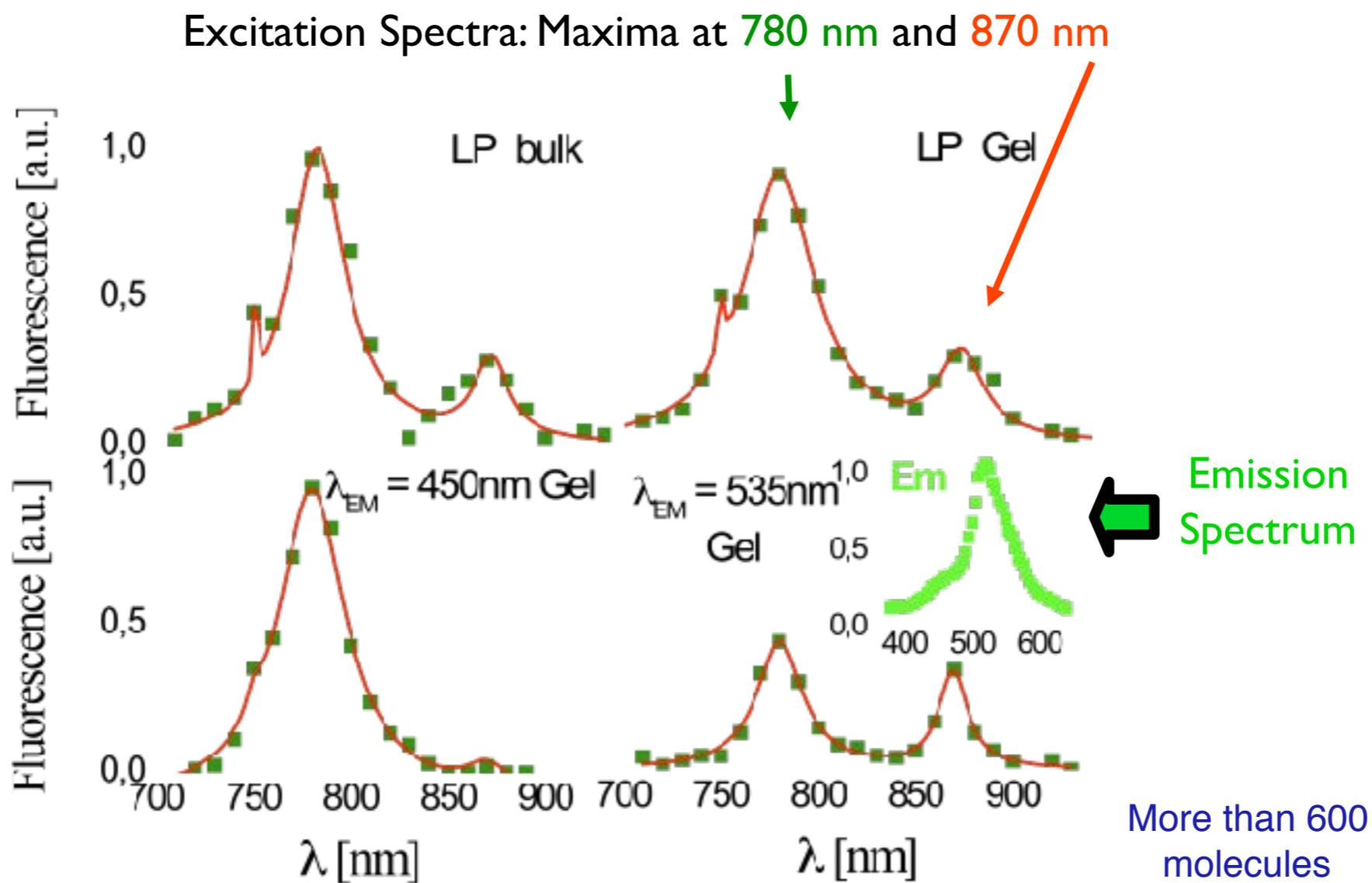
E²GFP

Mutations:
Ser65Thr + Phe64Leu
Thr203Tyr



2PE and GFP

Two-Photon Spectra

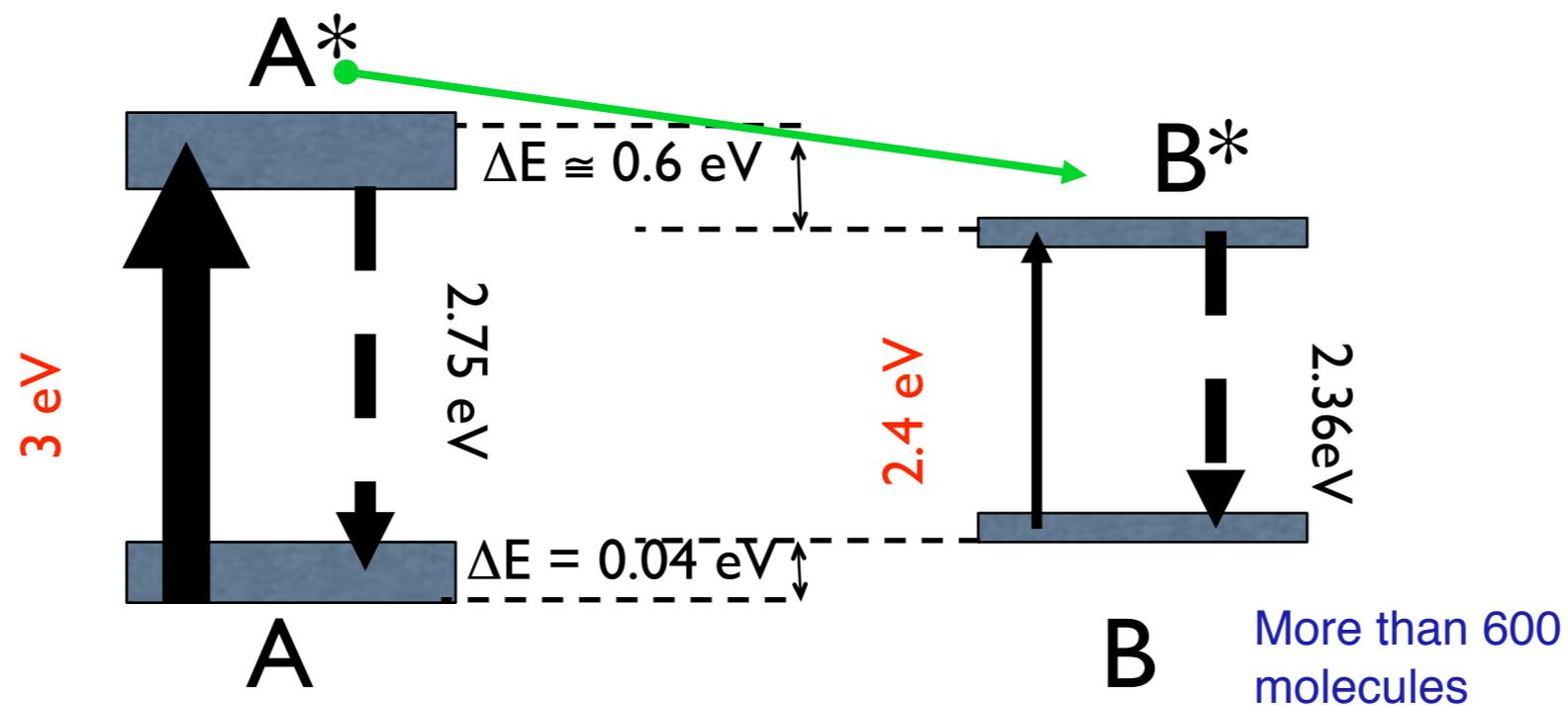


2PE and GFP

Ground States

State A Exc 780 nm
Neutral Em 450 nm
Lifetime 1.0 ns

State B Exc 870 nm
Anionic Em 535 nm
Lifetime 2.8 ns



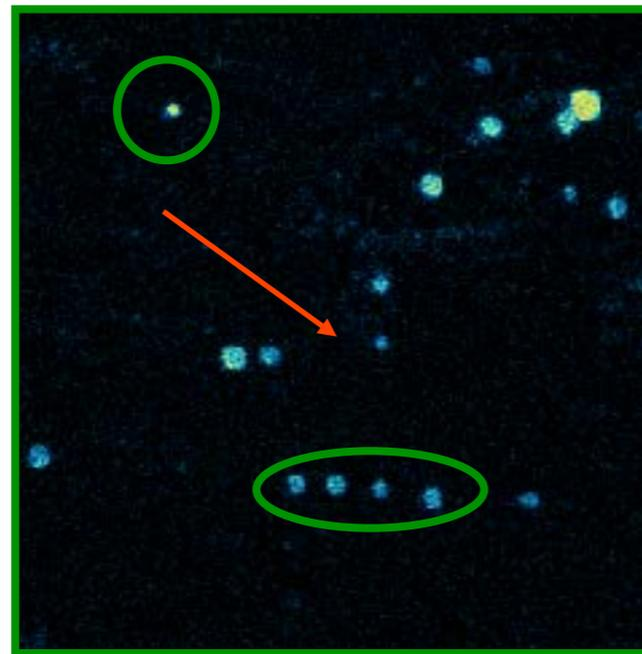
Slide credit: Fabio Cannone, Milano-Bicocca

Alberto Diaspro, Nanoscopy, Istituto Italiano di Tecnologia

2PE and GFP

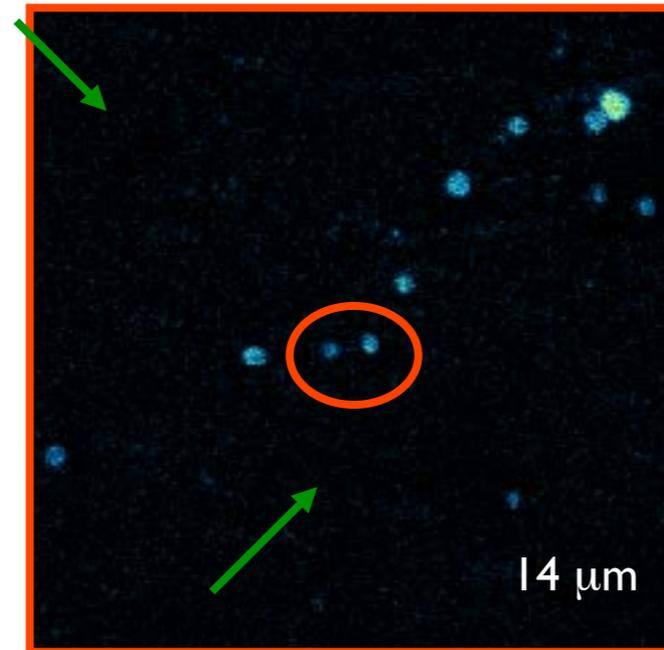
Ground States Distribution

$$n_A / n_B = 4.4 \pm 1.5$$



A

Exc 780 nm
Em 450 nm

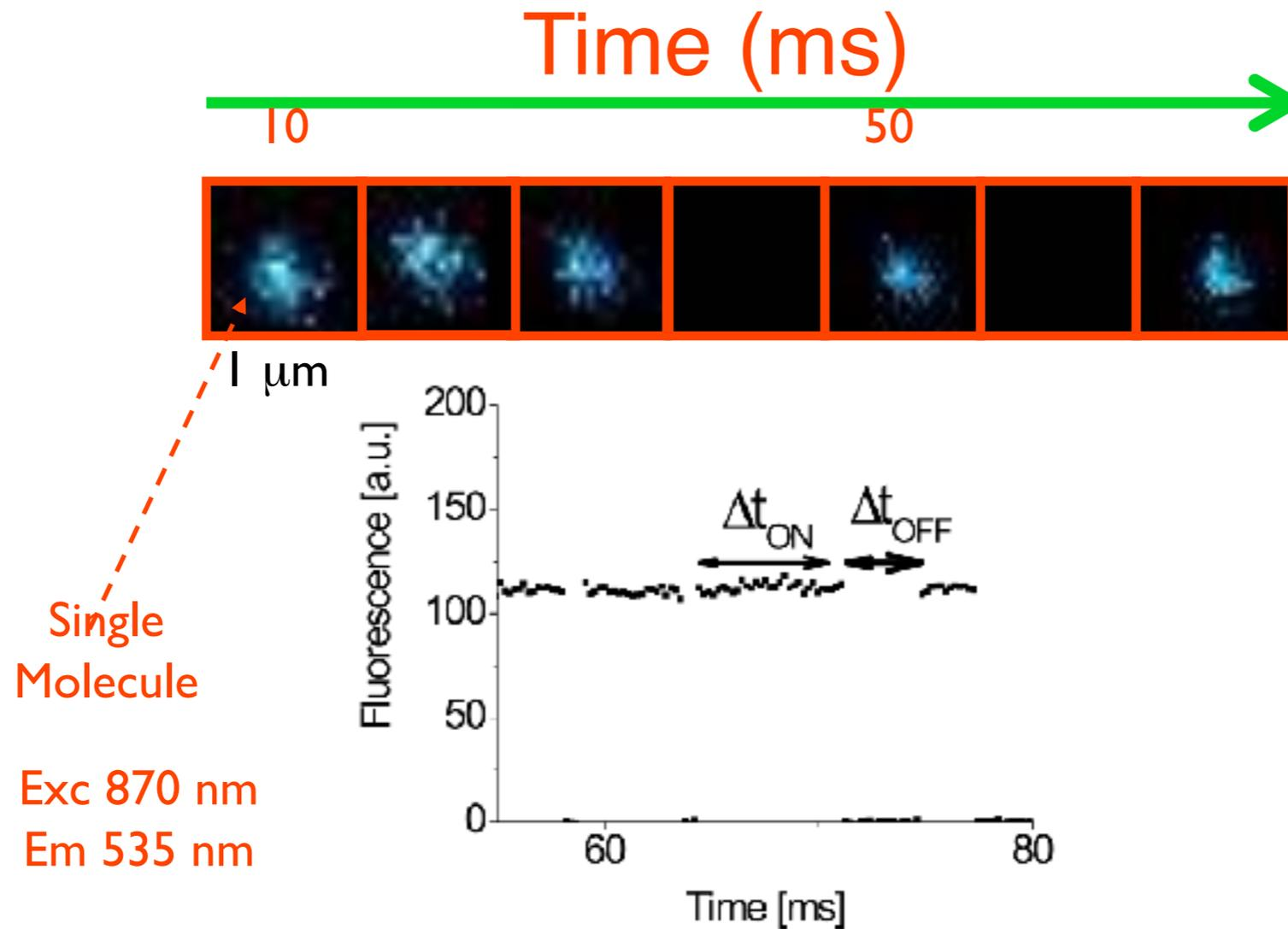


B

Exc 870 nm
Em 535 nm

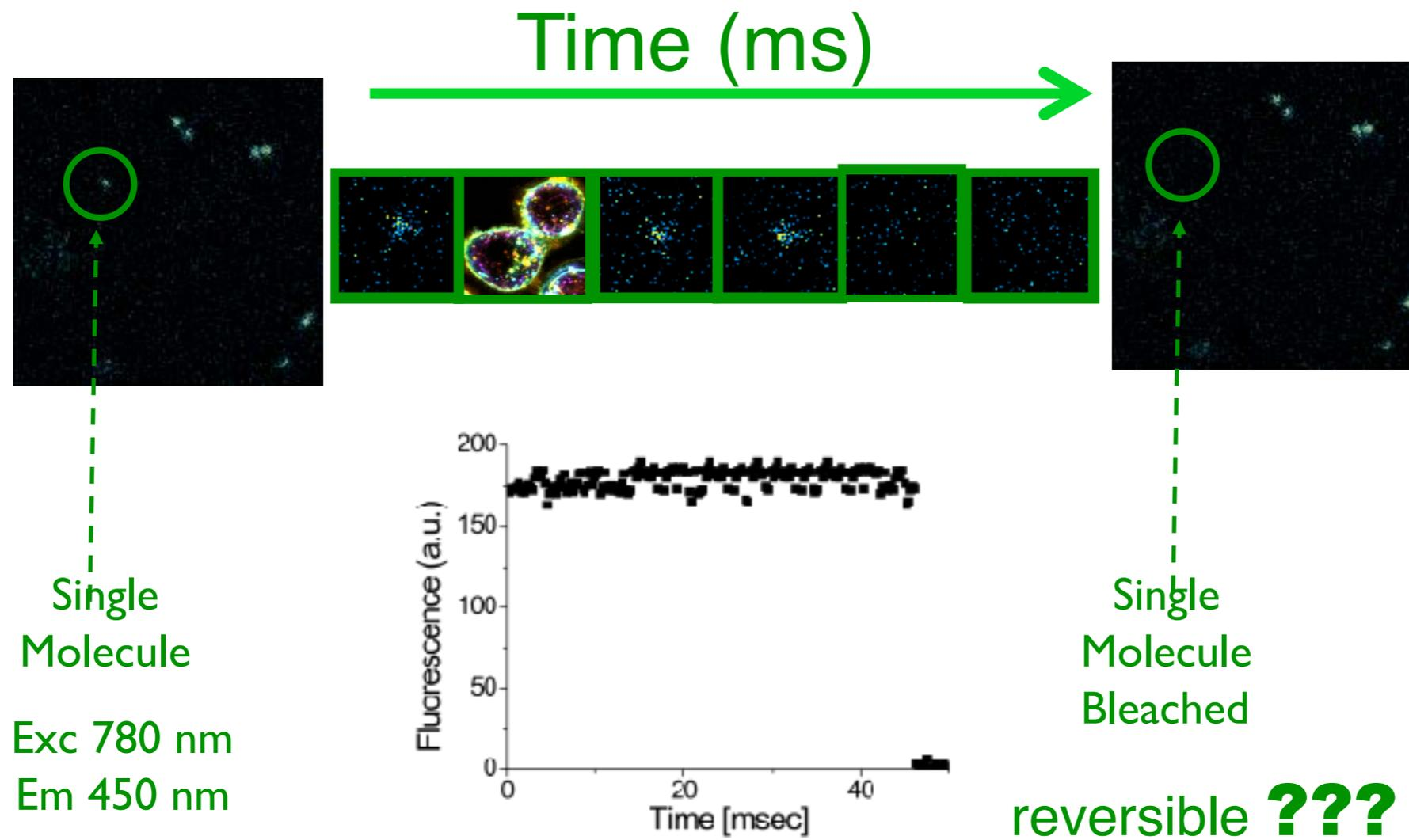
2PE and GFP

Blinking: State B



2PE and GFP

Bleaching: State A and B

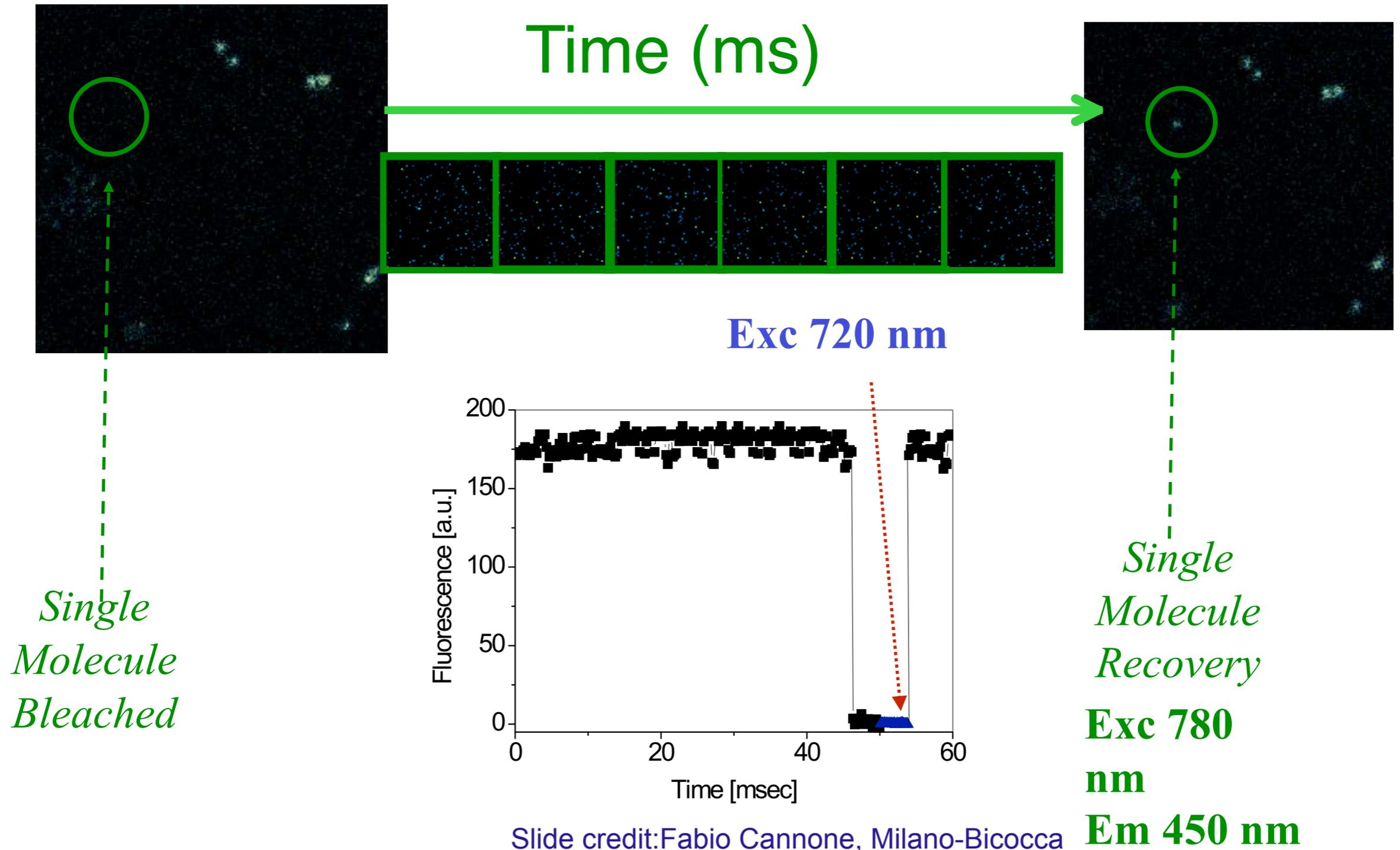


Slide credit: Fabio Cannone, Milano-Bicocca

Alberto Diaspro, Nanoscopy, Istituto Italiano di Tecnologia

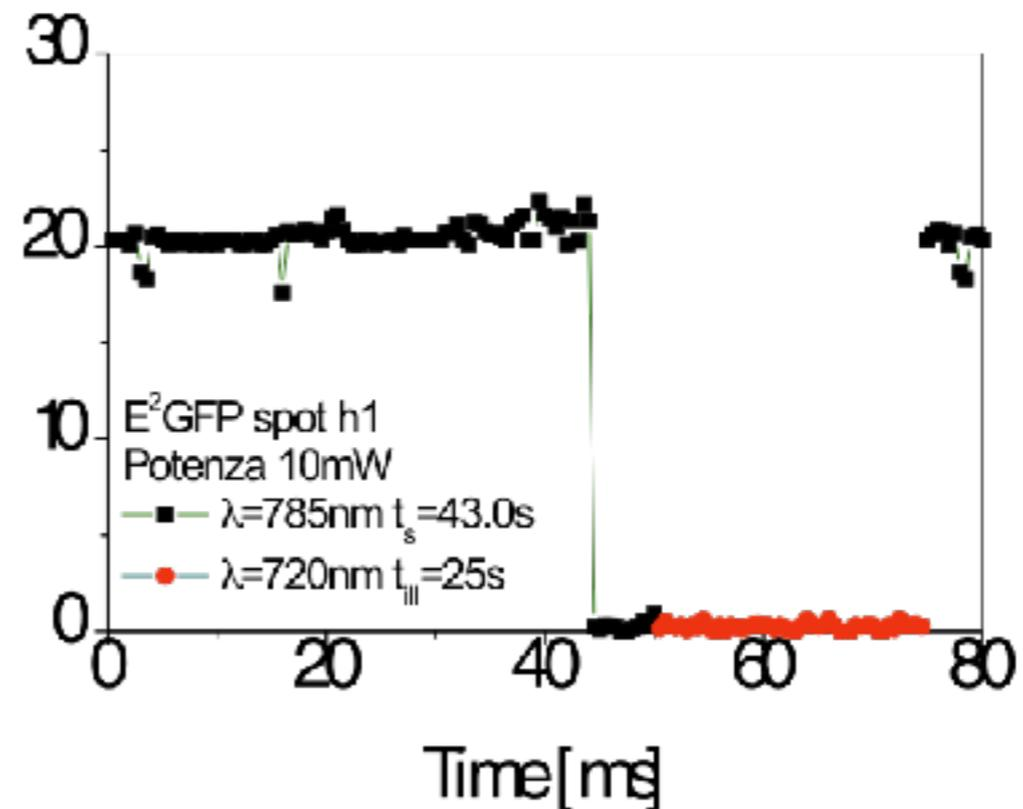
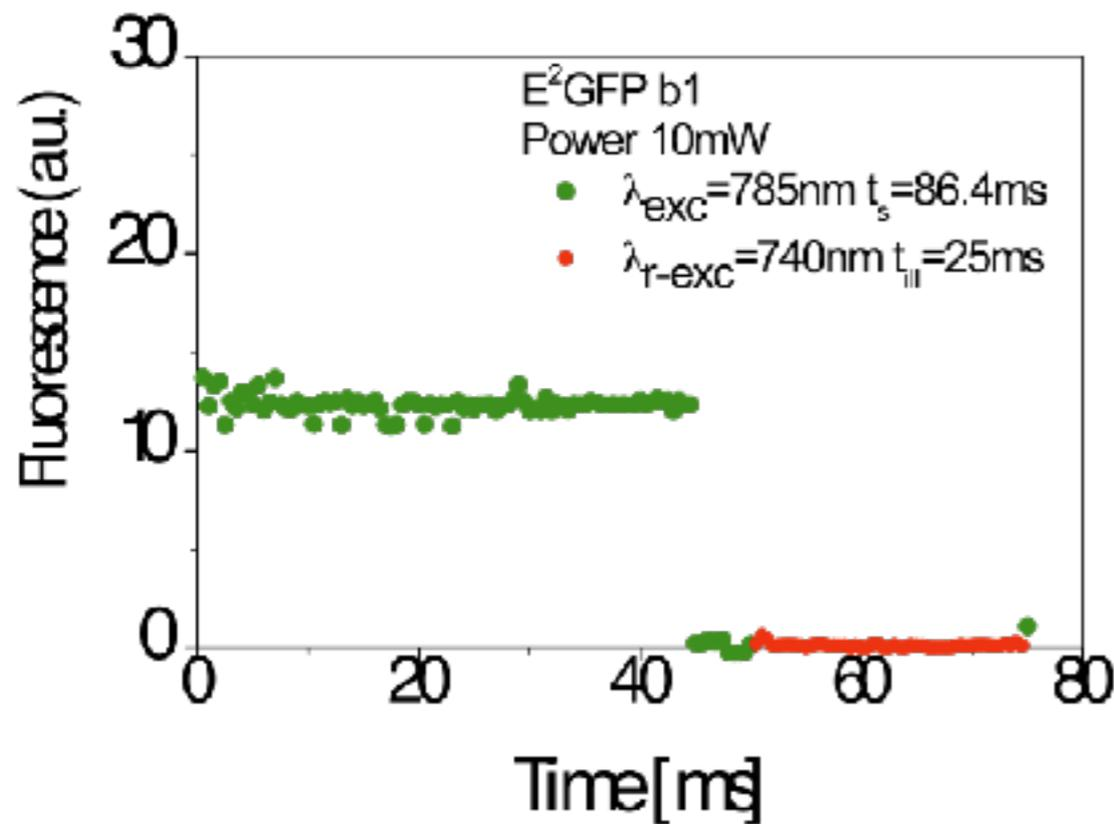
2PE and GFP

Fluorescence recovery



2PE and GFP

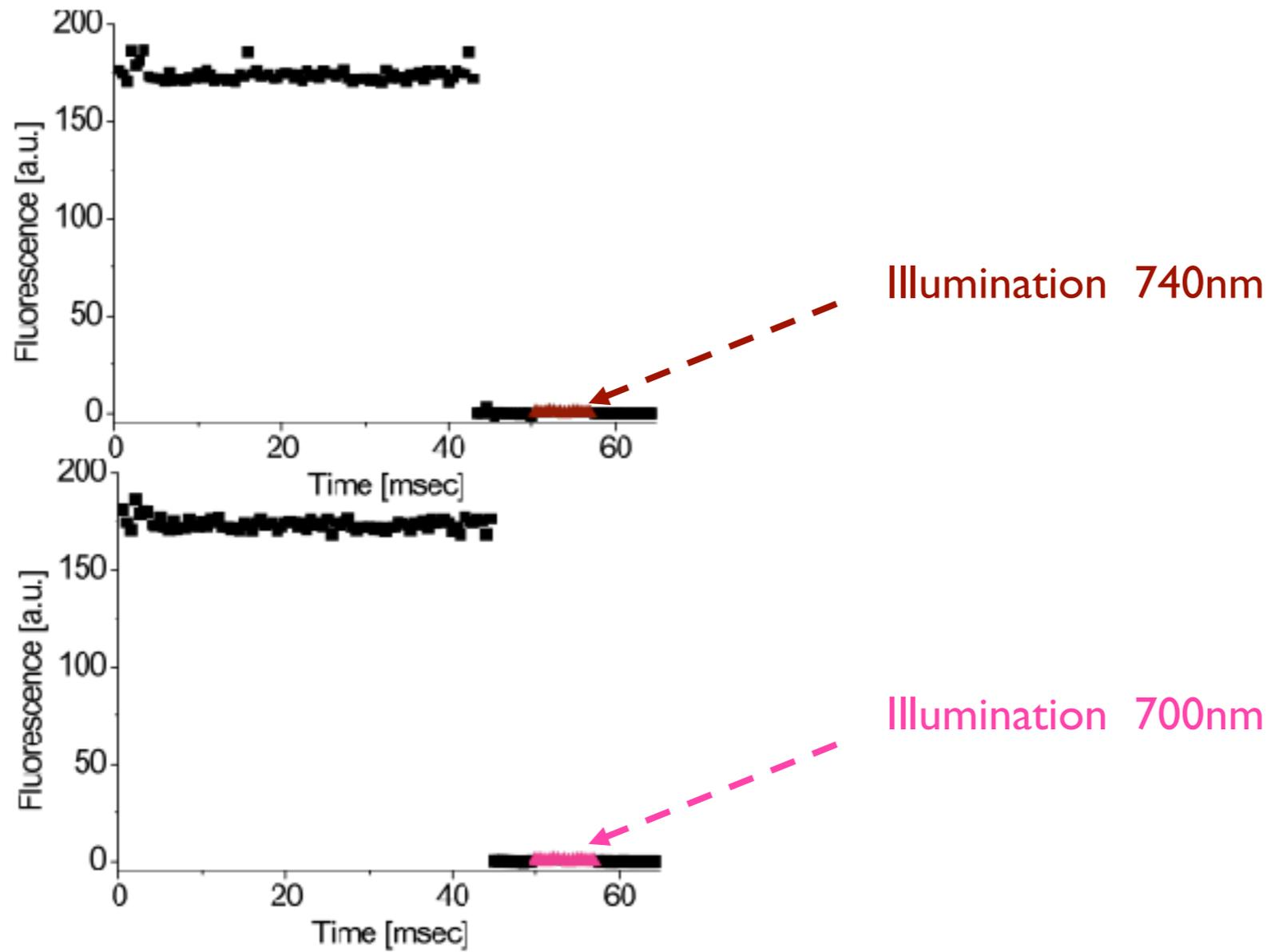
Fluorescence Recovery



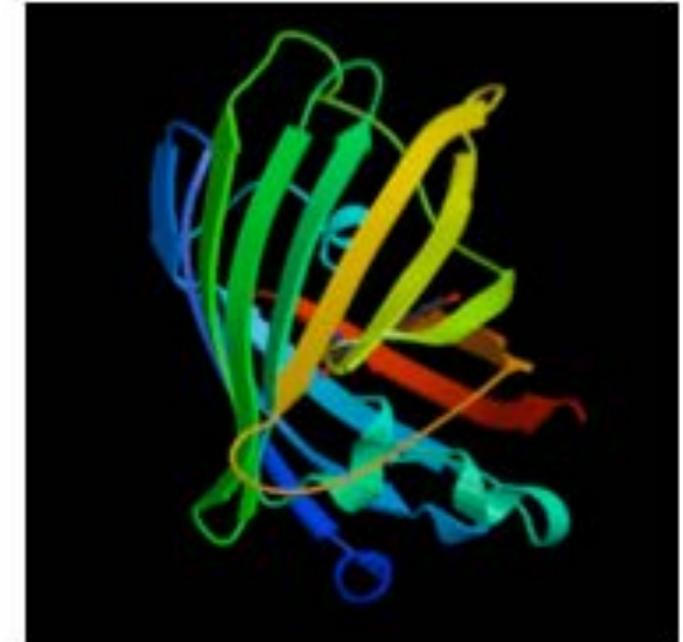
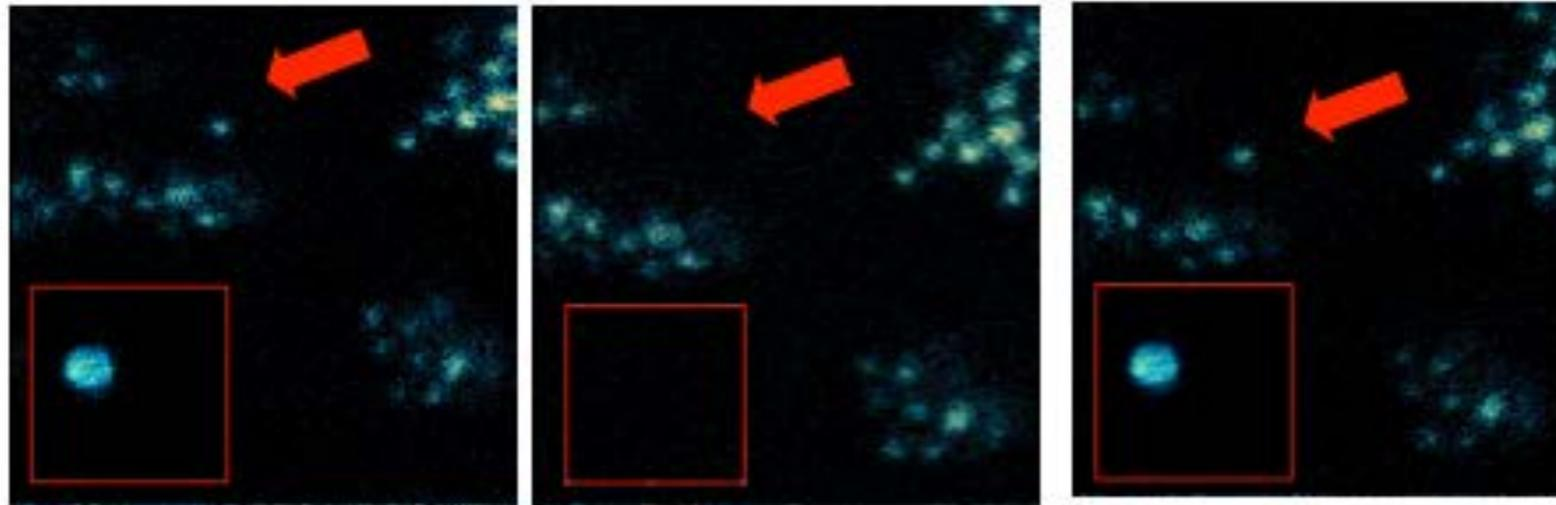
E²GFP

2PE and GFP

Fluorescence Recovery



2PE and GFP

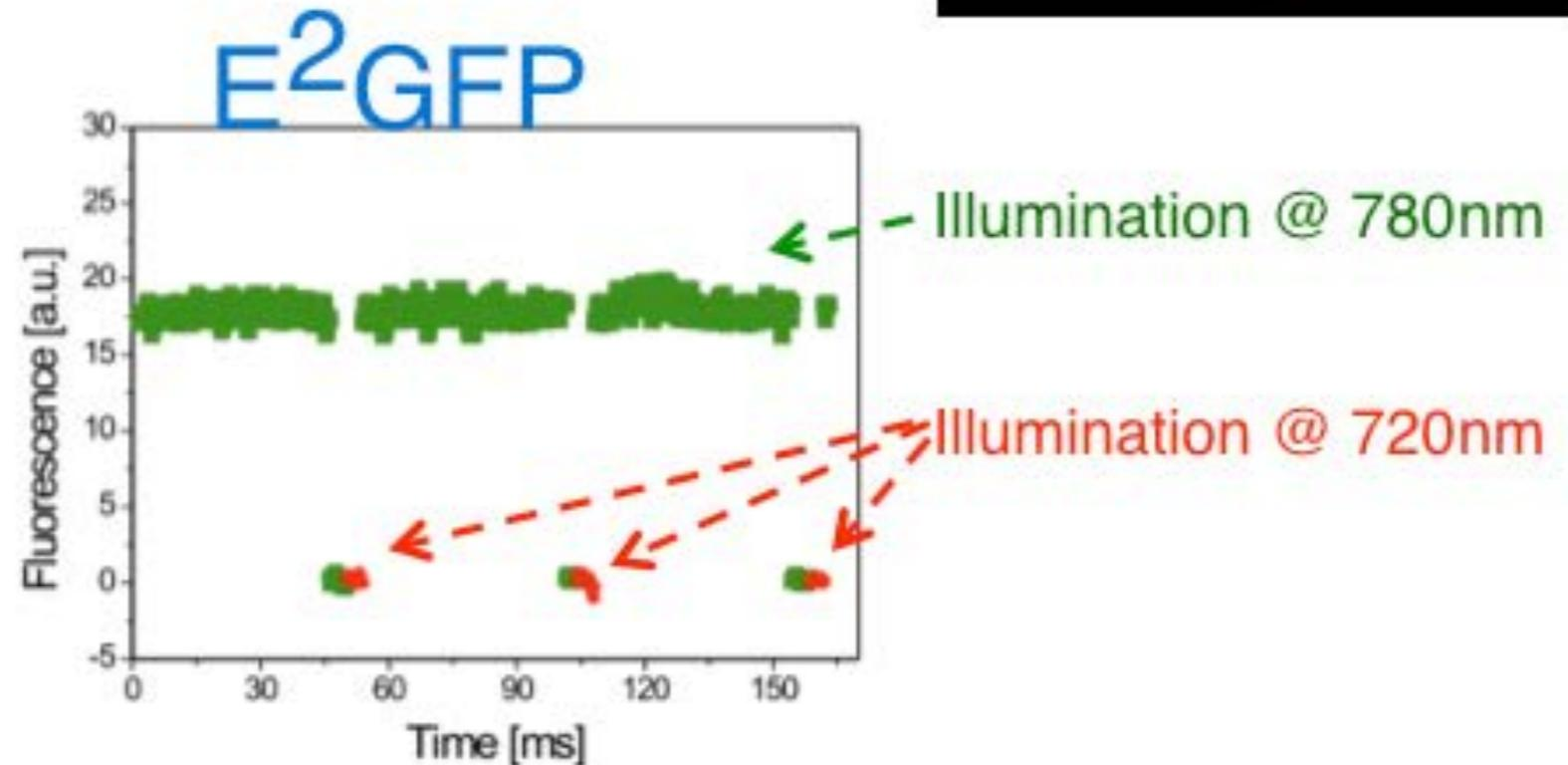


TPE @ 785 nm

TPE @ 720 nm

TPE @ 785 nm

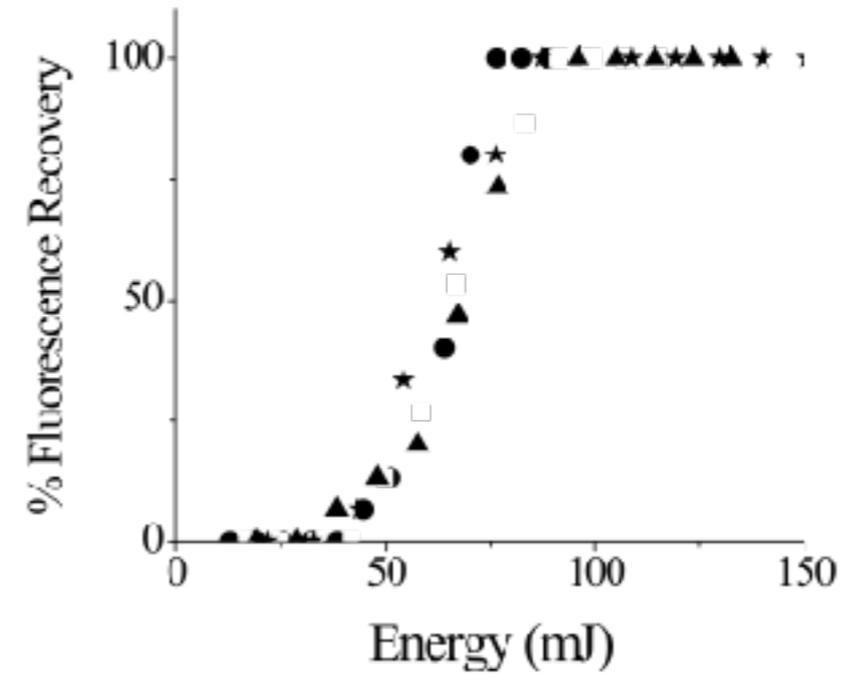
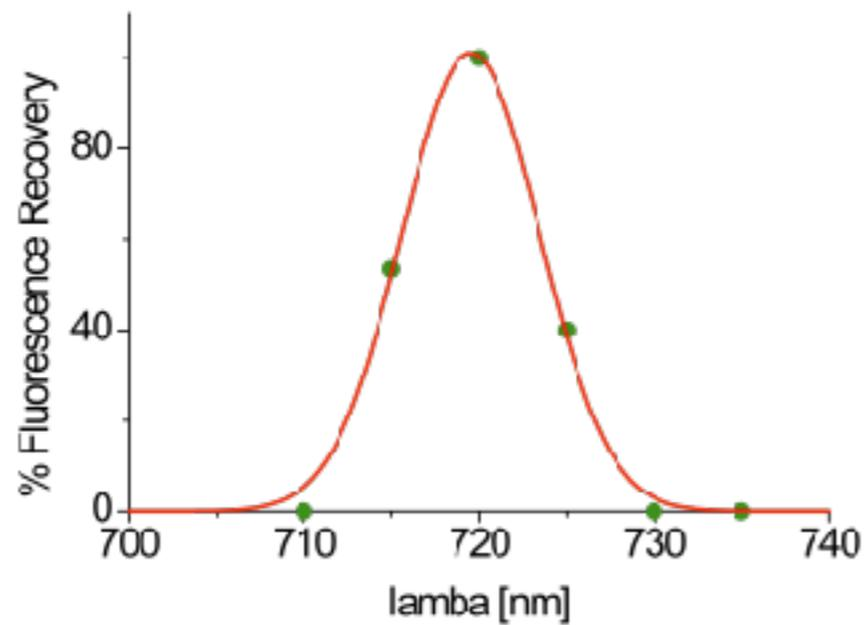
E²GFP in silica GEL, maximum excitation within 700-800 nm range @ 785; after imaging photobleaching @ 785; photocycling @ 720 nm - no photorecovery @ 710/730 -; final imaging @ 785.



PHYS REV E STAT NONLIN SOFT MATTER PHYS. 2004 SEP;70(3 PT 1):030901

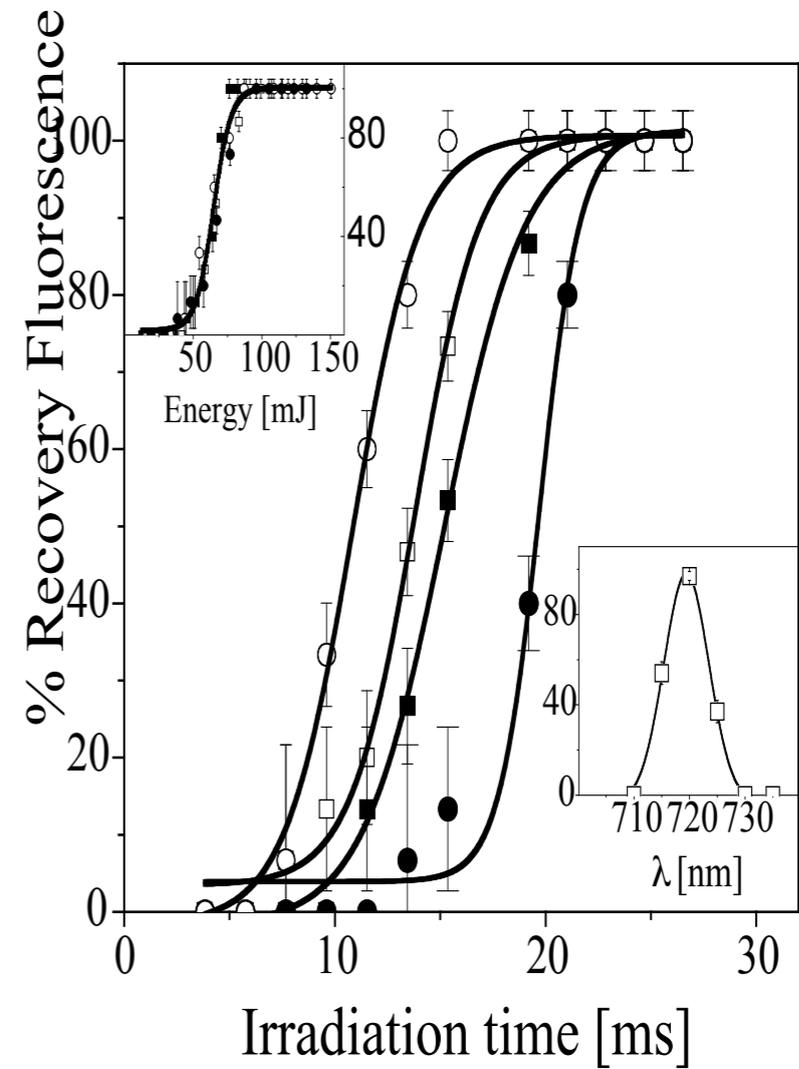
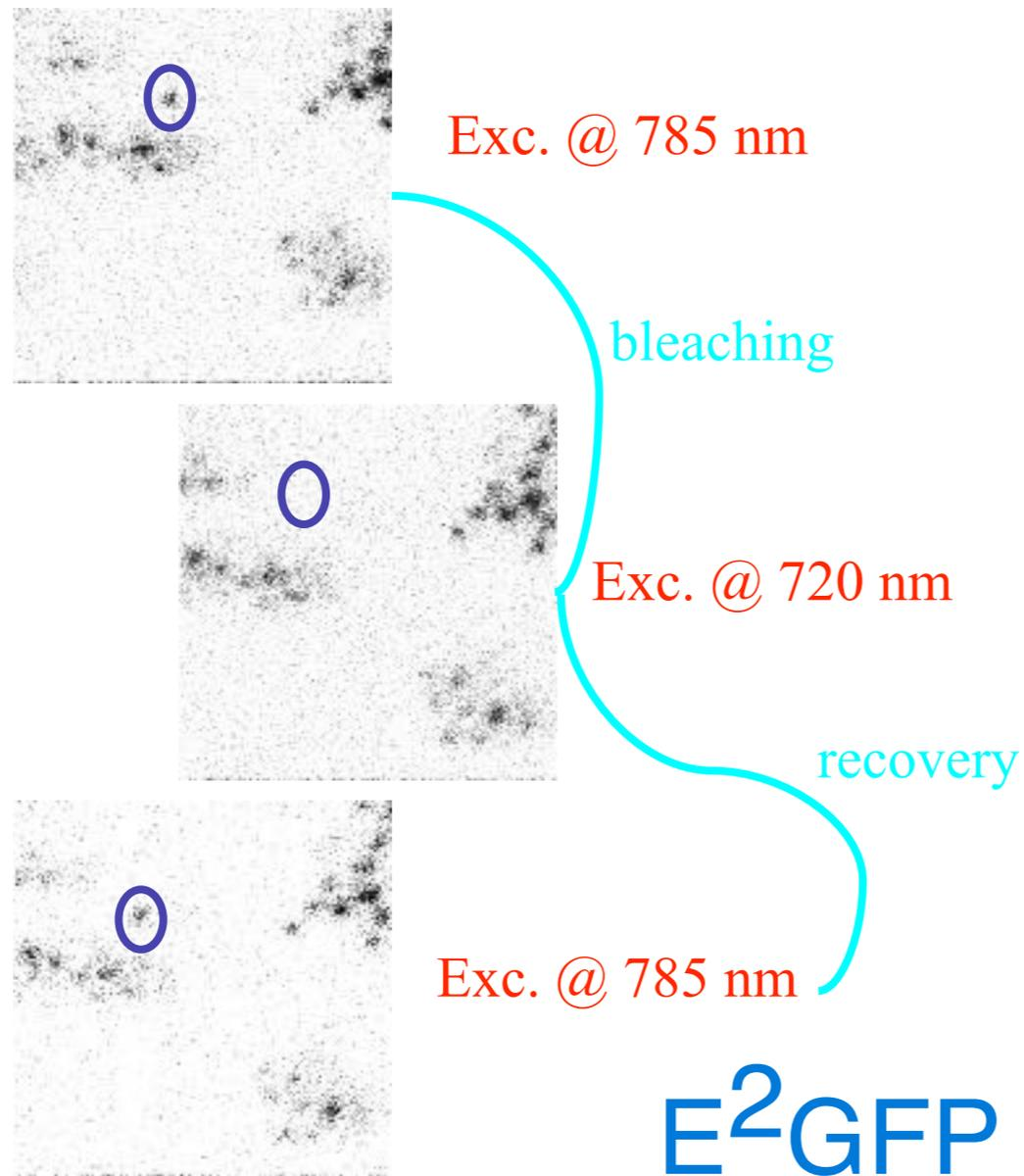
2PE and GFP

Recovery Threshold Energy



$$E = P_{720} \Delta t = \text{power} \times (\text{illumination time at 720 nm})$$

2PE and GFP

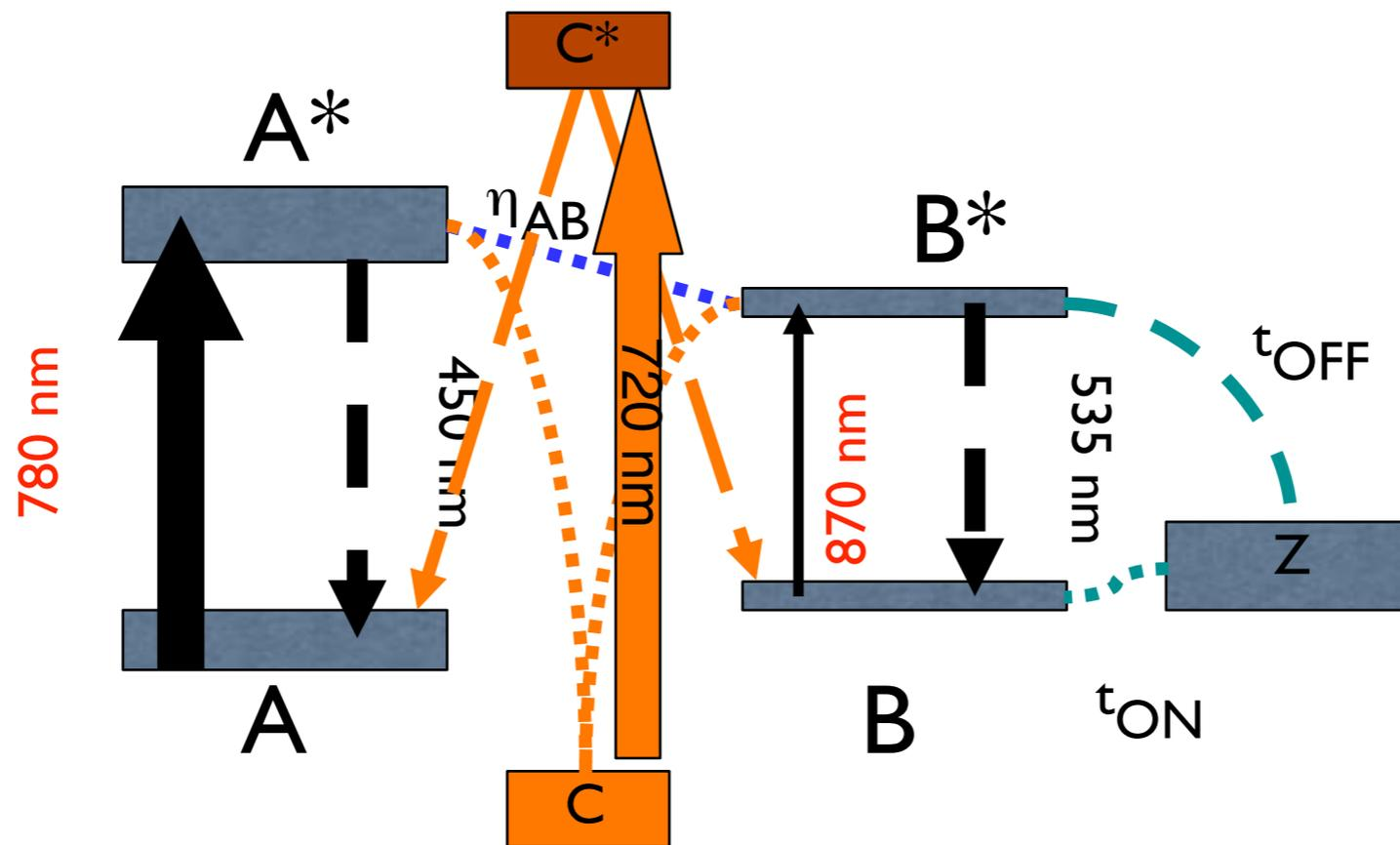


Slide credit: Giberto Chirico, Milano-Bicocca

Alberto Diaspro, Nanoscopy, Istituto Italiano di Tecnologia

2PE and GFP

Energy Level Diagram



PHYS REV E STAT NONLIN SOFT MATTER PHYS. 2004 SEP;70(3 PT 1):030901

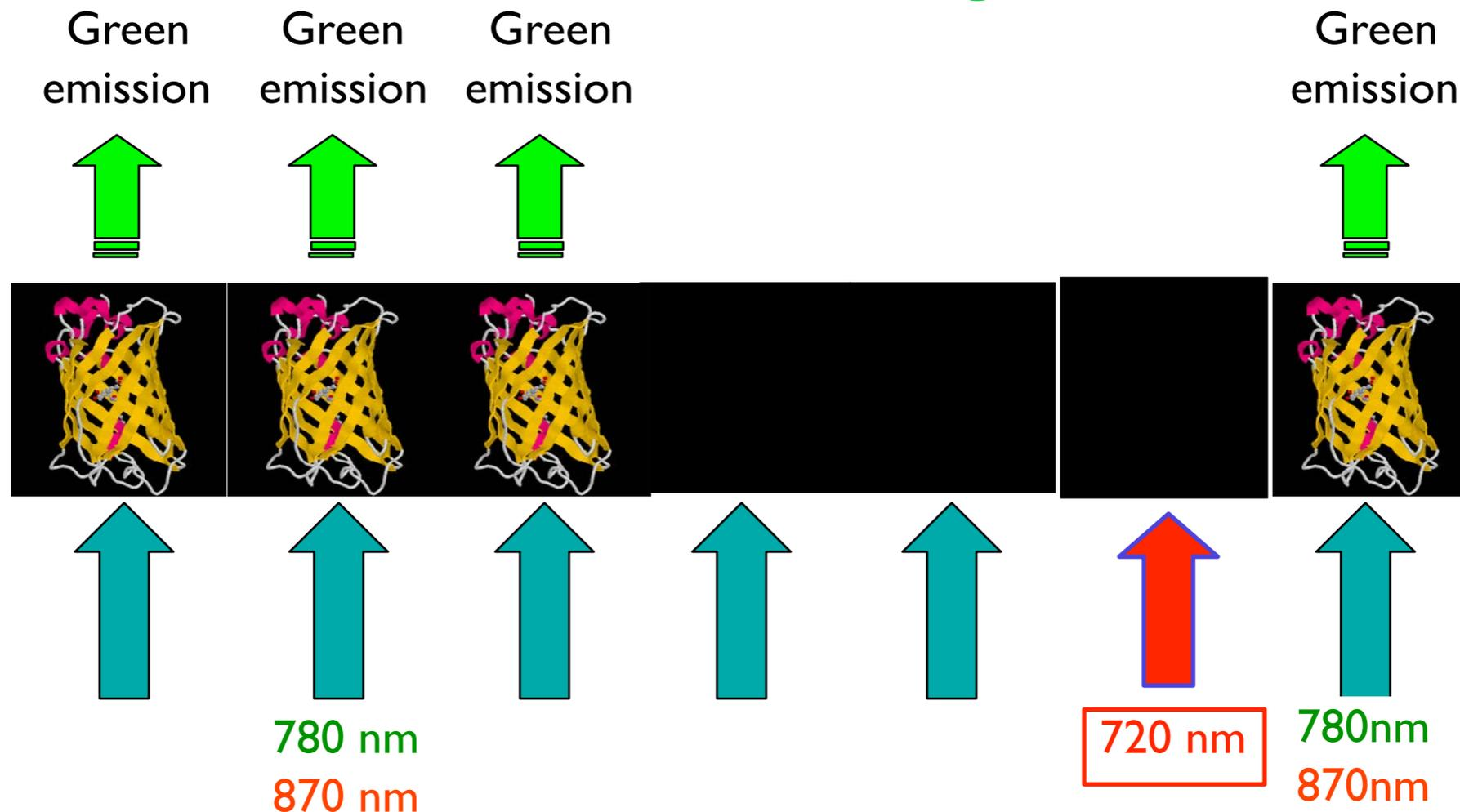
Slide credit:Giberto Chirico, Milano-Bicocca

Alberto Diaspro, Nanoscopy, Istituto Italiano di Tecnologia

2PE and GFP

E^2 GFP

Two Photon Switching Protein



Switchable - GFP - Single molecule

PHYS REV E STAT NONLIN SOFT MATTER PHYS. 2004 SEP;70(3 PT 1):030901

2PE and GFP PA-GFP

(green fluorescent protein → photo activatable green fluorescent protein)

1346

Biophysical Journal Volume 89 August 2005 1346–1352

Two-Photon Activation and Excitation Properties of PA-GFP in the 720–920-nm Region

Marc Schneider,^{*} Sara Barozzi,[†] Ilaria Testa,^{*‡} Mario Faretta,[†] and Alberto Diaspro^{*‡§}

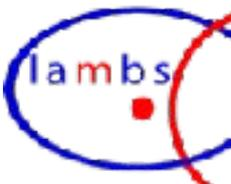
^{*}INFM Genoa, Department of Physics, University of Genoa, I-16146 Genoa, Italy; [†]European Institute of Oncology, Department of Experimental Oncology, 20141 Milan, Italy; [‡]LAMBS-MicroScoBio Research Center, University of Genoa, 16146 Genoa, Italy; and [§]IFOM, Istituto FIRC di Oncologia Molecolare, 20139 Milan, Italy

ABSTRACT This report covers the two-photon activation and excitation properties of the PA-GFP, a photoactivatable variant of the *Aequorea victoria* green fluorescent protein in the spectral region from 720 to 920 nm. It is known from this special form of the molecule that it has an increased level of fluorescence emission when excited at 488 nm after irradiation at $\lambda \sim 413$ nm, under single-photon excitation conditions. Here, we show that upon two-photon irradiation, PA-GFP yields activation in the spectral region from 720 to 840 nm. After photoactivation, the excitation spectrum shifts maintaining the very same emission spectrum of the single-photon case for the native and photoactivated protein. Additionally, when comparing the conventional photoactivation at $\lambda = 405$ nm with a two-photon one, a sharper and better controllable three-dimensional volume of activation is obtained.

Submitted October 14, 2004, and accepted for publication May 16, 2005.



Alberto Diaspro, Nanoscopy, Istituto Italiano di Tecnologia



2PE and GFP PA-GFP

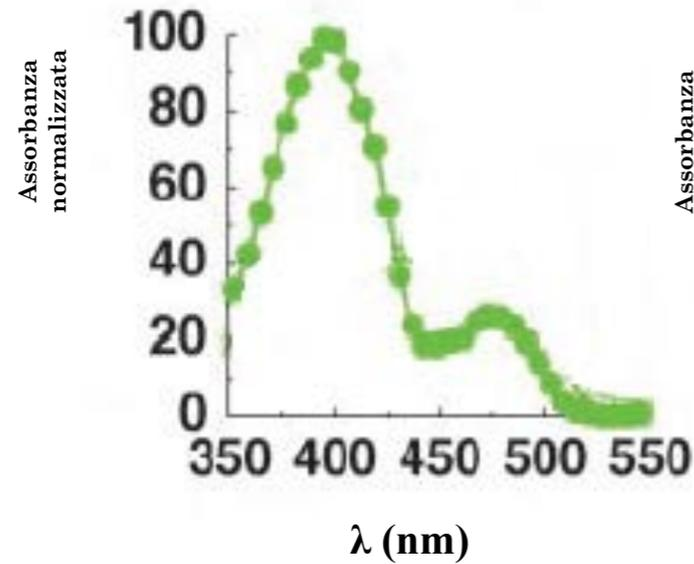
(green fluorescent protein → photo activatable green fluorescent protein)

Photoactivatable - Protein

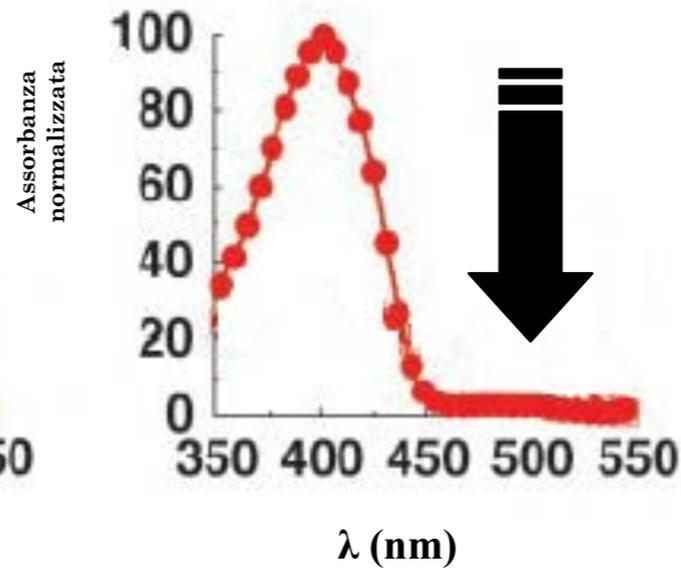
aa mutation at 203 position:

Treonina

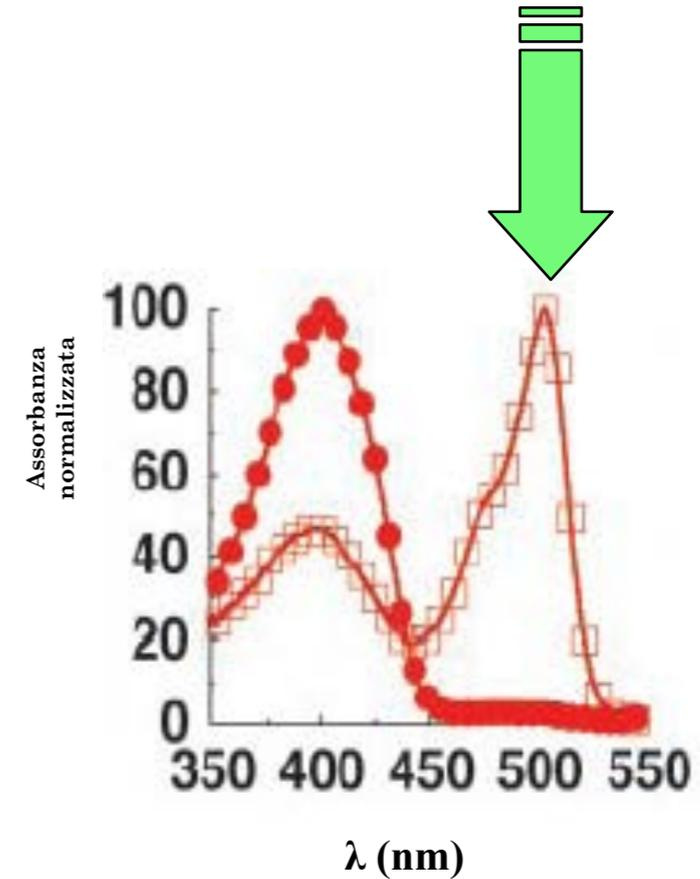
Istidina



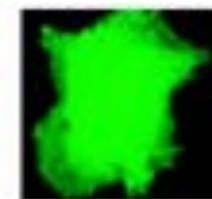
GFP



PA-GFP



PA-GFP*



Patterson GH, Lippincott-Schwarz J. (2002) Science 297:1873-1877.

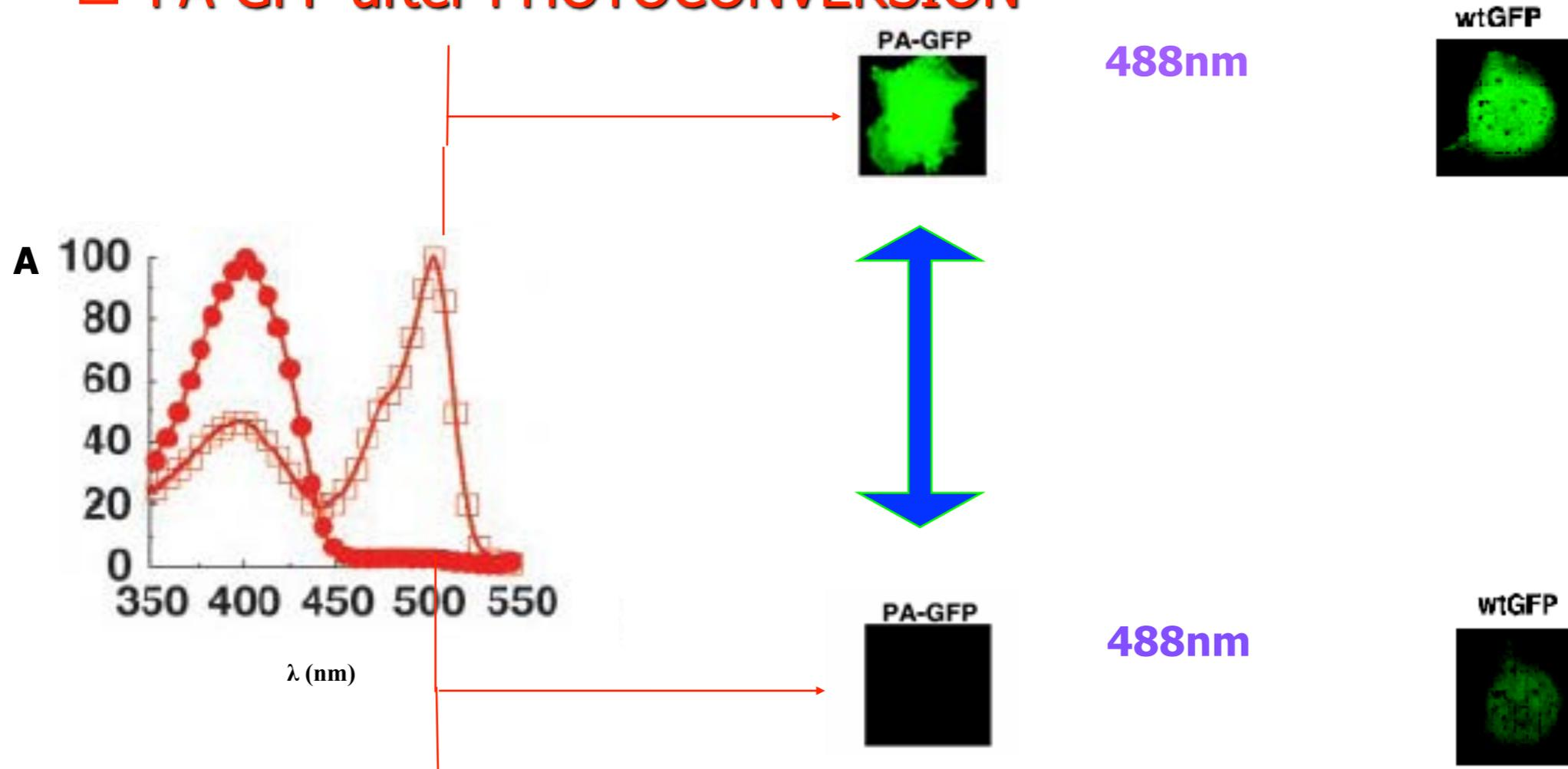
2PE and GFP PA-GFP

(green fluorescent protein → photo activatable green fluorescent protein)

Photoactivatable - Protein

What's new is the extraordinary enhancement achieved: wt-GFP shows a 2-3 fold increase in fluorescence after activation, PA-GFP fluorescence increases 50-100 fold.

□ PA-GFP after PHOTOCOVERSION

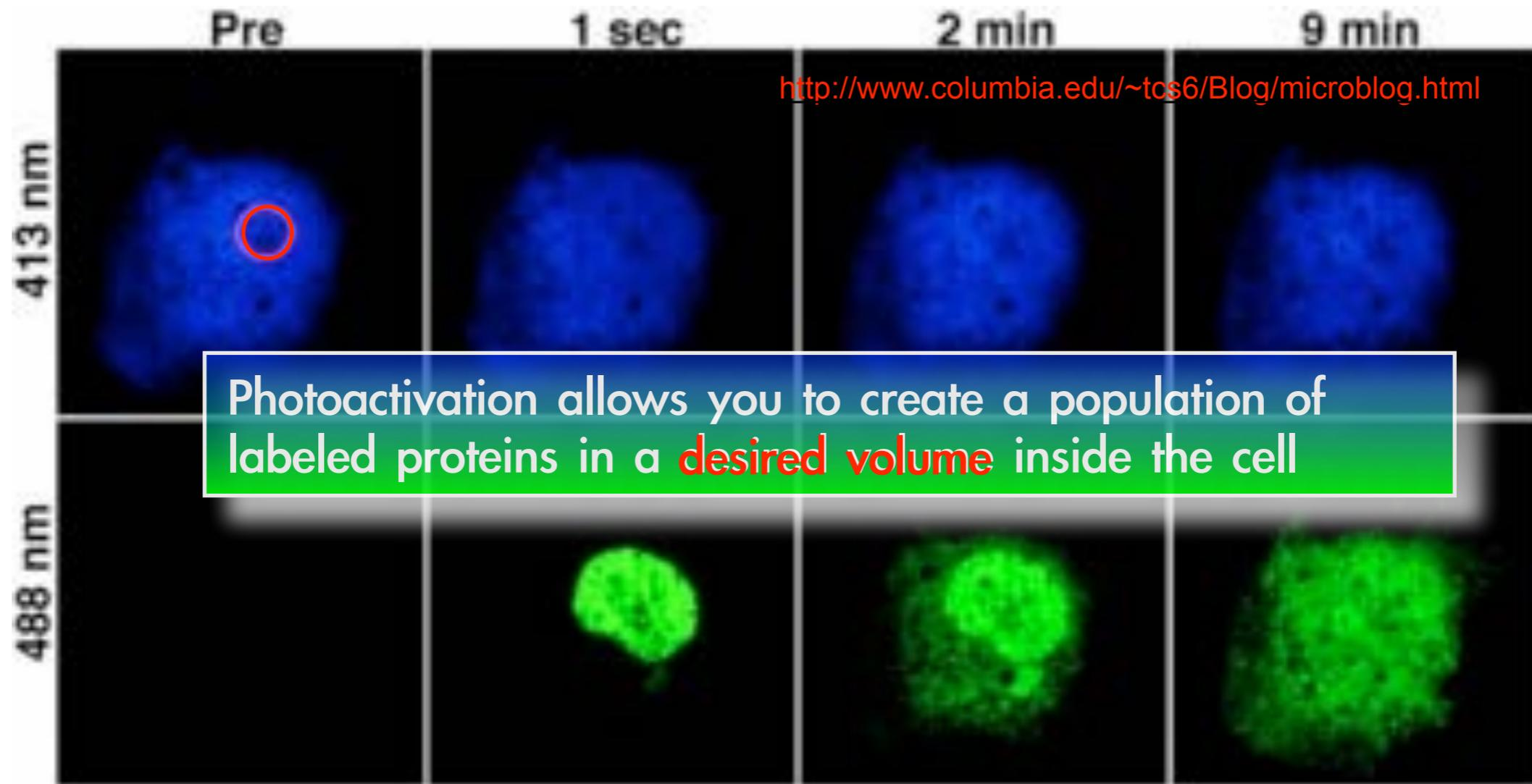


● PA-GFP before PHOTOCOVERSION

2PE and GFP PA-GFP

(green fluorescent protein → photo activatable green fluorescent protein)

Photoactivatable - Protein



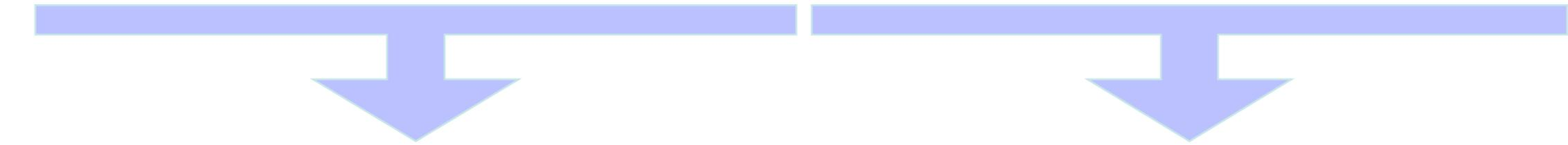
The area inside the red circle, which is within the cell nucleus, is photoactivated for ~1 s at 413 nm. After 1 second, GFP is seen throughout the nucleus. Between 2 and 9 minutes later, much of the GFP has distributed throughout the cytoplasm.

Patterson GH, Lippincott-Schwarz J. (2002) Science 297:1873–1877.

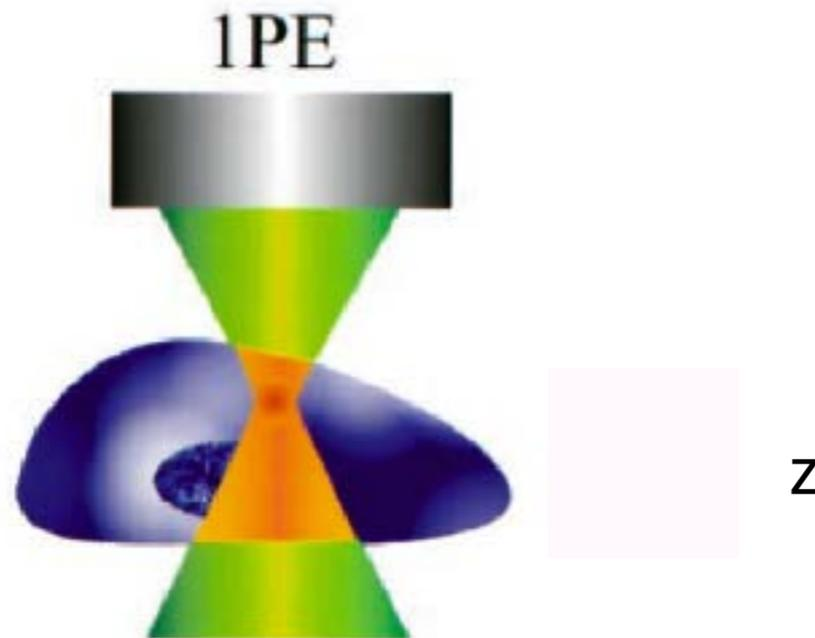
2PE and GFP PA-GFP

(green fluorescent protein → photo activatable green fluorescent protein)

Single-photon interaction

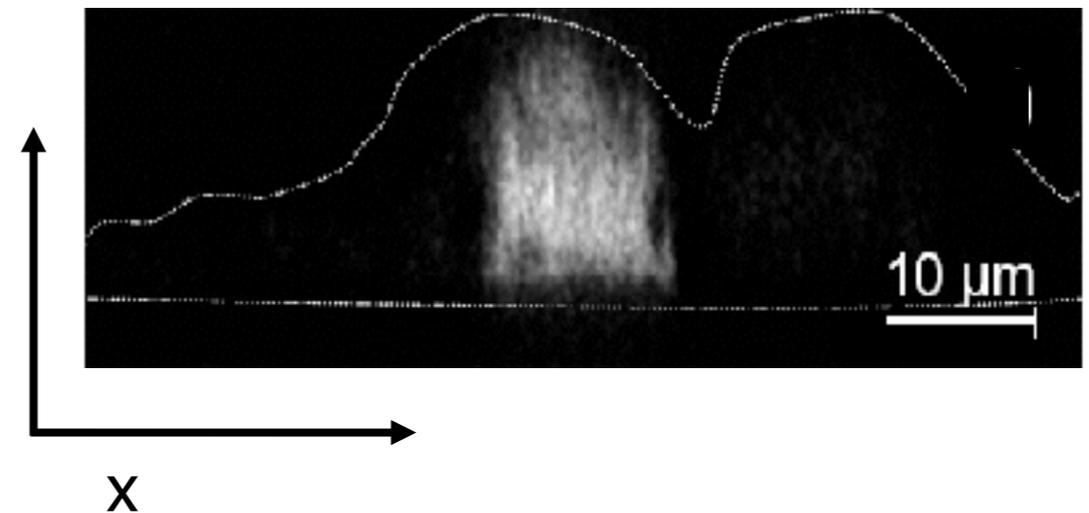


FLUORESCENCE MICROSCOPY



SINGLE-PHOTON ACTIVATION

UV-Vis
405-413 nm

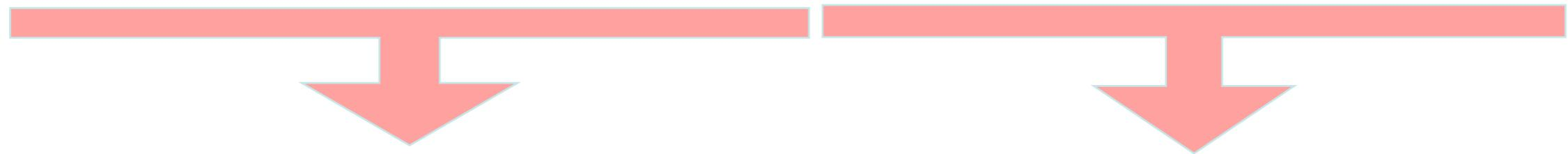


SCHNEIDER M., BAROZZI S., TESTA I., FARETTA M., DIASPRO A. (2005) BIOPHYS. J., vol.89(2)

2PE and GFP PA-GFP

(green fluorescent protein → photo activatable green fluorescent protein)

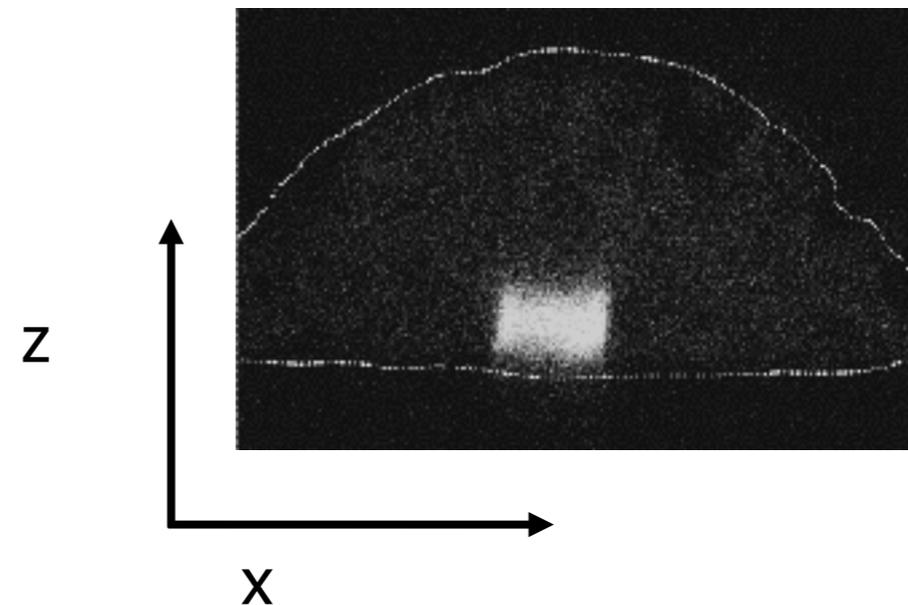
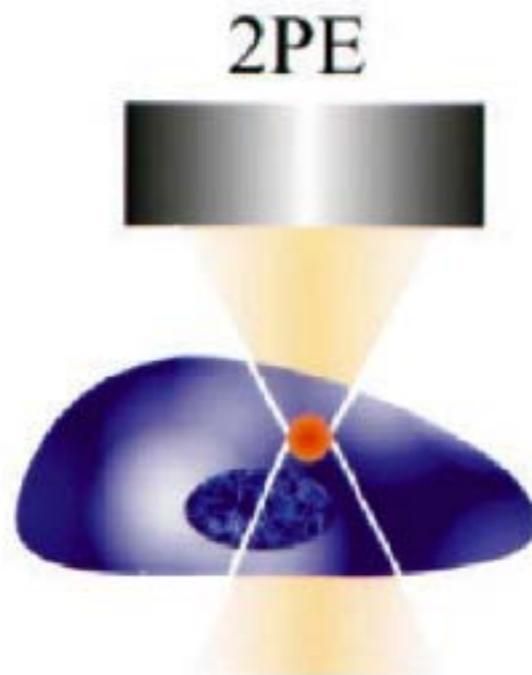
Two-photon interaction



TWO-PHOTON EXCITATION
MICROSCOPY

TWO-PHOTON ACTIVATION

IR-NIR



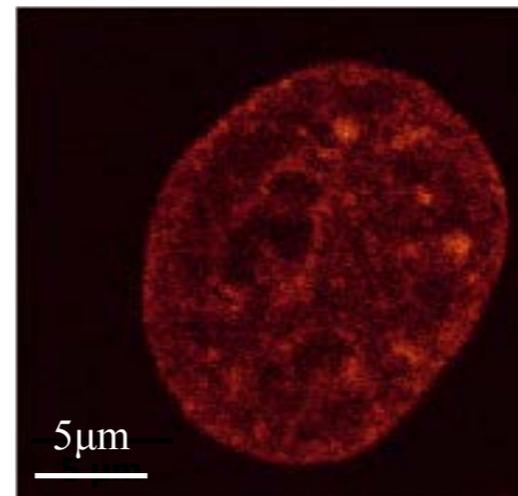
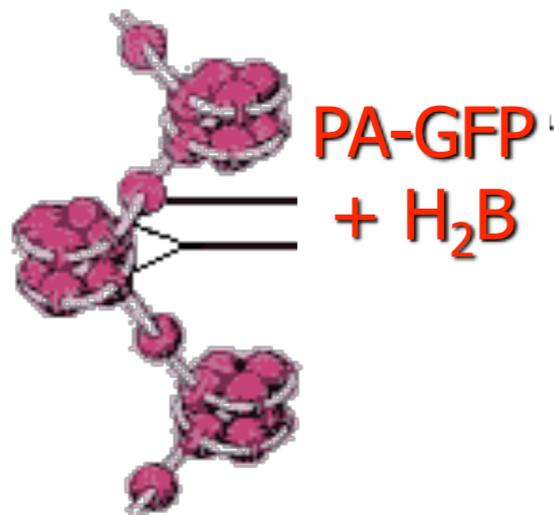
SCHNEIDER M., BAROZZI S., TESTA I., FARETTA M., DIASPRO A. (2005) BIOPHYS. J., vol.89(2)

2PE and GFP PA-GFP

(green fluorescent protein → photo activatable green fluorescent protein)

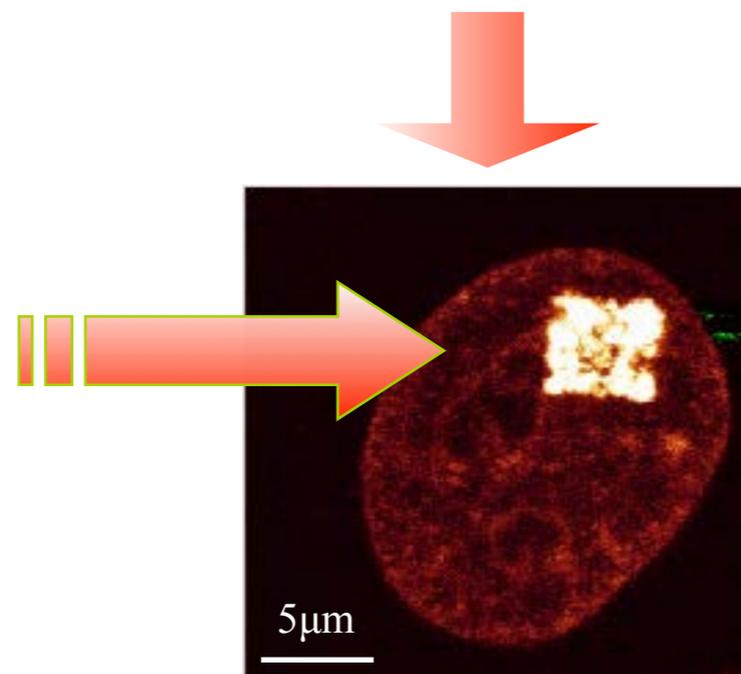
4D (x-y-z-t) switching

TAILOR YOUR OWN SET OF GFPs INTO THE CELL...TRACK IT!

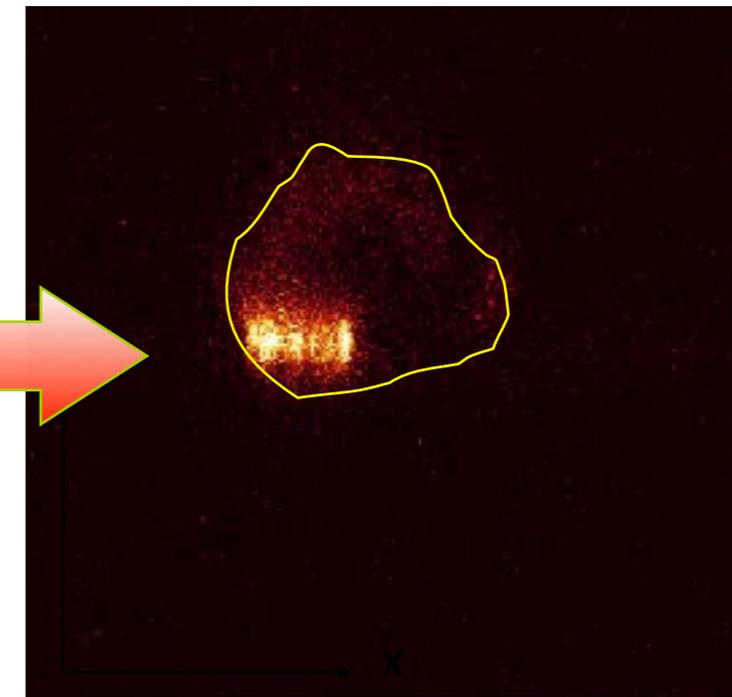


PRE / $\lambda_{vis} = 488 \text{ nm}$

PA into He-La
cell nucleus



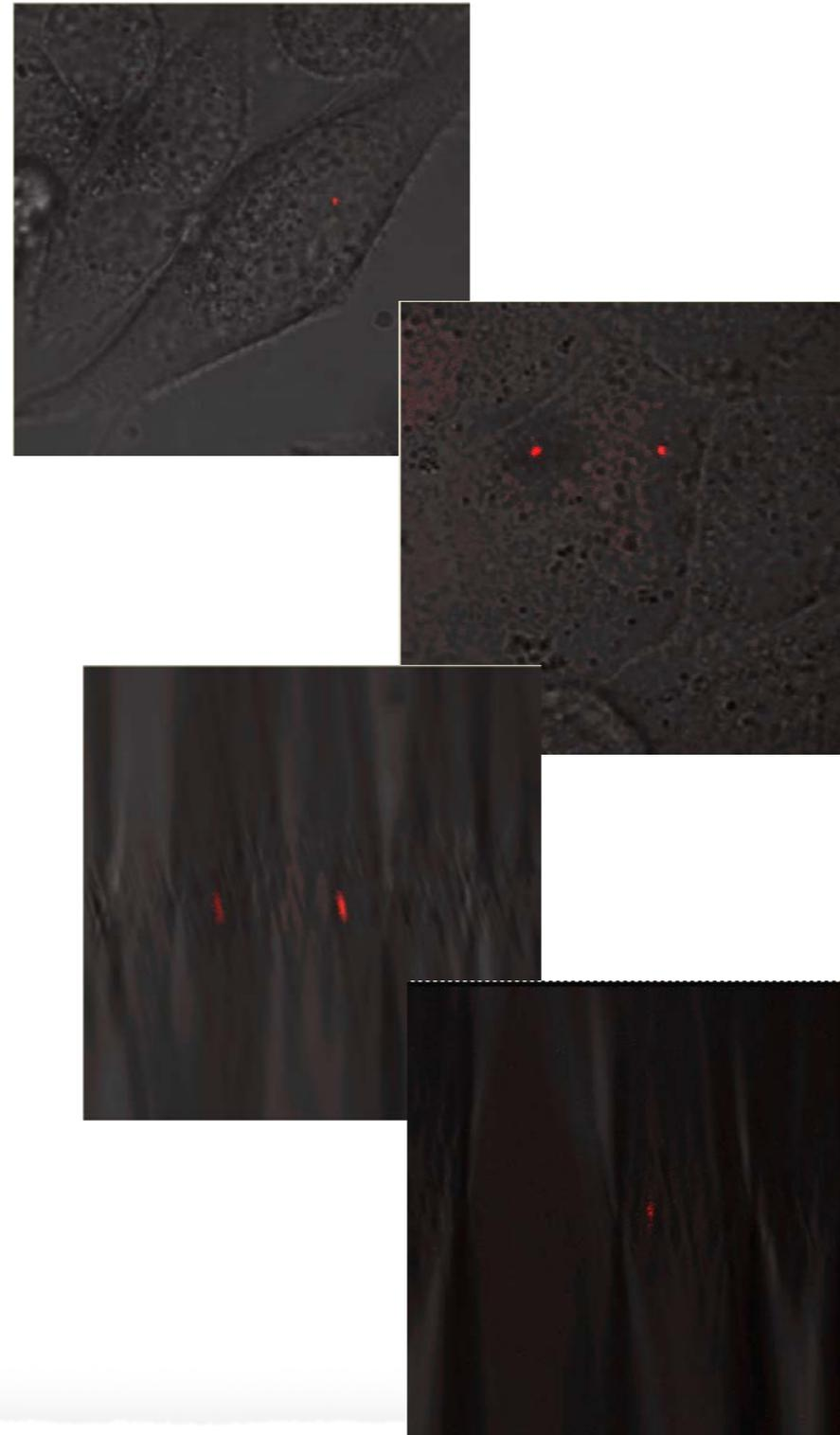
POST / $\lambda_{vis} = 488 \text{ nm}$



2PE and GFP PA-GFP

(green fluorescent protein \rightarrow photo activatable green fluorescent protein)

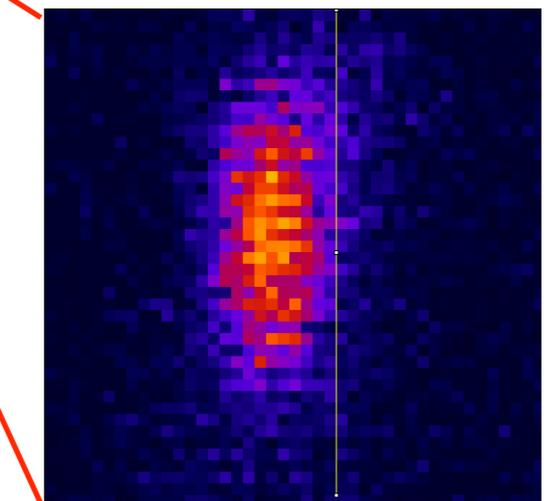
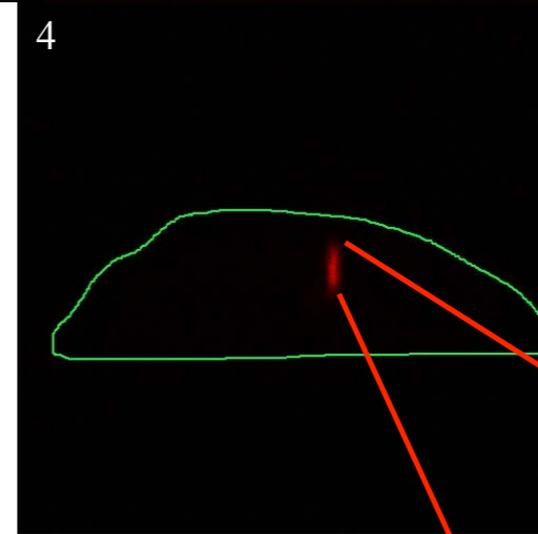
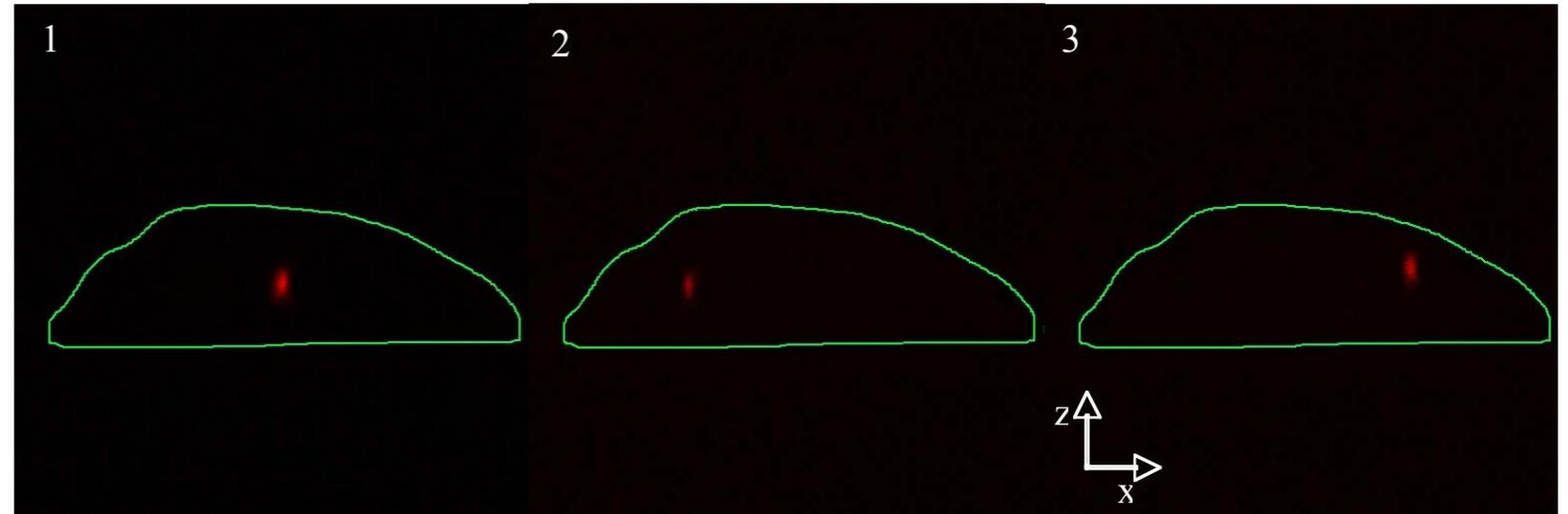
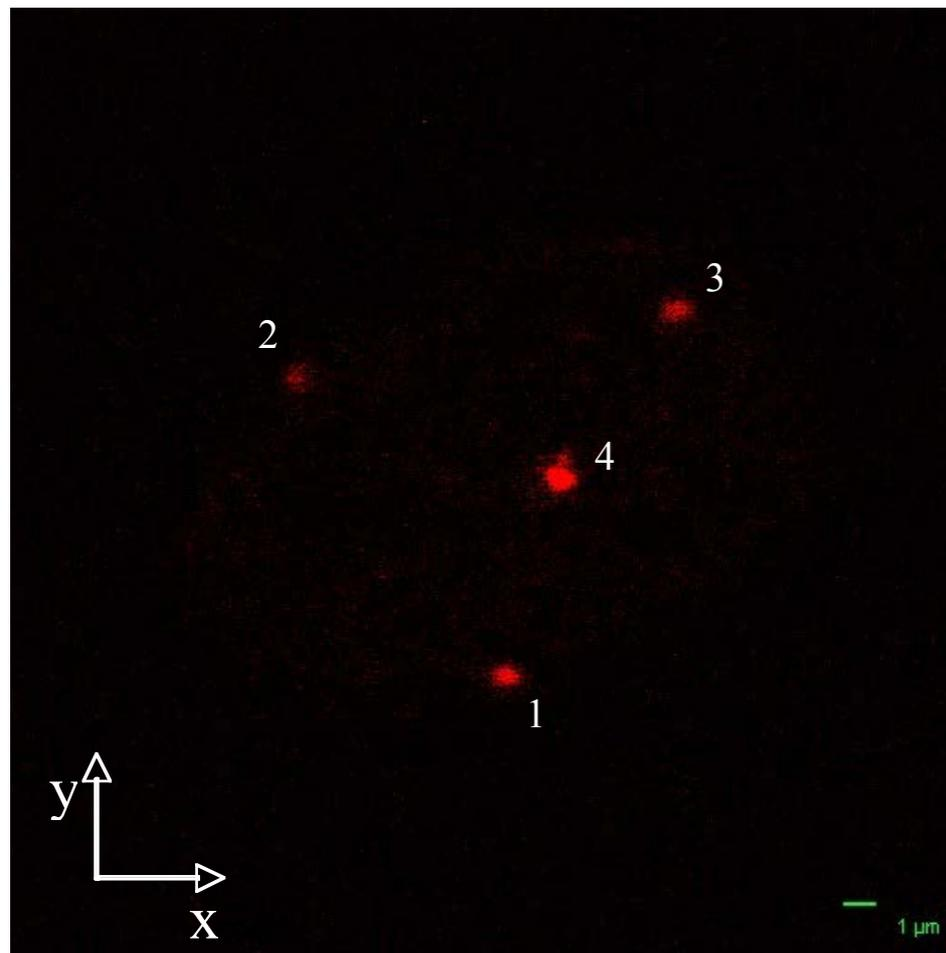
4D (x-y-z-t) switching



2PE and GFP PA-GFP

(green fluorescent protein → photo activatable green fluorescent protein)

4D (x-y-z-t) switching

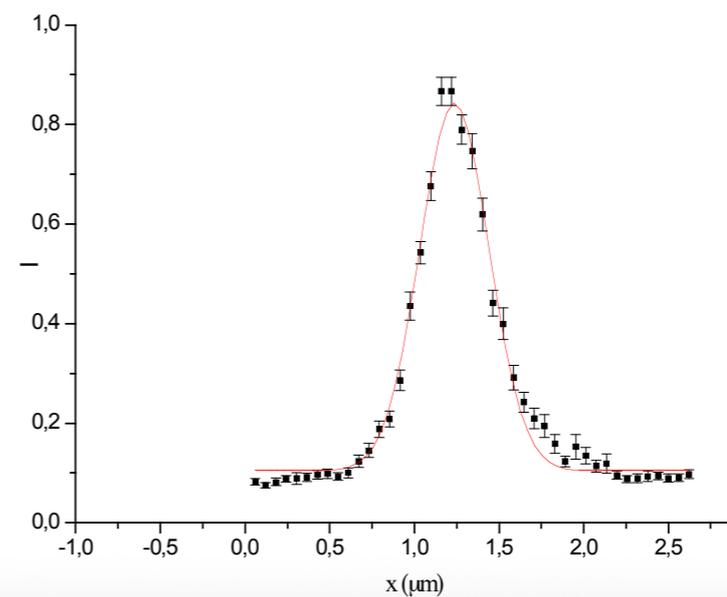
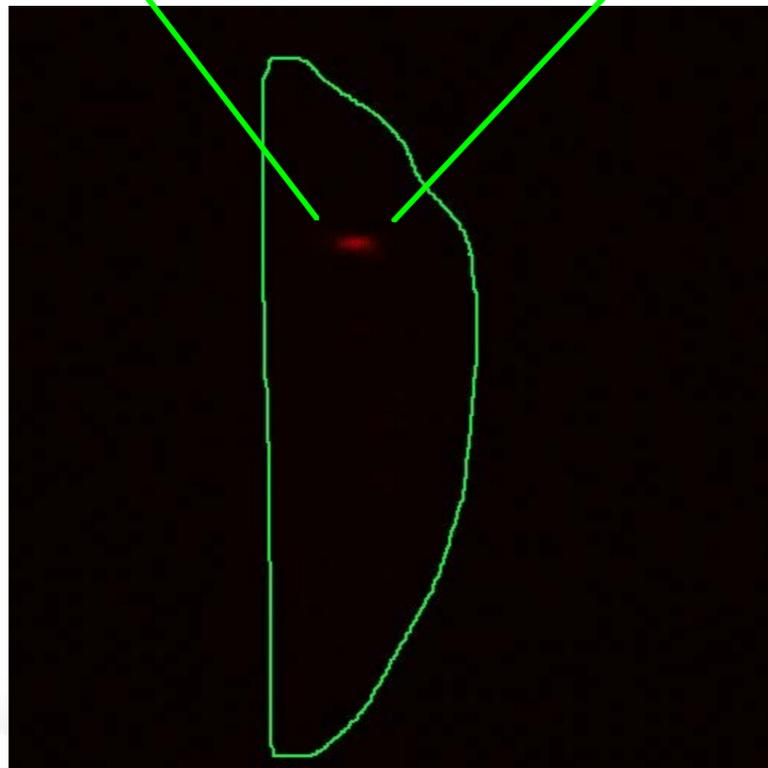
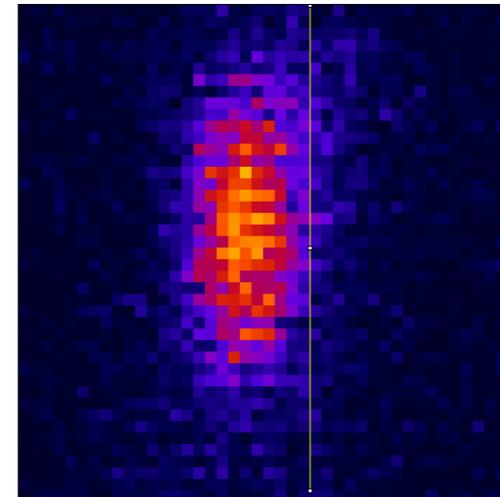
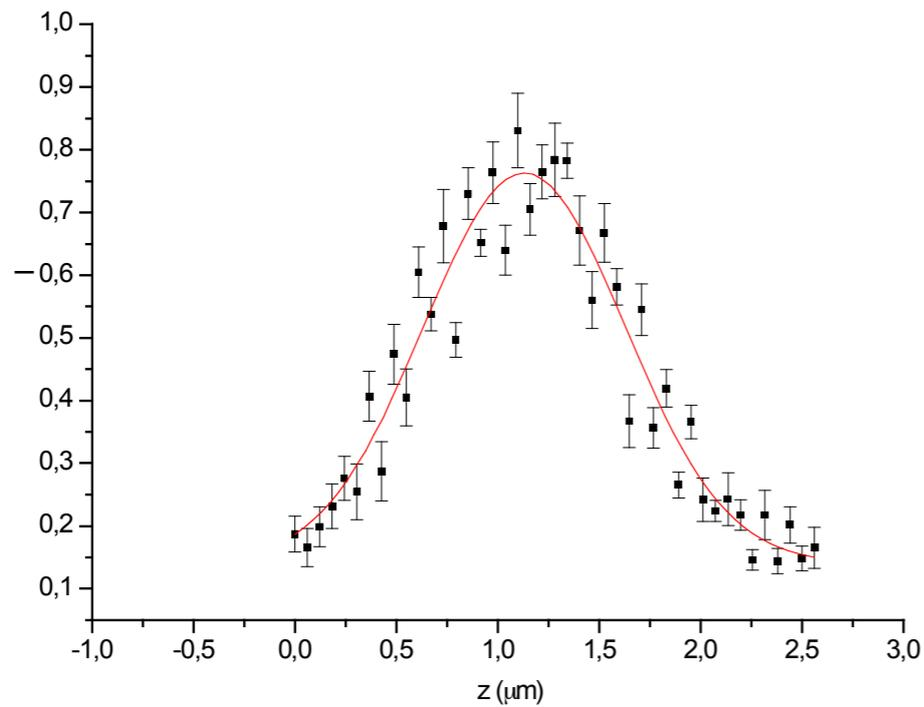


Ilaria Testa - LAMBS 2006

2PE and GFP PA-GFP

(green fluorescent protein \rightarrow photo activatable green fluorescent protein)

4D (x-y-z-t) switching



2PE and GFP PA-GFP

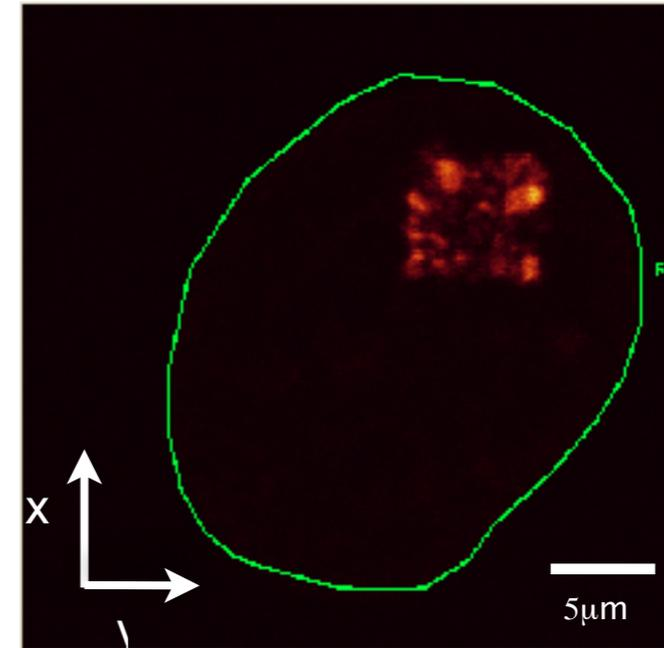
(green fluorescent protein \rightarrow photo activatable green fluorescent protein)

Two photon activation in living cells

PA-GFP +
H2B He-La
cell

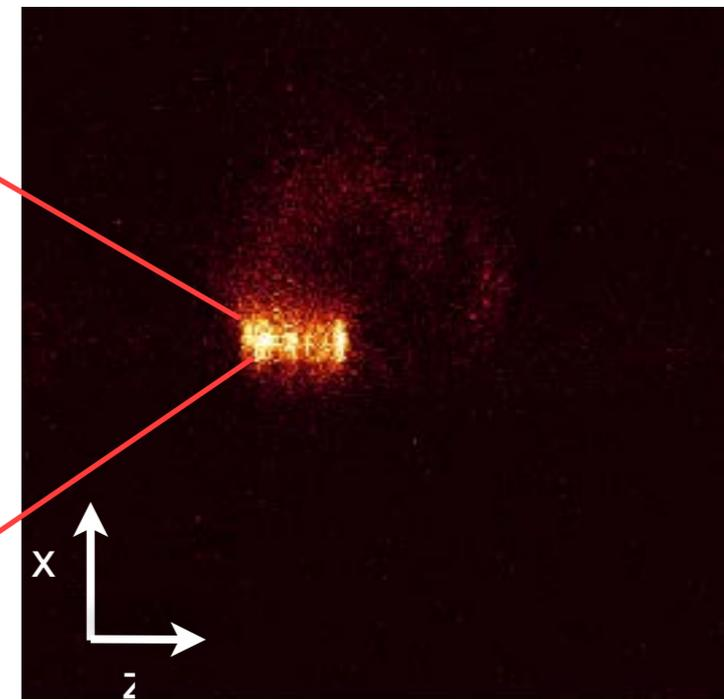
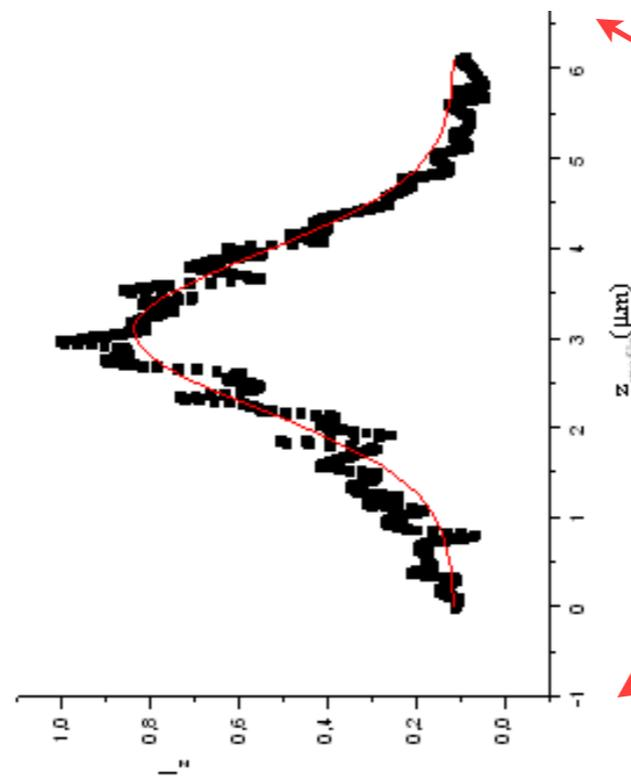


$\langle P_{\text{ACTIVATION}} \rangle =$
10mW
 $\lambda_{\text{ACTIVATION}} = 720\text{nm}$
Pixel time = 300 μs



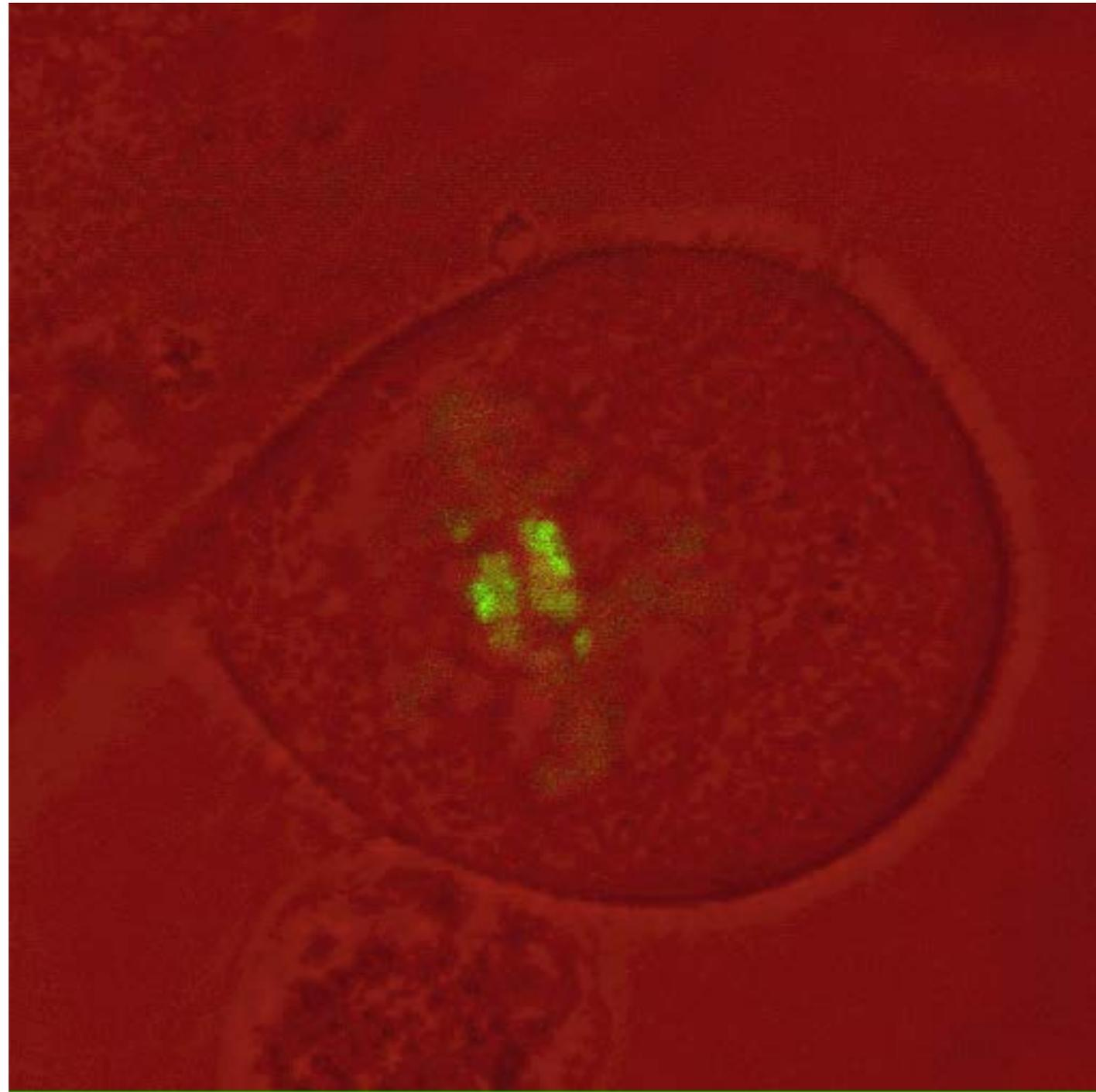
$\langle P_{\text{EXCITATION}} \rangle = 0,04 \text{ mW}$, $\lambda_{\text{EXCITATION}} = 488\text{nm}$
Pixel time = 4,9 μs , 512*512 pixels

LOCALIZED
INTERACTION



2PE and GFP PA-GFP

(green fluorescent protein → photo activatable green fluorescent protein)

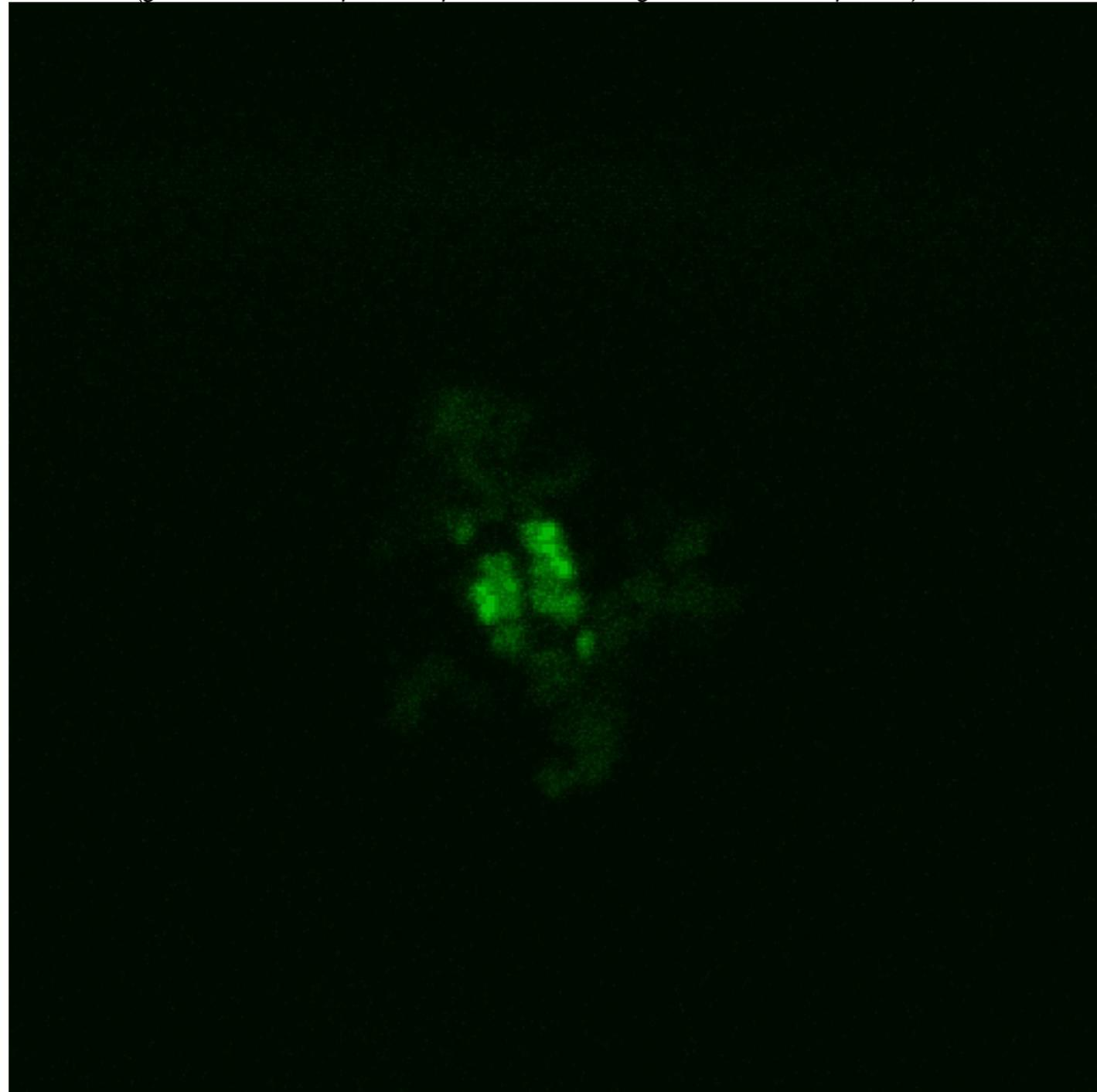


I. Testa, S. Barozzi, M. Faretta, A. Diaspro (2006)

PA-GFP, LEICA SP2 AOBS spectral system, Chameleon-XR Coherent tunable Ti-Sapphire laser

2PE and GFP PA-GFP

(green fluorescent protein → photo activatable green fluorescent protein)

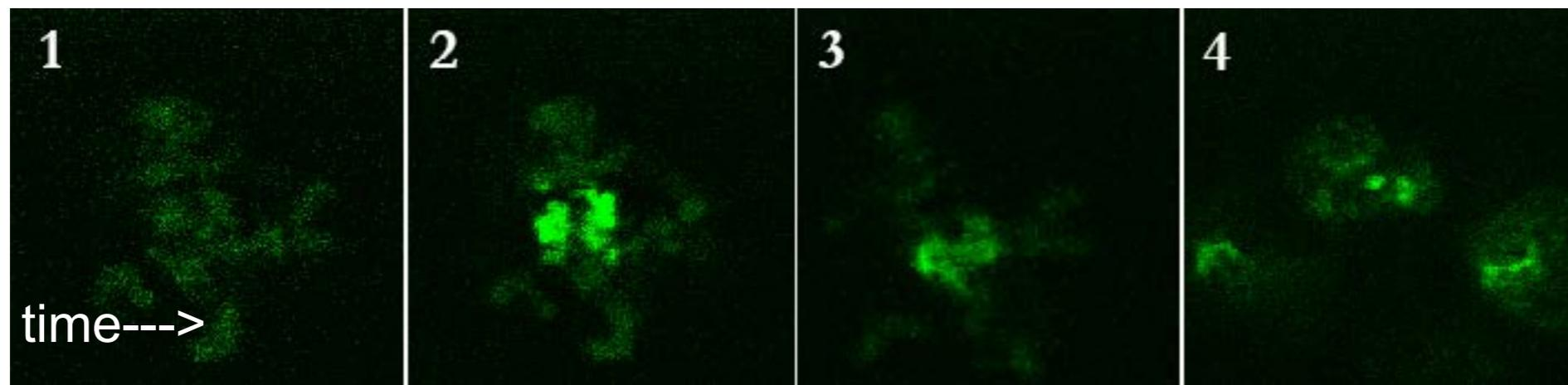
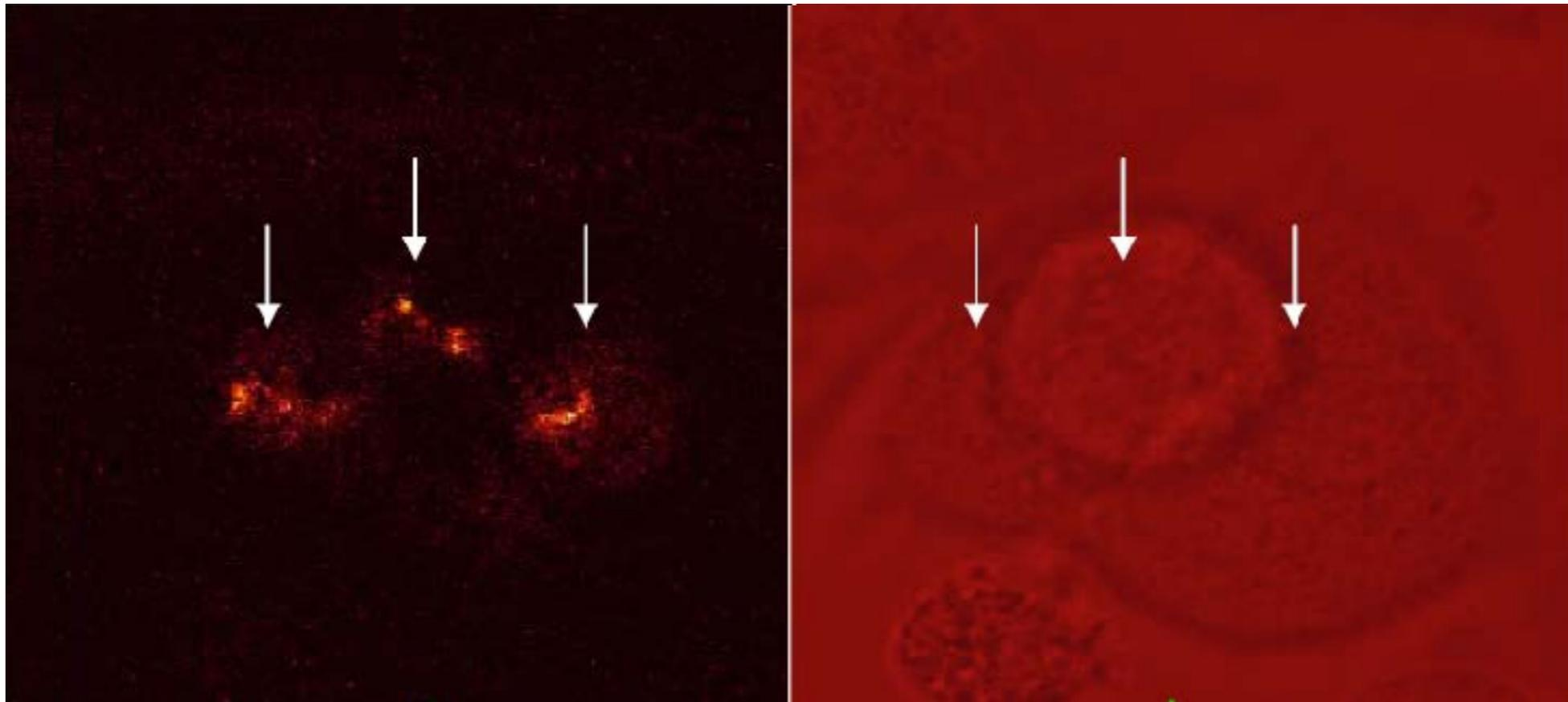


I. Testa, S. Barozzi, M. Faretta, A. Diaspro (2006)

PA-GFP, LEICA SP2 AOBS spectral system, Chameleon-XR Coherent tunable Ti-Sapphire laser

2PE and GFP PA-GFP

(green fluorescent protein → photo activatable green fluorescent protein)



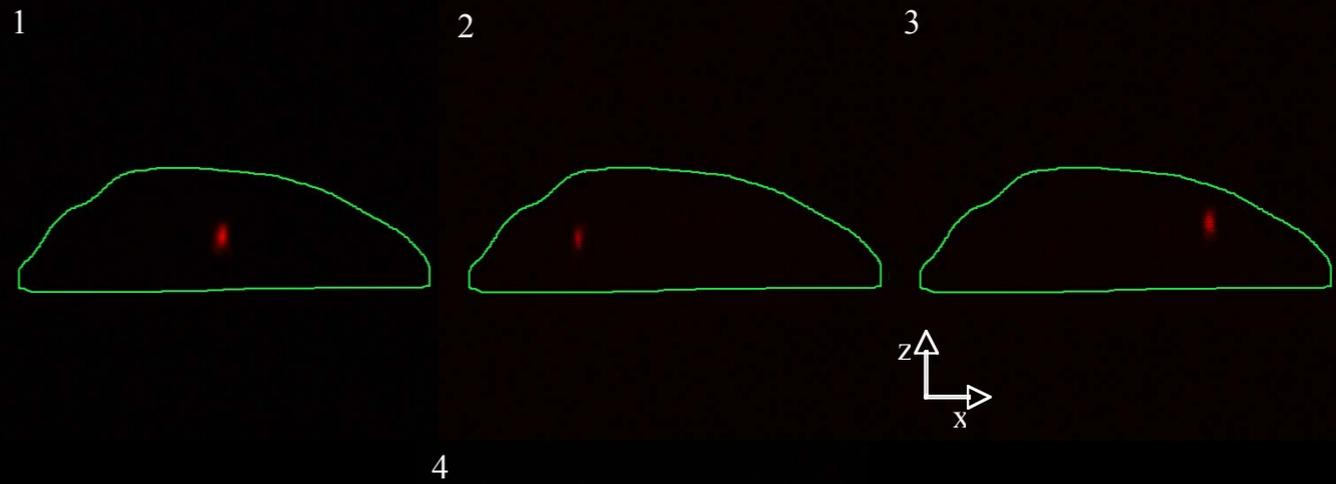
I. Testa, S. Barozzi, M. Faretta, A. Diaspro (2006)

PA-GFP, LEICA SP2 AOBS spectral system, Chameleon-XR Coherent tunable Ti-Sapphire laser

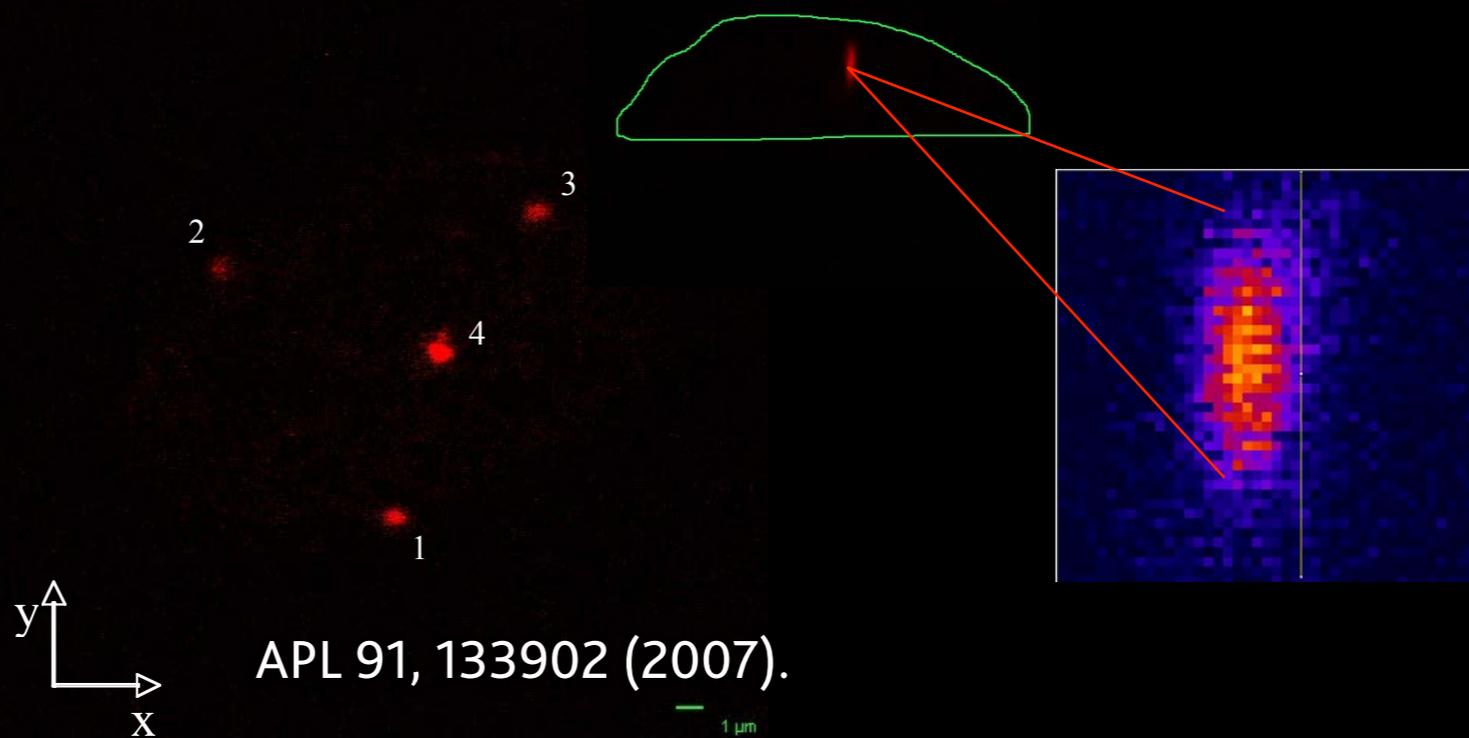
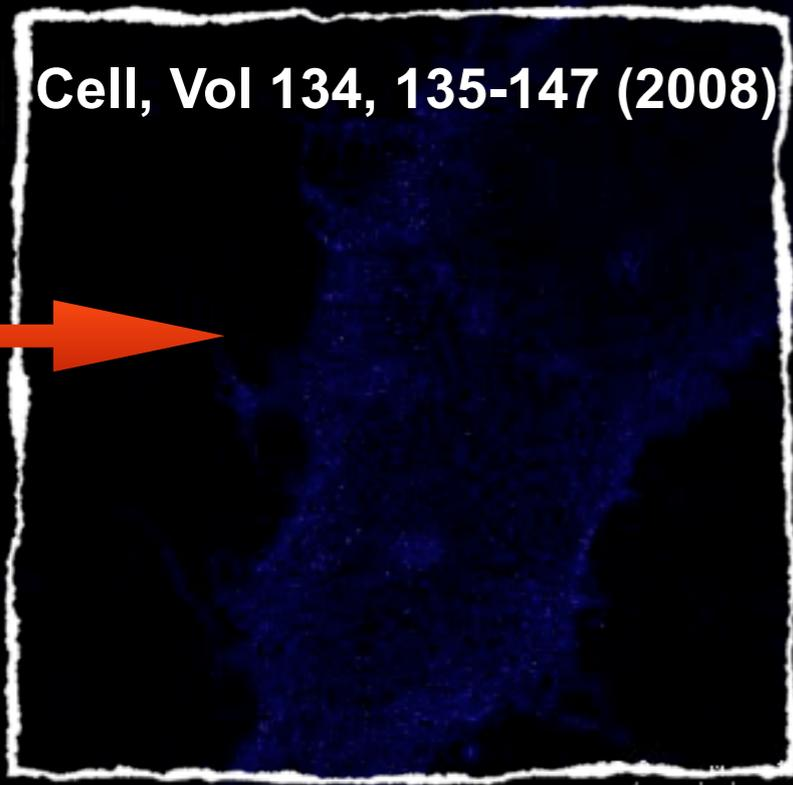
PA-GFP

4D (x-y-z-t) 2PE switching

Biophys. J., .89(2), 1346--1352 (2005).



Cell, Vol 134, 135-147 (2008)



APL 91, 133902 (2007).

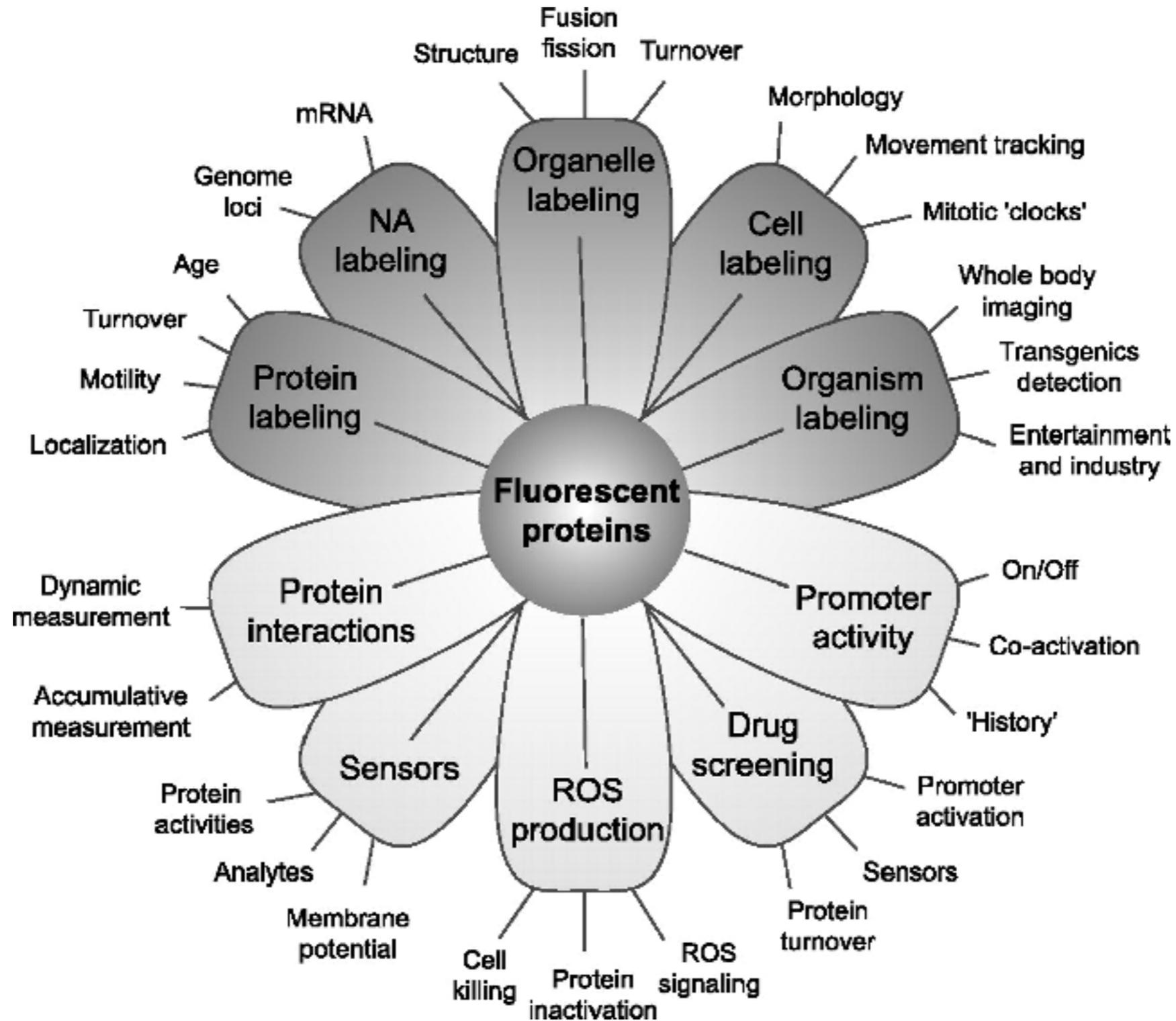
Diaspro Lab



Fluorescence is one of the basic processes that we use to access the 'nanoscale' information:

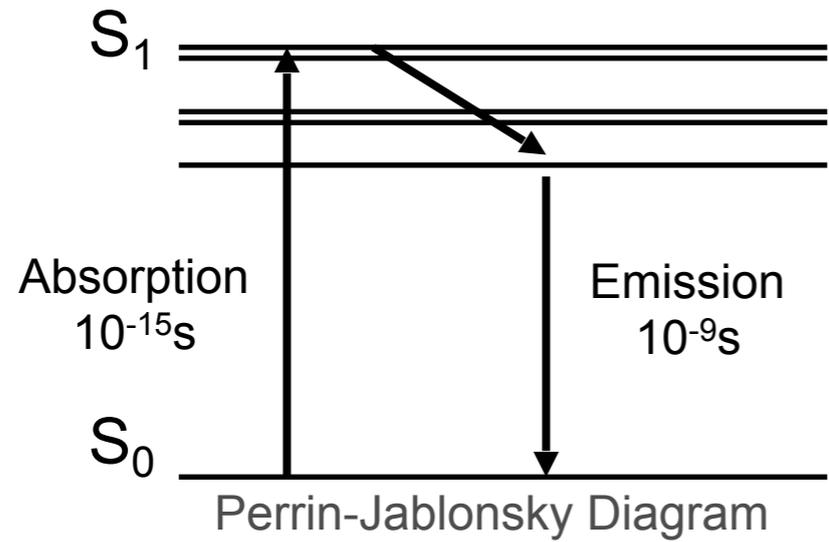
- Fluorescence spectroscopy
- Fluorescence microscopy

fluorescence and its surrounding



Dmitriy M. Chudakov, Mikhail V. Matz, Sergey Lukyanov, Konstantin A. Lukyanov, *Physiological Reviews* (2010) Vol. 90 no. 3, 1103-1163

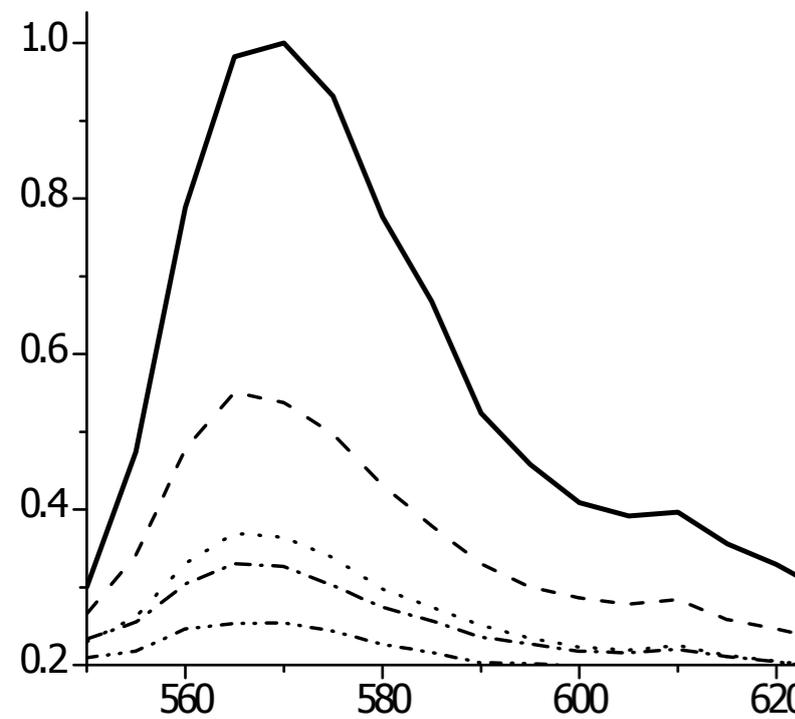
fluorescence and its surrounding



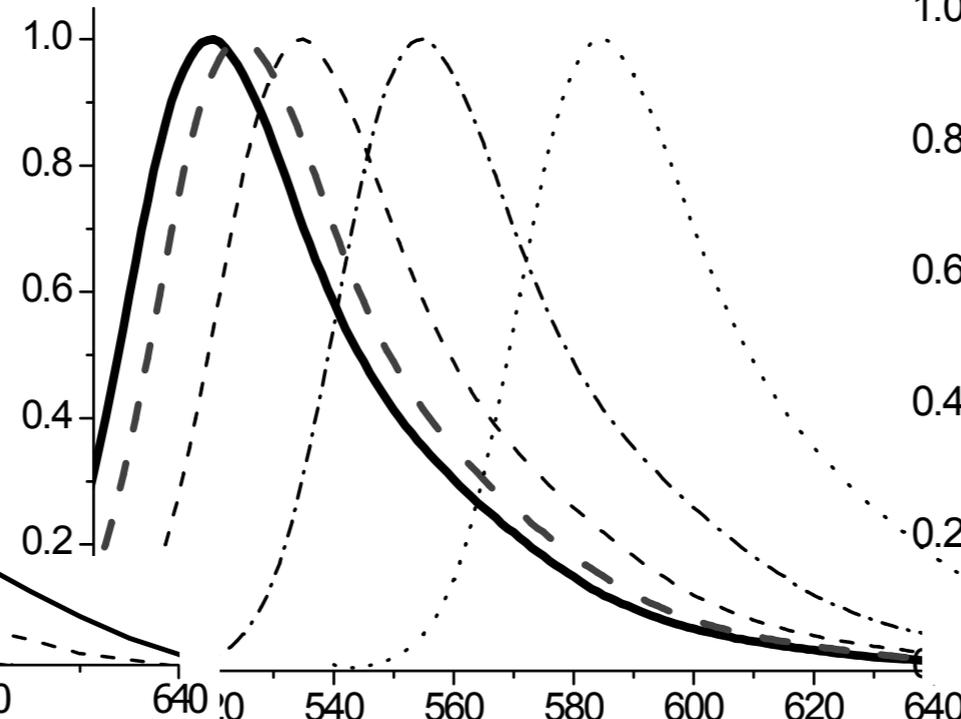
Interaction with surrounding environment

- Molecular interactions
- Molecular binding
- Fluorophore accessibility
- Conformational changes
- Rotational diffusion
- Interactions with solvent molecules
- ...

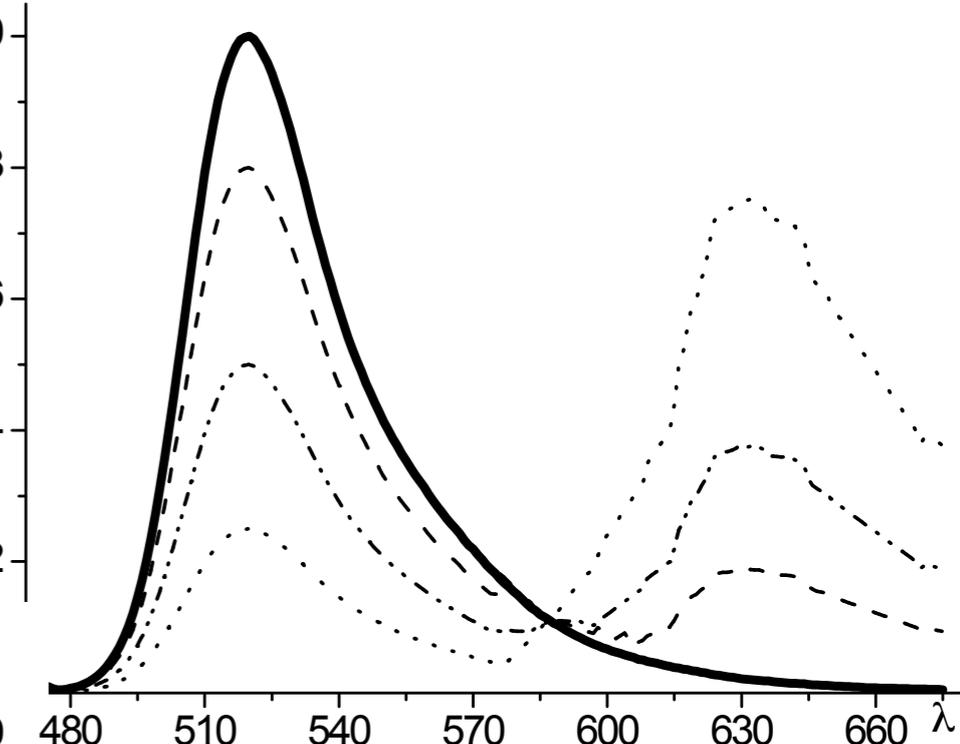
Fluorescence Decrease



Wavelength Shift



Shape Variations



Quenching and FRET

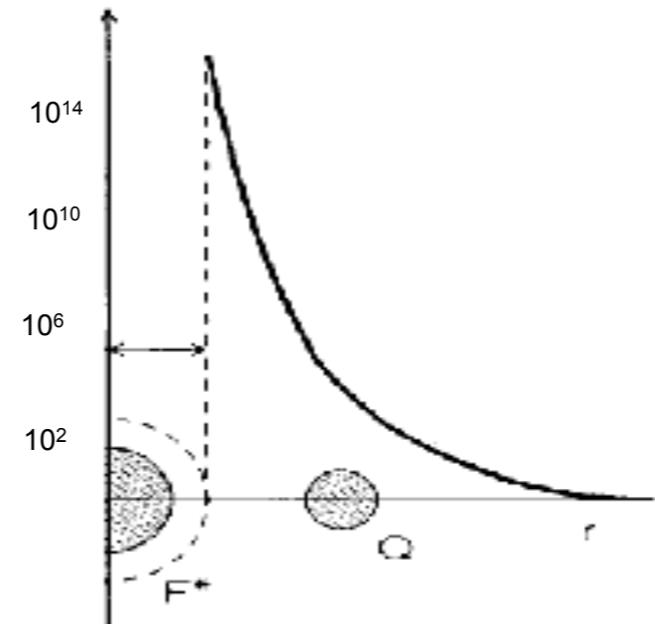
Quenching

Contact with diffusive encounters
Short-range interactions 1Å
Sensitive to steric shielding,
charge-charge interactions...

$$k_Q = \beta e^{-(r-r_c)}$$

FRET

events/s



Quenching and FRET

Quenching

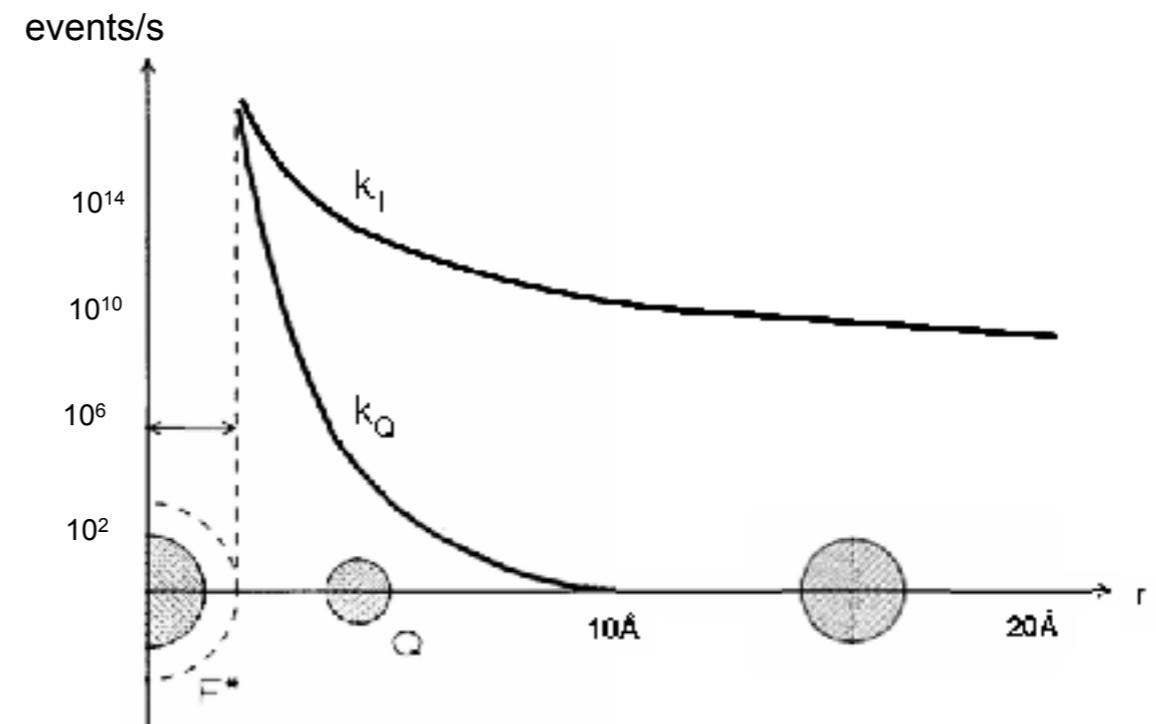
Contact with diffusive encounters
Short-range interactions 1Å
Sensitive to steric shielding,
charge-charge interactions...

$$k_Q = \beta e^{-(r-r_c)}$$

Resonance Energy Transfer
Long-range interactions 10-100 Å
Insensitive to steric factors,
electrostatic interactions...

FRET

$$k_T = \frac{1}{\tau_D} \left(\frac{R_0}{r} \right)^6$$



slide courtesy: Valentina Caorsi

Quenching and FRET

Quenching

Contact with diffusive encounters
Short-range interactions 1Å
Sensitive to steric shielding,
charge-charge interactions...

$$k_Q = \beta e^{-(r-r_c)}$$

FRET

Resonance Energy Transfer
Long-range interactions 10-100 Å
Insensitive to steric factors,
electrostatic interactions...

$$k_T = \frac{1}{\tau_D} \left(\frac{R_0}{r} \right)^6$$

Phenomenon studies
on model system

Biological Application
for protein-protein investigation

Quenching and FRET

Quenching

Contact with diffusive encounters
Short-range interactions 1Å
Sensitive to steric shielding,
charge-charge interactions...

$$k_Q = Ae^{-\beta(r-r_c)}$$

FRET

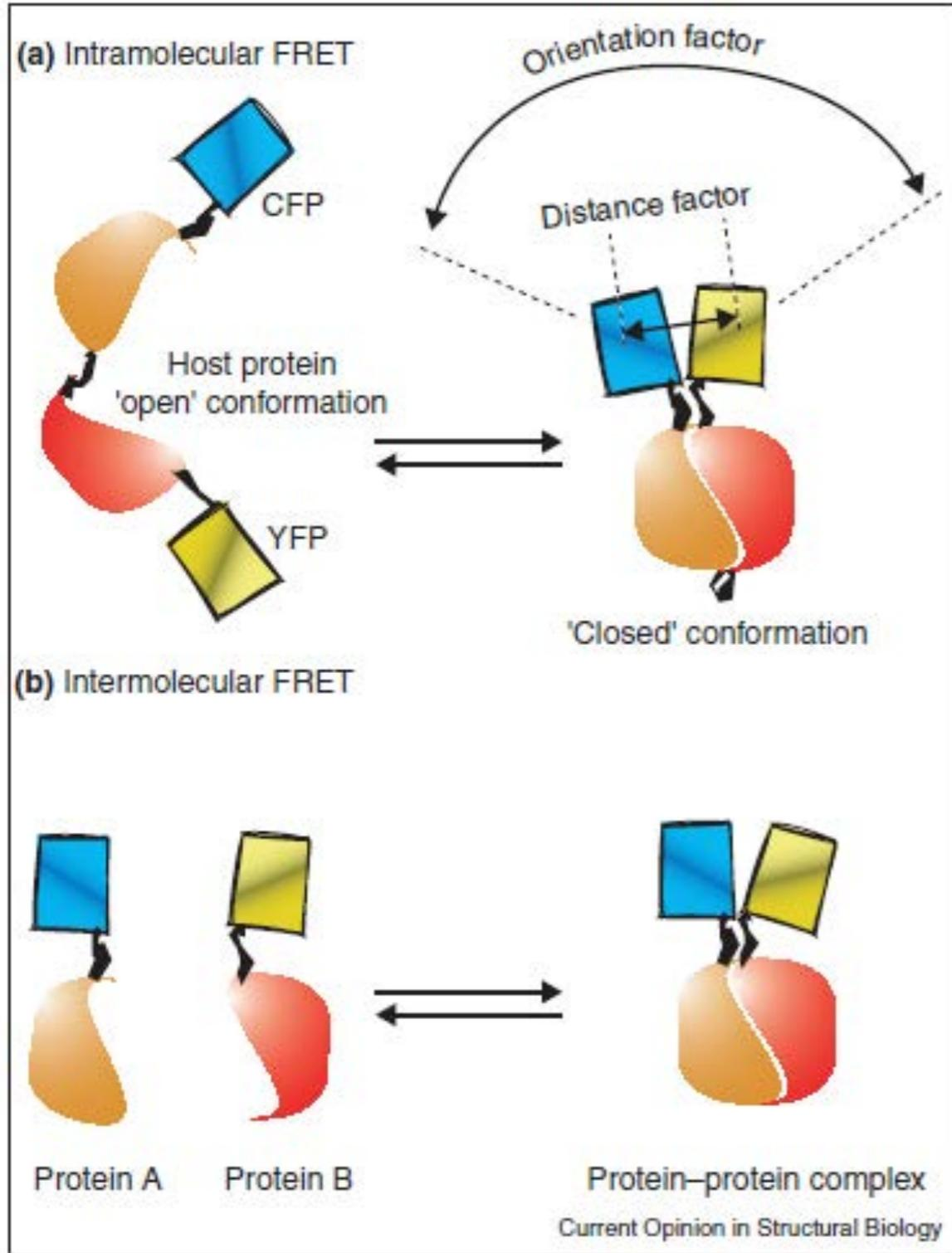
Resonance Energy Transfer
Long-range interactions 10-100 Å
Insensitive to steric factors,
electrostatic interactions...

$$k_T = \frac{1}{\tau_D} \left(\frac{R_0}{r} \right)^6$$

Phenomenon studies
on model system

Biological Application
for protein-protein investigation

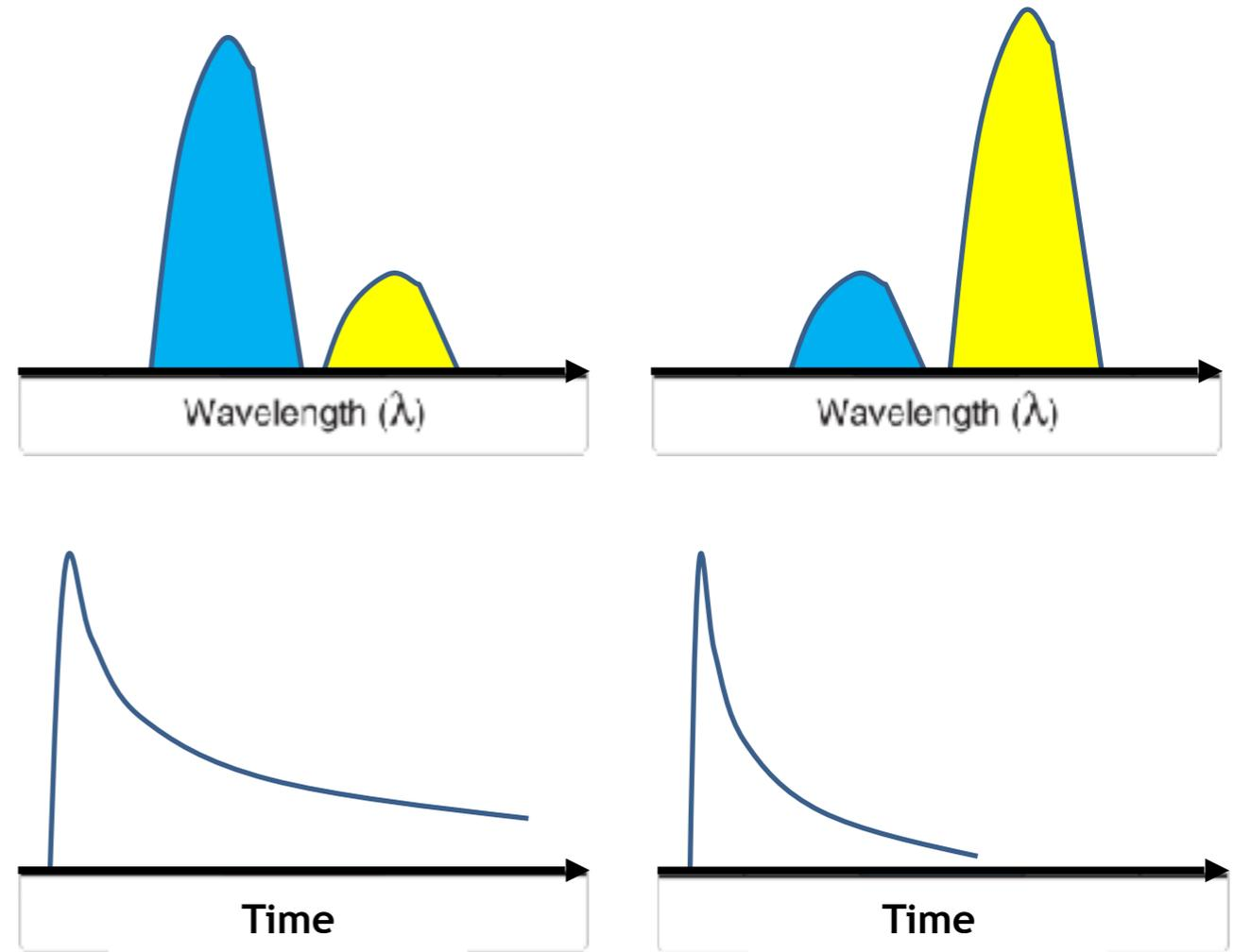
FRET



Truong and Ikura, 2001

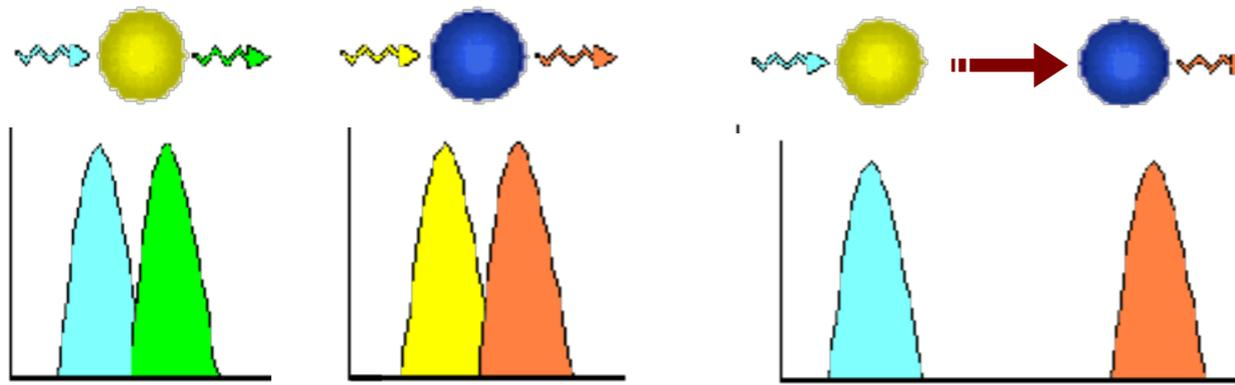
NO FRET
 $d > 10\text{nm}$

FRET
 $d < 10\text{nm}$

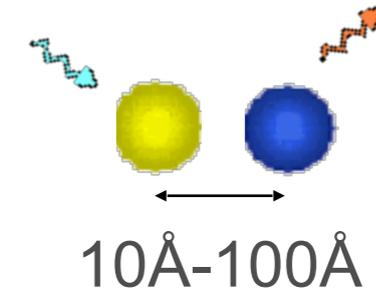


Detected measuring changes
in emission spectra or in
lifetime.

FRET

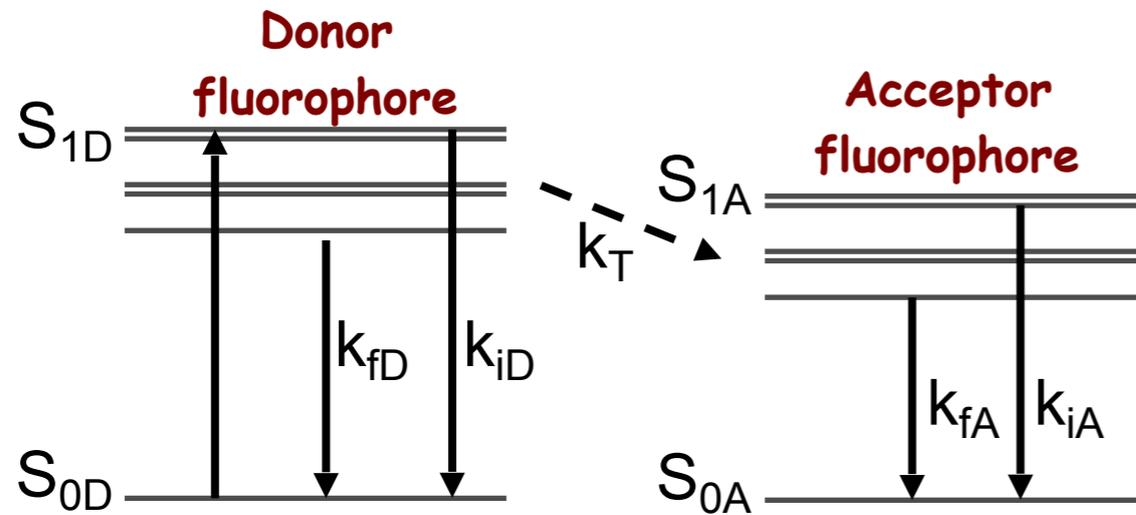
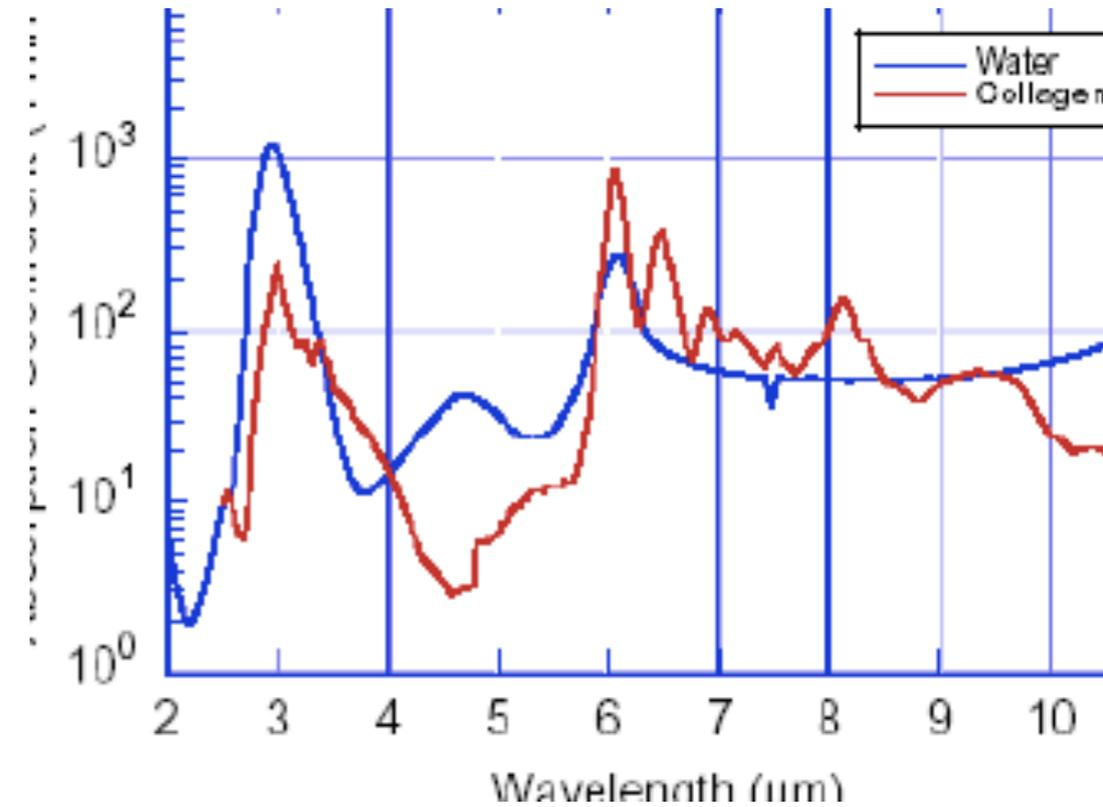


1) Distance

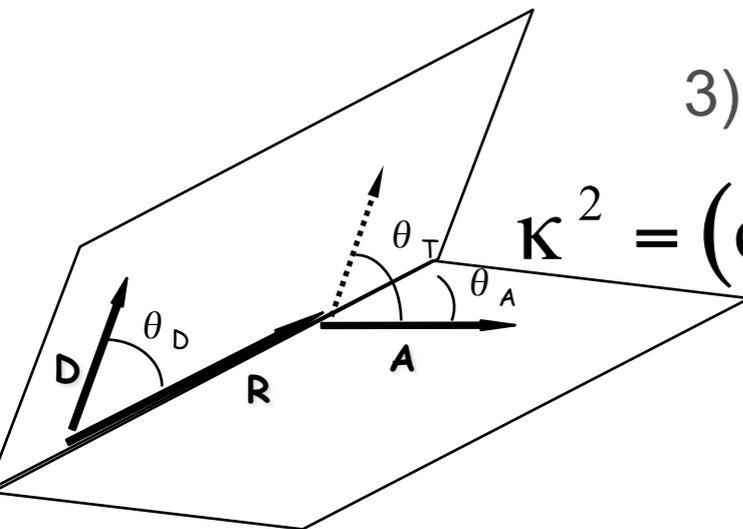


2) Spectral Overlap

$$J(\lambda) = \int F_D(\lambda) \epsilon_A(\lambda) \lambda^4 d\lambda$$



3) Dipole Orientation

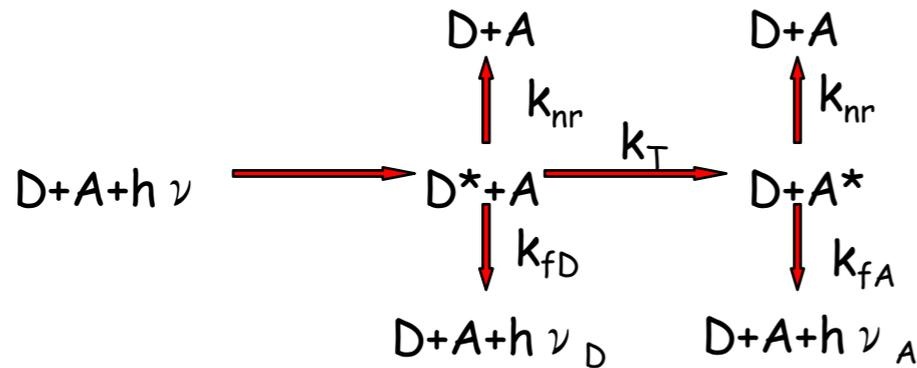


$$\kappa^2 = (\cos\theta_T - 3\cos\theta_D \cos\theta_A)^2$$

A. Periasamy and R. Day. Molecular Imaging FRET Microscopy and Spectroscopy Oxford University Press, 2005.

FRET

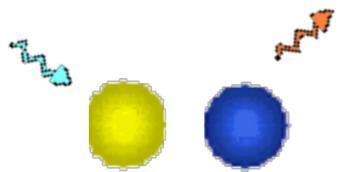
Rate constants for competing events:



$$E = \frac{K_T}{K_T + K_f + K_{nr}}$$

FRET as a nanometric ruler to investigate cellular process

Single pair

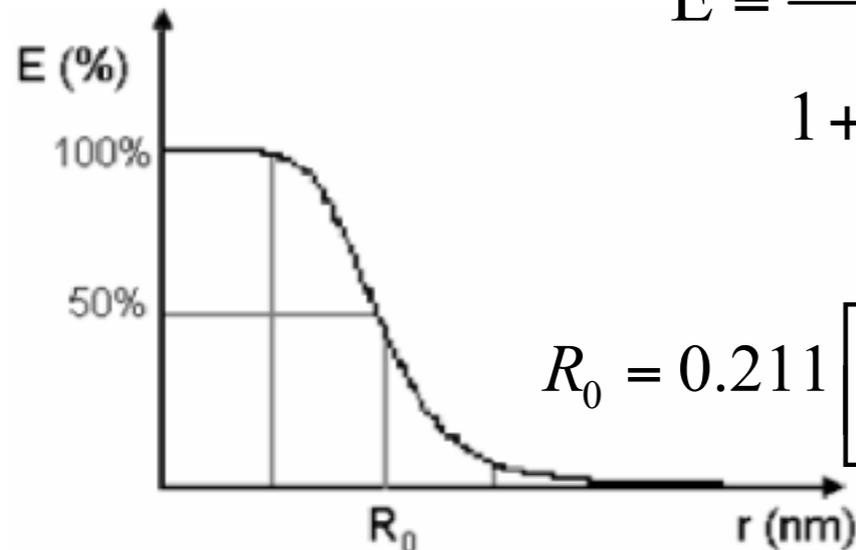


$$k_T = \frac{1}{\tau_D} \left(\frac{R_0}{r} \right)^6$$

$$E = \frac{1}{1 + \left(\frac{r}{R_0} \right)^6}$$

$$R_0 = 0.211 \left[\kappa^2 \frac{Q_D}{n^4} J(\lambda) \right]^{\frac{1}{6}}$$

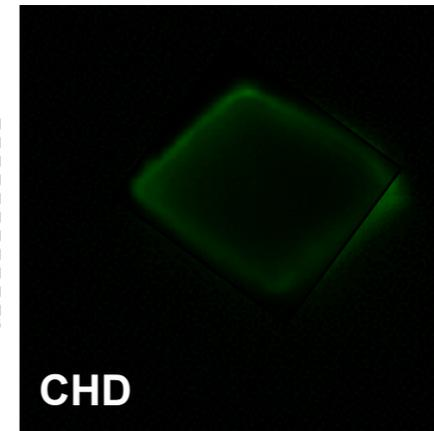
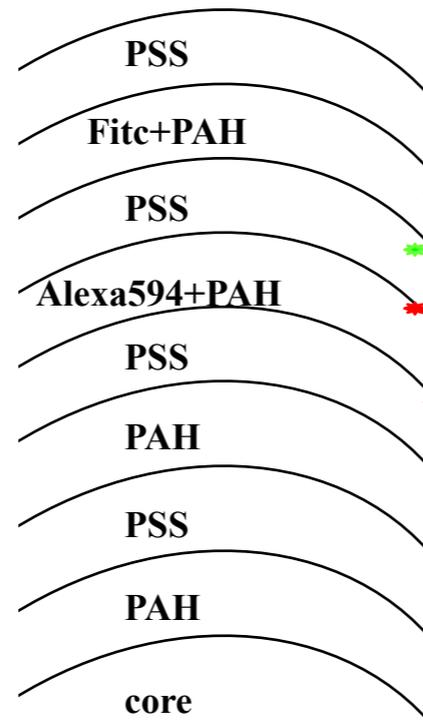
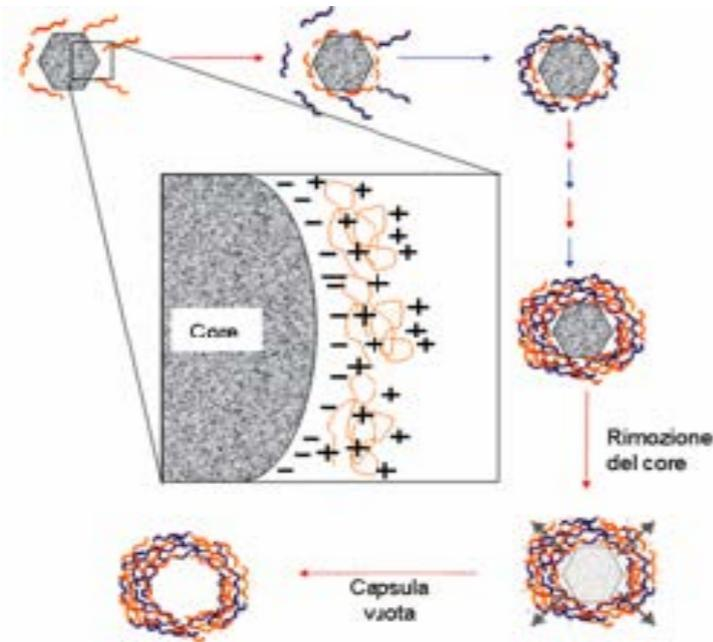
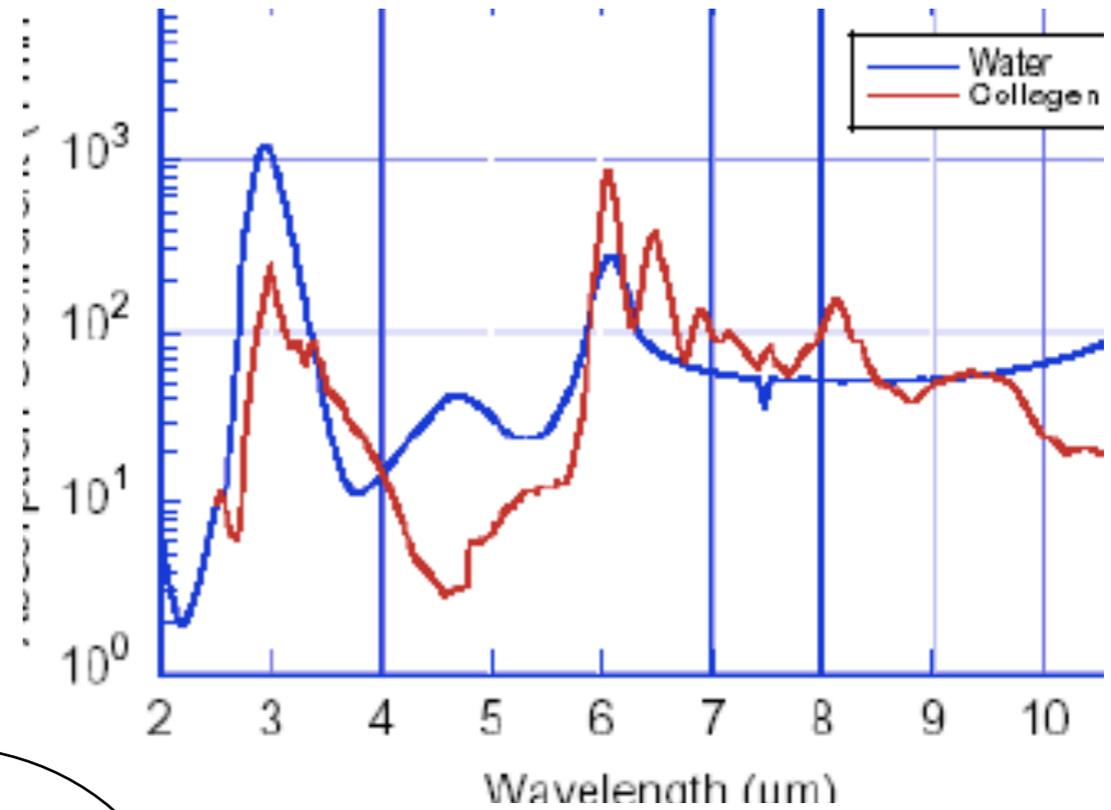
- Protein folding and complexations
- Receptor/ligand interactions
- Conformational Changes
- Structure and conformation of nucleic acids
- Distribution and transport of lipids
- Membrane fusion assays
- Membrane potential sensing



A. Periasamy and R. Day. Molecular Imaging FRET Microscopy and Spectroscopy Oxford University Press, 2005.

FRET

- Donor Emission
- Acceptor Photobleaching
- Cross talk and SBT corrections
- Spectrally Resolved
- Donor Lifetime



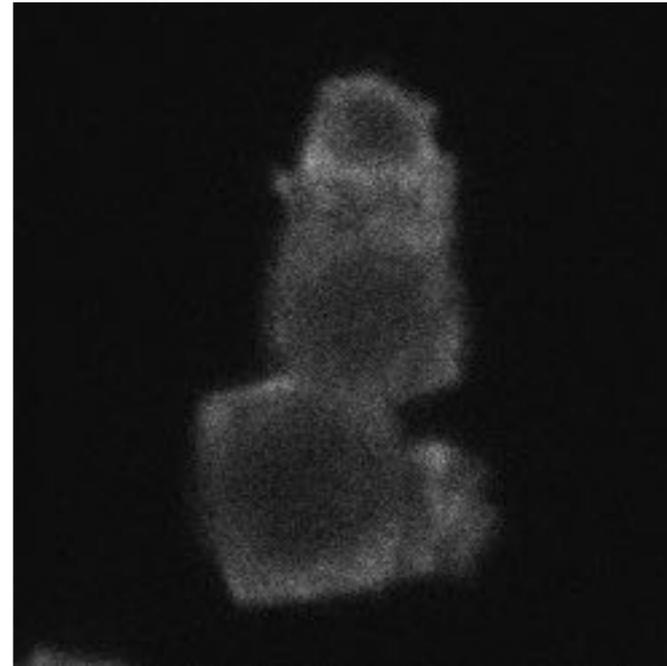
Caorsi V.,Ronzitti E.,Vicidomini G.,Krol S., McConnell G.and A. Diaspro. *FRET measurements on fuzzy fluorescent nano-structures*. MRT 2007 **70** (5):452-458.

slide courtesy: Valentina Caorsi

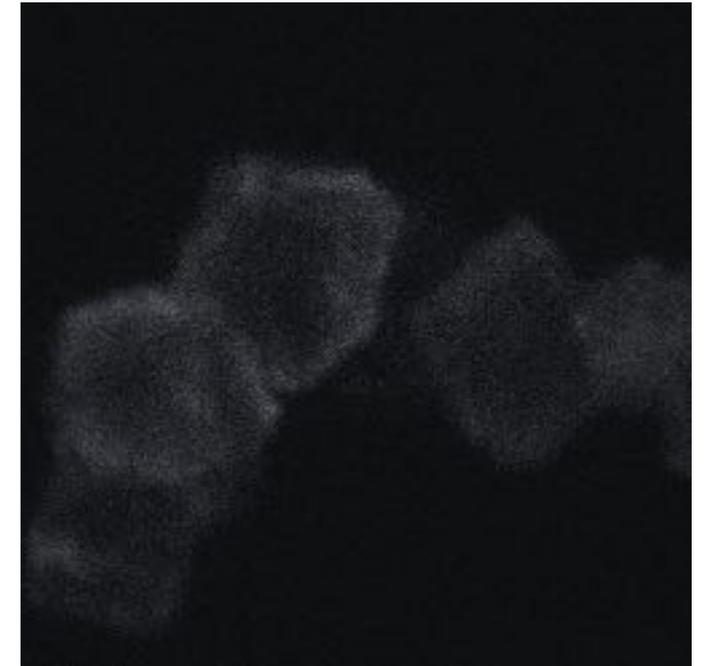
FRET

- Donor Emission
- Acceptor Photobleaching
- Cross talk and SBT corrections
- Spectrally Resolved
- Donor Lifetime

I_D



I_{DA}



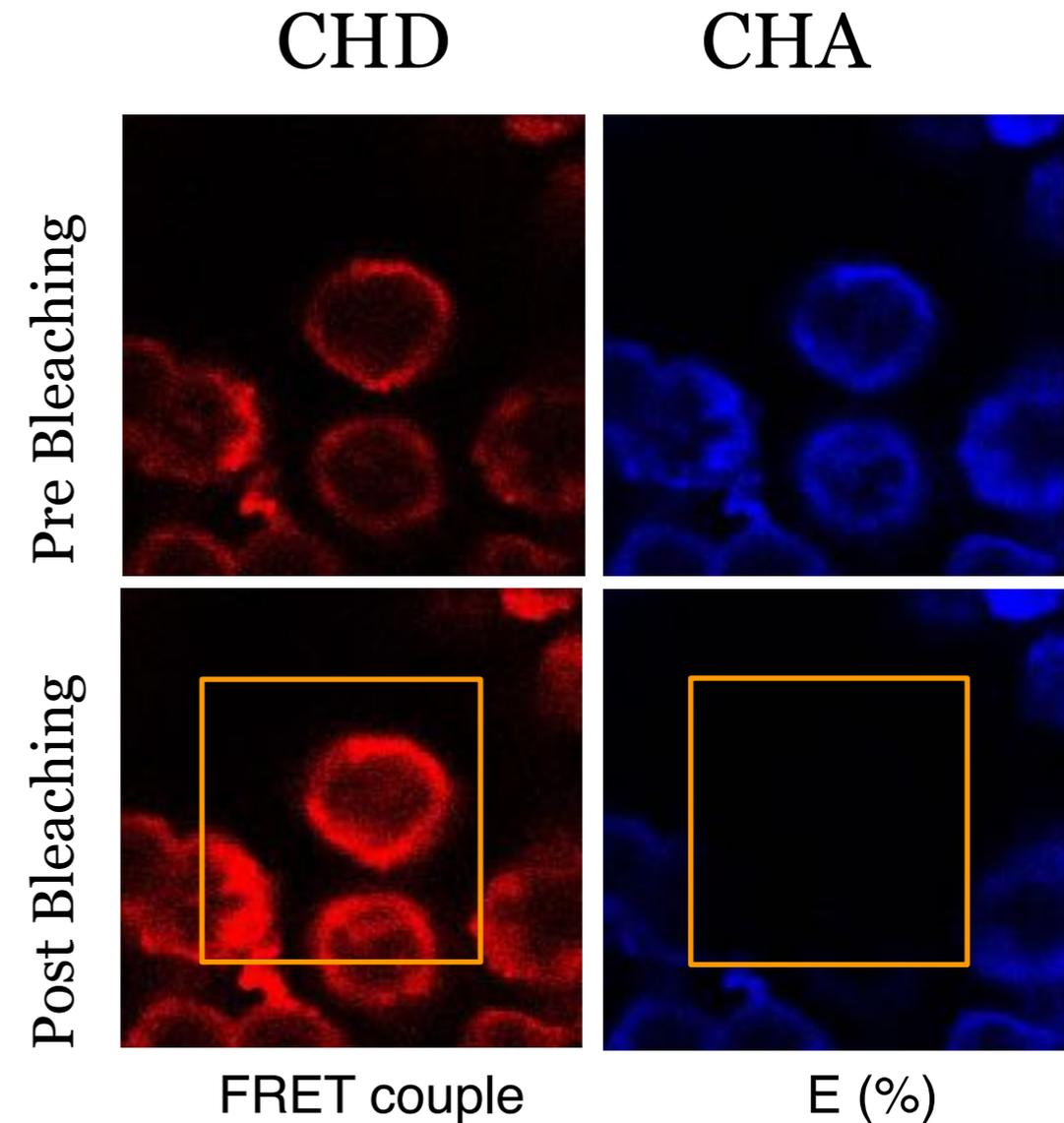
$$E = 1 - \frac{I_{DA}}{I_D}$$

FRET couple	E (%)
Fitc-Alexa594	33 ± 5
Alexa488-Alexa594	38 ± 3
Cy3-Cy5	37 ± 6

C.Berney and G.Danuser. FRET or no FRET: a quantitative comparison. Biophysical Journal 2003 **84** 3992--4010

FRET

- Donor Emission
- Acceptor Photobleaching
- Cross talk and SBT corrections
- Spectrally Resolved
- Donor Lifetime



$$E = 1 - \frac{I_{DA}}{I_{DA_{\text{afterphotobleaching}}}}$$

Cy3-Cy5

29 ± 5

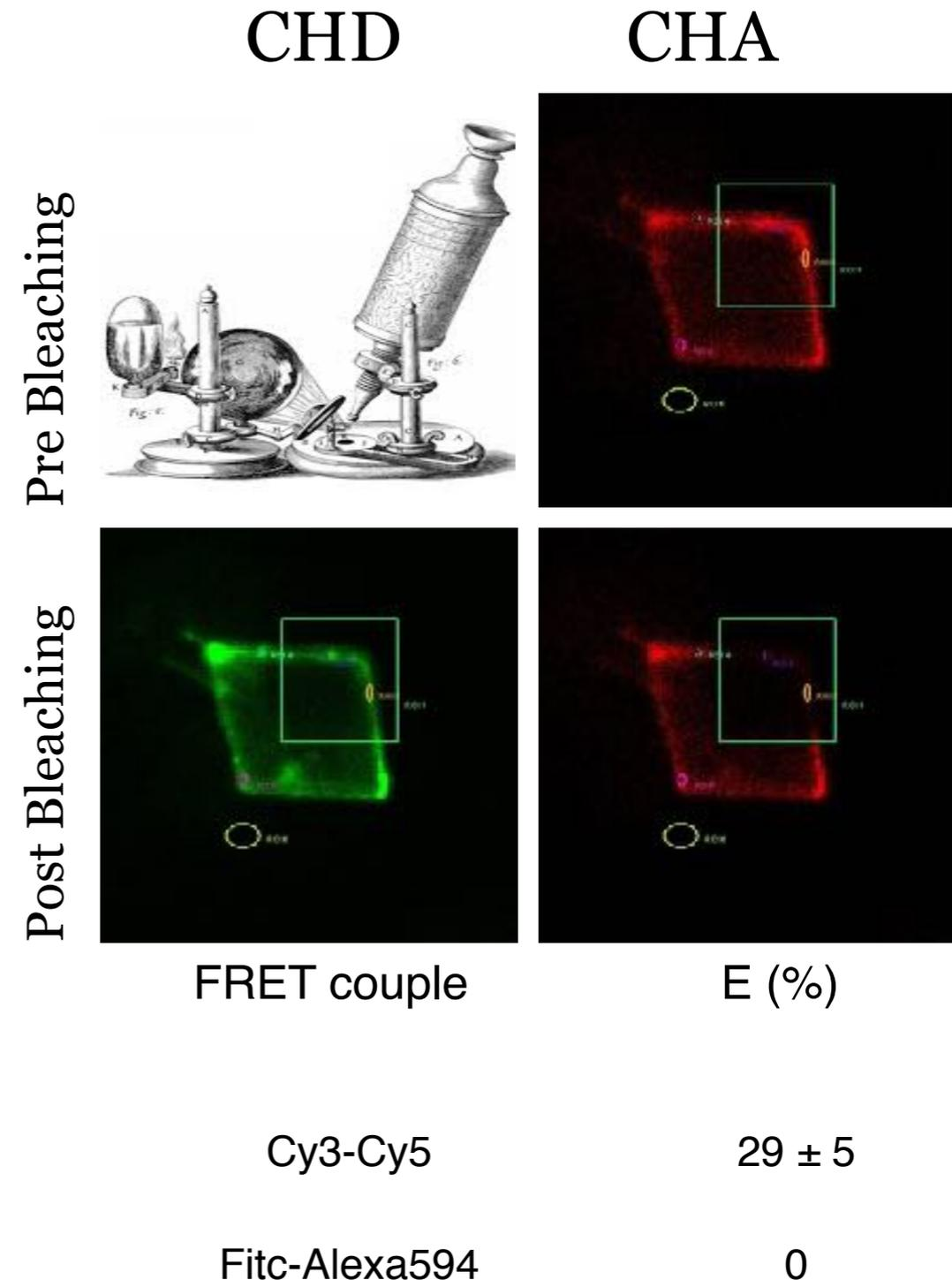
T. S. Karpova et Al. Fluorescence resonance energy transfer from cyan to yellow fluorescent protein detected by acceptor photobleaching using confocal microscopy and a single laser. J Microsc 2003 **209** 56--70

slide courtesy: Valentina Caorsi

FRET

- Donor Emission
- Acceptor Photobleaching
- Cross talk and SBT corrections
- Spectrally Resolved
- Donor Lifetime

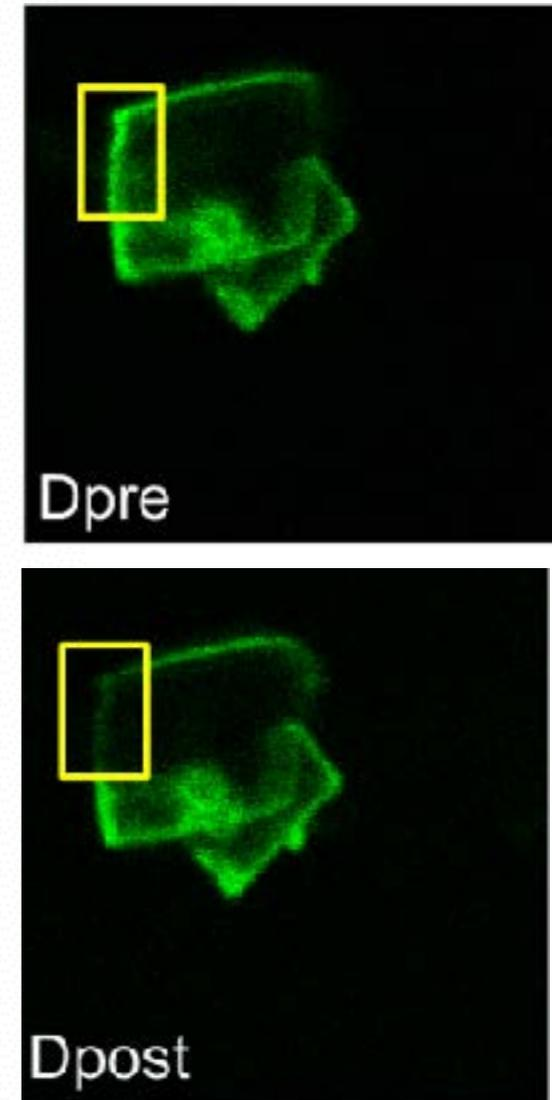
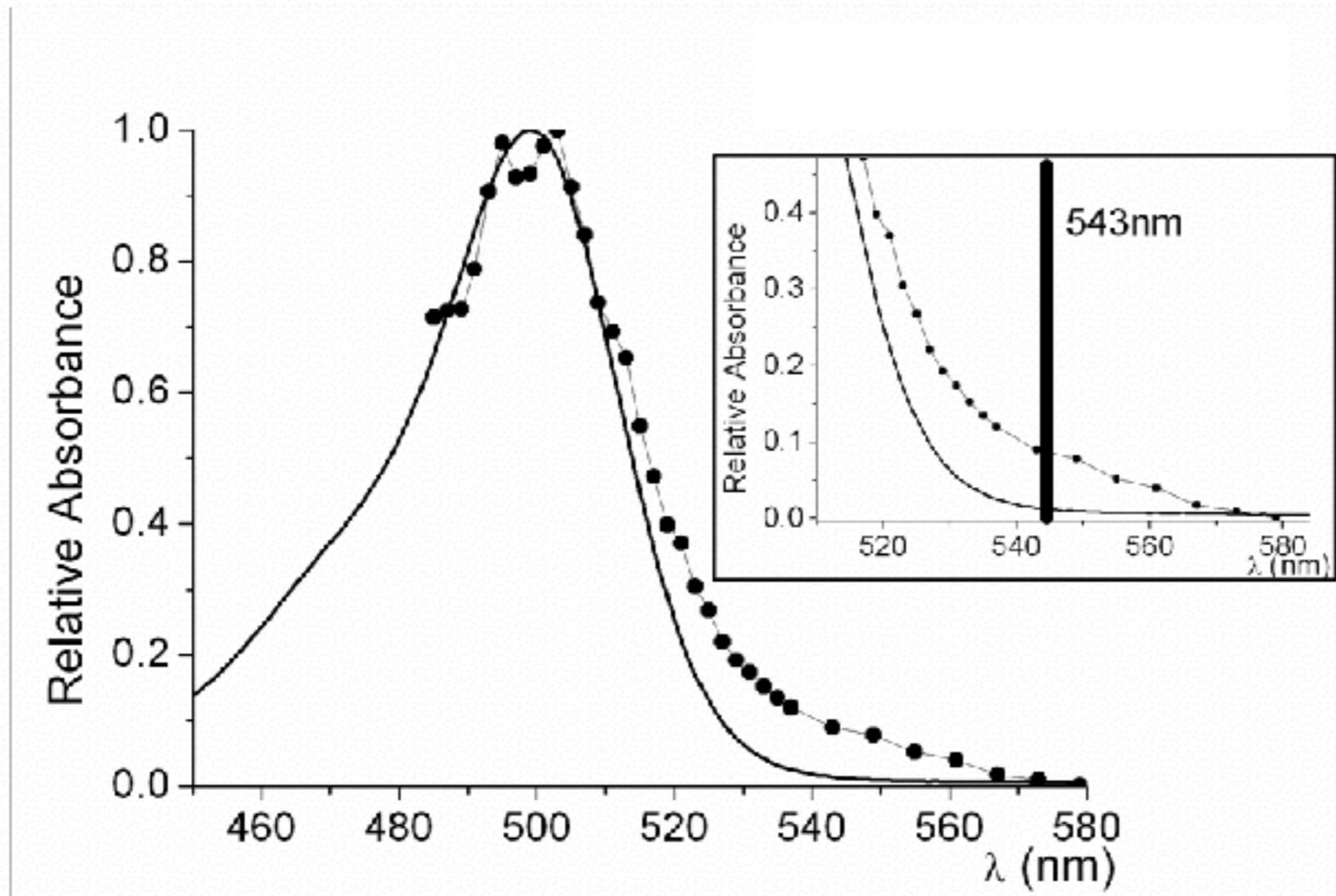
$$E = 1 - \frac{I_{DA}}{I_{DA_{\text{after photobleaching}}}}$$



T. S. Karpova et Al. Fluorescence resonance energy transfer from cyan to yellow fluorescent protein detected by acceptor photobleaching using confocal microscopy and a single laser. J Microsc 2003 **209** 56--70

slide courtesy: Valentina Caorsi

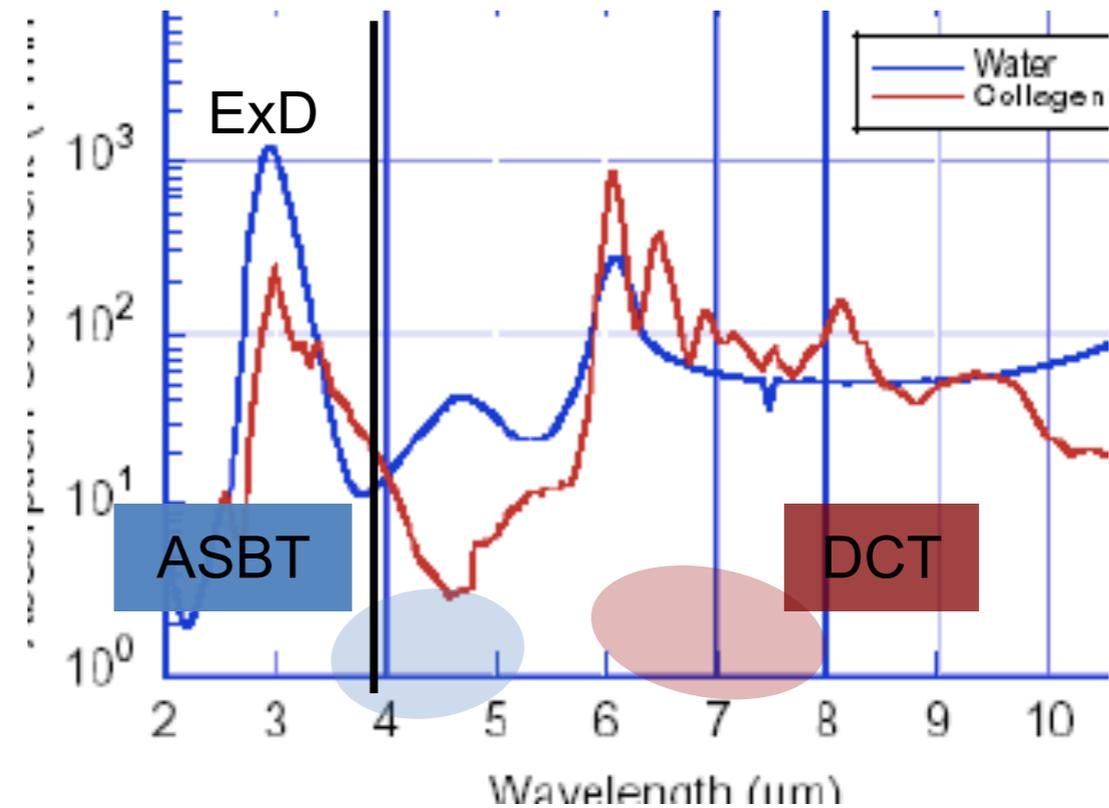
FRET



slide courtesy: Valentina Caorsi

FRET

- Donor Emission
- Acceptor Photobleaching
- Cross talk and SBT corrections
- Spectrally Resolved
- Donor Lifetime



M. Elangovan and H. Wallrabe and Y. Chen and R.N. Day and M. Barroso and A. Periasamy. Characterization of one- and two-photon excitation fluorescence resonance energy transfer microscopy. *Methods* 2003 29 58--73

slide courtesy: Valentina Caorsi

FRET

$$R_{Dn} = \left(\sum_i \frac{b_i}{a_i} \right)_n$$

$$R_{An} = \left(\sum_i \frac{c_i}{d_i} \right)_n$$

- Donor Emission
- Acceptor Photobleaching
- Cross talk and SBT corrections
- Spectrally Resolved
- Donor Lifetime

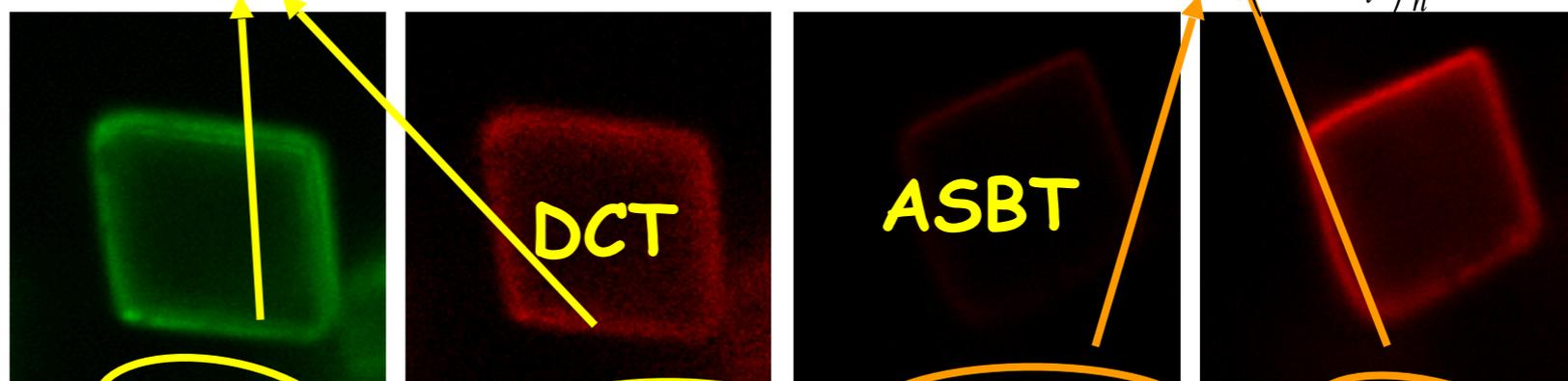


Image a Image b Image c Image d

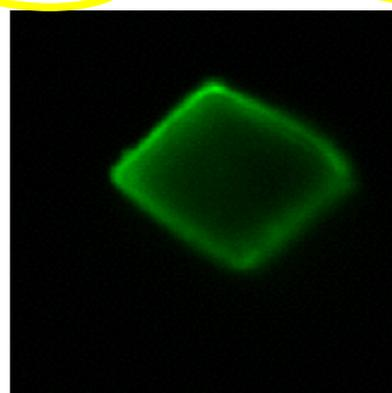


Image e



Image f

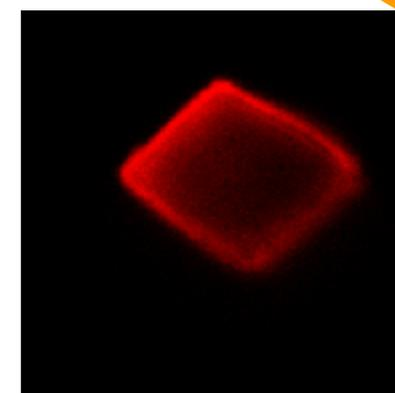


Image g

FRET couple

E (%)

Fitc-Alexa594

29 ± 7

Alexa488-Alexa594

24 ± 5

Cy3-Cy5

30 ± 6

$$E = 1 - \frac{I_{DA}}{I_{DA} + pFRET \frac{\Psi_{DD}}{\Psi_{AA}} Q_D}$$

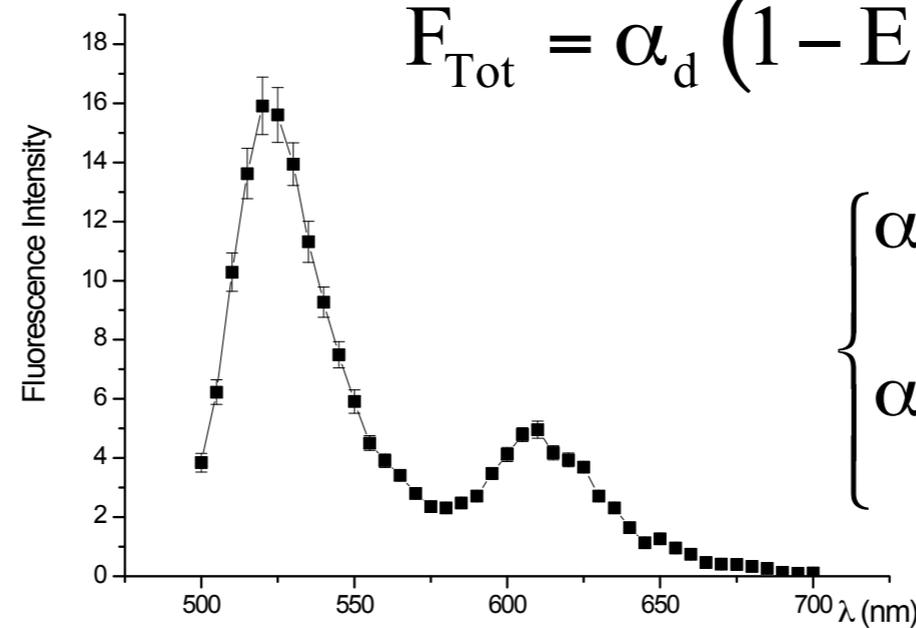
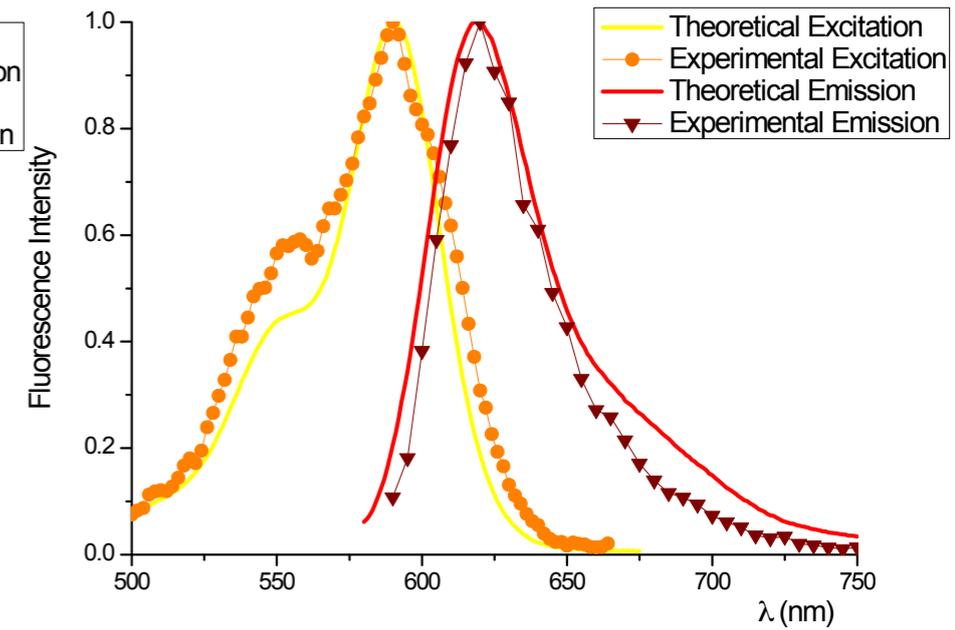
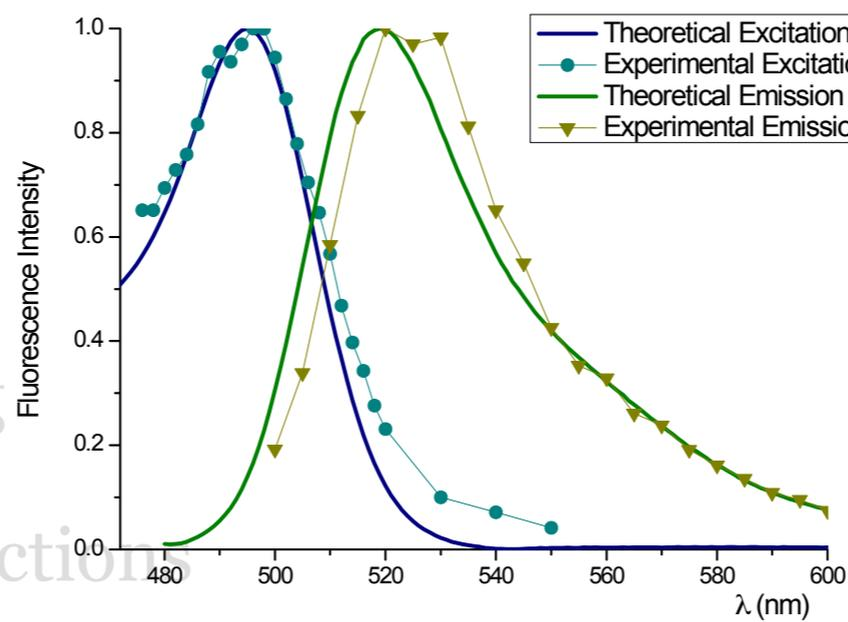
Eliminating Cross Talk and SBT

slide courtesy: Valentina Caorsi

Alberto Diaspro, Nanoscopy, Istituto Italiano di Tecnologia

FRET

- Donor Emission
- Acceptor Photobleaching
- Cross talk and SBT corrections
- Spectrally Resolved
- Donor Lifetime



$$F_{\text{Tot}} = \alpha_d (1 - E) F_d + \alpha_a F_a + \alpha_d E \frac{\epsilon_a}{\epsilon_d} F_a$$

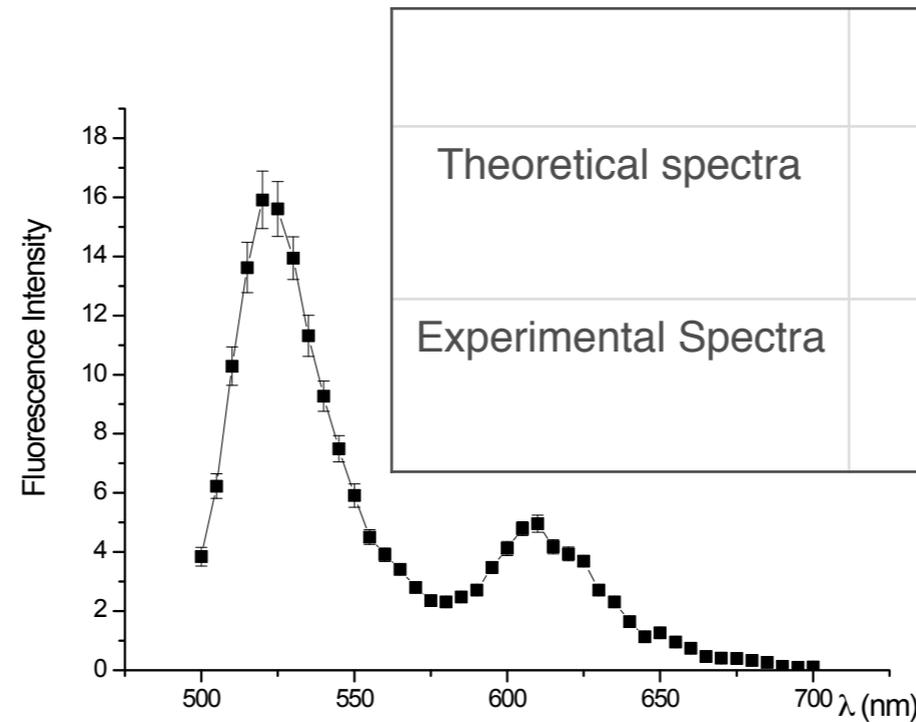
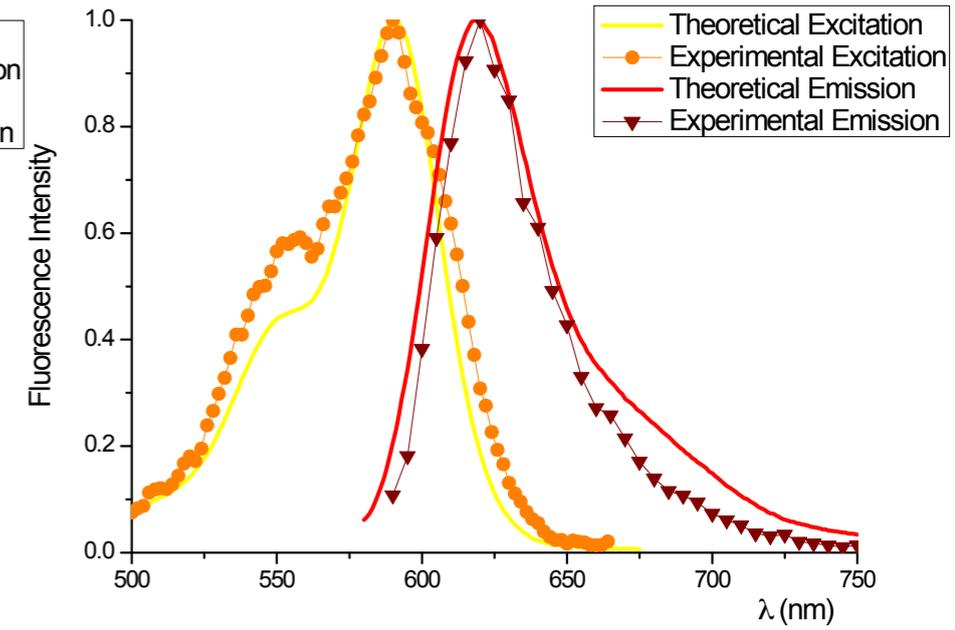
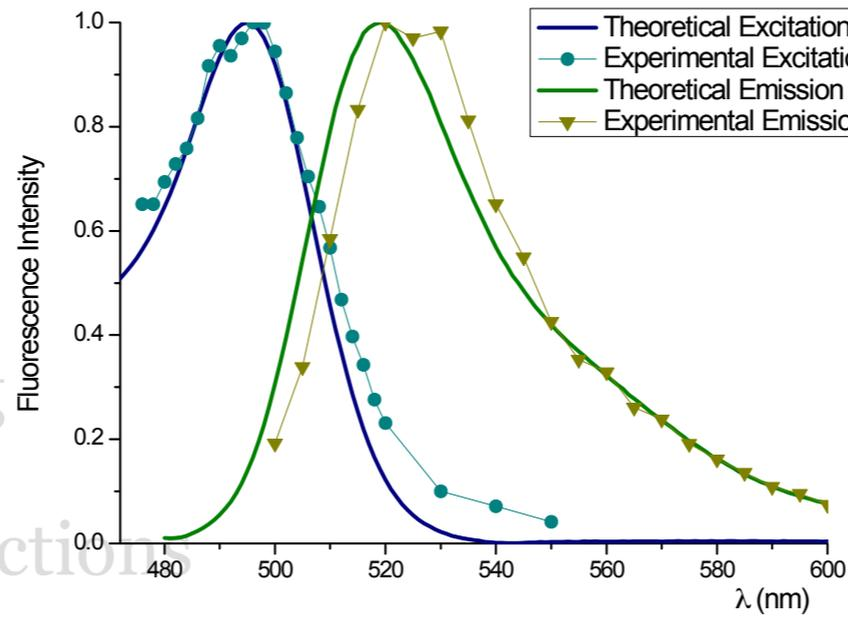
$$\begin{cases} \alpha_1 = \alpha_d (1 - E) \\ \alpha_2 = \alpha_a + \alpha_d E \frac{\epsilon_a}{\epsilon_d} \end{cases}$$

Neher, R.A. and Neher, E. Applying spectral fingerprinting to the analysis of FRET images. *Microsc Res Tech.* 2004 1;64(2):185-95.

slide courtesy: Valentina Caorsi

FRET

- Donor Emission
- Acceptor Photobleaching
- Cross talk and SBT corrections
- Spectrally Resolved
- Donor Lifetime



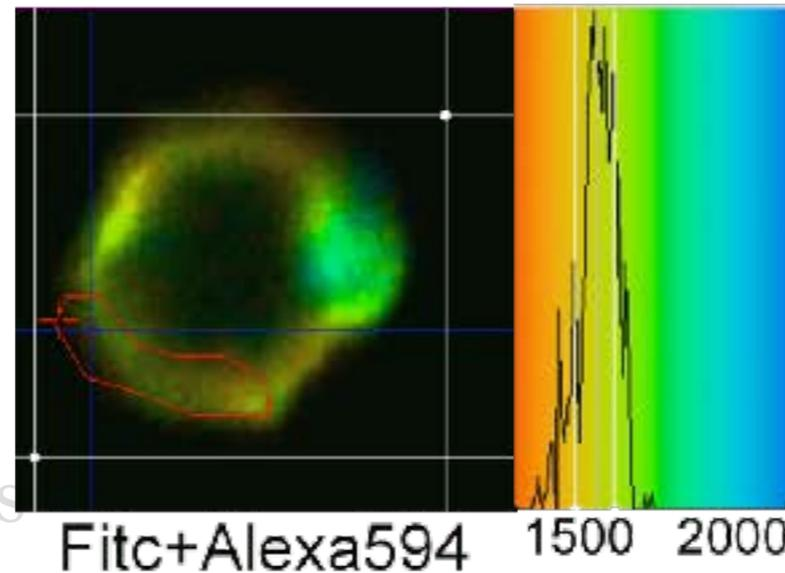
	E	d/a
Theoretical spectra	38 ± 3	3.2 ± 0.4
Experimental Spectra	25 ± 2	4.9 ± 0.9

Neher, R.A. and Neher, E. Applying spectral fingerprinting to the analysis of FRET images. *Microsc Res Tech.* 2004 1;64(2):185-95.

slide courtesy: Valentina Caorsi

FRET

- Donor Emission
- Acceptor Photobleaching
- Cross talk and SBT corrections
- Spectrally Resolved
- Donor Lifetime



τ_D Fitc 1.96±0.12 ns

τ_{DA} 1.28±0.06 ns

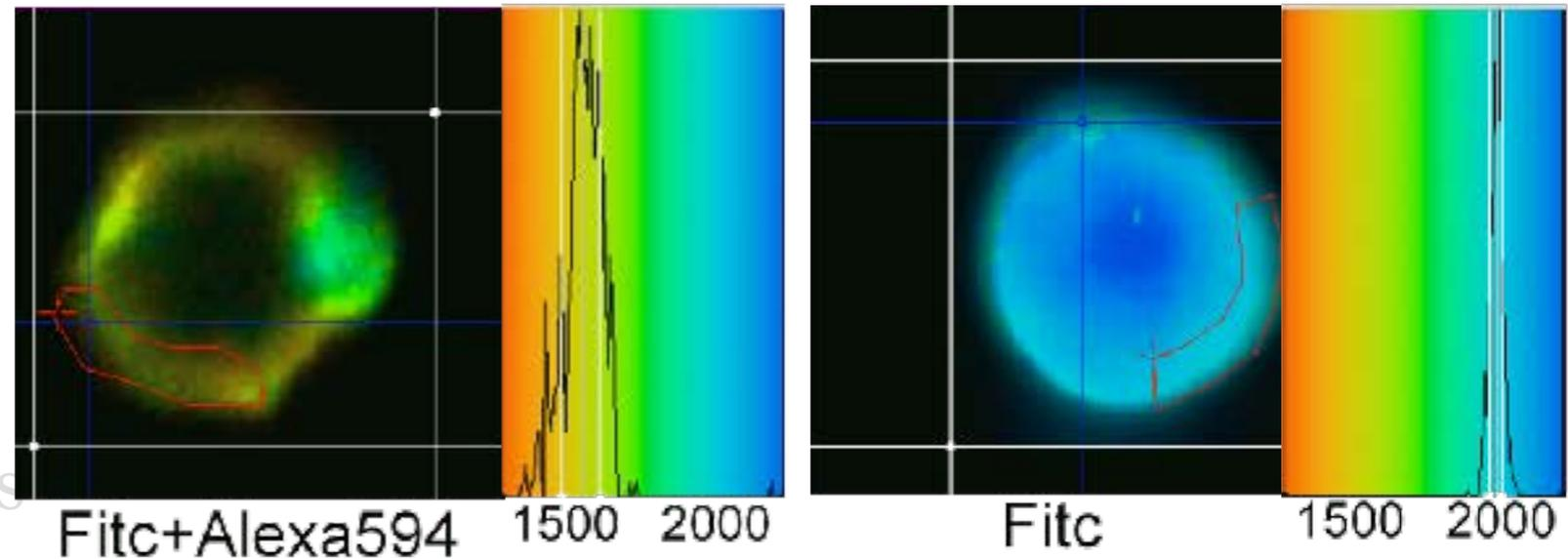
FRET efficiency 35±4 %

$$E = 1 - \frac{\tau_{DA}}{\tau_D}$$

W. Becker et al. Fluorescence lifetime images and correlation spectra obtained by multidimensional time-correlated single photon counting. *Microsc Res Tech* 2006 **69** 186--195

FRET

- Donor Emission
- Acceptor Photobleaching
- Cross talk and SBT corrections
- Spectrally Resolved
- Donor Lifetime



τ_D Fitc 1.96 ± 0.12 ns

τ_{DA} 1.28 ± 0.06 ns

FRET efficiency 35 ± 4 %

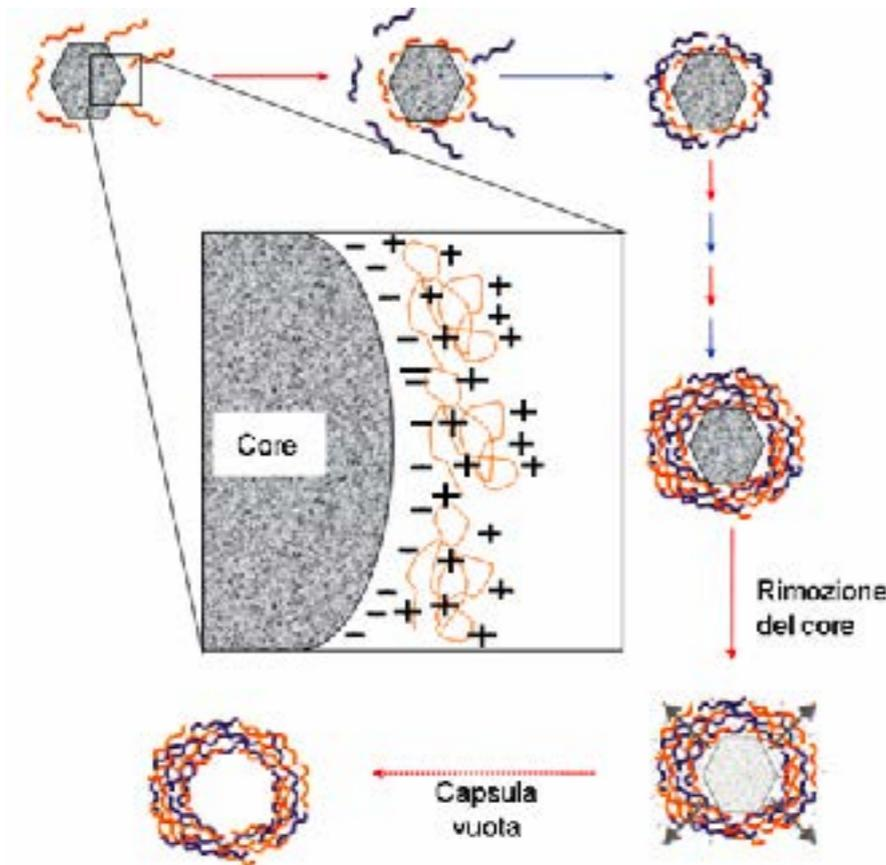
τ_D Fitc 2.02 ± 0.04 ns

$$E = 1 - \frac{\tau_{DA}}{\tau_D}$$

W. Becker et al. Fluorescence lifetime images and correlation spectra obtained by multidimensional time-correlated single photon counting. *Microsc Res Tech* 2006 **69** 186--195

slide courtesy: Valentina Caorsi

A model system (nanocapsules)

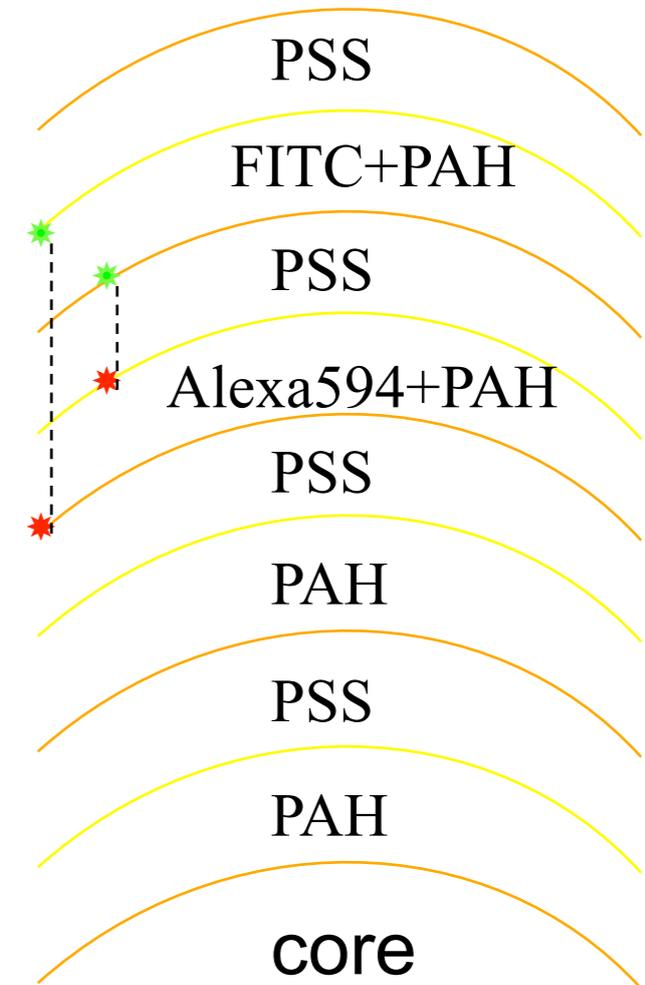


Distance

D-A

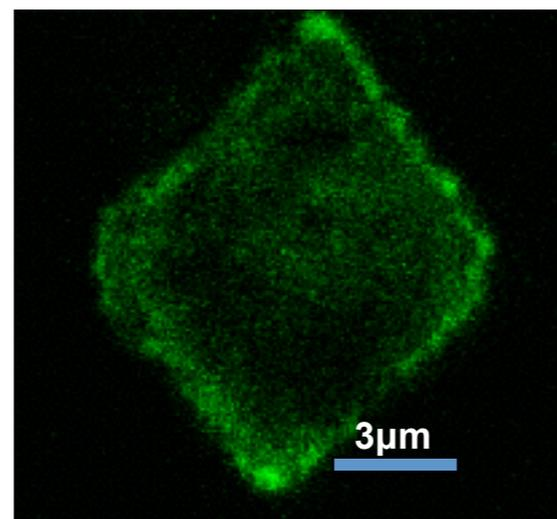
2.5-7.5 nm

Polyelectrolytes with opposite charges



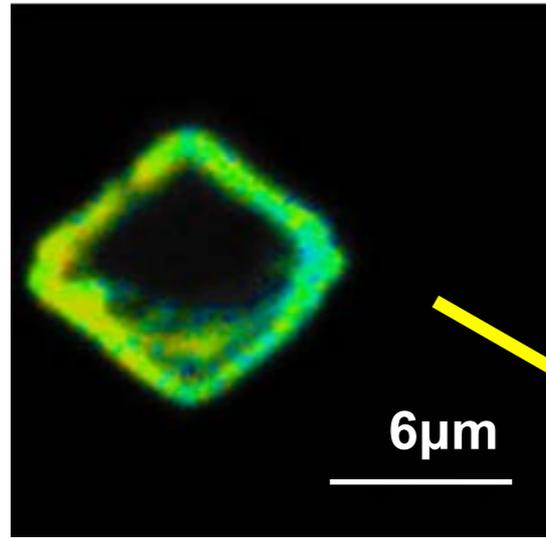
Nanocapsules of 8 layers labelled at 5° and 7° layer

Two photon excitation imaging



FRET and FLIM on nanocapsules

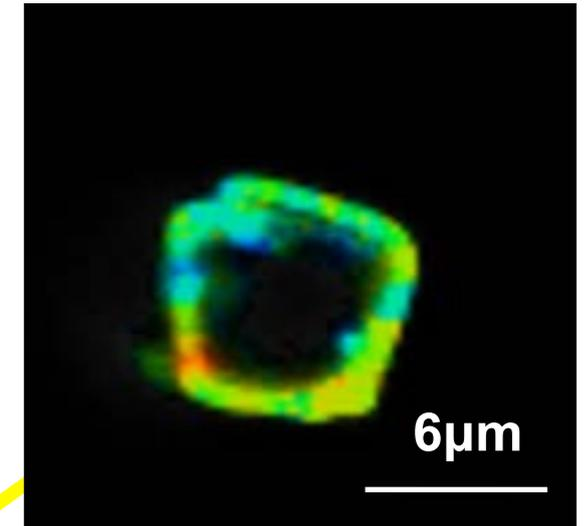
Donor FITC +
Acceptor Alexa594



150ps

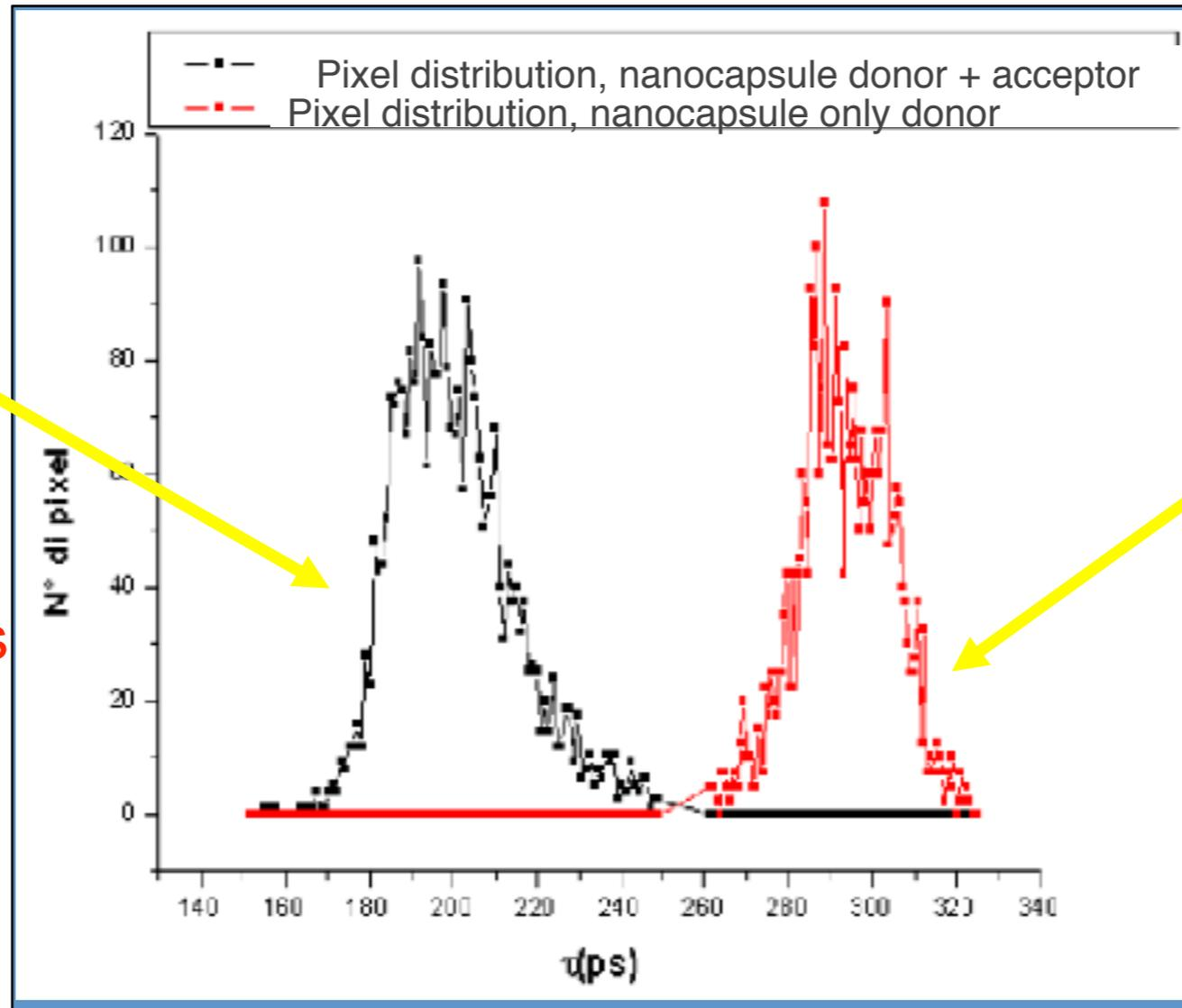
250ps

Donor FITC



270ps

320ps



Translation due to **FRET**

Caorsi V., Ronzitti E., Vicidomini G., Krol S., McConnell G., Diaspro A. (2007) *Micr. Res. Tech.*, 70
Nizzari M., Caorsi V., et al., Diaspro A. (2007) *JBC*

Fluorescence recovery after photobleaching

From ensemble average experiments to single molecule imaging

Slide credit for FRAP slides (adapted): Davide Mazza

Loren...Diaspro et al., **Q Rev Biophys.** 2015 Aug;48(3):323-87.

Slide credits: Davide Mazza - mazza.davide@hsr.it

Alberto Diaspro, Nanoscopy, Istituto Italiano di Tecnologia

xVivo – The inner life of cell



<http://www.xvivo.net/animation/the-inner-life-of-the-cell/>

WHY

IS STUDYING THE DYNAMICS OF YOUR PROTEIN IMPORTANT?

I – CARRIES INFORMATION ABOUT UNDERLYING MOLECULAR MECHANISMS.

Interactions, transport processes, oligomerization states...

II – CELLULAR OUTCOMES DEPEND ON PROTEIN DYNAMICS

Eg. Circadian rhythms, Response to inflammation, to DNA damage...

Oscillations in NF- κ B Signaling Control the Dynamics of Gene Expression

D. E. Nelson,¹ A. E. C. Ihekwaba,² M. Elliott,¹ J. R. Johnson,¹
C. A. Gibney,¹ B. E. Foreman,¹ G. Nelson,¹ V. See,¹ C. A. Horton,¹
D. G. Spiller,¹ S. W. Edwards,¹ H. P. McDowell,⁴ J. F. Unitt,⁵
E. Sullivan,⁶ R. Grimley,⁷ N. Benson,⁷ D. Broomhead,³
D. B. Kell,² M. R. H. White^{1*}

p53 Dynamics Control Cell Fate

Jeremy E. Purvis, Kyle W. Karhohs, Caroline Mock, Eric Batchelor,*
Alexander Loewer,† Galit Lahav‡



In vivo dynamics of RNA polymerase II transcription

Xavier Darzacq^{1,2}, Yaron Shav-Tal^{1,2}, Valeria de Turris¹, Yehuda Brody³, Shailesh M Shenoy¹,
Robert D Phair⁴ & Robert H Singer¹

WHAT

INSTRUMENT TO USE?

OPTICAL MICROSCOPY looks like a good candidate.

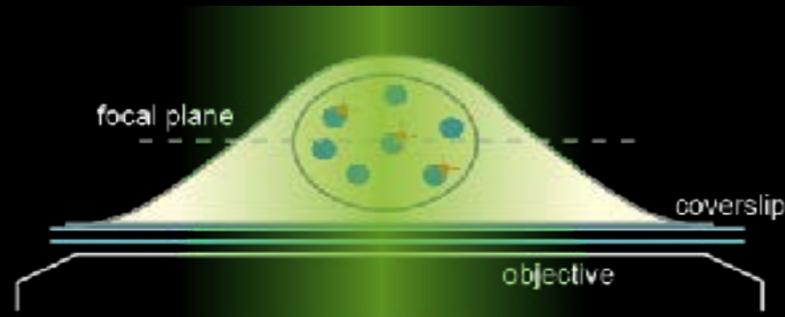
Cells are transparent to visible light.

Relatively low phototoxicity (but beware of near UV radiation).

With sufficient resolution (~200nm) to visualize intracellular compartments

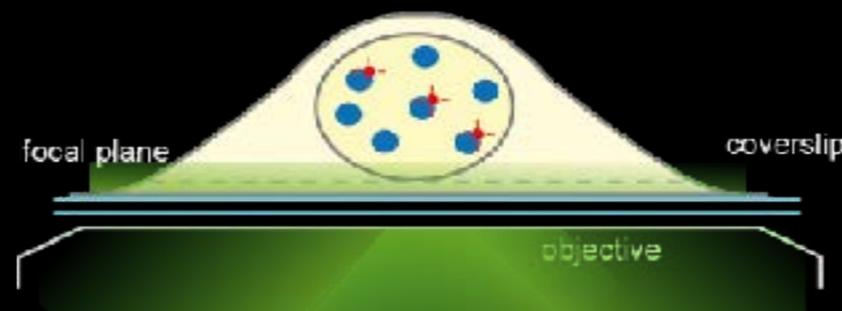
What kind of microscopy?

WIDEFIELD
ILLUMINATION



- + Sensitive
- + Fast
- Out of focus blur

TIRF
ILLUMINATION



- + Sensitive
- + No out of focus blur
- Limited to surface

LASER SCANNING
(e.g. CONFOCAL)



- + No out of focus blur
- Not that fast
- Not that sensitive

The missing link.

Light microscopy



© T. Hatano, NIG, Japan

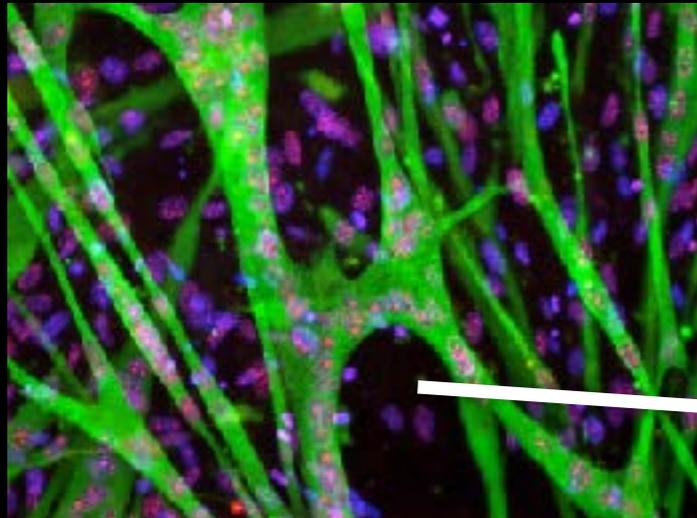
Viability

Electron microscopy



© CBIM, Imperial College, UK

Immunofluorescence

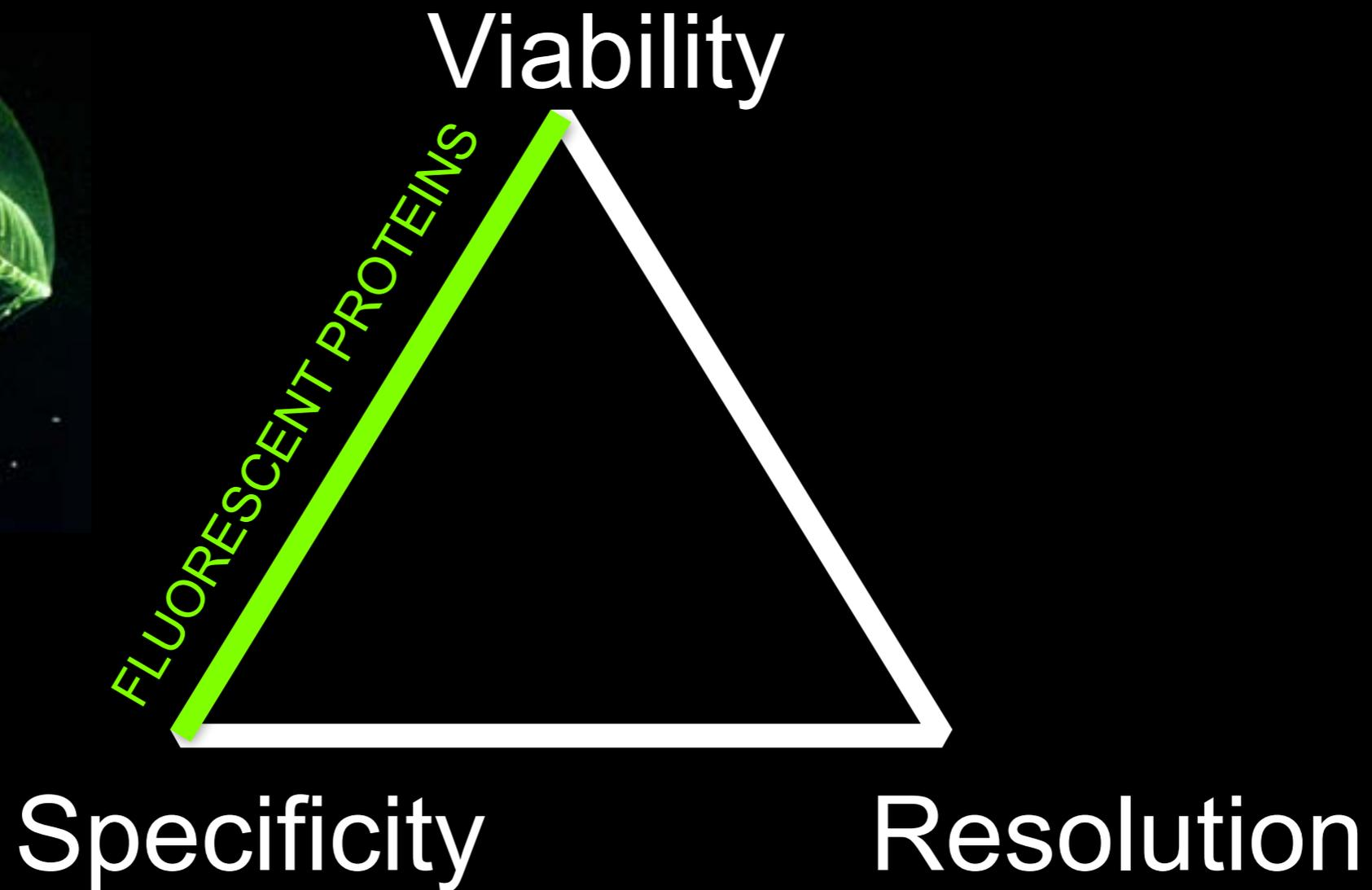


© M.Neguembor, HSR.

Specificity

Resolution

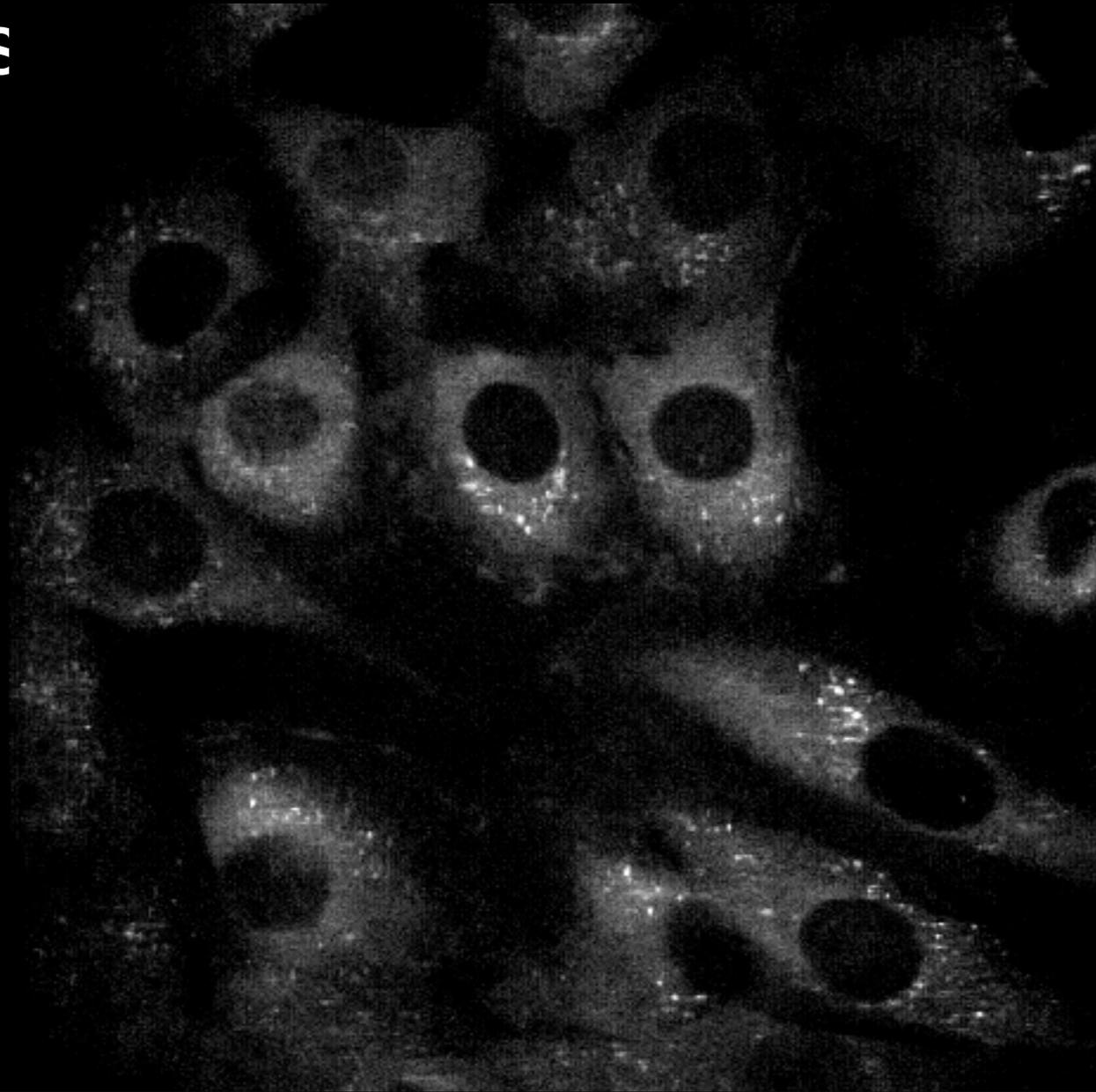
GFP: bridging viability and specificity



Von Dassow, 200

Some dynamics can be measured directly

Example: massive translocations between different compartments

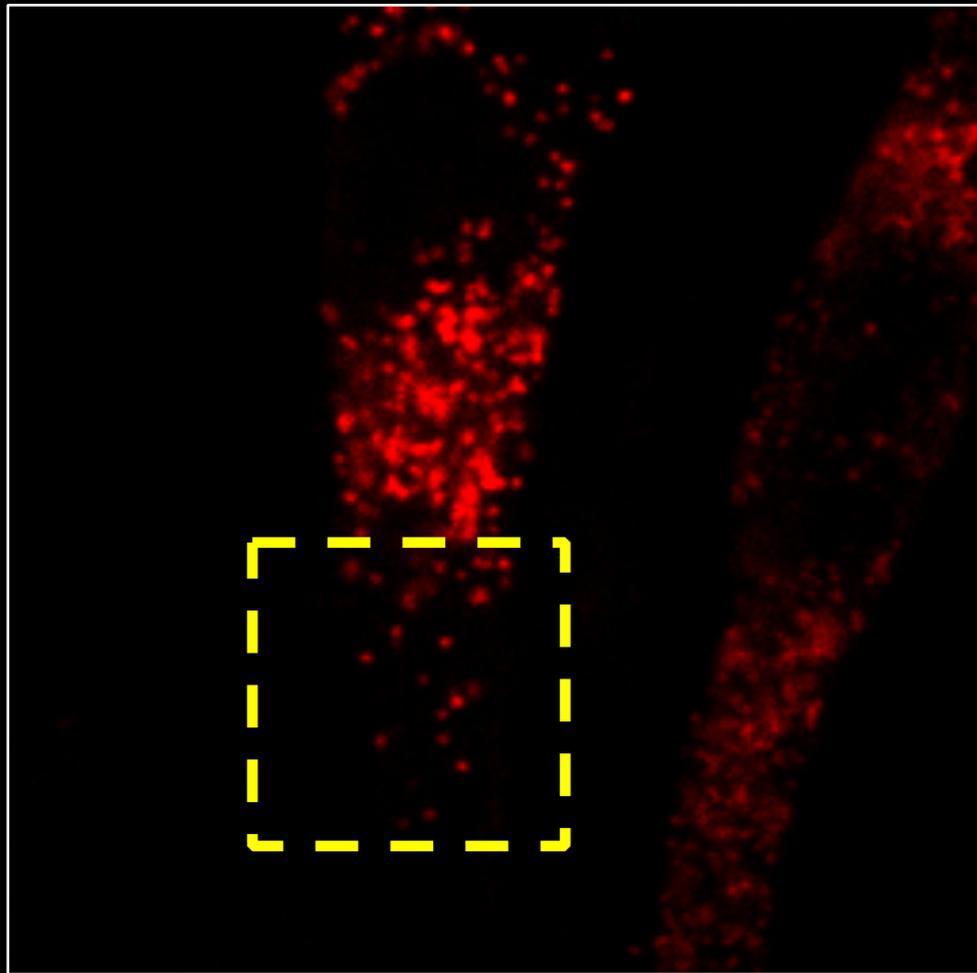


NF-kB translocation

(Sung and Agresti, 2009)

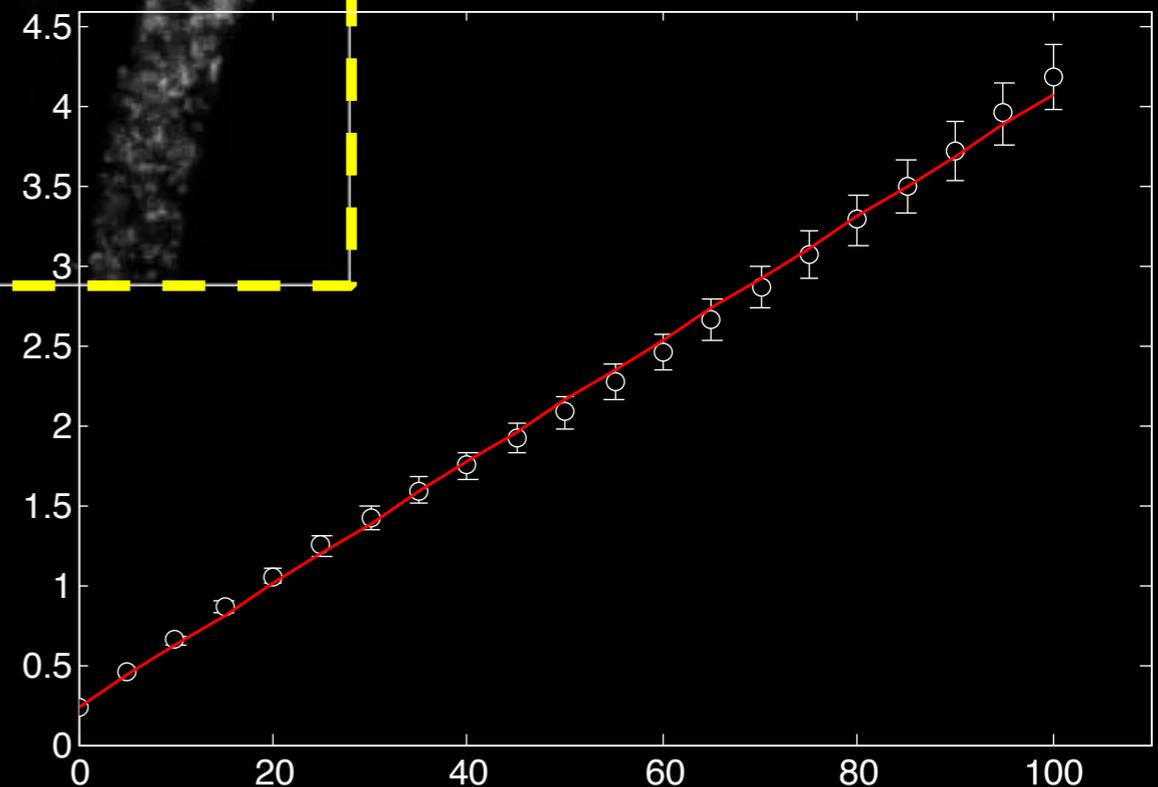
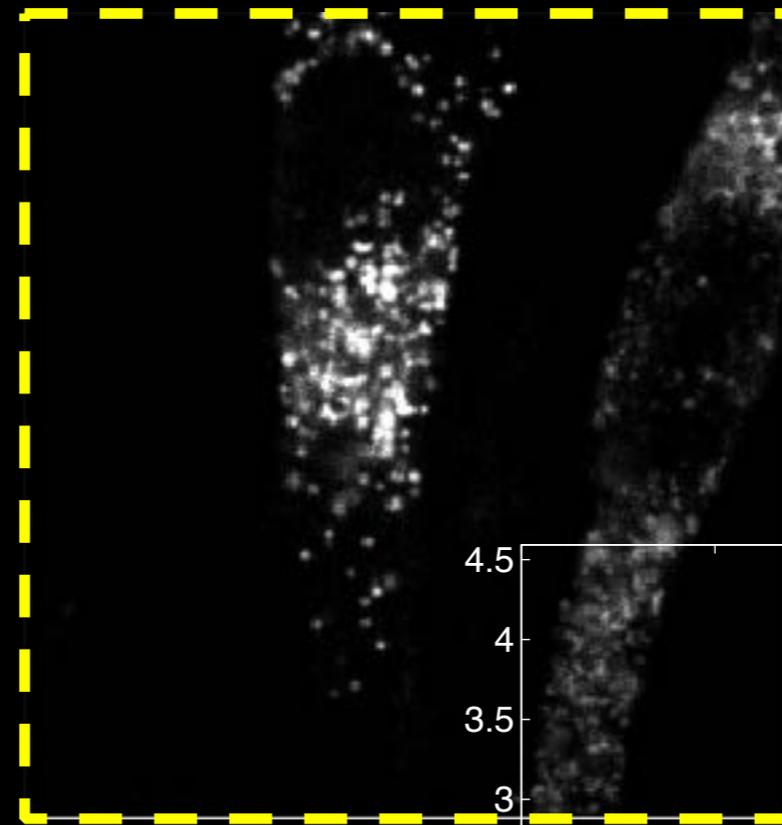
Mobility of dispersed particles

one image every 5 sec
whole movie ~ 500s



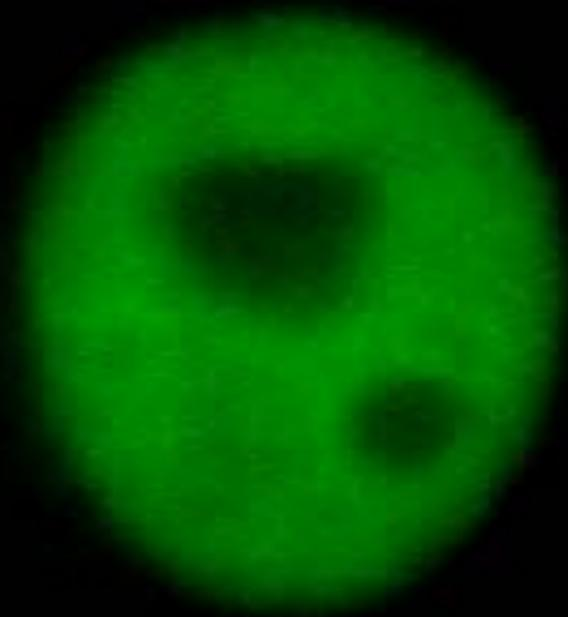
Aggregates of Ab heavy chain.
(w/ M. Mossuto and R. Sitia, HSR)

Tracked particles



Equilibrium: a molecular Where's Waldo

It can be difficult to understand what individual molecules do,
even when selectively labelling your protein of interest.

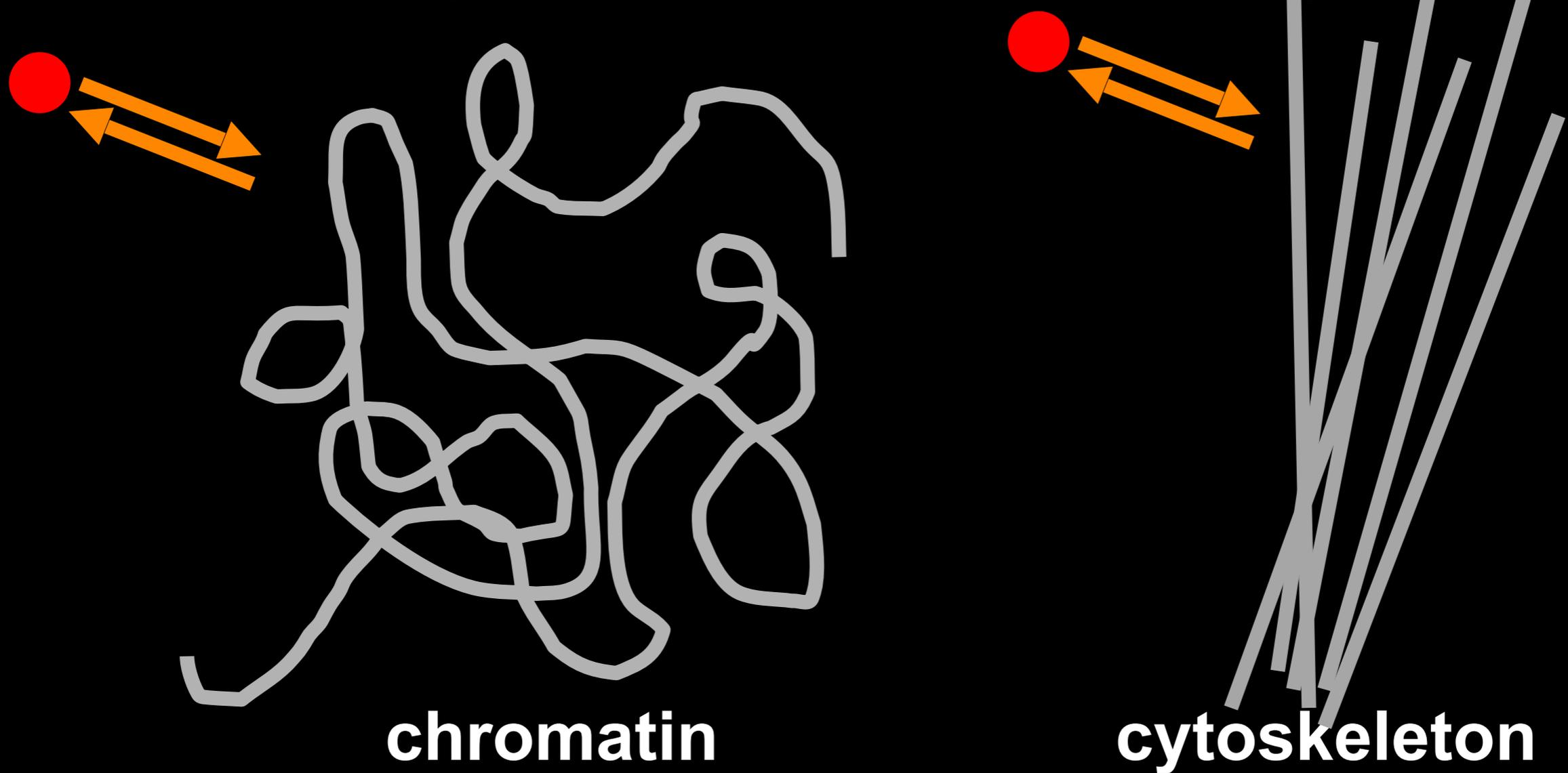


Tumor suppressor p53-GFP
in live fibroblasts (30 min after dex stimuli)



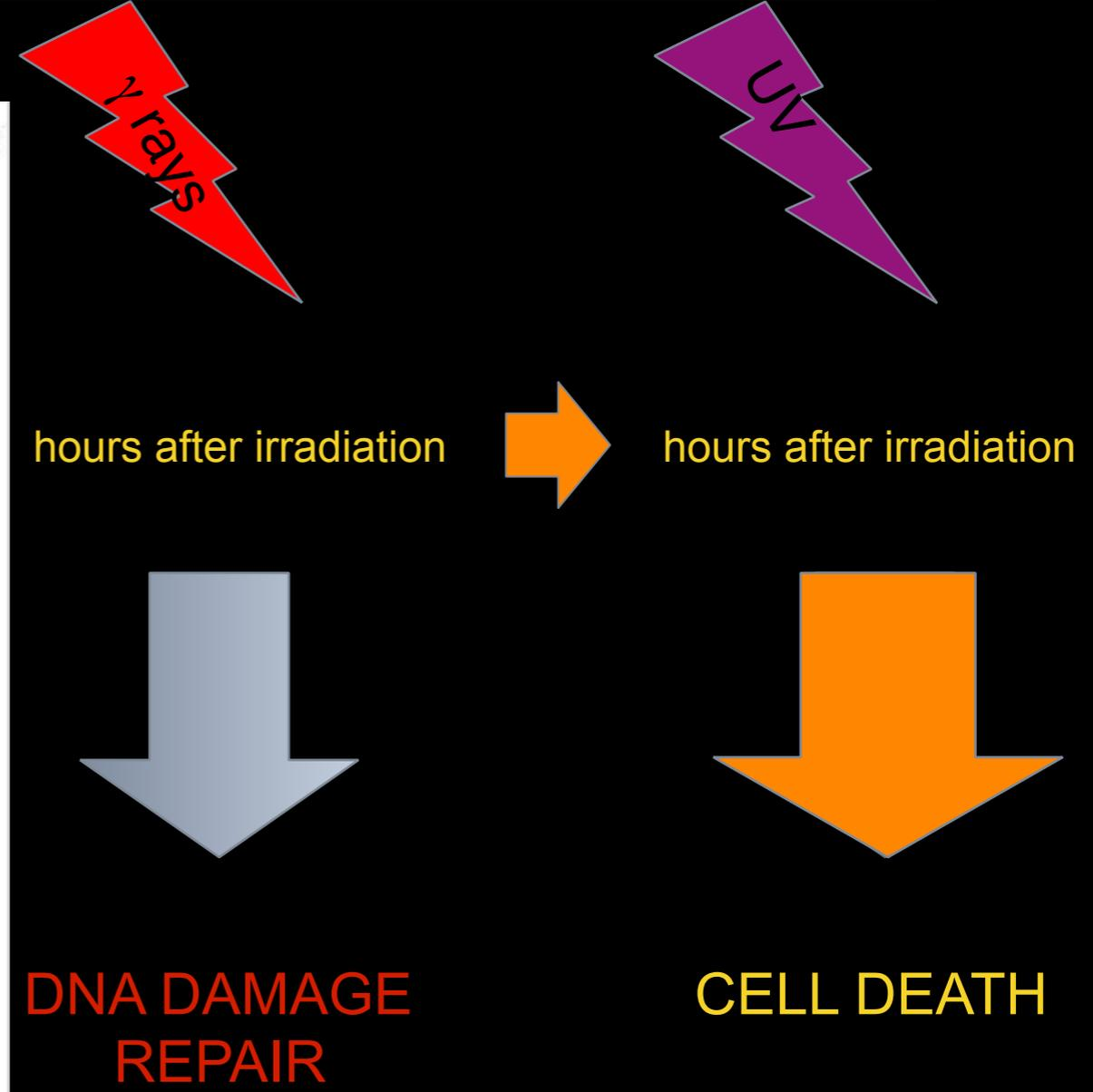
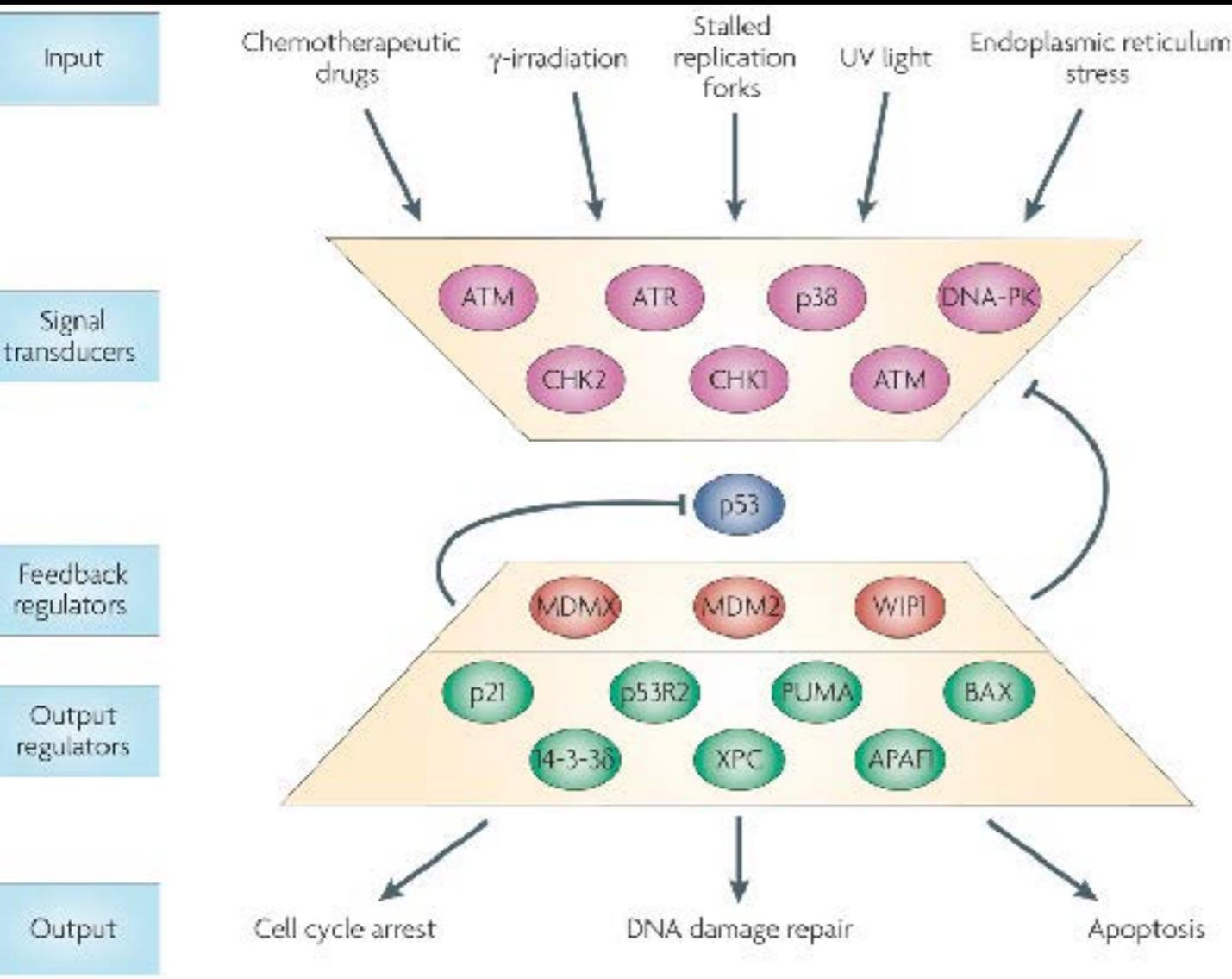
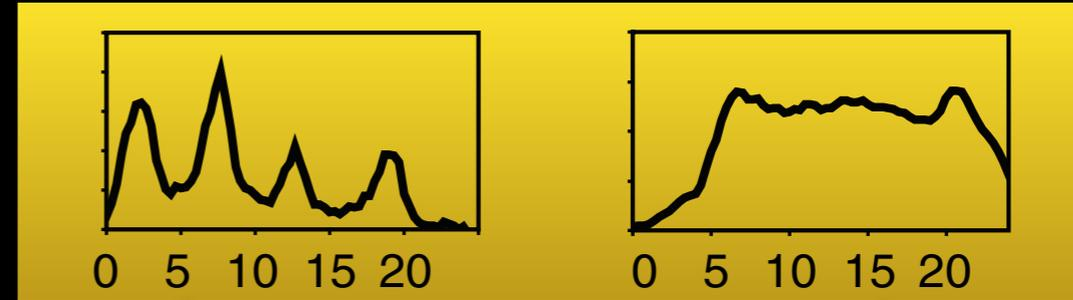
Binding to ~immobile scaffolds is a widespread event in the cells

In the nucleus, these interactions regulate transcription, translation and DNA repair.



Long term experiments?

Interfering with protein dynamics allows interfering with cellular fate.



(Batchelor et al., Mol Sys Biol, 2011) (Purvis et al., Science, 2012)

(Batchelor et al., Nat. Cancer Rev, 2009)

Perturbation control

Modify the fluorescence properties of a subpopulation of molecules by using a pulse of intense light.

Fluorescence Perturbation techniques (FPT)

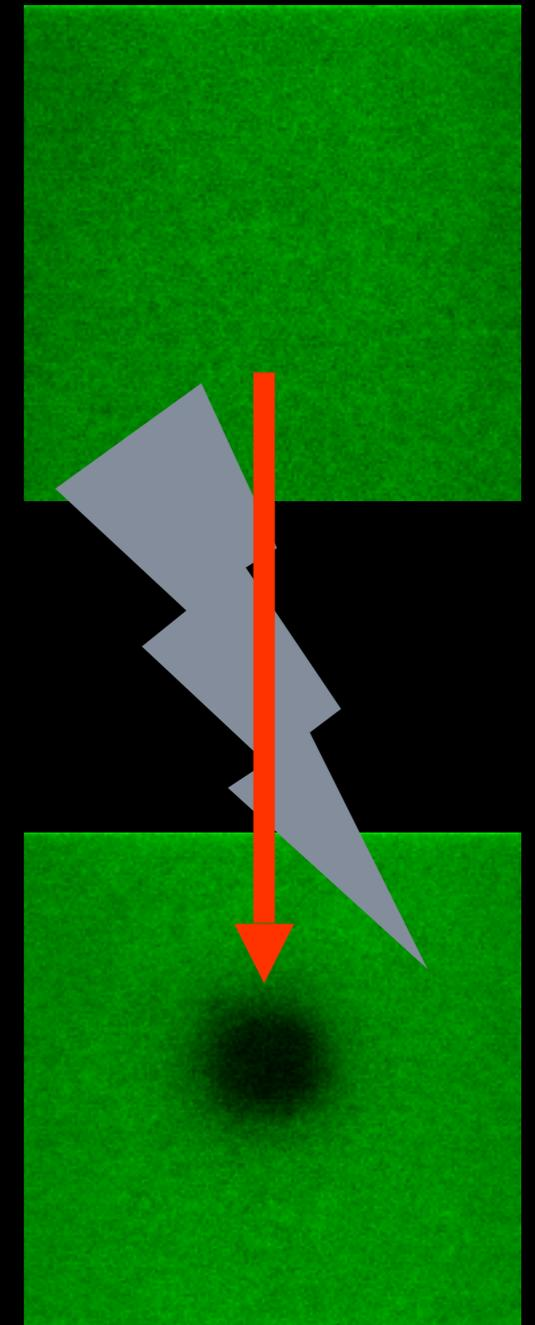
Photobleaching
Techniques

Photoactivation
Techniques

i-FRAP
Inverse FRAP

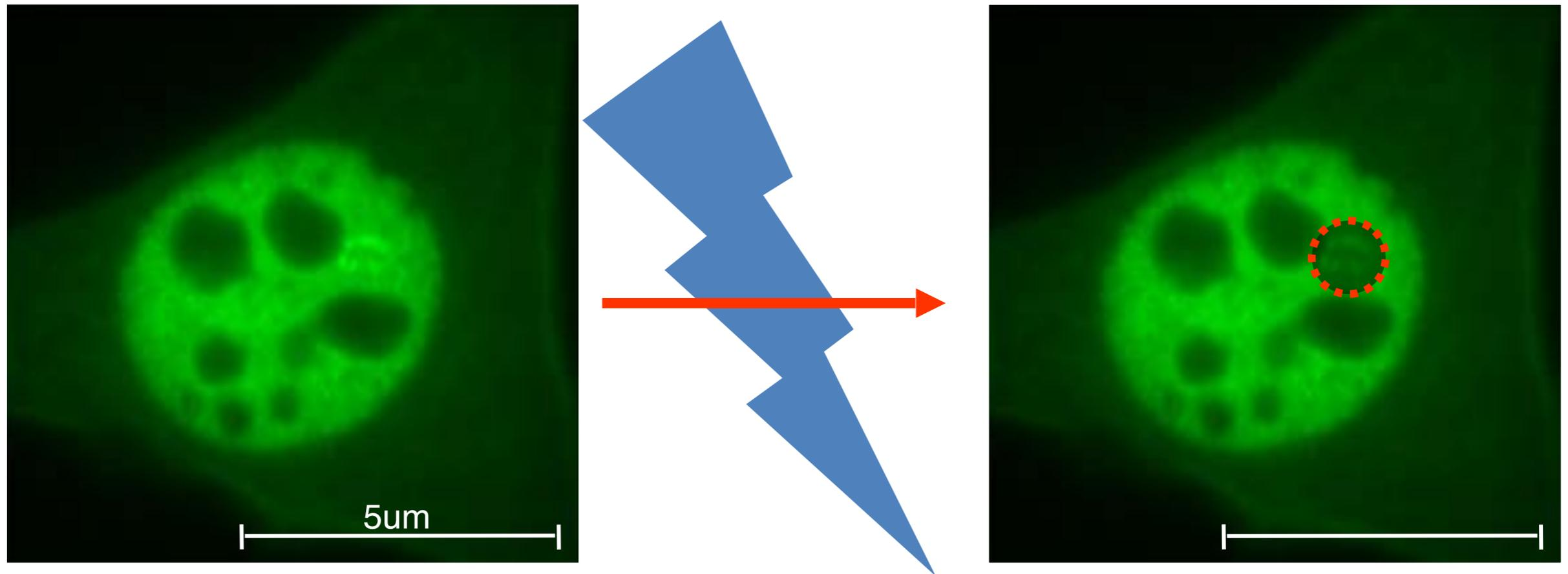
FRAP
Fluorescence Recovery
after Photobleaching

FLIP
Fluorescence Loss
Into Photobleaching



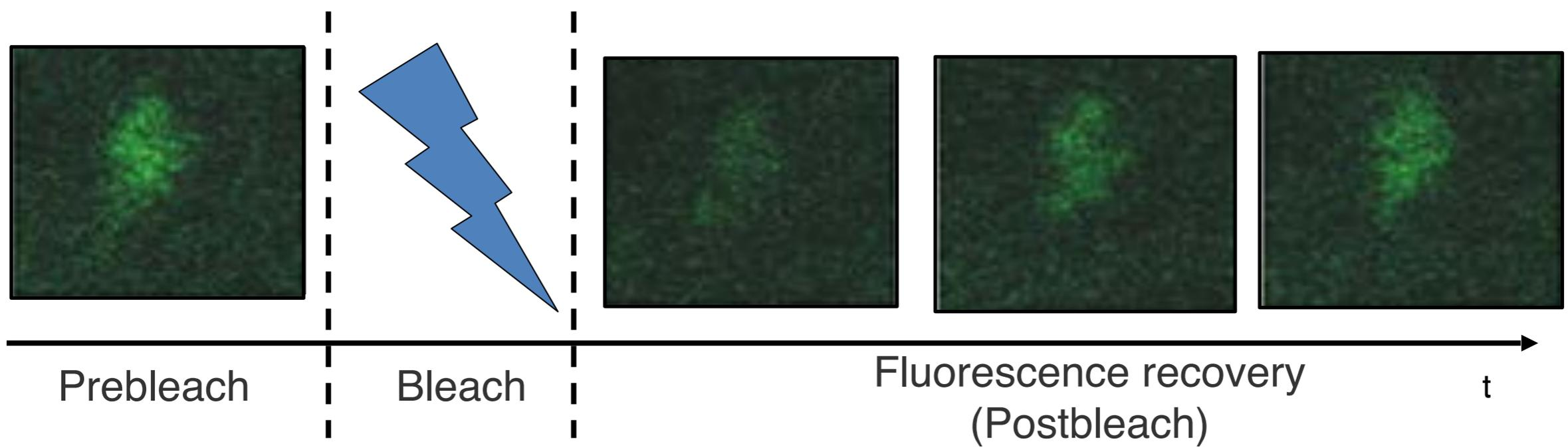
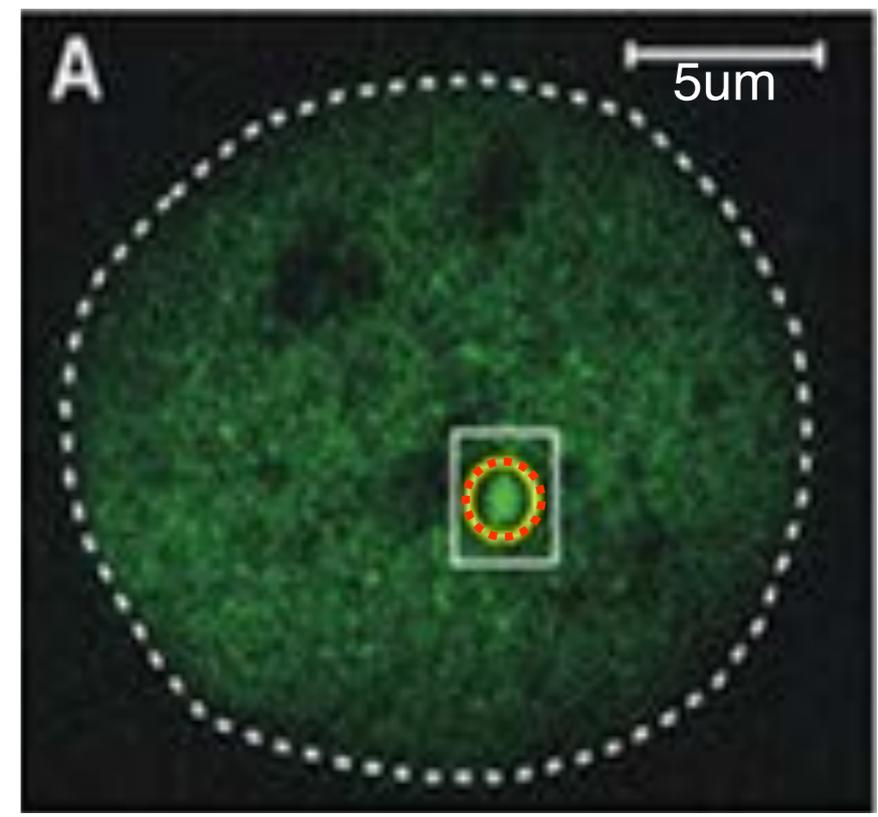
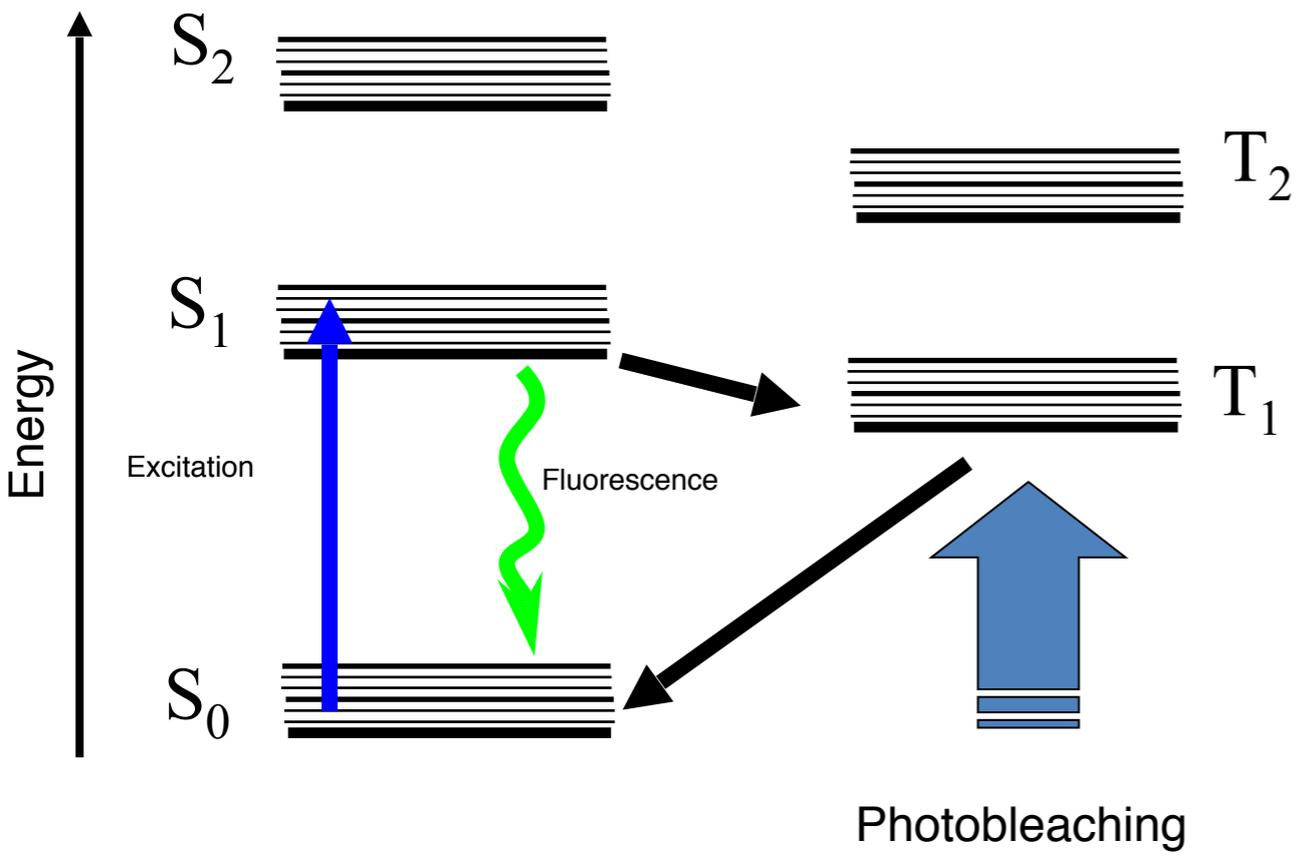
FRAP

Perturbation control:



slide credit: Davide Mazza, LAMBS

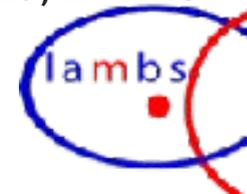
FRAP



slide credit: Davide Mazza, LAMBS

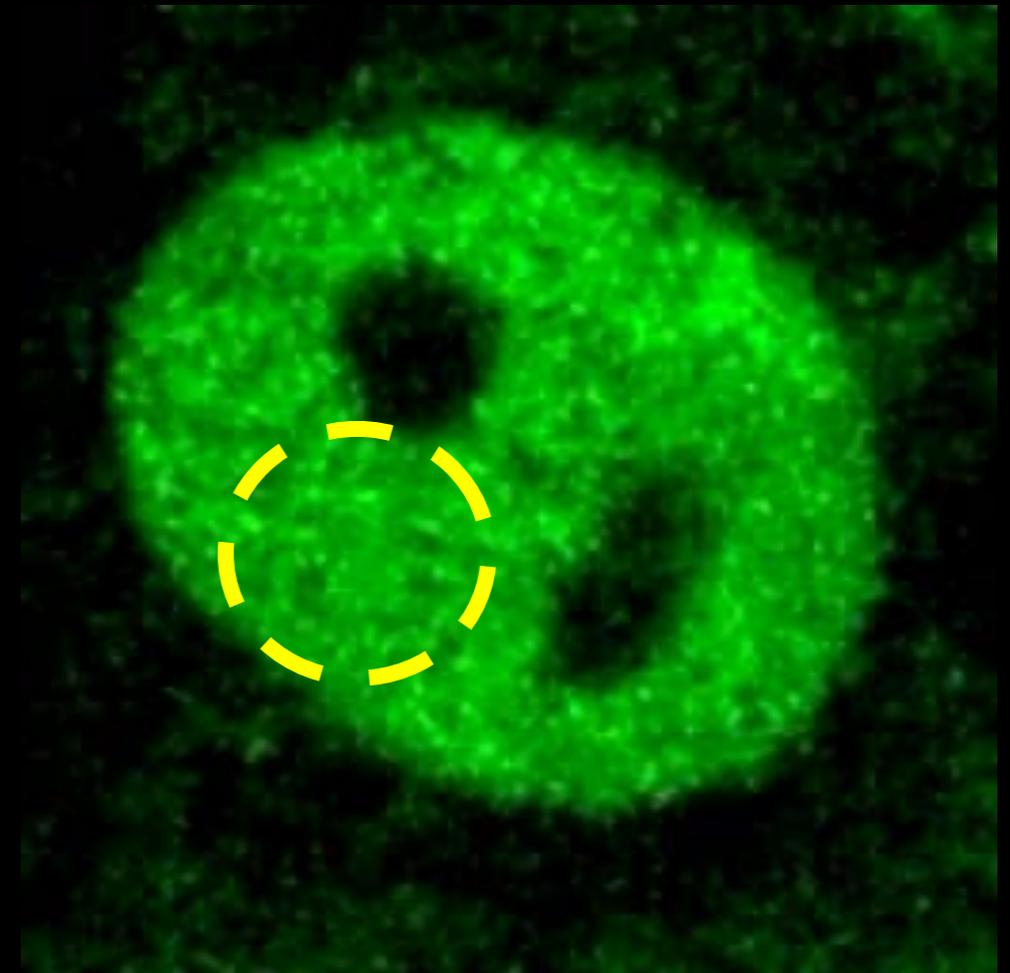
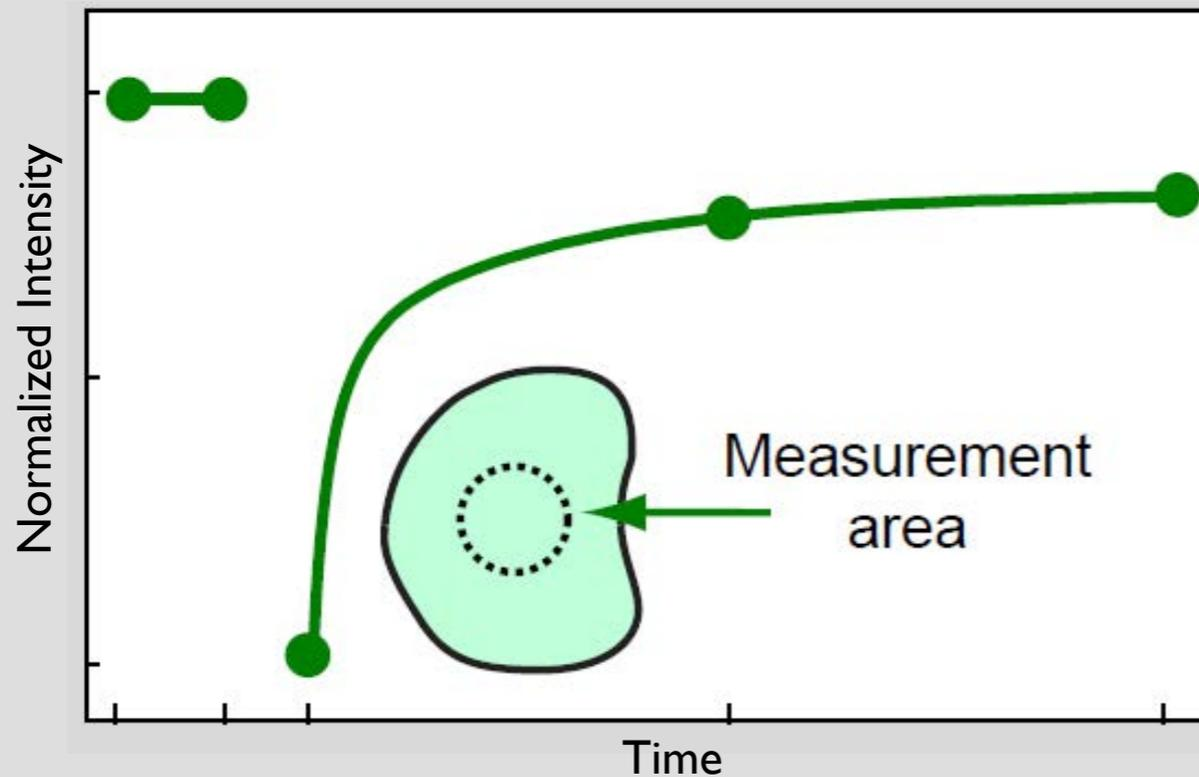
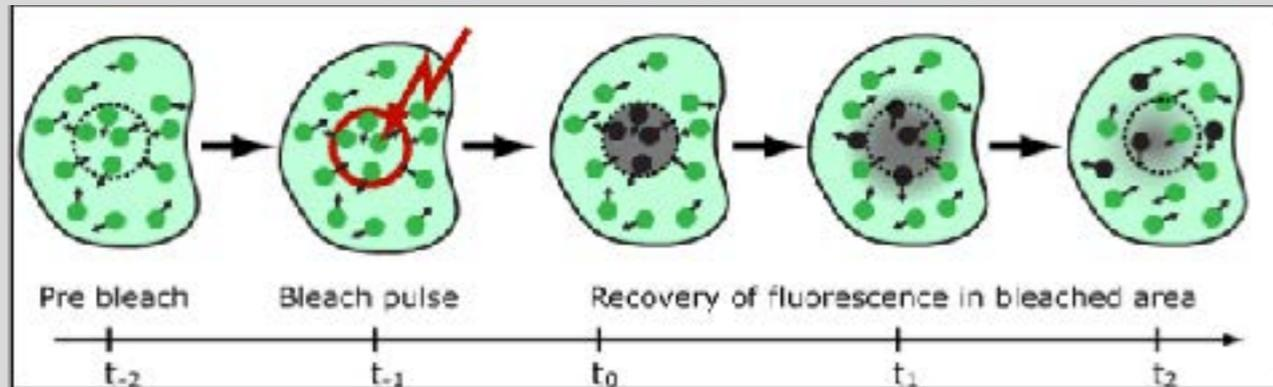


Alberto Diaspro, Nanoscopy, Istituto Italiano di Tecnologia



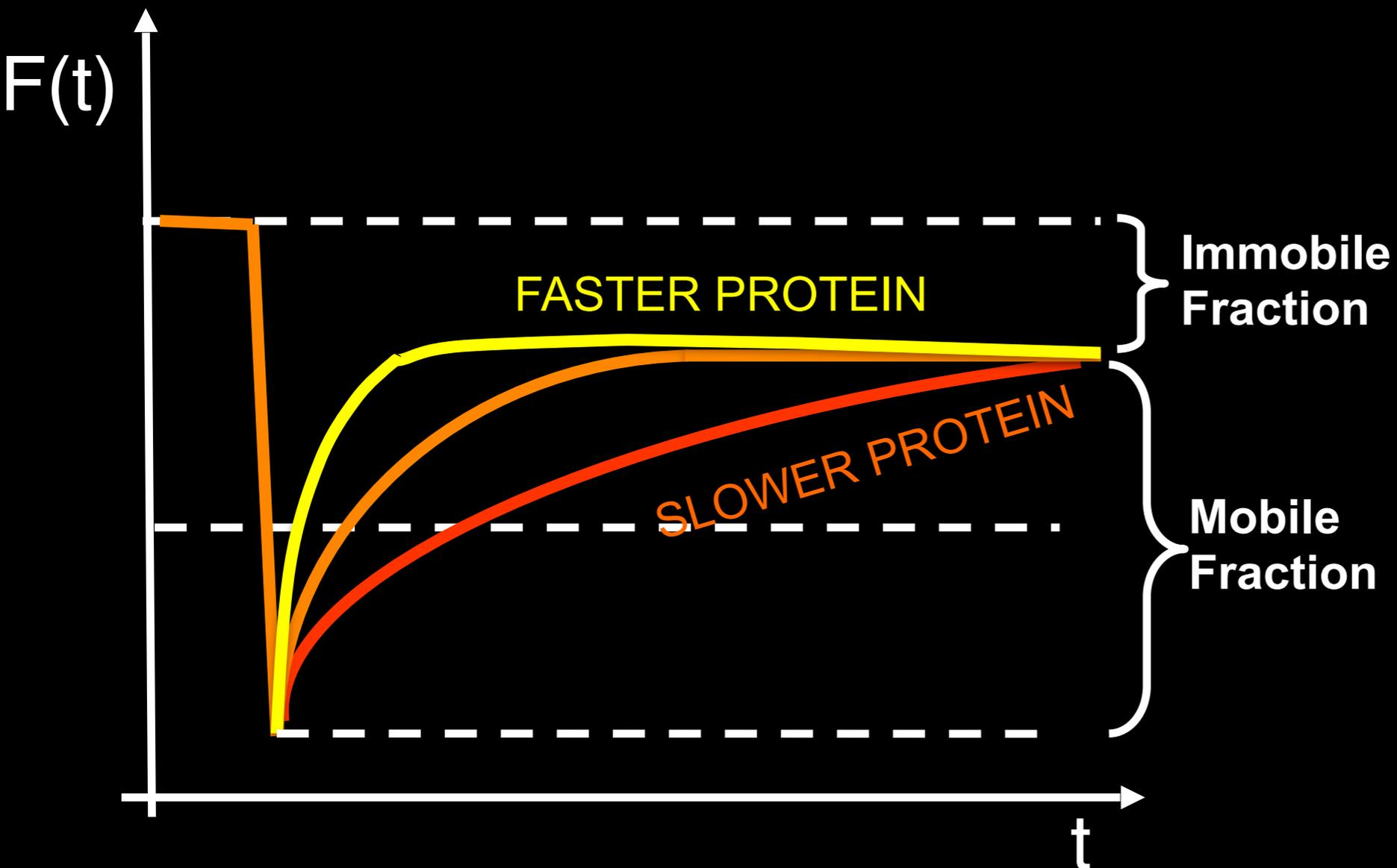
Fluorescence recovery after photobleaching

Fluorescence Recovery After Photobleaching (FRAP)



p53 dynamics in living cells
(whole movie 30 s)

Qualitative analysis of FRAP data



$$t_{50} > t_{50} > t_{50}$$

Can we be more quantitative?

YES BUT WE NEED SOME MATH

Free diffusion

Axelrod, D et al.(1976), Biophys J 16, 1055--1069.
Soumpasis, D. M. (1983), Biophys J 41, 95--97.

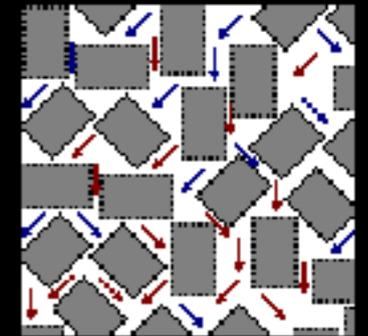


Anomalous sub-diffusion

Saxton, M. J. (2001), Biophys J 81, 2226--2240.

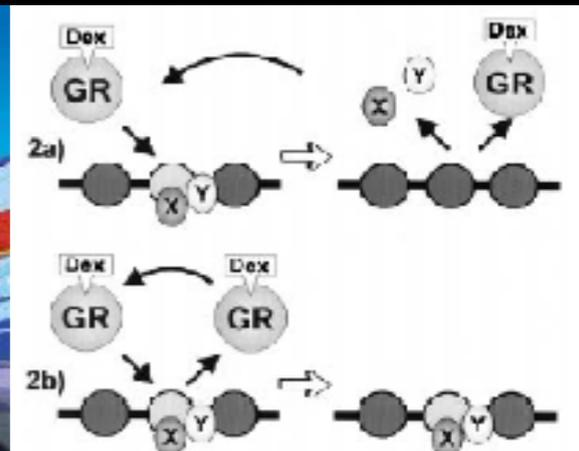
Diffusion in heterogeneous systems

Siggia, E. D. et al. (2000), Biophys J 79(4), 1761--1770.

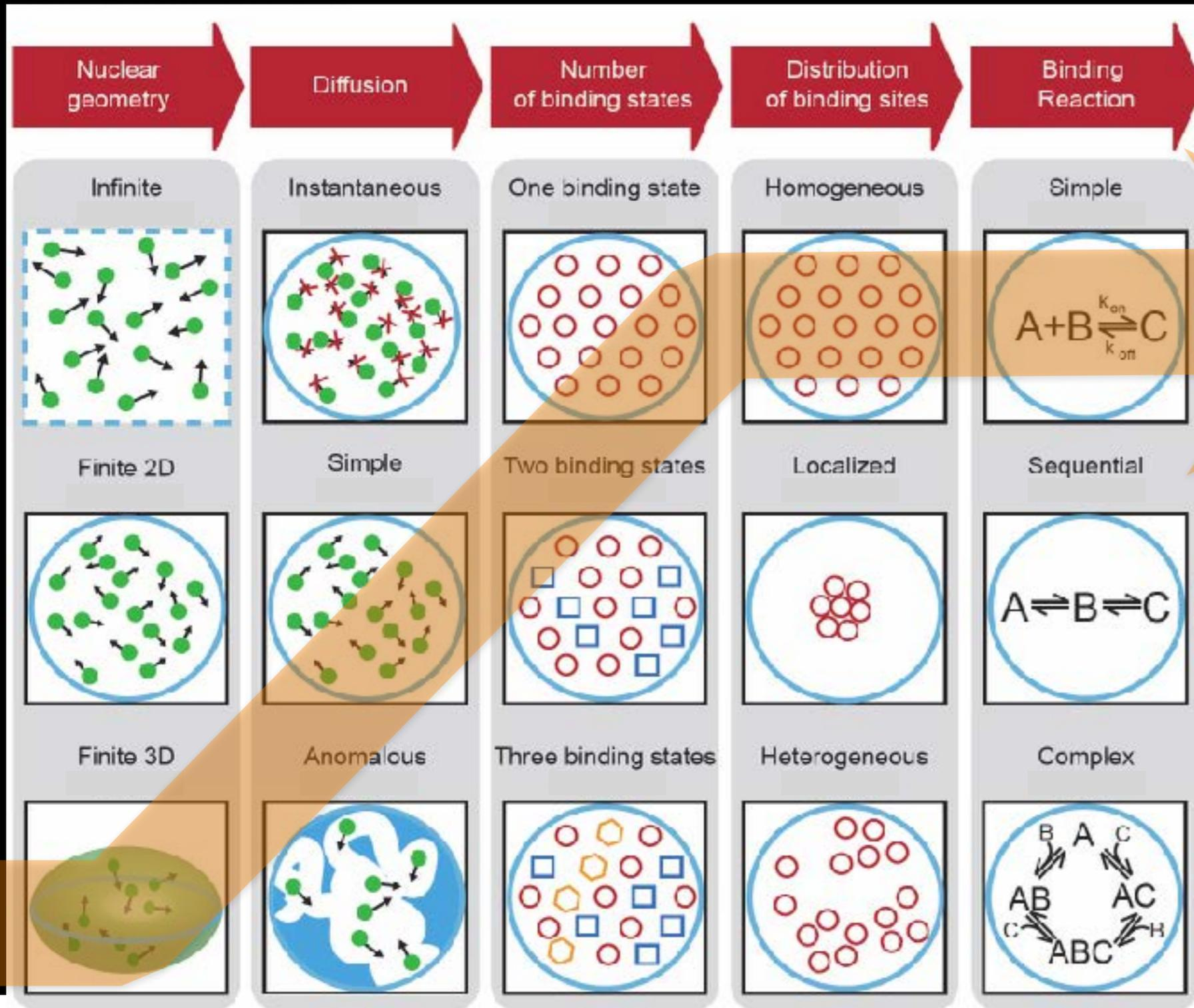


Diffusion and binding problems (hit and run)

Sprague, B. L.; et al. (2004) Biophys J, 86, 3473--3495.
Mueller et al. , B. L. et al. (2008), Biophys J.



Selecting a model for the FRAP experiments

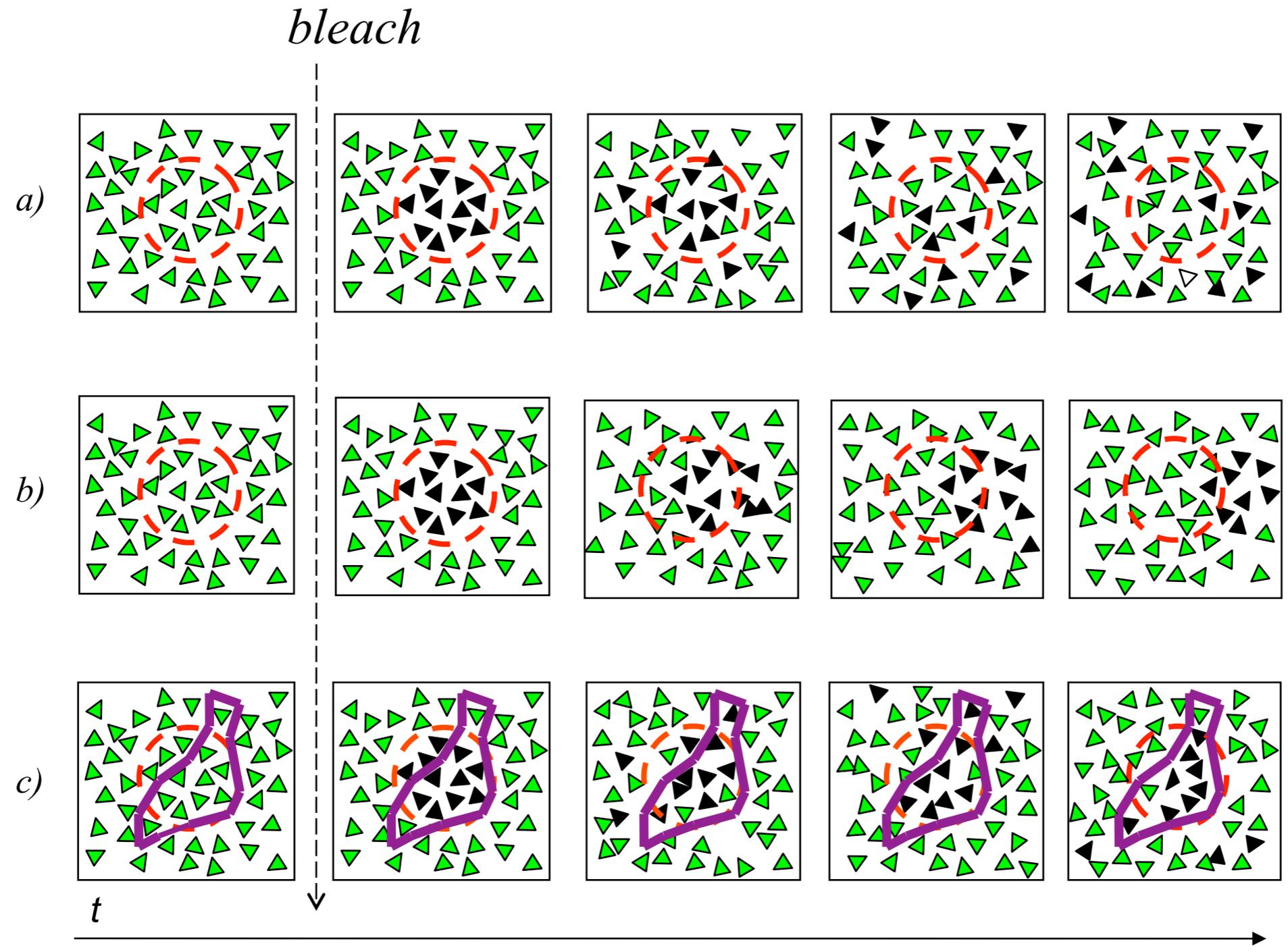


Equations deduced from the choices made

$$\begin{cases} \frac{\partial F}{\partial t} = D_F \nabla^2 F - k_{on}^* F + k_{off} C \\ \frac{\partial C}{\partial t} = + k_{on}^* F - k_{off} C \end{cases}$$

With proper initial and boundary conditions lead to model for experimental data

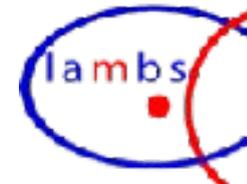
FRAP



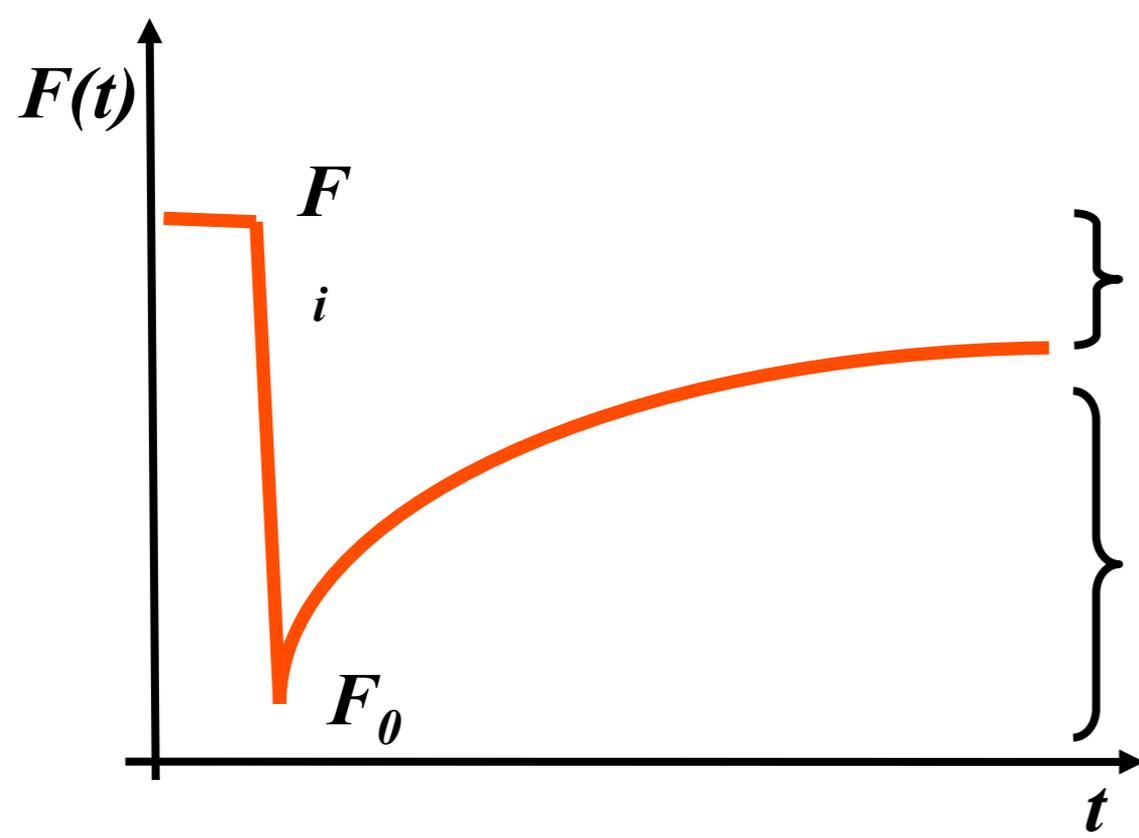
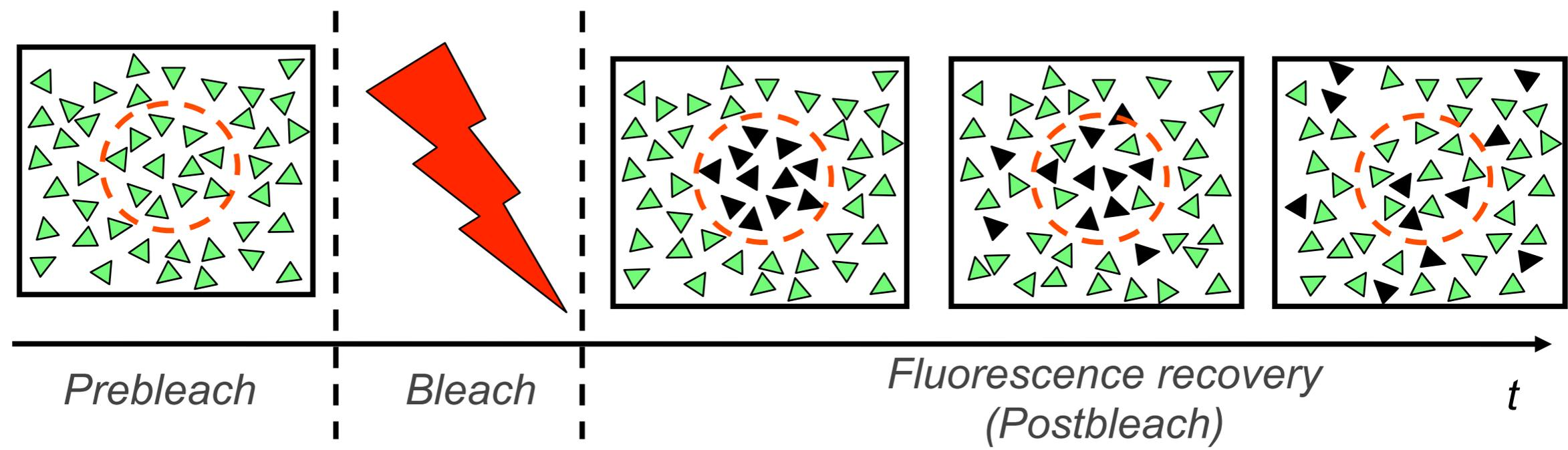
Slide credits: Davide Mazza, Francesca Cella, LAMBS



Alberto Diaspro, Nanoscopy, Istituto Italiano di Tecnologia



FRAP



Immobile Fraction

$$M_i = 1 - M_f$$

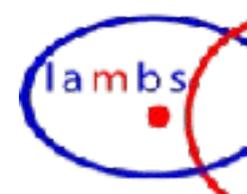
Mobile Fraction

$$M_f = \frac{F_\infty - F_0}{F_i - F_0}$$

Slide credits: Davide Mazza, Francesca Cella, LAMBS

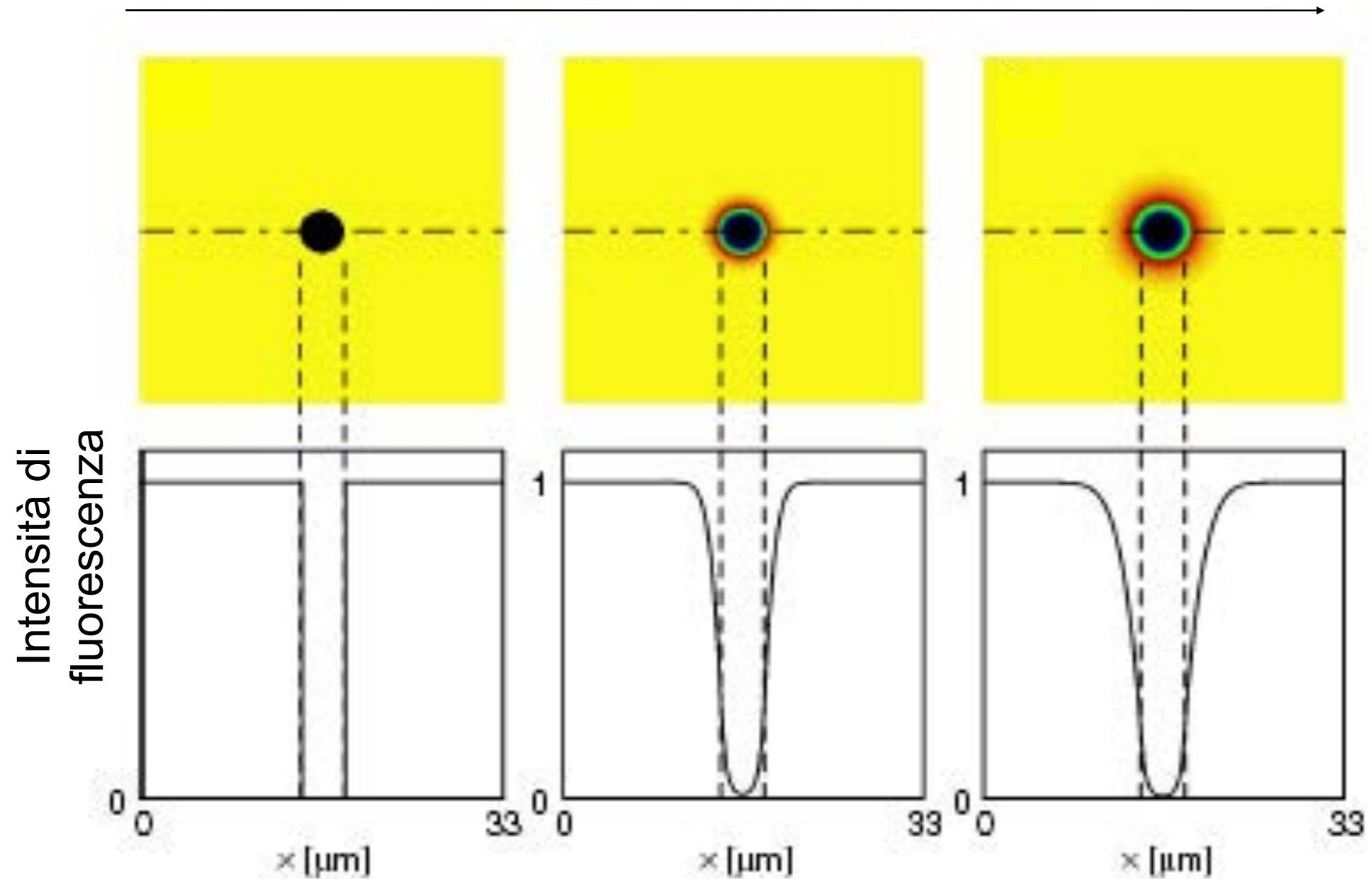


Alberto Diaspro, Nanoscopy, Istituto Italiano di Tecnologia



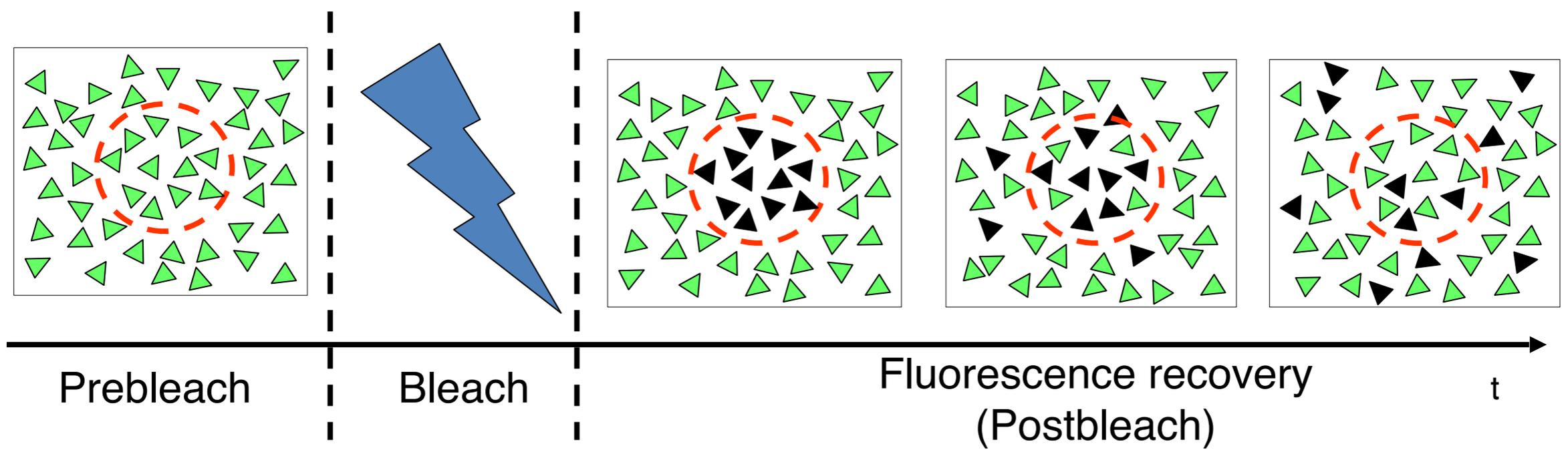
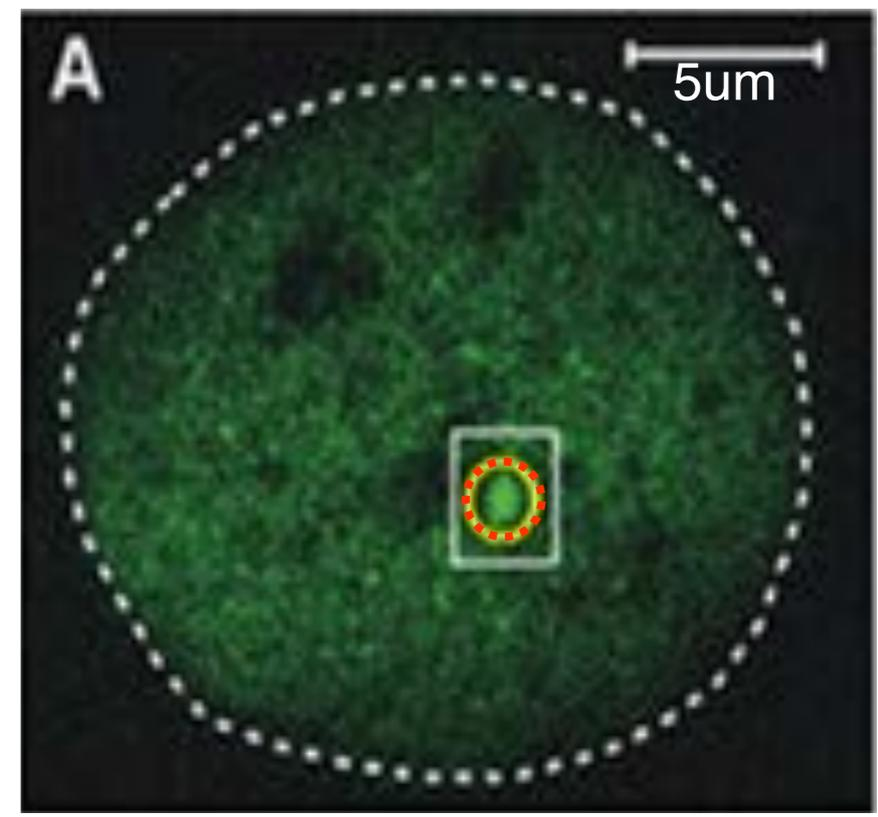
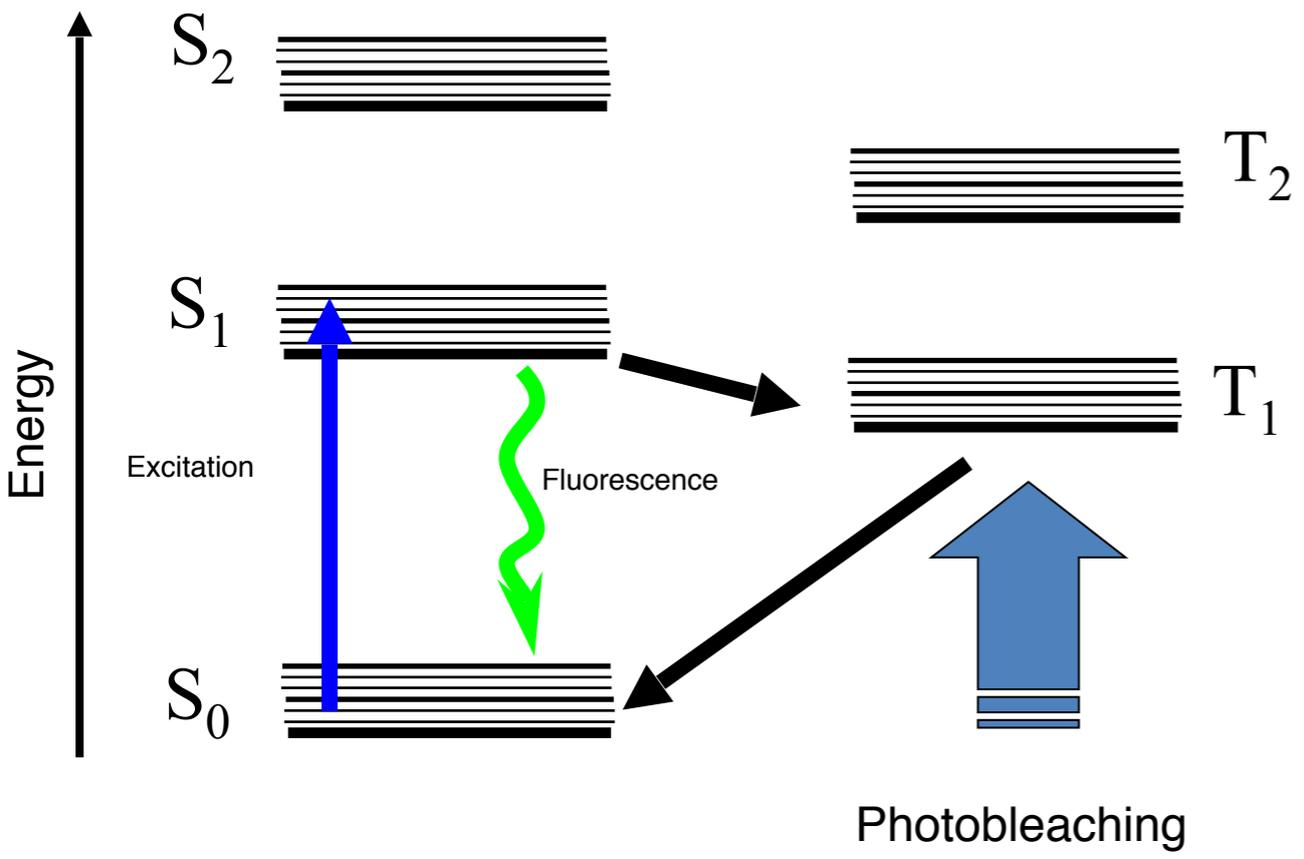
FRAP

By Increasing the bleach time



Weiss, M. (2004), *Traffic* 5(9), 662--671.

FRAP



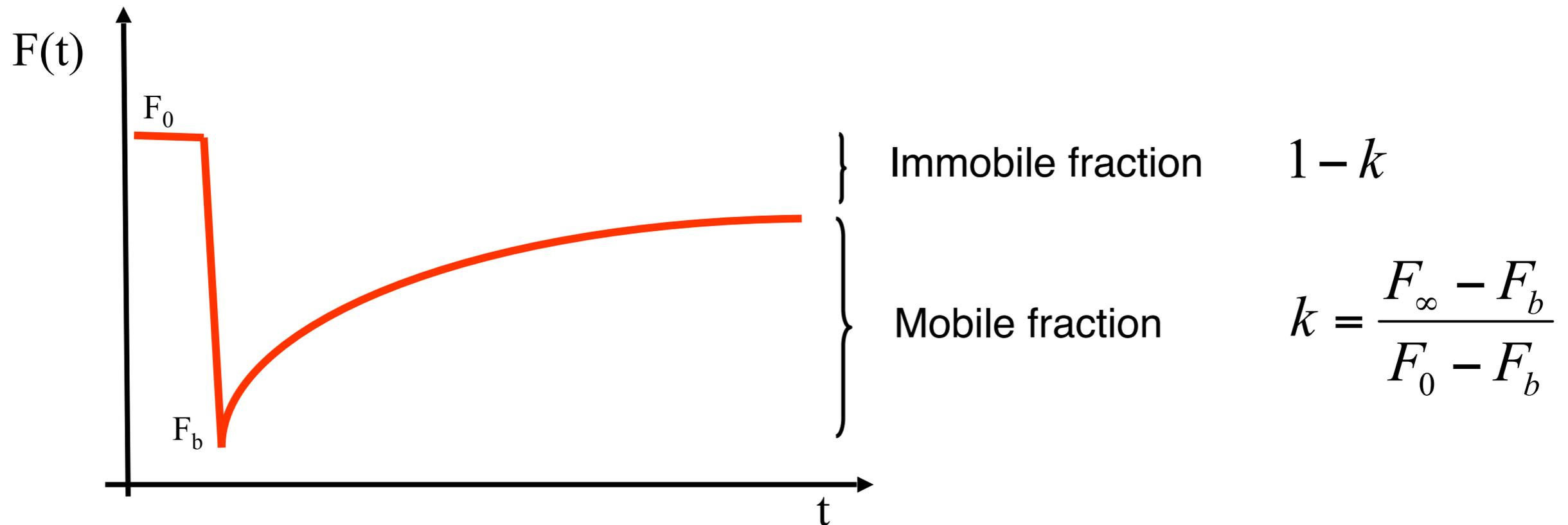
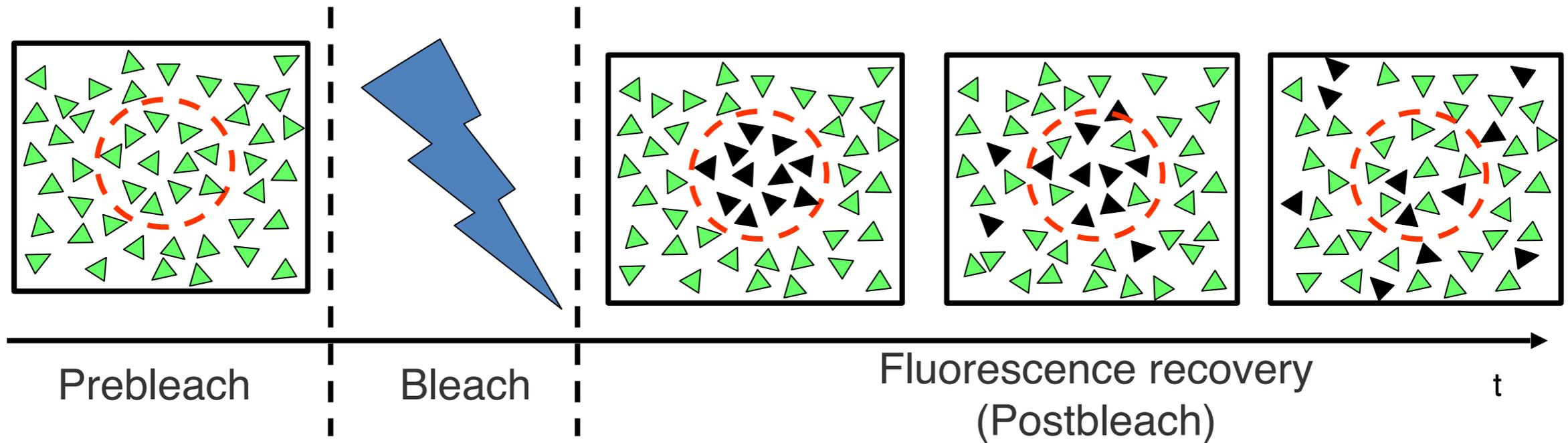
McNally, J. & Smith, C. (2001), in Confocal and two-photon microscopy, ed. A. Diaspro



Alberto Diaspro, Nanoscopy, Istituto Italiano di Tecnologia

slide credit: Davide Mazza, LAMBS

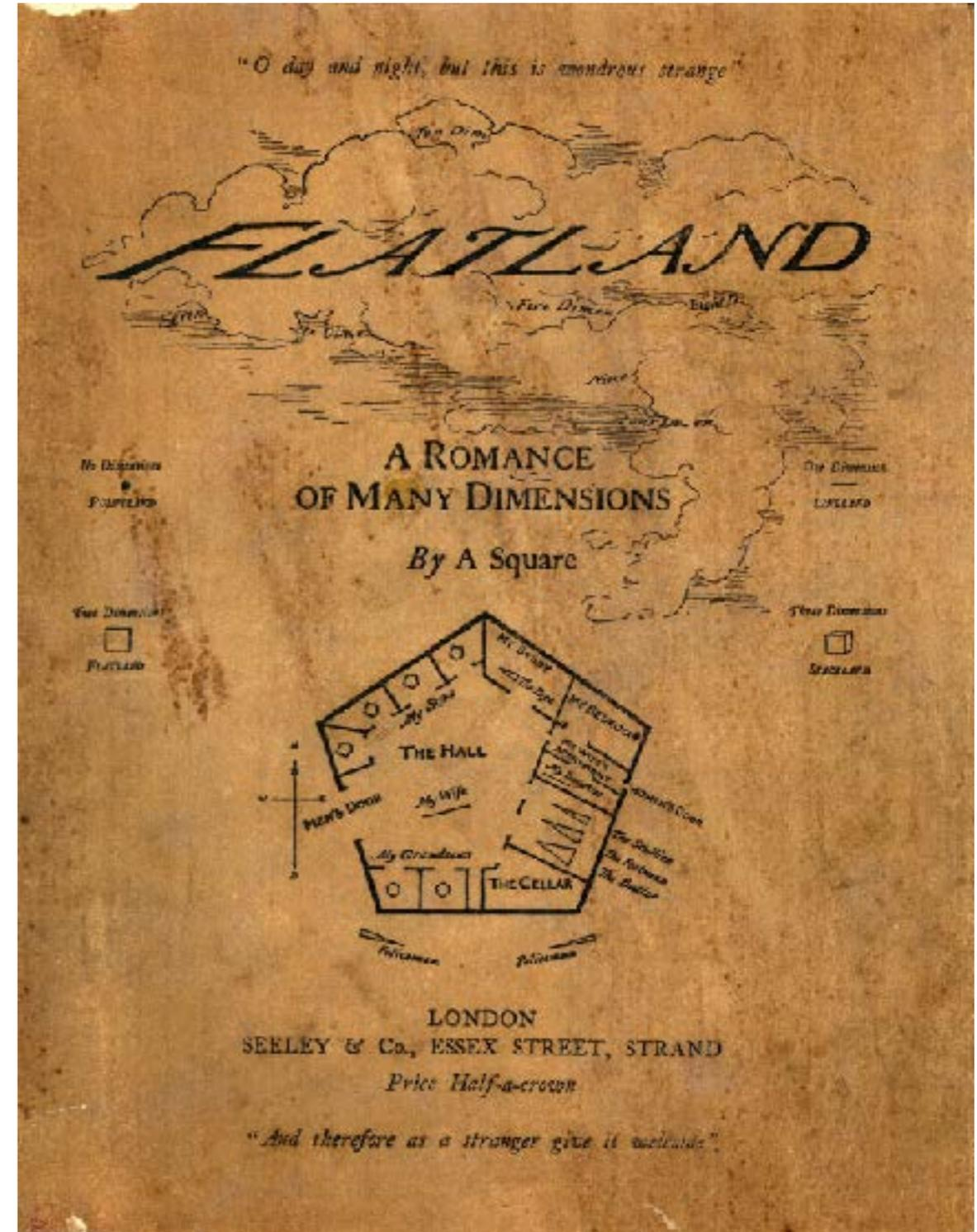
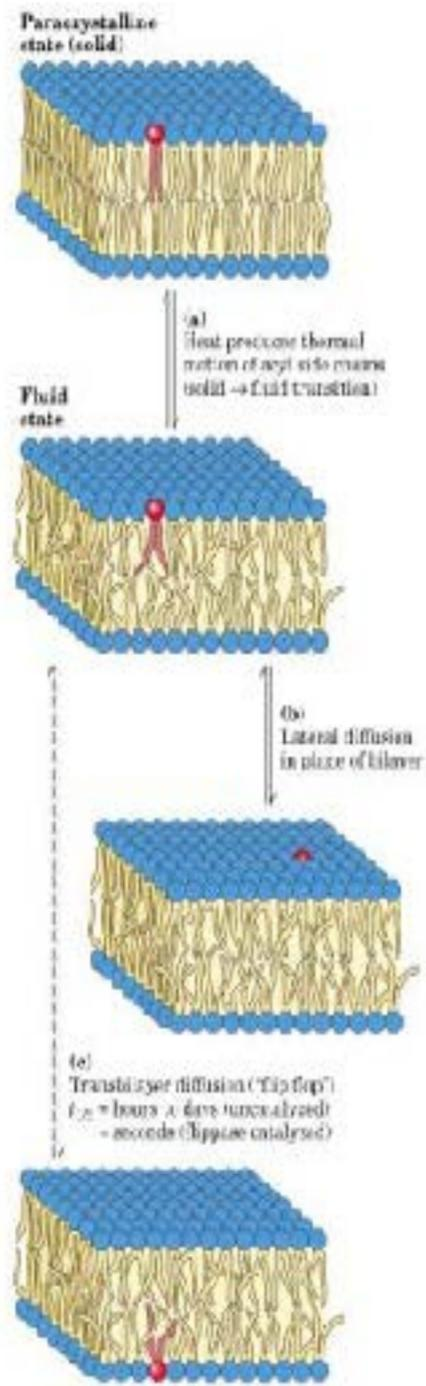




slide credit: Davide Mazza, LAMBS

FRAP

Cell territories are not FLATLAND...

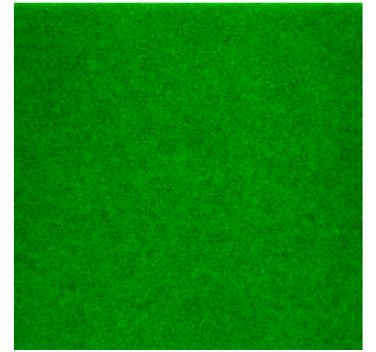


slide credit: Davide Mazza, LAMBS

FRAP

Condizione Iniziale

Distribuzione Uniforme di
molecole fluorescenti

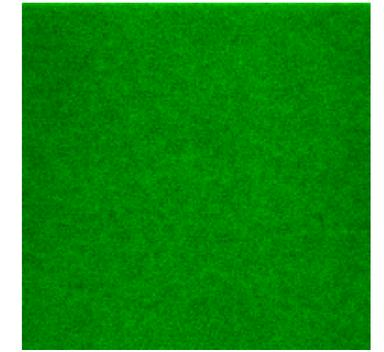


slide credit: Davide Mazza, LAMBS

FRAP

Condizione Iniziale

Distribuzione Uniforme di
molecole fluorescenti



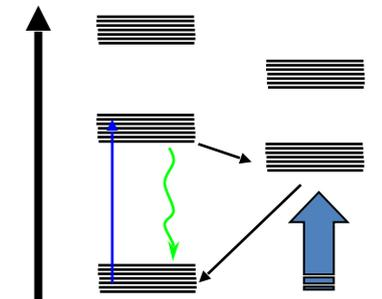
Photobleaching

Reazione Irreversibile del primo ordine

$$\frac{dC(x, y, t)}{dt} = -\alpha I_b(x, y)C(x, y, t)$$

Rate di Photobleaching

Distribuzione d'illuminazione

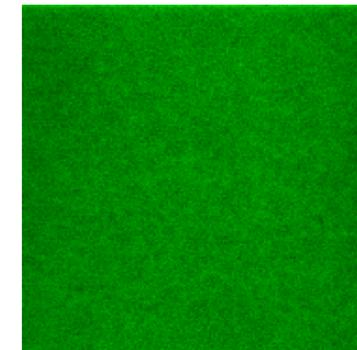


slide credit: Davide Mazza, LAMBS

FRAP

Condizione Iniziale

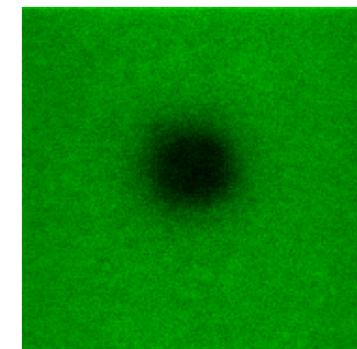
Distribuzione Uniforme di
molecole fluorescenti



Photobleaching

Reazione Irreversibile del primo ordine

$$\frac{dC(x, y, t)}{dt} = -\alpha I_b C(x, y, t)$$



Fluorescenza finale al
termine della fase di bleach

=

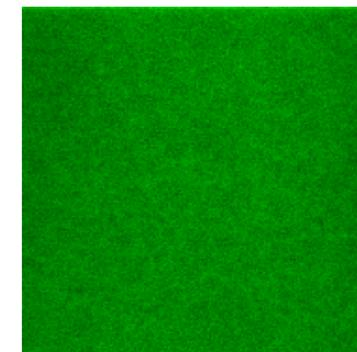
Condizione Iniziale per la
fase di Recovery

slide credit: Davide Mazza, LAMBS

FRAP

Condizione Iniziale

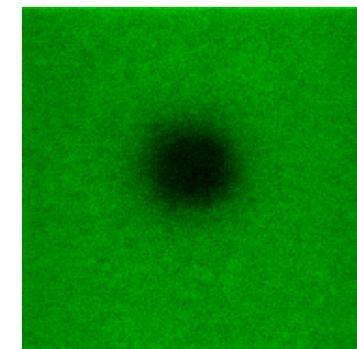
Distribuzione Uniforme di
molecole fluorescenti



Photobleaching

Reazione Irreversibile del primo ordine

$$\frac{dC(x, y, t)}{dt} = -\alpha I_b C(x, y, t)$$



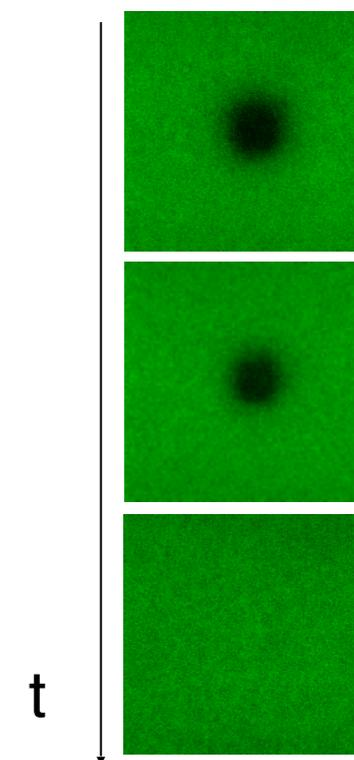
Fluorescenza finale al
termine della fase di bleach

Recovery

Equazione che descriva il
moto delle molecole

$$\frac{\partial C(x, y, t)}{\partial t} = D \nabla^2 C(x, y, t)$$

(la legge di Fick)

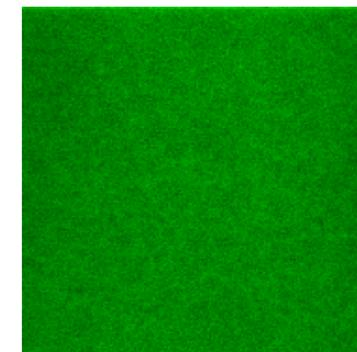


slide credit: Davide Mazza, LAMBS

FRAP

Condizione Iniziale

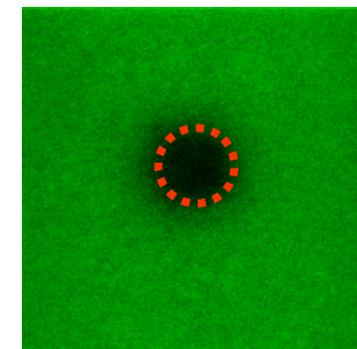
Distribuzione Uniforme di
molecole fluorescenti



Photobleaching

Reazione Irreversibile del primo ordine

$$\frac{dC(x, y, t)}{dt} = -\alpha I_b C(x, y, t)$$



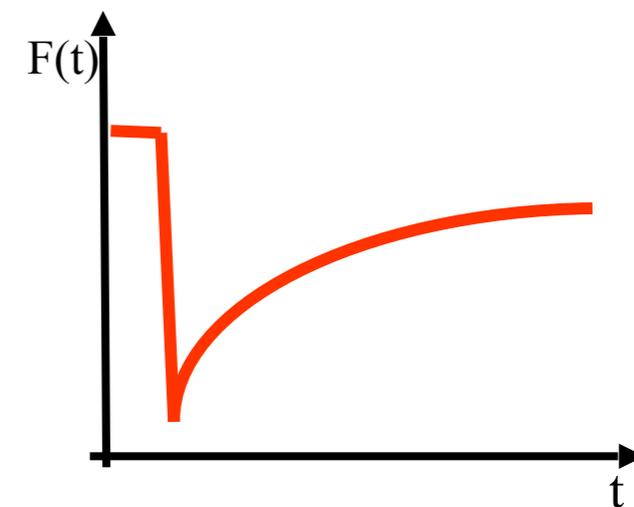
Fluorescenza finale al
termine della fase di bleach

Recovery

$$\frac{\partial C(x, y, t)}{\partial t} = D \nabla^2 C(x, y, t)$$

Equazione che descriva il
moto delle molecole

Fluorescenza media in
funzione del tempo



slide credit: Davide Mazza, LAMBS

Condizione Iniziale

Photobleaching

$$\frac{dC(x, y, t)}{dt} = -\alpha I_b C(x, y, t)$$

Fluorescenza finale al termine della fase di bleach

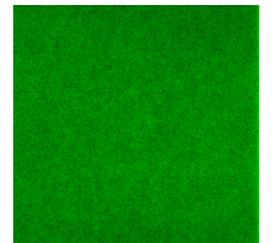
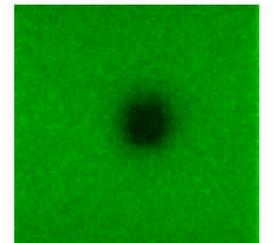
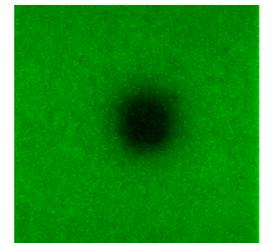
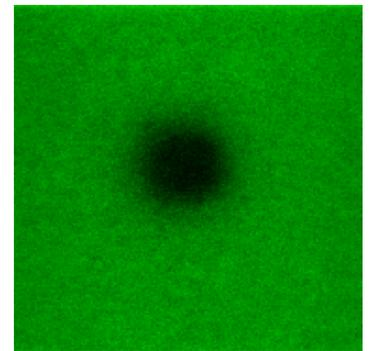
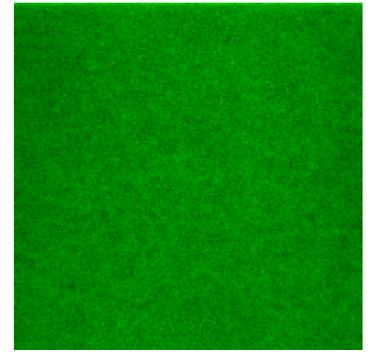
Recovery

$$\frac{\partial C(x, y, t)}{\partial t} = D \nabla^2 C(x, y, t)$$

Questa descrizione considera **bleaching** and **recovery** disaccoppiati

Niente **bleaching** durante la fase di **recovery**

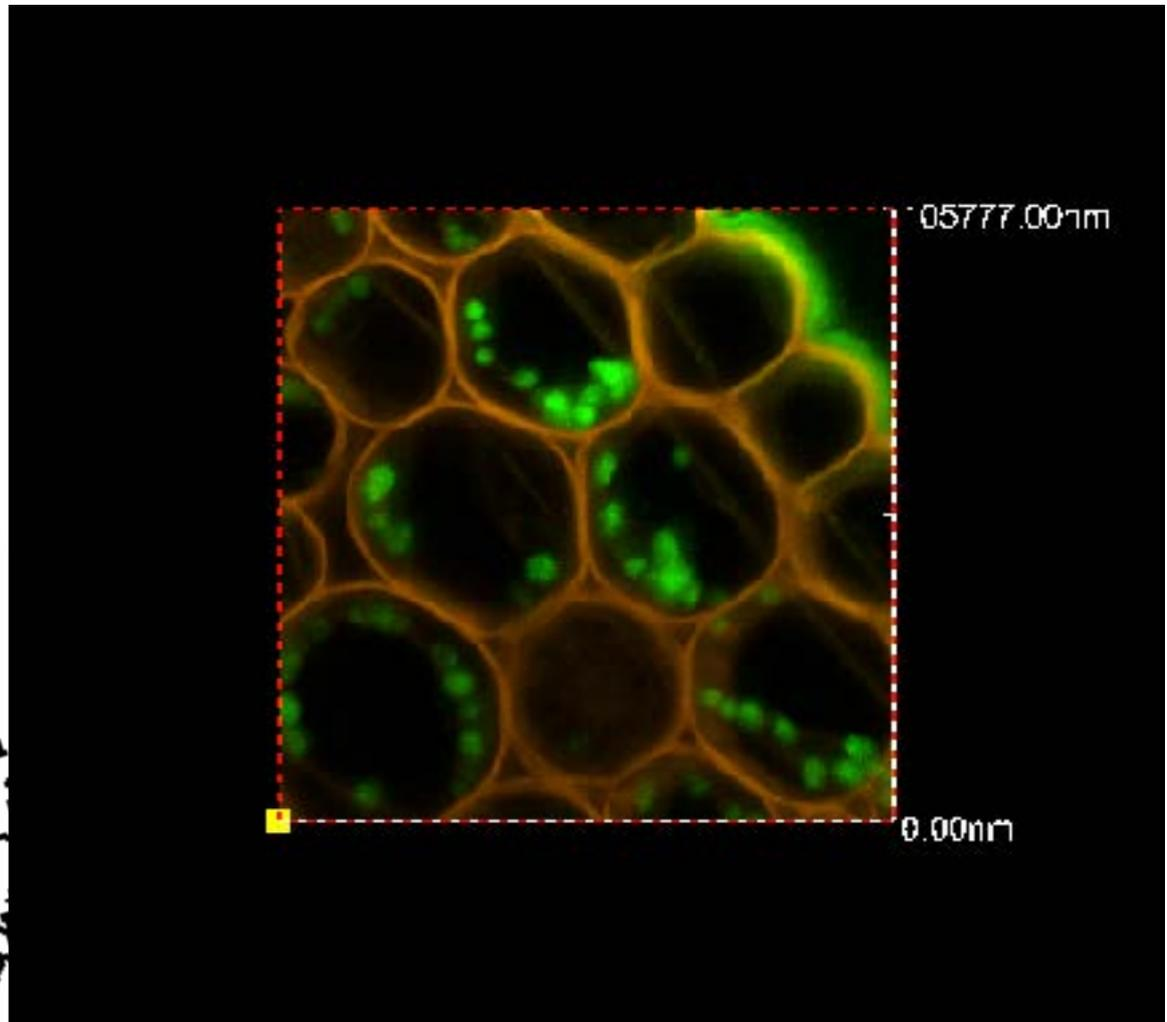
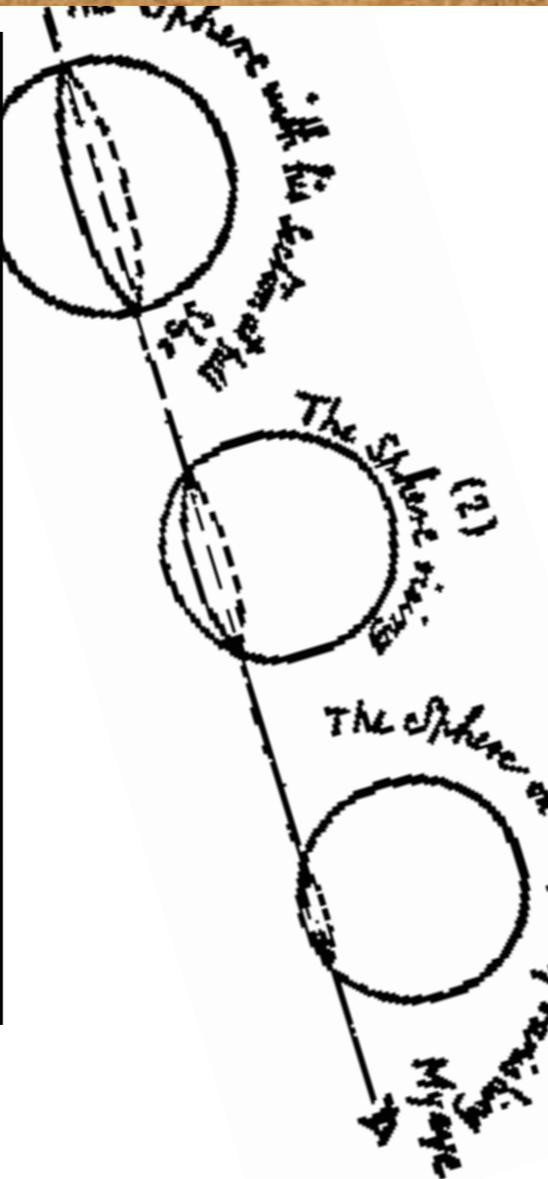
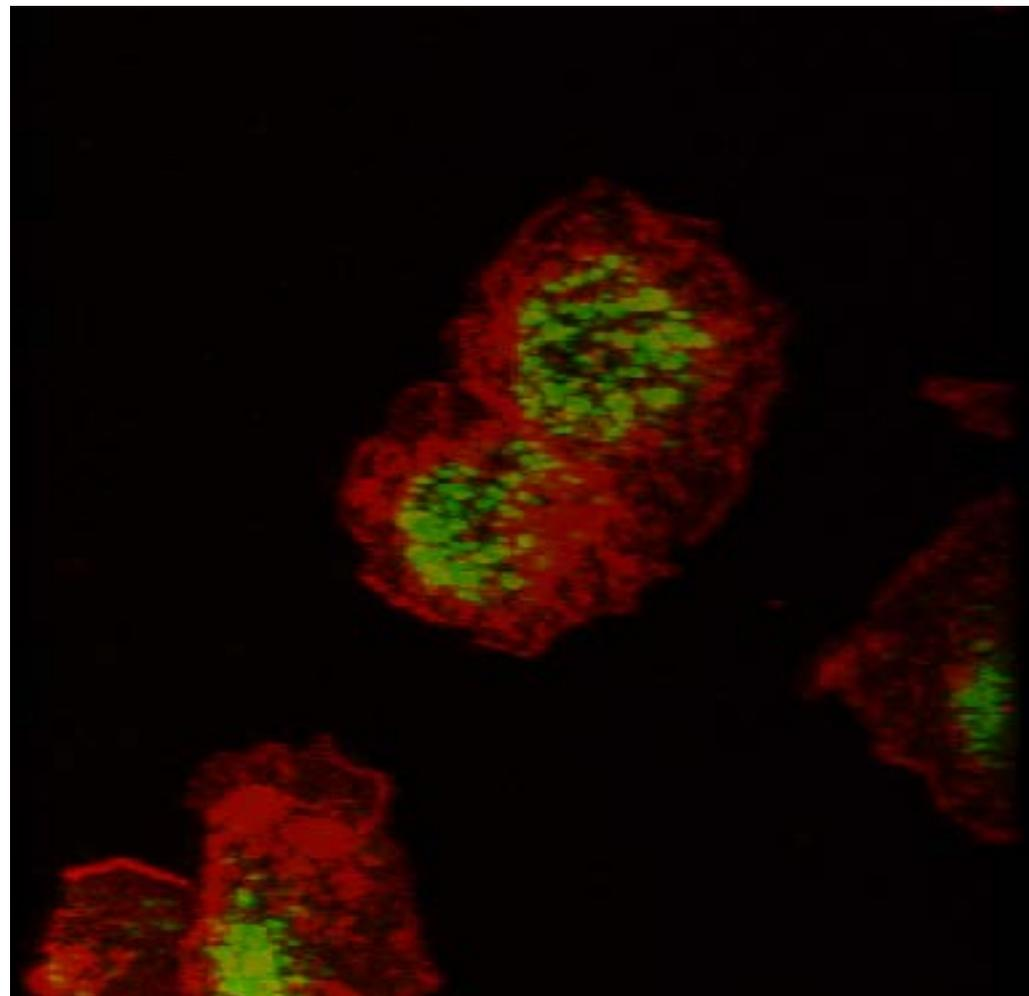
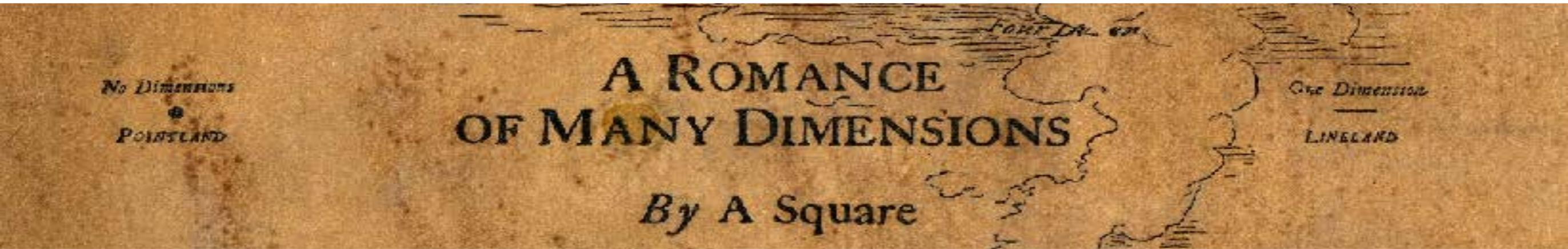
Niente **diffusione** durante la fase di **bleaching**
(massimo D misurabile)



t

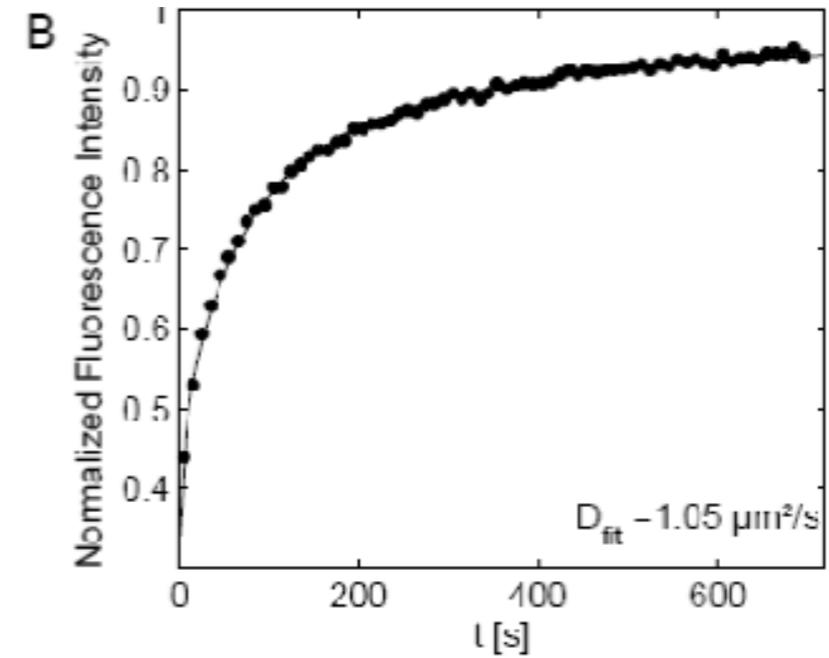
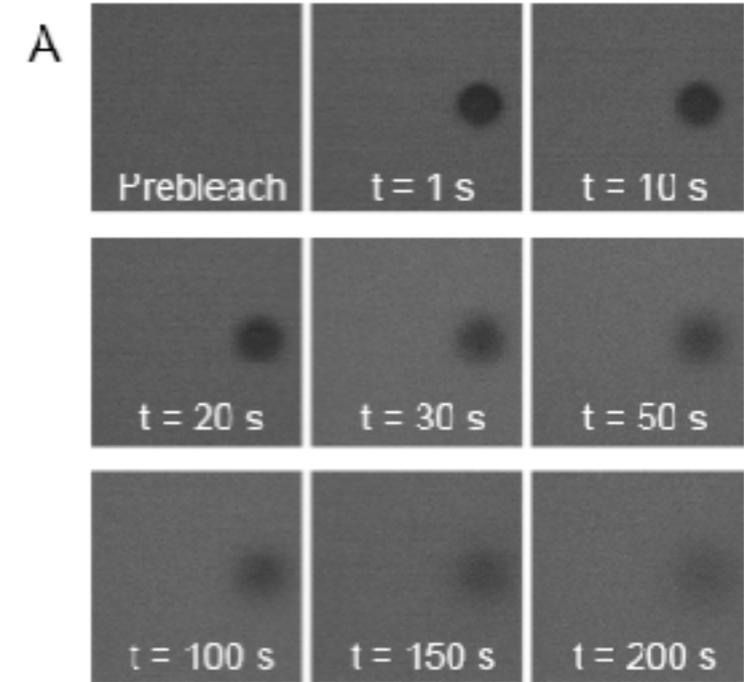
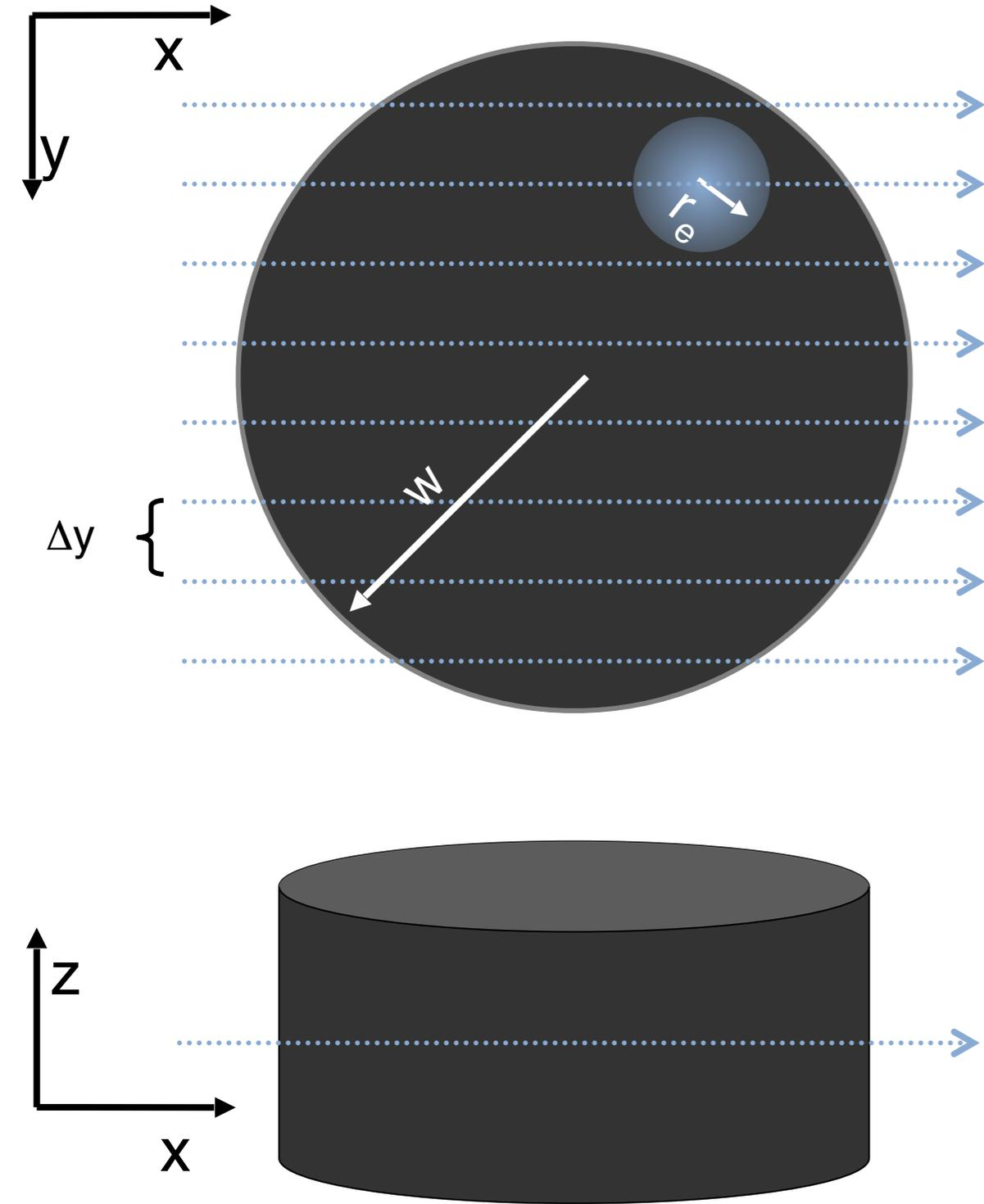
slide credit: Davide Mazza, LAMB

FRAP



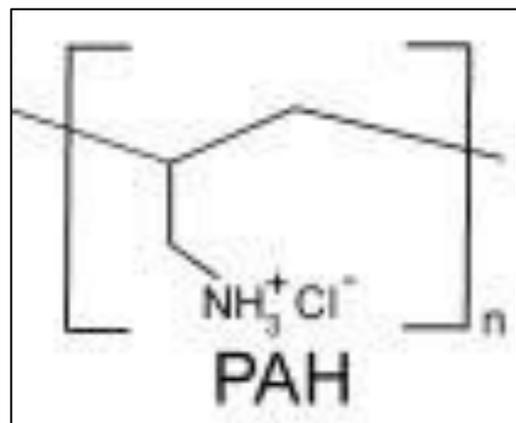
FRAP

Obiettivo a bassa apertura numerica (Profilo cilindrico)



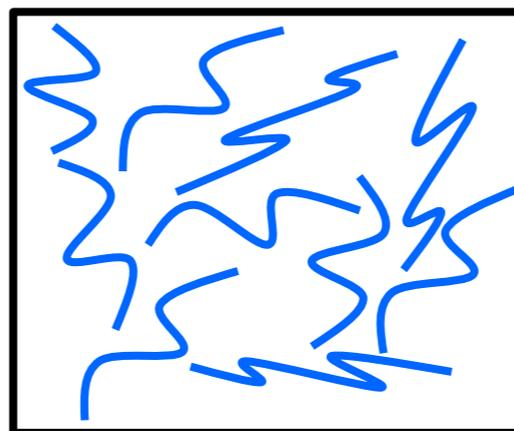
Applicabile per regioni di bleach con $w > 10 \mu\text{m}$

FRAP

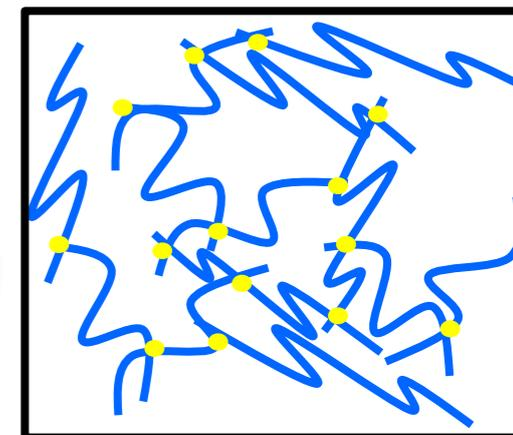


PAH (15KDa, 170mg/ml)

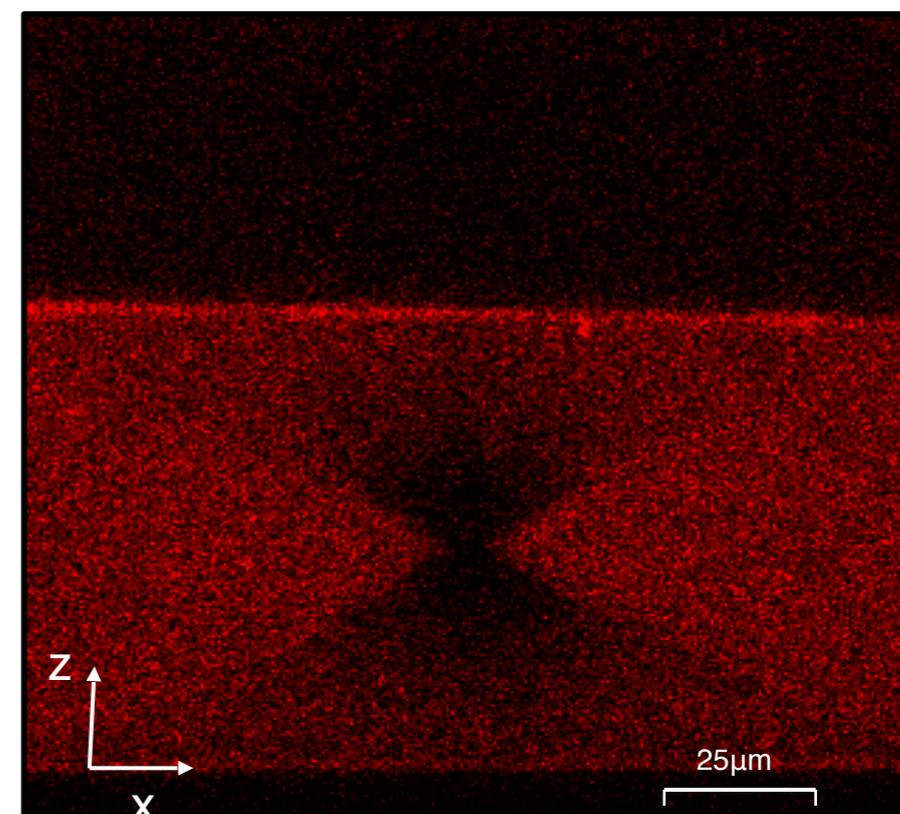
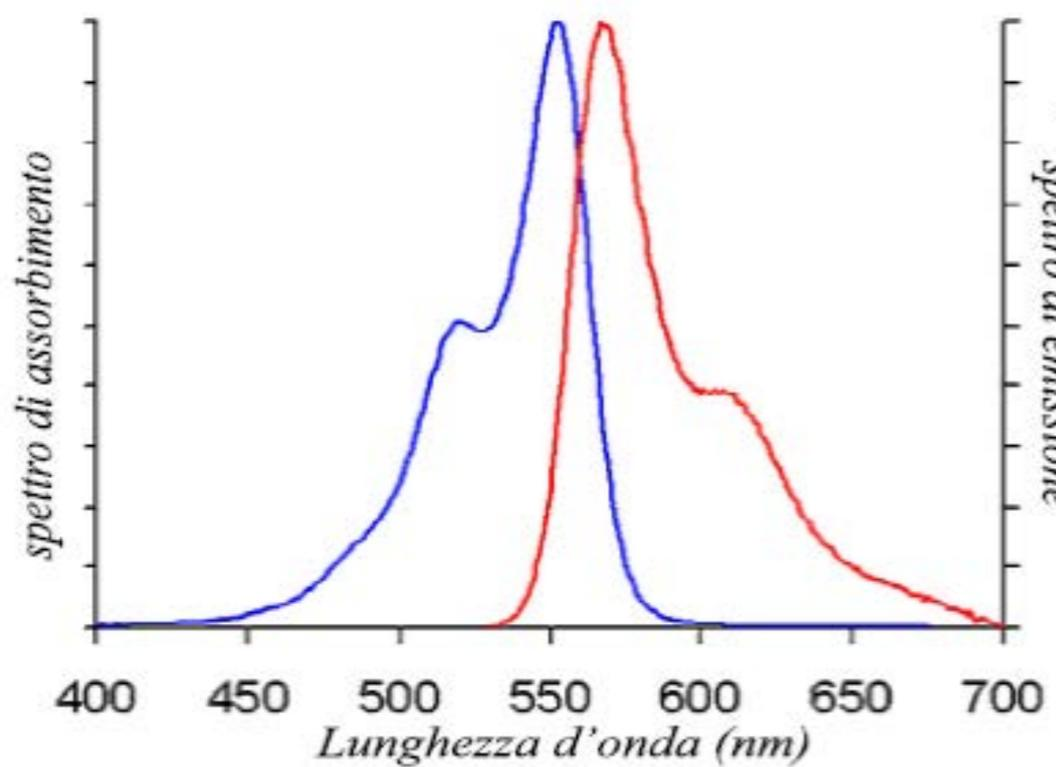
Crosslinker:
 NaH_2PO_4



→
Crosslinking
ionico

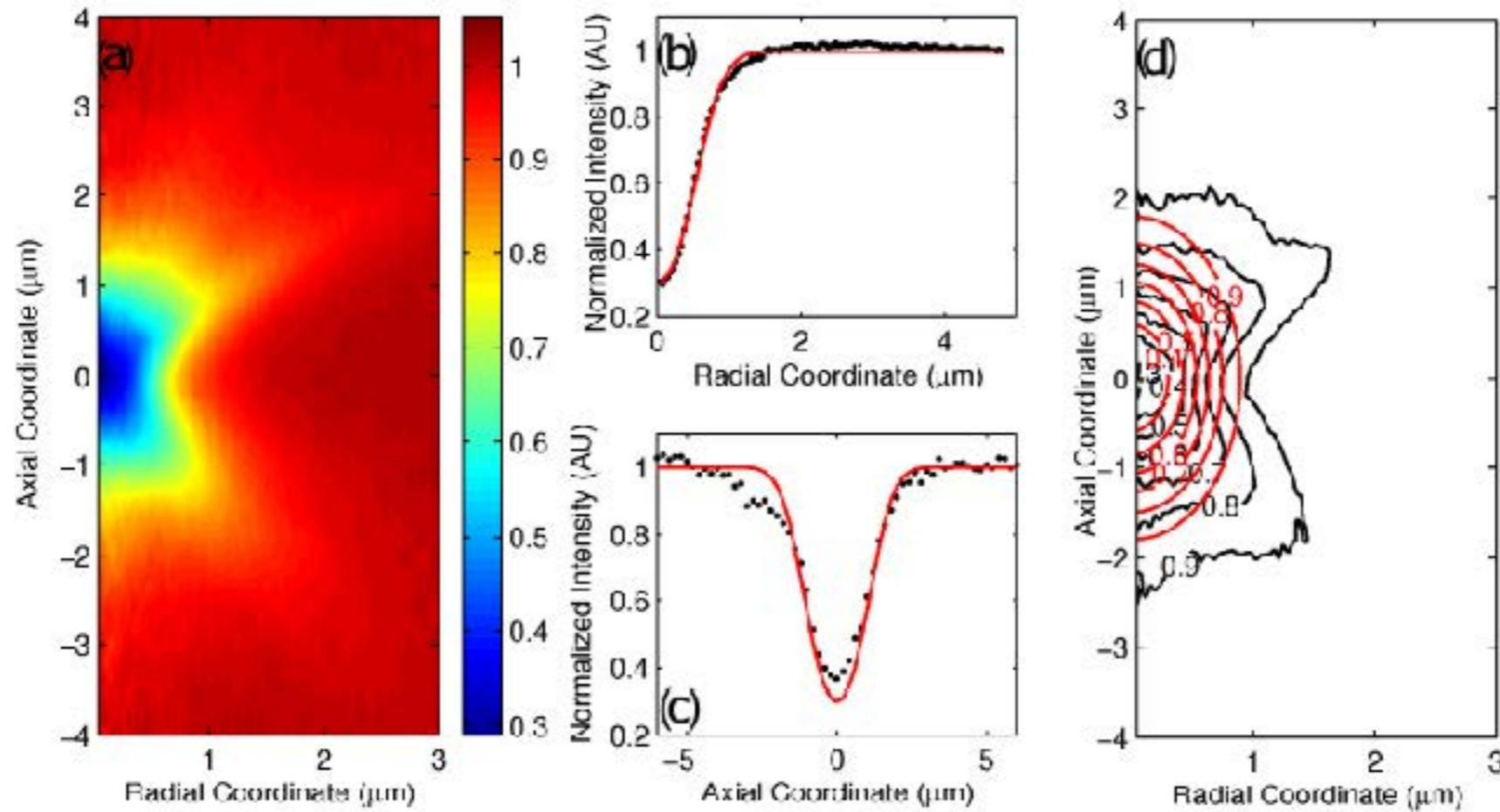


Molecola fluorescente: **ALEXA 555**



slide credit: Davide Mazza, LAMBS

FRAP



Approssimazione Gaussiana del profilo di Illuminazione:

$$\langle I_b(r, z) \rangle = \langle I_b(0, 0) \rangle e^{-\left(\frac{2r^2}{r_e^2} + \frac{2z^2}{z_e^2}\right)}$$

$$\frac{dC(x, y, t)}{dt} = -\alpha I_b C(x, y, t)$$



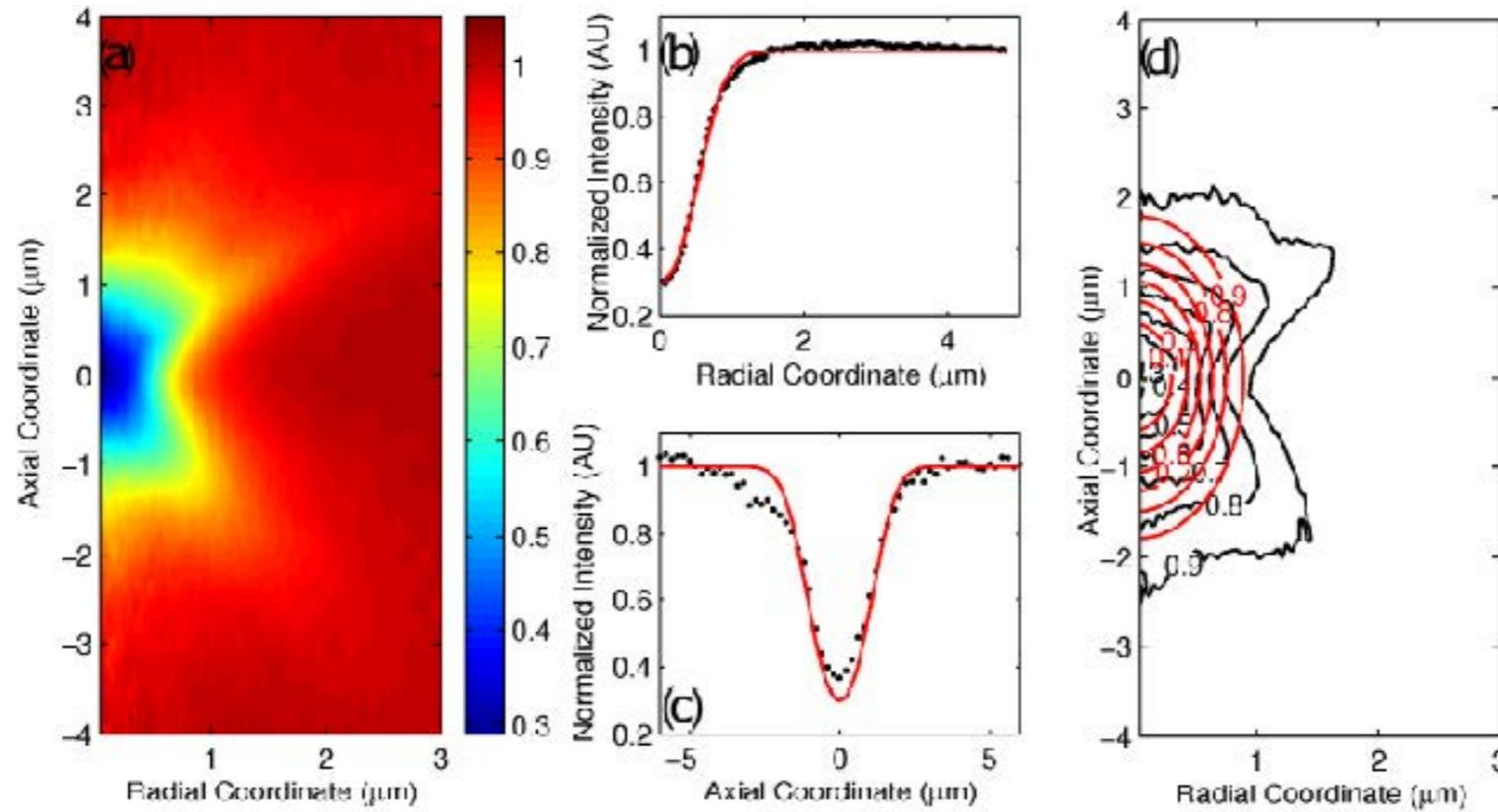
Profilo di Photobleaching

$$C_B(r, z) = C_0 e^{-K_{1ph} e^{-\left(\frac{2r^2}{r_e^2} + \frac{2z^2}{z_e^2}\right)}}$$

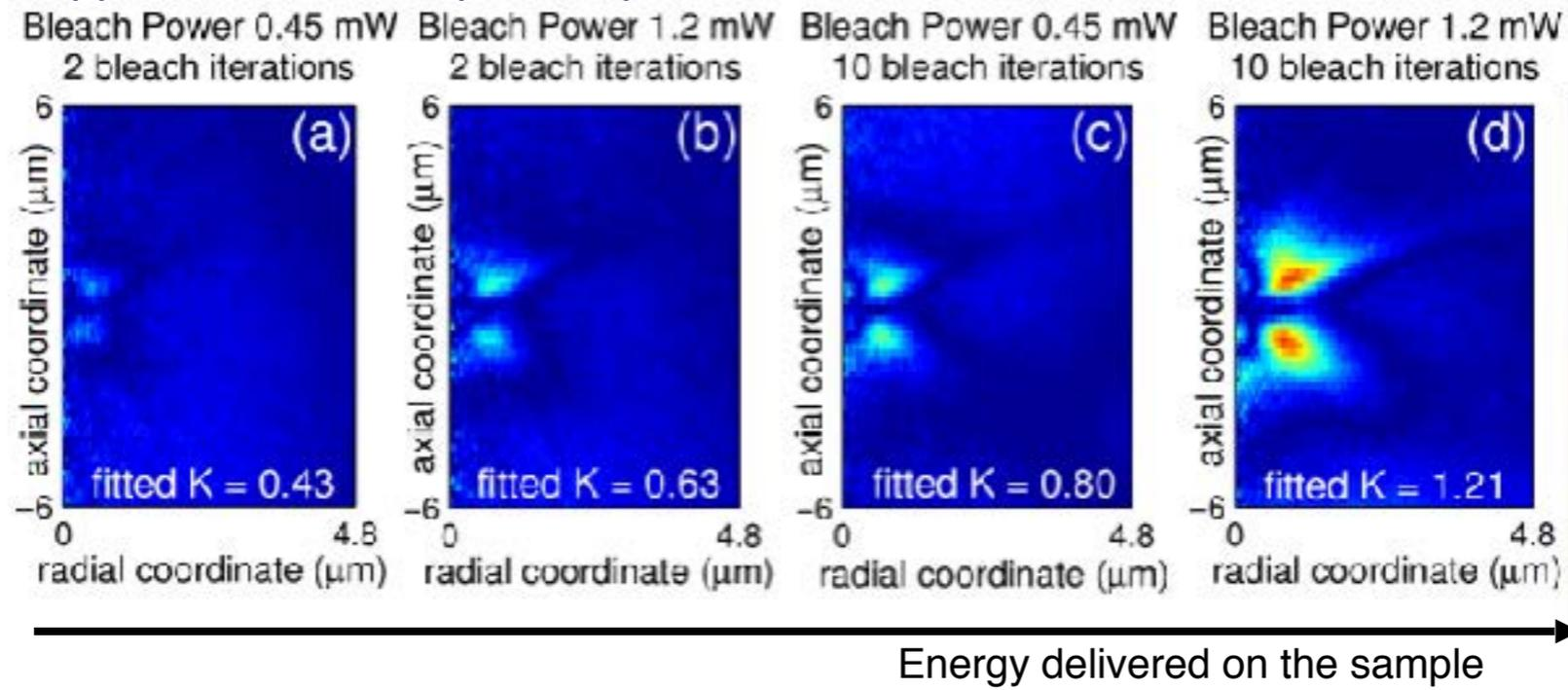
slide credit: Davide Mazza, LAMBS

Mazza D. et al, Applied Optics, 2007

FRAP



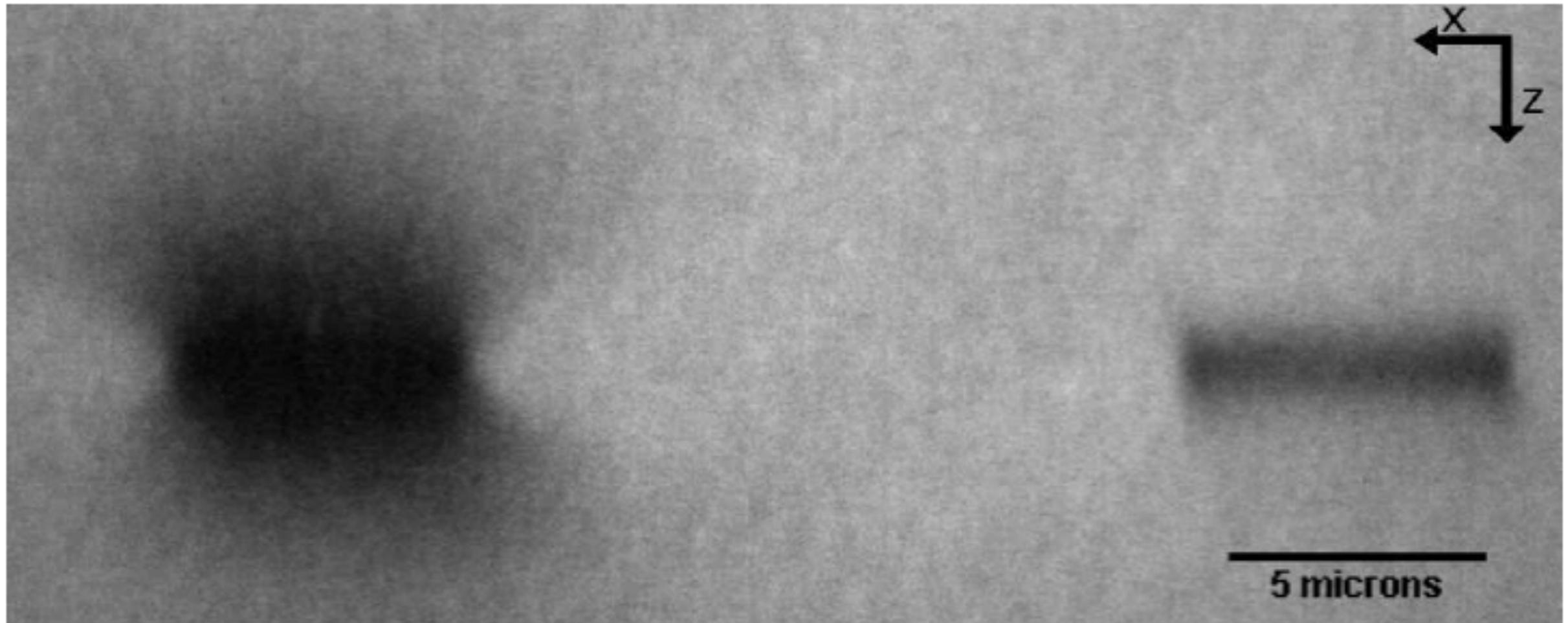
Mappa dei residui tra profilo sperimentale e modello



slide credit: Davide Mazza, LAMBS

FRAP

Loren...Diaspro et al., *Q Rev Biophys.* 2015 Aug;48(3):323-87.



1PE

$$\frac{dC(x, y, t)}{dt} = -\alpha I_b C(x, y, t)$$

2PE

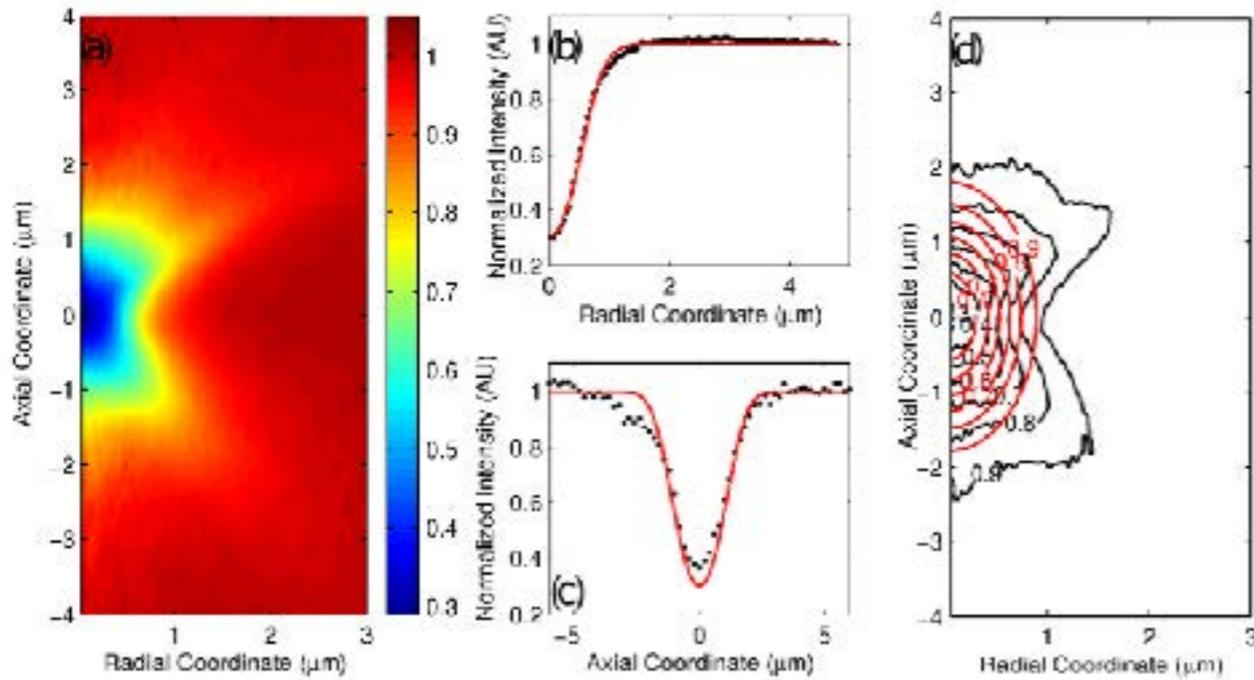
$$\frac{dC(x, y, t)}{dt} = -\alpha \langle I_b^2 \rangle C(x, y, t)$$

Mazza D, Braeckmans K, Cella F, Testa I, Vercauteren D, Demeester J, De Smedt SS, **Diaspro A.**
***Biophys J.* 2008 Oct;95(7):3457-69.**

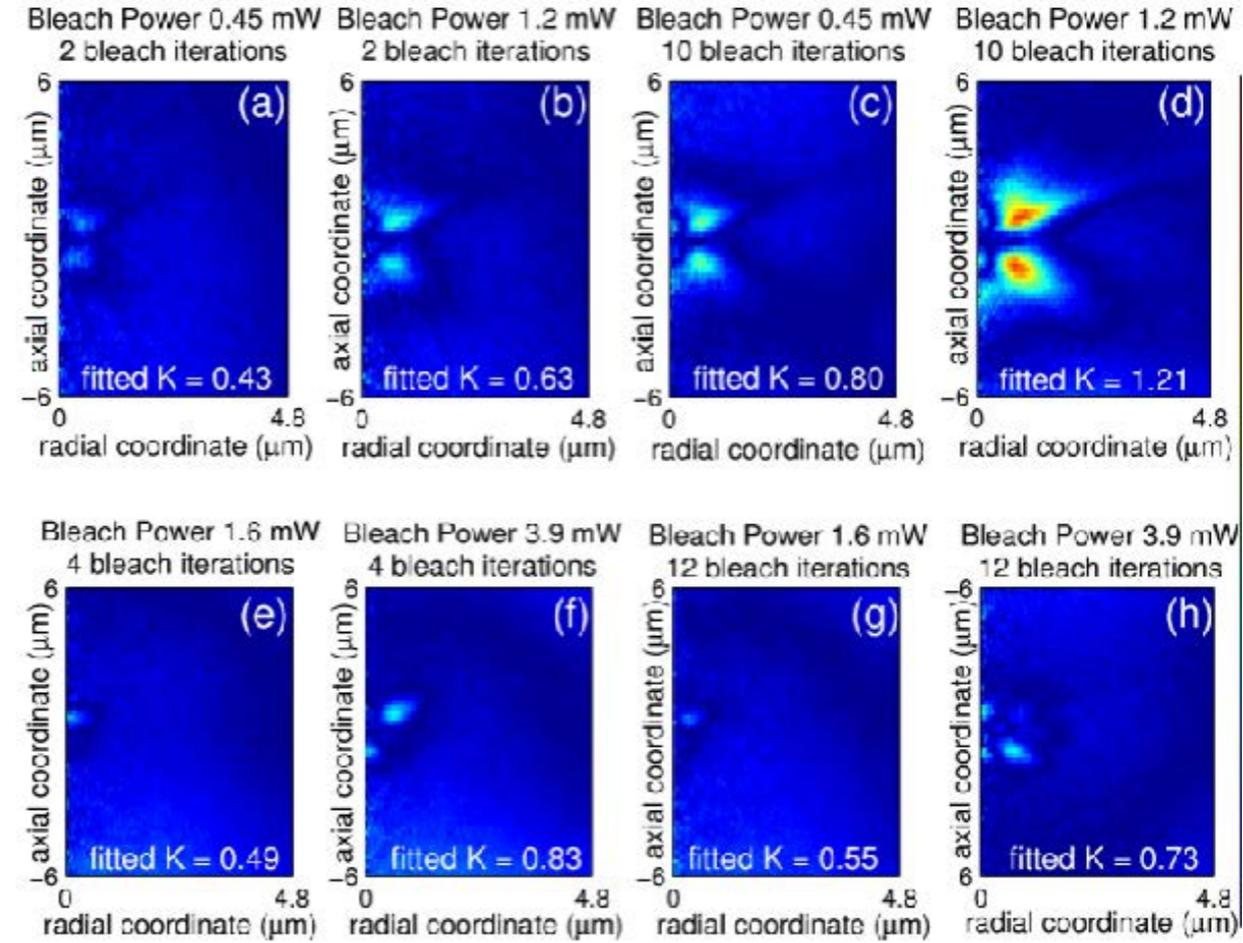
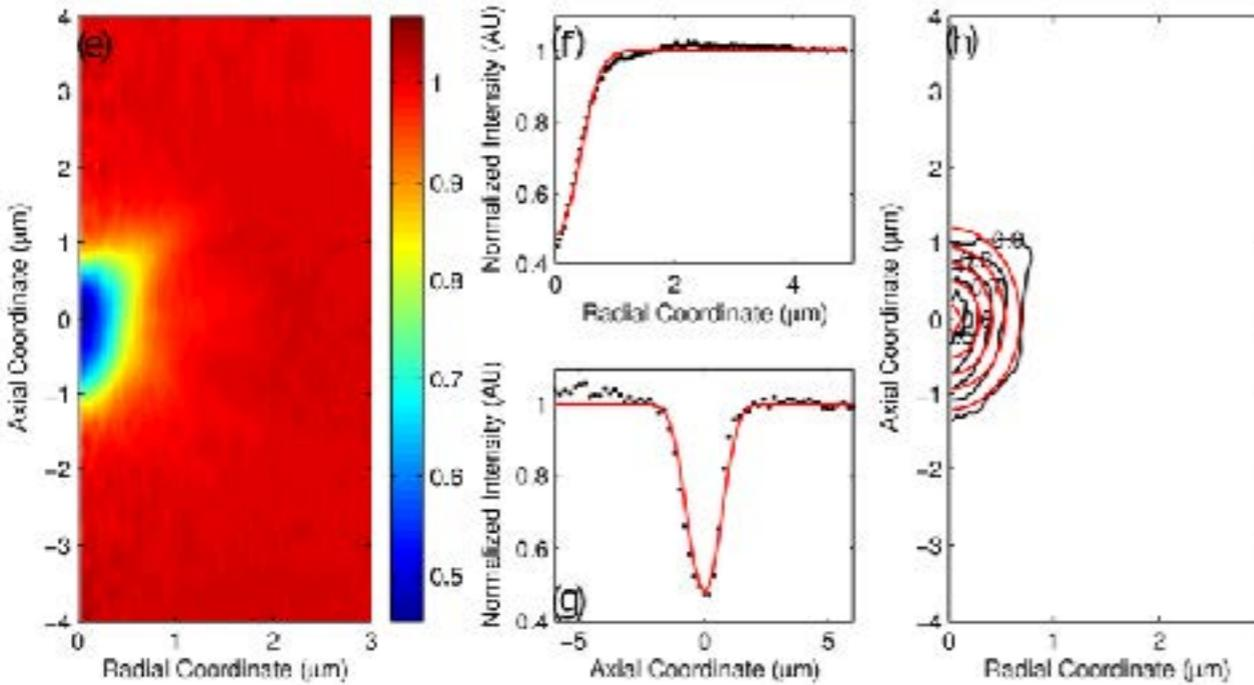
slide credit: Davide Mazza, LAMBS

FRAP

Eccitazione convenzionale



Eccitazione a due fotoni



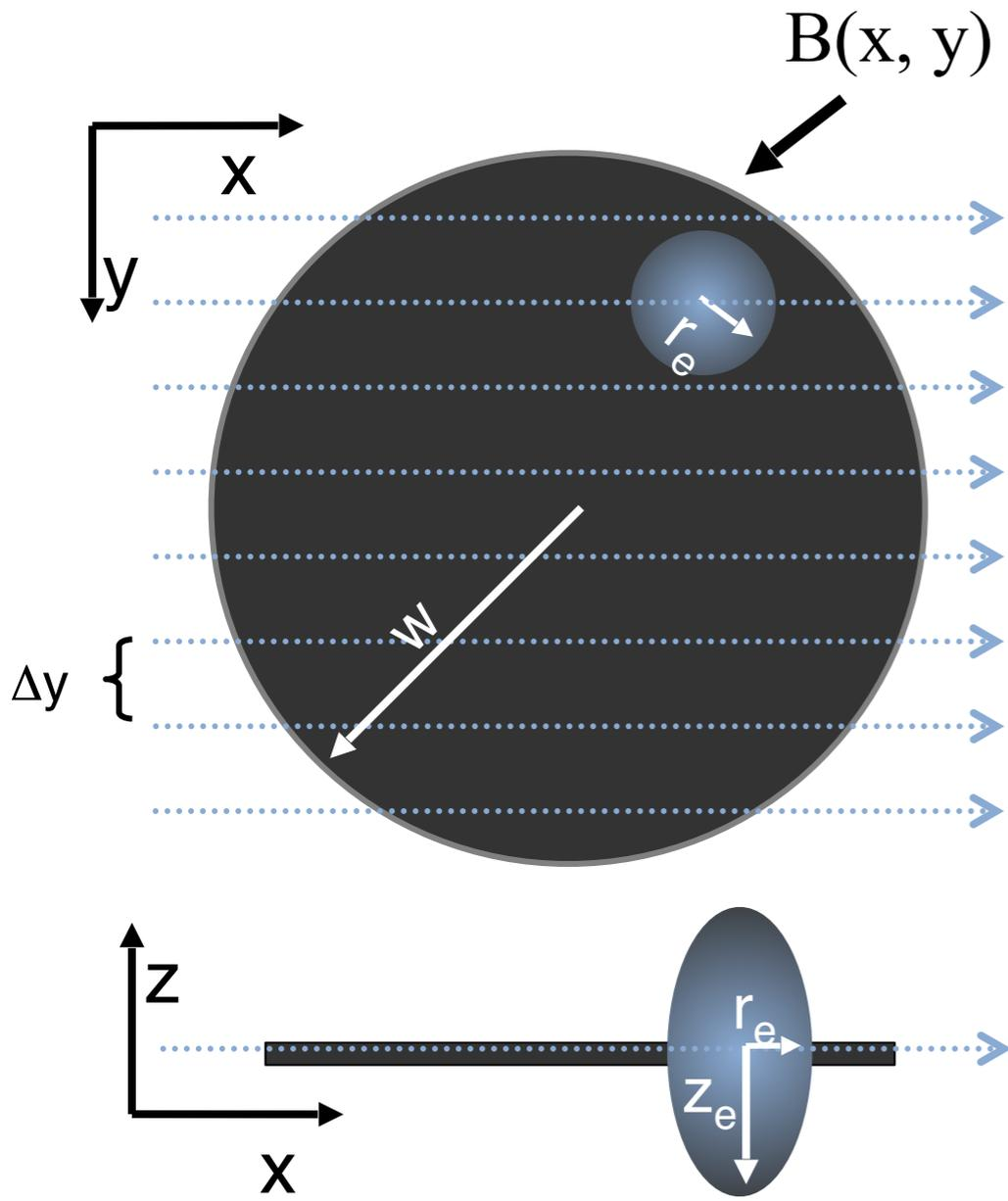
Profilo di Photobleaching

$$C_B(r, z) = C_0 e^{-K_{2ph} e^{-\left(\frac{4r^2}{r_e^2} + \frac{4z^2}{z_e^2}\right)}}$$

slide credit: Davide Mazza, LAMBS

Mazza D. et al, Applied Optics, 2007

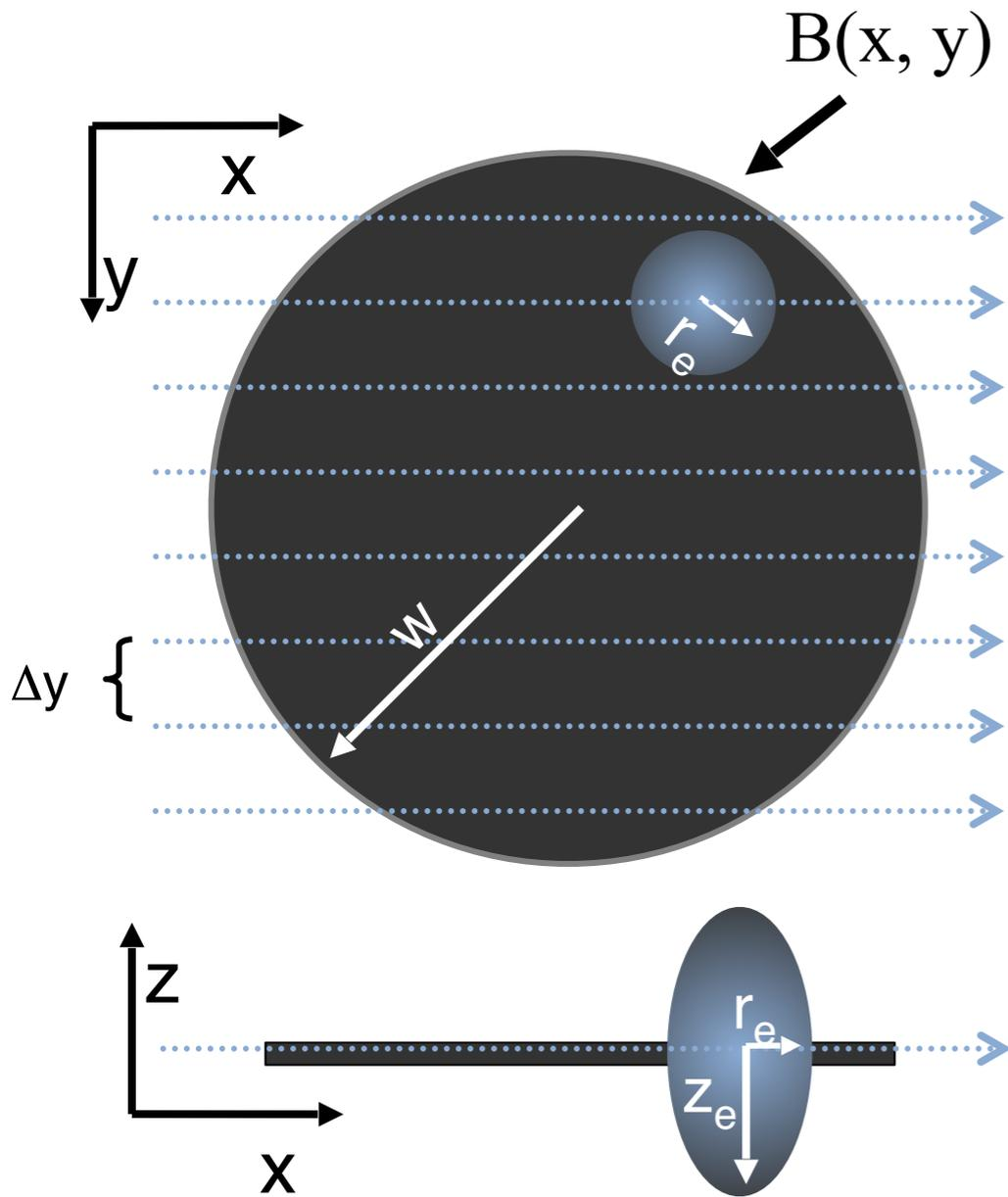
FRAP



slide credit: Davide Mazza, LAMBS

Mazza D. et al., BJ 2008

FRAP



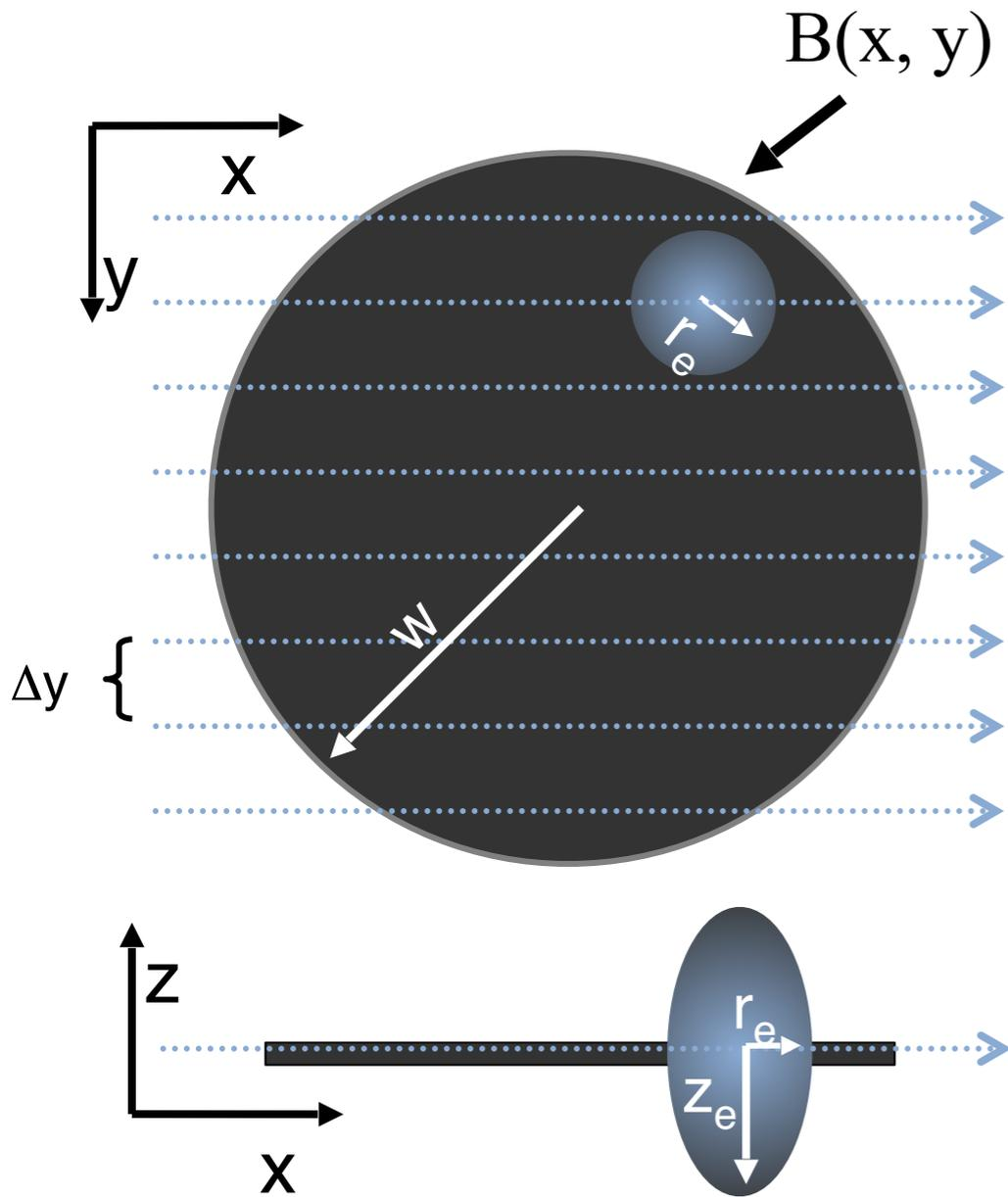
Condizione Iniziale

$$C(r, z) = C_0$$

slide credit: Davide Mazza, LAMBS

Mazza D. et al., BJ 2008

FRAP



Condizione Iniziale

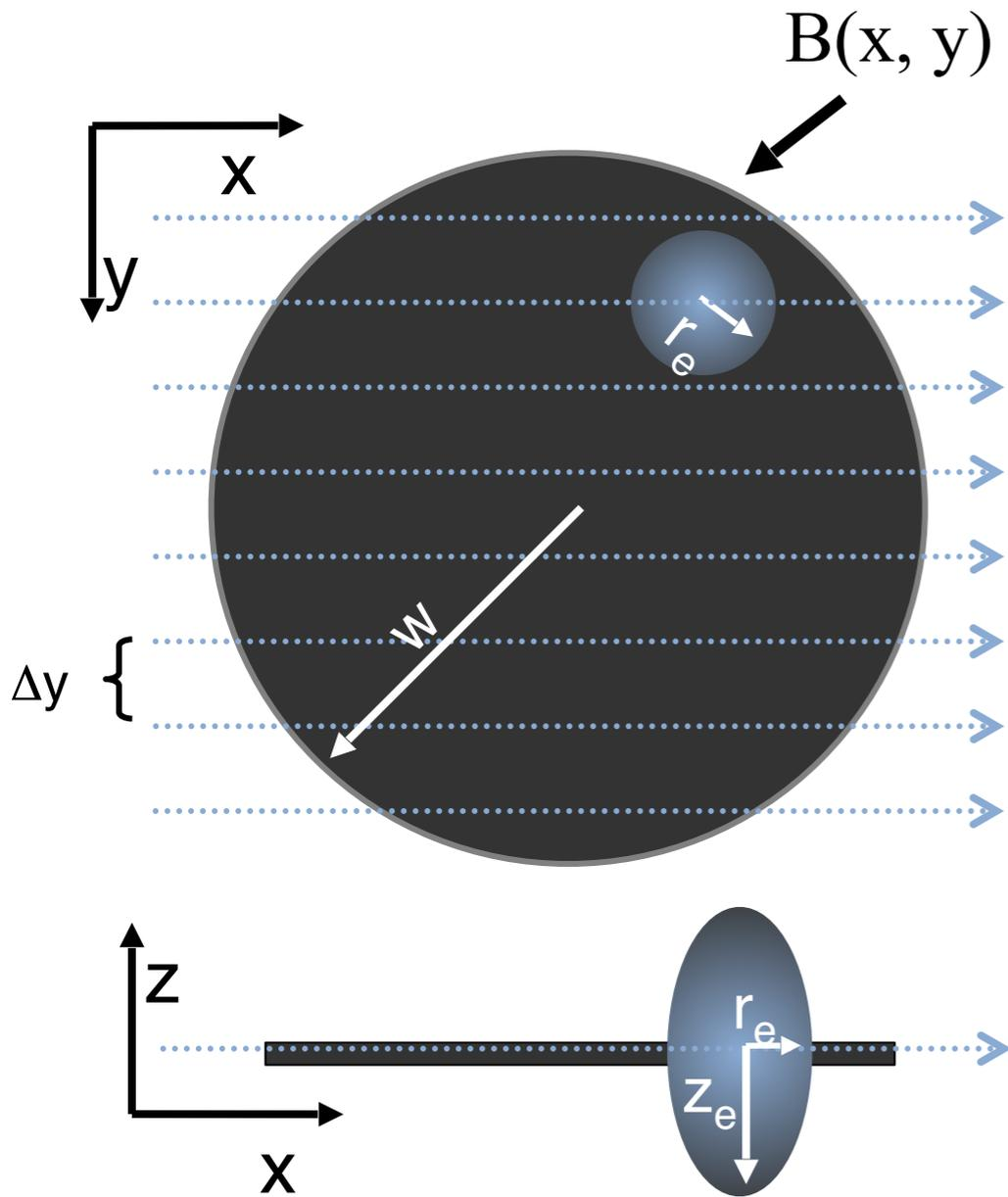
$$C(r, z) = C_0$$

Photobleaching

$$\frac{dC(r, z, t)}{dt} = -\alpha \langle I_b^2(r, z, t) \rangle C(r, z, t)$$

Mazza D. et al., BJ

FRAP



Condizione Iniziale

$$C(r, z) = C_0$$

Photobleaching

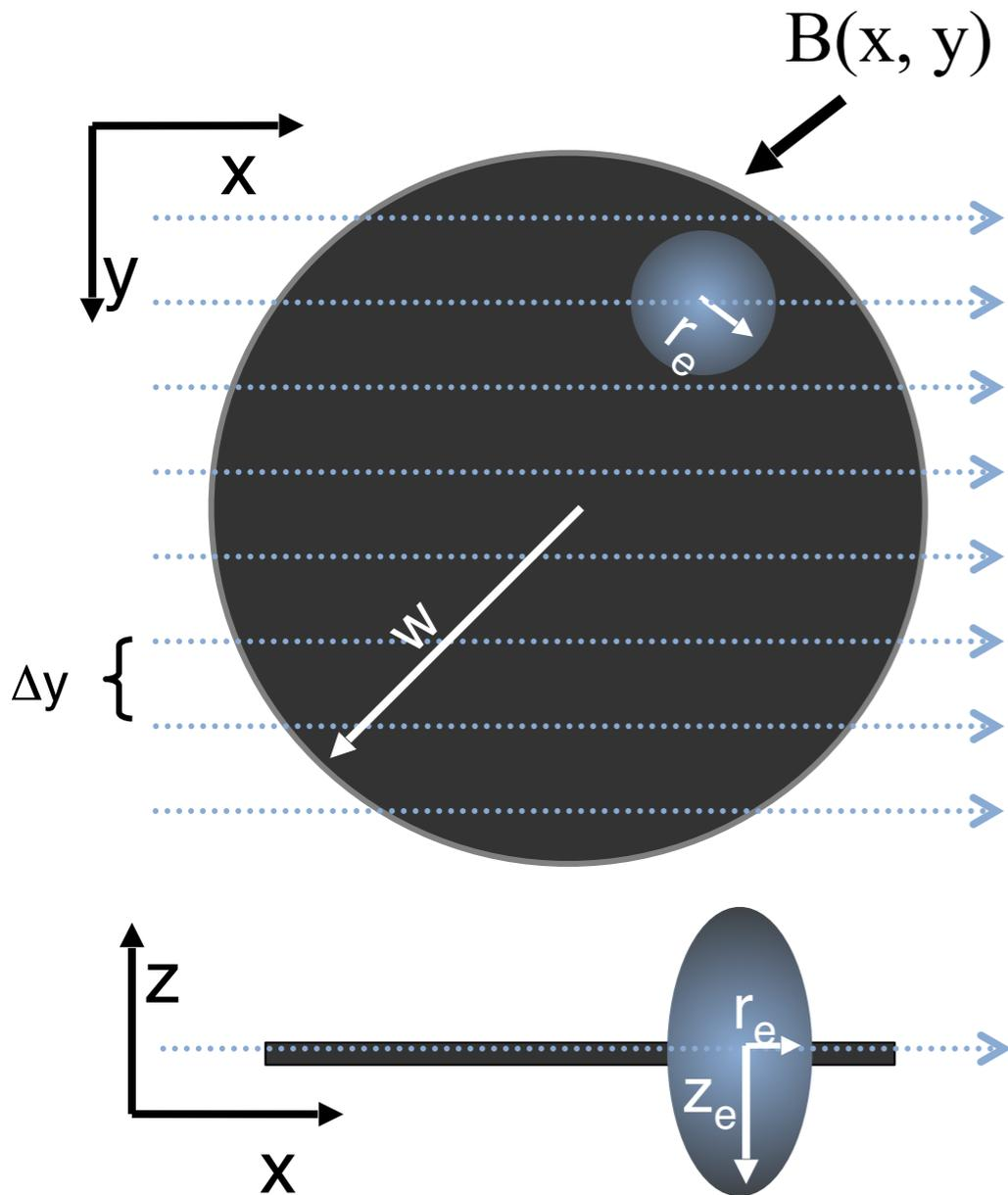
$$\frac{dC(r, z, t)}{dt} = -\alpha \langle I_b^2(r, z, t) \rangle C(r, z, t)$$

$$C_b(r, z) = C_0 e^{-\frac{\alpha}{v\Delta y} K(r, z)}$$

$$K(x, y, z) = B(x, y) \otimes_{x, y} I_b^2(x, y, z)$$

Mazza D. et al., BJ 2008

FRAP



Condizione Iniziale

$$C(r, z) = C_0$$

Photobleaching

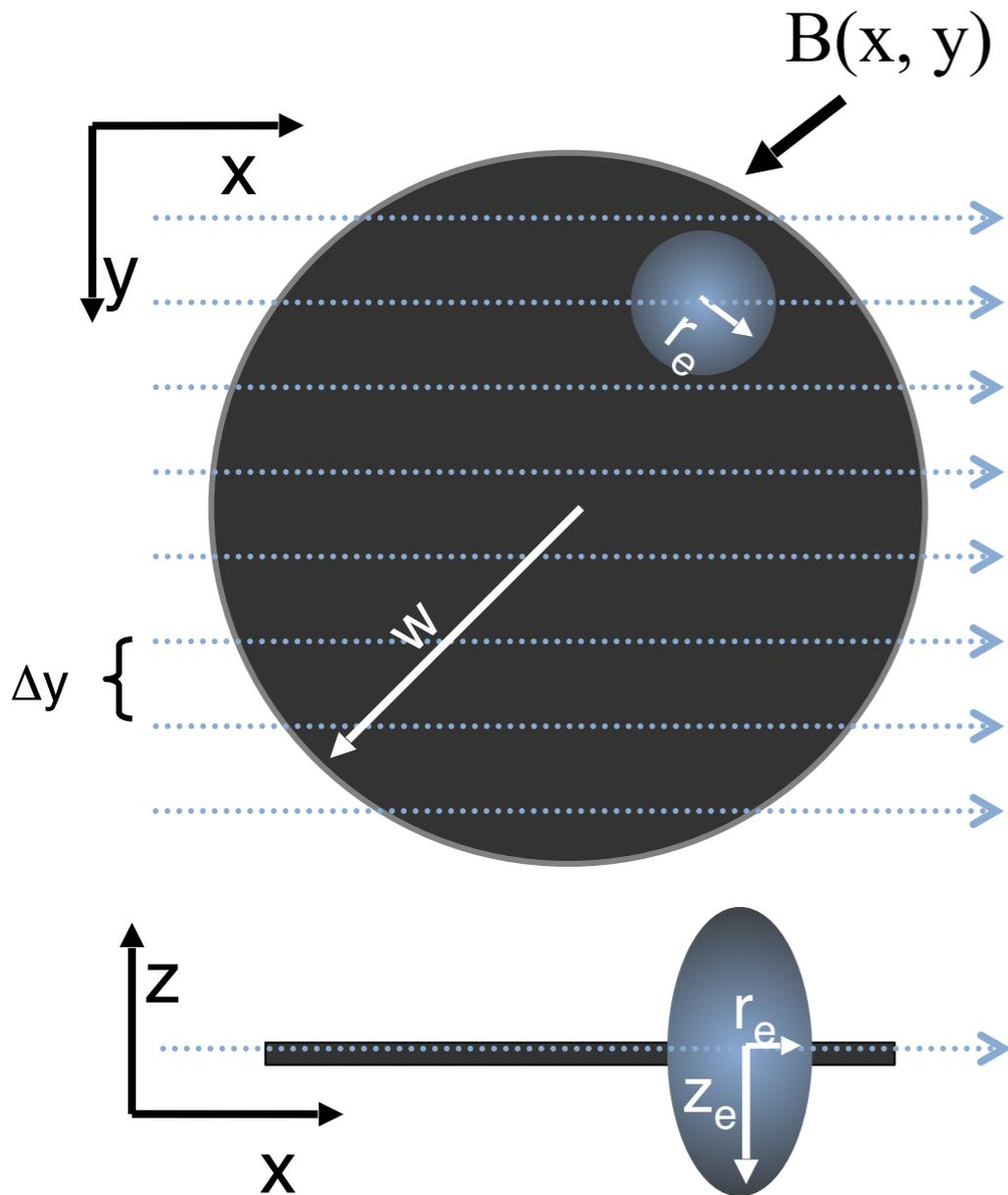
$$C_b(r, z) = C_0 e^{-\frac{\alpha}{v\Delta y} K(r, z)}$$

Diffusione

$$\frac{\partial C(r, z, t)}{\partial t} = D\nabla^2 C(r, z, t)$$

Mazza D. et al., BJ 2008

FRAP



Condizione Iniziale

$$C(r, z) = C_0$$

Photobleaching

$$C_b(r, z) = C_0 e^{-\frac{\alpha}{v\Delta y} K(r, z)}$$

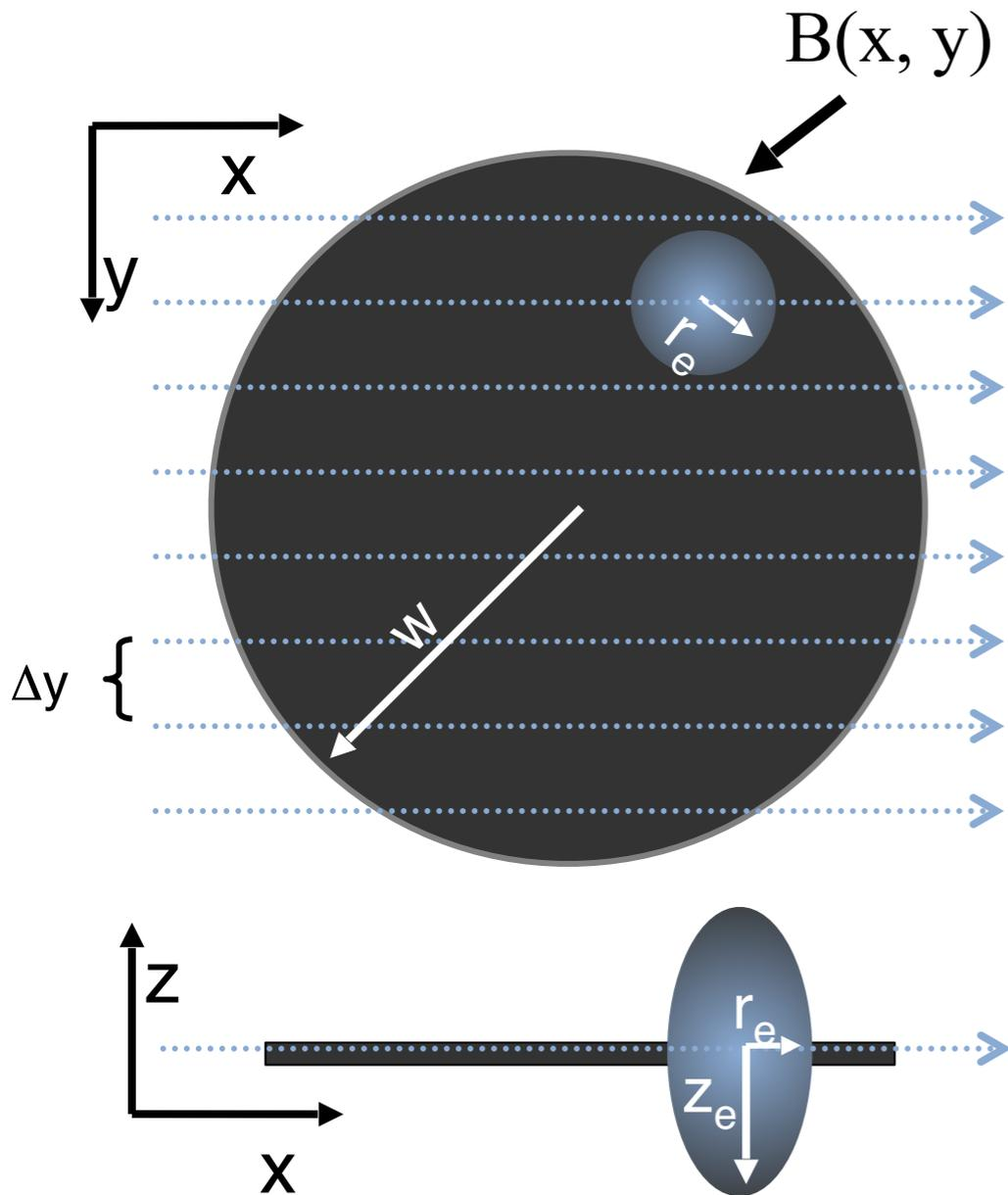
Diffusione

$$\frac{\partial C(r, z, t)}{\partial t} = D \nabla^2 C(r, z, t)$$

$$C(r, z, t) = C_0 - C_0 \left[1 - \sum_{i=0}^{+\infty} \frac{(-K_{0n})^i}{i!} \frac{z_e}{\sqrt{z_e^2 + 8iDt}} e^{-\frac{2iz^2}{z_e^2 + 8iDt}} \right] \\ \times \frac{1}{2Dt} e^{-\frac{r^2}{4Dt}} \int_{r'=0}^w e^{-\frac{r'^2}{4Dt}} I_0 \left(\frac{rr'}{2Dt} \right) r' dr'$$

Mazza D. et al., BJ 2008

FRAP



Condizione Iniziale

$$C(r, z) = C_0$$

Photobleaching

$$C_b(r, z) = C_0 e^{-\frac{\alpha}{v\Delta y} K(r, z)}$$

Diffusione

$$\frac{\partial C(r, z, t)}{\partial t} = D \nabla^2 C(r, z, t)$$

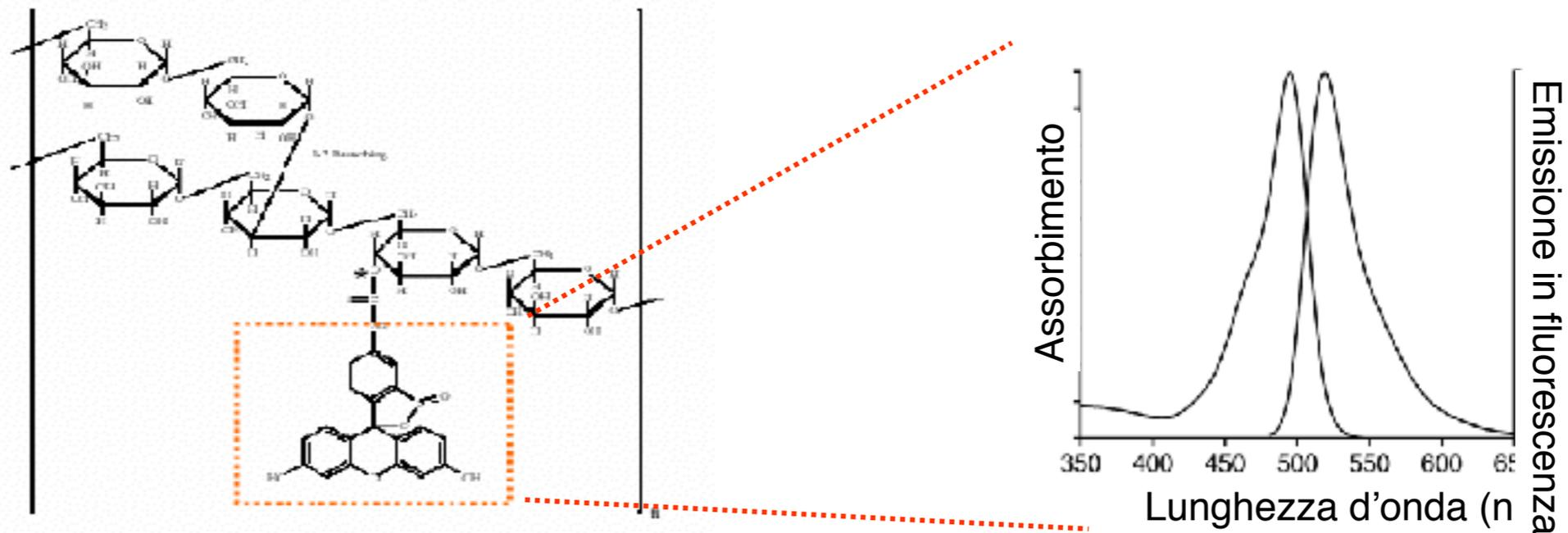
$$\frac{F_{tot}(t)}{F_{tot,0}} = 1 + \sum_{i=1}^{+\infty} \frac{(-K_{0n})^i}{i!} \frac{z_e}{\sqrt{8iDt + z_e^2 + iz_d^2}} \times \left[1 - e^{-\frac{w^2}{2Dt}} \left(I_0 \left(\frac{w^2}{2Dt} \right) + I_1 \left(\frac{w^2}{2Dt} \right) \right) \right]$$

Mazza D. et al., BJ 2008

FRAP

$$\frac{F_{tot}(t)}{F_{tot,0}} = 1 + \sum_{i=1}^{+\infty} \frac{(-K_{0n})^i}{i!} \frac{z_e}{\sqrt{8iDt + z_e^2 + iz_d^2}} \times \left[1 - e^{-\frac{w^2}{2Dt}} \left(I_0\left(\frac{w^2}{2Dt}\right) + I_1\left(\frac{w^2}{2Dt}\right) \right) \right]$$

Validazione sperimentale su soluzioni a viscosità controllata di Fluoresceina-Destrani

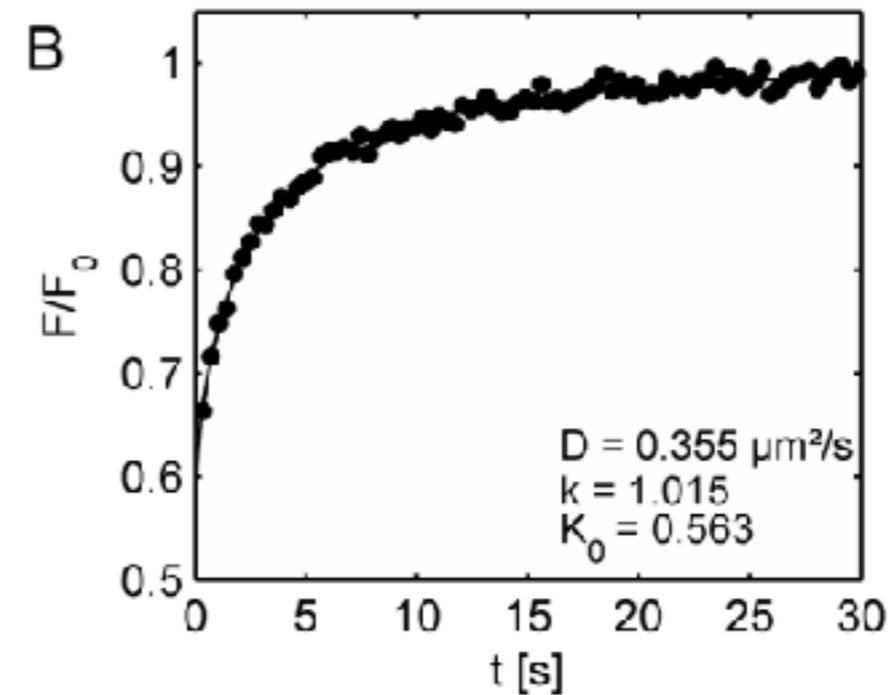
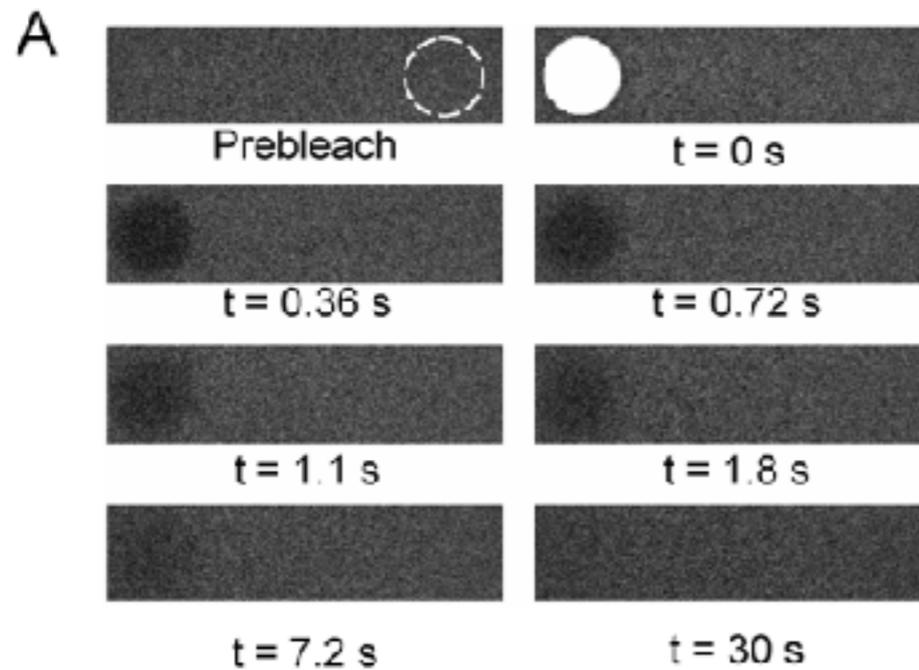


Mazza D. et al., BJ 2008

FRAP

$$\frac{F_{tot}(t)}{F_{tot,0}} = 1 + \sum_{i=1}^{+\infty} \frac{(-K_{0n})^i}{i!} \frac{z_e}{\sqrt{8iDt + z_e^2 + iz_d^2}} \times \left[1 - e^{-\frac{w^2}{2Dt}} \left(I_0\left(\frac{w^2}{2Dt}\right) + I_1\left(\frac{w^2}{2Dt}\right) \right) \right]$$

Validazione sperimentale su soluzioni a viscosità controllata di Fluoresceina-Destrani

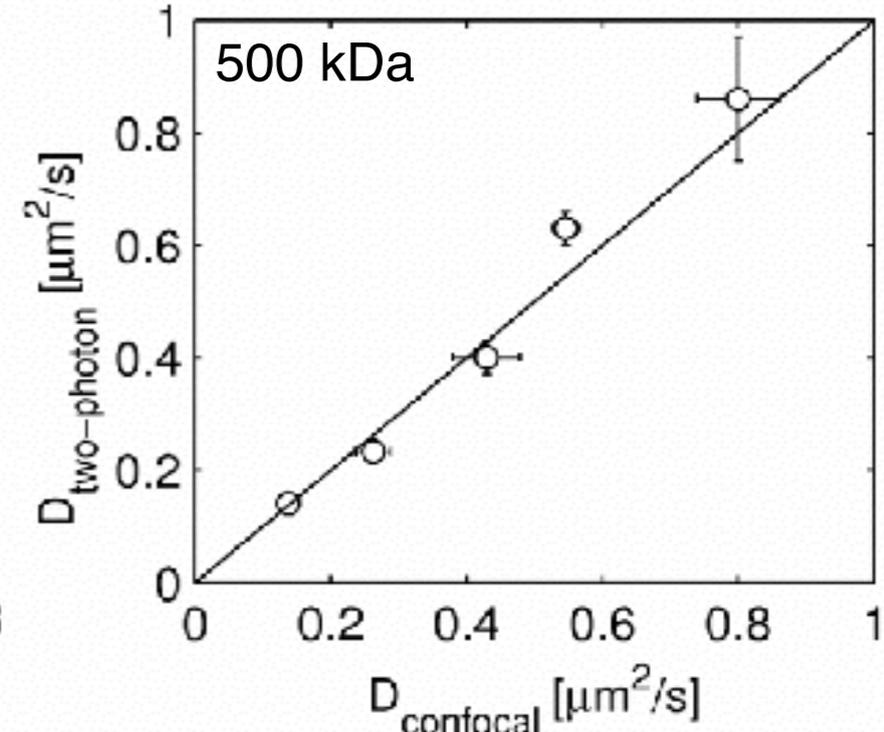
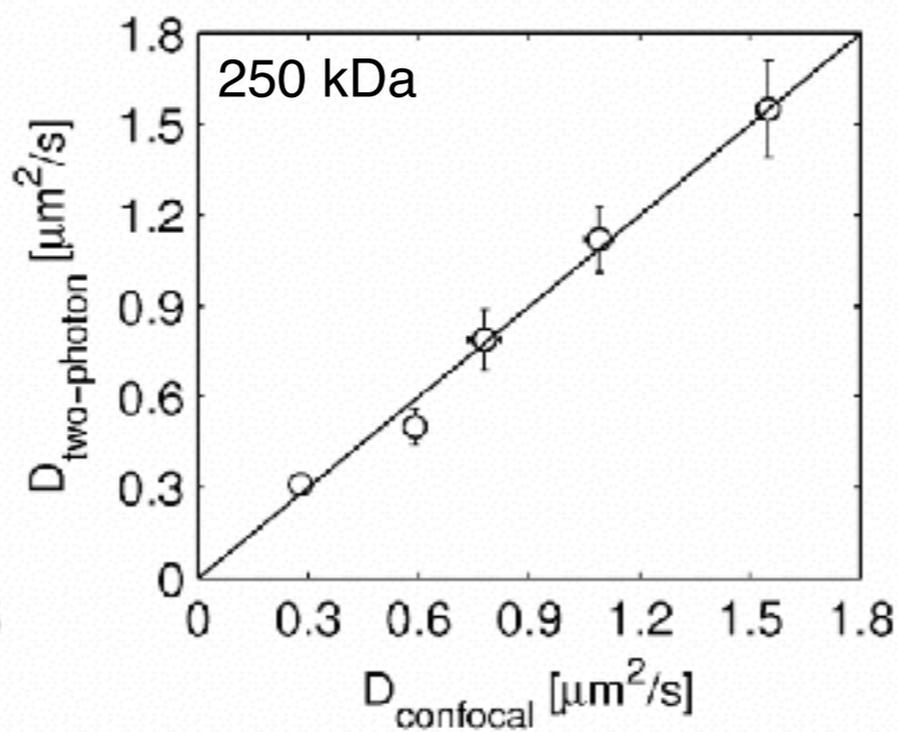
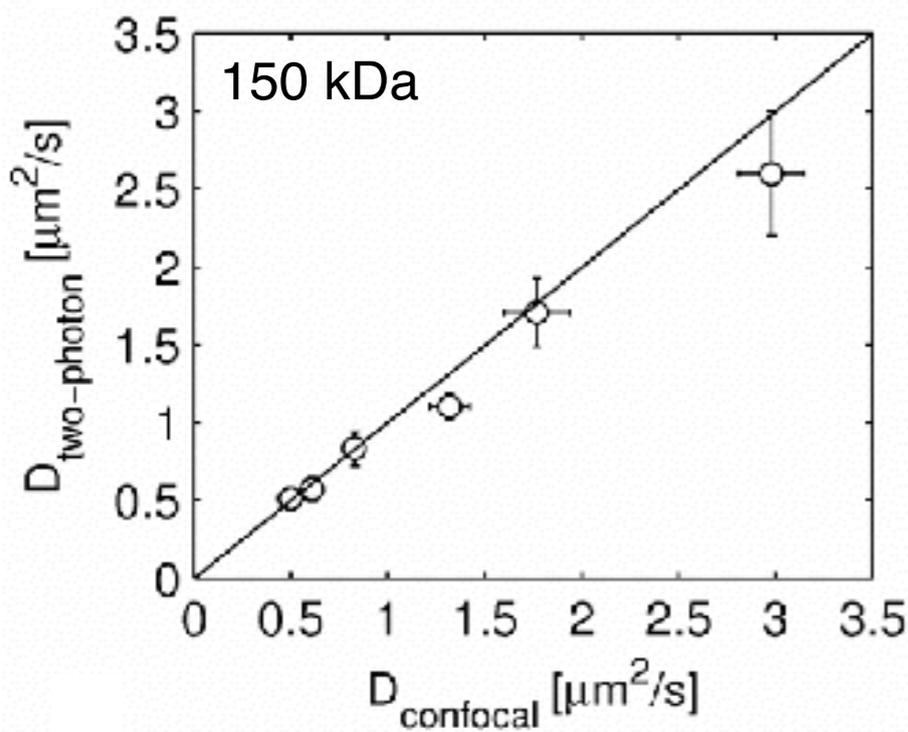


Mazza D. et al., BJ 2008

FRAP

$$\frac{F_{tot}(t)}{F_{tot,0}} = 1 + \sum_{i=1}^{+\infty} \frac{(-K_{0n})^i}{i!} \frac{z_e}{\sqrt{8iDt + z_e^2 + iz_d^2}} \times \left[1 - e^{-\frac{w^2}{2Dt}} \left(I_0 \left(\frac{w^2}{2Dt} \right) + I_1 \left(\frac{w^2}{2Dt} \right) \right) \right]$$

Confronto tra diffusione 2D (FRAP confocale – bassa apertura numerica)
e diffusione 3D (FRAP a 2 fotoni – alta apertura numerica)



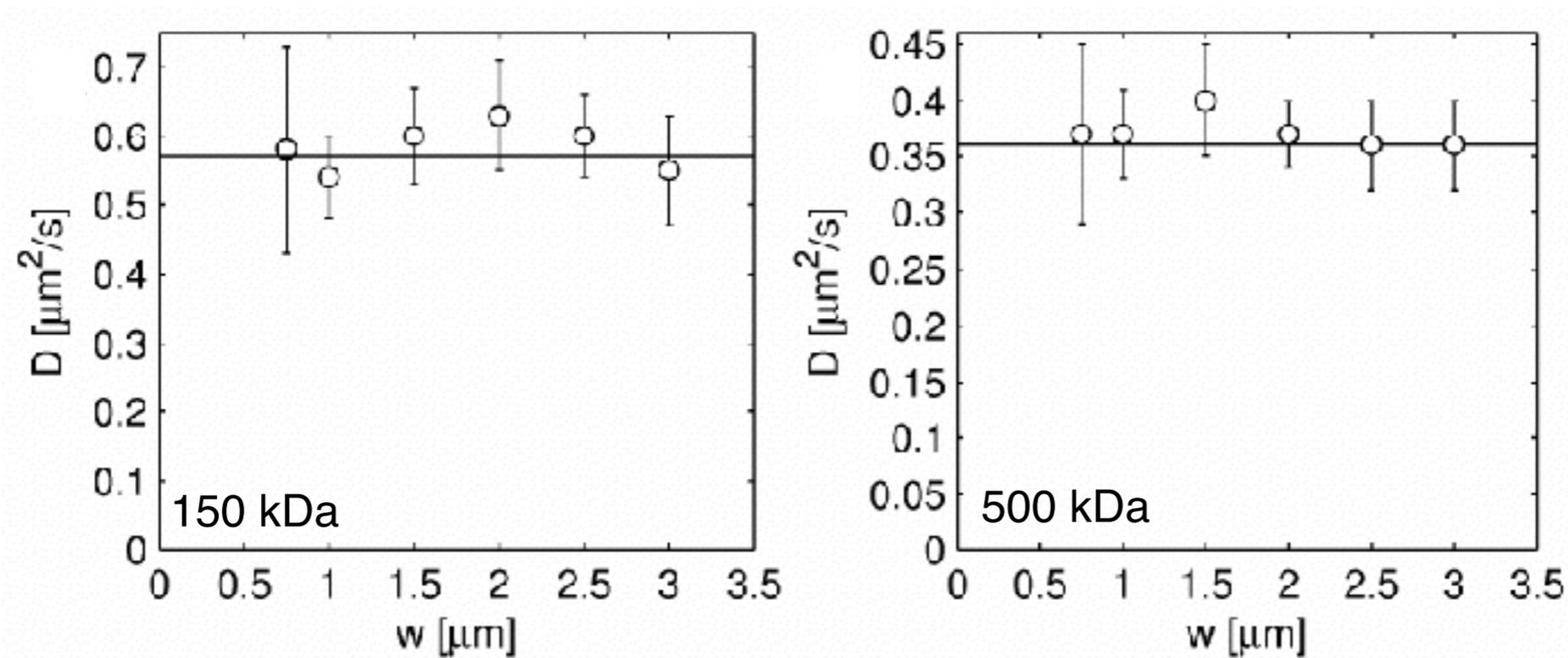
+ Obiettivo ad Alta apertura Numerica

Mazza D. et al., BJ 2008

FRAP

$$\frac{F_{tot}(t)}{F_{tot,0}} = 1 + \sum_{i=1}^{+\infty} \frac{(-K_{0n})^i}{i!} \frac{z_e}{\sqrt{8iDt + z_e^2 + iz_d^2}} \times \left[1 - e^{-\frac{w^2}{2Dt}} \left(I_0\left(\frac{w^2}{2Dt}\right) + I_1\left(\frac{w^2}{2Dt}\right) \right) \right]$$

Qualità del modello in dipendenza della dimensione della regione di bleach



+ Obiettivo ad Alta apertura Numerica

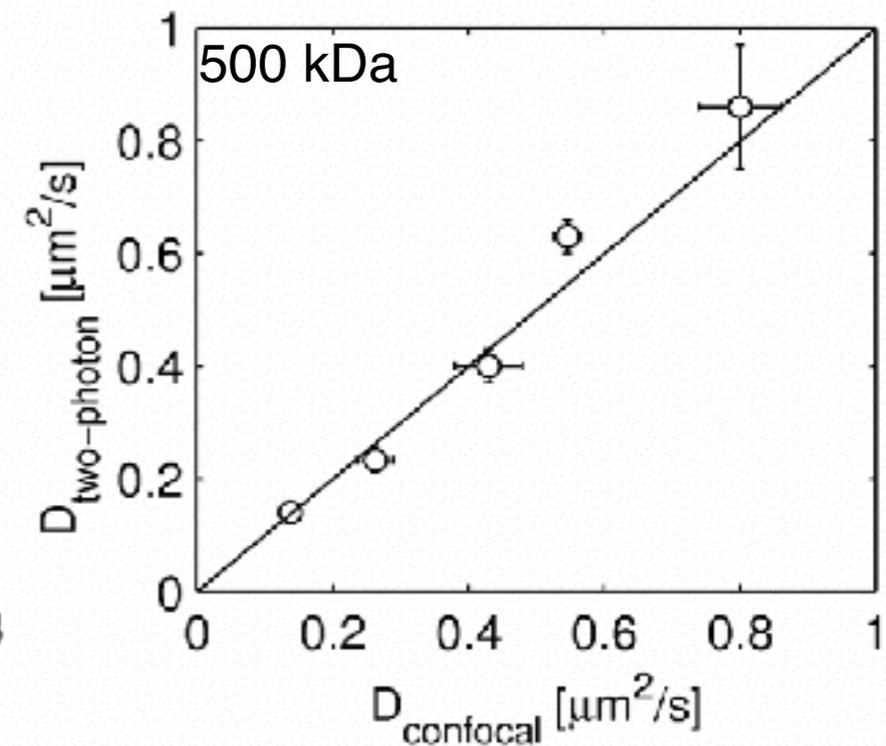
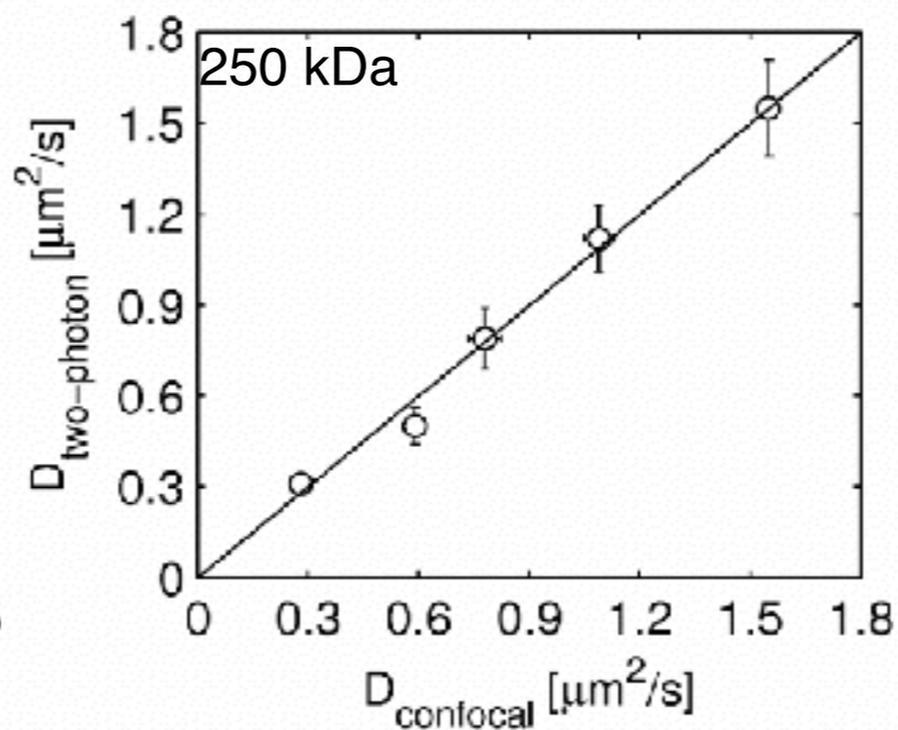
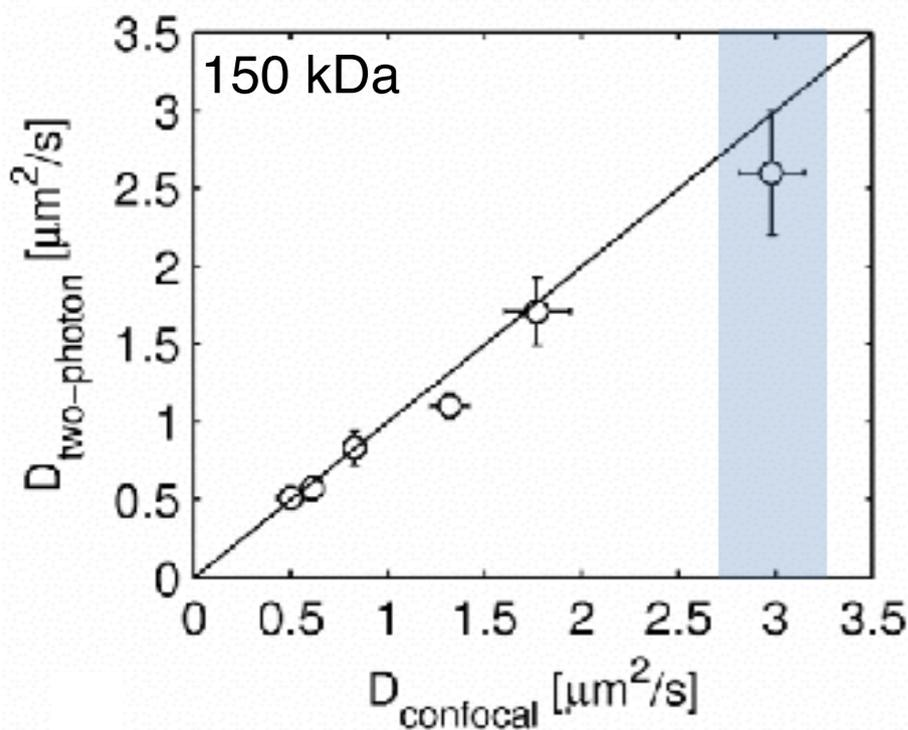
+ Controllo nelle dimensioni della regione di bleach

Mazza D. et al., BJ 2008

FRAP

$$\frac{F_{tot}(t)}{F_{tot,0}} = 1 + \sum_{i=1}^{+\infty} \frac{(-K_{0n})^i}{i!} \frac{z_e}{\sqrt{8iDt + z_e^2 + iz_d^2}} \times \left[1 - e^{-\frac{w^2}{2Dt}} \left(I_0\left(\frac{w^2}{2Dt}\right) + I_1\left(\frac{w^2}{2Dt}\right) \right) \right]$$

Validazione sperimentale su soluzioni a viscosità controllata di Fluoresceina-Destrani



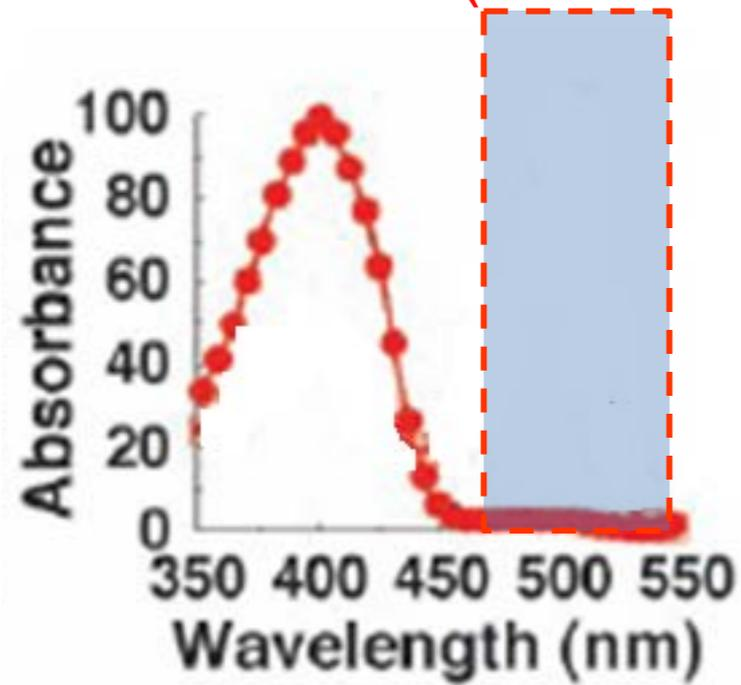
+ Obiettivo ad Alta apertura Numerica

- Limiti nella misura dei coefficienti di diffusione misurabili

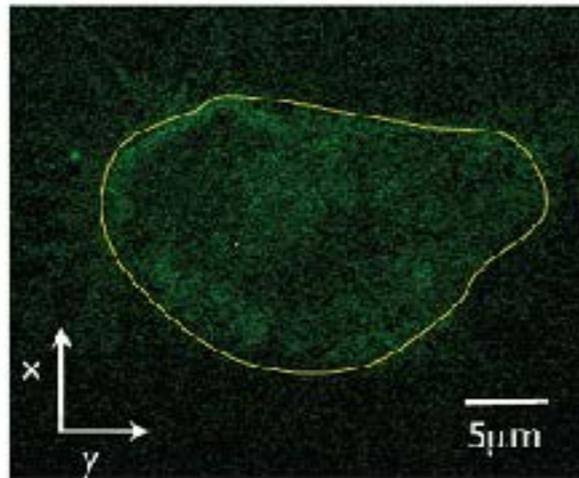
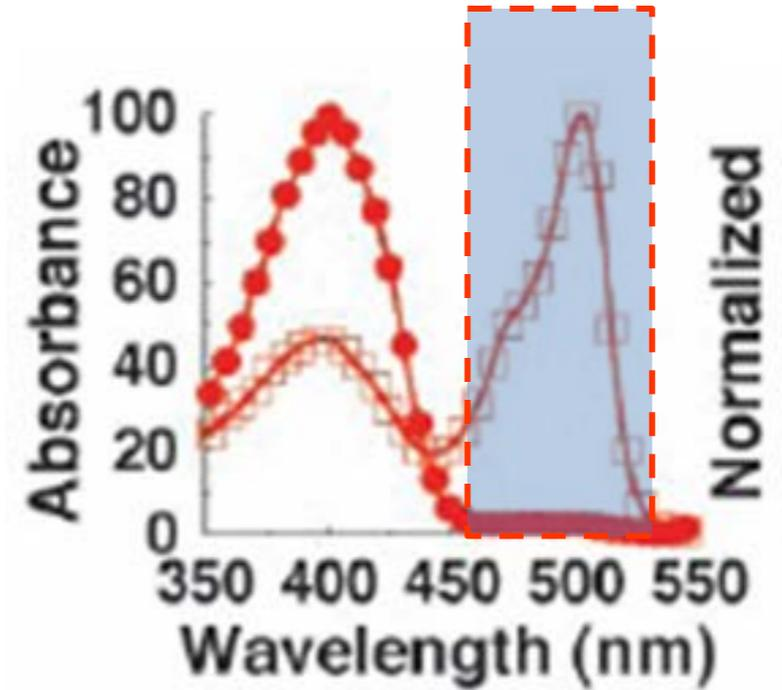
+ Controllo nelle dimensioni della regione di bleach

FRAP

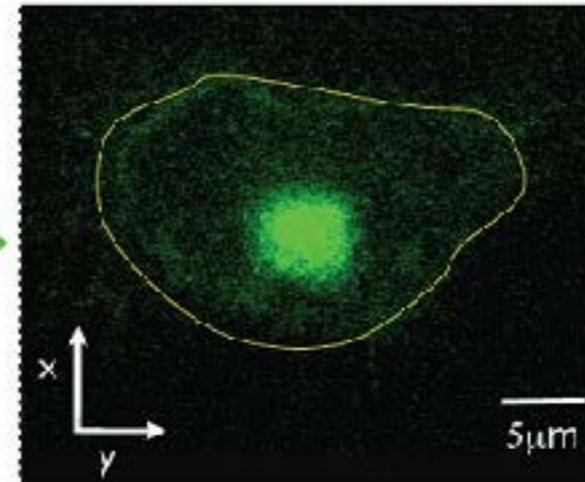
Photoactivatable GFP (PA-GFP)



PHOTOACTIVATION



PHOTOACTIVATION



PRE ACTIVATION

$\langle P_{\text{EXCITATION}} \rangle = 0,04 \text{ mW}$, $\lambda_{\text{EXCITATION}} = 488 \text{ nm}$
Pixel time = 4,9 μs, 512*512 pixels

POST ACTIVATION

$\langle P_{\text{EXCITATION}} \rangle = 0,04 \text{ mW}$, $\lambda_{\text{EXCITATION}} = 488 \text{ nm}$
Pixel time = 4,9 μs, 512*512 pixels

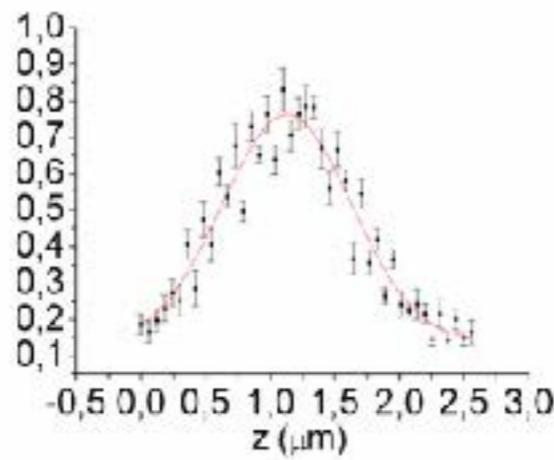
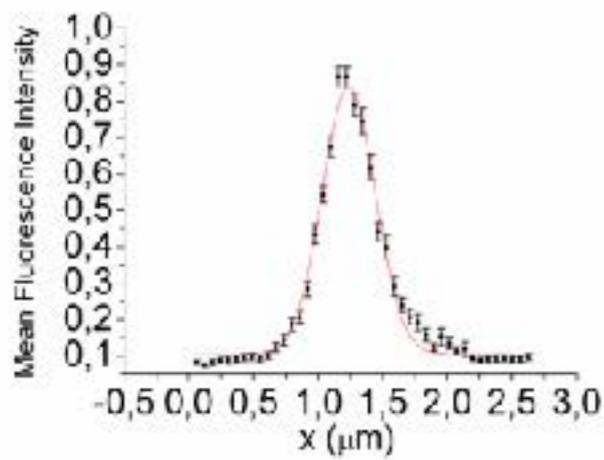
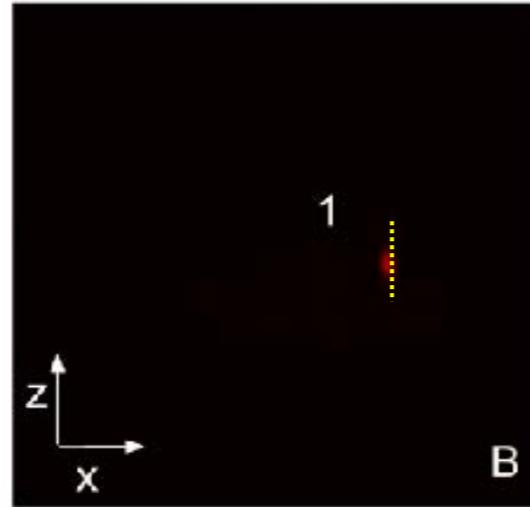
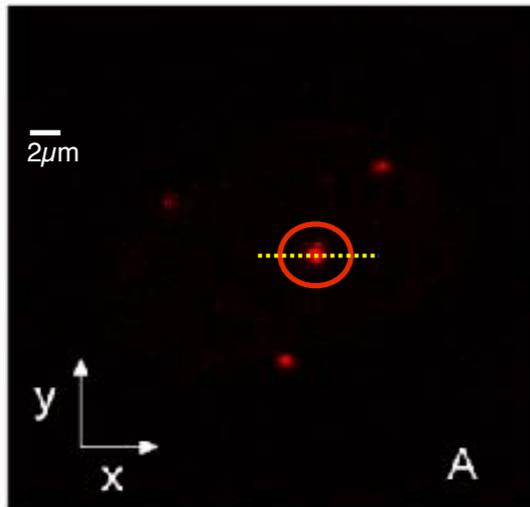
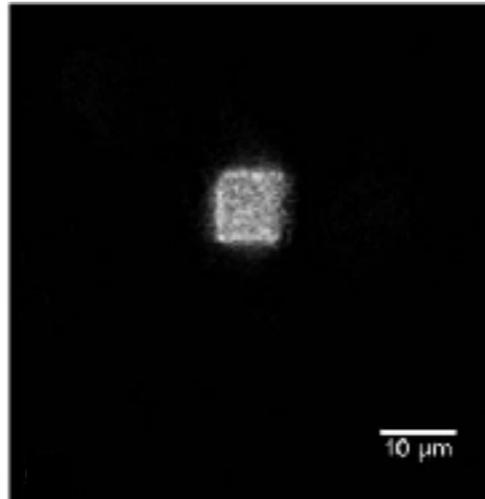
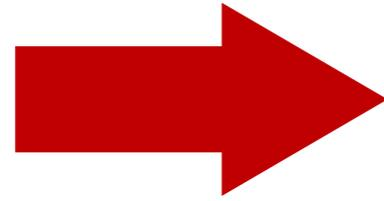
Patterson and Lippincott-Schwartz, Methods, 2003

slide credit: Davide Mazza, LAMBS

FRAP



ATTIVAZIONE
A DUE FOTONI

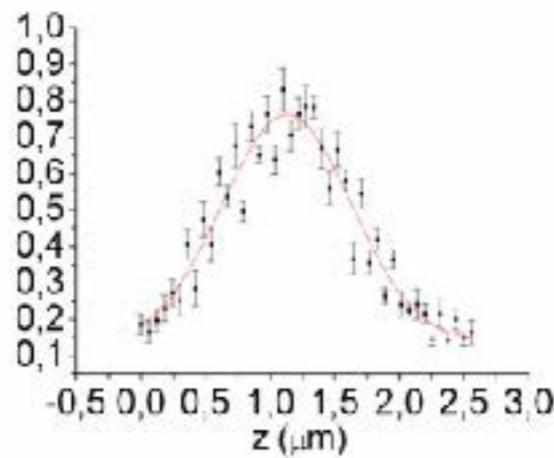
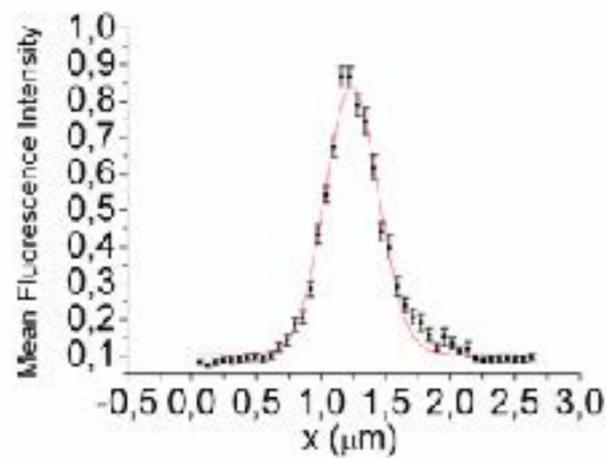
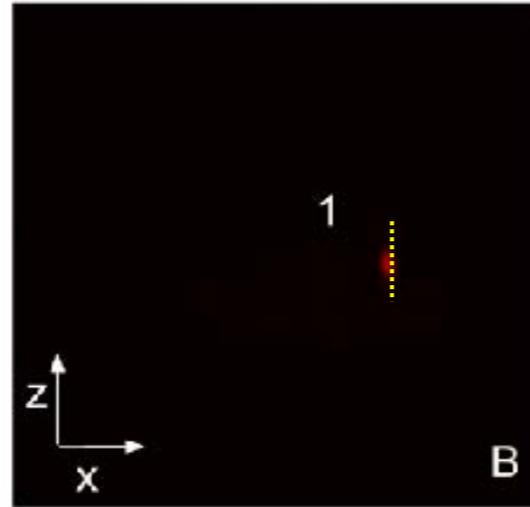
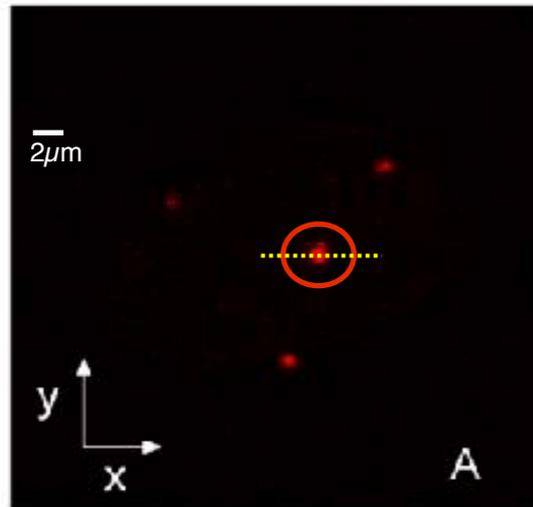
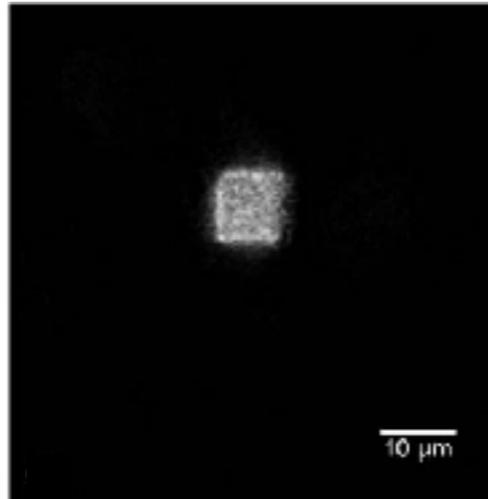
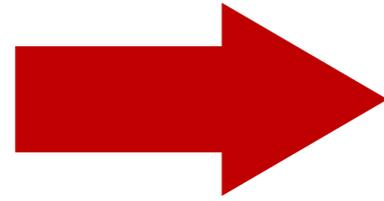


Schneider M, et al., Biophys J, 2004

Testa I, et al., J Microscopy, 2008

FRAP

ATTIVAZIONE
A DUE FOTONI



Estensione del modello alla fotoattivazione

Diffusione di proteine native
e proteine attivate

$$\frac{F_{tot}(t)}{F_{tot,0}} = 1 + \frac{(\sigma_m - \sigma_{A,m})C_0}{\sigma_m C_0 + \sigma_{A,m} C_{A,0}} \sum_{i=1}^{+\infty} \frac{(-K_{0n})^i}{i!} \frac{z_e}{\sqrt{8iDt + z_e^2 + iz_d^2}} \times \left[1 - e^{-\frac{w^2}{2Dt}} \left(I_0\left(\frac{w^2}{2Dt}\right) + I_1\left(\frac{w^2}{2Dt}\right) \right) \right]$$

Schneider M, et al., Biophys J, 2004

Testa I, et al., J Microscopy, 2008

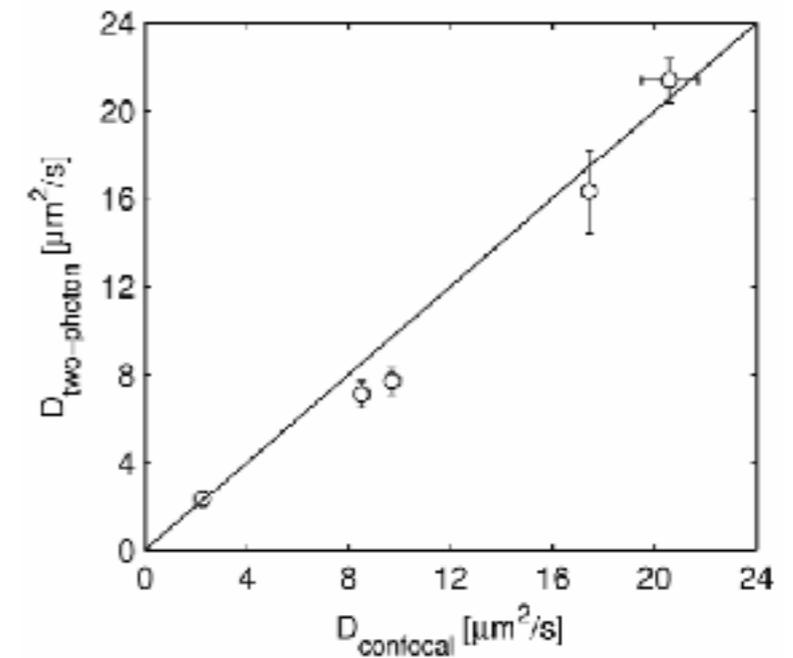
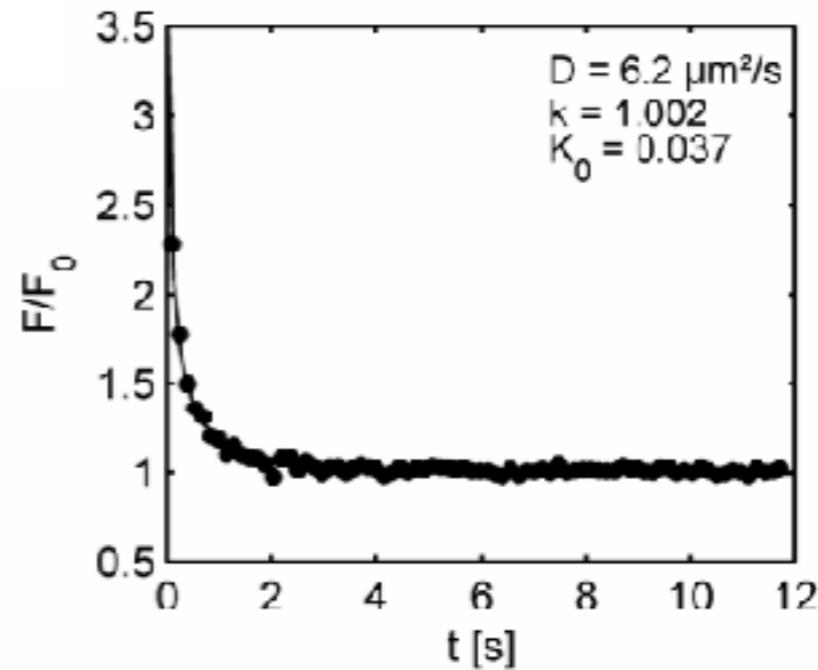
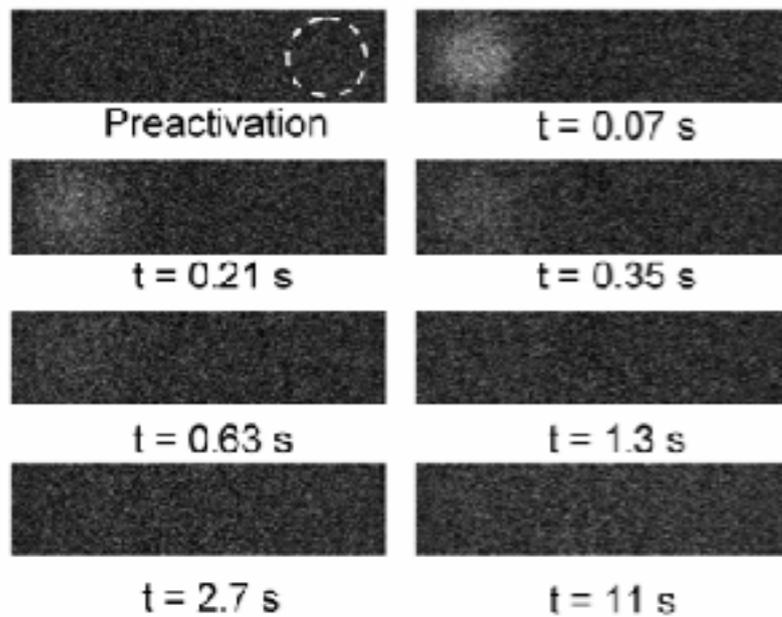
FRAP

Photoactivatable GFP (PA-GFP)

$$\frac{F_{tot}(t)}{F_{tot,0}} = 1 + \frac{(\sigma_m - \sigma_{A,m})C_0}{\sigma_m C_0 + \sigma_{A,m} C_{A,0}} \sum_{i=1}^{+\infty} \frac{(-K_{0n})^i}{i!} \frac{z_e}{\sqrt{8iDt + z_e^2 + iz_d^2}}$$

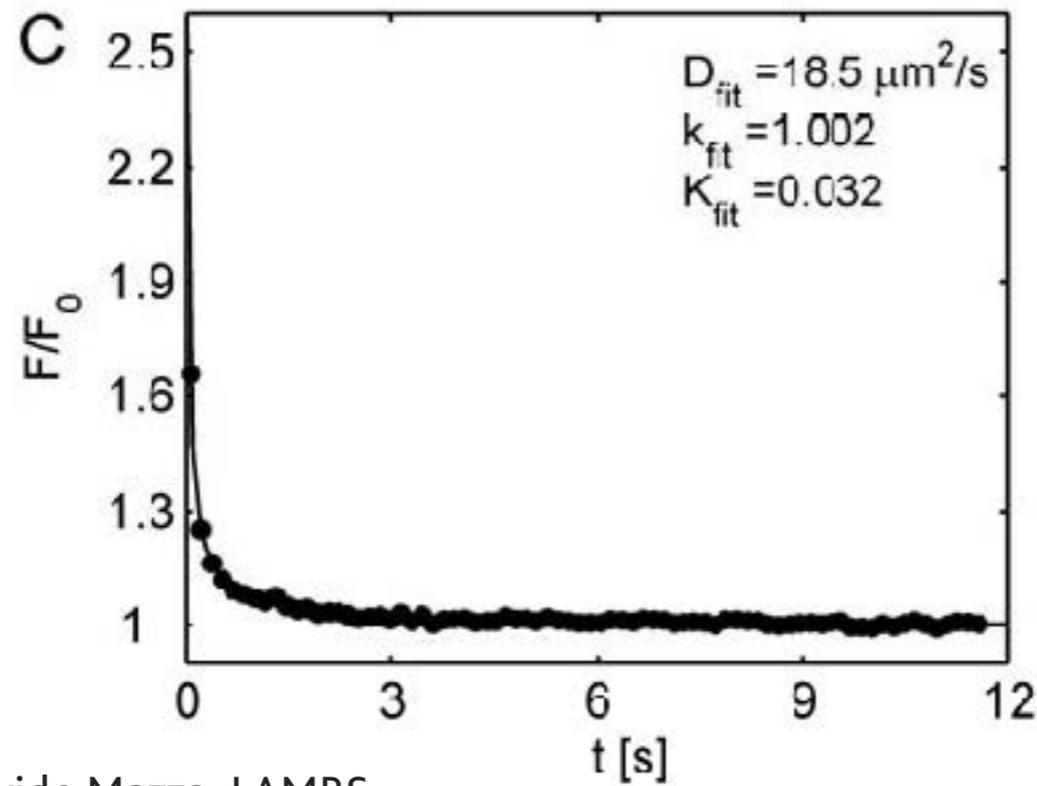
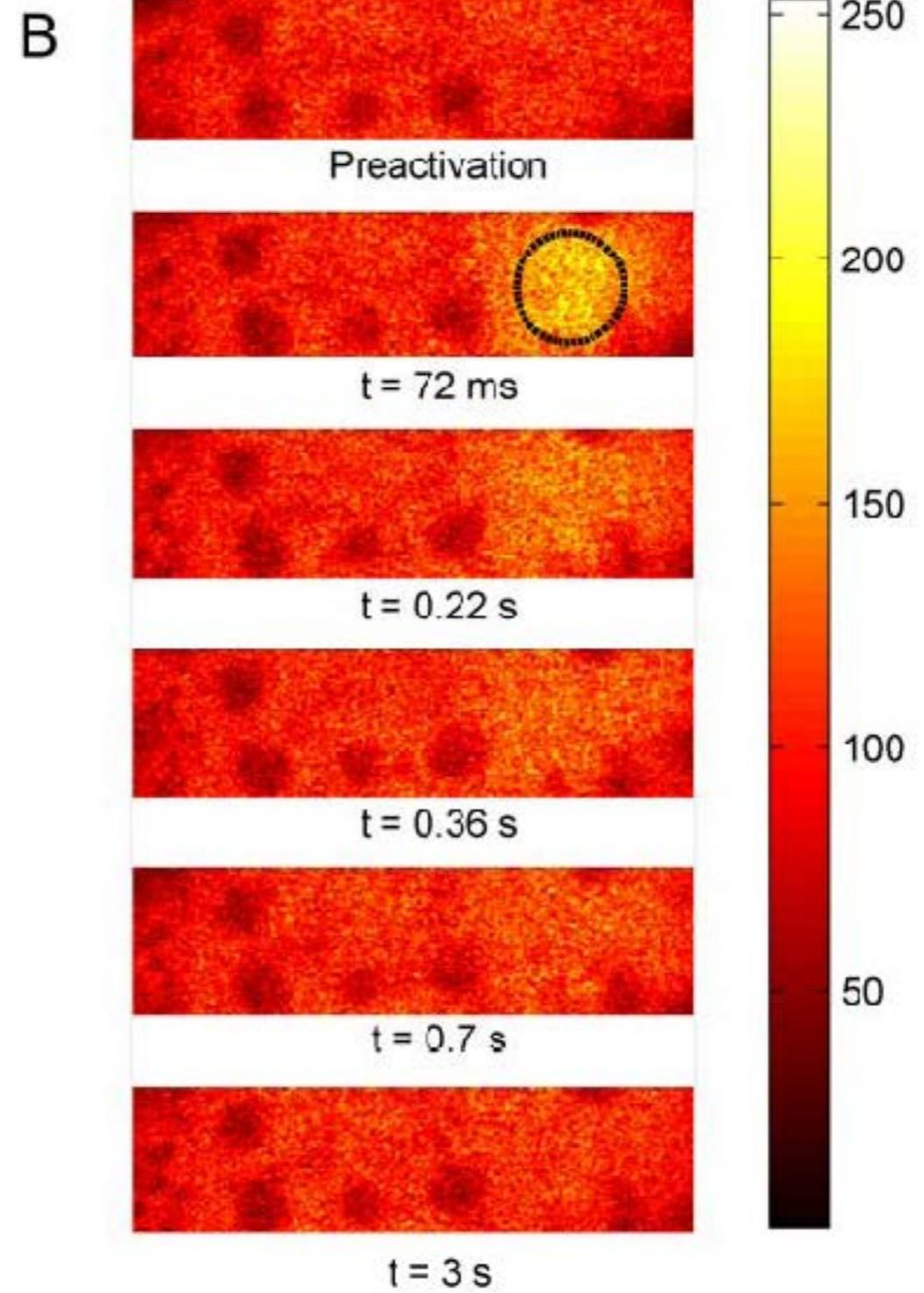
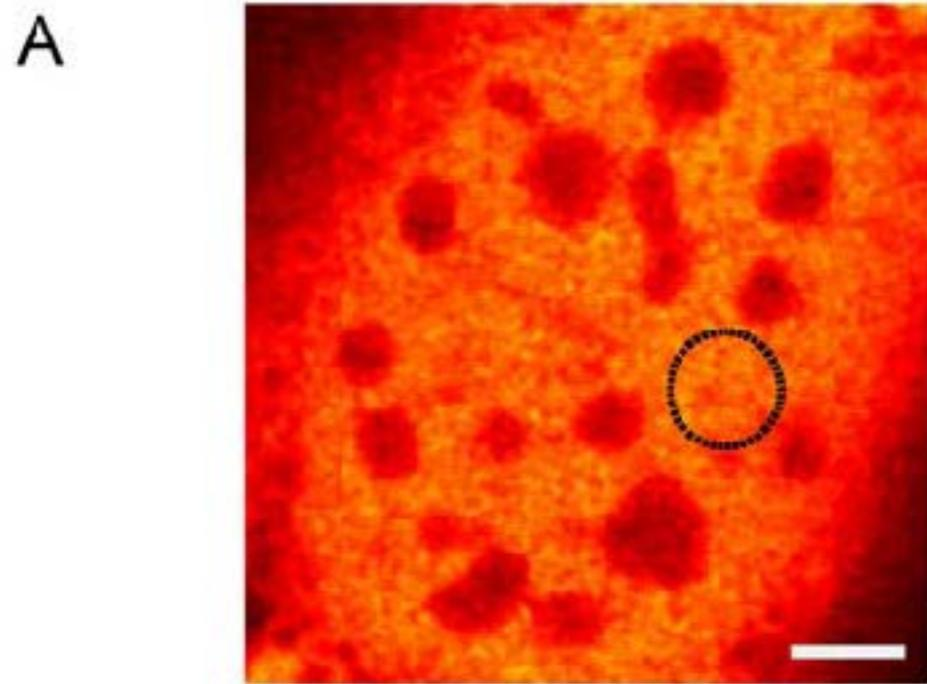
$$\times \left[1 - e^{-\frac{w^2}{2Dt}} \left(I_0\left(\frac{w^2}{2Dt}\right) + I_1\left(\frac{w^2}{2Dt}\right) \right) \right]$$

Validazione sperimentale su soluzioni a viscosità controllata di paGFP



slide credit: Davide Mazza, LAMBS

FRAP



slide credit: Davide Mazza, LAMBS

Mouse Embryo Fibroblasts NIH-3T3

FRAP

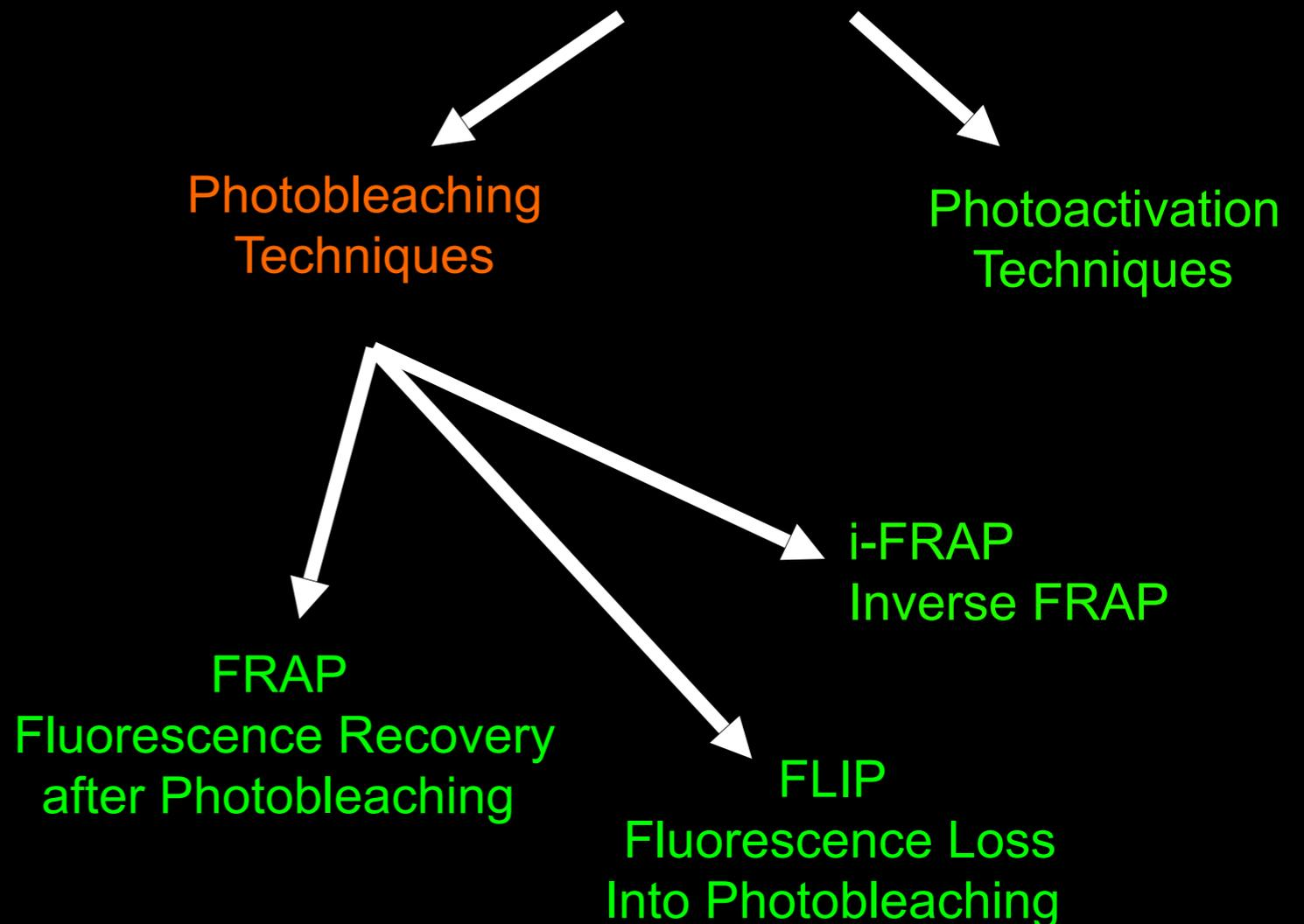
Loren...Diaspro et al., *Q Rev Biophys.* 2015 Aug;48(3):323-87.

Dendra2 photoactivation
in HEPg2 cells



with Dr. M. Crippa

Fluorescence Perturbation techniques (FPT)

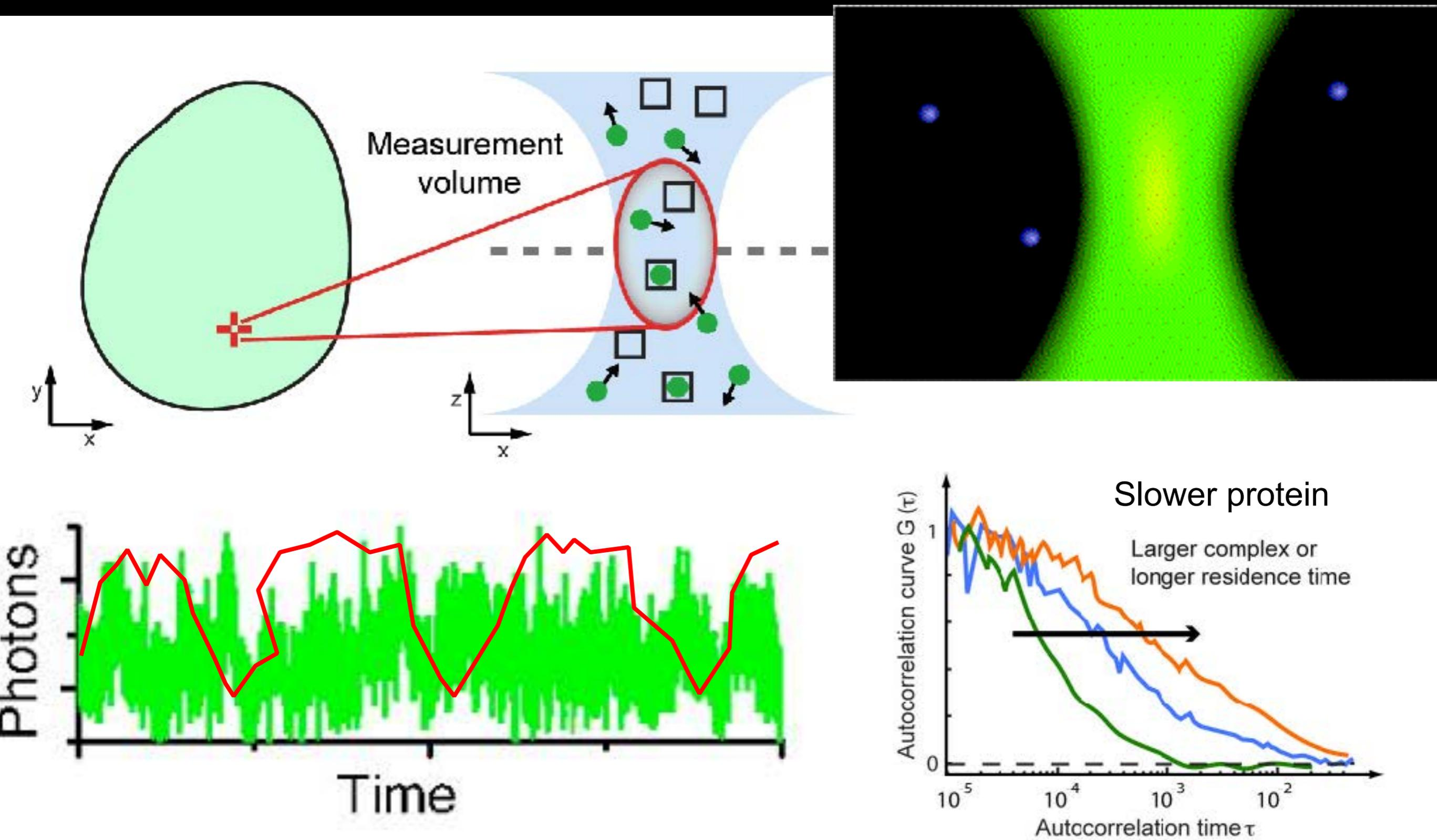


SOMETIMES LESS IT'S BETTER

DECREASING CONCENTRATION
OF FLUORESCENT PROBE

	FRAP	FLIP	Fluorescence fluctuation techniques	Single molecule
Probe concentration	μM	μM	nM	pM to nM
Photobleaching	Yes	Yes	No	No
Resolution	$1 \mu m$	$>1 \mu m$	$0.2 \mu m$	$0.02 \mu m$
Local measurement	Yes	No	Yes/no	No
Bulk technique	Yes	Yes	Yes	No

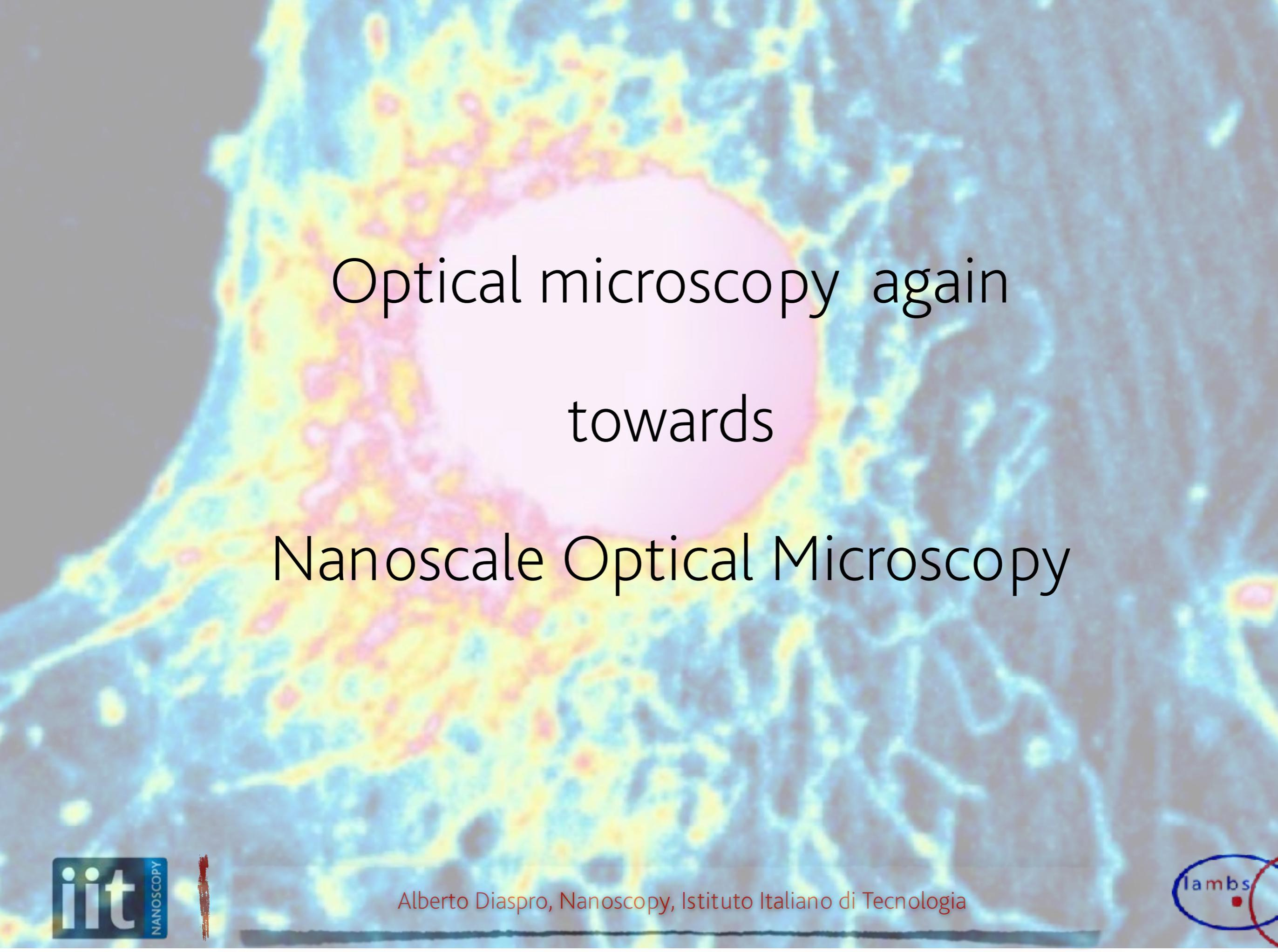
Fluorescence fluctuation spectroscopy (FCS)



SOMETIMES LESS IT'S BETTER

DECREASING CONCENTRATION
OF FLUORESCENT PROBE

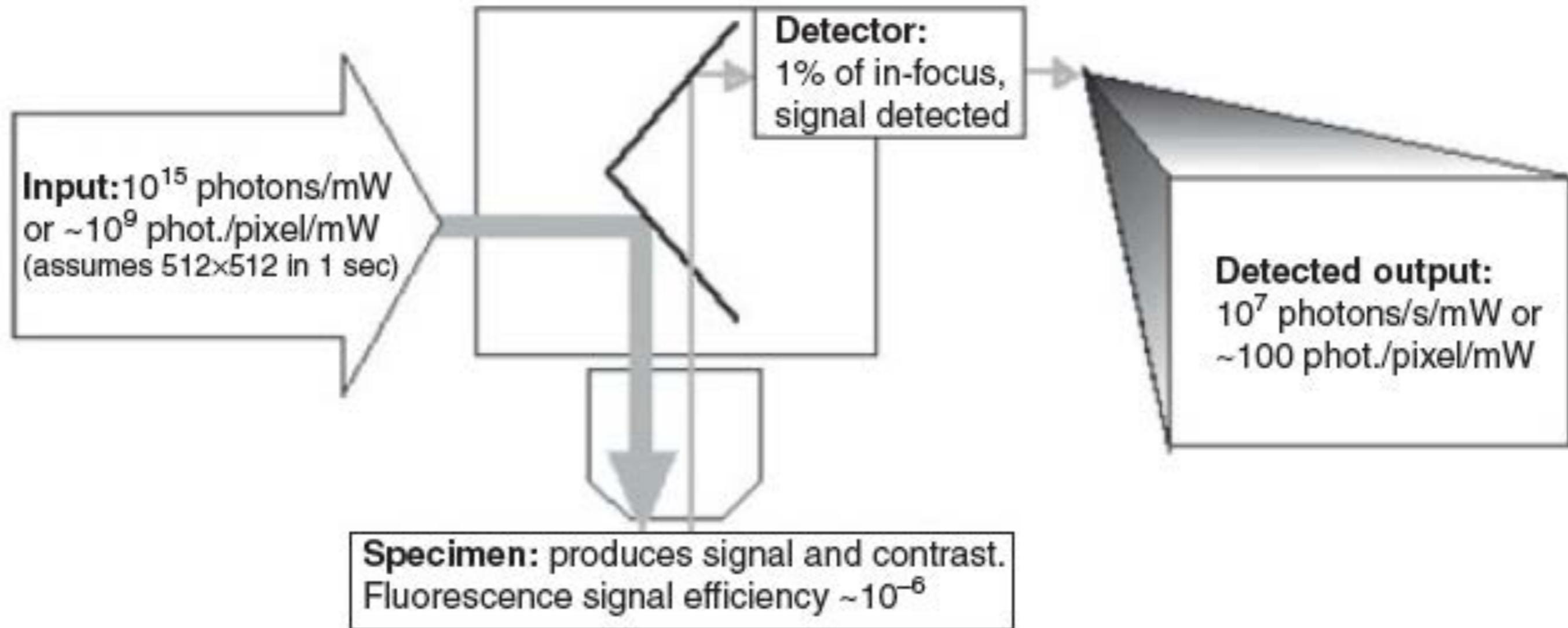
	FRAP	FLIP	Fluorescence fluctuation techniques	Single molecule
<i>Probe concentration</i>	μM	μM	nM	pM to nM
<i>Photobleaching</i>	Yes	Yes	No	No
<i>Resolution</i>	$1 \mu m$	$>1 \mu m$	$0.2 \mu m$	$0.02 \mu m$
<i>Local measurement</i>	Yes	No	Yes	No
<i>Bulk technique</i>	Yes	Yes	Yes	No



Optical microscopy again
towards

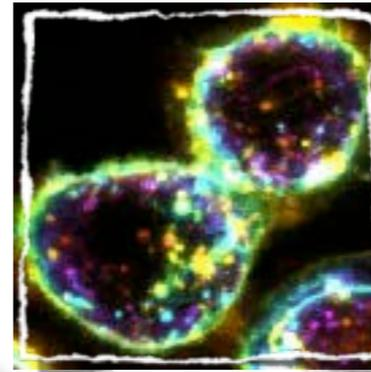
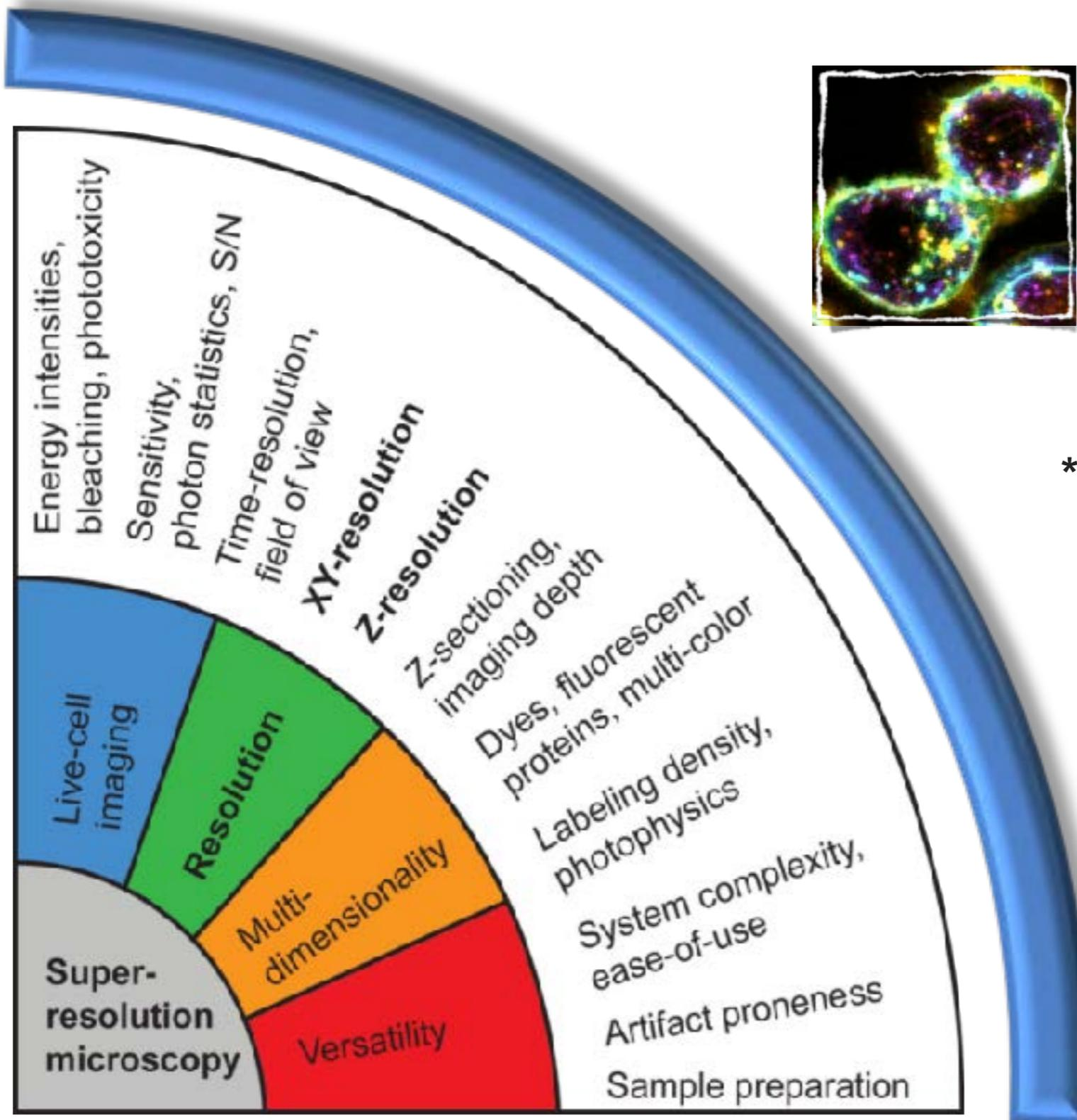
Nanoscale Optical Microscopy

optical microscopy scenario



Slide credit: Handbook of Confocal Microscopy (J.Pawley ed.), Plenum, 2006

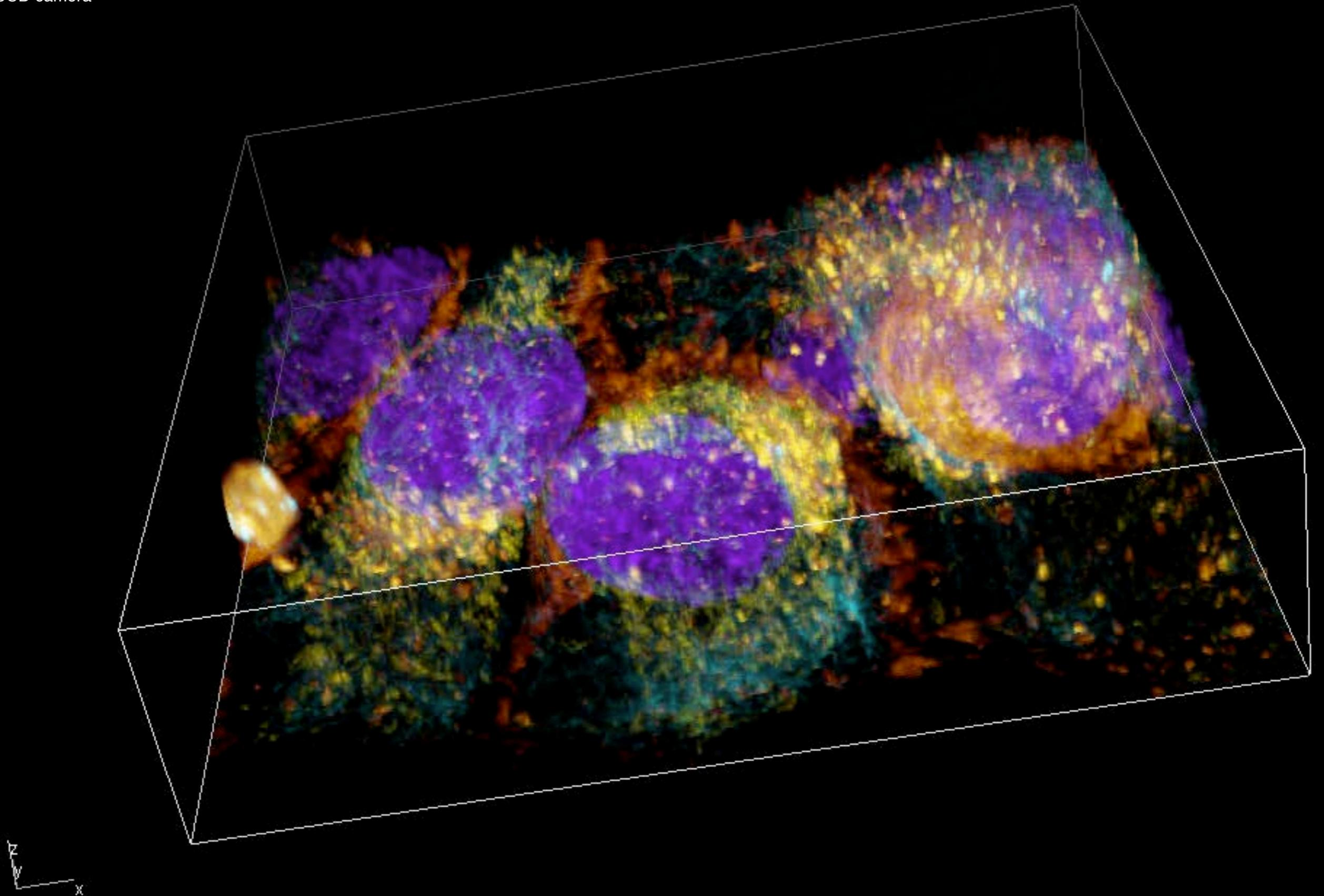
Optical Microscopy Framework



- *wide field optical sectioning microscopy
- *confocal laser scanning microscopy
- *two-photon excitation microscopy
- *SHG, Raman, Phase, Polarisation
- *light sheet fluorescence microscopy
- *near-field fluorescence microscopy
- ...
- *optofluidics, origami, lab on a chip microscopy
- *expansion microscopy

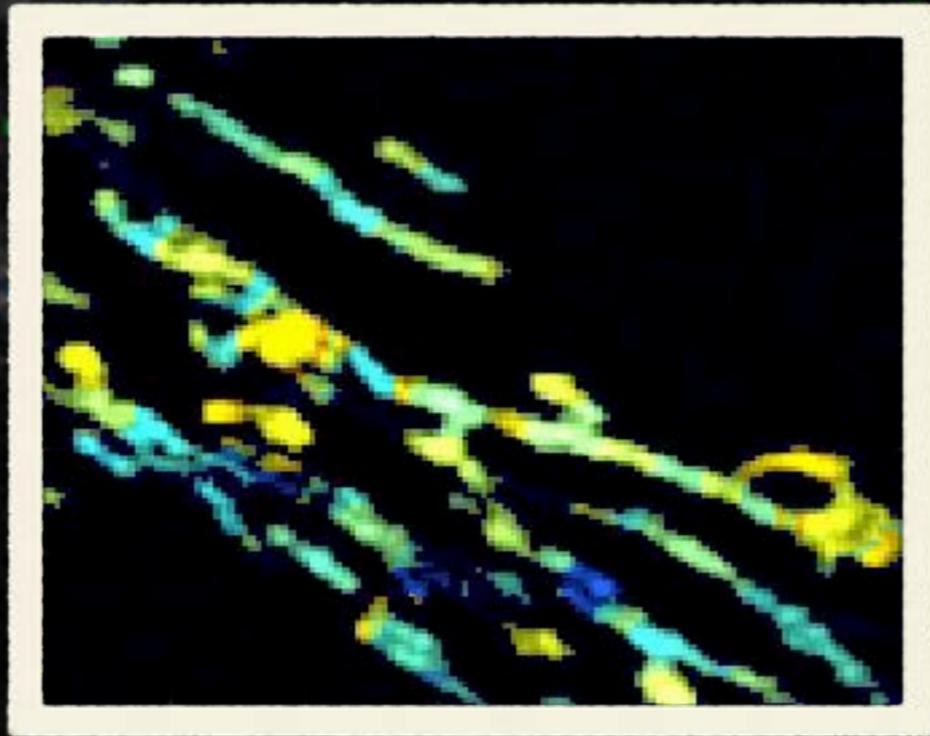
JBC Review 2010 by Lothar Schermelleh, Rainer Heintzmann and Heinrich Leonhardt

Sample preparation: Luca Pesce
Image Acquisition: Lorenzo Scipioni
Microscope: Nikon Ti Eclipse
Spinning Disk, equipped with Andor
iXon3 EMCCD camera



Width: 71.80 μm Height: 71.80 μm Depth: 17.00 μm

3D 4-colors confocal microscopy images of live HeLa cells. Cell staining shows DNA (Hoechst 33342 - Magenta), tubulin (Tubulin Tracker - Cyan), mitochondria (Mitotracker Orange - Yellow) and plasma membrane (Cell Mask - Red). image size is 512x512, pixels size is 140 nm/pixel.



3D

Optical Sectioning
Confocal
Light Sheet
Liquid Lens
2PE

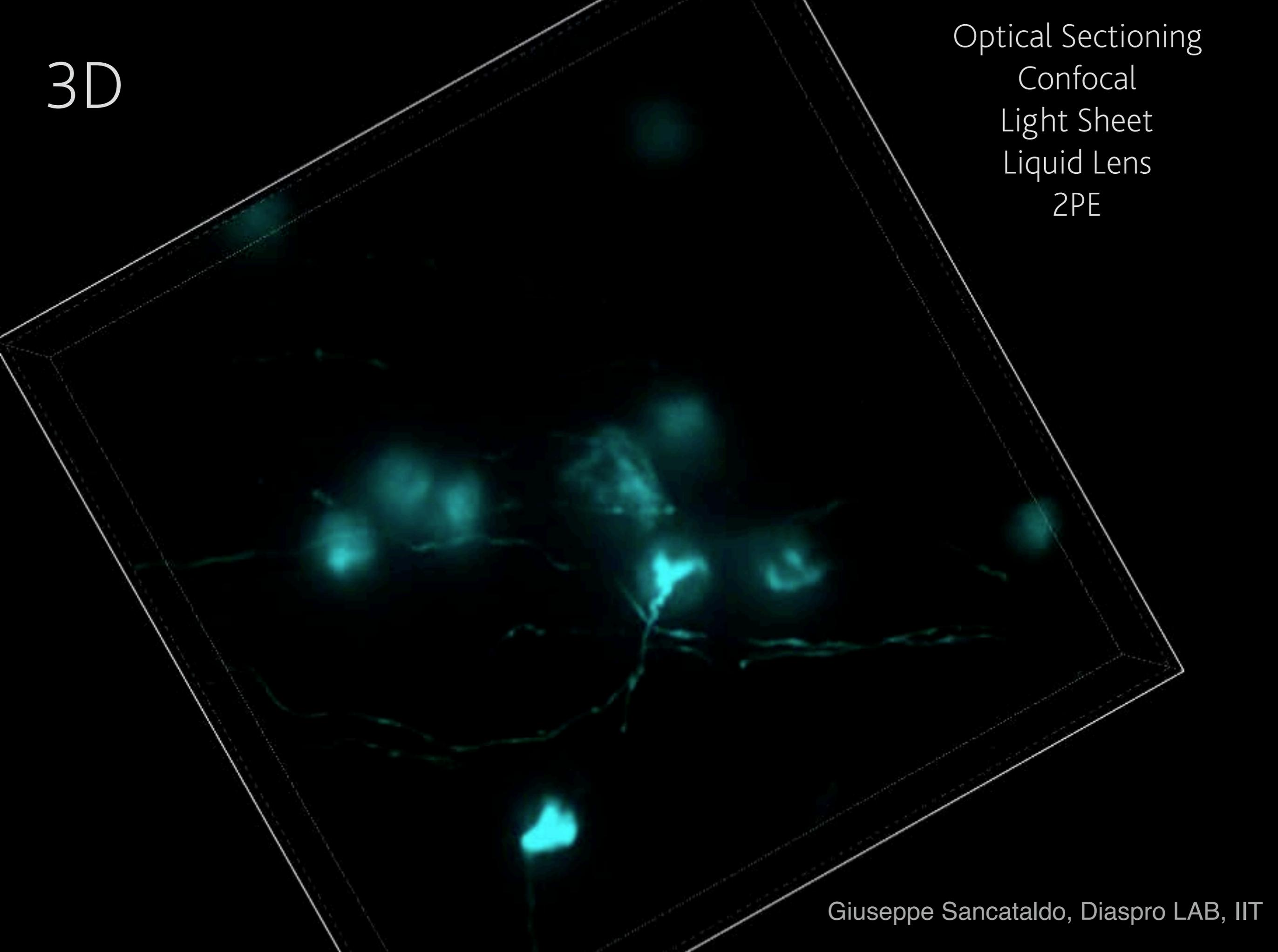
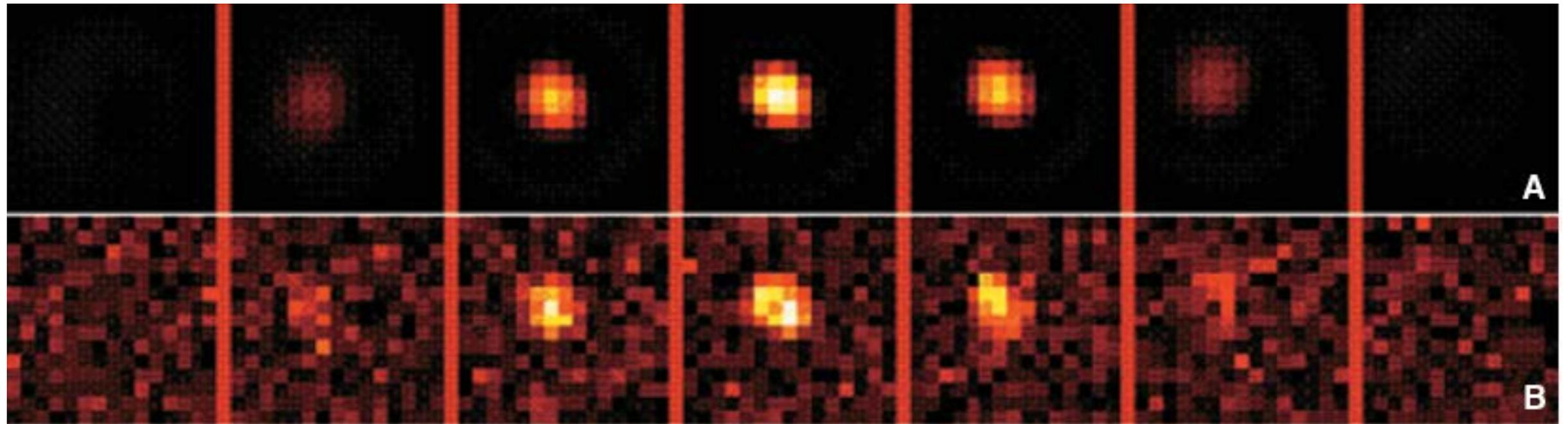
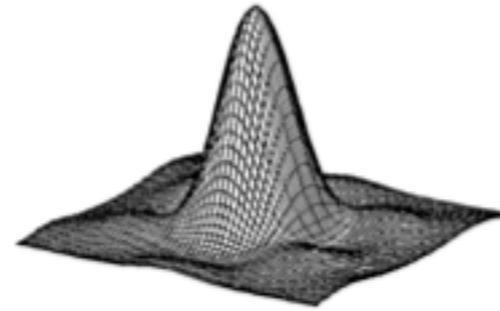


Image formation process

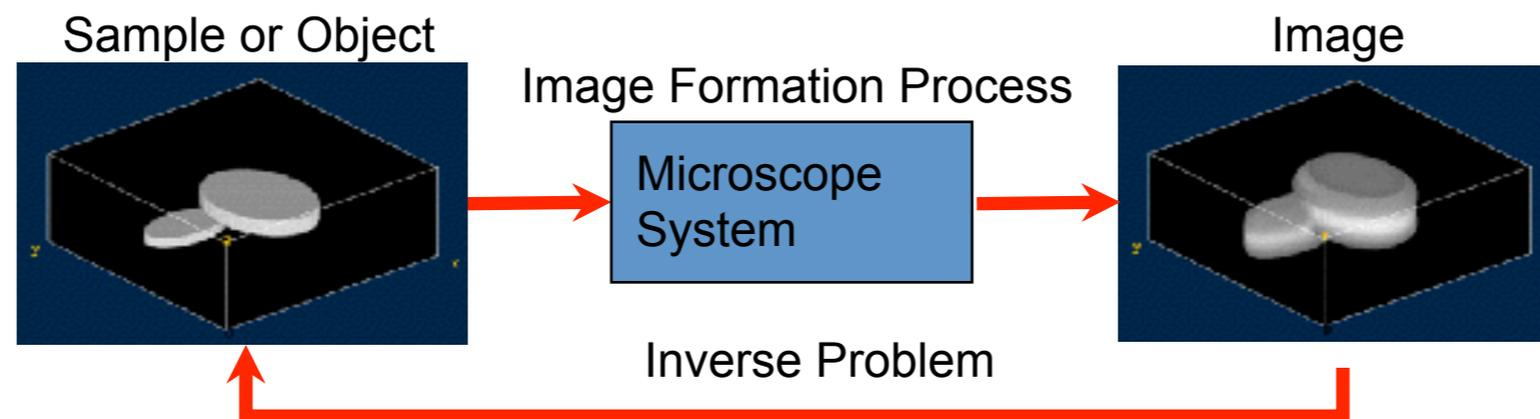
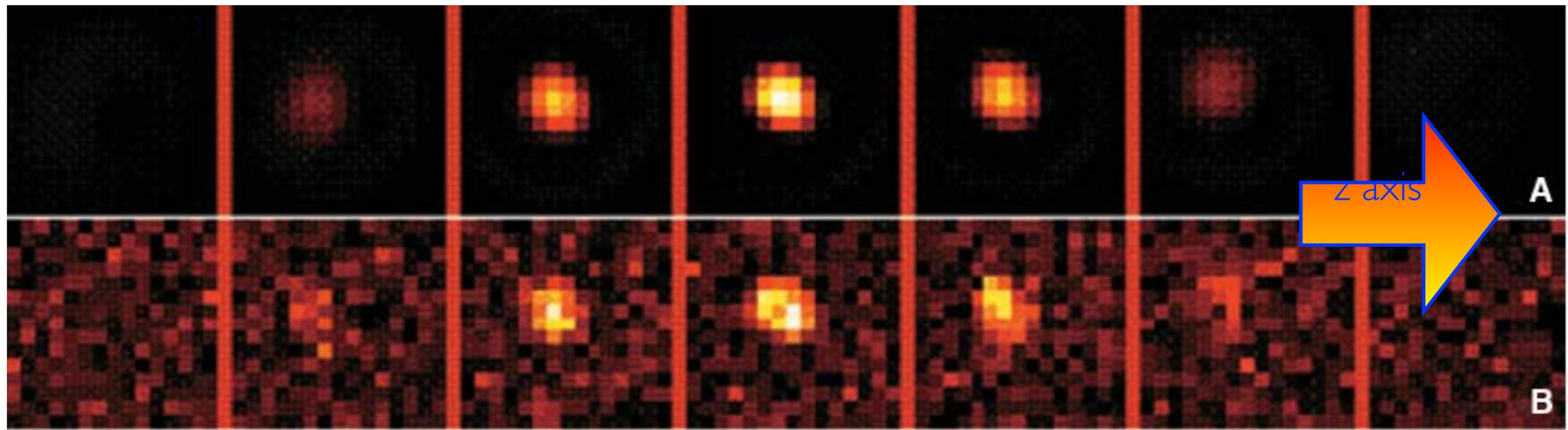
Linear and space invariant system fully described by its PSF (point spread function)



$z=0$

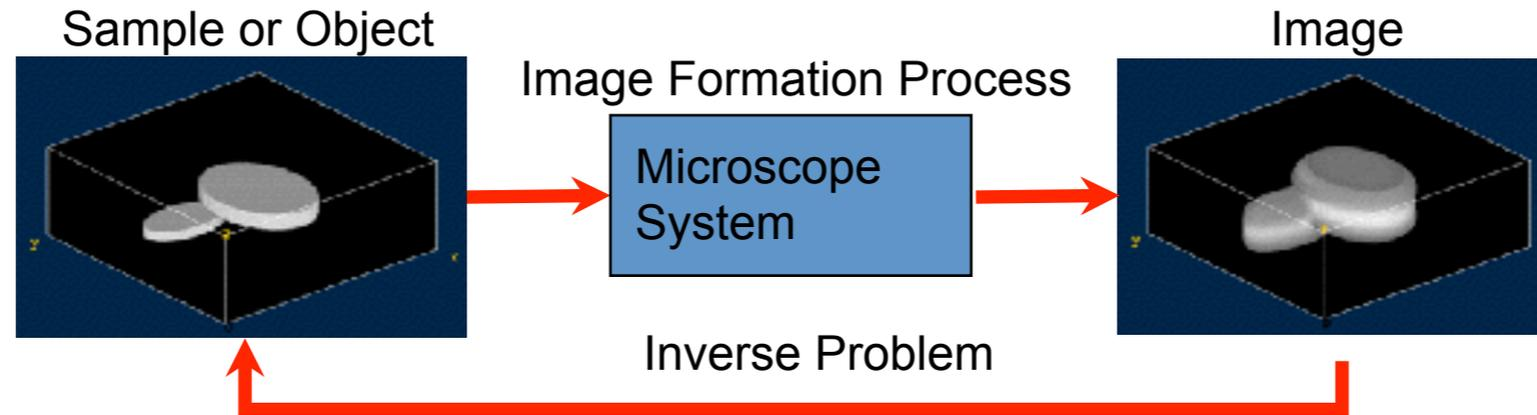
Slide credit: Handbook of Confocal Microscopy (J.Pawley ed.), Plenum, NEW edition, 2006

Linear and space invariant system fully described by its PSF (point spread function)

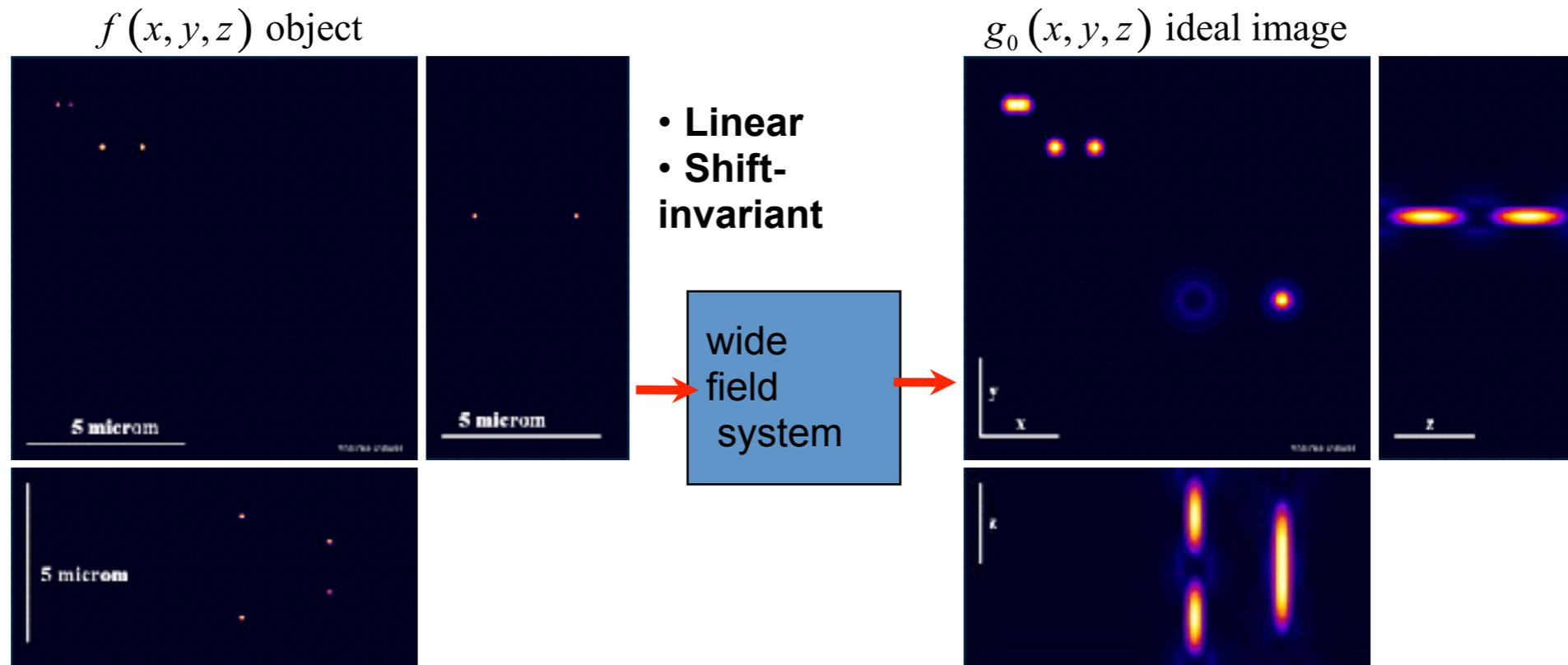


Slide credits: Giuseppe Vicidomini, Jim Pawley

Image formation process



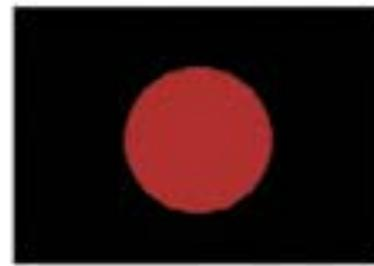
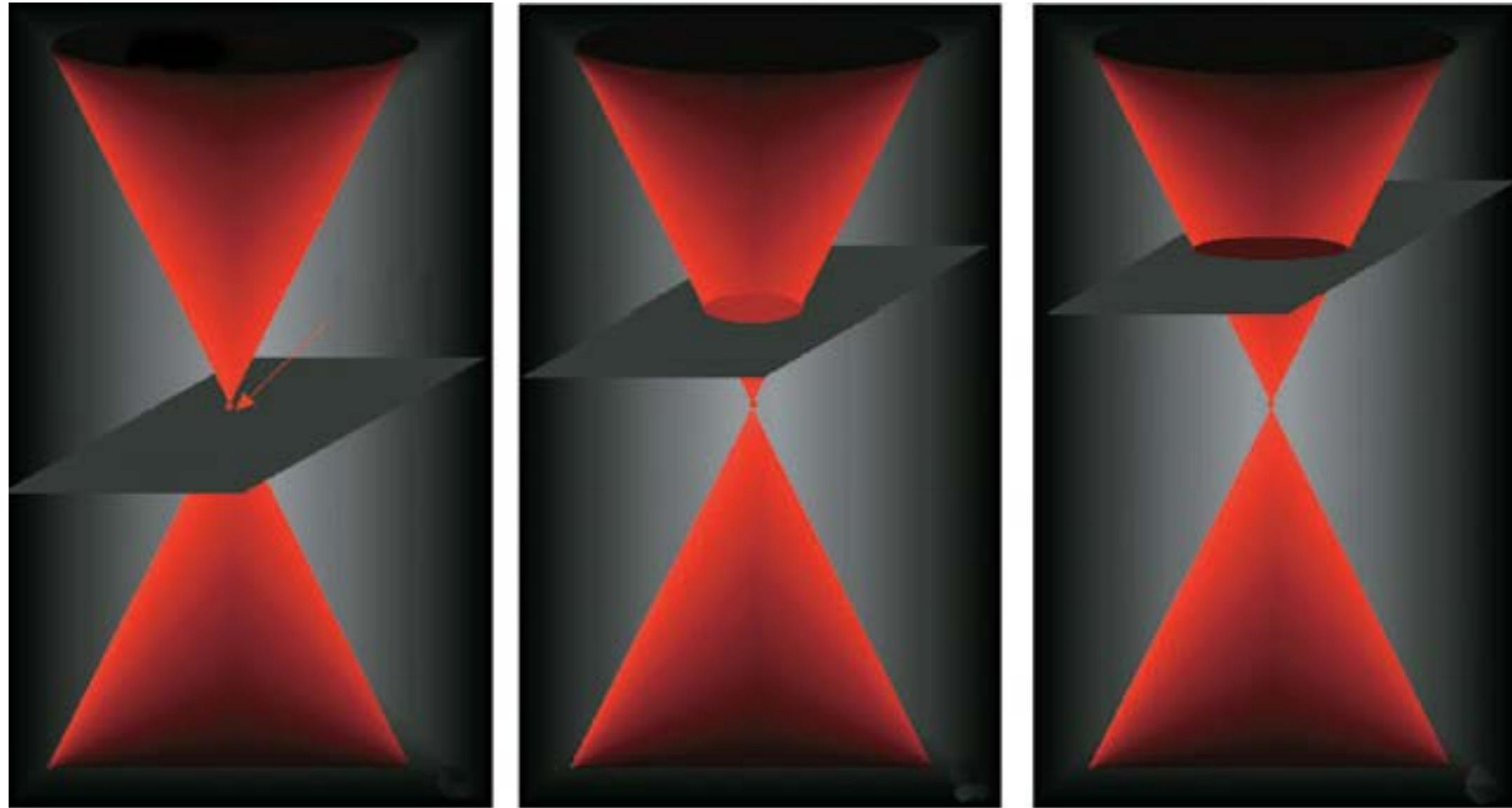
$$g_0(x, y, z) = f(x, y, z) *_{3D} PSF(x, y, z) = \int_{-\infty}^{+\infty} \int_{-\infty}^{+\infty} \int_{-\infty}^{+\infty} f(x-\xi, y-\eta, z-\zeta) PSF(\xi, \eta, \zeta) d\xi d\eta d\zeta$$



Process image formation simulation of a wide-field microscopy.
Simulation parameters: objective 100x NA 1.3 oil, $n=1.518$, λ_{ex} 488nm, λ_{em} 520nm.



Image formation process



Alberto Diaspro, Nanoscopy, Istituto Italiano di Tecnologia

Image formation process

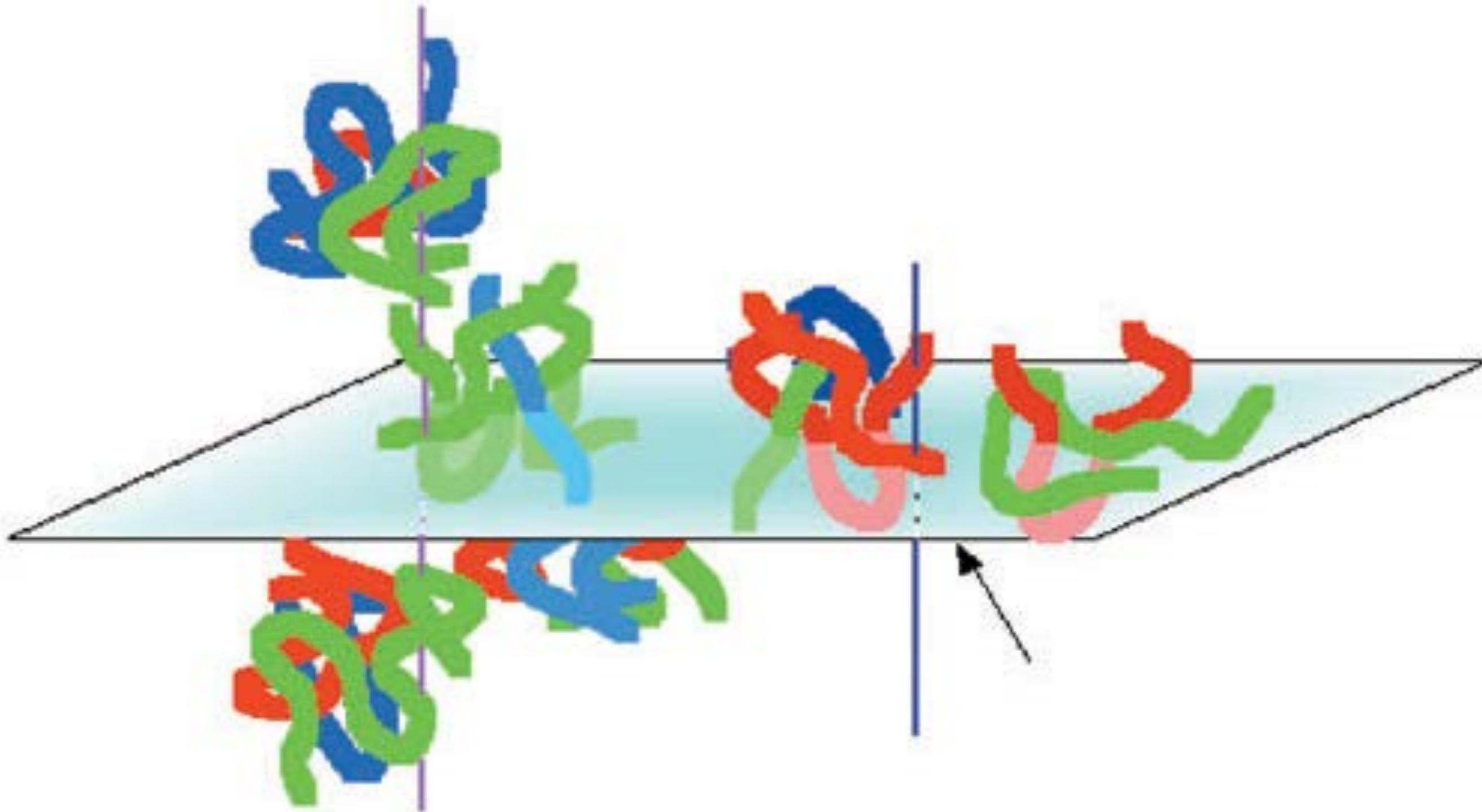
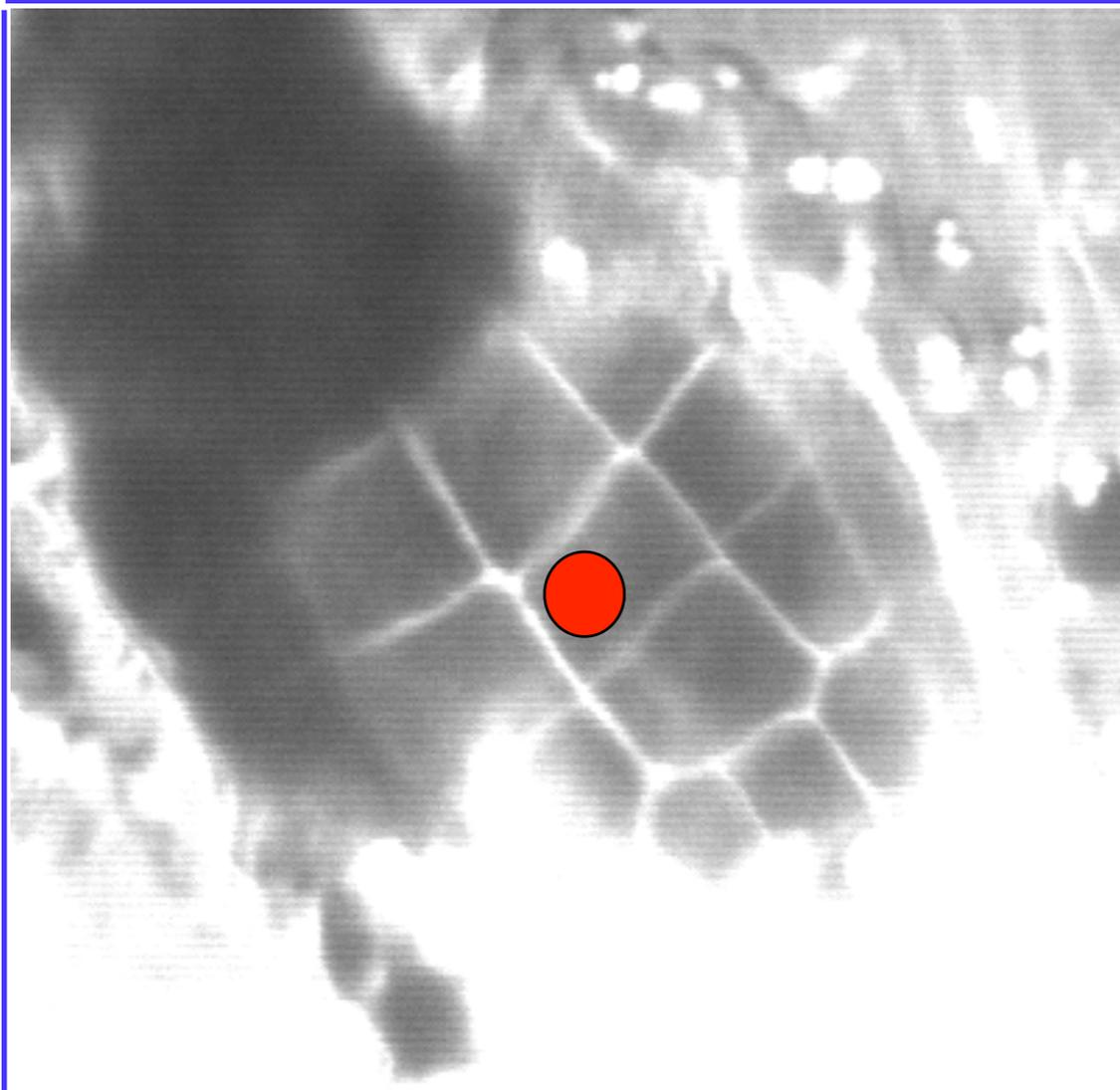
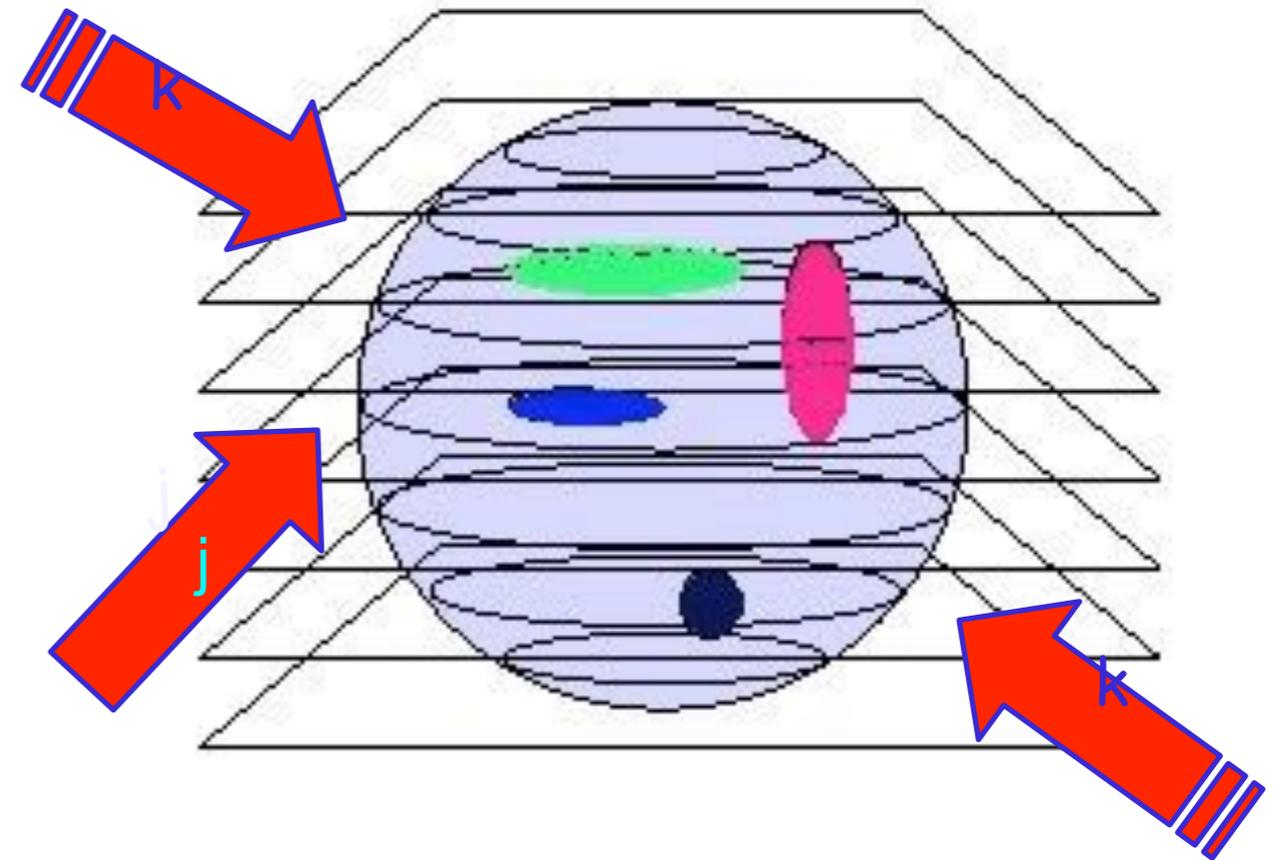


Image formation process



NAVIGATING INTO CELLS AND TISSUES

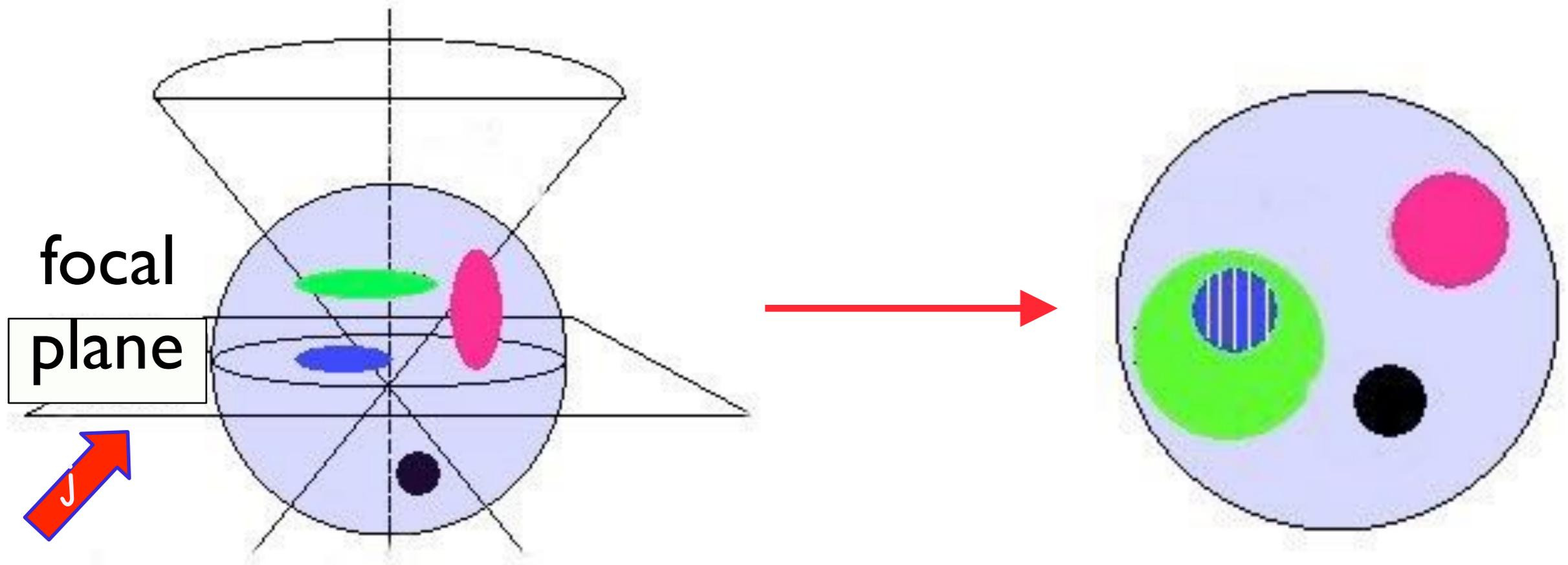


B. Bianco, A. Diaspro, Cell Biophysics, 15 (3), pp.189-200, 1989.

A. Diaspro, et al., Image Vision and Computing, 8 (2), pp.130-141, 1990.

Image formation process

OPTICAL SECTIONING RESULT



B. Bianco, A. Diaspro, Cell Biophysics, 15 (3), pp.189-200, 1989.

A. Diaspro, et al., Image Vision and Computing, 8 (2), pp.130-141, 1990.

Image formation process

OPTICAL SECTIONING

Within the optical sectioning scheme the situation is that the observed image O at a plane j is produced by the true fluorescence distribution at plane j , distorted by the microscope through S , plus contributions from adjacent k planes and noise N .

$$O_j = I_j S_j + \sum_{k \neq j} I_k S_k + N$$

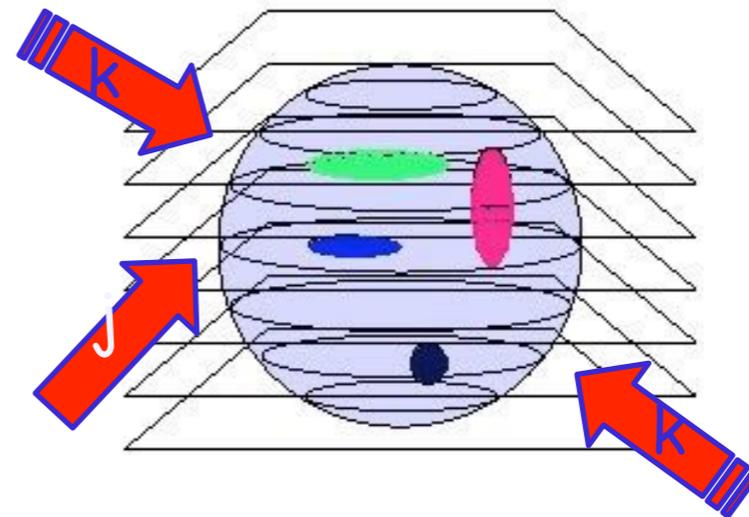
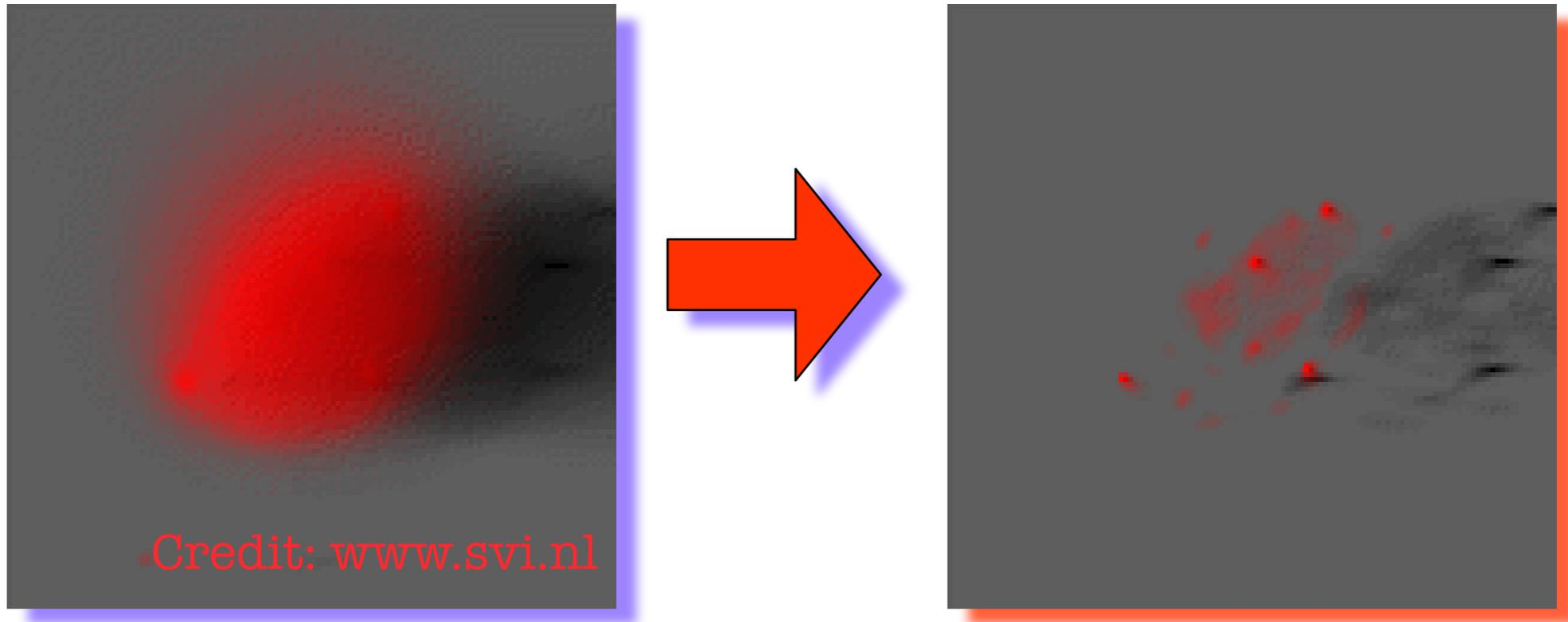


Image formation process

Solving the equation set...

$$O_j = I_j S_j + \sum_{k \neq j} I_k S_k + N$$



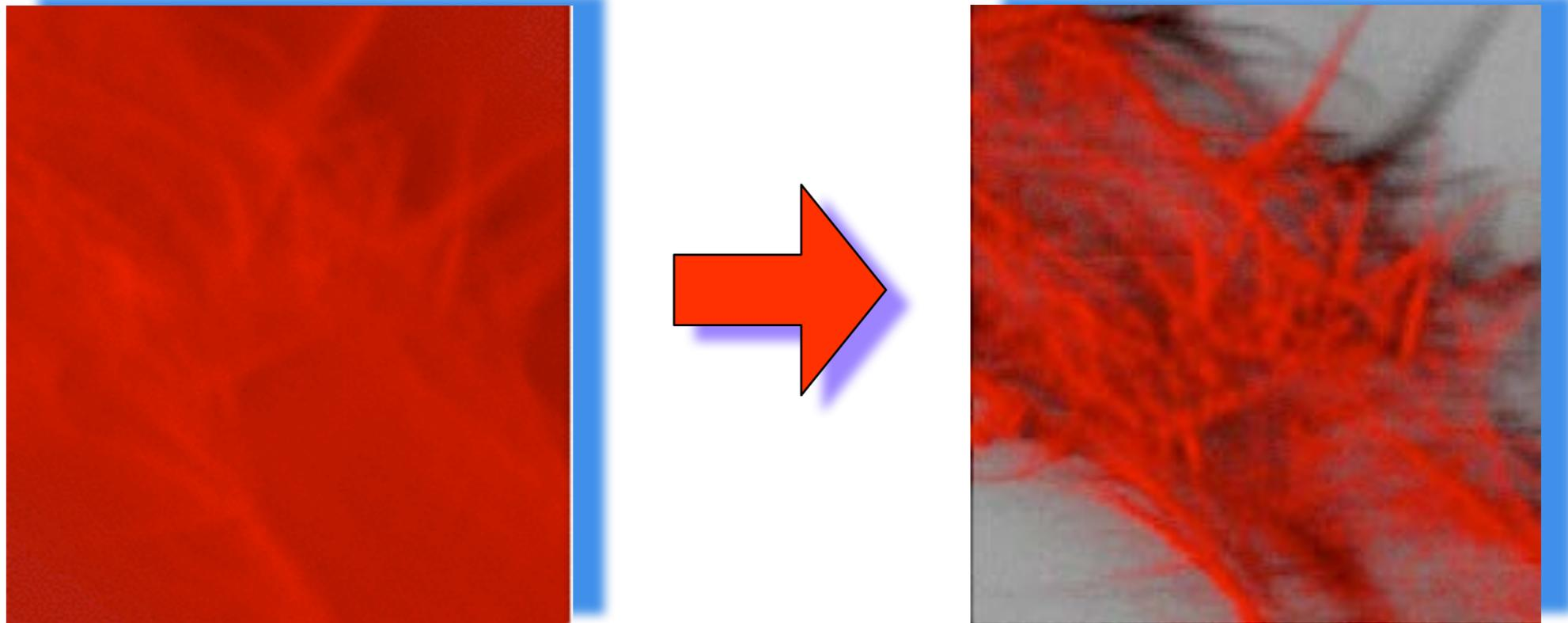
$$h(x, y, z) * f(x, y, z) + n(x, y, z) + b(x, y, z) = g(x, y, z)$$

www.powermicroscope.com

Image formation process

Solving the equation set...

$$O_j = I_j S_j + \sum_{k \neq j} I_k S_k + N$$



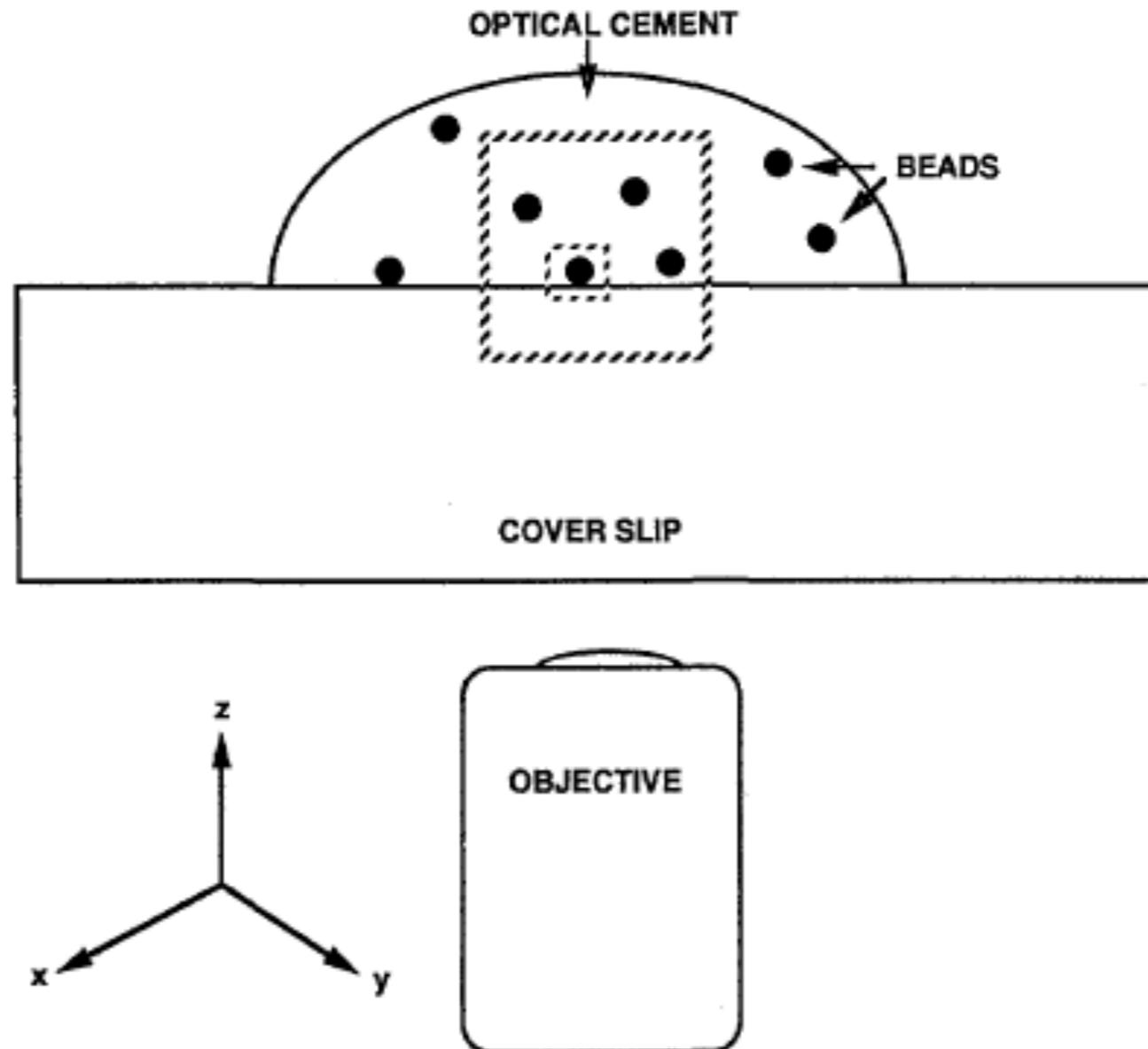
BONETTO P., BOCCACCI P., SCARITO M., DAVOLIO M., EPIFANI M., VICIDOMINI G., TACCHETTI C., RAMOINO P., USAI C., DIASPRO A.
(2004) MICROSCOPY RESEARCH AND TECHNIQUE. vol. 64, pp. 196-203.

www.powermicroscope.com

OPTICAL RESOLUTION

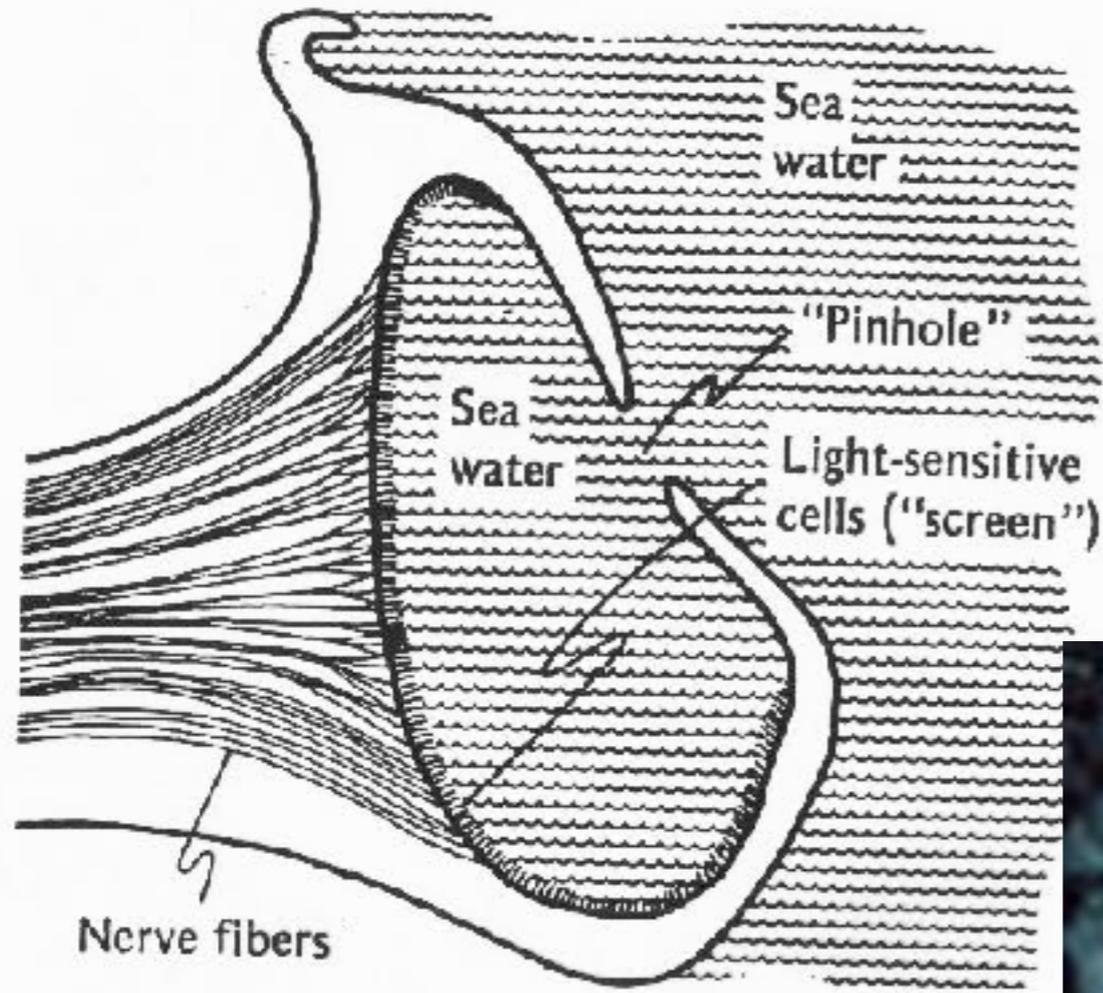
Artifacts in computational optical-sectioning microscopy

James G. McNally, Chrysanthe Preza, José-Angel Conchello, and Lewis J. Thomas, Jr.

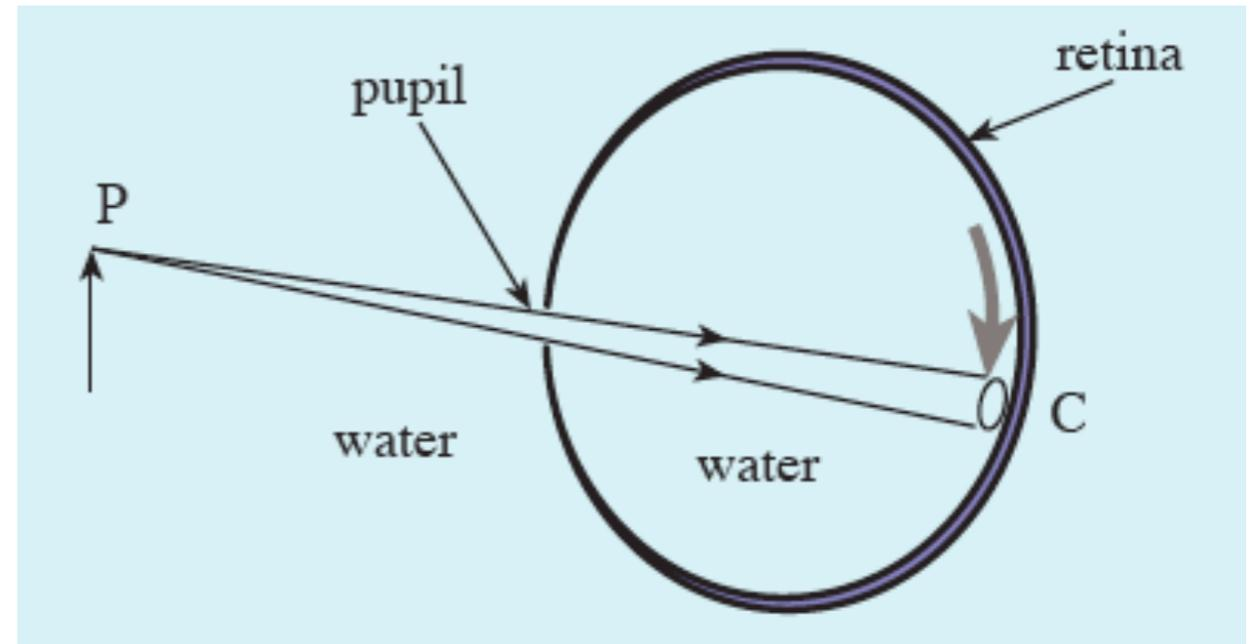


Alberto Diaspro, Nanoscopy, Istituto Italiano di Tecnologia

Image formation process



Nautilus



Giuseppe Colicchia 2006 *Phys. Educ.* **41** 15-17

Slide credit idea: Paolo Sapuppo, Leica Microsystems

Image formation process

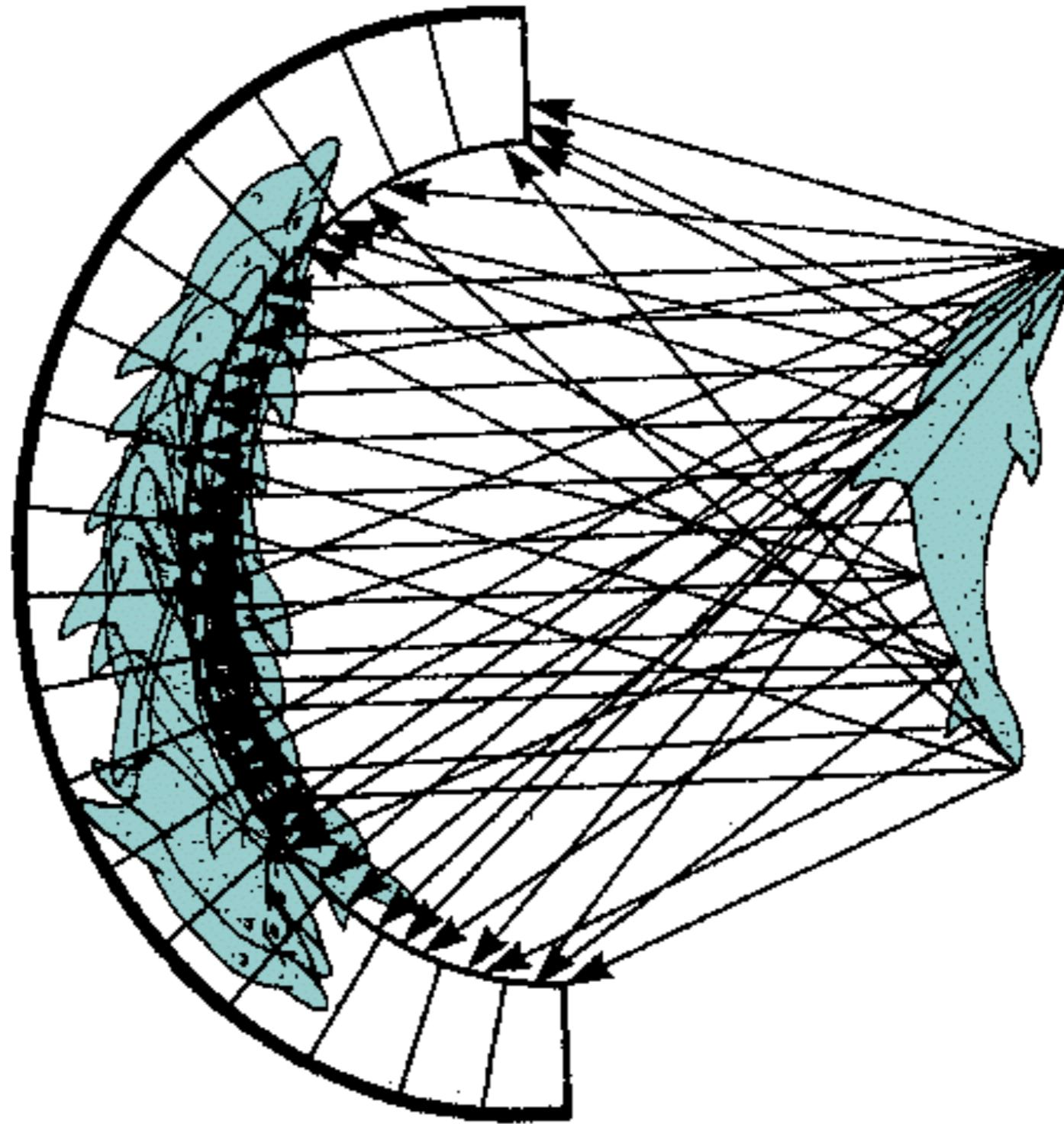


Image formation process

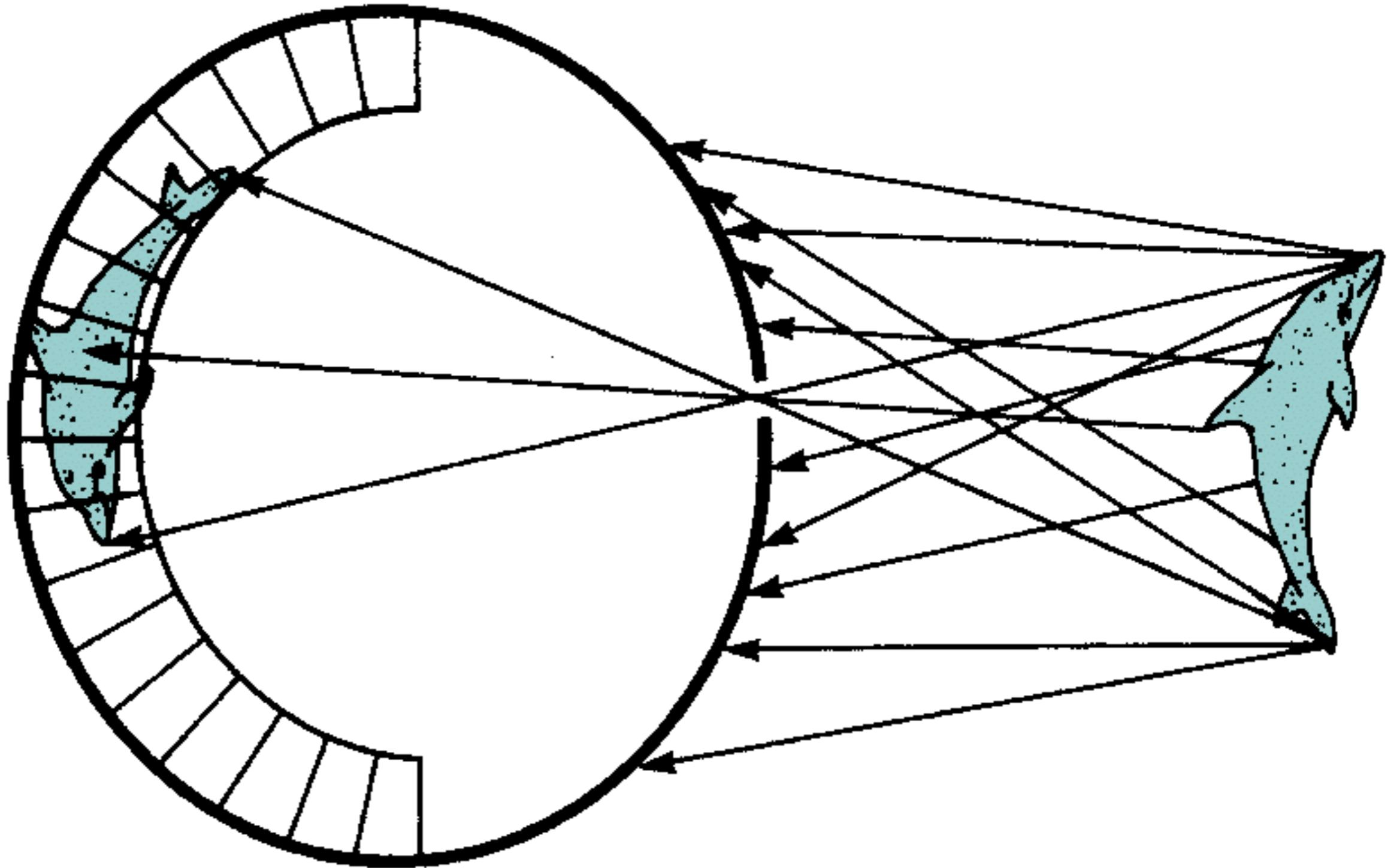


Image formation process



Anacapri- La Grotta Azzurra

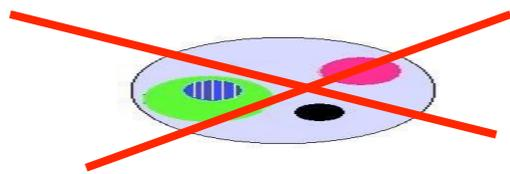
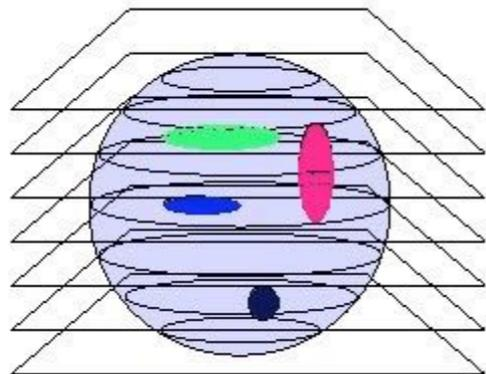
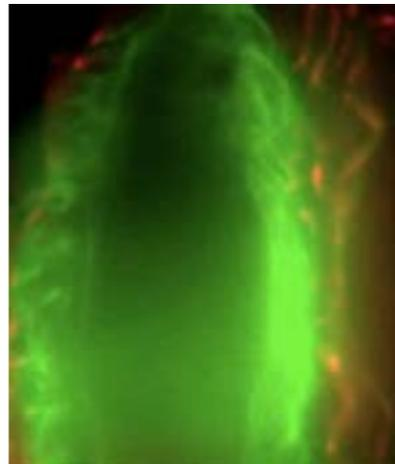
confocal laser scanning microscopy

Solving the equation set...by means of a confocal set-up

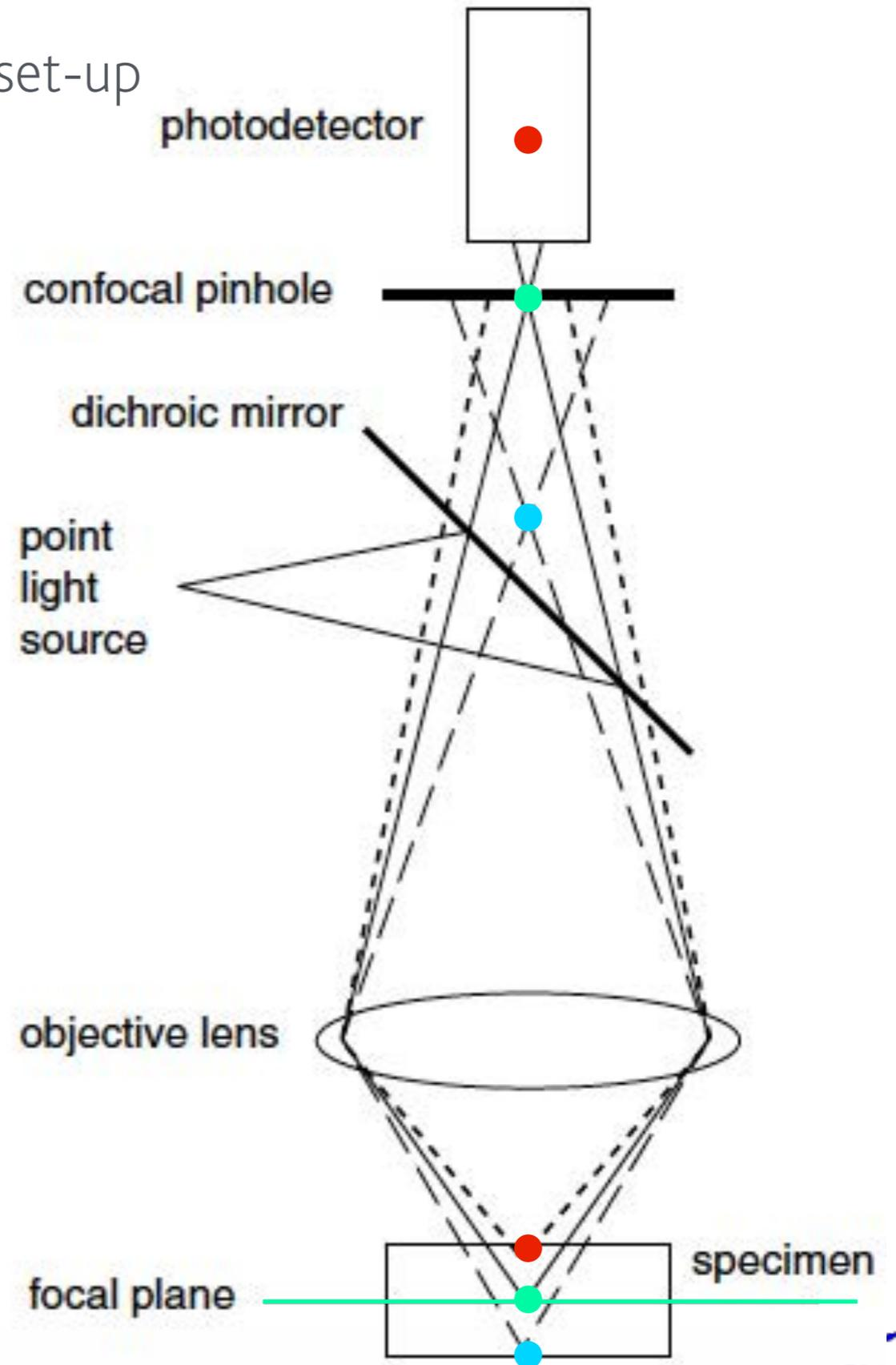
$$\sum I_k S_k \quad \rightarrow \quad 0$$

$$S_j \quad \rightarrow \quad 1$$

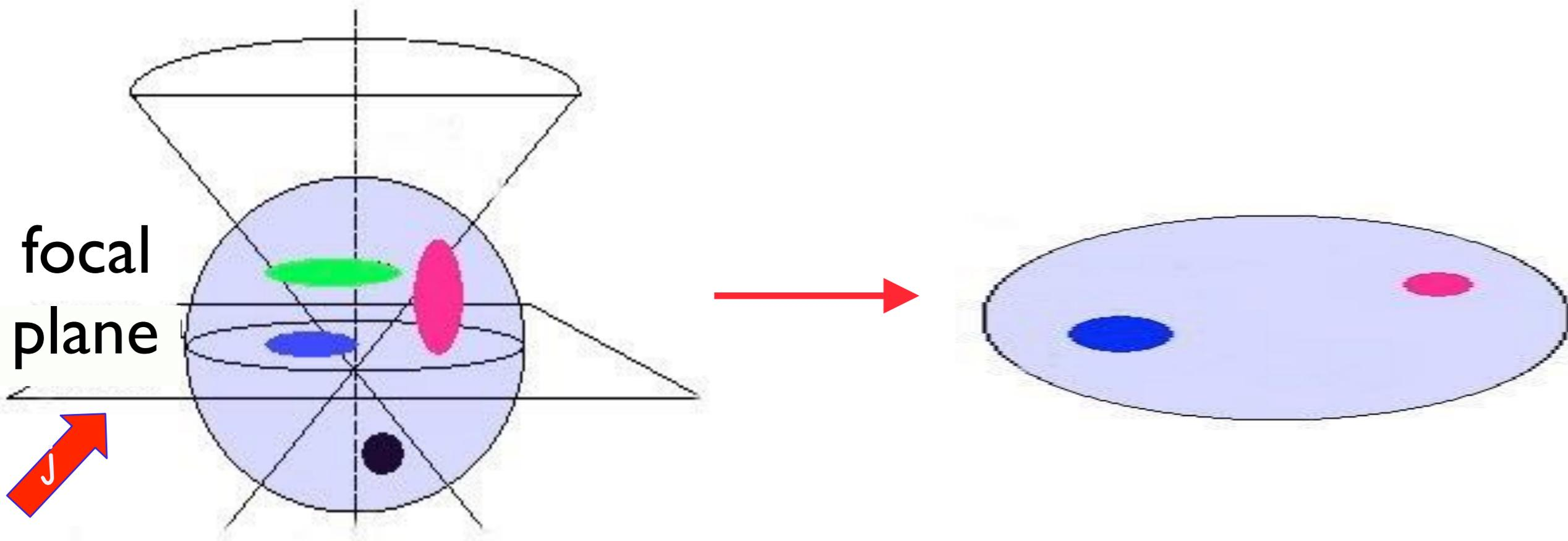
$$O_j \quad \rightarrow \quad I_j$$



~~$$O_j = I_j S_j + \sum_{k \neq j} I_k S_k + N$$~~

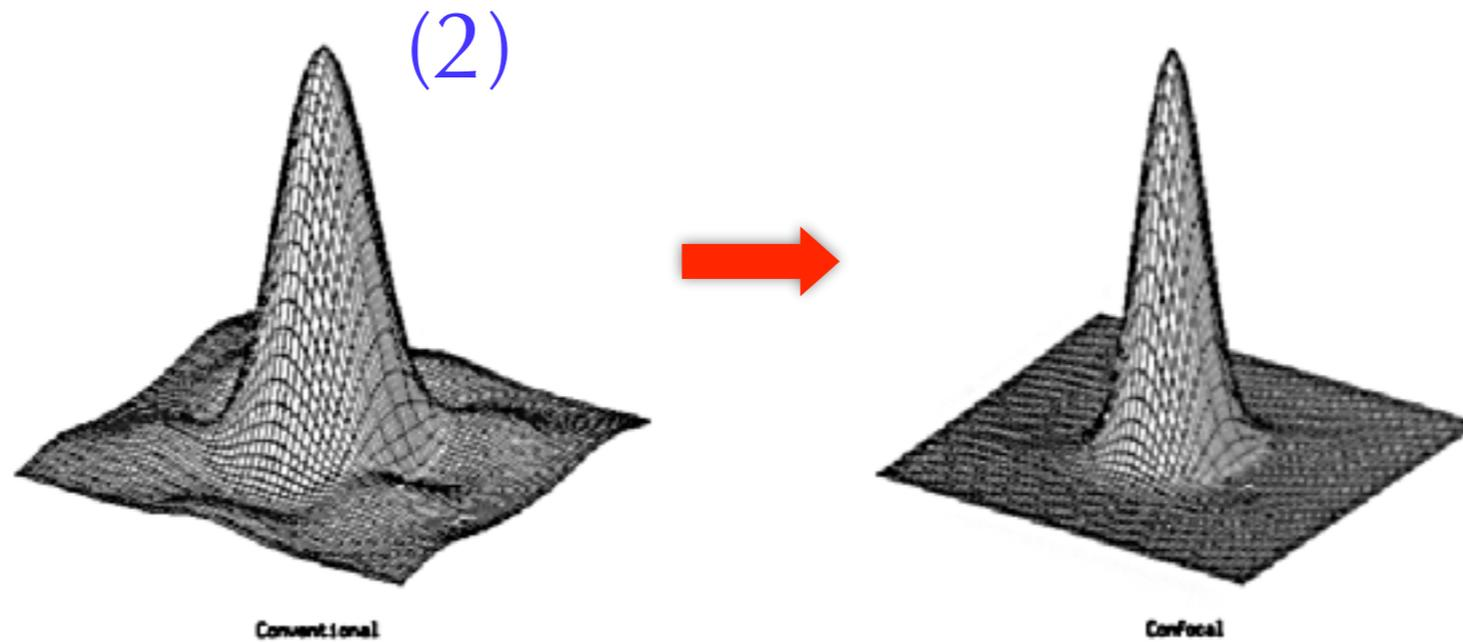


Modified from D. Shotton, 1993 and C.L. Smith, 2011

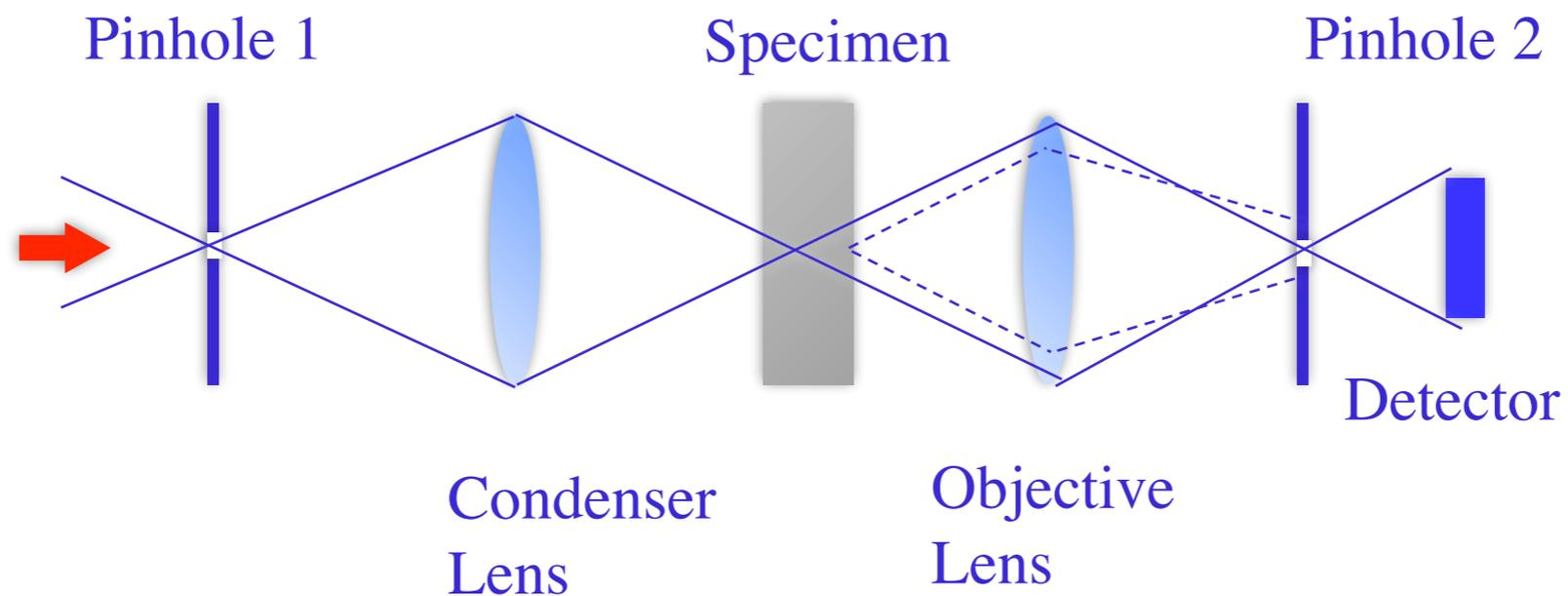


Slide credit: Giuseppe Vicidomini, LAMBS-MicroScoBio, Genova

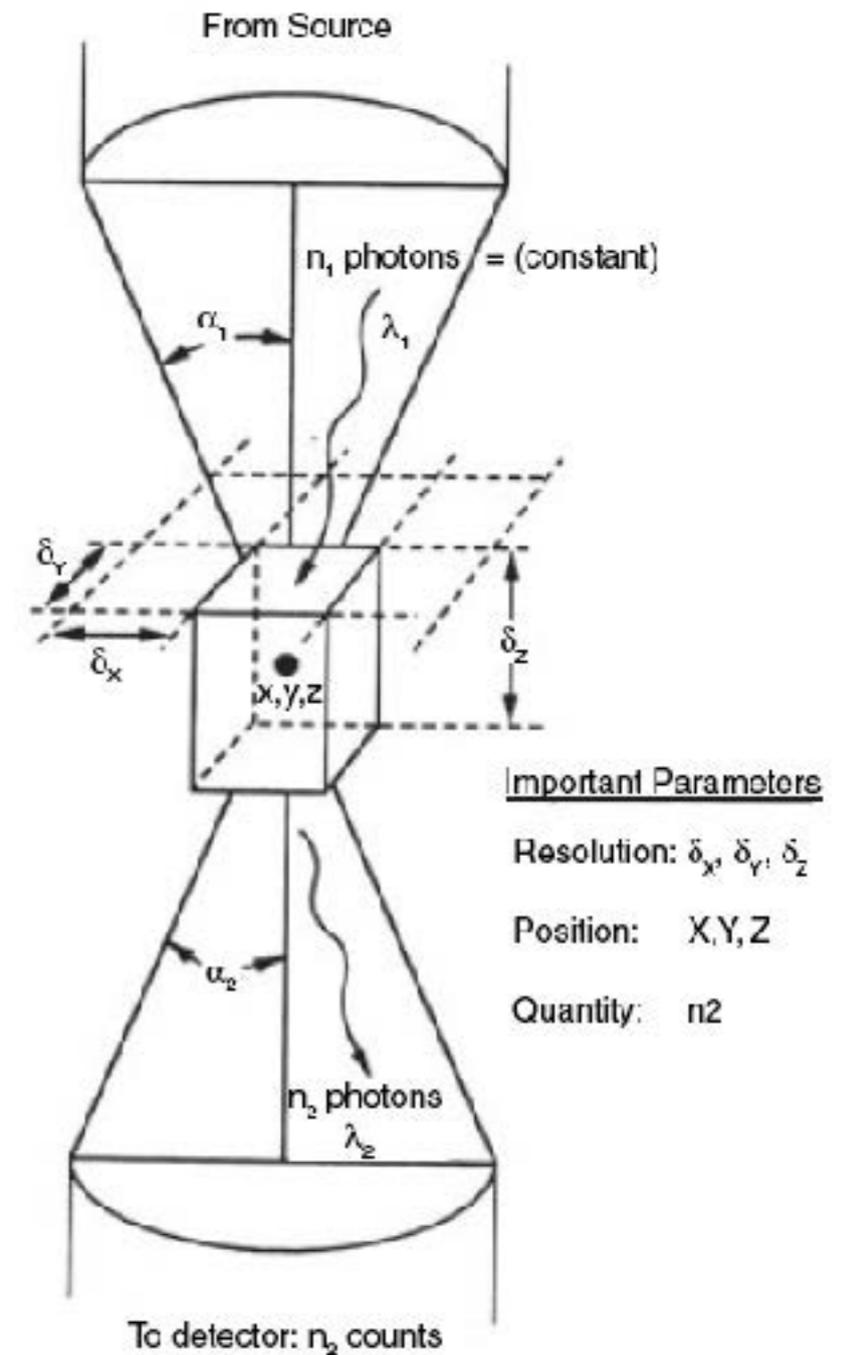
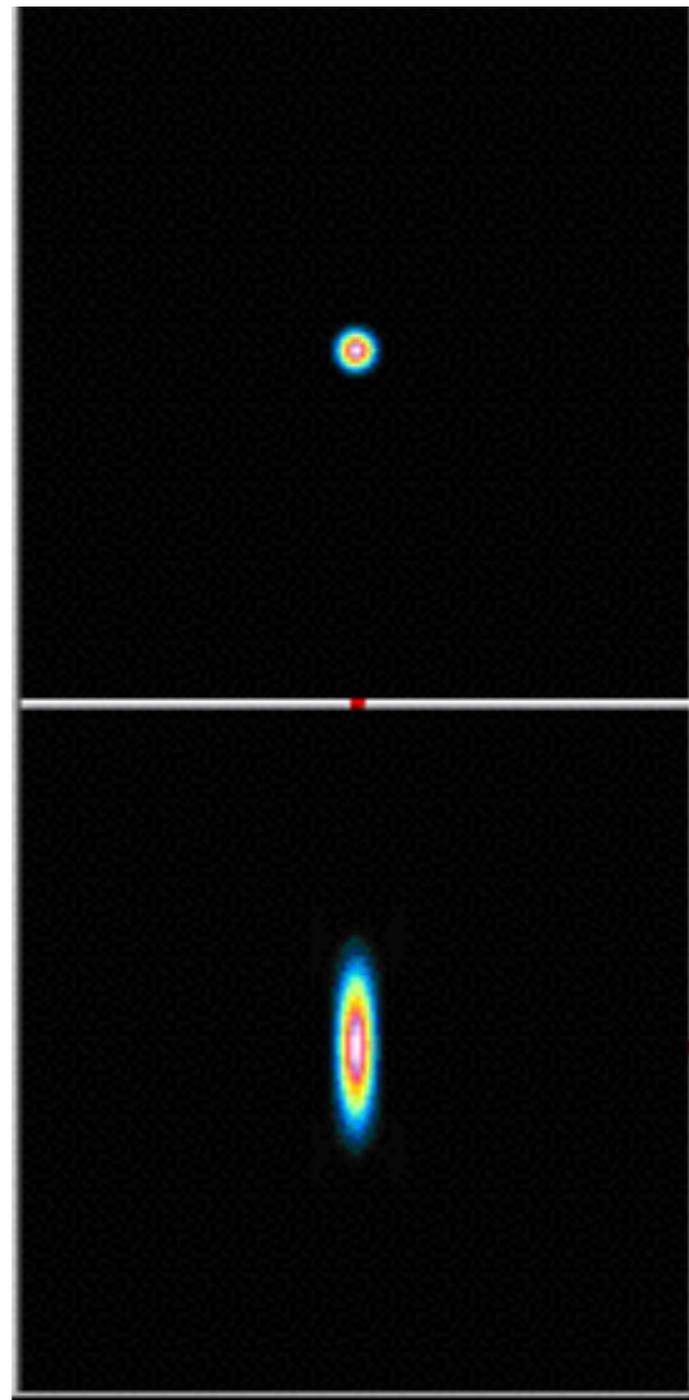
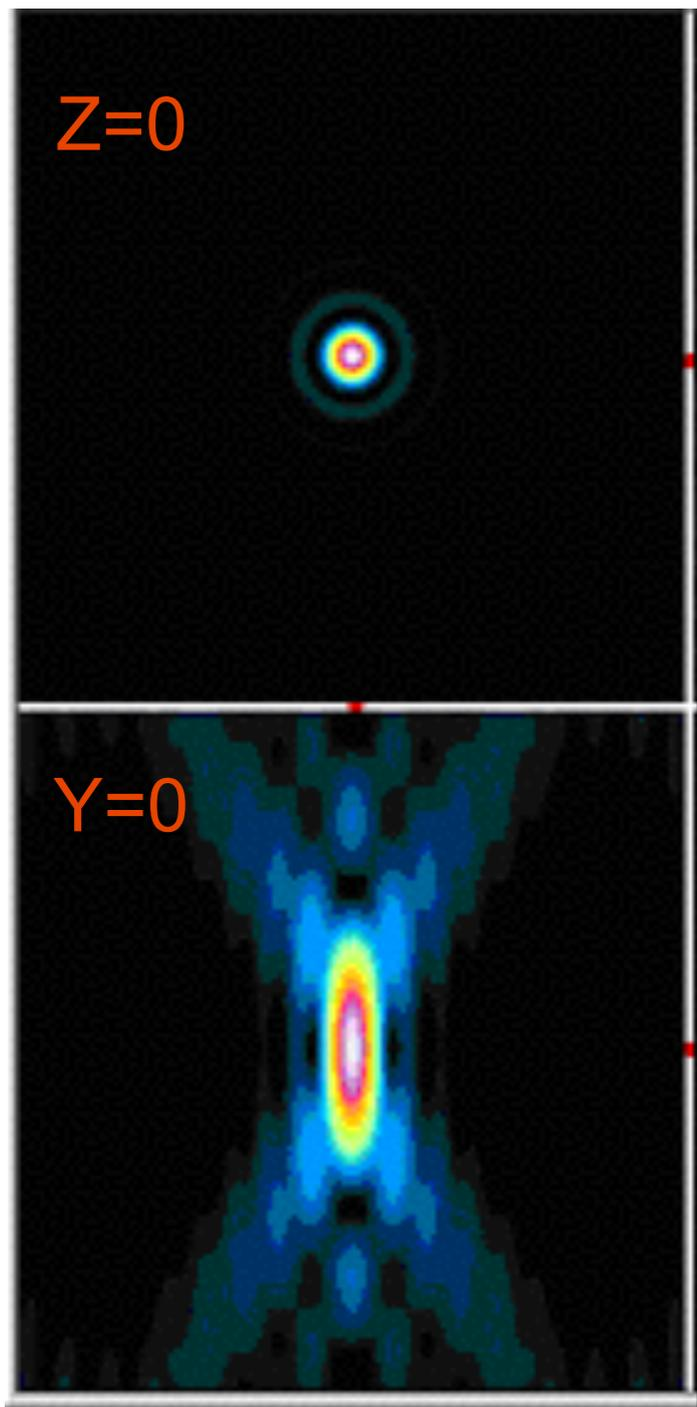
confocal laser scanning microscopy



$$I_{fluor-conf} = I_{det} I_{ill} \rightarrow I^2 \propto \frac{1}{z^4}$$



confocal laser scanning microscopy



POINTLIKE OBJECT VS. QUASI POINTLIKE IMAGE

confocal laser scanning microscopy



Available online at www.sciencedirect.com

SCIENCE @ DIRECT®

Biology of the Cell 95 (2003) 335–342

Biology
of the Cell

www.elsevier.com/locate/bicell

Scientiae Forum / History of biology of the cell

How the Confocal Laser Scanning Microscope entered Biological Research

W. B. Amos^{a,*}, J.G. White^b

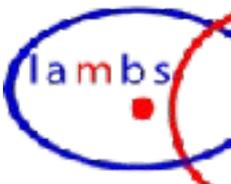
^a *MRC Laboratory of Molecular Biology, Cambridge, UK*

^b *Laboratory of Molecular Biology, University of Wisconsin, Madison, USA*

Received 21 May 2003; accepted 27 May 2003



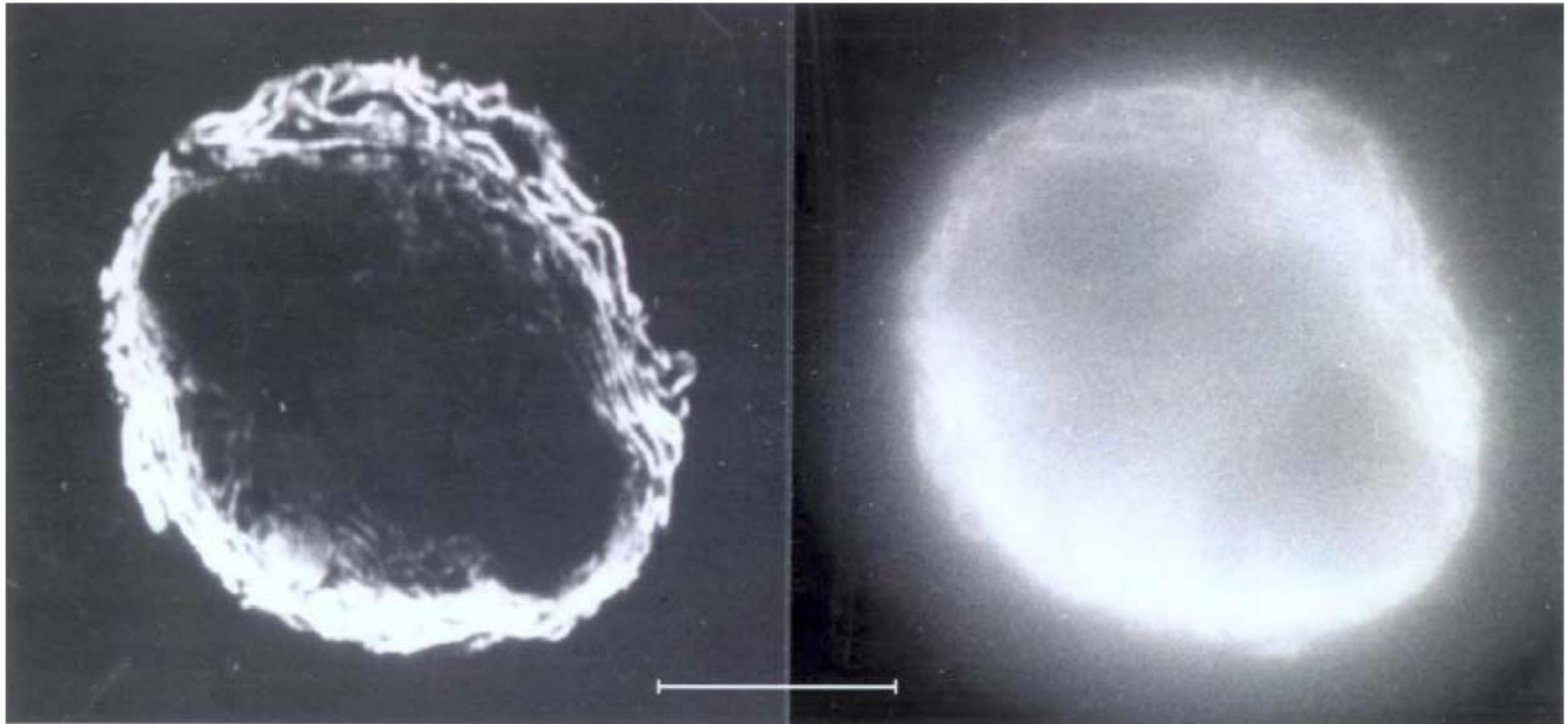
Alberto Diaspro, Nanoscopy, Istituto Italiano di Tecnologia



confocal laser scanning microscopy

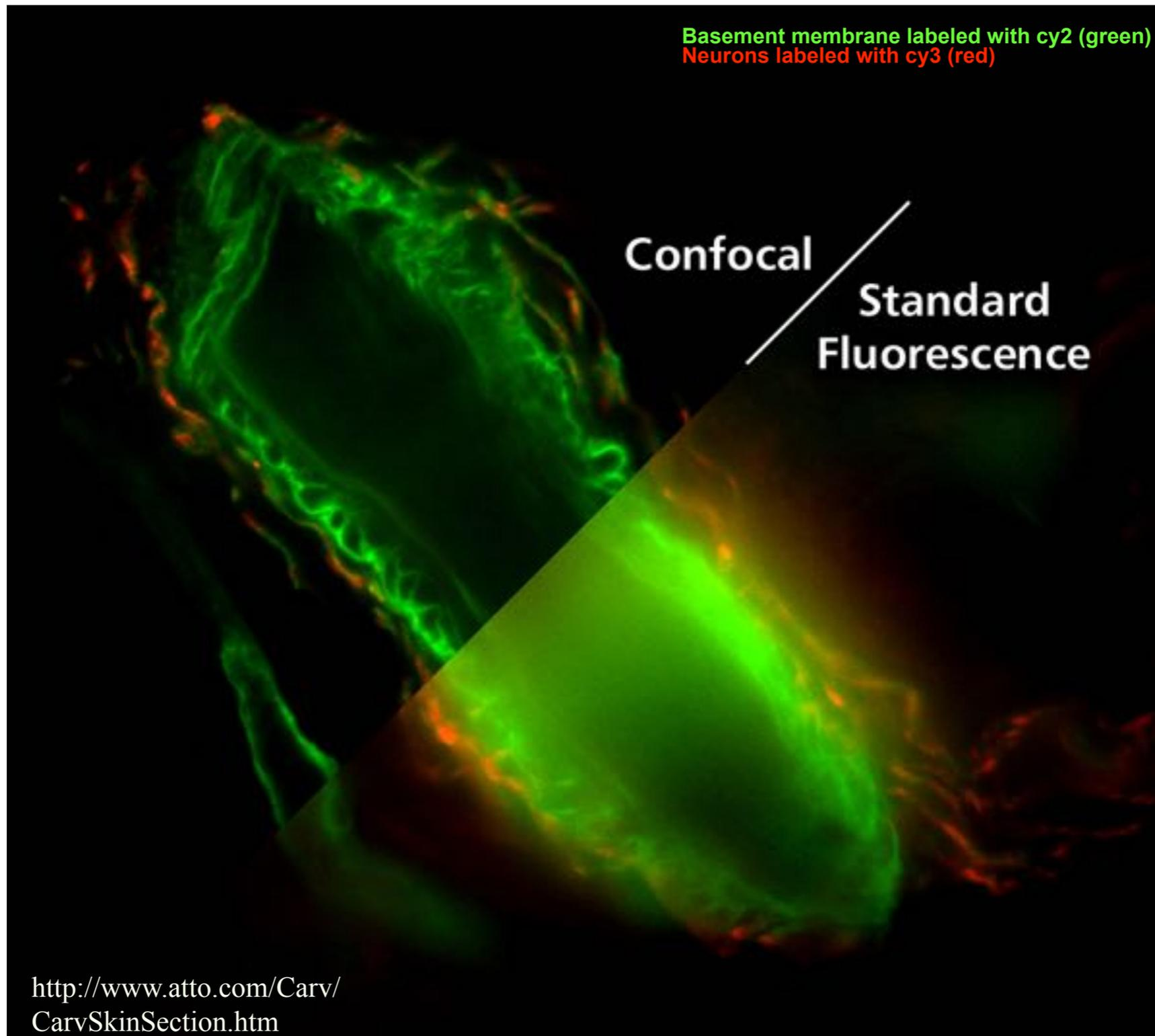
W.B. Amos, J.G. White / *Biology of the Cell* 95 (2003) 335–342

339



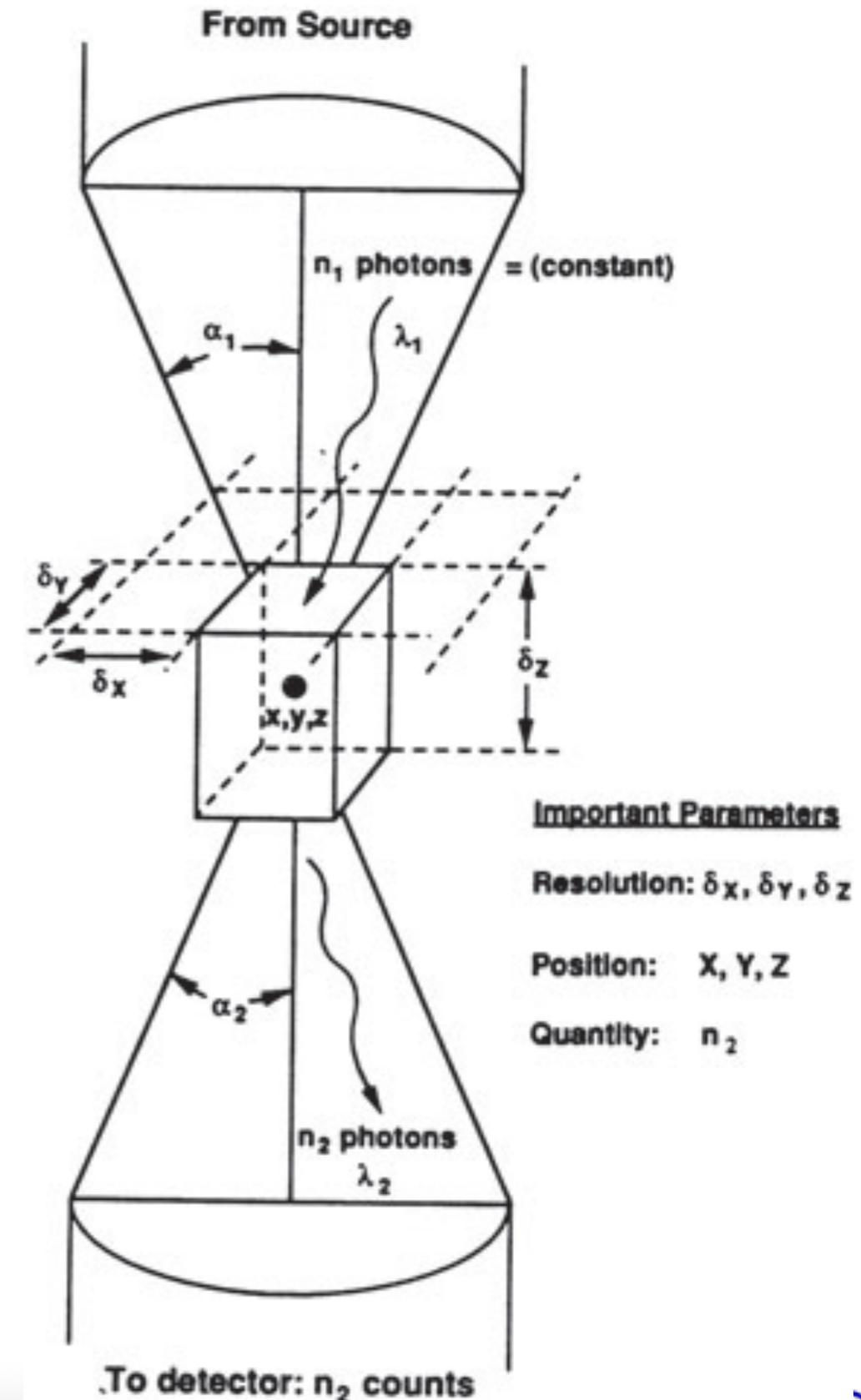
An early comparison of a conventional epi-fluorescence image with a confocal one obtained with the polygon scanner. The specimen is a plasmacytoma labelled with anti-endoplasmic reticulum, which binds chiefly to cisternae of the endoplasmic reticulum. In the conventional image it is not possible to establish whether the central nucleus lacks endoplasmic reticulum and the individual cisternae are unclear. Scale bar = 10 μm . (Specimen prepared by Gordon Koch. Image previously published in the *Journal of Cell Biology*, 105, p44 (1987)).

confocal laser scanning microscopy

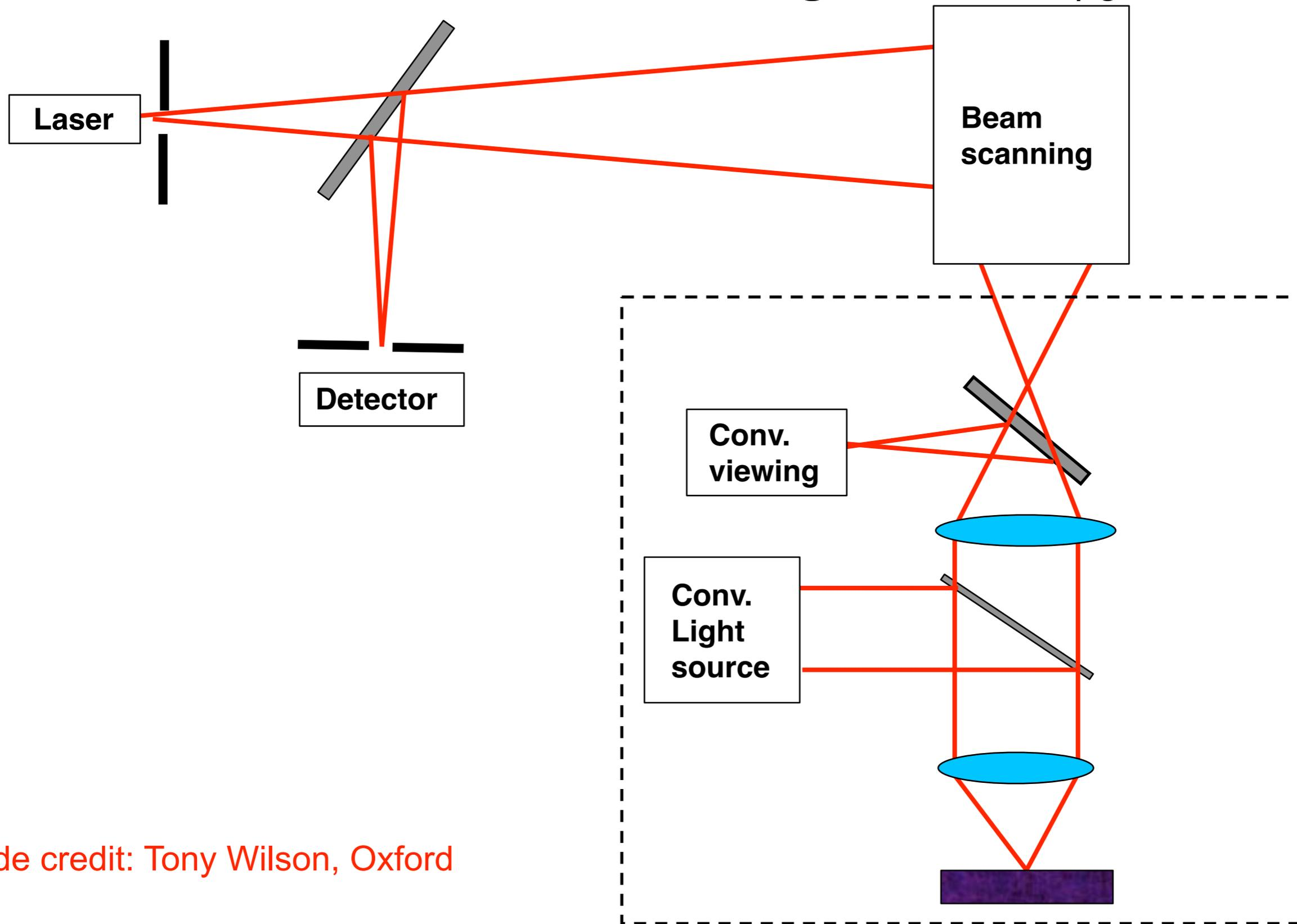


confocal laser scanning microscopy

- Reduced blurring of the image from light scattering
- Increased effective resolution
- Improved signal to noise ratio
- Clear examination of thick specimens
- Z-axis scanning
- Depth perception in Z-sectioned images



confocal laser scanning microscopy



Slide credit: Tony Wilson, Oxford

confocal laser scanning microscopy

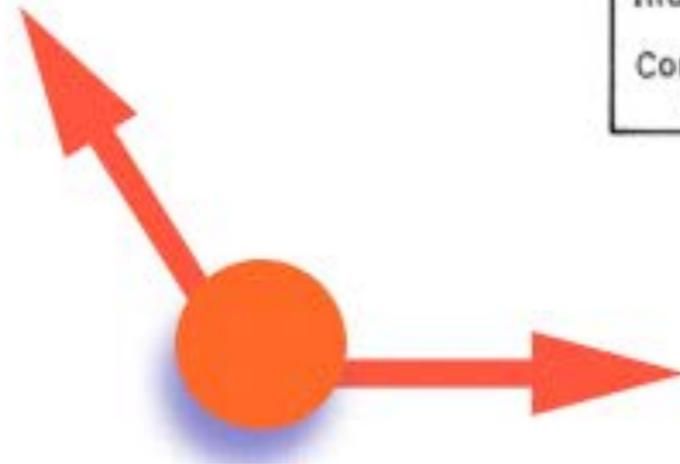
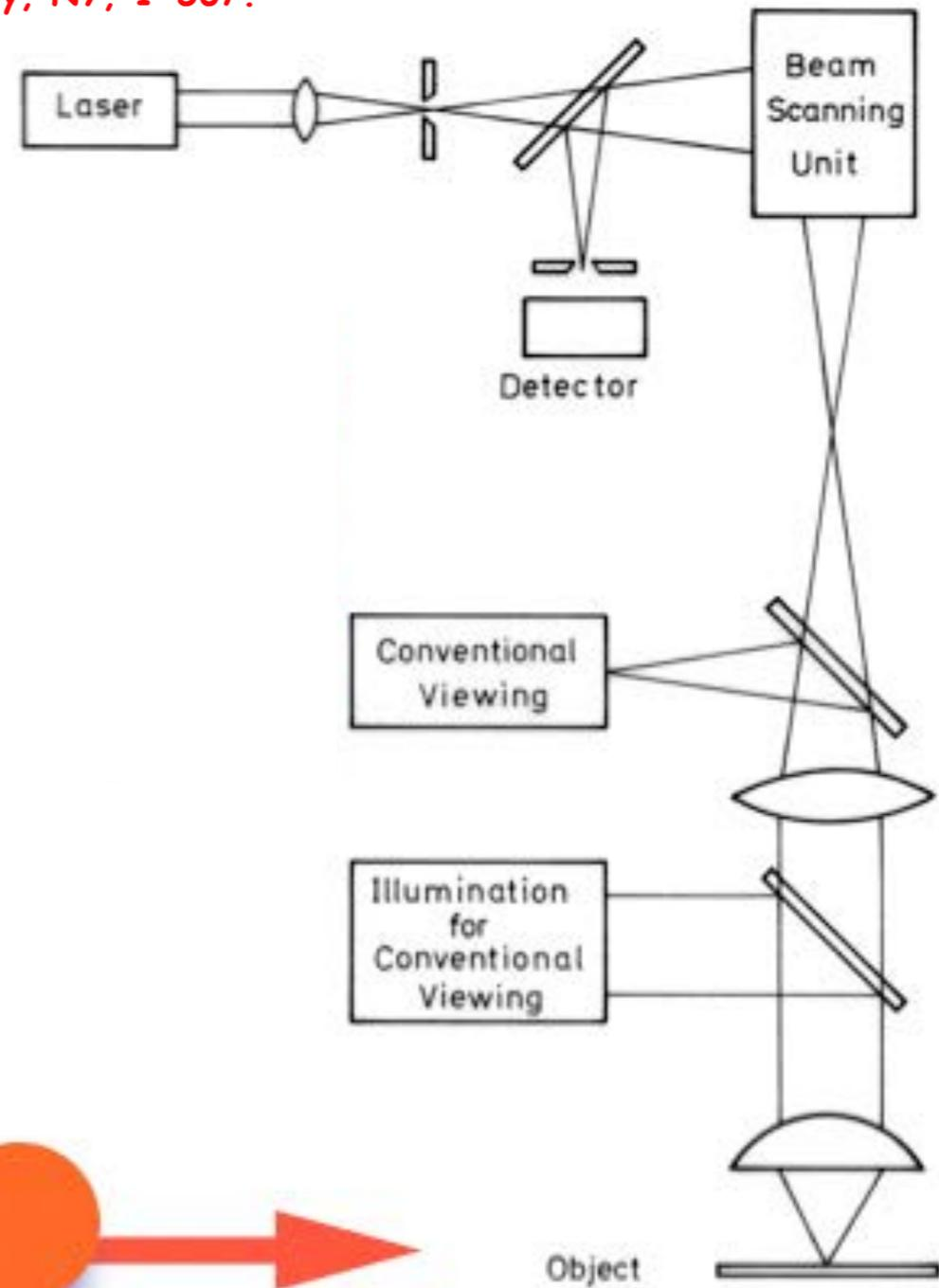
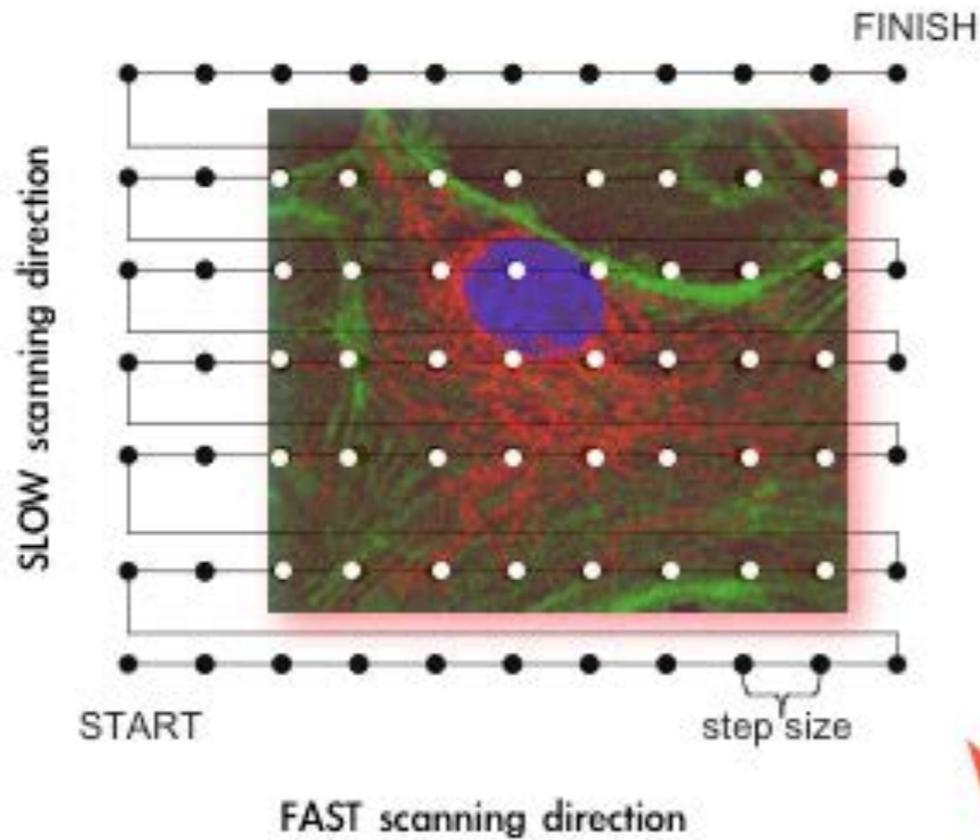


Giuseppe Pellizza da Volpedo (1868-1907)

Panni al sole (1894), olio su tela, 87x131 cm, Domodossola, collezione privata

confocal laser scanning microscopy

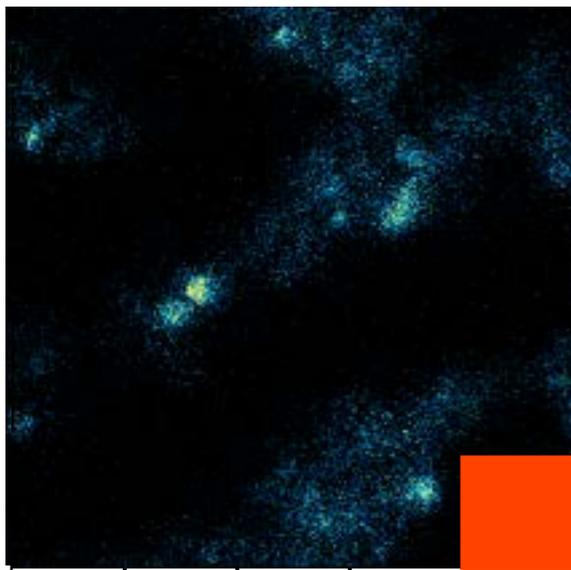
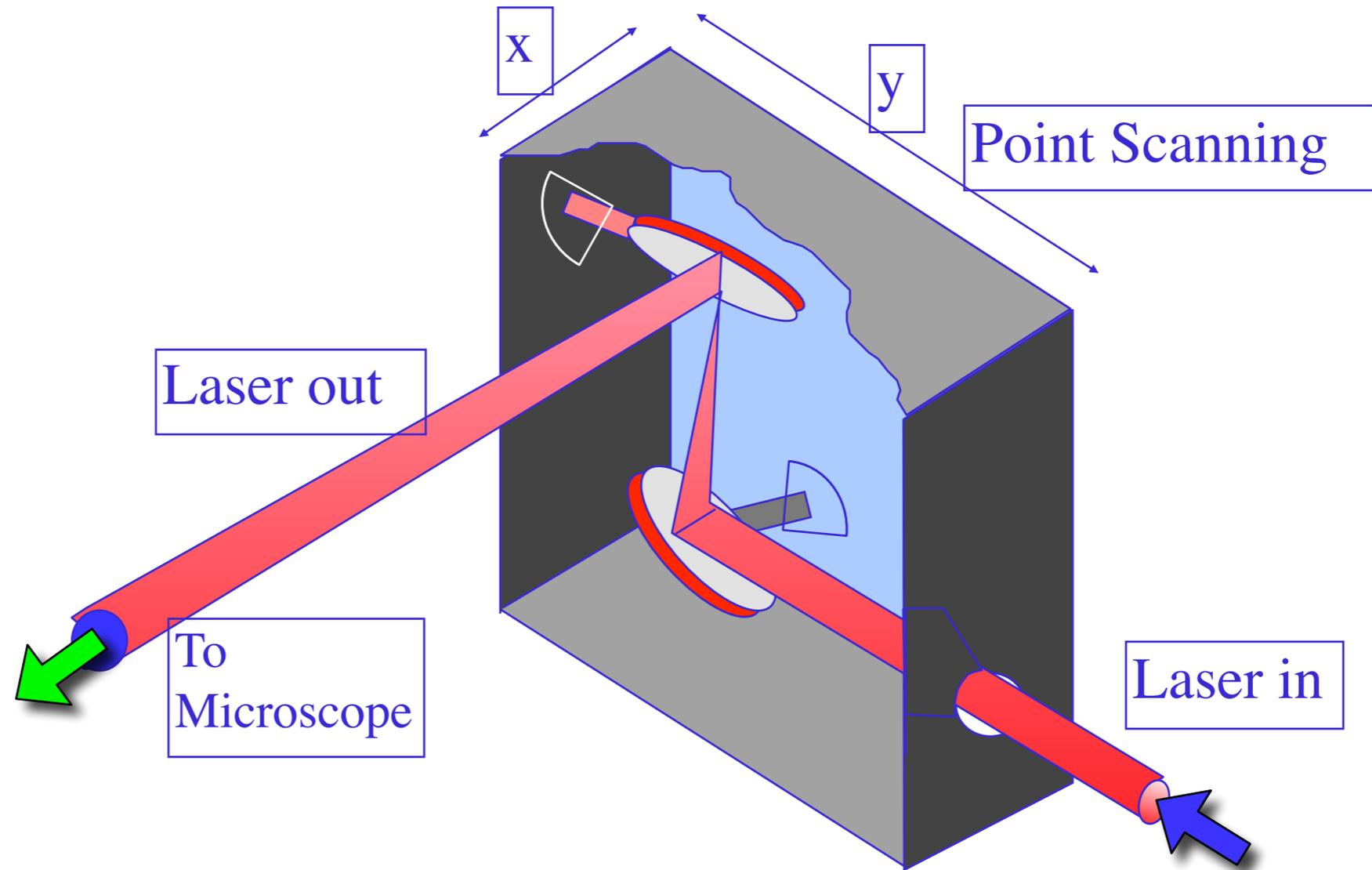
A. Diaspro (ed.), (2001) "Confocal and Two-photon Microscopy. Wiley, NY, 1-567.



confocal laser scanning microscopy

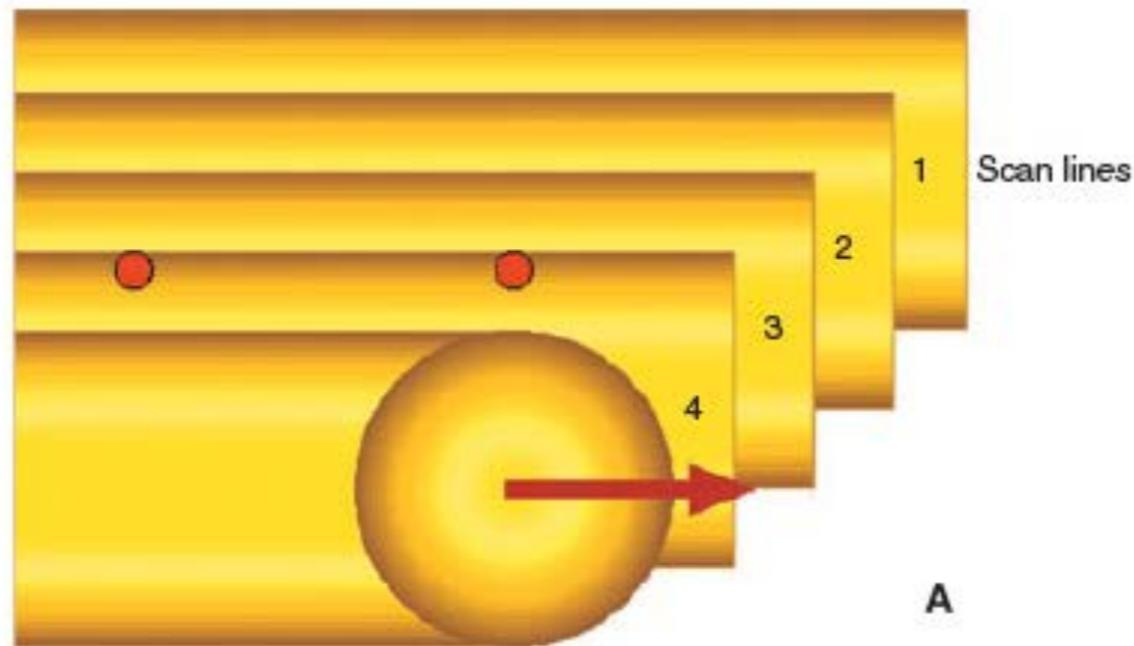
LIKE A FLORIAN'S COFFE IN VENICE

2 ms/line

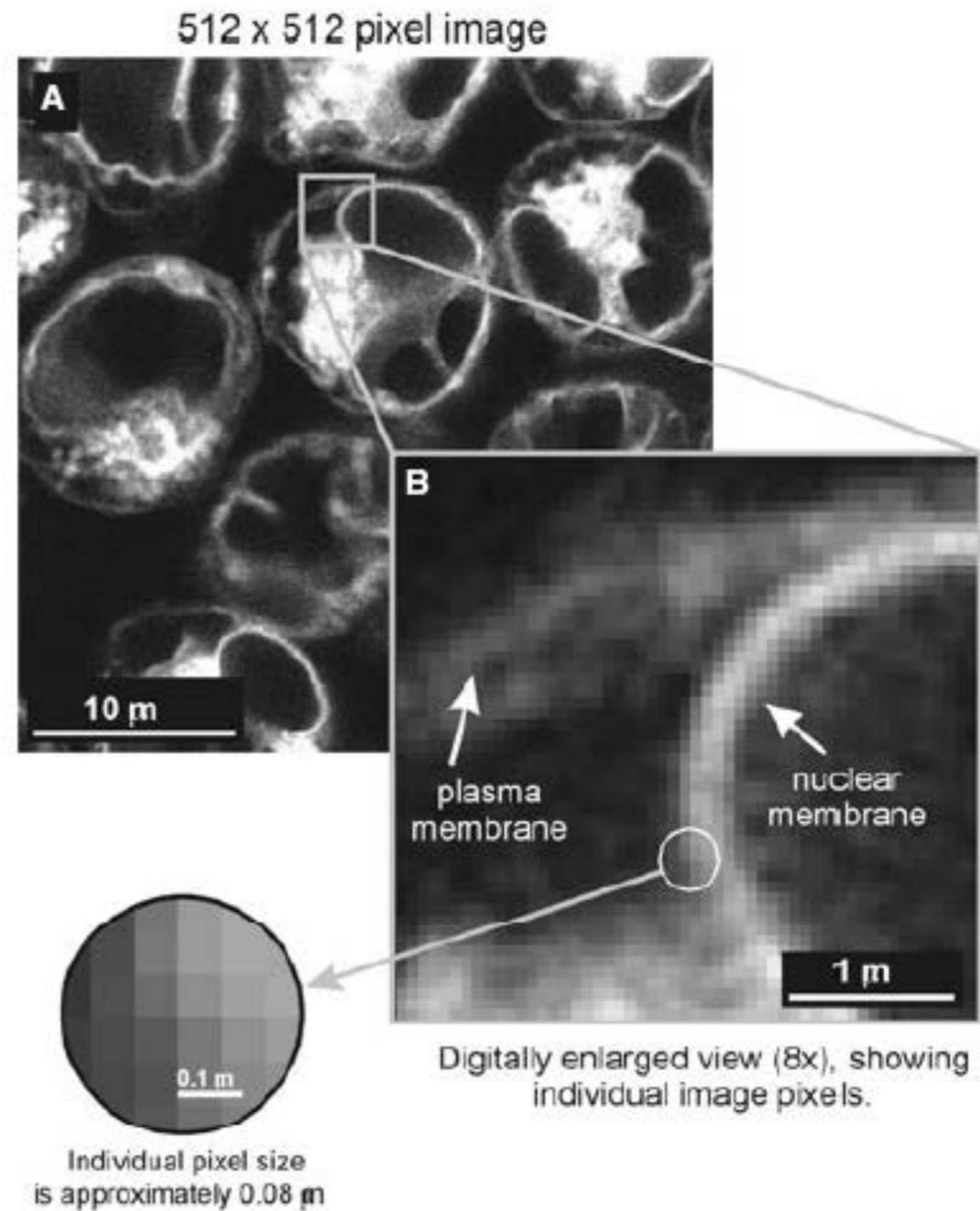
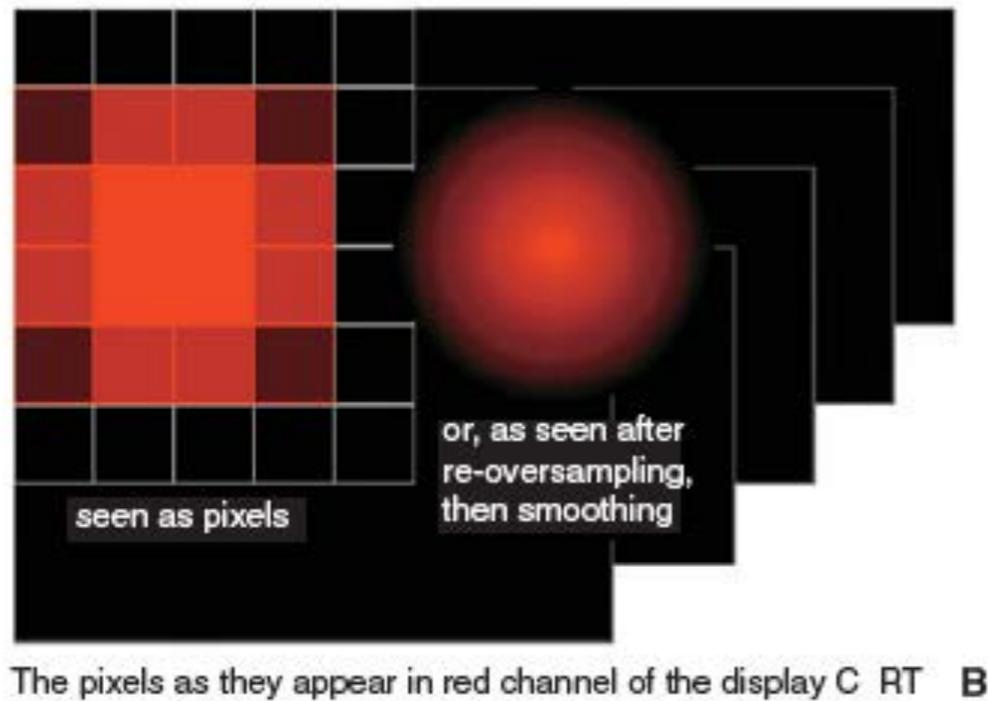


Slide credit: Fabio Cannone

confocal laser scanning microscopy



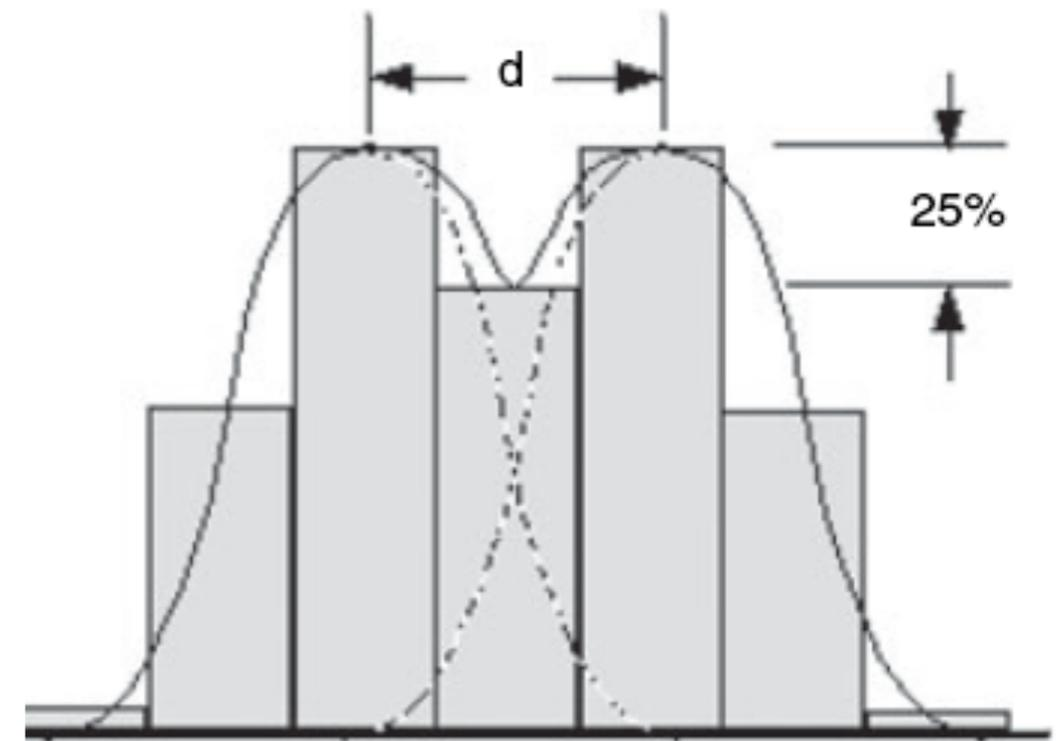
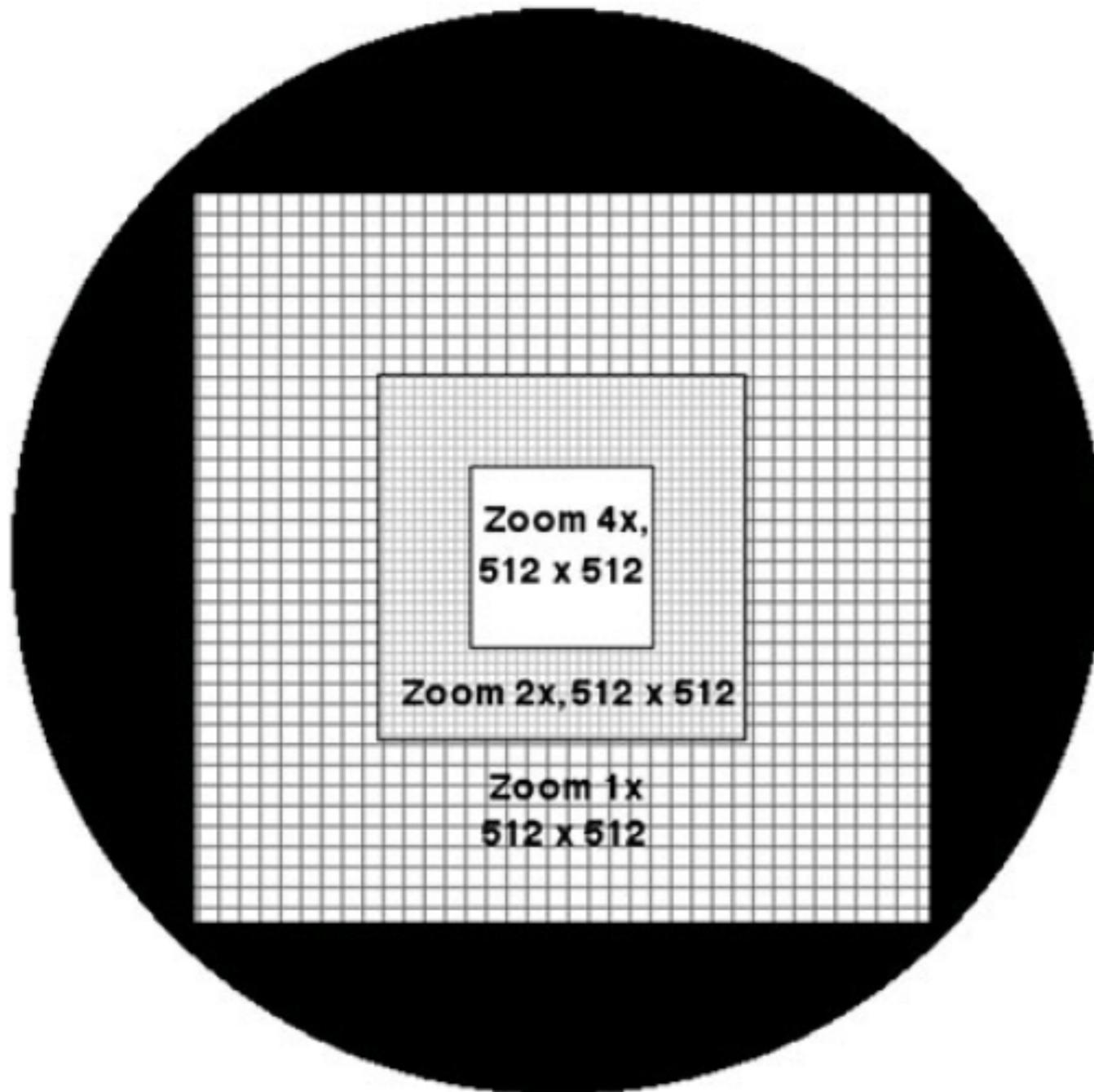
The geometry of the beam scanning the specimen



Slide credit: Handbook of Confocal Microscopy (J.Pawley ed.), Plenum, NEW edition, 2006

Alberto Diaspro, Nanoscopy, Istituto Italiano di Tecnologia

confocal laser scanning microscopy



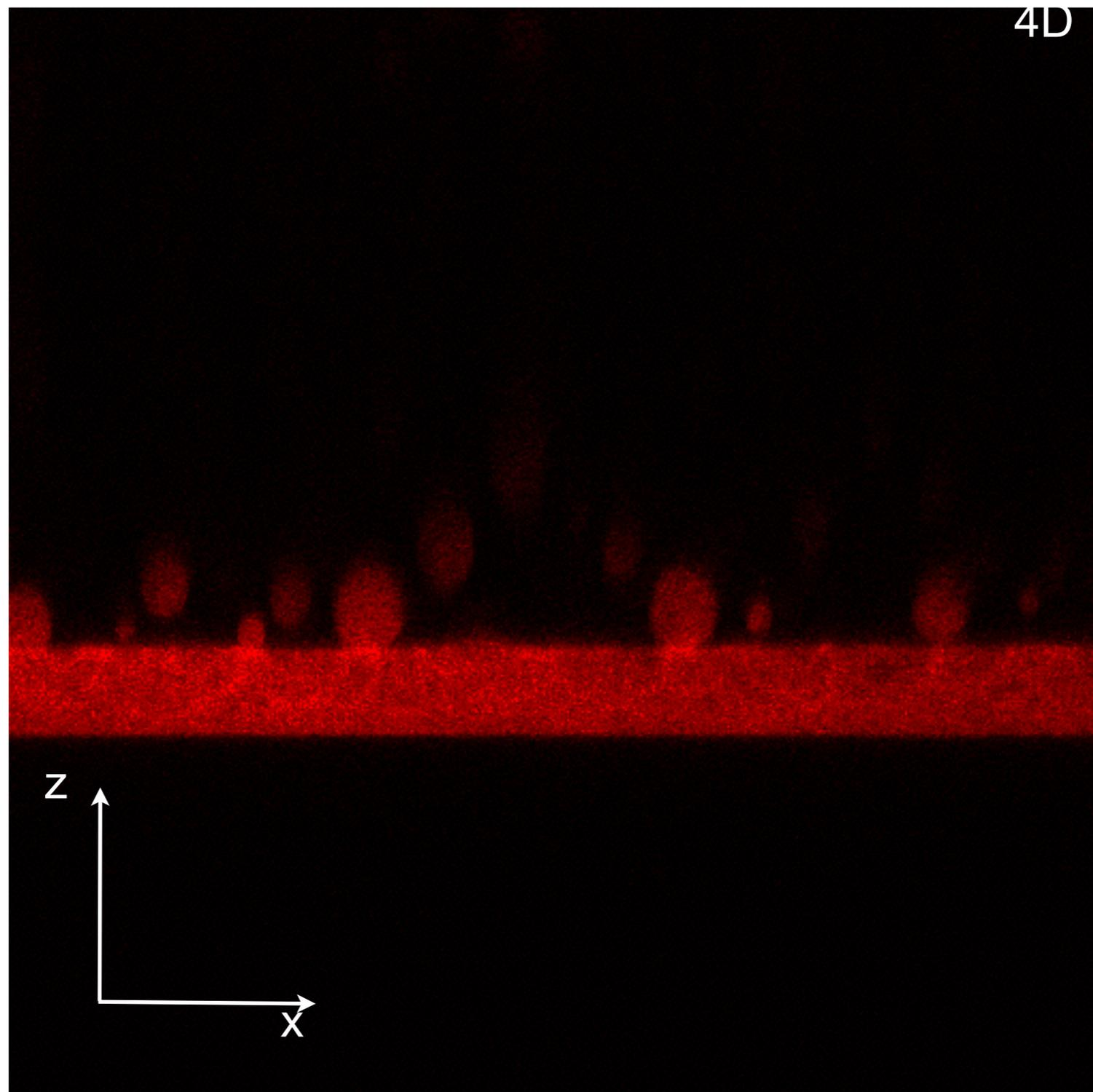
Rayleigh resolution, d ,
and Nyquist digitizing

Slide credit: Handbook of Confocal Microscopy (J.Pawley ed.), Plenum, NEW edition, 2006

confocal laser scanning microscopy

POINT BY POINT IMAGING
LIKE A FLORIAN'S COFFE IN VENICE

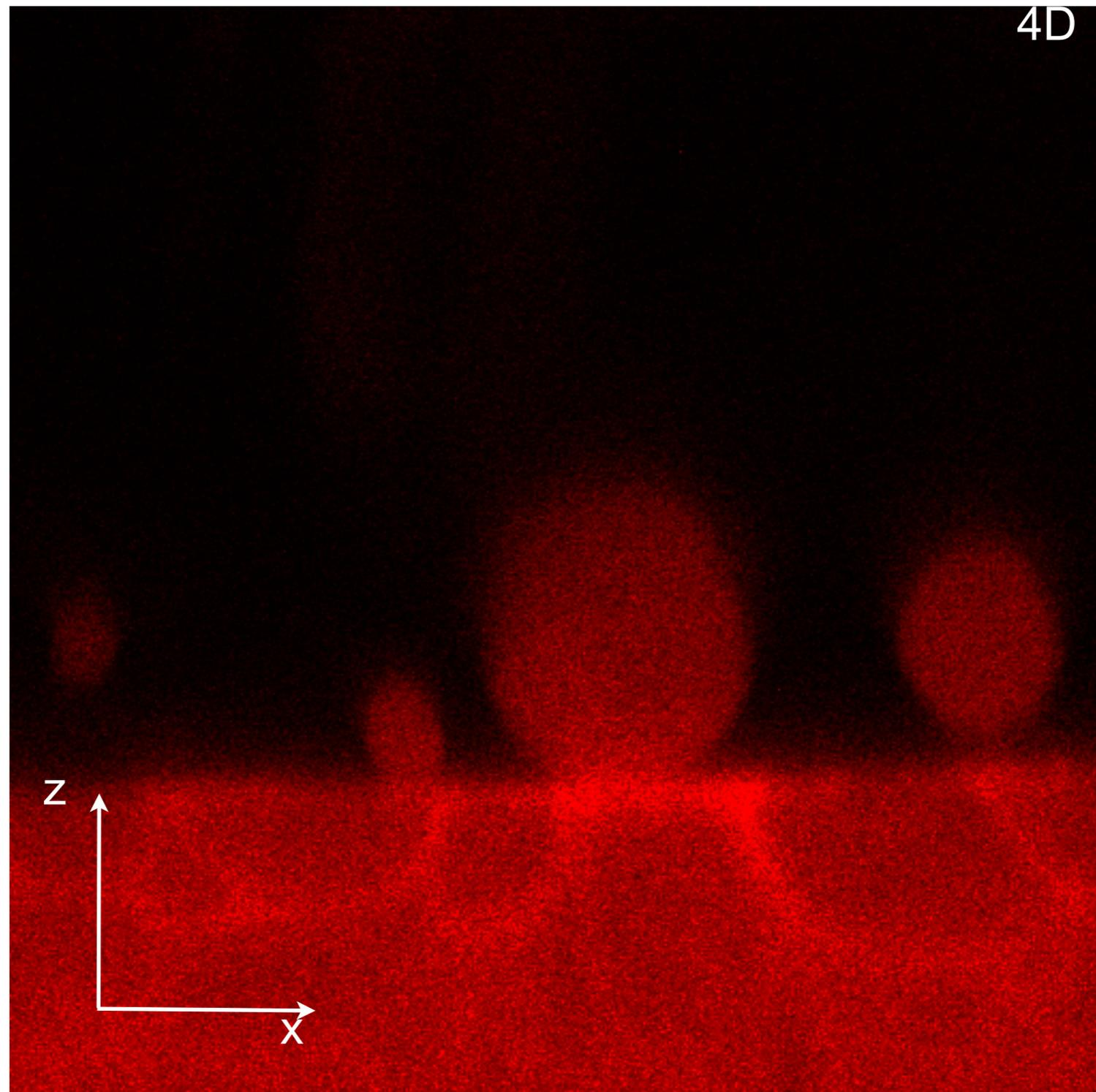
2 ms/line



confocal laser scanning microscopy

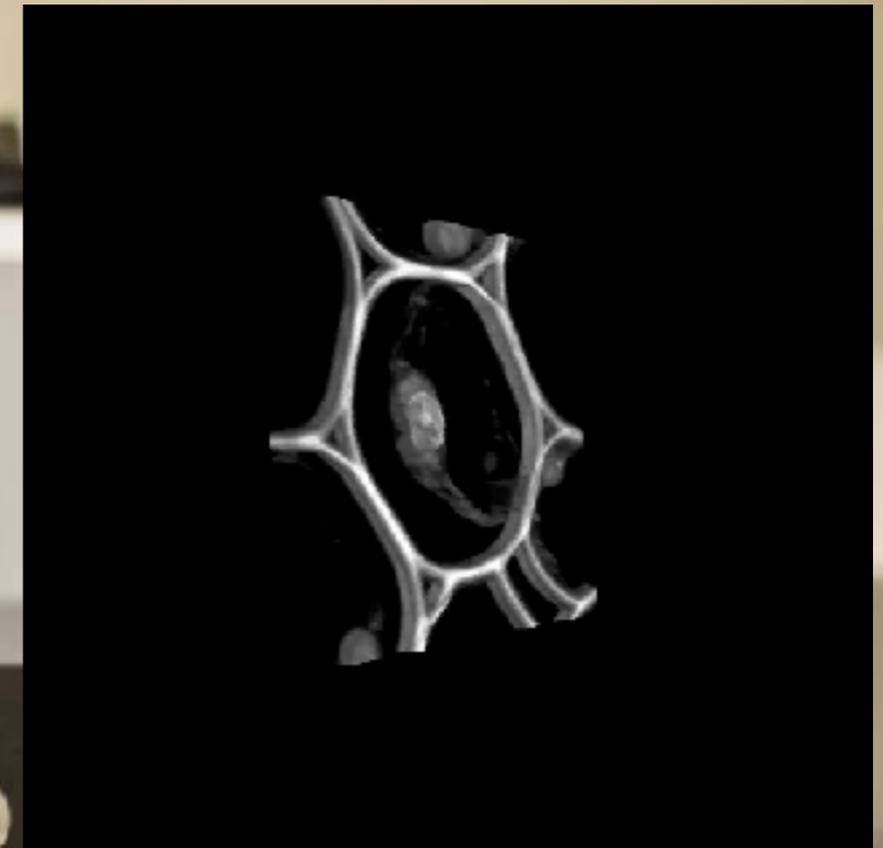
POINT BY POINT IMAGING
LIKE A FLORIAN'S COFFE IN VENICE

2 ms/line



3D/4D SUPER FAST Z-SCANNING - liquid lens

Use sound to periodically modulate the refractive index of a fluid at 100 kHz – 1 MHz

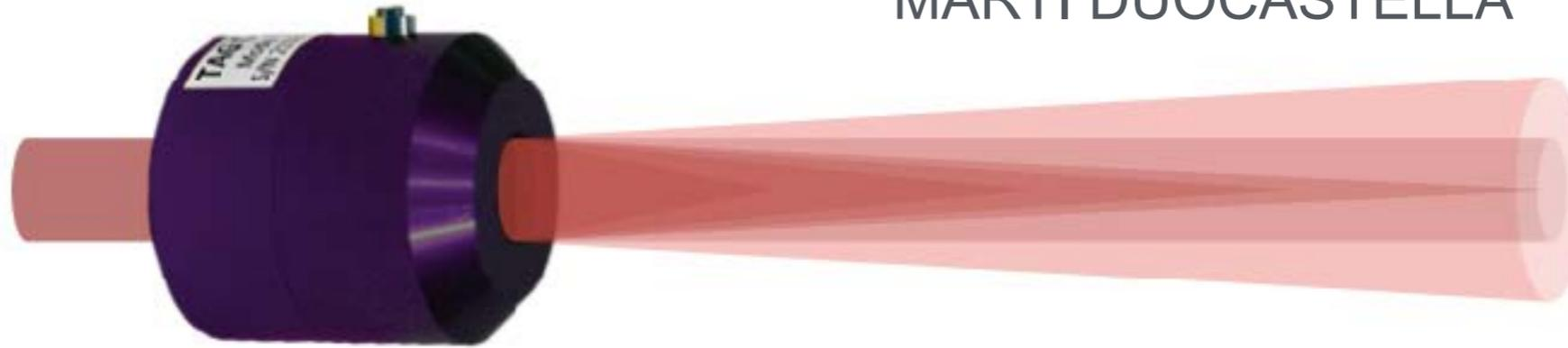


Martí Duocastella, Giuseppe Vicidomini, and Alberto Diaspro, "Simultaneous multiplane confocal microscopy using acoustic tunable lenses," *Opt. Express* 22, 19293-19301 (2014)

Photo: Agnese Abrisci, Istituto Italiano di Tecnologia © IIT

Ultra-high speed varifocal liquid lens

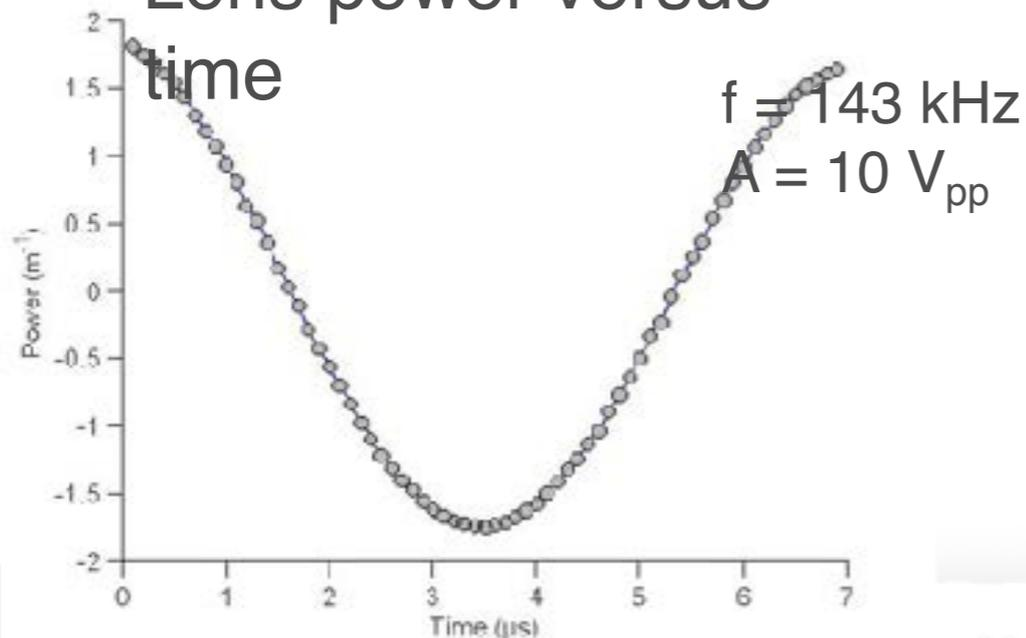
MARTI DUOCASTELLA



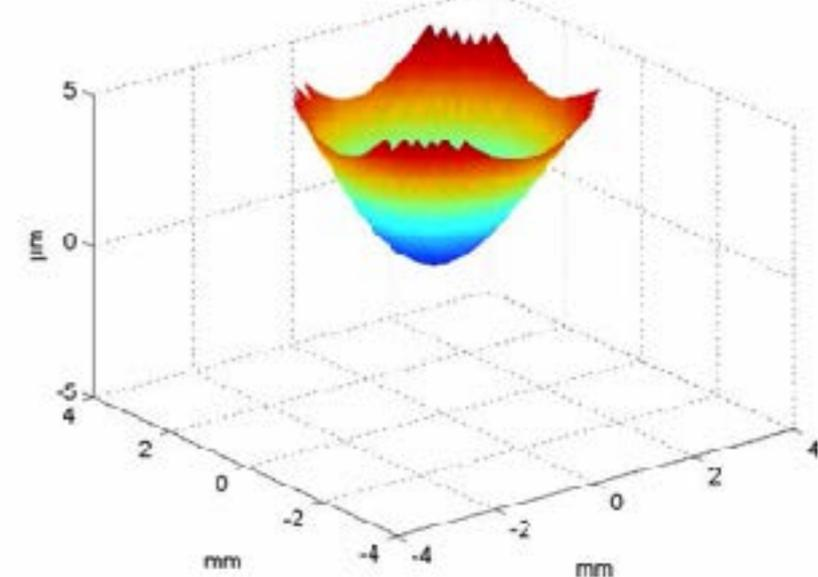
TAG lens → Tunable acoustic gradient index of refraction lens

Use sound to periodically modulate the refractive index of a fluid at 100 kHz – 1 MHz

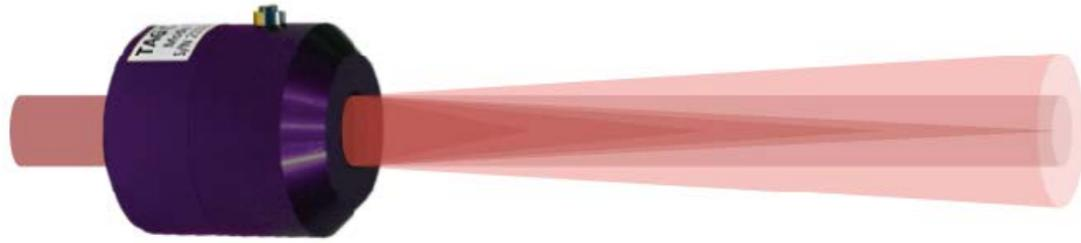
Lens power versus time



Wavefront versus time



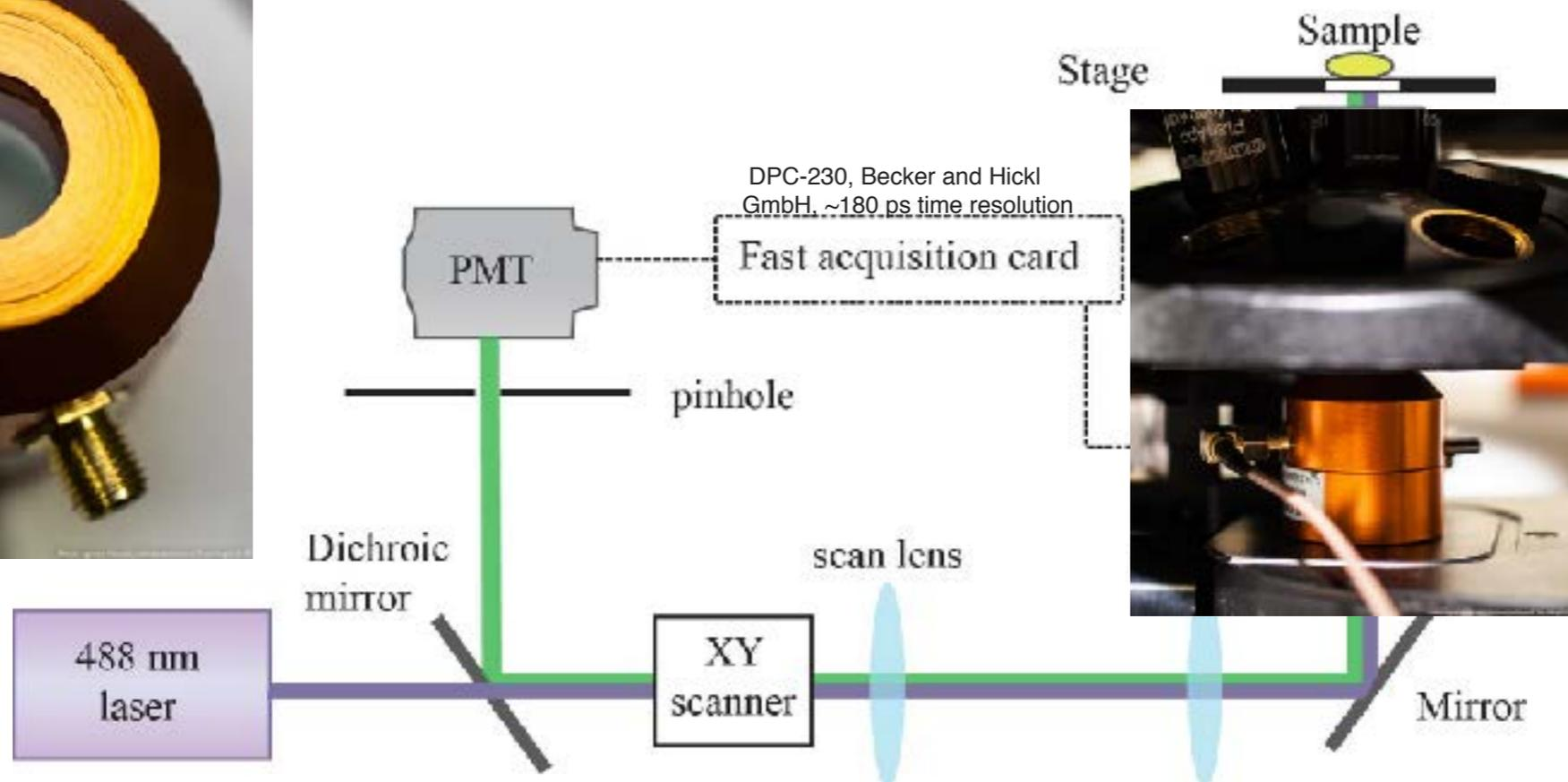
Ultra-high speed varifocal liquid lens



MARTI DUOCASTELLA

TAG lens → Tunable acoustic gradient index of refraction lens

Use sound to periodically modulate the refractive index of a fluid at 100 kHz – 1 MHz

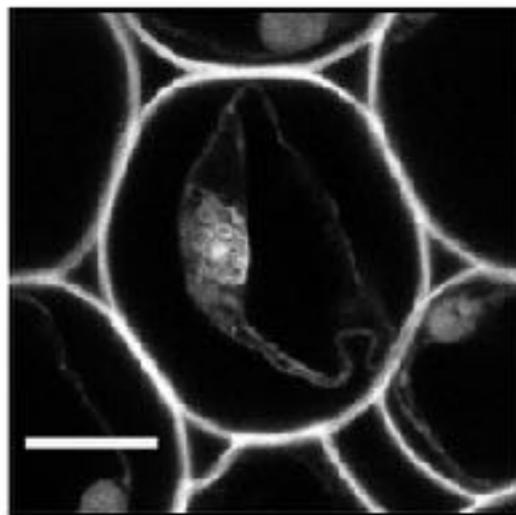
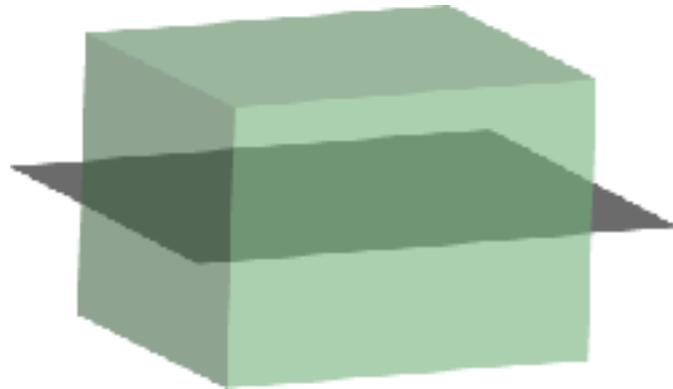


Opt. Express 22, 19293-19301 (2014)

Multiplane imaging

In a single XY scan...

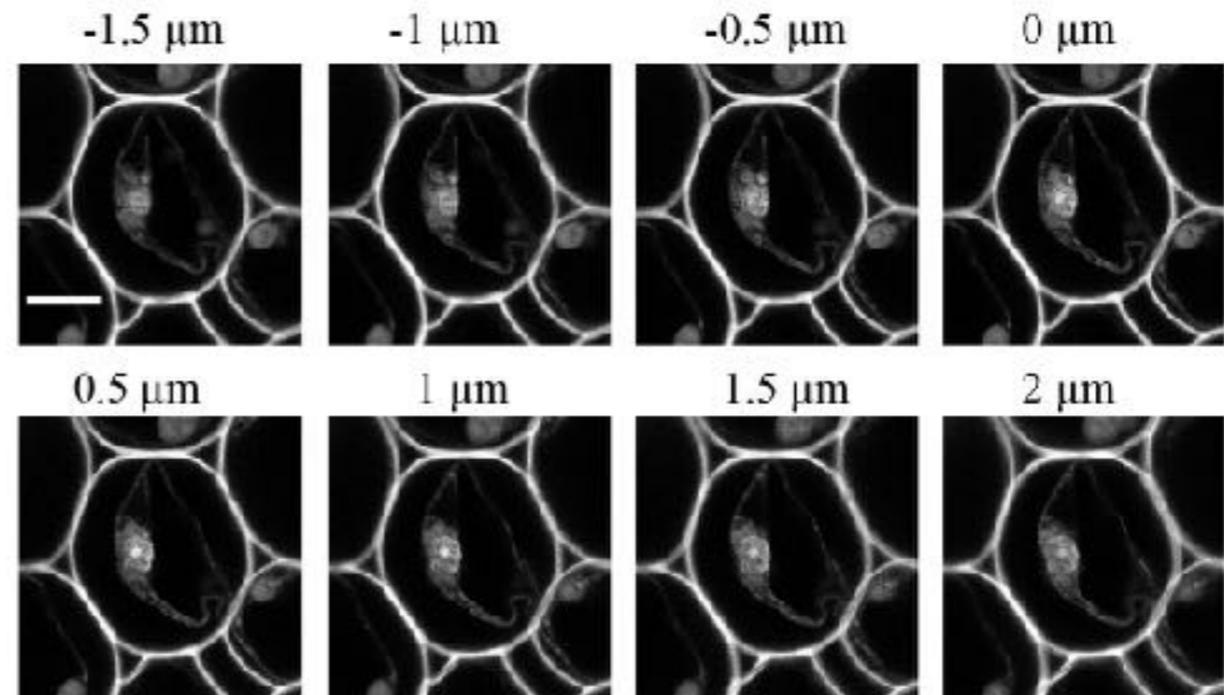
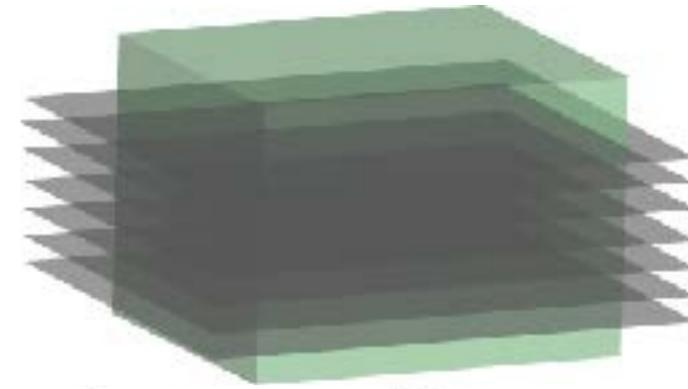
Without the TAG lens



One single plane

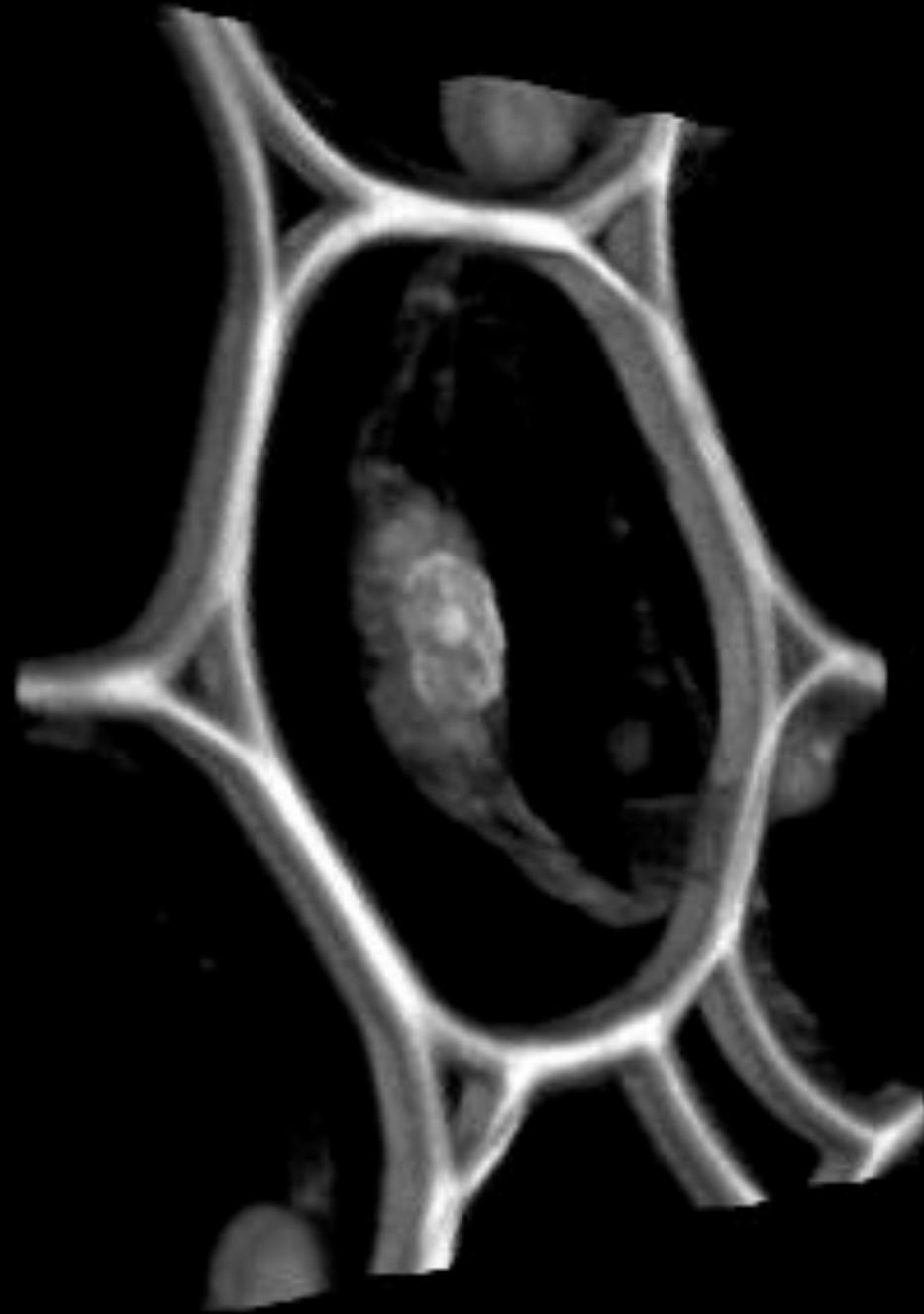
With the TAG lens

Multiple planes, **only** limited by SNR



Martí Duocastella, Giuseppe Vicidomini, and Alberto Diaspro, "Simultaneous multiplane confocal microscopy using acoustic tunable lenses," *Opt. Express* 22, 19293-19301 (2014)

Martí Duocastella, Giuseppe Vicidomini, and Alberto Diaspro, "Simultaneous multiplane confocal microscopy using acoustic tunable lenses," *Opt. Express* **22**, 19293-19301 (2014)



Volumetric imaging of neurons:

- mouse brain axial slice
150um thick

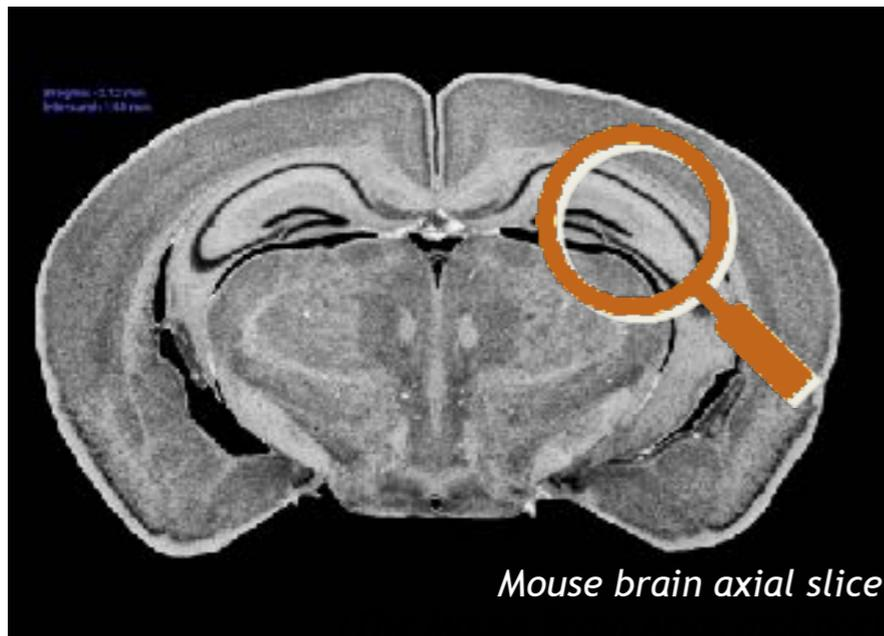
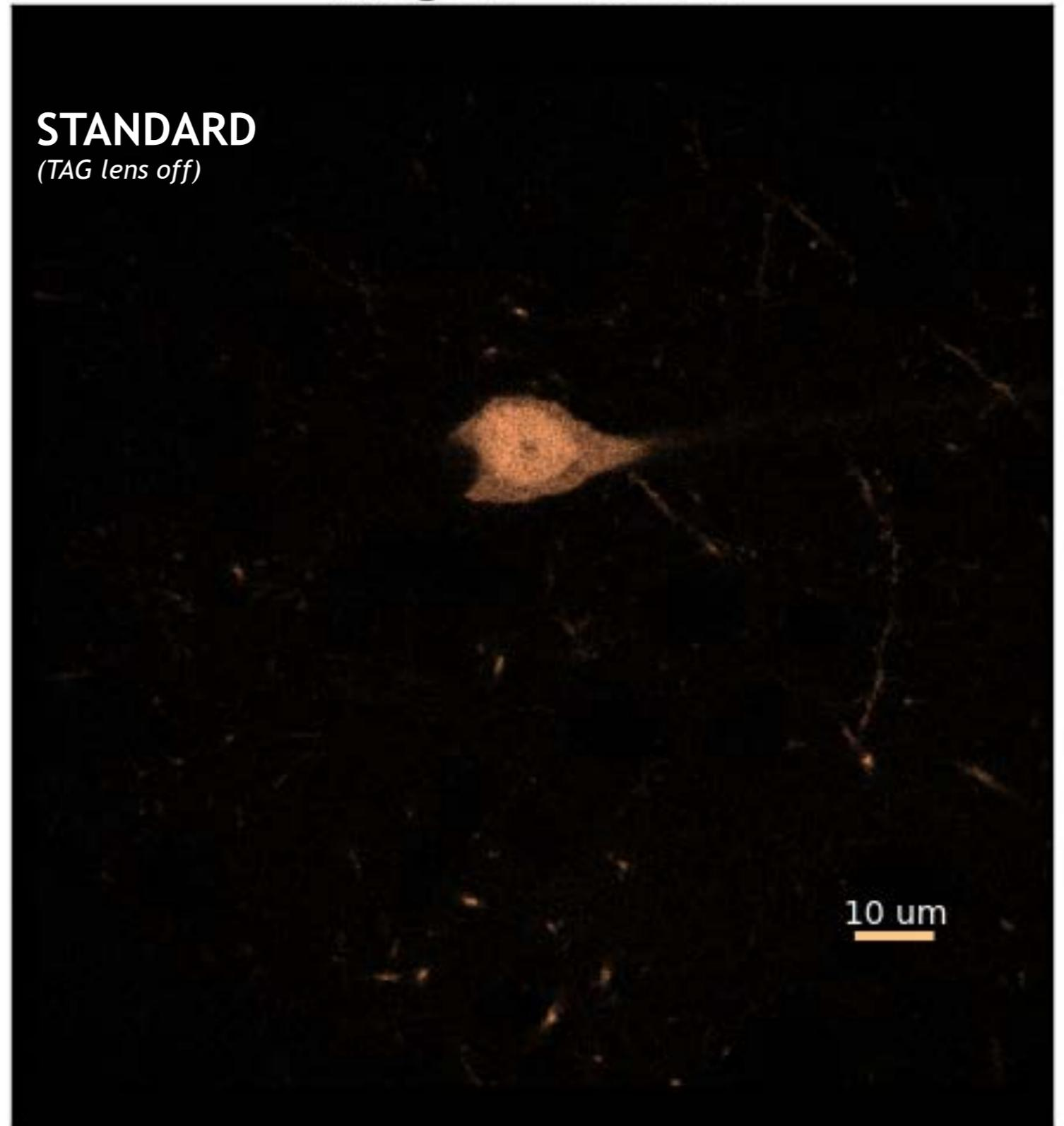


Image 1 - TAG off

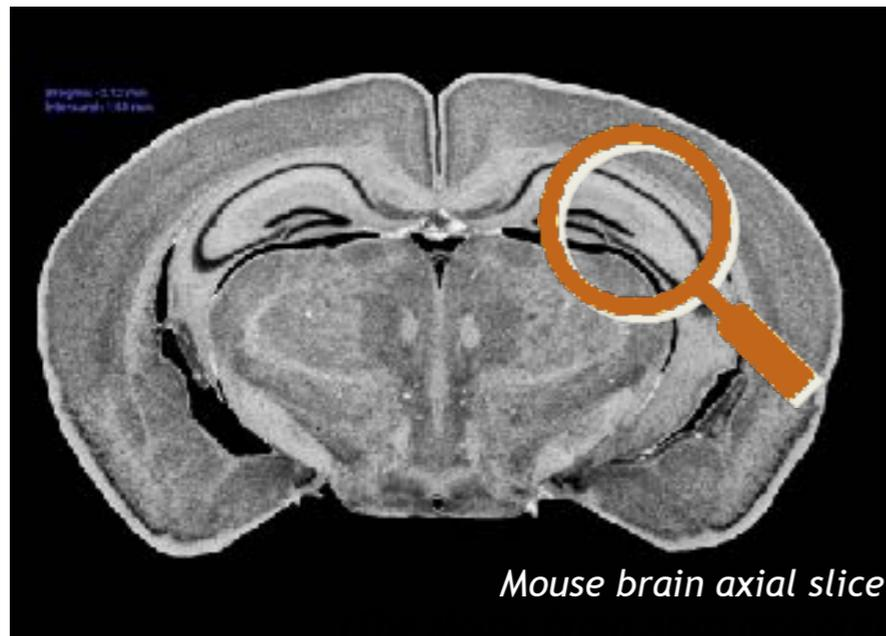
STANDARD
(TAG lens off)



slide credit: Simonluca Piazza, Diaspro Lab, IIT

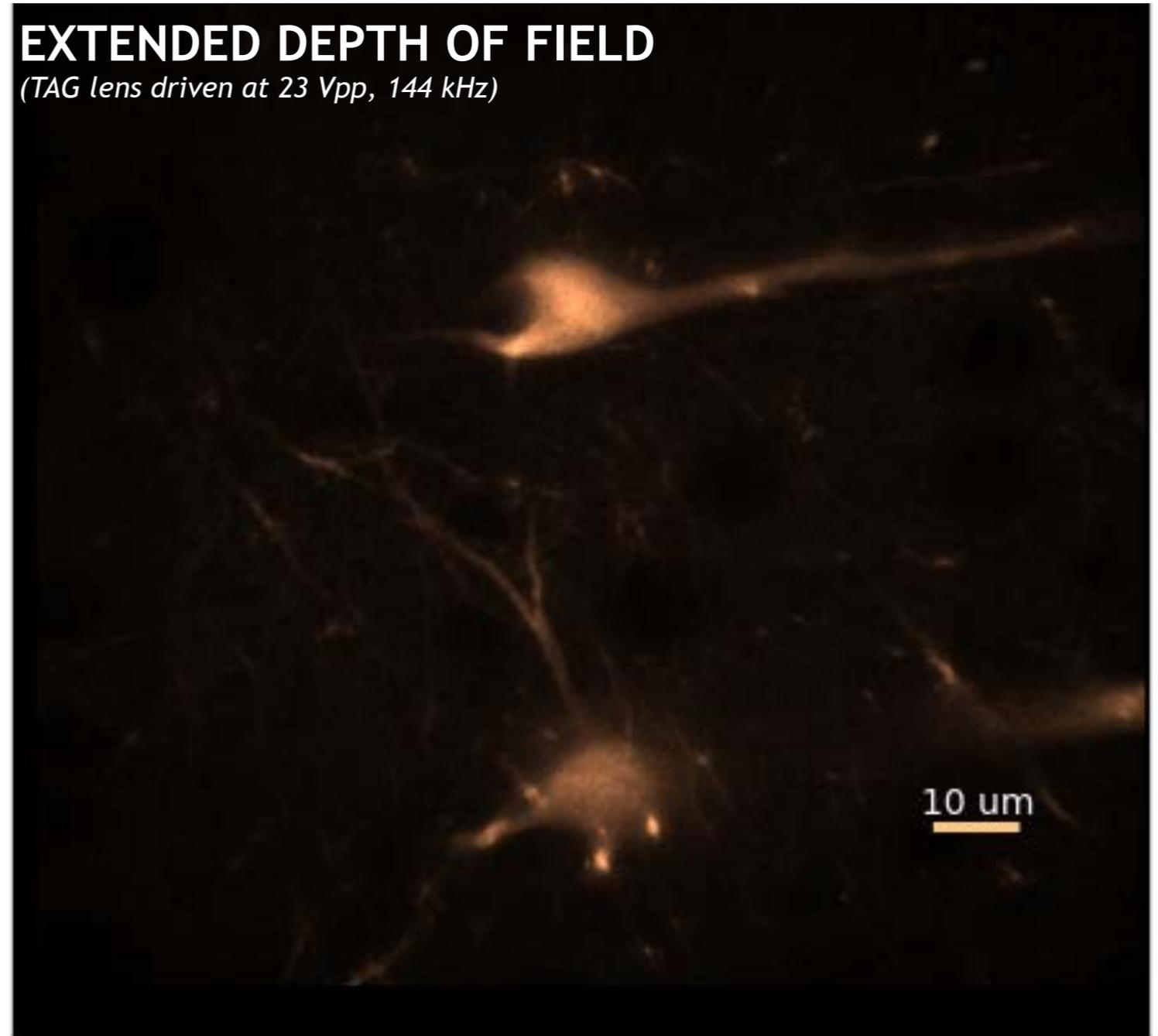
Volumetric imaging of neurons:

- mouse brain axial slice
150um thick



EXTENDED DEPTH OF FIELD

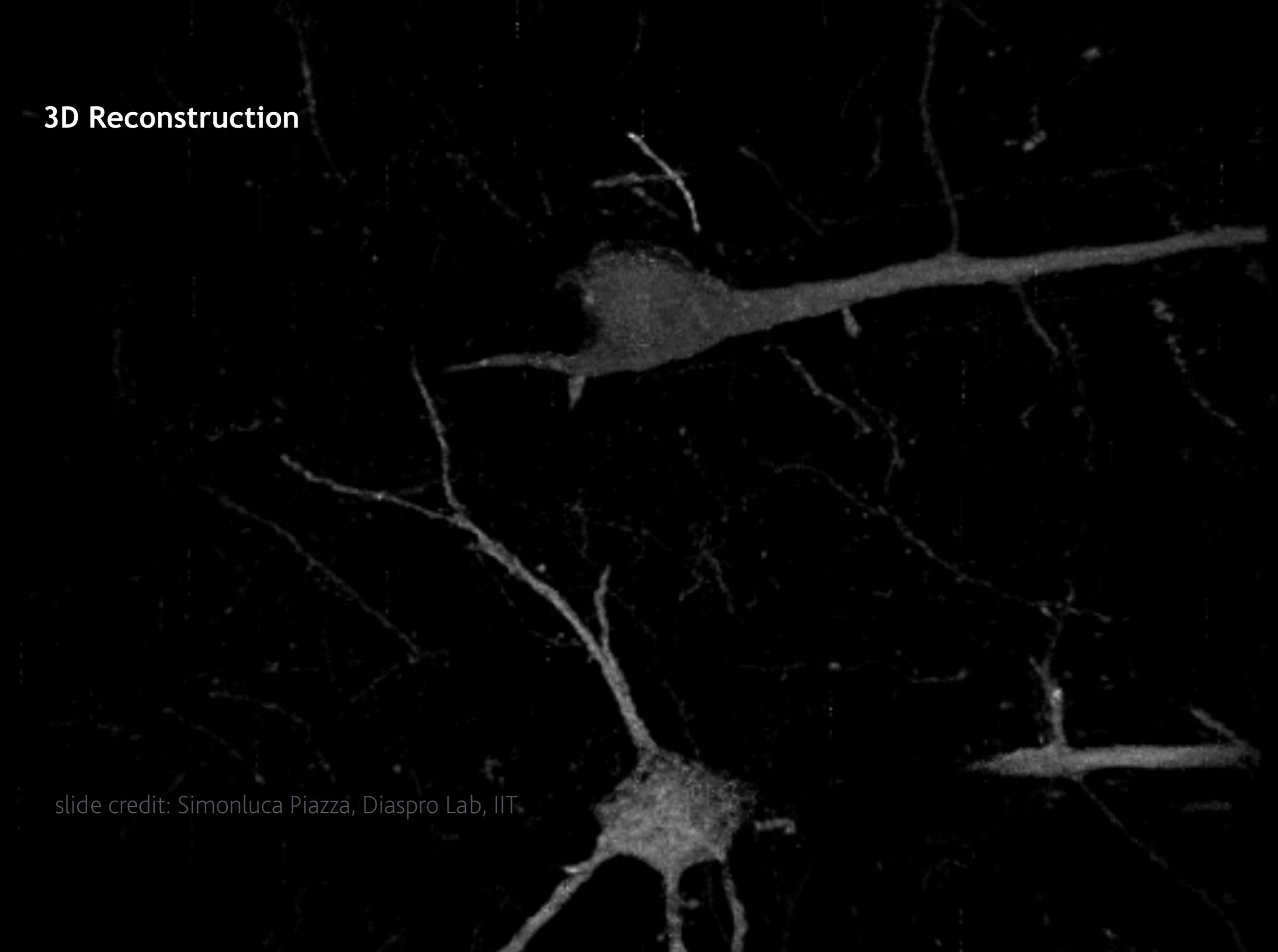
(TAG lens driven at 23 V_{pp}, 144 kHz)



slide credit: Simonluca Piazza, Diaspro Lab, IIT

3D Reconstruction

slide credit: Simonluca Piazza, Diaspro Lab, IIT



SPIM - liquid lens

Paolo Bianchini, Diaspro Lab, set-up 2016



Collaboration with Peter Saggau,



Ducros M et al, (2013) *Proc Natl Acad Sci U S A* 110(32):13138-13143.
Diaspro, A. (2013) *Microsc. Res. Tech.* 76: 985–987.

“less lazy” ...3D



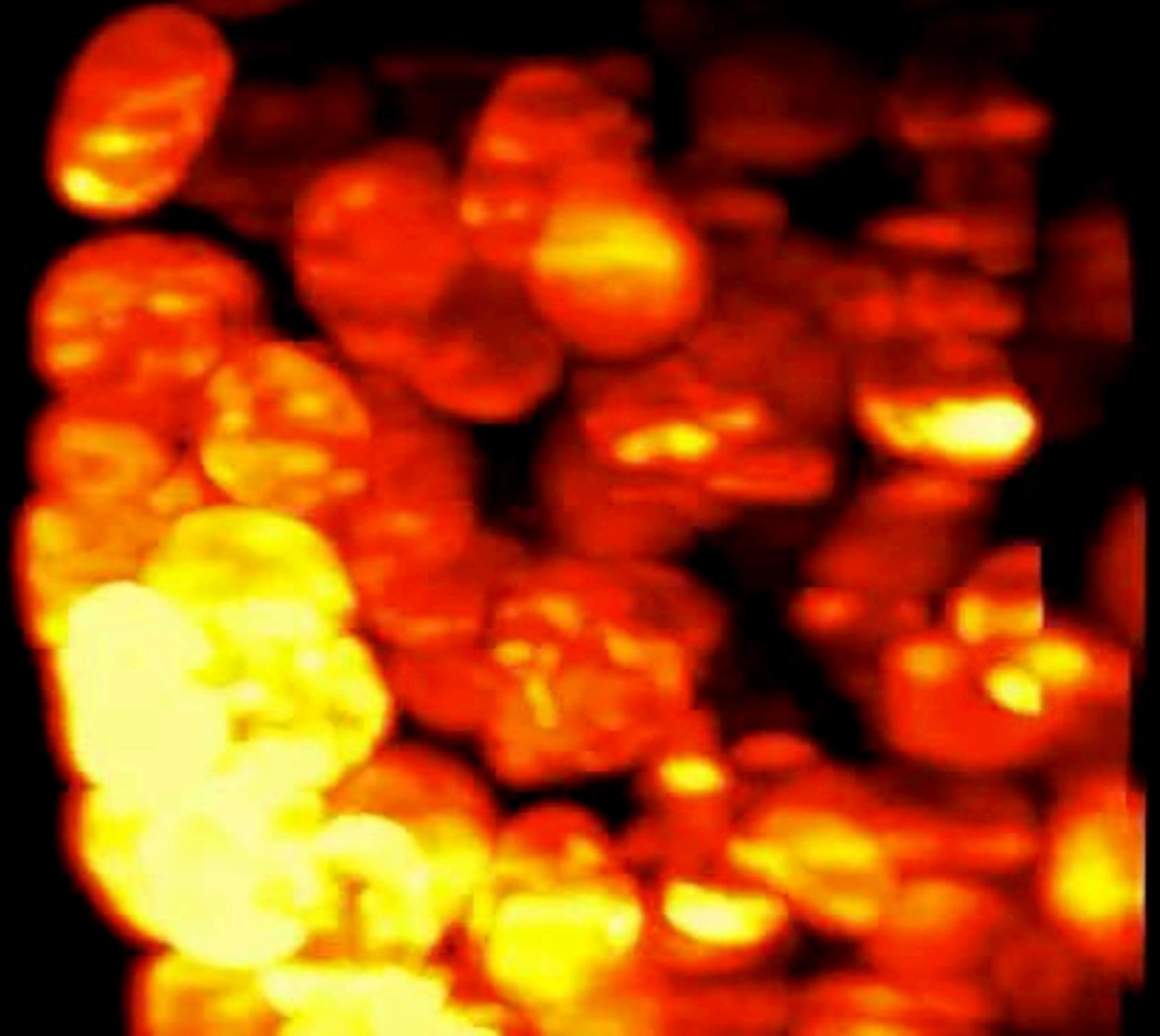
3D Thick objects

SPIM -human
mammary MCF10A
cell spheroid

Sample credit: Laura Furia,
Mario Faretta - IEO Milan



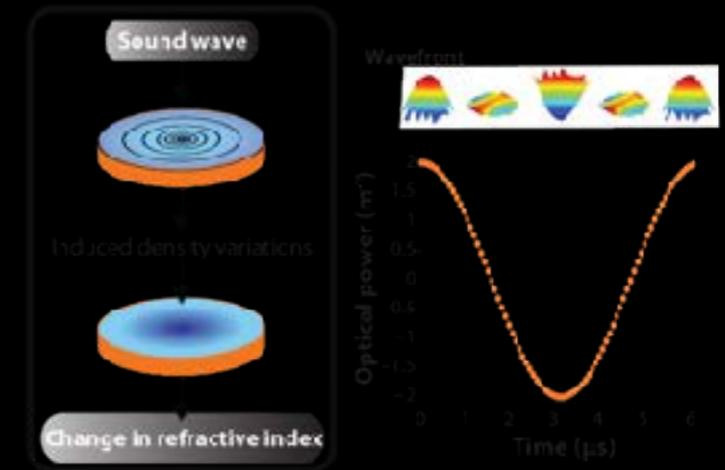
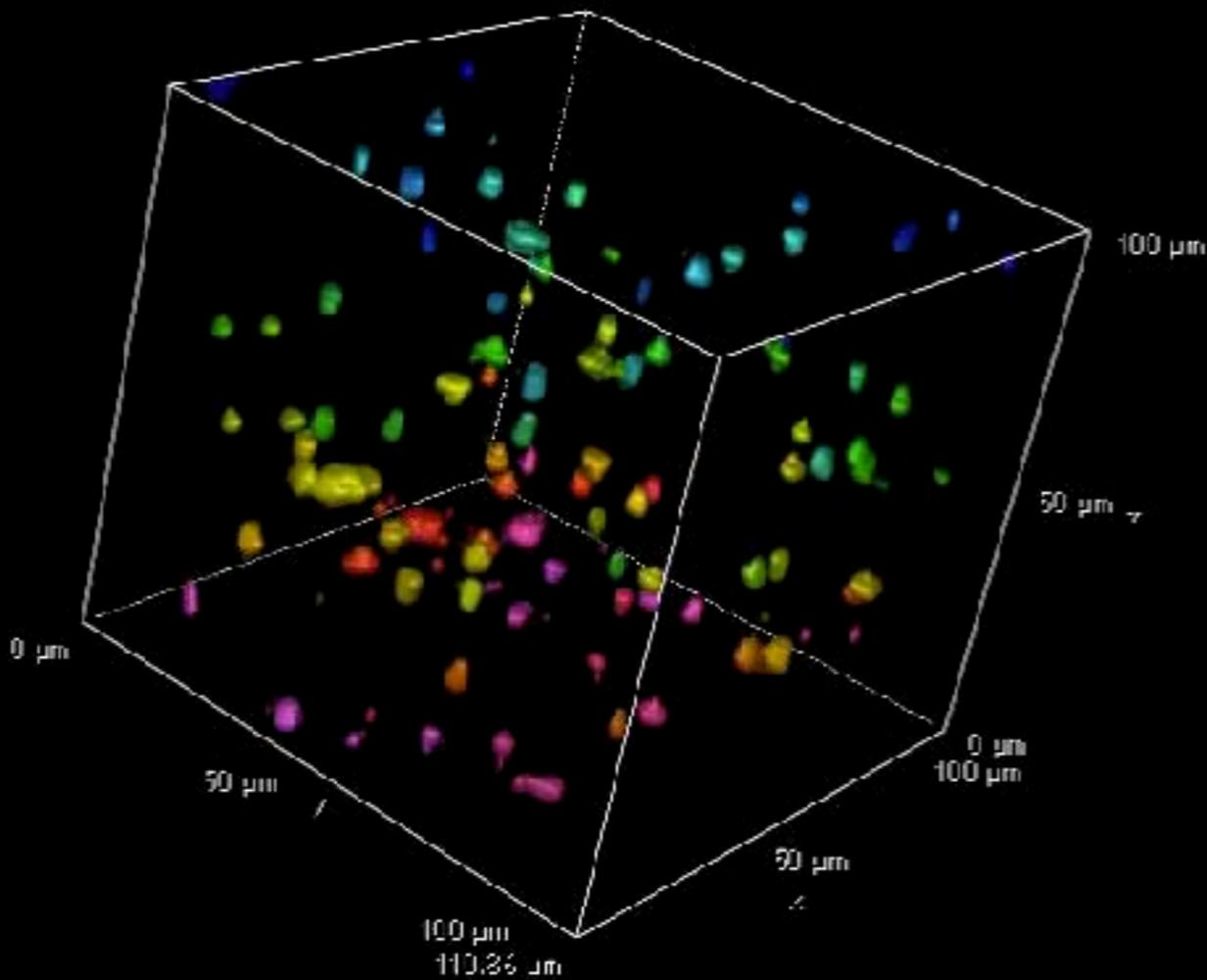
Credits: Zeno Lavagnino, Francesca
Cella Zancchi - Diaspro Lab, IIT



200 Volumes per Second
10000 Frames per Second
 $600 \cdot 10^6$ Voxels per Second

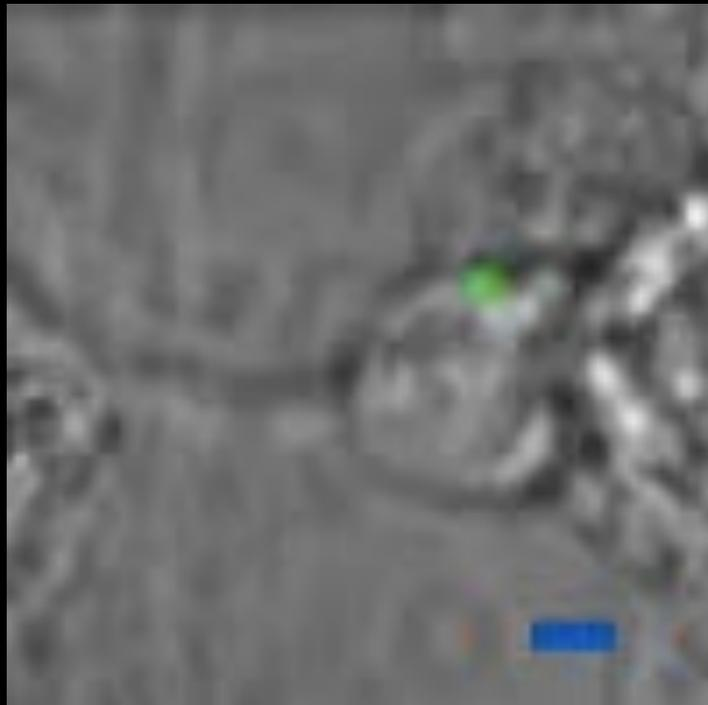
SPIM - liquid lens

0.000 sec

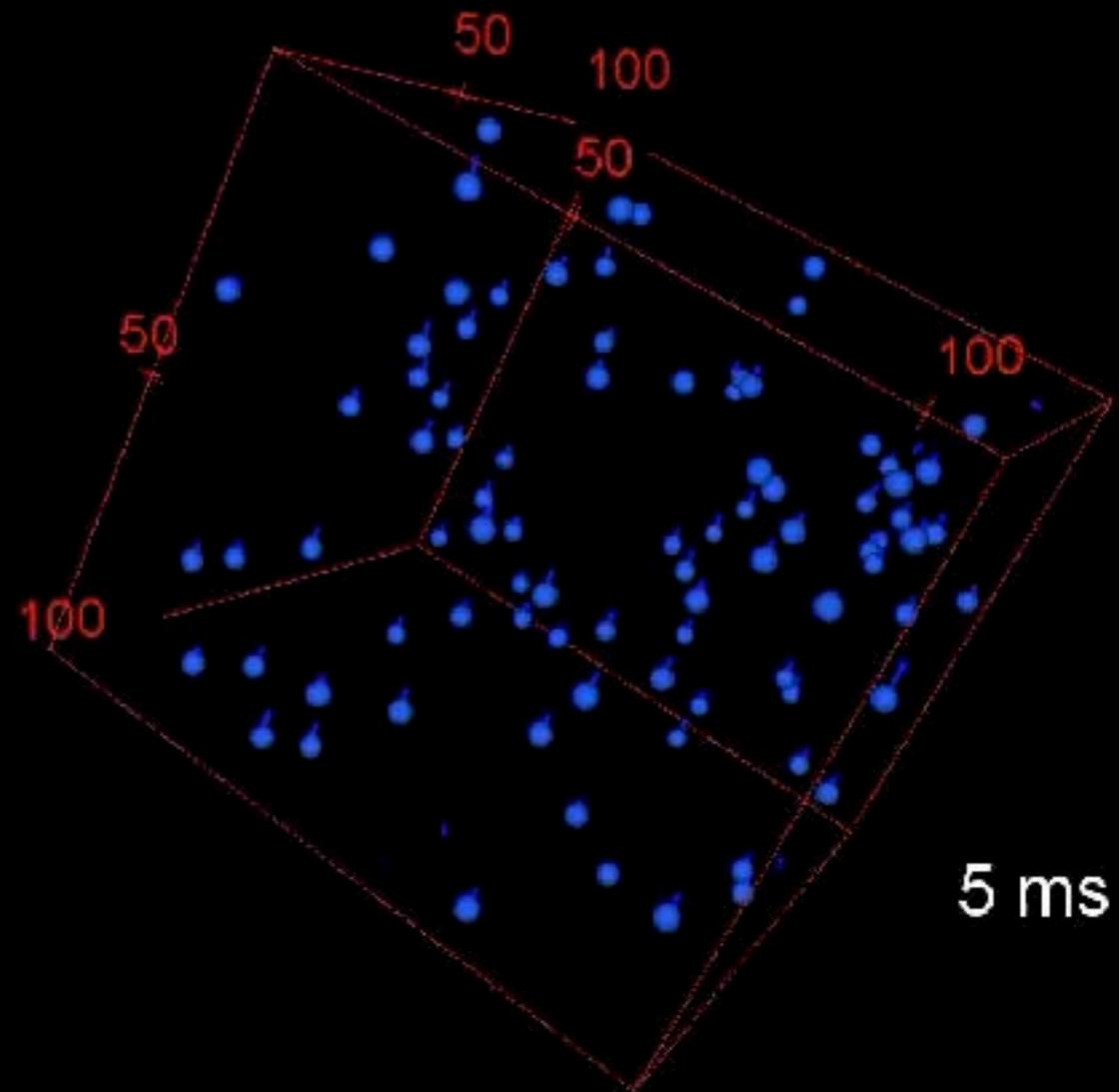


Credits: Giuseppe Sancataldo, Paolo Bianchini,
Marti Duocastella - Diaspro Lab, IIT - 2016

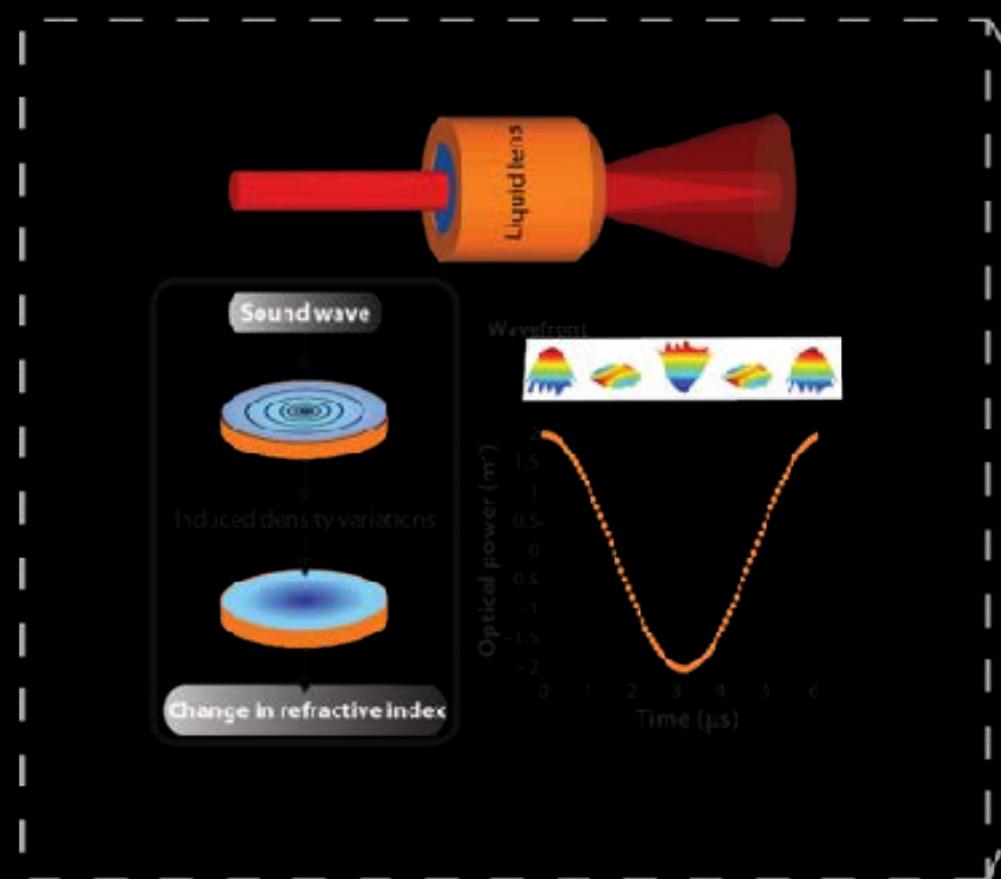
Particle Tracking



Diffusion of GABA receptor in living neuron



Credit: Giuseppe Sancatldo, Diaspro Lab, 2017



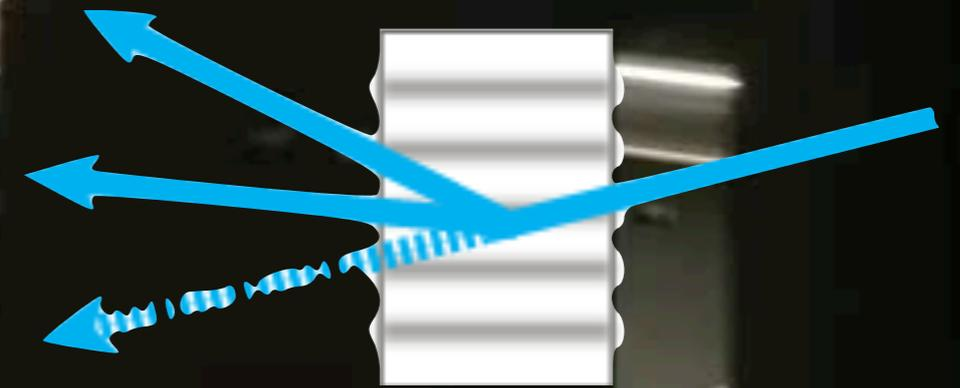
Volume Size $138 \times 138 \times 60 \mu\text{m}^3$ (XYZ)
 11 Volumes/Second
 333 Frame/Second
 3 ms/frame
 30 planes/Volume
 Nile Red Fluorescence Signal
 Andor NEO 5.5 camera
 Sample credit: Paola Ramoino

Credits: Giuseppe Sancataldo, Paolo Bianchini,
 Marti Duocastella - Diaspro Lab, IIT - 2016

Simultaneous Planes



ϑ_2
 ϑ_1
0

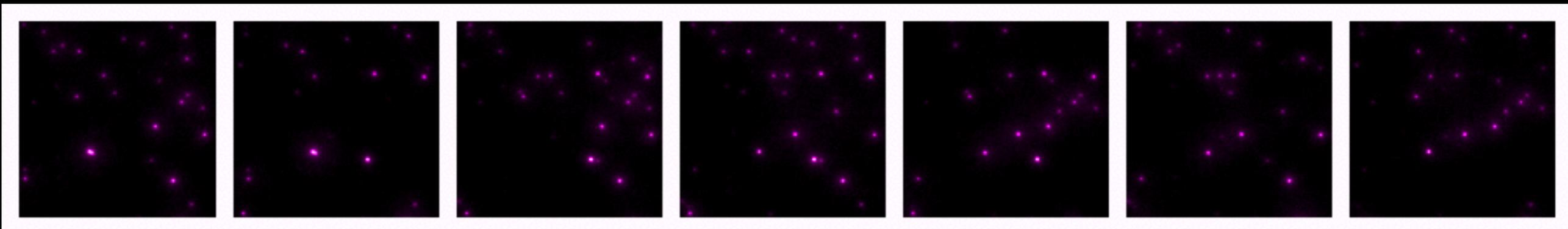


Seven Simultaneous Planes

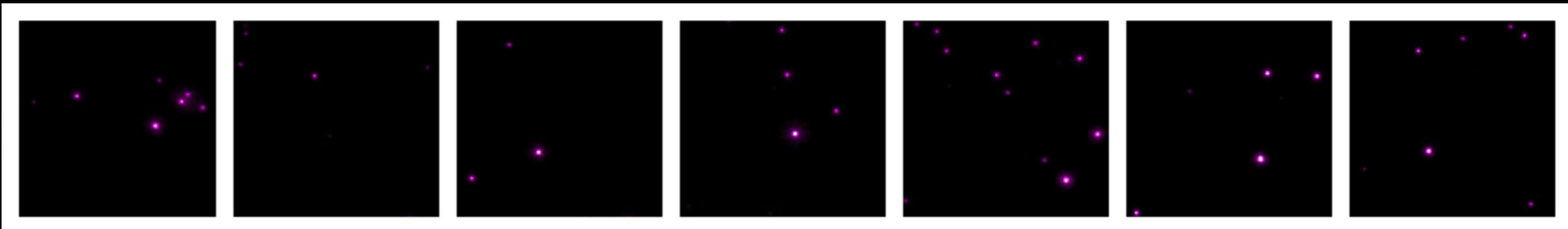
1 LIGHT ON
0 LIGHT OFF

$$\begin{bmatrix} 1 & 0 & 1 & 0 & 1 & 0 & 1 \\ 0 & 1 & 1 & 0 & 0 & 1 & 1 \\ 1 & 1 & 0 & 0 & 1 & 1 & 0 \\ 0 & 0 & 0 & 1 & 1 & 1 & 1 \\ 1 & 0 & 1 & 1 & 0 & 1 & 0 \\ 0 & 1 & 1 & 1 & 1 & 0 & 0 \\ 1 & 1 & 0 & 1 & 0 & 0 & 1 \end{bmatrix}$$

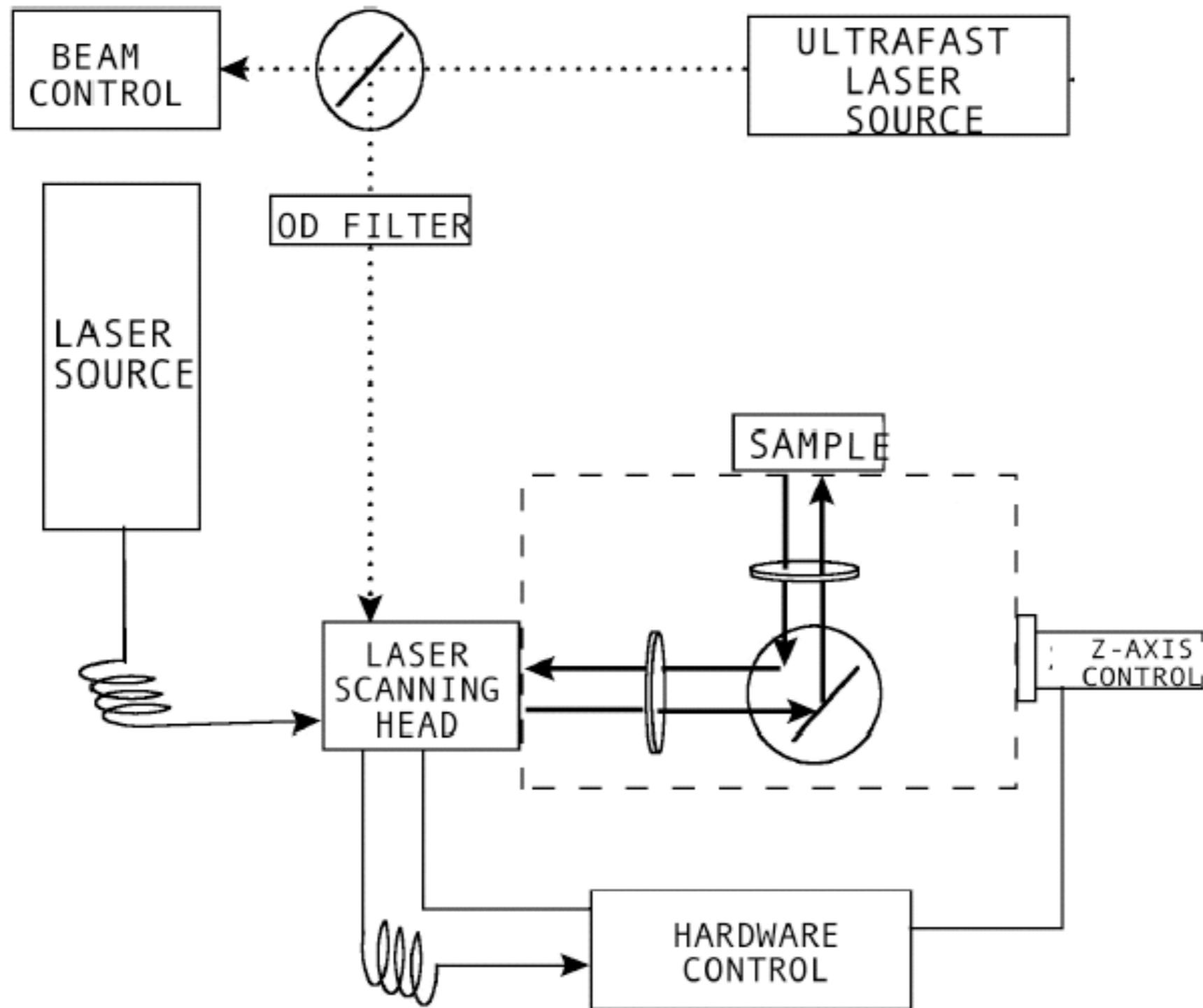

ENCODED



DECODED

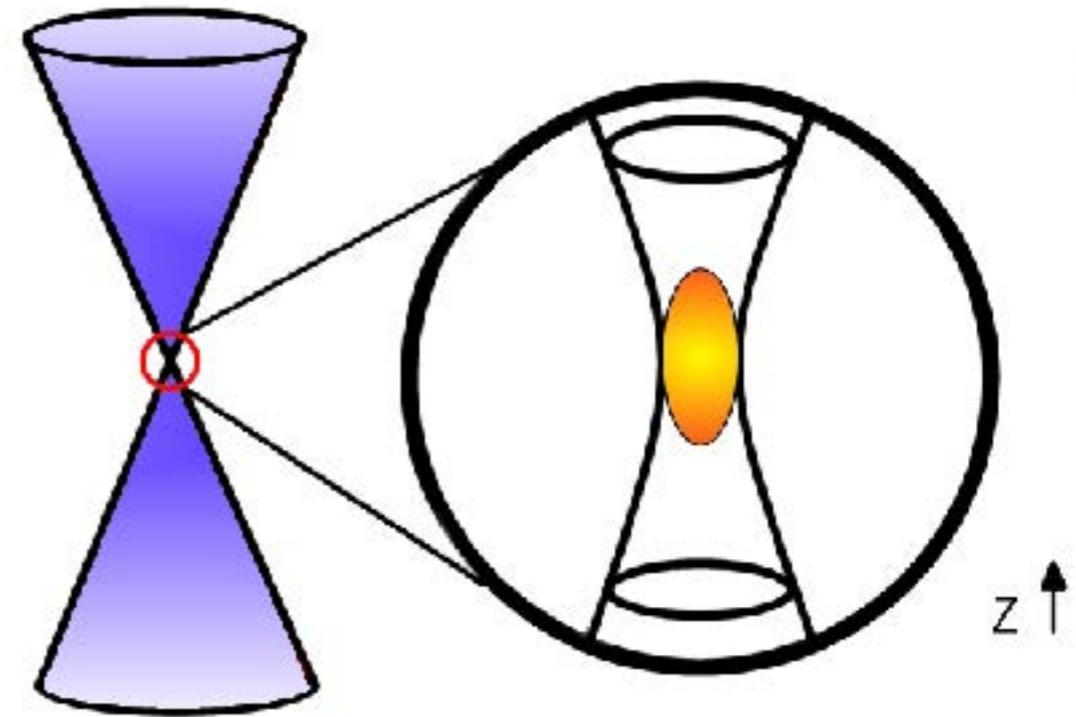
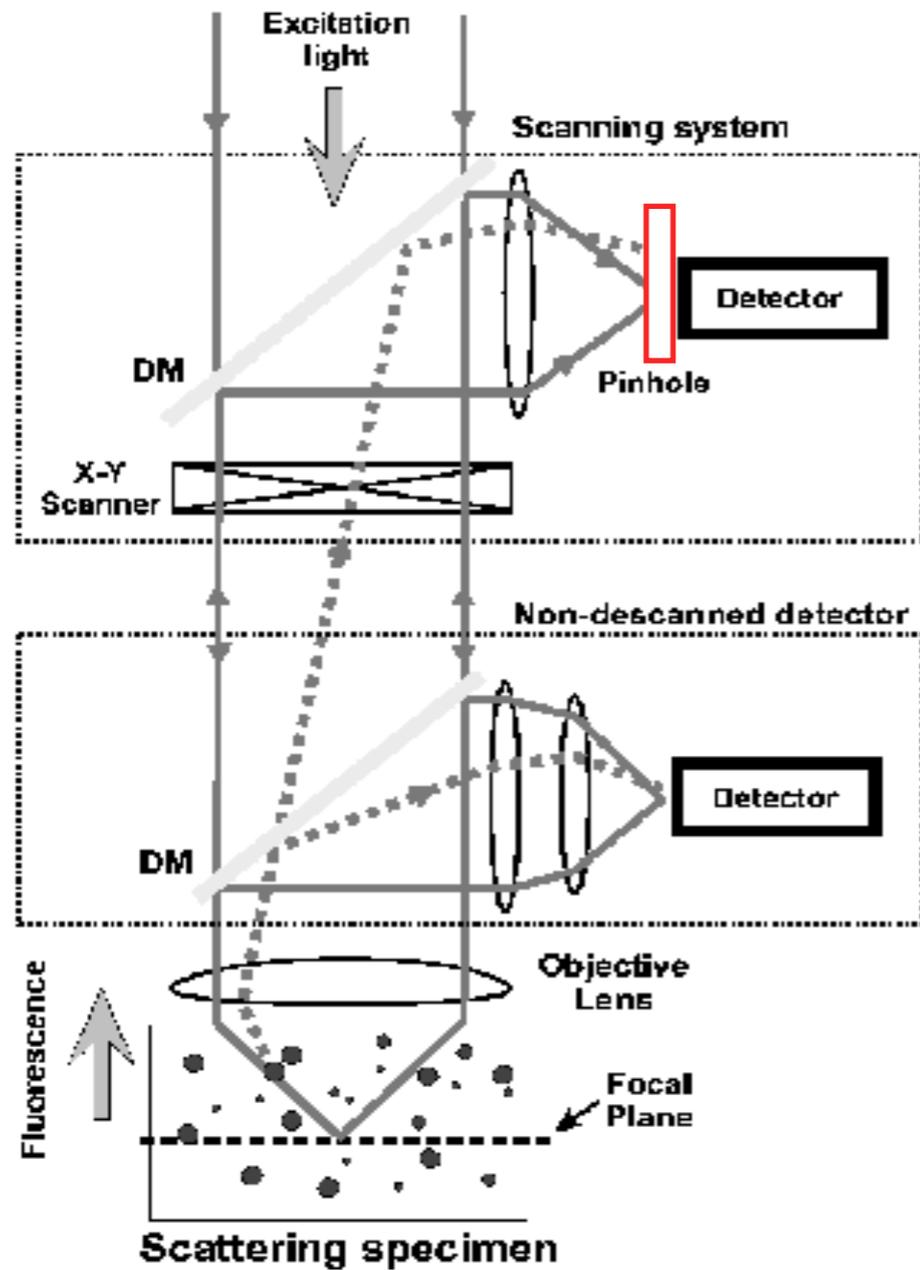


two-photon excitation (2pe) microscopy



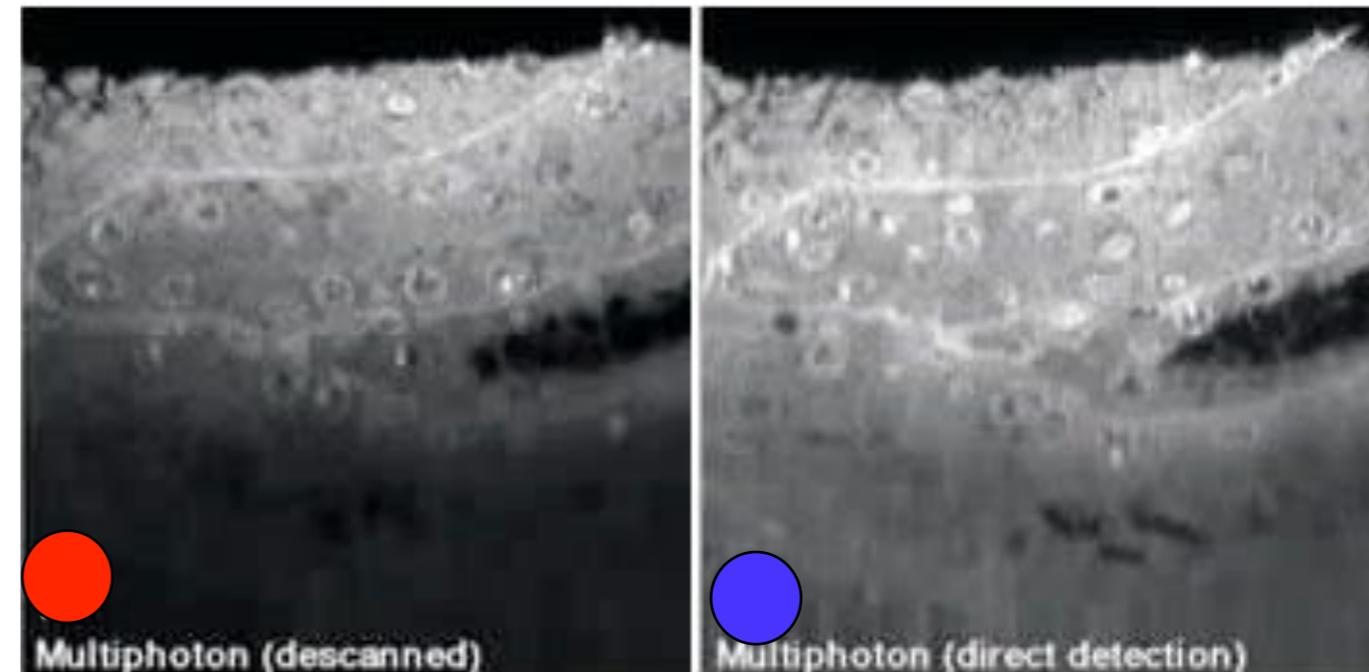
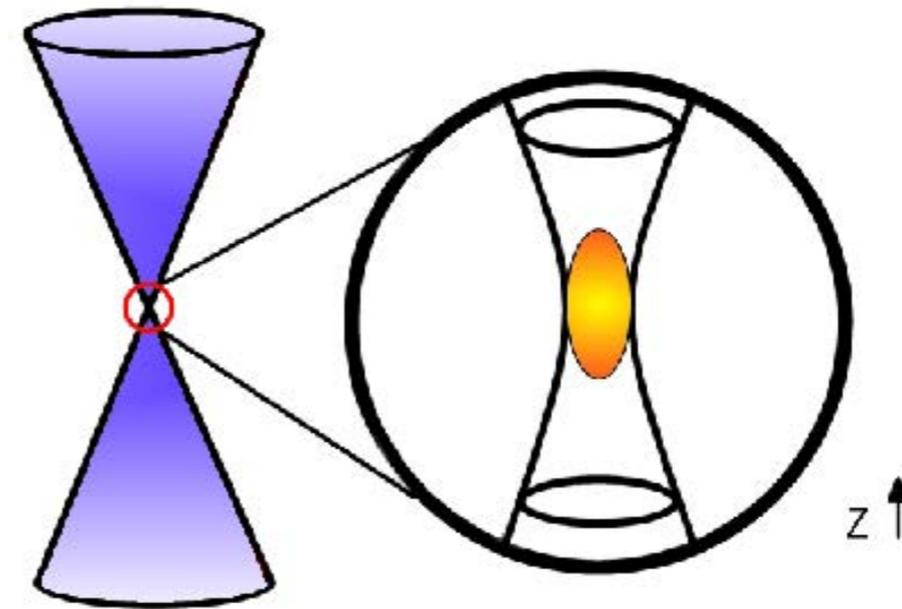
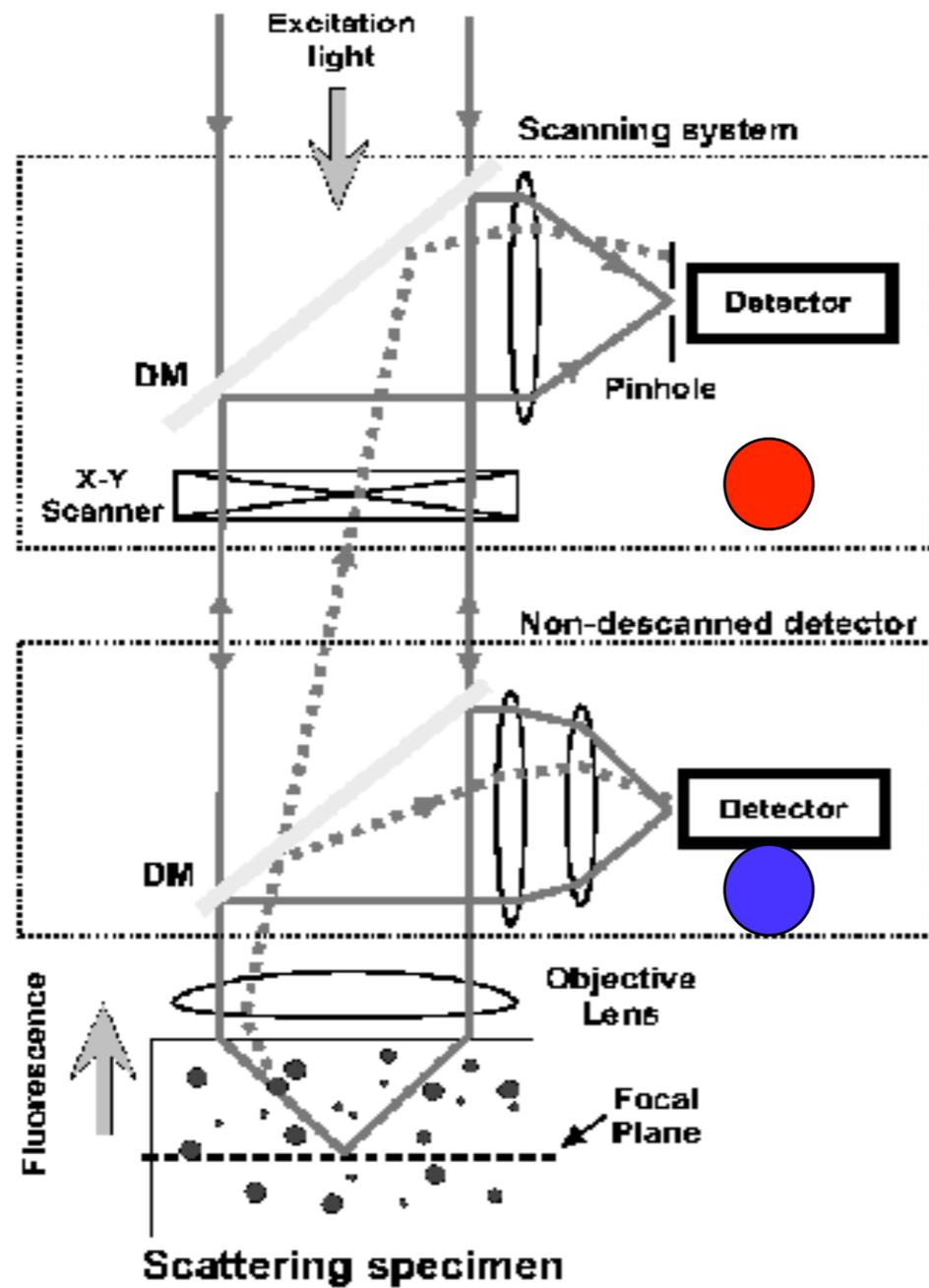
DIASPRO ET AL., MICROSC.RES.TECH., 47(3), 196-205, 1999

two-photon excitation (2pe) microscopy



C.SOELLER & M.B.CANNEL,
MICROSC.RES.TECH., 47(3), 182-195,
1999

two-photon excitation (2pe) microscopy



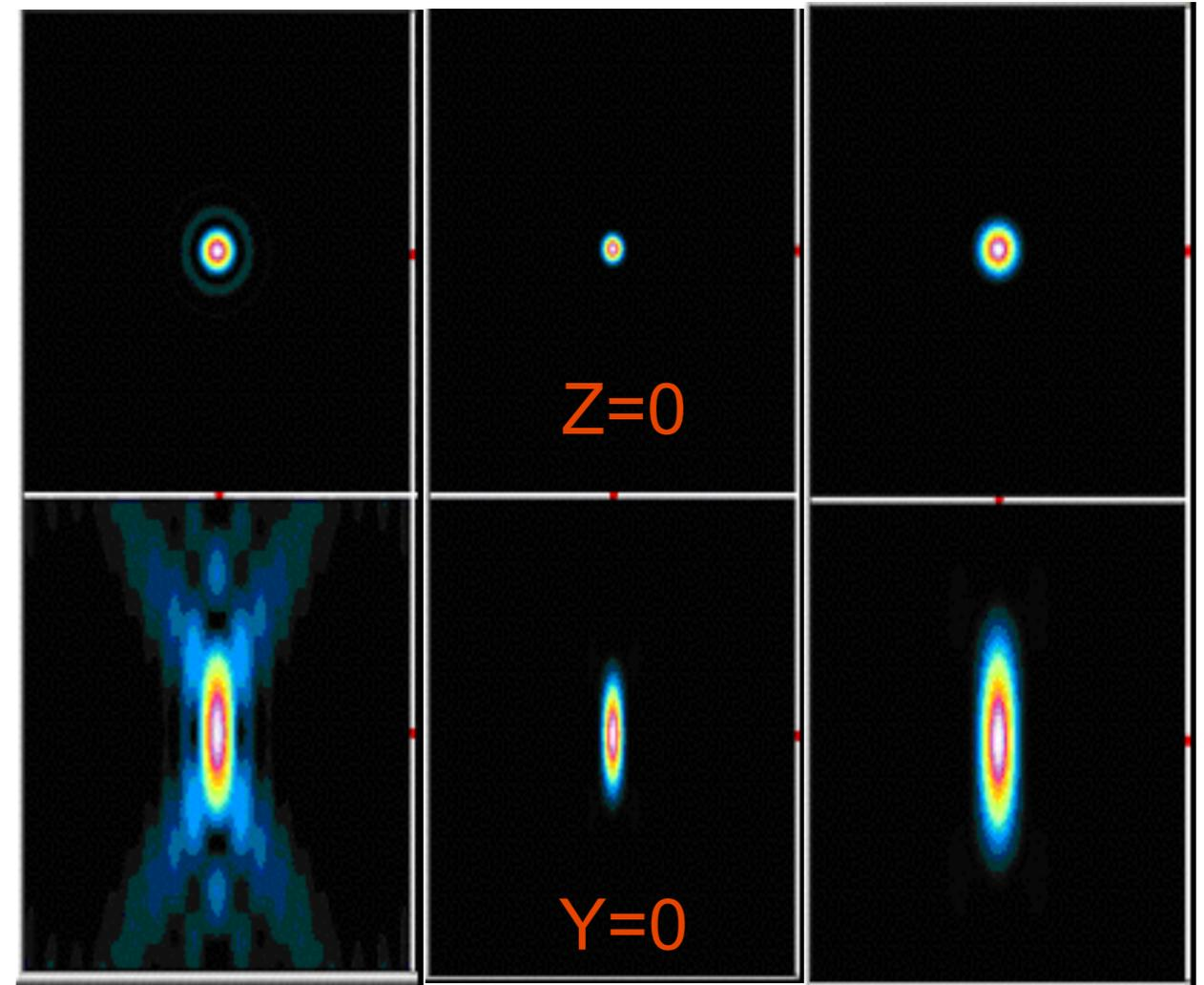
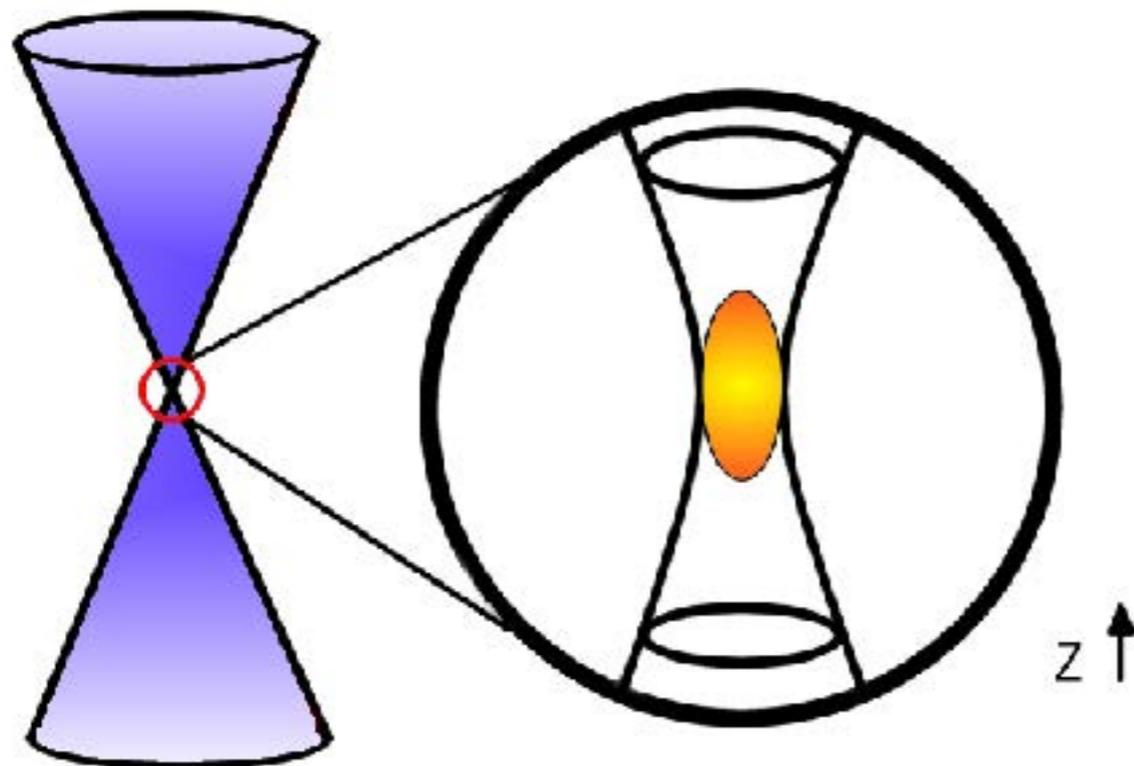
two-photon excitation (2pe) microscopy

➤ Confocal PSF:

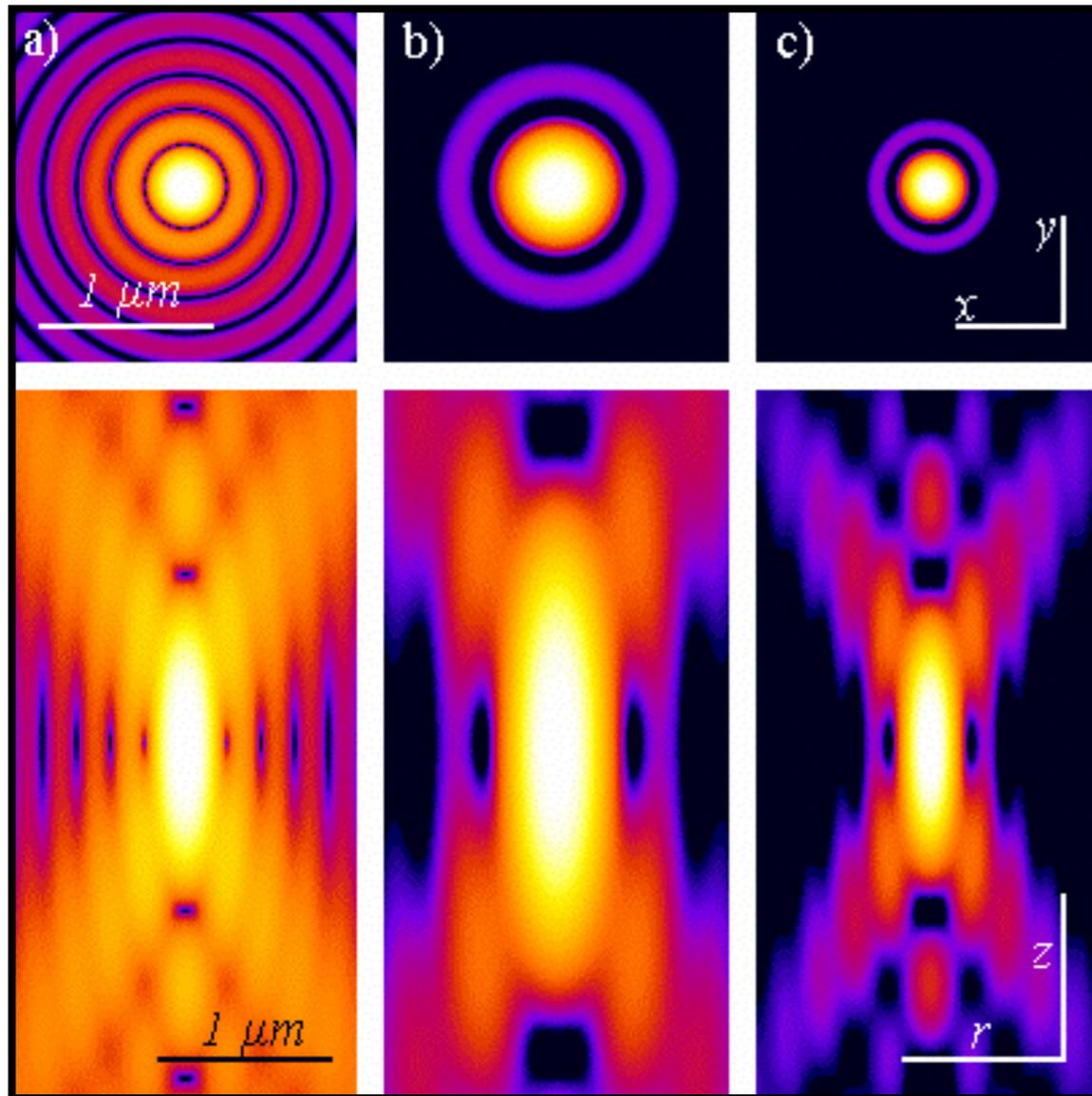
$$I_{fluor-conf} = I_{det} I_{ill} \rightarrow I^2 \propto \frac{1}{z^2} \frac{1}{z^2}$$

➤ 2-photon PSF:

$$I_{fluor-2\gamma} = [I_{ill}]^2 \rightarrow I^2 \propto \frac{1}{z^4}$$



two-photon excitation (2pe) microscopy



hi

$$PSF_{WF}(x, y, z) = h_{em}(x, y, z)$$

$$PSF_{CLS}(x, y, z) = h_{ex}(x, y, z) \times h_{em}(x, y, z) \cong$$

$$\cong (h_{ex}(x, y, z))^2$$

lo

$$PSF_{TPE}(x, y, z) = (h_{ex}(x, y, z))^2$$

FWHM	WF	CLS	TPE
Axial (μm)	0.83	0.58	1.03
Lateral (μm)	0.20	0.14	0.25

Computed PSFs (a) Wide-field (b) Two-photon (c) Confocal. All PSFs are computed using 100x/ 1.3 NA, $n=1.518$, single-photon λ_{ex} 488nm, two-photon λ_{ex} 900nm, λ_{em} 520nm. Logarithmic contrast.

Slide credit: Giuseppe Vicidomini, LAMBS-MicroScoBio, Genova

methods

Technique	Three-dimensional resolution	Acquisition speed	Photodamage, photobleaching	Tissue imaging depth
Deconvolution microscopy	Submicron resolution, but algorithms are computationally intensive	Depends on camera; fast acquisition, but slow deconvolution	High (depends on excitation wave-length). Whole sample exposed	Superficial (<40 μm), owing to light scattering
Confocal microscopy	Submicron resolution with pinhole aperture	Limited by scanhead design (typically two frames per second (2 fps), but 30 fps with resonant mirror or spinning disk)	High (depends on excitation wave-length). Whole sample exposed	Moderate (<80 μm), owing to light scattering
Two-photon microscopy	Submicron resolution, but slightly less than for confocal microscopy. Inherent optical sectioning with two-photon effect	Limited by scanhead design (typically 2 fps, but 30 fps with resonant mirror)	Low (long excitation wavelength). Excitation only in focal plane	Hundreds of microns (<500 μm , depends on tissue)

two-photon excitation (2pe) microscopy



This article can be downloaded for free from: <http://www.biomedical-engineering-online.com/content/5/1/36>

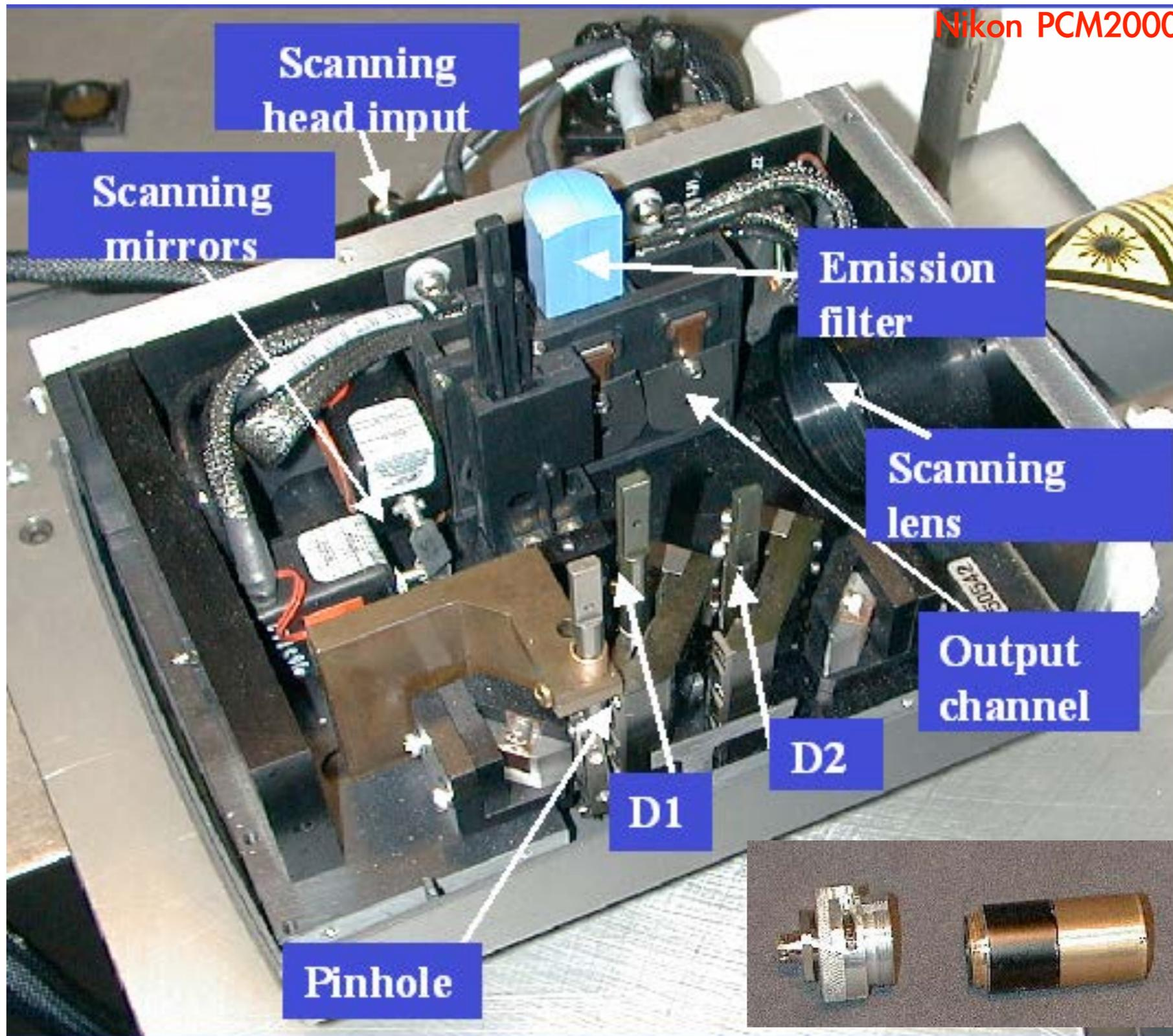
two-photon excitation (2pe) microscopy



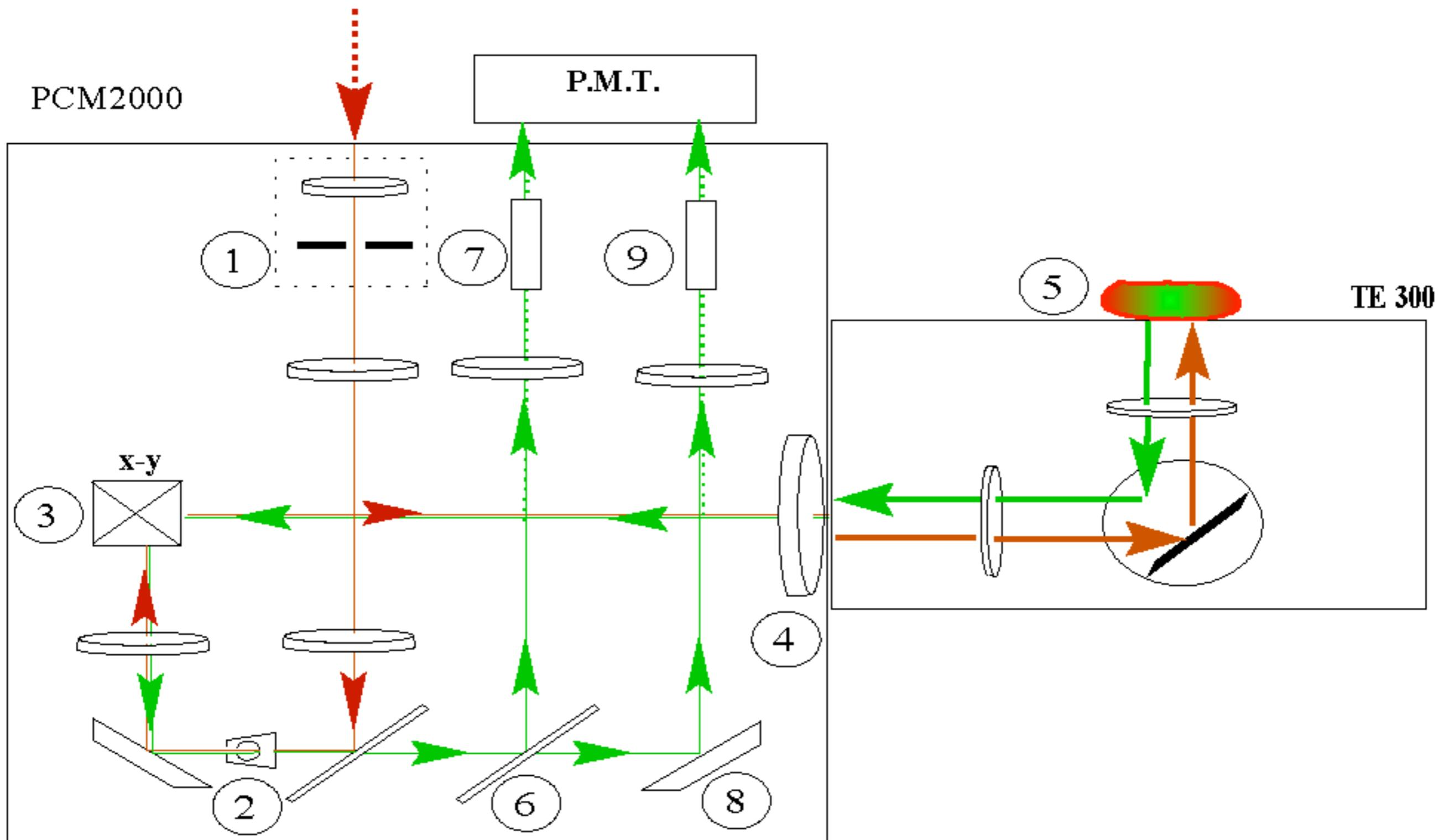
DIASPRO ET AL., MICROSC.RES.TECH., 47(3), 196-205, 1999

Alberto Diaspro, Nanoscopy, Istituto Italiano di Tecnologia

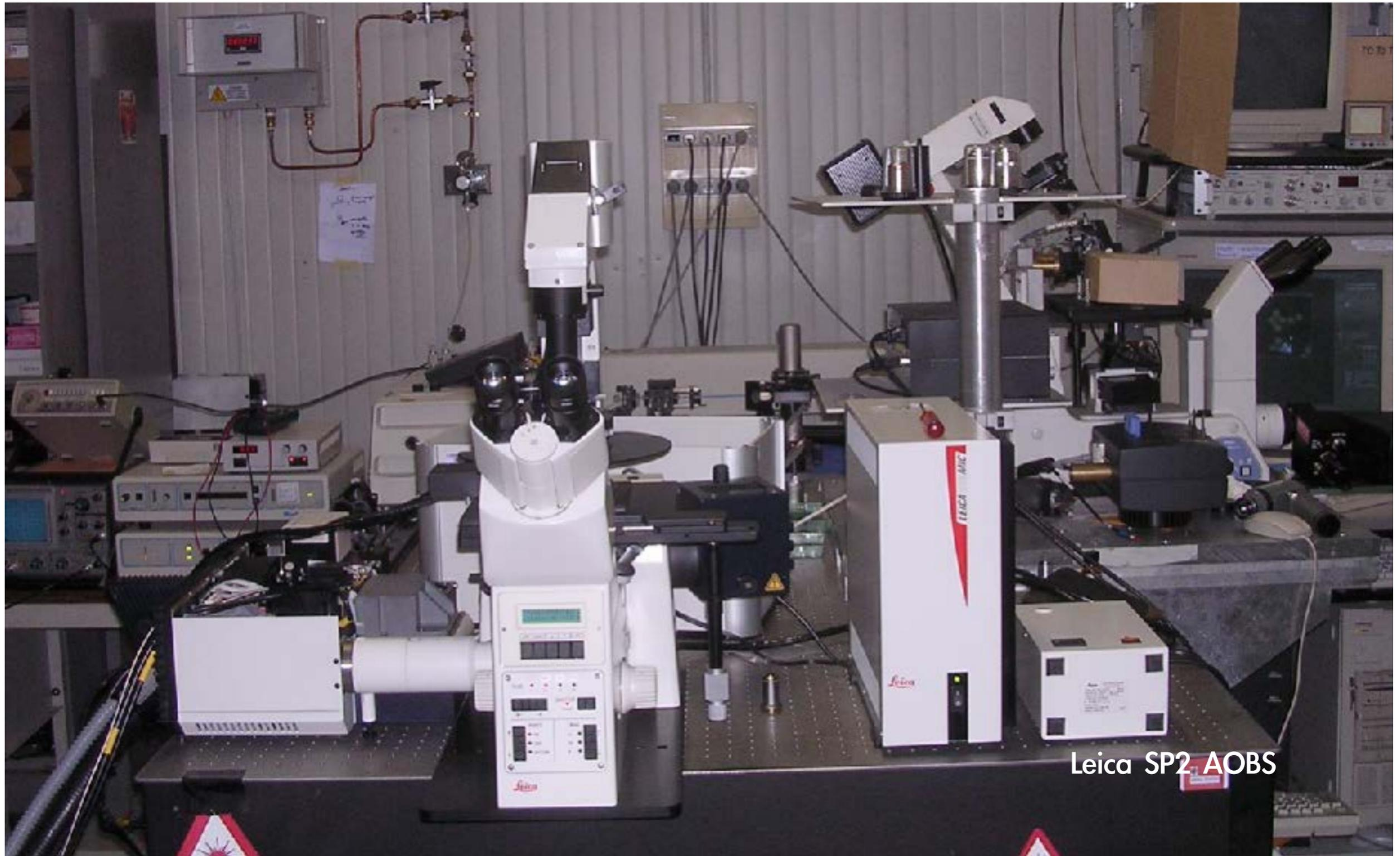
two-photon excitation (2pe) microscopy



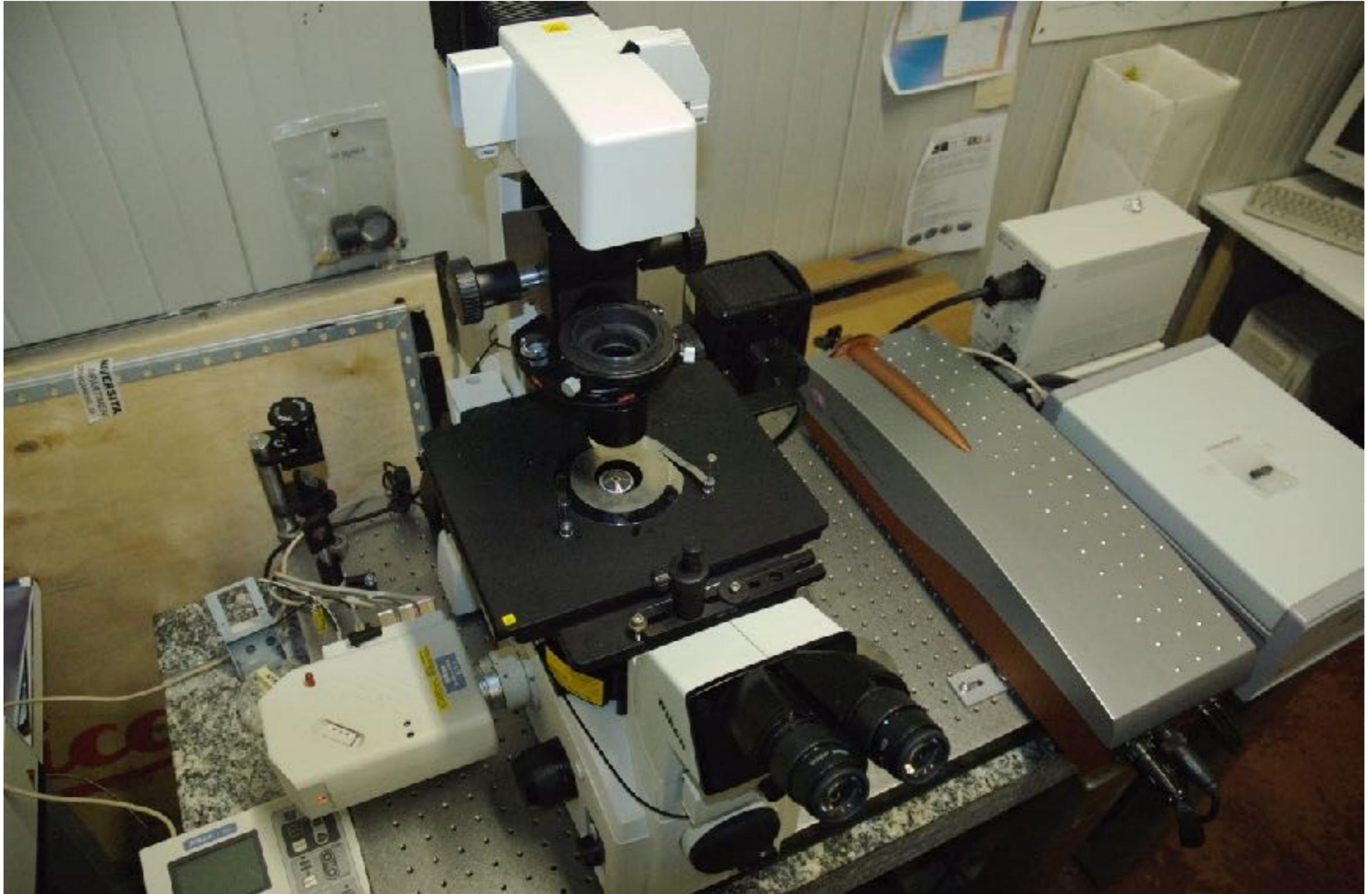
two-photon excitation (2pe) microscopy



two-photon excitation (2pe) microscopy



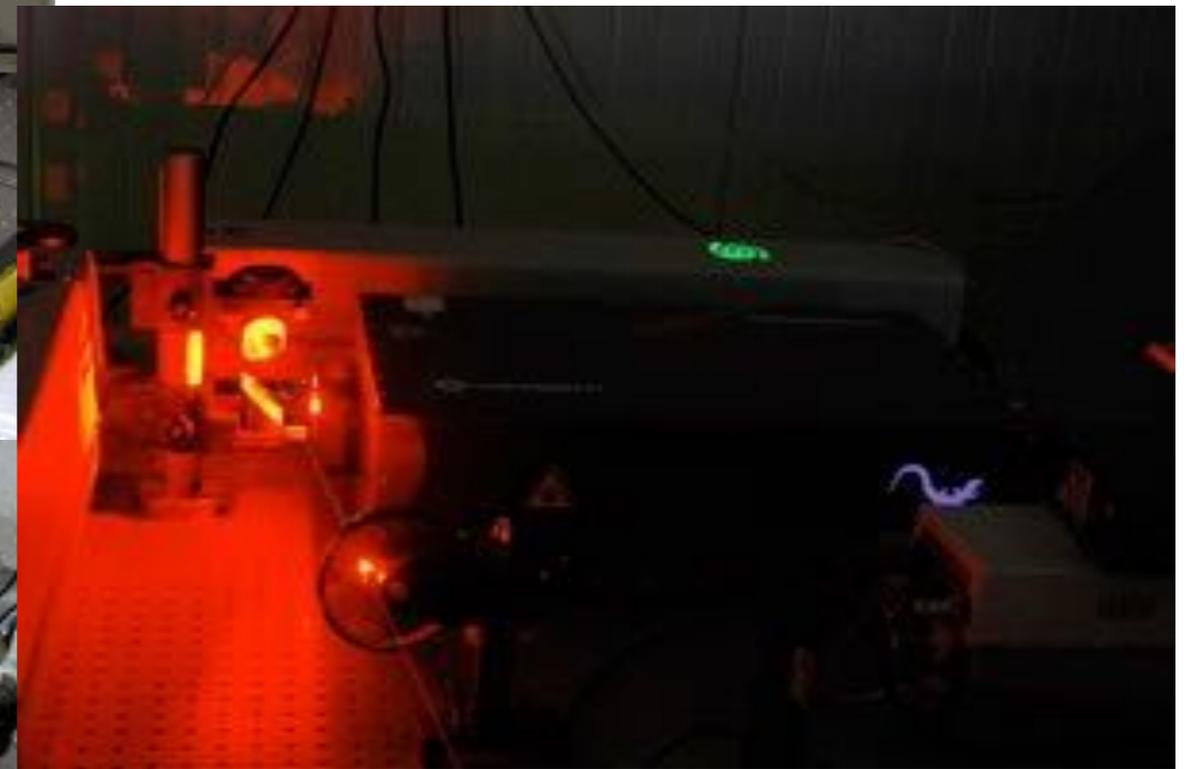
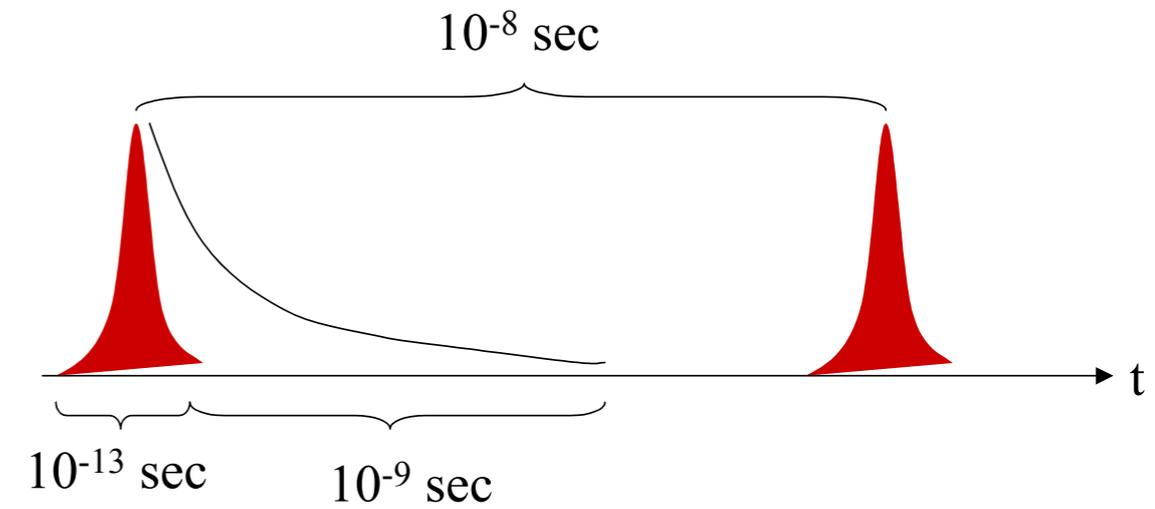
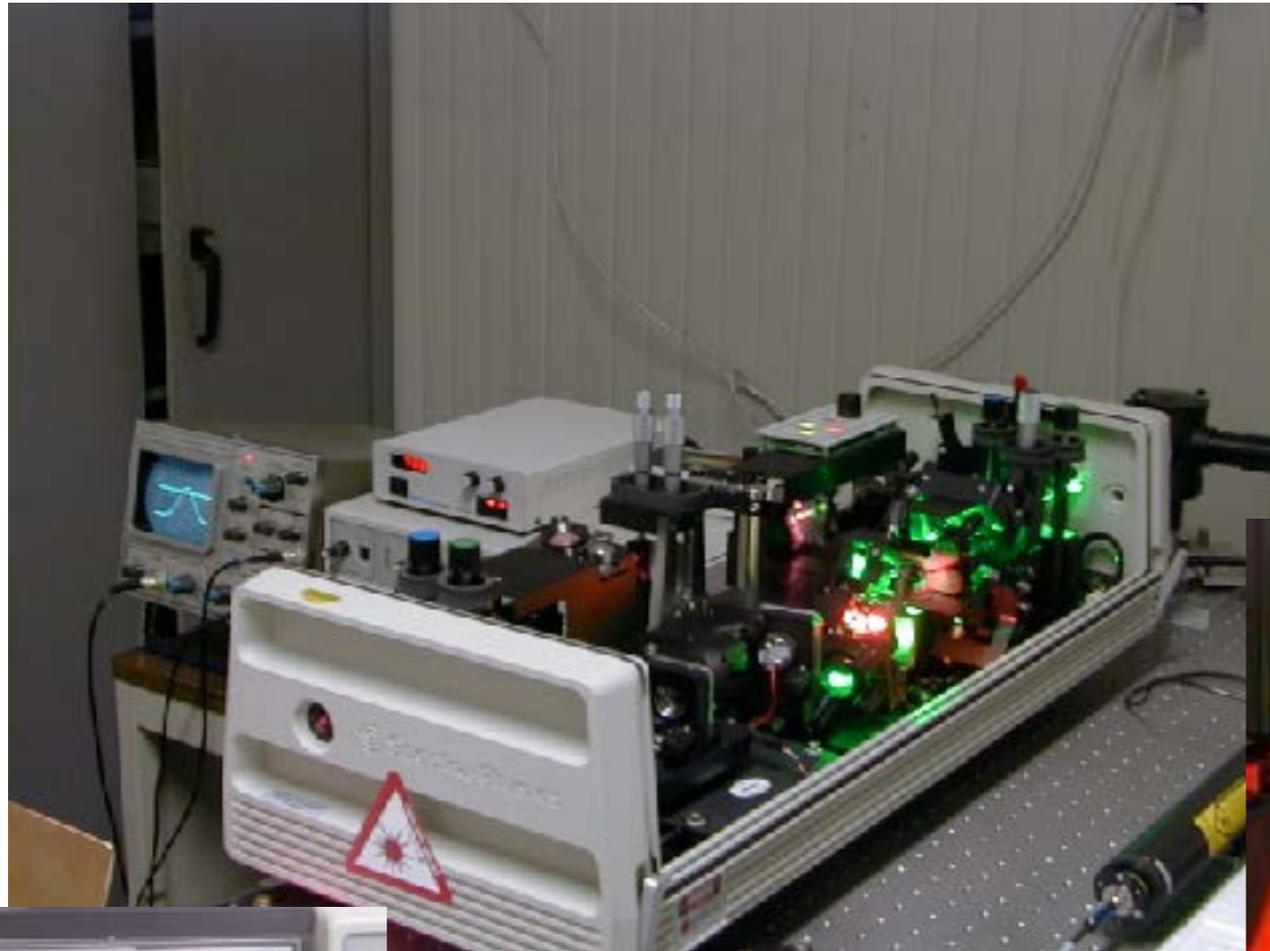
two-photon excitation (2pe) microscopy



Nikon spectral C1 - Two-photon Amplitude laser

Alberto Diaspro, Nanoscopy, Istituto Italiano di Tecnologia

two-photon excitation (2pe) microscopy



Tsunami-Millennia
(680-830/780-930),
Chameleon XR (720-980)

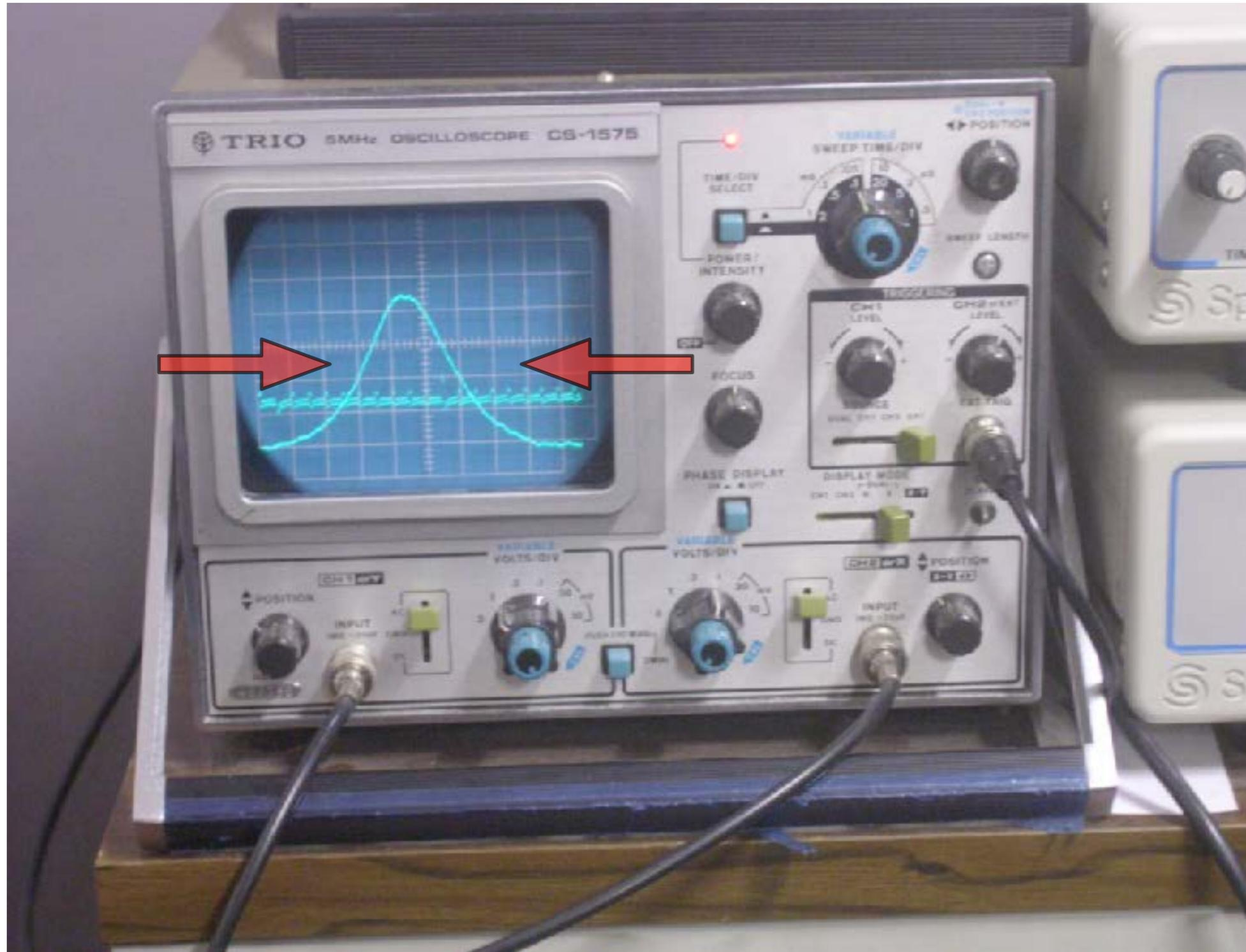
two-photon excitation (2pe) microscopy

copyright LAMBS/Paolo Bianchini



Ultrafast Laser Sources for Multiphoton excitation

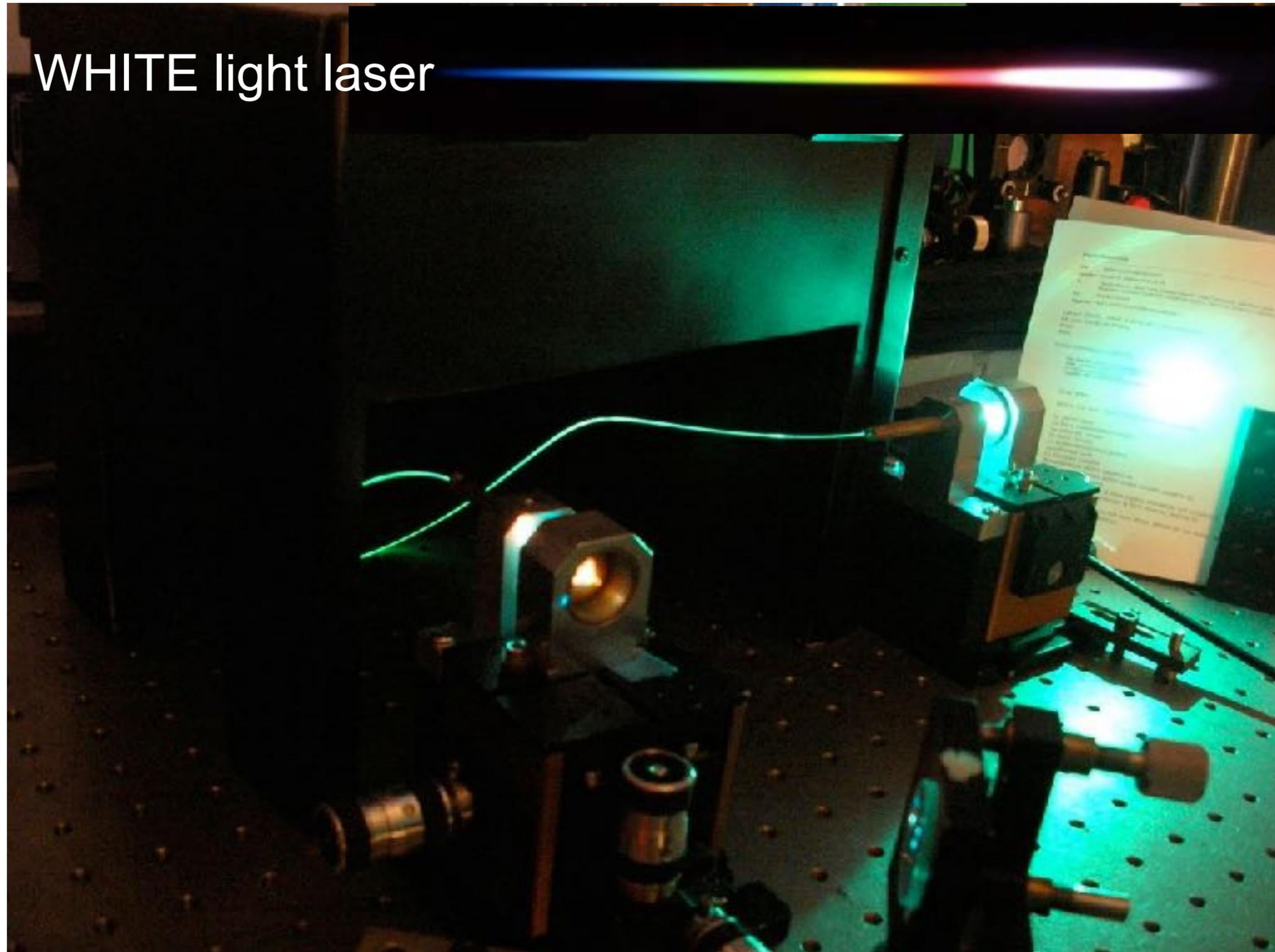
two-photon excitation (2pe) microscopy



A.DIASPRO, ET AL. QUART. REV. .BIOPHYS.,VOL.38, NR.2, PP.1-72 (2005).

Slide credit:Mario Arace, 1978

two-photon excitation (2pe) microscopy



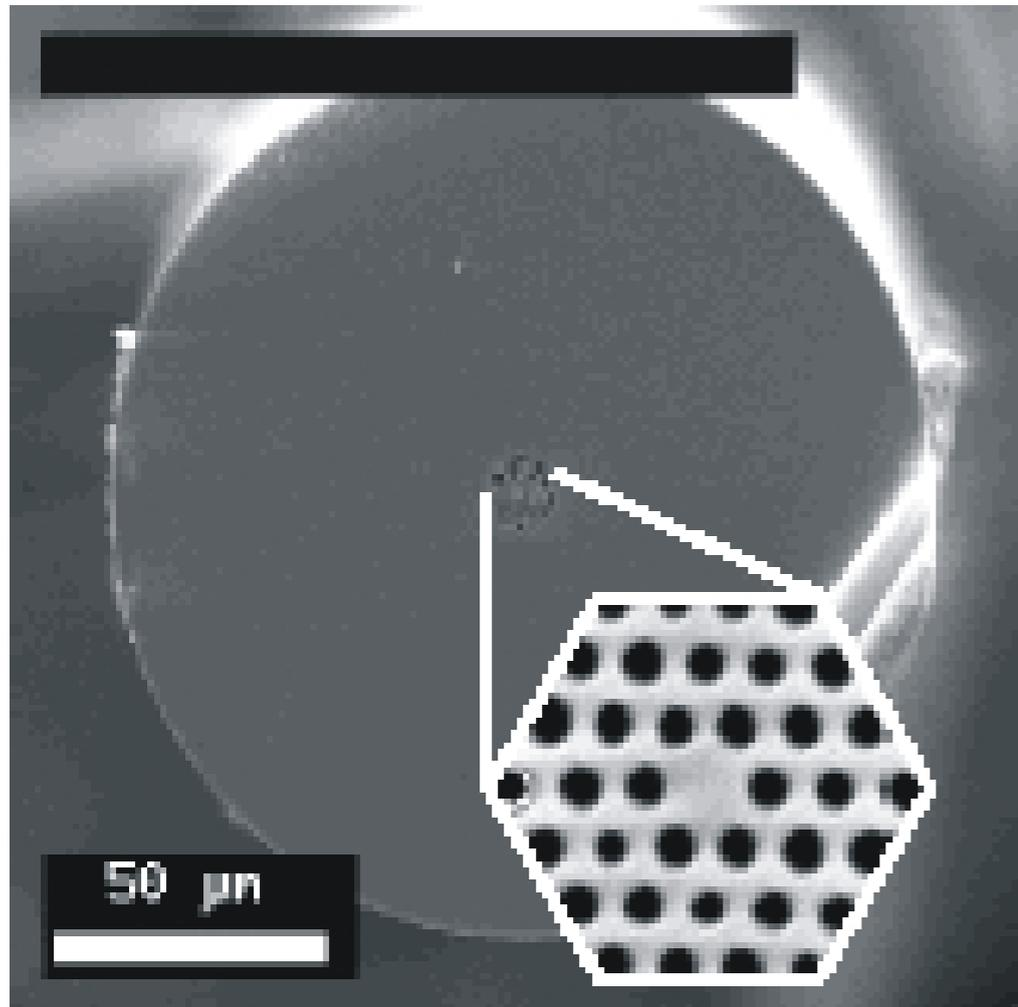
Caorsi V., Ronzitti E., Vicidomini G., Krol S., McConnell G., Diaspro A. (2007) *Micr. Res. Tech.*, 70

two-photon excitation (2pe) microscopy

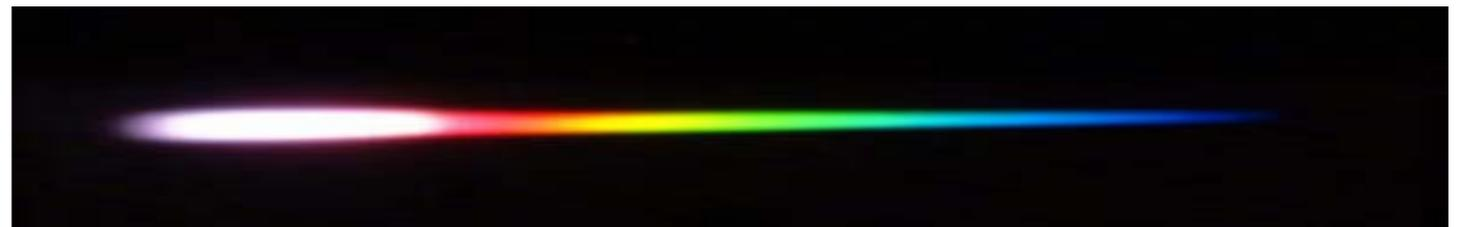
High propagating peak intensity from fs-pulsed sources enhances nonlinear processes:

Self-phase modulation + Raman shifting + four-wave mixing + other =

White-light supercontinuum

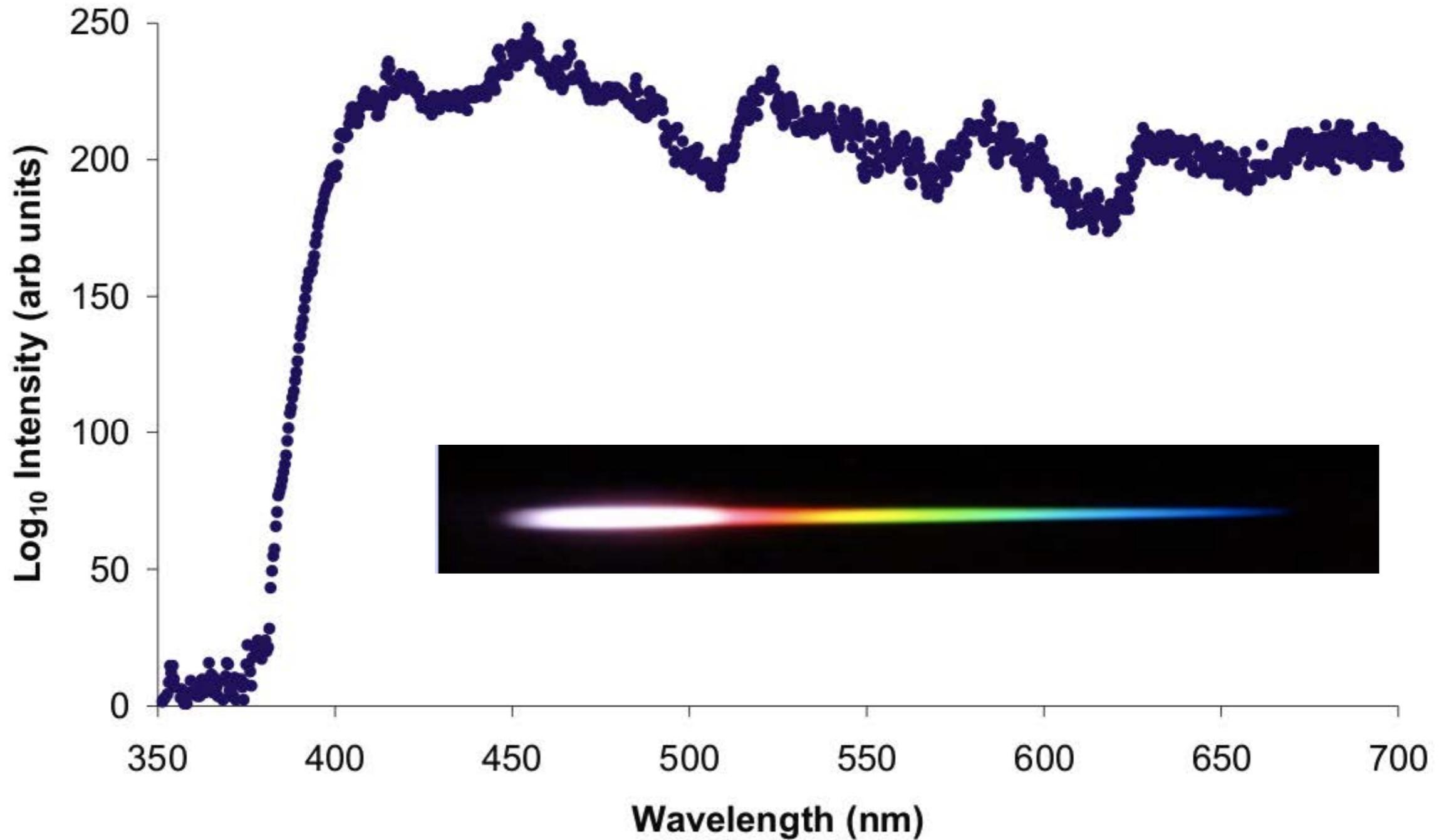


Courtesy of Crystal Fibre A/S



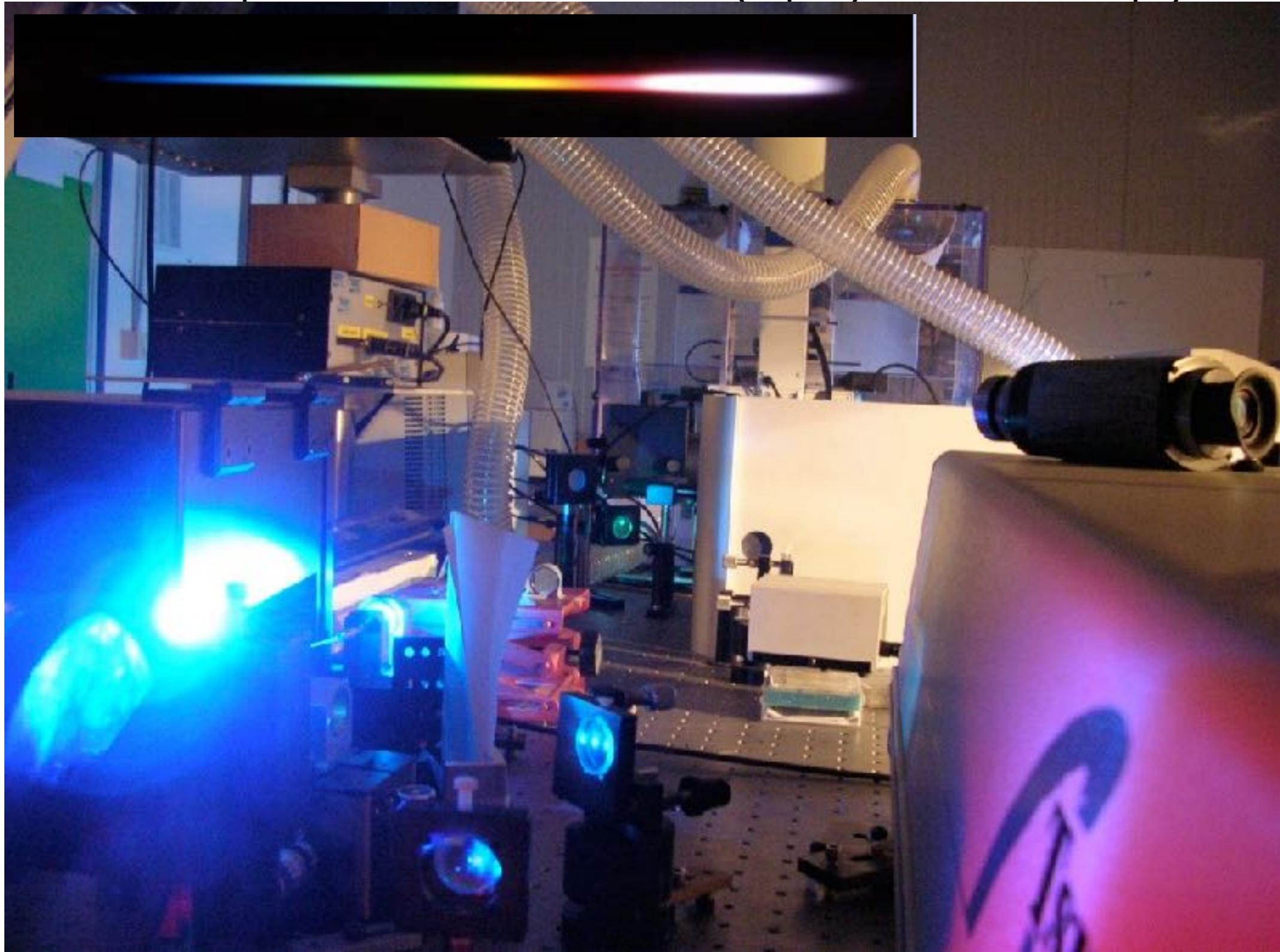
Courtesy Gail Mc Connel, John Girkin

two-photon excitation (2pe) microscopy



Courtesy Gail Mc Connel, John Girkin

two-photon excitation (2pe) microscopy



Caorsi V., Ronzitti E., Vicidomini G., Krol S., McConnell G., Diaspro A. (2007) Micr. Res. Tech., 70

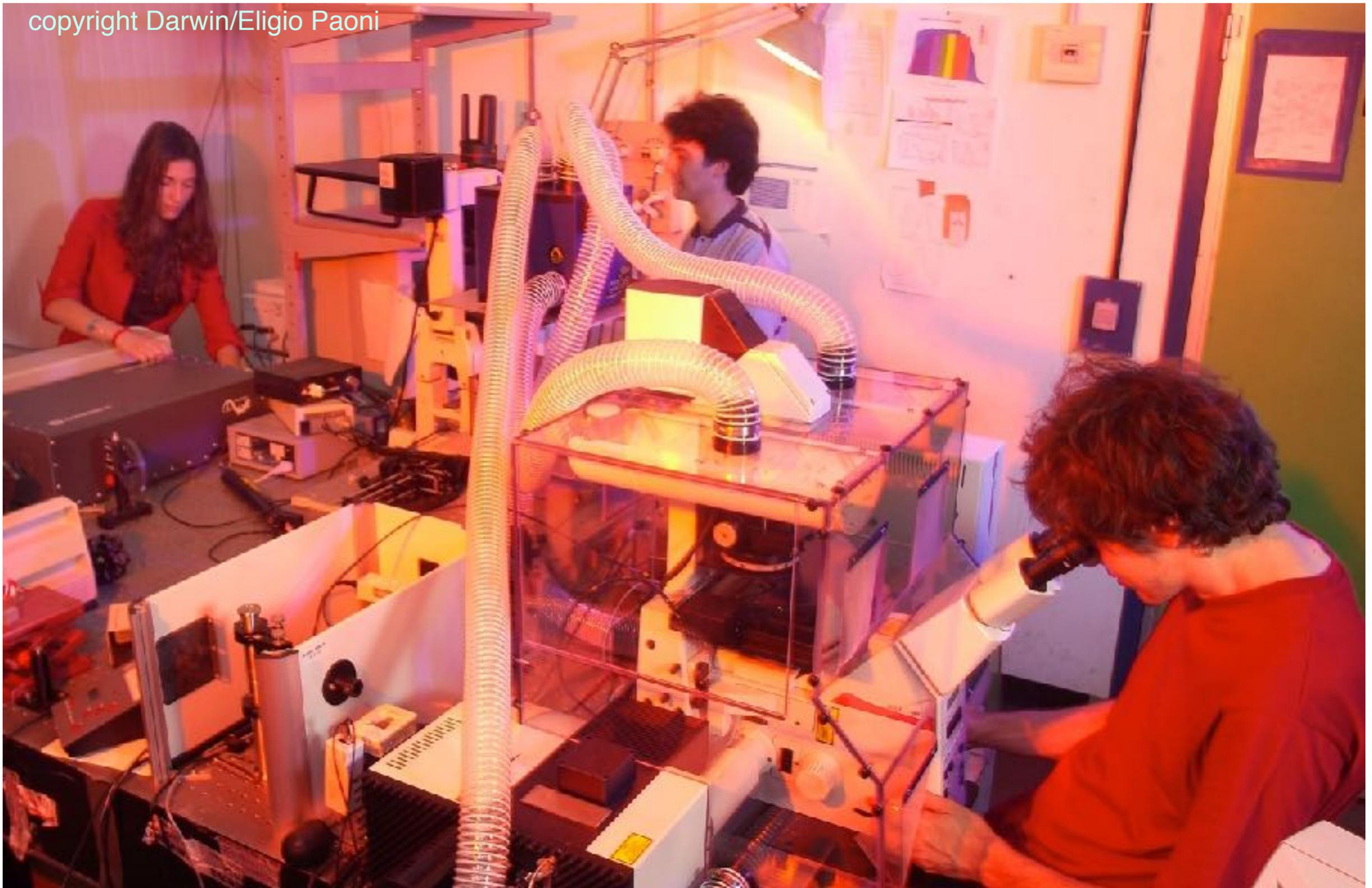
two-photon excitation (2pe) microscopy

Laser Material	Company; Model	Wavelength /nm	Pulse Length	Repetition Rate	Power	Comments
Ti:Sapphire	Coherent; Mira	700-980	<200fs	76MHz	0.7W 1.3W	May require mirror change for full tuning
	Spectra Physics; Tsunami	700-1000	<100fs (or 2ps as option)	80MHz	0.8W 1.4W	May require mirror change for full tuning
	Coherent; Chameleon - XR	705-980	<140fs	90MHz	1.7W	Hands free operation, computer controlled, compact design, single box
	Spectra Physics; Mai Tai	710-990	120fs	80MHz	1.5W	Hands free operation, computer controlled, compact design, single box
	Time Bandwidth; Pallas	780-860	<100fs	75MHz	500mW	
	Time Bandwidth; Tiger	780-860	<100fs	100MHz	400mW	
	Femtosource	750-850	<12fs	75MHz	400mW 600mW	
Nd:YLF	MicroLase/Coherent Scotland; BioLite	1047	200fs	120MHz	500mW	Not presently available
Nd:Glass	Time Bandwidth; GLX200	1058	<250fs	100MHz	>400mW	
Ytterbium	Amplitude Systems	1030	<200fs	50MHz	1W	Demonstrated on dyes inc Texas Red and GFP; optional 950-1150 selectable
Cr:LiSAF	Highglasers	850nm	100fs	50MHz	>1--mW	
OPO	Coherent and Spectra Physics	350-1200	100fs		~200mW	Exact parameters depends crystal selected. Requires TiSapphire as pump source

A.DIASPRO, ET AL. QUART. REV. .BIOPHYS.,VOL.38, NR.2, PP.1-72 (2005).

two-photon excitation (2pe) microscopy

copyright Darwin/Eligio Paoni



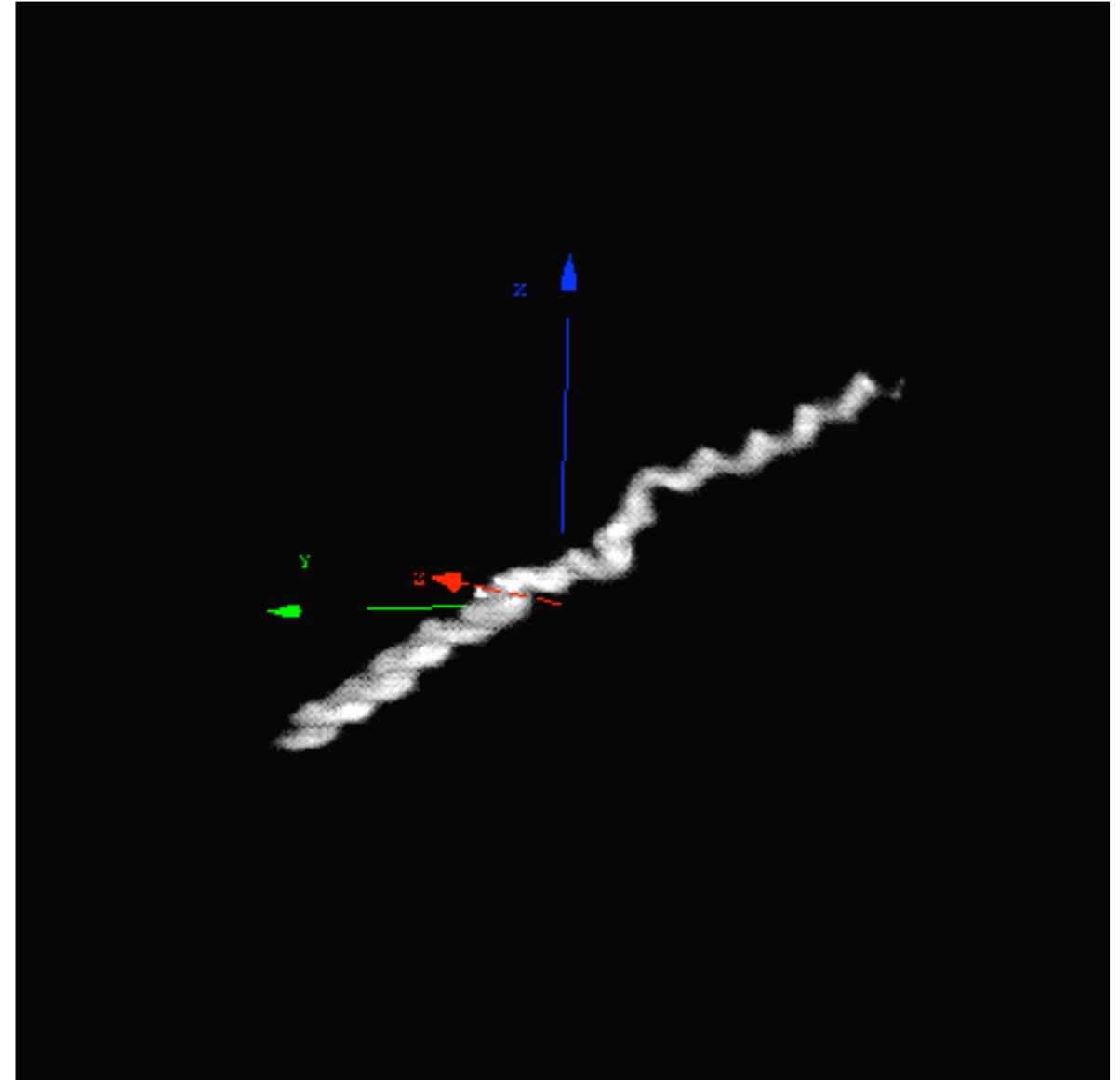
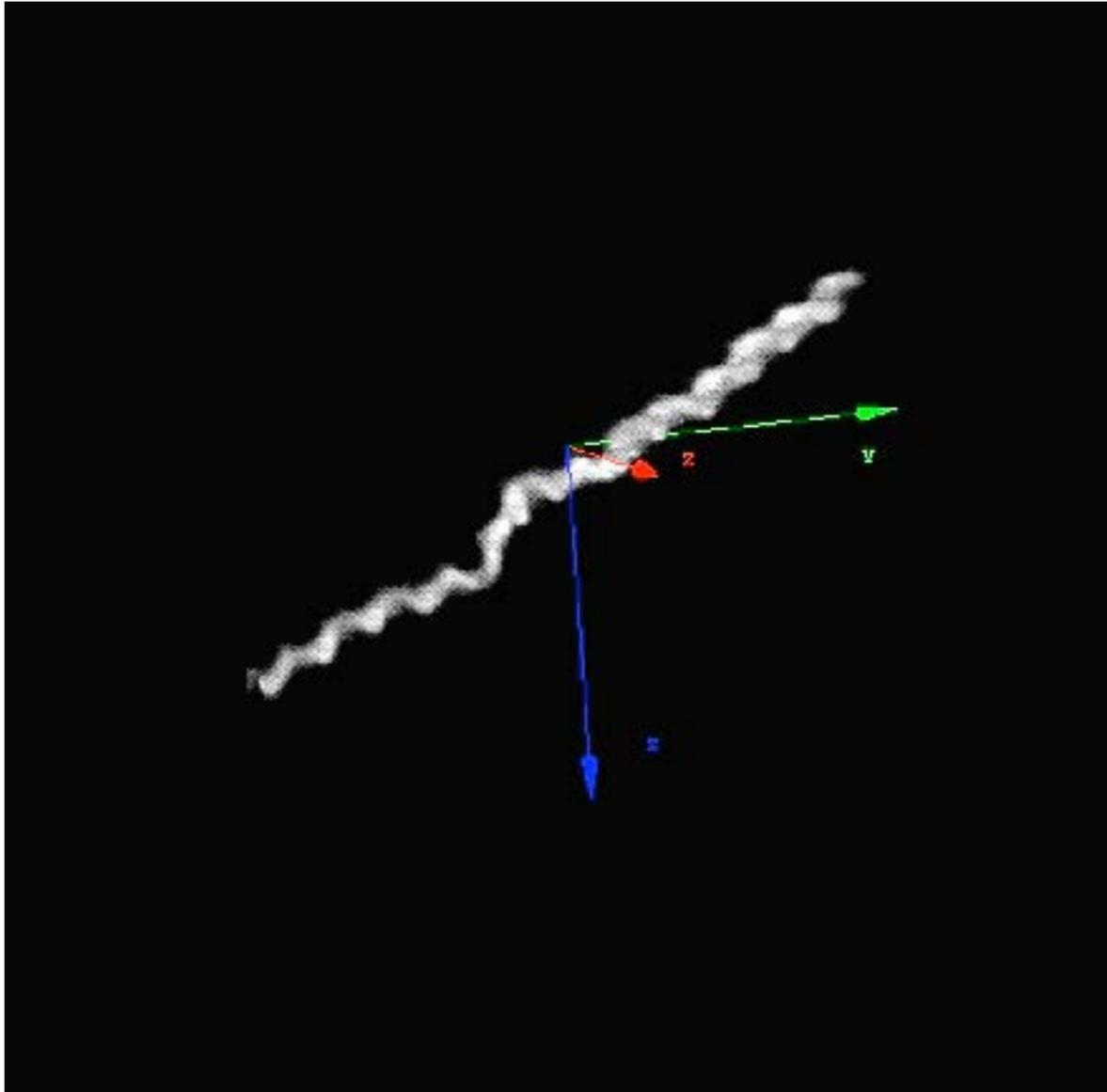
two-photon excitation (2pe) microscopy



DIASPRO ET AL., MICROSC.RES.TECH., 47(3), 196-205, 1999

Alberto Diaspro, Nanoscopy, Istituto Italiano di Tecnologia

two-photon excitation (2pe) microscopy

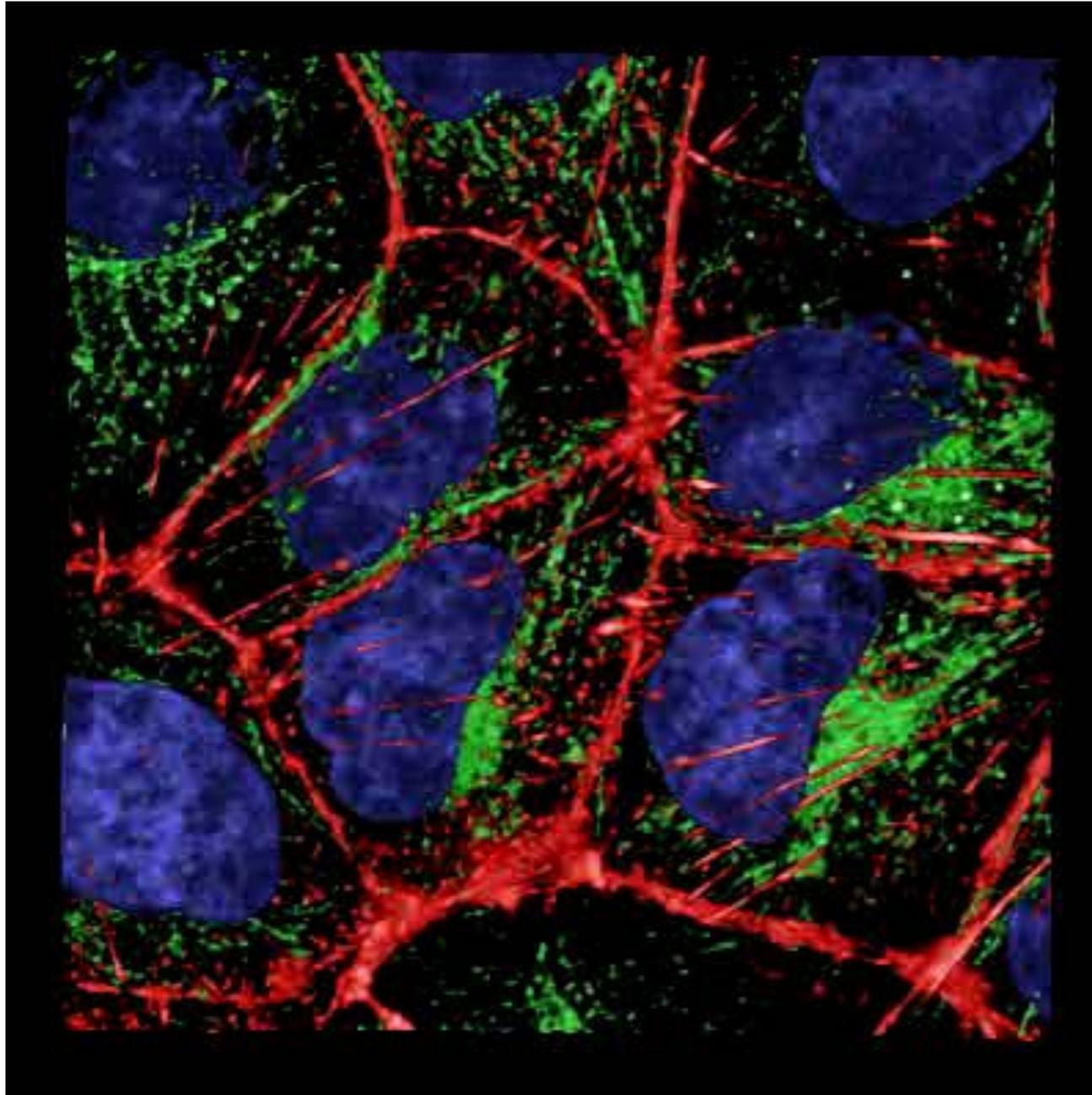


Eledone cirrhosa (octopus) sperm heads

DIASPRO ET AL., MICROSC.RES.TECH., 47(3), 196-205, 1999

Slide credit: Silvia Scaglione, Francesco Difato

two-photon excitation (2pe) microscopy



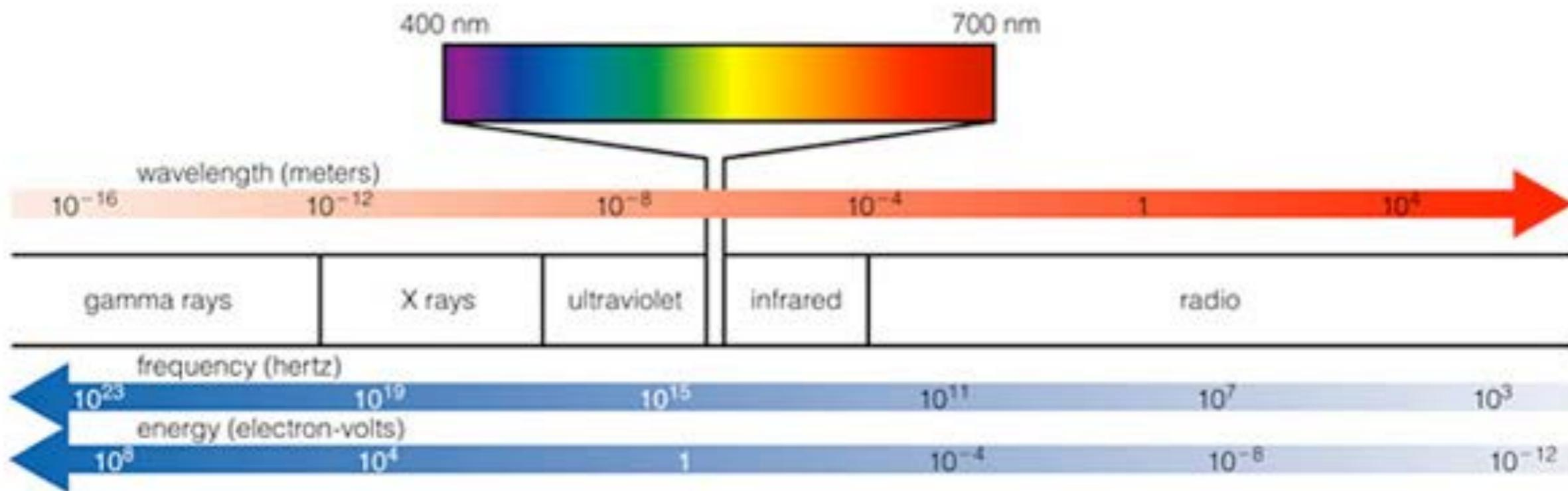
Tissue cultured PTR cells, TexasRed-Phalloidin, FITC-a tubulin, and DAPI.
(Drs. Wang and Dunn, ICBM)



Two photon volume of dapi labeled nuclei and fluorescein labeled anti-cadherin.
(Dr. Dunn, ICBM)

two-photon excitation (2pe) microscopy

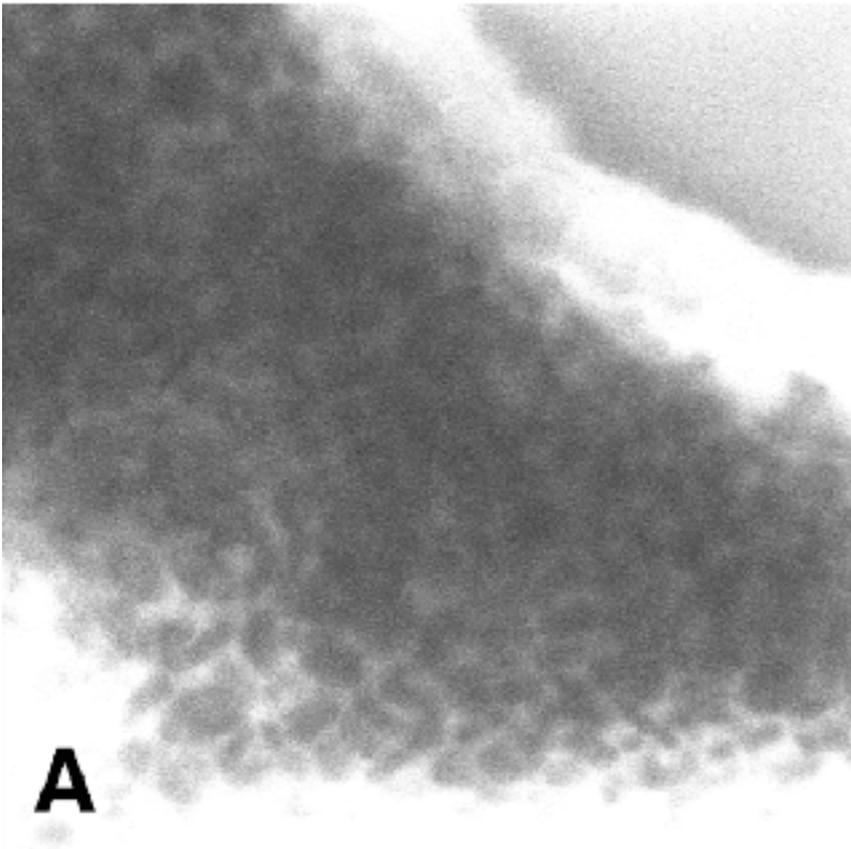
Wavelengths shifted to the red



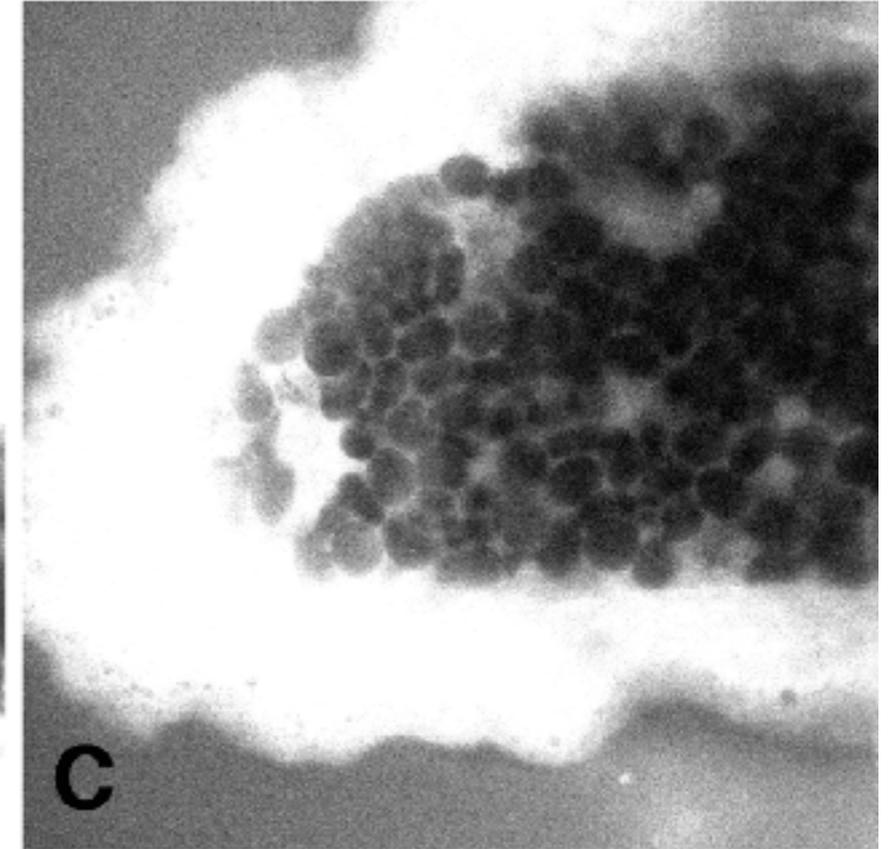
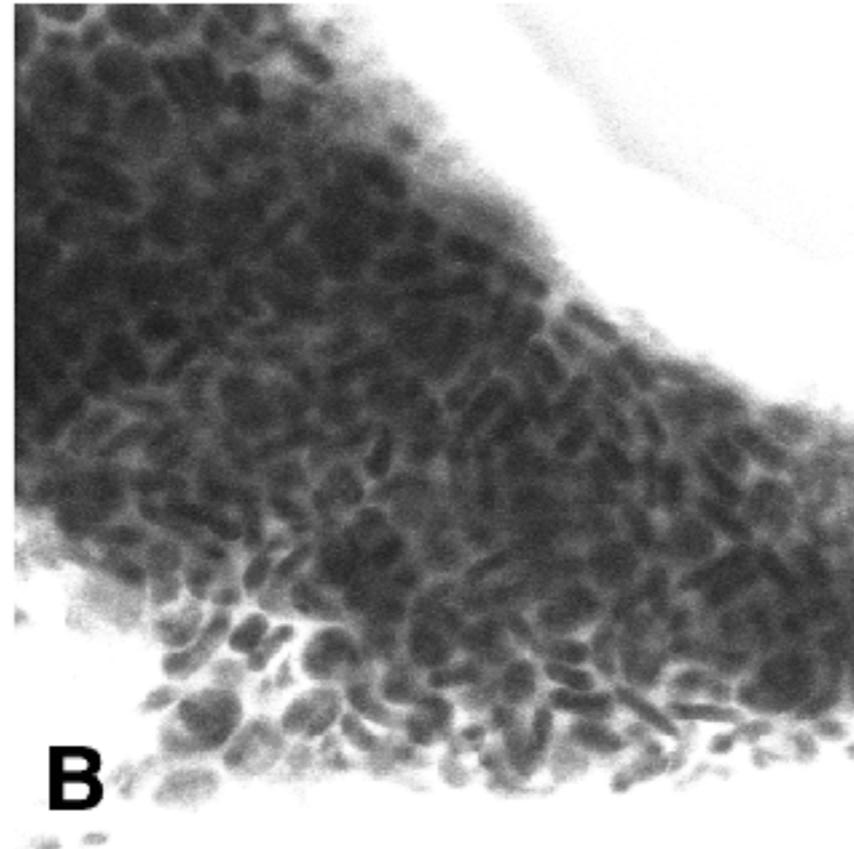
two-photon excitation (2pe) microscopy

One-Photon

Two-Photon



70 μm Deep

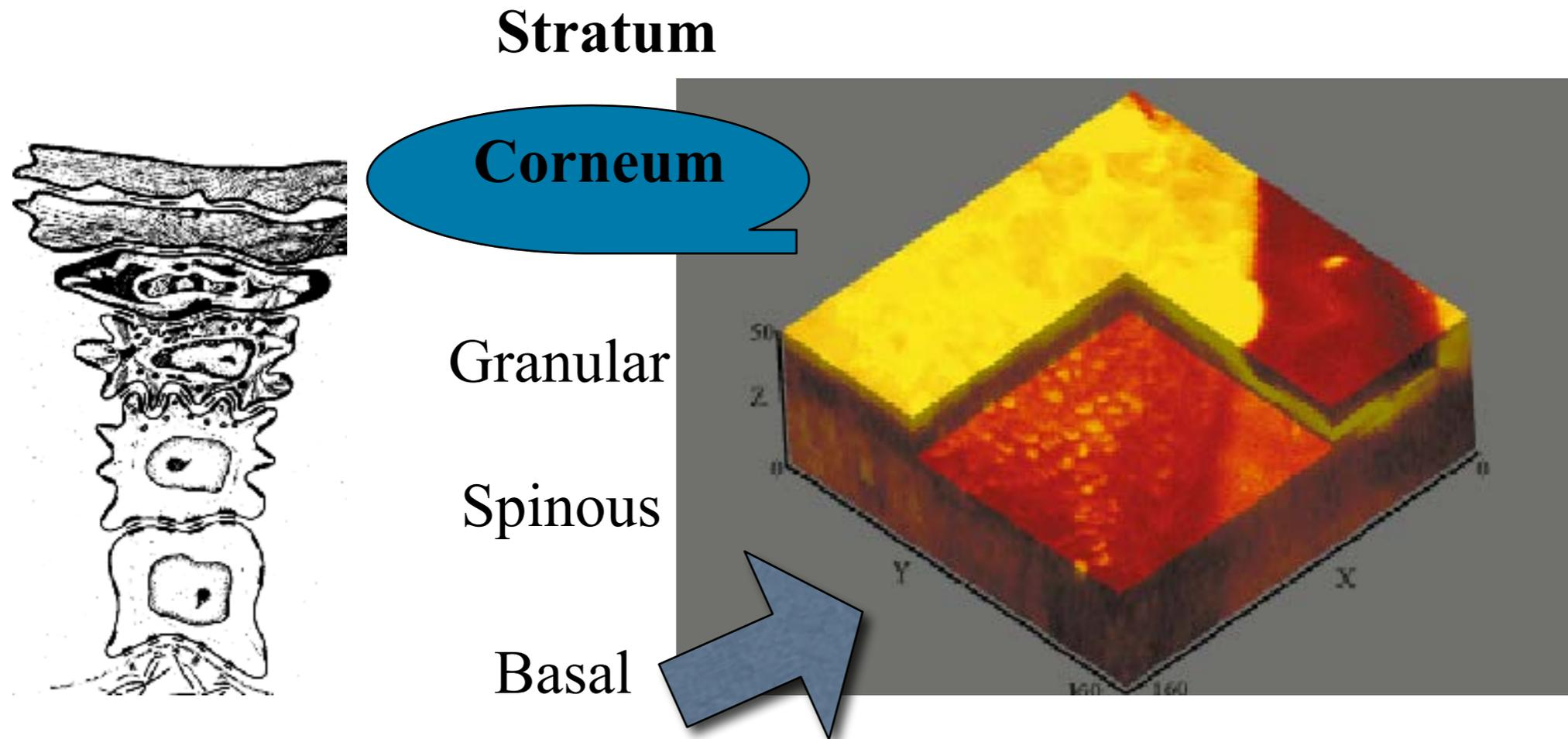


140 μm Deep

Images of a Shark Choroid Plexus Stained with Fluorescein

Piston DW (2005), PLoS Biol 3(6): e207

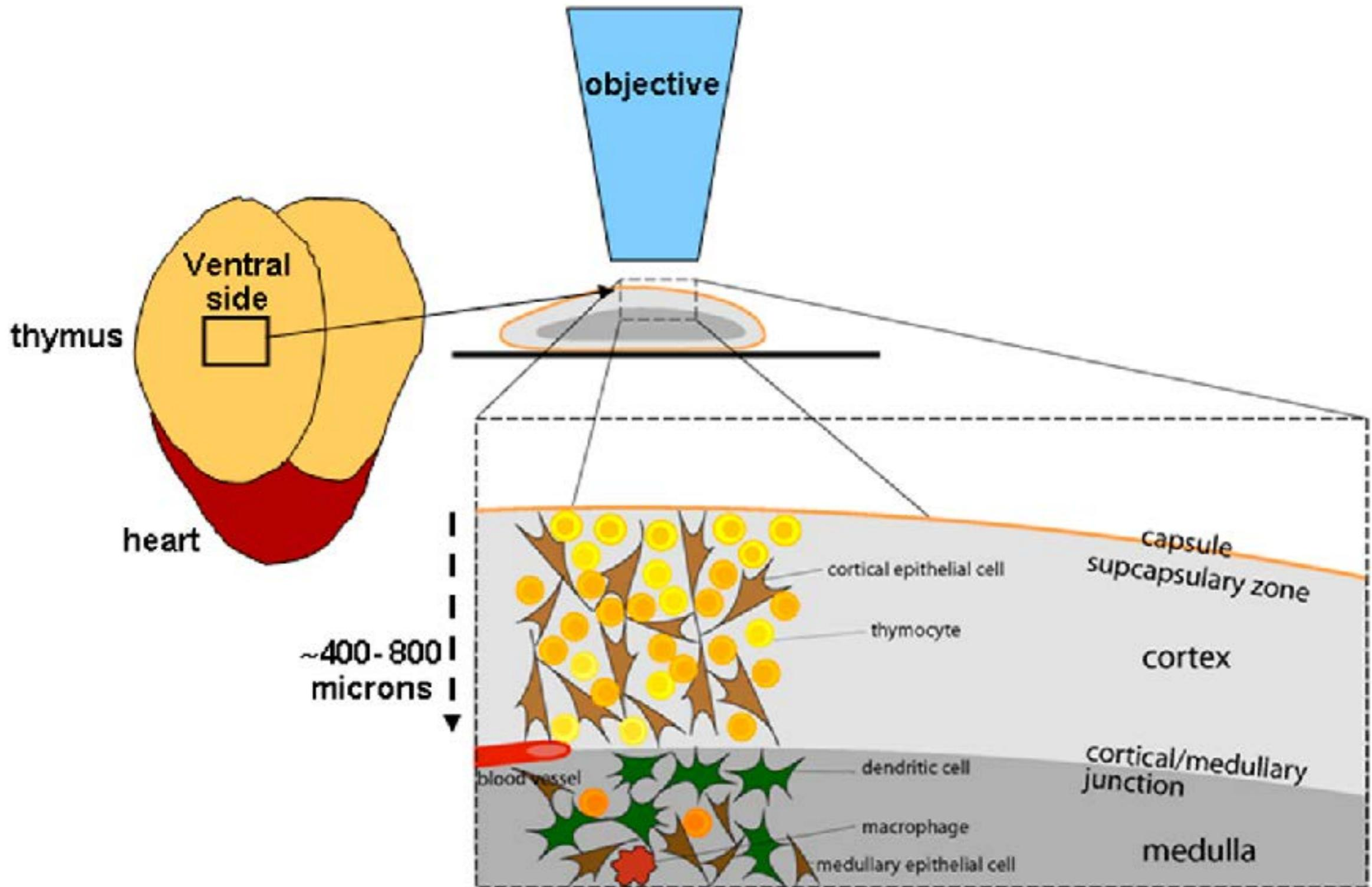
two-photon excitation (2pe) microscopy



Three-dimensional reconstructed two-photon images of in vivo human skin. The strata corneum and the basal layers are clearly visible.

(Image credit: PETER SO, BARRY MASTERS)

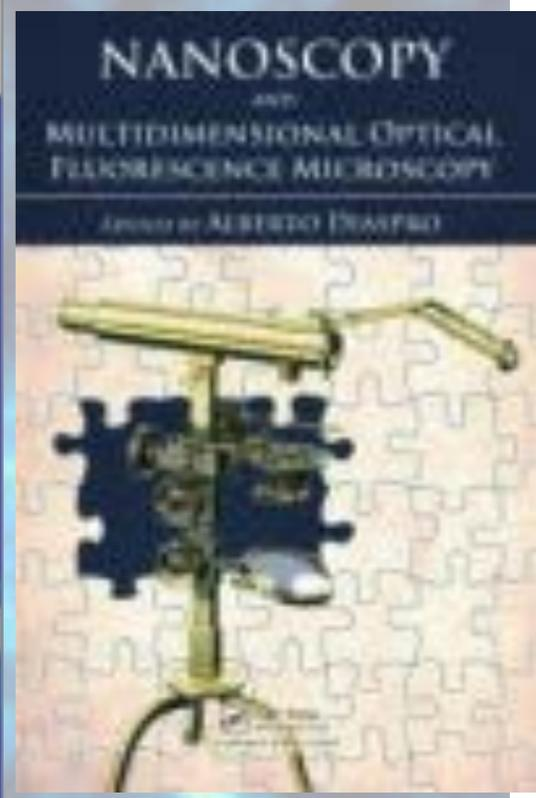
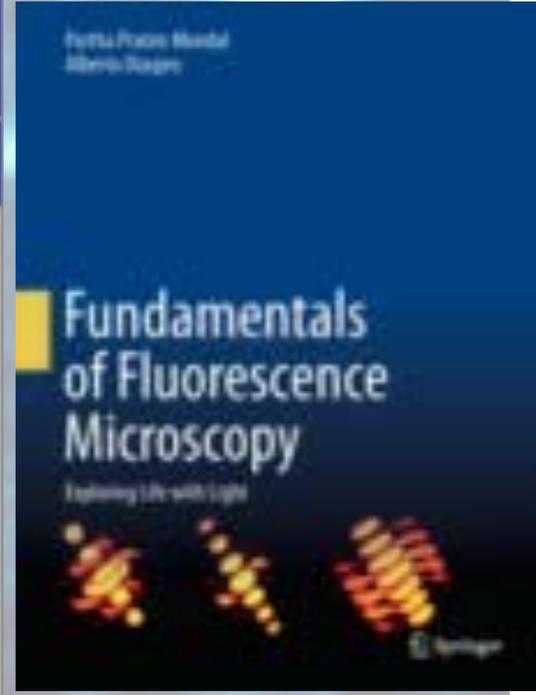
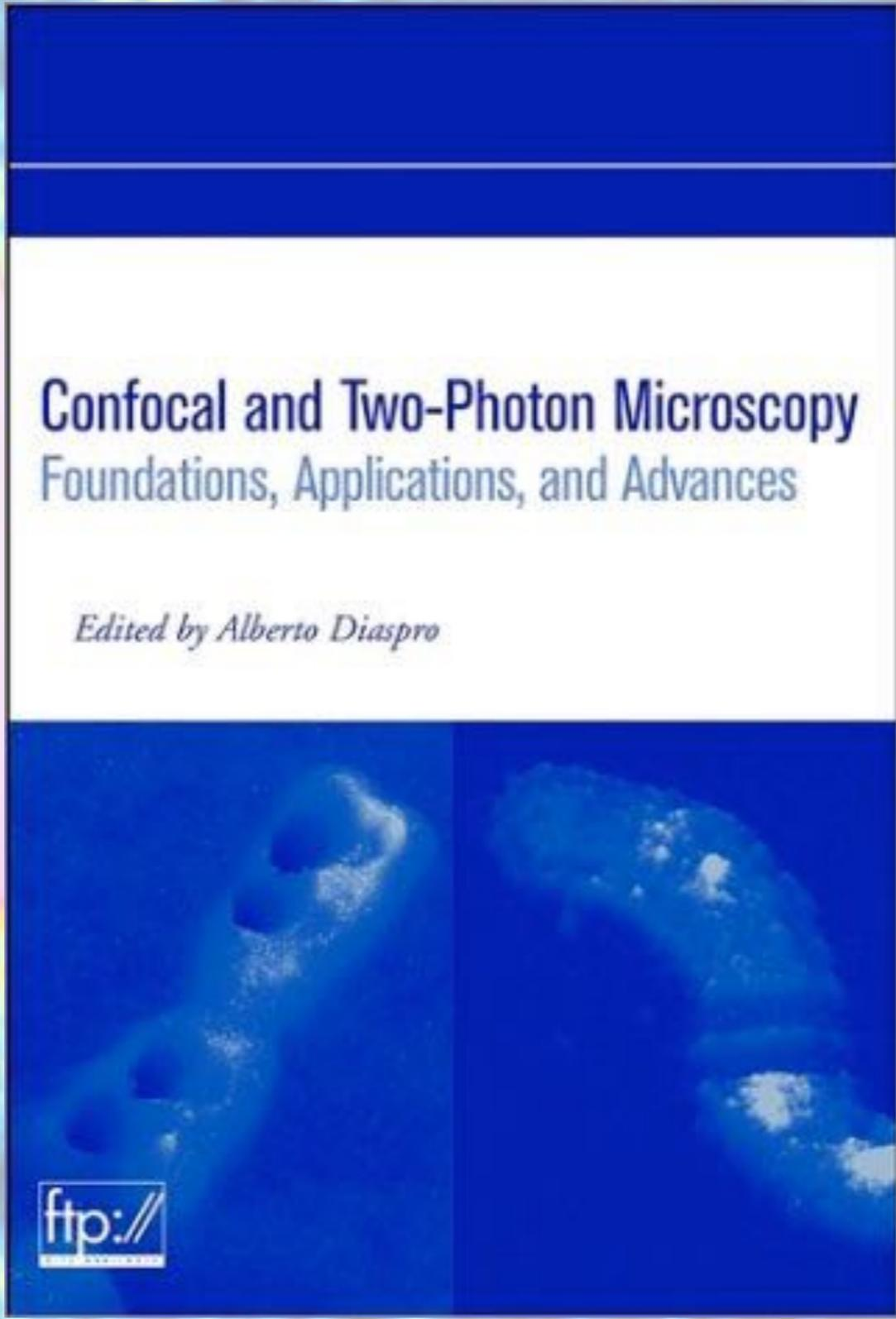
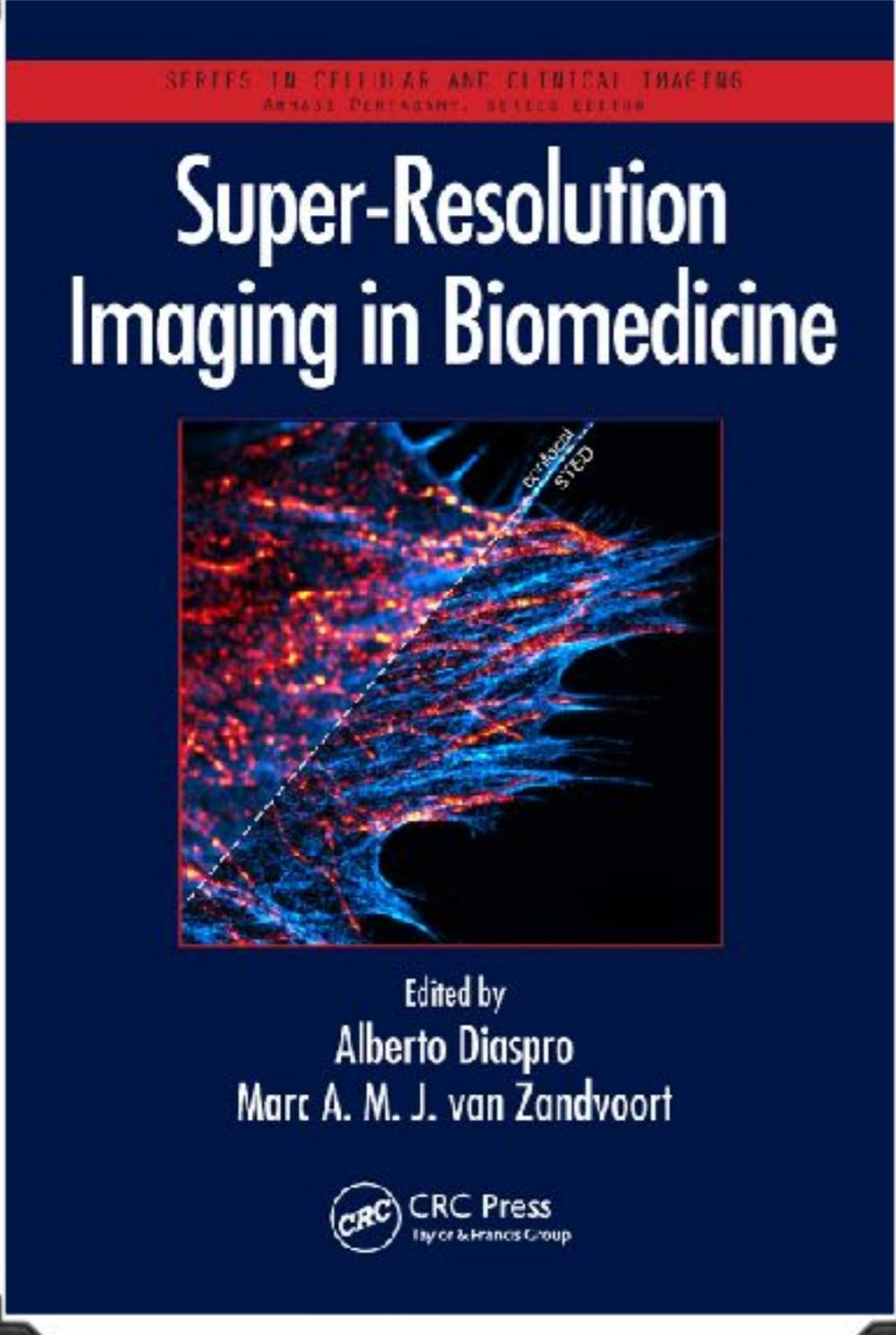
two-photon excitation (2pe) microscopy



Real-time visualization of thymocytes within intact thymic lobes using two-photon microscopy

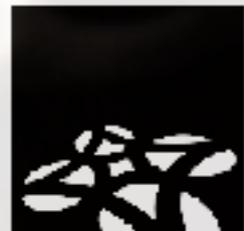
From: (2005) Tracking Migrating T Cells in Real Time. PLoS Biol 3(6): e205

Alberto Diaspro, Nanoscopy, Istituto Italiano di Tecnologia



Alberto Diaspro, Nanoscopy, Istituto Italiano di Tecnologia





Istituto Veneto
di Scienze Lettere
ed Arti

Nanoscale Optical Microscopy

6-9 June 2017
Venice, Italy

Arti
Lettere
Scienze

VENICE